UNIVERSITÁ DEGLI STUDI DI UDINE

CORSO DI DOTTORATO DI RICERCA IN
SCIENZE BIOMEDICHE E BIOTECNOLOGICHE

CICLO XXVI

TESI DI DOTTORATO DI RICERCA

FUNCTIONAL MODULATION OF BASE EXCISION REPAIR (BER) BY NON-CANONICAL DNA REPAIR ENZYMES: THE CASE OF NUCLEOPHOSMIN

Dottorando: MATTIA POLETTO

Relatore: Prof. GIANLUCA TELL

ANNO ACCADEMICO 2013/2014

To Michela

TABLE OF CONTENTS

TABLE OF CONTENTS

PREFACE

The stability of our genome is granted by a complex array of DNA repair systems that counteract DNA damage. DNA damage and DNA repair are necessarily linked to oncology, as the vast majority of genomic mutations originate from unrepaired or aberrantly repaired DNA lesions. Genome instability is an initiating factor during tumorigenesis, but plays also a fundamental role during tumor progression, because certain tumors can become reliant on a subset of DNA repair pathways to thrive. Interestingly, in the current clinical practice almost every therapeutic approach to cancer induces DNA damage. The study of DNA repair pathways is therefore crucial to understand the tumor response to conventional anti-cancer therapy and to develop novel approaches that exploit DNA repair pathway weaknesses in tumor cells.

This thesis work will focus on one particular DNA repair pathway (namely, the base excision repair – BER) that, in the last decade, has emerged as novel and appealing target for anti-cancer therapy. One of the components of BER that might be suitable for drug development is the apurinic/apyrimidinic endonuclease 1 (APE1), an enzyme that is critical to the pathway. APE1, in fact, is the major abasic endonuclease in mammalian cells, but it also regulates gene expression through redox-dependent and independent modulation of transcription. Currently, many laboratories are focusing on the development of specific APE1 inhibitors targeting the many functions of the protein: these molecules are very promising candidates for anti-cancer therapy, both as single agents and as adjuvants in combination therapy. However, the main limitation in translating these inhibitors from bench top to bedside is represented by the fact that APE1 is ubiquitously expressed, and systemic inhibition of this essential protein would likely have deleterious consequences.

A proteomic study carried out in the laboratory that hosted me during my PhD project revealed that the APE1 interactome is far more diverse than expected; among the proteins interacting with APE1, in fact, there are factors involved in the ribosome biogenesis and in different RNA processing steps. APE1, moreover, was unexpectedly found to accumulate within nucleoli through the interaction with the phosphoprotein nucleophosmin (NPM1), thus suggesting a putative role for APE1 during ribosome biogenesis. These studies are rather pioneering, as in this decade the scientific community is strongly reconsidering the view of the nucleolus as a mere ribosome factory. A novel concept of the nucleolus as a stress sensor is emerging, and a growing number of studies are revealing the presence of DNA repair factors among the proteins populating this organelle. Yet, their precise function still represents a question mark.

PREFACE

During my PhD studies I contributed to the thorough characterization of the APE1/NPM1 interaction, revealing its relevance to cancer. We discovered that this protein-protein association controls the APE1 catalytic activity during BER and, importantly, we observed that an aberrant APE1/NPM1 interaction occurring in a subset of acute myeloid leukemia (AML) patients sensitizes cells to DNA-damaging agents. Crucially, impairment of the APE1/NPM1 interaction hinders cancer cell proliferation. Therefore, we believe that targeting this molecular association might prove efficacious in treating cancers that overexpress both APE1 and NPM1, because these tumors might rely on an increased APE1/NPM1 interaction for survival and proliferation.

The characterization of the APE1/NPM1 interaction revealed a substantial gap into our knowledge of the NPM1 biology. Many evidences in literature point to a function of this multifunctional protein during the DNA damage response (DDR); nevertheless our knowledge concerning the exact role(s) of NPM1 in this context is still scanty. The discovery of the APE1/NPM1 association represented the first relevant hint to a possible direct role for NPM1 in the BER pathway. As it will become clear in this thesis, however, working on the sole APE1/NPM1 interaction was like scratching the tip of an iceberg.

ABSTRACT

The base excision DNA repair pathway (BER) is an essential cellular process that deals with small lesions originating from oxidation and alkylation of DNA, which occurs spontaneously, as a result of the intracellular metabolism, or after exposure to genotoxins (e.g. anti-tumor drugs). Unfortunately, dysregulation of BER enzymes is observed in some tumors and can foster cancer cells survival upon DNA damage caused by chemo- and radio-therapy. Recent findings highlighted an unexpected complexity of BER. Apparently unrelated protein components are now listed as novel modulators of the pathway; in addition, the individuation of BER factors within nucleoli opens questions on potential roles for BER proteins beyond DNA repair.

The interaction between the apurinic/apyrimidinic endonuclease 1 (APE1) and nucleophosmin (NPM1) is a perfect example of the BER complexity. As the main AP-endonuclease in mammalians, APE1 is central to BER; yet, through the association with NPM1, APE1 accumulates within nucleoli in tumor cells. Here it possibly takes part to RNA processing, a function that is somehow unrelated to the canonical APE1 role in BER. Furthermore, the APE1/NPM1 interaction modulates both the BER and the nucleolar roles of APE1, being essential for the proliferation of cancer cells. On the other hand, despite the growing body of evidence linking NPM1 and the DNA damage response, it is not clear whether NPM1 could play a direct role in the modulation of the overall BER.

My PhD project was aimed at the thorough characterization of the APE1/NPM1 association and of the general role of NPM1 in BER. A first part of this thesis will describe the development of small molecules able to disrupt the APE1/NPM1 interaction in tumor cells as novel tools for investigation and for translational purposes. The second part of this work will focus on the characterization of NPM1 as modulator of the BER. This thesis work led to the individuation of low molecular weight compounds targeting the APE1/NPM1 interaction and displaying anti-tumor properties. In addition, I demonstrate here for the first time the implication of NPM1 as multi-level modulator of the BER pathway, providing new insights into the role of BER proteins within nucleoli.

INTRODUCTION

1. The endless knot: DNA damage and DNA repair systems

The genetic information required to build a functional organism is carved on an intrinsically unstable substrate called DNA. The chemical nature of the DNA makes this molecule a powerful system to carry information; yet the very same composition of nucleic acids renders our genes susceptible to alterations. Byproducts of cellular metabolism, chemotherapeutic drugs, UV-radiation continuously expose our genome to life-threatening mutations. Consequently, in order to grant the integrity of DNA, cells have evolved an array of DNA repair systems. This chapter will introduce the concept of DNA damage, briefly reviewing our current knowledge of the complex network of pathways that are commonly referred to as "DNA repair systems".

1.1. Seek and destroy: from DNA lesions to repair systems

The cellular environment is constantly targeted by DNA-damaging threats; endogenous (e.g. reactive oxygen species – ROS[1]) as well as exogenous (e.g. ionizing radiation – IR) stimuli are common sources of DNA lesions [1]. The magnitude of the issue is nicely exemplified by a crude estimate of 10^5 DNA-damaging events per day in a single human cell; this implies that DNA repair systems must work at the striking rate of roughly 10^{16}-10^{18} repair events per day in an adult human organism [2]. Unrestricted accumulation of DNA lesions can induce mutagenesis (base substitutions, insertions, deletions and chromosomal rearrangements), contributing to cell death, cancer, neurodegeneration and aging. For this reason our cells possess several DNA repair systems; each of them operates on a particular subtype of DNA lesion, often with overlaps in the damage selectivity [3]. The spectrum of possible DNA lesions is wide: at a first glimpse DNA damage can be broadly categorized into (i) single nucleobases modifications (e.g. oxidation, alkylation, generation of abasic (AP) sites), (ii) damage to the phosphate backbone (i.e. single and double-strand breaks) and (iii) inter/intra-strand crosslinks [2]. Fig. 1 schematically lists the main DNA repair pathways, along with the type of lesion that is usually dealt with by each pathway.

[1] A list of the abbreviations has been placed at the end of the thesis, for clarity.

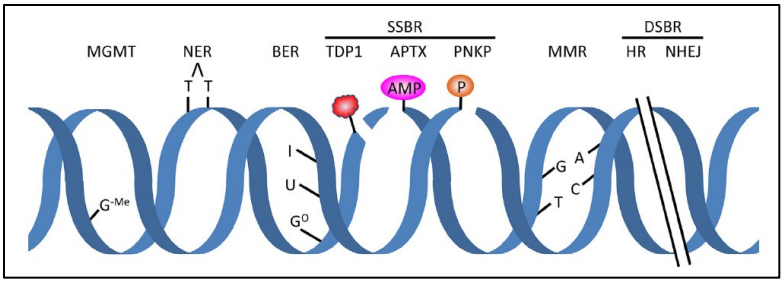

Fig. 1 – Schematic representation of the major DNA repair pathways in eukaryotic cells. Repair pathways or crucial enzymes are reported at the top, while the respective lesion is indicated at the bottom. APTX: aprataxin; BER: base excision repair; DSBR: double-strand break repair; HR: homologous recombination; MGMT: O^6-methylguanine-DNA methyltransferase; MMR: mismatch repair; NER: nucleotide excision repair; NHEJ: nonhomologous end joining; PNKP: polynucleotide kinase 3'-phosphatase; SSBR: single-strand break repair; TDP1: tyrosyl-DNA phosphodiesterase 1; G^{-Me}: O^6-methylguanine; T^T: thymine dimer; I: inosine; U: uracil; G^o: 8-oxoguanine. Source: [3].

The DNA repair systems acting in eukaryotic cells are usually organized into multi-step pathways, where groups of enzymes work in serial manner in order to resolve specific target lesions. Indeed, while prokaryotes and lower eukaryotes display several direct reversal enzymes, the only lesions directly reverted in mammals are O^6-alkylguanine adducts. This kind of damage, mainly introduced by endogenous and exogenous methylating agents (e.g. S-adenosylmethionine [1] and N-methylnitrosourea [4], respectively), is generally removed by a single suicide enzyme, namely MGMT [5]. Complex photo-adducts and other helix-distorting lesions are usually produced by environmental mutagens (e.g. UV irradiation, benzopyrene) by reactions with endogenous products of lipid peroxidation (e.g. malendialdehyde) or by certain chemotherapeutic drugs (e.g. cisplatin). The nucleotide excision repair (NER) pathway deals with such bulky lesions, removing a patch of DNA spanning several nucleotides around the site of damage and replacing it with undamaged nucleotides [6]. Bases mismatches and insertion-deletion loops are generally removed by the mismatch repair system (MMR); this pathway is in charge for the detection and elimination of replication errors, as well as of deleterious repair intermediates arising from the homologous recombination (HR) repair [7]. Single nucleotide lesions constitute a subtle modification of the DNA sequence that seldom leads to significant distortion in the double-helix structure. Bases modifications occur very frequently in eukaryotic cells, as mitochondrial respiration can foster the production of ROS, leading to nucleotides oxidation. Typical examples of nucleobase lesions are oxidation derivatives (e.g. 7,8-dihydro-8-oxoguanine – 8-oxo-dG) or alkylation byproducts (e.g. 3-methyladenine); the latter being mainly introduced by chemotherapeutic alkylating agents (e.g. temozolomide). The base excision repair (BER) pathway is the DNA repair system that detects these small lesions and removes the damaged nucleotide(s). This particular DNA repair pathway is central to this thesis and will be described in great detail in the next chapter. DNA strand breaks are very toxic and mutagenic lesions which can

induce chromosomal rearrangements. It has been calculated that a single double-strand break (DSB) is sufficient to arrest the cell cycle of a eukaryotic cell [8]. In order to cope with such cytotoxic lesions our cells have two DSB repair systems, namely the nonhomologous end joining (NHEJ) and the HR pathways. The two enzymatic systems are preferentially used in distinct cell cycle phases (i.e. HR prevails over NHEJ during the S and G2 phases); with NHEJ being the major DSBs repair system in higher eukaryotes [3].

Notably, each DNA damaging agent induces a widespread spectrum of lesions, and this is particularly evident for anti-cancer agents. Cisplatin, for instance, generates DNA adducts, interstrand crosslinks (ICLs) and oxidative-stress [9, 10]. It is therefore clear that a single DNA repair pathway cannot cope with a DNA damaging challenge as an isolated entity. Accordingly, several evidences point to the existence of diverse cross-talks between DNA repair pathways. BER, just to name one, is tightly and dynamically connected to the single-strand break repair (SSBR) pathway, as single-strand breaks (SSBs) are repair intermediates generated during the BER process itself [11]. In addition, also the NER and the MMR pathways have recently been suggested to share connection points with the BER, especially when DNA lesions are very heterogeneous, as in the case of cisplatin [10-13] or 5-fluorouracil [14].

In conclusion, the description of DNA repair pathways as static arrays of sequential operations is nowadays outdated. Rather, DNA repair pathways must be regarded as dynamic systems that co-operate and sometimes compete to repair DNA with extreme plasticity, adapting to the existing damage load and characteristics.

1.2. The DNA damage response

As our knowledge of DNA repair pathways deepened, the definition of "DNA repair system" itself evolved. Currently it seems more appropriate to name "DNA damage response" (DDR) the complex signaling network that is responsible for the maintenance of the genome stability. The current concept of DDR is centered onto DNA checkpoints as key entities that monitor DNA integrity throughout the cell cycle, working together with canonical DNA repair pathways. DNA checkpoints are therefore not responsible for DNA damage sensing *per se* (this is a task carried out by DNA repair pathways), their role is rather to grant an appropriate response to any kind of insult the cell genome might take. The typical behavior of a coordinated DDR involves: halting the cell cycle to allow adequate time to repair DNA or to trigger apoptosis; preventing the generation of secondary lesions, by directing the primary lesion to the most appropriate repair pathway and by boosting that pathway; modifying transcription [5].

The DDR works at least at five levels (Fig. 2): sensors recognize DNA lesions and chromatin abnormalities. Usually, the detection of the lesion is directly carried out by DNA repair proteins. Proximal transducer kinases, such as the ataxia telangiectasia mutated (ATM) and the ataxia telangiectasia and Rad3 related (ATR), mediate the very first DNA damage signaling event. Distal transducer kinases (e.g. Chk1 and Chk2) are then responsible for the amplification of the signaling cascade. The importance of phosphorylation at this stage of the DDR is highlighted by the finding that DNA damage elicits over 900 distinct phosphorylation events, involving more than 700 substrates [15]. Mediators determine both the temporal and the spatial progression of the DDR by coordination of the phosphorylation events, whereas effectors determine the outcome of the DDR. A typical example of effector molecule is the p53 tumor suppressor, the stabilization of which is quantitatively linked to the DNA damage load and may lead to cell cycle arrest, apoptosis or senescence [16, 17].

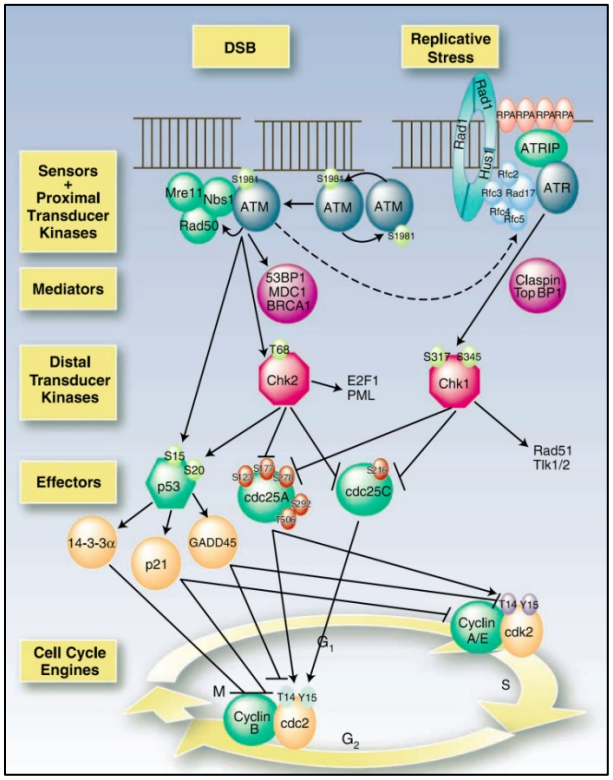

Fig. 2 – Schematic description of the canonical DNA damage response. Genomic instability induced either by direct DNA damage (here represented by a DSB) or by replicative stress is detected by specific sensors (e.g. the Mre11-Rad50-Nbs1 or "MRN complex", or the Rad9-Rad1-Hus1 or "911 complex") and immediately transduced to proximal kinases (i.e. ATM, ATR). Mediators determine the spatial and temporal activation of the DDR through coordination of the phosphorylation cascade to the distal transducers (i.e. Chk1, Chk2). Effectors govern the final outcome of the response through direct and indirect modulation of the cell cycle engines. Adapted from [18].

It is worth mentioning that in the last decades the nucleolus has emerged as novel and unusual site where the DDR might originate. In particular, it appears that some kinds of cell stress, DNA damage in particular, are sensed through this organelle, leading to p53 stabilization [19-21]. This topic is central to this thesis and it will be thoroughly discussed in a dedicate paragraph (2.4 "*Nucleoli and BER. The ribosome factory revisited*").

2. *Base excision repair. A pathway for sneaky lesions*

As mentioned in the first chapter, the BER pathway canonically deals with small non-bulky lesions that do not induce major distortion in the double-helix structure. Examples of such lesions are oxidized or alkylated DNA nucleobases, but also deamination products, such as uracil or inosine [3]. The importance of this pathway is underlined by the fact that DNA damage resolved by BER is very common in our cells; current estimates suggest that there are more than 100 kinds of oxidative base modifications, potentially arising as the result of ROS attack ([22] and references therein). In addition, the occurrence of abnormal nucleobases can be highly mutagenic, as some lesions do not block the DNA polymerase, which can incorporate the wrong nucleotide. This can lead, for instance, to transversion mutations in the case of 8-oxo-dG:A mispairings [23, 24]. Other modified bases (e.g. thymine glycol), conversely, directly hinder the progression of DNA or RNA polymerase, triggering apoptotic responses ([3] and Fig. 3).

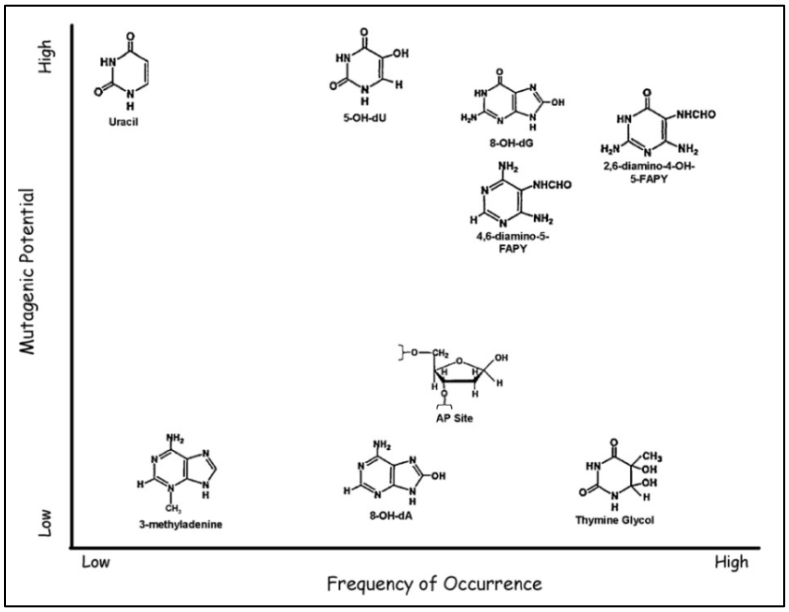

Fig. 3 – Frequency and mutagenic potential of some common bases and sugar lesions. The graph depicts the chemical composition of a subset of canonical BER substrates. The mutagenic potential refers to the likelihood of inaccurate duplication or bypass over the lesion; as a general rule, with few exceptions, the greater the blocking potential, the lower the mutagenic capacity. Source: [25].

The following paragraphs will give an overview of the BER pathway, with particular emphasis on the coordination of this complex DNA repair system. The current implication of BER enzymes in tumorigenesis and therapy resistance, as well as the possibility to target BER enzymes for

anti-cancer therapy, will be briefly outlined. This section will end with a short glimpse on our current knowledge of the non-canonical roles of the BER proteins, providing some preliminary consideration concerning the still puzzling presence of BER enzymes within nucleoli.

2.1. Exploring the BER pathway

The BER pathway is an essential DNA repair system in higher eukaryotes; accordingly, homozygous knockout of the core BER factors (apurinic/apyrimidinic endonuclease 1 – APE1, DNA polymerase β – Polβ, X-ray repair cross-complementing 1 – XRCC1, DNA ligase I – LigI and DNA ligase III – LigIII) results in embryonic or early post-natal lethality [3]. Enzymatic and non-enzymatic components of the pathway co-operate in a sequential manner following five major steps: (i) recognition and excision of the damaged base, (ii) incision of the resulting AP site to generate a nick on the DNA backbone, (iii) processing of the DNA ends surrounding the nick, (iv) filling of the nucleotide gap and (v) sealing of the nick ([3, 26] and Fig. 4).

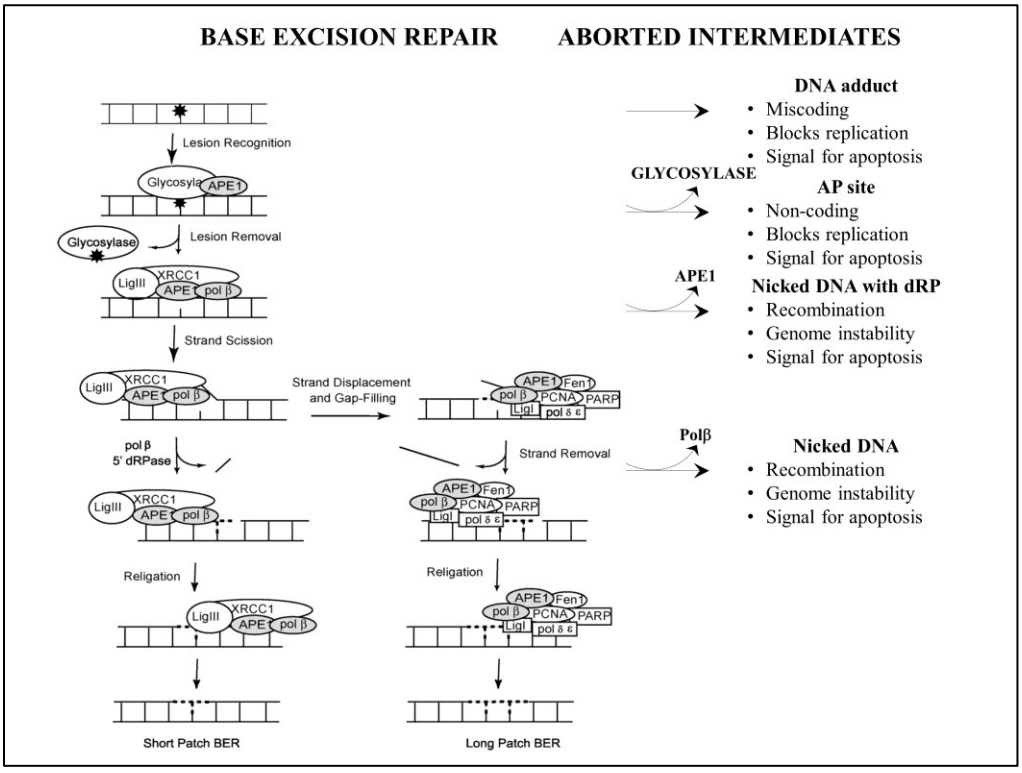

Fig. 4 – The BER pathway: importance of its modulation to avoid the formation of aborted intermediates. Schematic representation of the BER-mediated DNA repair. Each stage involves the intervention of one or more proteins (indicated by ellipses and boxes). The canonical separation of the pathway in two sub-pathways (short and long patch BER) is depicted. Note that in the absence of proper coordination of the BER, each enzymatic step can generate an aborted intermediate that, in turn, can lead to different deleterious consequences. Adapted from [11, 27].

As already mentioned, BER copes with small and non-bulky damaged bases; therefore, in order to detect such "sneaky" lesions, cells possess a pool of specialized enzymes called DNA glycosylases. These proteins are thought to scan the DNA helix, recognizing and excising the damaged base in a lesion-specific manner. DNA glycosylases can be categorized into monofunctional or bifunctional, depending on their mechanism of action. While monofunctional DNA glycosylases (e.g. the uracil-DNA glycosylase – UNG) simply cleave the C1'-N-glycosidic bond, generating an AP-site, bifunctional enzymes have an associated β-lyase activity (e.g. the 8-oxoguanine DNA glycosylase – OGG1) that, in addition to the elimination of the damaged base, cleaves the DNA backbone leaving a 3'-α,β-unsaturated aldehyde blocking moiety. An additional family of DNA glycosylases (represented by the human NEIL1 and NEIL2 enzymes) is also able to operate a β,δ-elimination reaction, leaving a 3'-phosphate-blocked nick on the DNA backbone [28]. Higher eukaryotes display a vast array of DNA glycosylases (at least 11 in human [28]), with significant redundancy in their damage selectivity. Accordingly, single knockout of many enzymes of this class is not lethal *per se*, even if accumulation of unrepaired DNA lesions occurs [29, 30].

The base excision step generally leaves behind an AP-site that is immediately recognized and processed by an AP-endonuclease, which cleaves 5' to the baseless site, nicking the DNA backbone and generating a 3'-OH and a 5'-dRP (deoxyribonucleotide-phosphate) moiety. In metazoans the major AP-endonuclease activity is ascribed to APE1, a multifunctional enzyme that will be described in great detail in the following chapter of this thesis. APE1 incision is usually sufficient to generate the DNA ends suitable for the conclusion of the repair process; further oxidation of the DNA termini, base-excision operated by bifunctional glycosylases, or complex repair intermediates, however, require the intervention of other end-processing enzymes such as aprataxin (APTX), the polynucleotide kinase 3'-phosphatase (PNKP) or the tyrosyl-DNA phosphodiesterase 1 (TDP1). The dRP-lyase activity of Polβ and minor APE1 activities (see below) may also contribute to the "end-cleaning" process. These end-tailoring enzymes convert the SSB to a single-nucleotide gap that can be efficiently filled in and re-ligated [26, 28, 31-34].

After the end-processing step, the repair process can take two different sub-pathways. Typically, BER proceeds via the short-patch (SP) pathway, engaging Polβ to replace the missing nucleotide, followed by the XRCC1-LigIII complex which is responsible for the ligation of the nick [35]. Under some circumstances, such as the presence of a 5'-moiety that is refractory to the Polβ lyase activity, low ligation efficiency, or during the S phase of the cell cycle (i.e. when replication-associated proteins are more abundant), BER can be completed through a strand displacement-dependent gap filling process called long-patch (LP) pathway [3, 36]. LP-BER relies on replicating polymerases such as DNA polymerase δ and ε, in a complex with the sliding clamp PCNA

(proliferating cell nuclear antigen); Polβ is able to carry out a strand displacement-dependent gap filling as well, but only after stimulation by specific protein-protein interactions [37]. During LP-BER a stretch of 2-12 nucleotides generated during the synthesis process is removed by the flap endonuclease FEN1 and subsequent intervention of the PCNA-associated LigI seals the nick [37, 38].

As mentioned in the first chapter, the BER is not an isolated process, but it shares protein components with at least two sub-pathways, namely SSBR and nucleotide incision repair (NIR) [27]. SSBs are generated by a plethora of cues, including ROS, ionizing radiation, radiomimetic drugs and topoisomerase I inhibitors, but are also unavoidable intermediates generated during BER processing. The SSBR pathway initiates through recruitment of the poly(ADP-ribose) polymerase PARP1, which recognizes exposed SSBs and modulates the repair process through enzymatic ADP-ribosylation of protein substrates. Interestingly, many BER proteins (e.g. XRCC1, Polβ) interact with PARP1 ([37] and Fig. 5). Moreover, PARP1 has been shown to enhance the BER processing of uracil and AP-sites overall [39], highlighting the tight connection between BER and SSBR. More recently, Ischenko and Saparbaev individuated a glycosylase-independent branch of the BER that specifically deals with a subset of base lesions (e.g. 5-hydroxy-2'-deoxycytidine, uracil). The so called NIR pathway requires intervention of APE1 as entry-point enzyme, through a direct incision step at the damaged base [40-42]. Although very interesting, the physiological impact of the NIR pathway is still undergoing investigation, as within the intracellular milieu the presence of specific DNA glycosylases would likely render the NIR process poorly efficient.

2.2. Coordination of BER. The power is nothing without control

The concept of BER as a streamline process in which isolated enzymes carry out sequential reactions independently of one another is well outdated. The current view of BER is that of a dynamic intertwining of different enzymes and auxiliary proteins that operate in a highly orchestrated manner. Temporal and spatial coordination of BER (and, in general, of any DNA repair pathway) is essential for at least two reasons:

i. Imbalance in the BER components has been linked to genetic instability. In particular, overexpression of several core elements of the pathway is a hallmark of cancer progression and resistance to therapy [43-46]. These observations are possibly explained by the fact that increased expression of a single BER factor results in competition or excessive enzymatic activity, which is not buffered by sufficient amounts of the other proteins in the pathway. This has been formally shown, for instance, for APE1 [47], N-alkyladenine DNA glycosylase (AAG) [48] and Polβ [49, 50].

ii. Abortive intermediates of the pathway display intrinsic cytotoxicity. As introduced in the previous paragraph, in the absence of coordination the BER pathway may expose toxic reaction products to the cellular environment. Paradoxically, unprotected intermediates (e.g. SSBs) are much more toxic than the initial damaged bases (Fig. 4 and [51]). Therefore, the fine synchronization of the pathway is possibly the result of an evolutionary tradeoff between the rapid repair of mutagenic lesions and the potential hazard of deleterious intermediates that such repair generates.

Several models have been proposed in order to explain the mechanisms that have evolved to optimize the repair efficiency of the BER pathway. A first hypothesis dates back to 2000, when Wilson and Kunkel presented the so called "passing the baton" model for the BER coordination [11]. This model was based on the evidence that many BER factors are tightly associated by means of direct protein-protein interaction, or through DNA-protein interaction. Wilson and Kunkel suggested that the reaction substrate is channeled from the DNA glycosylase to the DNA ligase without any interruption that would expose toxic intermediates [11]. This model is supported by the evidence that many BER proteins interact with each other, displaying increased affinity for the reaction product of the upstream enzyme, rather than for their own substrate. A subsequent model proposed by Allinson and colleagues suggested that reaction rates of enzymatic activities within the pathway are concurrently tuned in order to achieve the required synchronization [39]. This model, for instance, postulates that the DNA glycosylases turnover rate and PARP1 contribute to the coordination of the repair process. According to this model, each kind of lesion affects differently the downstream pathway, which flexibly optimizes the repair rates with oscillations as great as one order of magnitude in terms of repair capacity [39].

A model that was somehow opposing the "passing the baton" paradigm postulated the existence of pre-formed complexes of BER factors (BERosomes) that process the DNA lesion as separate units [52, 53]. This concept was further elaborated to a "unified model", which separated the whole BER process into three functional processes (lesion recognition, strand scission/gap tailoring and DNA synthesis/ligation) each carried out by one or more transient multi-protein complexes and coordinated by scaffold proteins and post-translational modifications (PTMs) [27].

Despite the apparent divergence among the models that have been put forward to explain the complexity of BER, each of them probably describes different aspects of a unique and highly dynamic process. It is currently clear that the fine modulation of the BER pathway is achieved through a complex network of more or less stable protein-protein interactions and PTMs. Phosphorylation, acetylation, methylation, SUMOylation, as well as ubiquitination of almost every BER component have been suggested to play a role in the modulation of the pathway [27, 37, 54].

Moreover, direct as well as DNA-mediated interactions among BER enzymes and non-enzymatic scaffolds (e.g. XRCC1, PCNA) coordinate catalytic activities and dictate the selection of the sub-pathway appropriate for each situation ([27, 37] and Fig. 5).

An emerging concept is the role of non-canonical proteins as BER modulators. Several proteins apparently unrelated to the pathway have recently been discovered as novel unexpected coordinators of the BER [19]. p53, for instance has been implicated in the modulation of both APE1 and Polβ [37], whereas our laboratory discovered nucleophosmin (NPM1) as a new modulator of the APE1 enzymatic activity (see below). Additional modulation of the BER pathway is also achieved through evolutionarily acquired disordered extensions of some BER components, as will be discussed later.

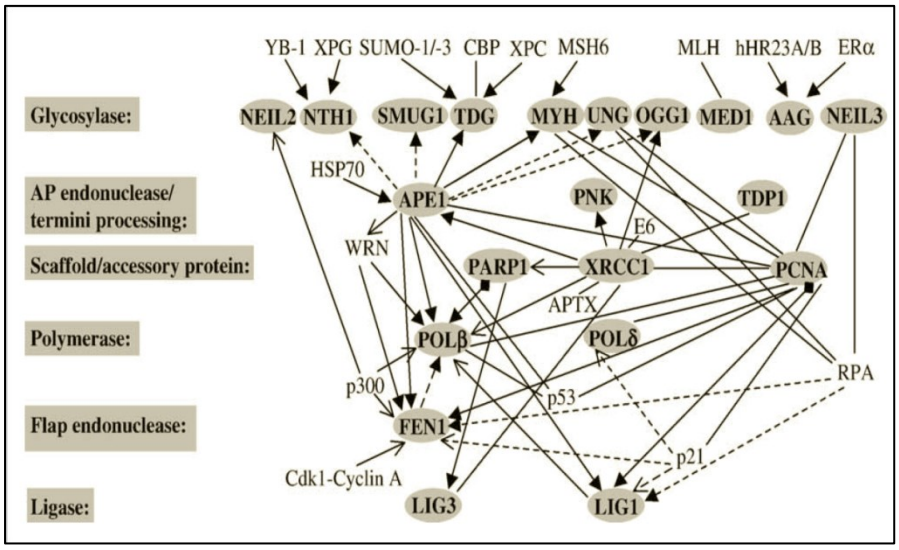

Fig. 5 – The complexity of the BER protein-protein interaction network. Canonical BER proteins are highlighted. Proteins detected within the same complex are connected by solid lines. Dashed lines connect proteins that do not share a complex, but that functionally influence each other. Stimulatory (closed arrows), inhibitory (open arrows) or stimulatory/inhibitory (closed arrows with a rectangle) effects are indicated. Lines without arrows indicate interaction in the absence of known effect. Source: [37].

BER enzymes are generally abundant proteins endowed with a relatively long half-life. Given the highly dynamic environment that every organism faces, it is clear that the amount of BER proteins must constantly oscillate and adjust to the steady-state DNA damage load. It is currently accepted that the enzymes engaged in the repair process are stabilized, while excessive components not involved in DNA repair are targeted for proteasomal degradation. The recent identification of several factors belonging to the ubiquitin-proteasome system as modulators of the BER stability shed new light on

the quick regulation of the BER dynamics ([28, 54, 55] and references therein). The turnover of Polβ, for instance, is the result of a balance between mono- or poly-ubiquitination reactions (mediated by the Mcl-1 ubiquitin ligase E3 – Mule and CHIP, respectively) and de-ubiquitination activities (carried out by the ubiquitin specific protease USP47) [56-58]. Interestingly, Mule activity is modulated through direct binding to the p14 alternative reading frame ($p14^{Arf}$) tumor suppressor [55], a DNA damage-responsive factor ([59-62] and Fig. 6) that is involved in the cellular protection against DNA damage and oncogenic activation. The mechanisms controlling $p14^{Arf}$ activation are only beginning to be elucidated, and it has been proposed that, under stress conditions, this protein is able to trigger a cell cycle delay through the stabilization of p53. This process is likely mediated by concurrent inhibition of the E3-ligases Mule and of the mouse double minute homolog 2 (Mdm2) which, under basal condition, target p53 for proteasomal degradation [63]. The $p14^{Arf}$/Mule axis, therefore, appears an interesting connection point between DNA damage sensing and the modulation of the BER protein amount; the fine mechanisms controlling these fluctuations, however, still need thorough explanation.

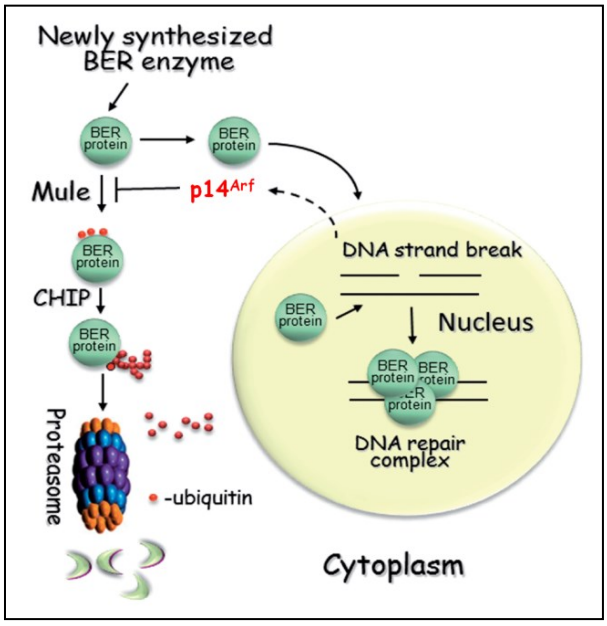

Fig. 6 – Modulation of the BER protein stability through the $p14^{Arf}$/Mule axis. Schematic representation of the pathway that regulates the steady-state levels of the core BER components (i.e. Polβ, XRCC1 and LigIII). BER proteins not engaged in DNA repair are constantly targeted for proteasomal degradation through Mule-mediated mono-ubiquitination and CHIP-mediated poly-ubiquitination. Upon DNA damage sensing, activation of the $p14^{Arf}$ tumor suppressor inhibits Mule, thus allowing quick stabilization of the BER proteins required to repair the lesion. Adapted from [28].

2.3. BER as a target for anti-cancer therapy

Very few diseases have been directly associated with defects in the BER pathway, perhaps as a consequence of the already mentioned importance of the core BER components for life. Among the few enzymes that have been linked to disease it is worth mentioning the glycosylases MUTYH and UNG, associated with cancer predisposition and immunological disorders, respectively [3]. Several investigators are pursuing the hypothesis that subtle variations among individuals, rather than overt inactivation of the BER capacity, are associated with disease occurrence, likely in an environmental exposure-dependent manner [64, 65].

A crucial feature of many cancer types is the overexpression of BER proteins, which frequently leads to the onset of chemo- and radio-resistance ([5] and references therein). Overexpression of APE1, for instance, has been reported to confer resistance to several chemotherapeutics (e.g. cisplatin, bleomycin) [66, 67] as well as to ionizing radiation [45]. In addition to these "macroscopic" expression phenotypes, more subtle variations, such as polymorphisms have been suggested to affect predisposition to tumor development. Polymorphic variants of APE1, XRCC1, OGG1 and Polβ, for instance, have been shown to affect DNA repair capacity, increasing susceptibility to cancer and negatively impacting on the overall survival [5, 68, 69].

Despite the presence of conflicting reports, it is possible to conclude that polymorphic variants, as well as expression patterns of BER proteins, might be important prognostic and predictive indicators in cancer. Several preclinical studies, moreover, have shown that downregulation of BER components sensitizes cells to different chemotherapeutics. For these reasons it has been suggested that the BER pathway might prove an effective druggable target to induce chemo-sensitization in specific tumor subtypes [30, 70]. Several laboratories are currently working in order to develop inhibitors of the core enzymes of the pathway (i.e. APE1, Polβ and FEN1) that display features suitable for translational applications [70].

2.4. Nucleoli and BER. The ribosome factory revisited

Before the turn of the century the nucleolus was merely considered the "ribosome factory" of the cell; strikingly, proteomics analyses of the nucleolar proteome revealed that these organelles contain a plethora of proteins that are not directly related to the classical ribosome processing machinery [71-74]. Among these were identified several DNA repair factors (e.g. LigIII, BRCA1, the Ku70/80 antigens, XRCC1), although their precise function in nucleoli was (and still is) poorly understood (reviewed in [19]). Nowadays, the presence of DNA repair proteins within nucleoli is well established ([19] and references therein). Several BER enzymes have been found to accumulate in these subnuclear compartments and their nucleolar localization has usually been linked to functions

that are uncoupled from their canonical role in the BER pathway. A paradigmatic example is given by APE1, which accumulates within nucleoli through the interaction with NPM1 and ribosomal RNA (rRNA). The nucleolar fraction of APE1 has been suggested to play a role in the RNA quality control processes [75] although the detailed molecular mechanisms of this non-canonical APE1 activity still remain elusive (the reader is referred to the next chapter for further details). Very recently, also the single-strand-selective monofunctional uracil-DNA glycosylase 1 (SMUG1) was shown to localize within nucleoli and to take part to the rRNA processing steps [76].

An emerging aspect in the biology of the nucleolus is the function of this organelle as a sensor for cell stress [21]. Extensive analyses documented a broad rewiring of the nucleolar proteome upon DNA damage; DNA repair proteins, in particular, relocalize from nucleoli under stress conditions (see for example [77-79], while the topic has been recently reviewed in [19]. The observed reorganization of the nucleolar proteome, fascinatingly, appears to be highly specific and selective, depending on the DNA damaging stimulus and ranging widely terms of both order of magnitude and proteins involved [20, 80].

Two key questions are still in need of answer: what is the function of nucleolar DNA repair proteins? Is there any functional relevance for the observed relocalization of nucleolar DNA repair proteins upon DNA damage? This thesis will try to address these open points, with a particular emphasis on BER enzymes.

3. Planet of the APE1(s)

APE1 is a key enzyme in the BER pathway and in mammalian cells. Almost every DNA lesion processed through the BER generates a repair intermediate that eventually requires the intervention of this protein. APE1, moreover, interacts with several BER components, both upstream and downstream in the pathway, acting as a fundamental coordinator for the entire DNA repair process [81].

APE1 is an abundant protein, ubiquitously expressed in every tissue [82]; the first reports on the protein date back to the nineties, when APE1was independently discovered as the main abasic endonuclease in cells and as a protein able to activate through a redox-dependent mechanism the transcription factor AP-1 [83-85]. Thereafter APE1 was named APE1/Ref-1 (i.e. apurinic/apyrimidinic endonuclease 1/Redox effector factor 1) and regarded as a multifunctional protein, acting both as a central BER component and as a co-transcriptional modulator.

As many other core BER enzymes, the protein is essential for cell viability and embryo development [86], whereas haploinsufficiency for APE1 has been shown to render mice hypersensitive to oxidative stress and enhance spontaneous mutagenesis [87, 88]. Being APE1 a vital protein, no APE1-deficient cellular models are available to date, making *in vivo* studies challenging. Therefore, it is still a matter of debate which protein function (i.e. DNA repair, redox, or both) is required for cell survival. This chapter will thoroughly describe the functions of the protein, with particular emphasis on its overlooked and phylogenetically young N-terminal domain. The recent discovery of novel non-canonical roles of APE1 will be discussed, especially in relation with its unexpected nucleolar residence and its interaction with NPM1. The chapter will then summarize our knowledge about the modulation of APE1, eventually describing the current efforts aimed at the pharmacological targeting of APE1 in pathology.

3.1. Protein structure and function

APE1 is a relatively small protein encompassing 318 amino acids. X-ray diffraction analyses revealed a monomeric α/β-sandwich globular fold that is structurally related to the *E. coli* exonuclease III (ExoIII) [89]. The protein also presents an unstructured N-terminal extension (first 48 amino acids) which represents a phylogenetically young addition to the protein [90-92]. APE1 can conventionally be separated into two functionally independent, but structurally overlapping domains. The C-terminal globular region of the protein (residues 61-318) is mainly devoted to the enzymatic activity and nucleic acid binding function, whereas the N-terminal portion (residues 1-127) is mainly

committed to the redox-dependent activity towards different transcription factors ([82, 93] and Fig. 7).

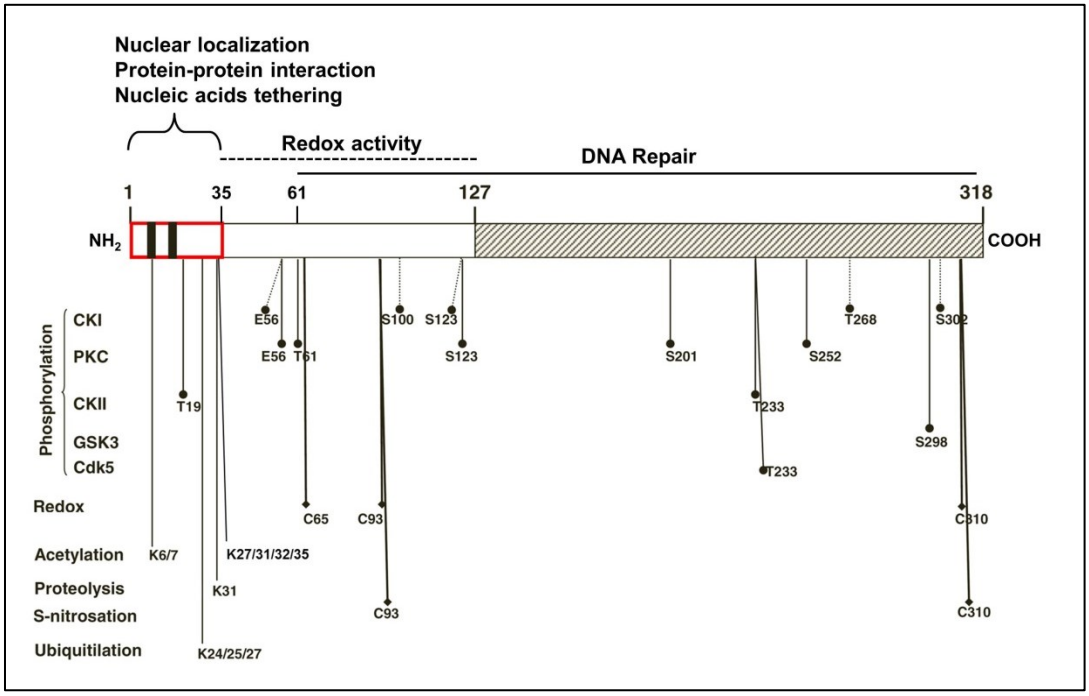

Fig. 7 – Schematic overview of the structural and functional organization of the APE1 protein. The APE1 tripartite functional arrangement is reported, along with the main activities ascribed to each domain. The lower part of the figure highlights the main residues known or predicted to undergo PTMs. Black bars at the N-terminus represent the bipartite nuclear localization signal. Adapted from [94-96].

The endonuclease function of APE1 on abasic DNA accounts for the vast majority of the total AP-site incision activity in a whole cell extract [83, 84]. The protein's C-terminal domain is highly conserved and shares extensive similarity with the *E. coli* homolog ExoIII [89]; this globular domain catalyzes the Mg^{2+}-dependent cleavage of the phosphodiester bond 5' to the AP-site, leaving a 3'-OH and a 5'-dRP group flanking the DNA nick. The enzymatic mechanism has been extensively analyzed and the fundamental amino-acids involved in the catalysis have been described by multiple mutagenesis studies [89, 92, 97, 98]. Beside the canonical activity on AP-site-containing DNA, APE1 has been reported to possess also additional functions such as 3'-phosphatase, 3'-5' exonuclease, 3'-phosphodiesterase, and RNaseH activity [97, 99, 100]. Most of these supplementary activities are very weak *in vitro* and likely contribute to very specific DNA end-tailoring events *in vivo*. The 3'-phosphodiesterase activity, for example, has been proposed to take part to the removal of fragmented sugar moieties at DNA strand breaks induced by bleomycin [101, 102]. The AP-site incision activity

and the additional APE1 functions likely share critical amino acids within the C-terminal domain, with few, reaction-specific, exceptions [103-105].

Recent and surprising findings revealed that APE1 exerts endonuclease activity also on RNA ([106] and references therein). The APE1-mediated cleavage of abasic RNA was observed concurrently with the unexpected nucleolar accumulation of the protein and was suggested to play a role in the rRNA processing mechanisms [75, 107, 108]. Accordingly, siRNA-mediated depletion of APE1 in HeLa cells resulted in an accumulation of oxidized RNA species and impairment of protein synthesis and cell growth [75]. In parallel studies APE1 was identified in rat liver polysomes as the endonuclease responsible for the cleavage of the c-myc mRNA, thus suggesting that the APE1 RNA-endonuclease activity might control the stability of selected target RNAs [108]. Additional mRNAs were also demonstrated to be target of APE1, the *in vivo* relevance of this overlooked APE1 function, however, remains to be elucidated [109].

APE1 is the only known DNA repair protein endowed with an associated redox function [110]. Since the first report identifying APE1 as the protein able to stimulate the DNA binding activity of AP-1 in a redox-dependent manner [85], several laboratories detected a long list of ubiquitous and tissue-specific transcription factors that are co-activated by APE1. Among these, there are factors relevant to cancer development and growth (e.g. nuclear factor-κB – NF-κB, HIF-1α, Egr-1, p53) suggesting that pharmacological targeting of the APE1 redox activity might be an interesting approach to anti-tumor treatment (refer to the paragraph 3.3 "*APE1 and pathology*") [110]. The mechanism underlying the APE1-mediated activation of so many structurally unrelated transcription factors is still poorly understood [110, 111]. The C65 residue has been implicated in catalysis, with C93 and/or C99 likely working as resolving cysteines during the reaction mechanism [110]. C65 is however solvent-inaccessible and a catalytic mechanism involving the partial unfolding of APE1 has been proposed [112, 113]. Curiously, the redox domain of APE1 appears to be a phylogenic gain of function of the protein, as the zebrafish ortholog (zAPE1) lacks any detectable redox activity. Substitution of the residue corresponding to C65 in zAPE1, however, completely restores the redox function of the mutant, further pointing to C65 as critical residue for this accessory APE1 activity [111]. APE1 has been suggested to modulate transcription factors with two distinct mechanisms; p53, for instance, undergoes both redox-dependent and redox-independent modulation by APE1. While the first mechanism enhances p53 DNA-binding activity through reduction of the transcription factor [114], the redox-independent action of APE1 promotes p53 tetramerization [115].

In addition to its canonical activities (i.e. DNA repair and redox), APE1 has been demonstrated to directly modulate the transcriptional rate of diverse genes. In particular, APE1 was initially discovered as a component of a protein complex binding to the negative calcium response

elements (nCaRE) on the parathyroid hormone gene promoter [116] and subsequently suggested to play a role in the modulation of the renin gene [117]. It has been proposed that the presence of nCaRE sequences upstream the APE1 gene contributes to a negative feedback-like modulation of the APE1 expression [118]; this hypothesis, however, has not been thoroughly investigated. As nCaRE sequences are present in many other genes, it is conceivable that the binding of APE1 to these sequences might play a role in the transcriptional modulation of several cellular components. This is indeed the case for the SIRT1 deacetylase, which transcription is induced upon oxidative stress by an nCaRE-binding complex containing APE1 itself [119, 120].

3.2. The N-terminal domain: an overlooked molecular device for APE1

Only very recently the N-terminal extension of APE1 roused the interest of the scientific community. This domain has long been barely considered in the structural analyses of the protein as its intrinsic lack of ordered structure impairs its ability to crystallize ([90] and references therein). Intrinsically disordered regions in DNA repair proteins are only now emerging as important regulation points of many aspects of the BER pathway, and several studies highlighted the recent phylogenic acquisition of disordered domains in different BER proteins [52, 90, 91].

The N-terminal region of APE1 (amino acids 1 to 48) has been shown to modulate diverse aspects of the biology of the protein, including its roles in abasic DNA/RNA cleavage (through regulation of the catalytic activity and the nucleic acids binding), its function as a transcriptional modulator, and its protein-protein interaction network. In particular, it is clear that the N-terminal extension of APE1 is required for its stable binding to several protein partners, including XRCC1, Polβ and NPM1 [75, 121, 122]. This protein region, moreover, is absolutely necessary for the discrimination of structural elements in undamaged nucleic acids, a feature that APE1 likely exploits during the nCaRE-mediated transcriptional modulation and to detect AP-sites [90, 119]. During part of my PhD project I systematically investigated the APE1 binding capacity toward undamaged nucleic acids, highlighting that secondary structures (e.g. double-stranded regions interrupted by single-stranded local distortions) strongly enhance the APE1 affinity for DNA/RNA [90]. These findings deepen our comprehension of the APE1-mediated transcriptional modulation through nCaRE sequences binding [119]. Moreover, our observations support a two-step mechanism explaining APE1 detection of DNA damage: a first, low-affinity, quasi-processive scanning [123] is carried out by the unstructured N-terminal region of APE1, which recognizes a local distortion (or an AP-site); the interaction is then stabilized by an higher-affinity binding event that is carried out by the whole globular domain of APE1 [90].

The phylogenic acquisition of critical lysine residues conferred additional flexibility to the APE1 N-terminal domain, as confirmed by both structural and biophysical studies [90, 124]. The presence of additional basic residues, in a very plastic structural context, suggest that APE1 could exploit its N-terminal extension as a sort of "tail", which can be easily adapted to bind very different interacting partners. Moreover, as observed for other BER components, the intrinsically disordered N-terminal region also includes residues target of PTMs and a bipartite nuclear localization signal ([125] and Fig. 7). APE1 is modulated by means of different PTMs (reviewed in [82, 126, 127]), most of which occur indeed within the N-terminal domain. Examples include ubiquitination [128, 129], acetylation and proteolysis [130-132]. Among the PTMs on this domain, acetylation at K6 and 7 has been demonstrated to modulate APE1 transactivation activity [133], while we showed that acetylation at K27, 31, 32 and 35 is important for the tuning of different activities of APE1. In particular, the charge status of these residues affects the nucleolar accumulation of the protein, its ability to interact with NPM1 and the catalytic activity on abasic DNA, possibly through the modulation of product release [90, 91, 124]. Very recently, we also demonstrated that acetylation at the K27-35 lysine cluster affects the acetylation status of the K6/7 residues, in a cross-talk involving the SIRT1 deacetylase [124]. Furthermore, during my PhD project I analyzed the APE1 K35 acetylation pattern in triple negative breast cancer specimens, highlighting a profound dysregulation of the APE1 PTMs status in tumor tissue [134] (Fig. 8).

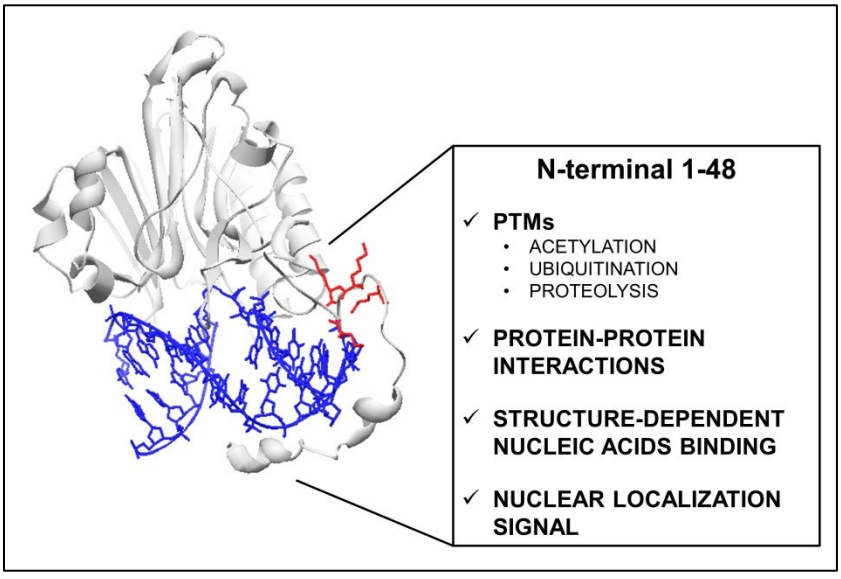

Fig. 8 – Schematic summary of the multiple regulatory functions exerted by the disordered N-terminal domain of APE1. The ribbon representation of APE1 (grey) bound to abasic DNA (blue) was obtained from the RCSB Protein Data Bank (1DEW) and edited using the SPDBV software (version 4.01). The 42 N-terminal amino acids, absent in the original structure, were manually inserted; side-chains of the critical lysine residues 27, 31, 32, 35 are highlighted (red). Adapted from [19].

In summary, the N-terminal extension of APE1 represents a novel molecular device that the protein acquired during phylogenesis. The evolutionary pressure exerted by an increasingly complex environment endowed APE1 with new residues which modulate the protein in many different ways (e.g. regulating APE1 activities, subcellular localization, interacting partners, PTMs). Due to its diverse effect on APE1, and based on the involvement of APE1 PTMs pattern in cancer, the N-terminal domain could be considered as a novel and interesting target to pharmacologically modulate different functions of the protein.

3.3. APE1 and pathology

The general importance of APE1 to the cell is conceivable, due to the multiplicity of cellular activities exerted by the protein. In accordance with its pivotal role, defects in APE1 activity and expression have been connected to cancer and neurodegeneration [135].

As already elucidated in the paragraph 2.3 ("*BER as a target for anti-cancer therapy*") alterations in the whole BER pathway and dysregulation of APE1, in particular, have been linked to cancer onset and progression. APE1 expression in human tumors shows a complex and heterogeneous pattern, being predominantly nuclear, with cytoplasmic and nuclear-cytoplasmic staining as well [82]. The endoribonuclease activity of APE1, its role in the mitochondrial BER, as well as its redox activity on newly synthesized transcription factors might in part explain its cytoplasmic localization [82, 105]. Alterations in the APE1 localization pattern have been observed in several tumors ([105] and references therein). Interestingly, an increased cytoplasmic localization of the protein has been linked to more aggressive cancer phenotypes and correlates with lower tumor differentiation, increased angiogenesis and lymph node status [46, 136]. Elevated APE1 expression levels, moreover, have been linked to tumor resistance to radiation- and platinum-based therapies [45, 67]. Taken together, these observations suggest that APE1 may have substantial prognostic significance in tumors.

Given the strong association existing between APE1 and cancer, pharmacological targeting of APE1 has been proposed as an appealing approach to improve the current anti-tumor therapy. Depletion or downregulation of APE1, in fact, has been show to induce apoptosis [137], cell growth defects [138] and sensitization to several DNA-damaging agents [105, 139]; whereas the redox activity of APE1 influences different mechanisms that are linked to cancer survival (e.g. growth, metastasis, angiogenesis, microenvironment) [110]. In the last decade a considerable effort has been made in order to develop small molecule inhibitors specifically targeting a single enzymatic activity of APE1 [110, 140]. To date, (2E)-3-[5-(2,3-dimethoxy-6-methyl 1,4-benzoquinoyl)]-2-nonyl-2-propenoic acid (E3330, APX3330) and few improved analogs are the most potent compounds

targeting the redox function of APE1 [141-144]. Potential applications for these inhibitors range from adjuvant to anti-tumor therapy to ophthalmological hyper-vascularization diseases [110]. Just to give an example, impairment of the APE1-mediated redox activation of AP-1, could have a profound effect on tumor resistance to cisplatin, as AP-1 has been suggested to induce the expression of DNA repair factors involved in the removal of cisplatin adducts [145]. Very recently, the specificity of action of E3330 has been the subject of a lively debate, as it appears that at high concentration the compound affects also the endonuclease activity of APE1 [112, 113, 146].

Parallel investigations by different groups have led to the design of potent small-molecule inhibitors of the APE1 endonuclease function. Optimized screening campaigns and structure-activity relationship studies have identified several structurally unrelated compounds with inhibitory activity in the single-digit micromolar range ([105, 140, 147-150] and references therein). Use of these inhibitors on cell lines potentiates the cytotoxicity of alkylating agents (e.g. methyl methanesulfonate – MMS, temozolomide), leading to an accumulation of AP-sites in treated cells. A couple of compounds (i.e. N-(3-(benzo[d]thiazol-2-yl)-6-isopropyl-4,5,6,7-tetrahydrothieno[2,3-c]pyridin-2-yl)acetamide – compound #3 and N-(3-(benzo[d]thiazol-2-yl)-5,6-dihydro-4H-thieno[2,3-c]pyrrol-2-yl)acetamide – compound #52), moreover, have been preliminarily tested *in vivo* and showed properties amenable for further pharmacological development [148]. At present, methoxyamine (MX) is the only APE1 inhibitor actively pursued in clinical trials for the management of advanced tumors [151]. The molecule, however, is formally to be considered an indirect BER inhibitor, as it forms covalent AP-site adducts that are refractory to APE1 cleavage [152].

Additional improvement and characterization of the existing APE1 inhibitors is warranted, as they will definitely reveal useful tools to depict the relative contribution of each APE1 activity to the cellular response to environmental stimuli. While valuable for *in vitro* studies, however, it is not clear whether unrestricted systemic inhibition of the APE1 functions could achieve specificity of action towards tumor cells. For this reason, my PhD project focused on the development and characterization of a new class of APE1 inhibitors targeting its protein-protein interaction network, and, in particular, the APE1/NPM1 molecular association.

4. *NPM1: a diverse protein*

Nucleophosmin (B23, numatrin, NO38, here referred to as NPM1) is a multifunctional phosphoprotein originally identified as a mitogen-induced factor in B lymphocytes [153]. The *NPM1* gene encodes for three splicing variants (B23.1, B23.2 and B23.3), that differ in their length and subcellular localization [154]. NPM1 (B23.1) is by far the best characterized isoform and in this thesis I will focus on this protein variant which, as previously explained, was identified as an interacting partner of APE1.

NPM1 is an essential protein that has been associated with several cellular functions, as well as to cancer onset and progression. From this standpoint, however, the overall picture of the role of NPM1 is still very blurred, as the protein has been described both as a proto-oncogene and as a tumor suppressor. Interestingly, the literature offers numerous hints pointing to a possible involvement of NPM1 in the DDR; nonetheless, our knowledge on the subject is still very poor.

This chapter will detail what is currently known about NPM1 functions, with particular emphasis on the still debated role of this protein in cancer. An entire section of this chapter (4.3 "*NPM1, a novel player in the DNA damage response?*") will focus on our current comprehension of NPM1 role(s) during the DDR, as this will be a central topic to this thesis.

4.1. Protein structure and function

NPM1 is synthesized as a 37 kDa polypeptide that can assemble into higher order oligomers. The NPM1 monomer shows a modular structure encompassing 294 amino acids and folds into two structurally independent domains (Fig. 9):

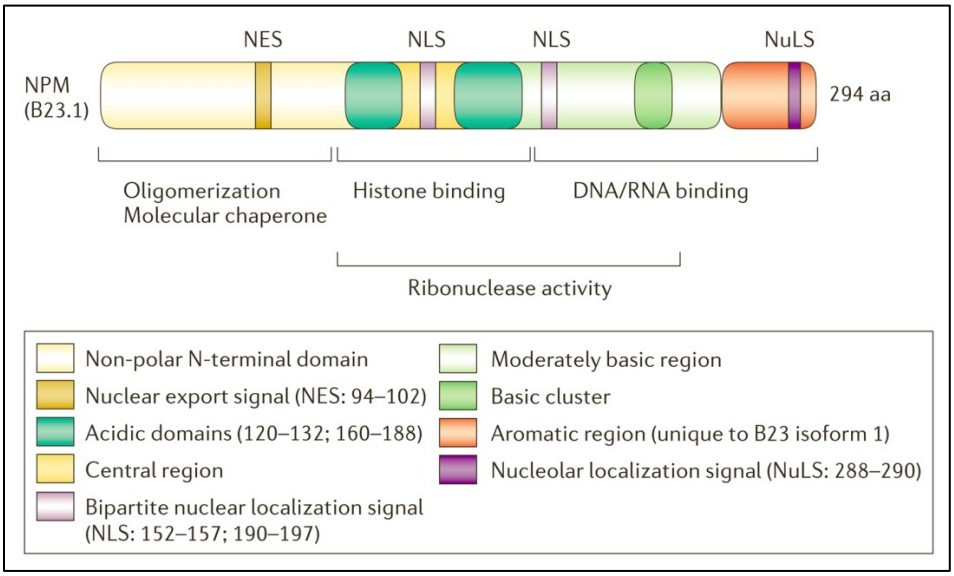

Fig. 9 – Schematic representation of the NPM1 primary structure. NPM1 contains two main structured regions (the N-terminal hydrophobic and the C-terminal DNA/RNA binding domains) that are separated by basic and acidic clusters. The subcellular localization of the protein is dynamically modulated by one nuclear export signal, a bipartite nuclear localization signal and a nucleolar localization signal. Source: [155].

The N-terminal part of the protein (amino acids 1-122) constitutes a highly conserved β-barrel core domain that is shared among the nucleoplasmin family of molecular chaperones; this region is responsible for the oligomerization of NPM1 [156-158]. Five monomers assemble into a ring-shaped oligomer; two pentamers, then, join head-to-head forming high molecular weight multimers [156, 157]. The N-terminal core is also responsible for several protein-protein interactions involving NPM1 (e.g. with $p14^{Arf}$ or APE1) [75, 159]. Mutual interactions between p53, Mdm2 and $p14^{Arf}$ are critical for the modulation of cell proliferation and apoptosis; NPM1 likely plays a key function in mediating the cross-talk among these factors. For instance, NPM1 regulates p53 levels and activity through direct interaction [160] and through competition with $p14^{Arf}$ for Mdm2 binding [161, 162]. On the other hand, NPM1 appears to be the focal link between nucleolar integrity and p53 activation. Although the functional significance of the NPM1/$p14^{Arf}$ interaction is still matter of debate, it is clear that the protein-protein association contributes to the stabilization of both

molecules. Whether the NPM1-mediated $p14^{Arf}$ sequestration within nucleoli has any functional significance is less understood [163]. It is however evident is that, upon triggering of nucleolar stress, redistribution of NPM1 to the nucleoplasm and ATM-induced dissociation from $p14^{Arf}$ are two crucial events leading to p53 stabilization [163, 164].

The C-terminal domain of NPM1 (amino acids 244-294) has been the subject of several structural studies, being the protein region most frequently mutated in acute myeloid leukemia (AML – see the next paragraph). This protein domain folds into a three-helix bundle that accounts for the nucleic acid binding activity of NPM1 [154, 165, 166]. The structural integrity of the NPM1 C-terminal region is tightly linked to the nucleolar localization of NPM1; it has been proposed that the high affinity of NPM1 for ribosomal particles and for G-quadruplex DNA structures is responsible for the nucleolar residence of the protein [154, 165, 167].

Analysis of the NPM1 primary sequence highlighted the presence of several targeting motifs that allow continuous shuttling of the protein from nucleoli to the cytoplasm (Fig. 9 and [168]). This feature, along with the high affinity of NPM1 for rRNA particles, and the reported involvement in the 28S rRNA maturation [169], strongly suggest a role for the protein in the ribosome processing. NPM1, in fact, has been proposed to provide the export signals and the chaperoning capabilities (see below) necessary for the transcription, maturation and transport of the ribosomal particles [170, 171].

There is no record of a comprehensive crystal structure of the full-length protein, so far. Nuclear magnetic resonance and circular dichroism analyses, however, shed insight into the dynamic organization of the unstructured regions containing one basic and two acidic stretches (Fig. 9) and linking the NPM1 N- and C-terminal domains [154, 172, 173]. These intrinsically disordered regions are important regulatory domains and acceptors of PTMs that modulate the NPM1 oligomerization status and its binding to RNA and G-quadruplex structures [154, 167, 173, 174].

The structural characteristics of NPM1 make this protein a paradigm to study protein folding dynamics. Recent analyses performed in collaboration with Dr. Marasco (University of Naples) allowed us to unveil the remarkable thermal and chemical stability of the NPM1 core domain. Notably, we showed that the folding of the C-terminal domain is stabilized by the presence of the surrounding disordered regions and by the N-terminal core. This suggests that future structural studies on NPM1 must take into account potential stabilizing effects given by the whole protein fold [172]. Different studies, moreover, demonstrated that NPM1 exerts chaperone-like activity on a variety of substrates, protecting specific target proteins from aggregation and denaturation *in vitro* [175]. The acidic portions of the protein appear necessary for the molecular chaperone activity of NPM1, especially on histones. NPM1, in fact, has been shown to assists the proper deposition of histones on

chromatin *in vivo*, thus modulating cellular processes such as transcription and, likely, DNA repair [176-180].

4.2. NPM1 and cancer: oncogene or tumor suppressor?

NPM1 role in cancer is multifaceted: the protein is known to suppress the early stages of tumorigenesis, while promoting cell growth in transformed cells. Moreover, tissue- and context-specific alterations characterize different aspects of NPM1 involvement in cancer [155]. Solid tumors, for instance, are often characterized by overexpression of NPM1, while hematological malignancies frequently bear mutations and chromosomal rearrangement involving the *NPM1* gene. These rearrangements have been reported to generate fusion proteins (e.g. NPM1-ALK, NPM1-MLF1, NPM1-RARα) that can sustain cell growth in acute promyelocytic leukemia, anaplastic large cell lymphoma and AML (reviewed in [163, 171]). The occurrence of *NPM1* alterations in about one third of adult AML patients, moreover, results in the concerted loss of one or two tryptophan residues that act as nucleolar targeting signals, along with the generation of an additional nuclear export signal and consequent delocalization of the protein to the cytoplasm (referred to as NPM1c+ mutation) [163]. The NPM1c+ mutation is considered a tumor initiating lesion in NPM1c+ AMLs [181, 182] and it is thought to promote transformation through overexpression of c-myc [183] and relocalization and/or inactivation of different interacting partners with tumor-suppressive function, such as $p14^{Arf}$ [184], Miz1 [185] and Fbw7γ [183]. NPM1c+ might also act as a dominant negative form, providing a dimerization interface and altering the subcellular localization of the wild-type protein, encoded by the non-mutated *NPM1* allele [163]. Interestingly, the NPM1c+ mutation identifies a prognostically favorable subgroup in AML (when present in the absence of mutations at the *FLT3-IDT* locus), showing higher relapse-free survival rates than AML with normal NPM1 [163]; a possible molecular explanation for the better response to therapy in NPM1c+ AML patient was recently suggested by our group. We demonstrated that NPM1c+ expression induces a cytoplasmic relocalization of APE1 in AML cells. The nuclear deprivation of APE1 and the consequent BER deficiency are likely to render AML cells more susceptible to genotoxins [186].

NPM1 levels generally correlate with proliferation; accordingly, overexpression of NPM1 is considered a prognostic marker of recurrence and progression in solid tumors [171, 187, 188]. The correlation between increased NPM1 levels and cancer has usually been linked to NPM1 roles in ribosome biogenesis [171], but the interaction of NPM1 with Mdm2, p53 and $p14^{Arf}$ might explain its involvement in the modulation of tumor cell proliferation. For instance, the elevated NPM1 levels observed in cancer may be oncogenic through negative regulation of the $p14^{Arf}$ anti-oncogenic functions [62]. NPM1, moreover, has been shown to cooperate with oncogenes in inducing cellular

transformation in mouse embryonic fibroblasts (MEFs) [189, 190]. Most of the conclusions drawn so far, however, result from experimental data from cell cultures; the lack of suitable mouse models of tumorigenesis renders our understanding of the *in vivo* NPM1 contribution to carcinogenesis controversial [171].

In conclusion, NPM1 could be considered as a tumor suppressor, in that loss of protein function (for instance, through impairment of physiological intracellular localization, or protein-protein interaction ability) may lead to selective pressure toward loss of p53 function and onset of tumorigenesis [63]. On the other hand, when considering the pro-proliferative role of NPM1 and the cross-activation of diverse pathway after fusion with different protein partners, one might envision NPM1 more as a proto-oncogene. For a comprehensive description of the duality of NPM1 in cancer the reader is referred to [155].

4.3. NPM1, a novel player in the DNA damage response?

Extensive work has been carried out in order to establish a link between NPM1 and the DDR; a clear picture of the exact function of NPM1 in this context, however, is still lacking. Perhaps one of the first evidences linking NPM1 and the maintenance of genome stability was the discovery that NPM1 associates with centrosomes during the G1 phase of the cell cycle, acting as a licensing factor. This function of NPM1 is controlled by cyclin E/Cdk2-dependent phosphorylation and prevents centrosome duplication prior to cell division [191, 192]. In accordance with these data, NPM1 knockout (KO) in mice leads to unrestricted centrosome duplication and overall genomic instability [193]. Studies performed on NPM1 KO mice revealed that NPM1 is essential for embryonic development and that NPM1 haploinsufficiency accelerates oncogenesis [193]. Loss of NPM1 function in MEFs results in stabilization of p53 and increased susceptibility to oncogenic transformation, with parallel accumulation of DDR markers (i.e. γ-H2AX and phospho-ATM) [194]. These observations are consistent with several reports showing that DNA damage induces the expression and/or the nucleoplasmic relocalization of NPM1 [21, 161, 195-198]. More recently, NPM1 was shown to undergo phosphorylation-mediated relocalization to sites of DSBs upon IR. Moreover, pharmacological interference with NPM1 translocation to DNA lesions prolongs DNA damage persistence [199, 200]. In summary, there are many hints that point to a role for NPM1 during the DDR; in particular, it appears clear that NPM1 function(s) are linked to the cell capacity to deal with DNA strand breaks.

Very recently, our laboratory proposed a possible involvement of NPM1 as novel modulator of the BER pathway. Specifically, we demonstrated that NPM1 modulates the AP-site incision activity of APE1 [91, 186]. Accordingly, NPM1-deficient MEFs display an increased sensitivity to

genotoxins that elicit a BER response (e.g. MMS, oxidizing agents, and bleomycin) [186]. These data suggest that NPM1 may play an important role in the modulation of the early BER steps, although no information is available on the effect of NPM1 on the overall BER capacity. This thesis work is aimed at filling this gap, investigating the connection between NPM1 and the BER.

5. *The APE1/NPM1 interaction in pathology*

In the last few years we demonstrated that the interaction between APE1 and NPM1 affects multiple aspects of the APE1 biology. Vice versa, the impact of this interaction on NPM1 functions, if any, is still unknown. The characterization of the APE1/NPM1 association in different tumor cell lines highlighted the pivotal role played by this molecular interaction in cancer cells. Existing evidences suggest that the APE1/NPM1 interaction could be considered a novel and interesting target for cancer therapy. Based on available data it is possible to summarize the effects of NPM1 on APE1 as follows:

- NPM1 positively modulates the endonuclease function of APE1 on DNA, but decreases its activity on AP-site-containing RNA. The result of this balance affects both cell growth and DNA repair capacity in response to genotoxins [75, 91, 186].
- NPM1 promotes the accumulation of a fraction of APE1 within nucleoli, where it possibly functions as rRNA processing enzyme [75]. Accordingly, interfering with the nucleolar localization of APE1 strongly impairs tumor cell growth [124].

These observations led us to propose a model explaining the APE1/NPM1 cross-talk in tumor cells, both under basal conditions and after genotoxic stress (Fig. 10).

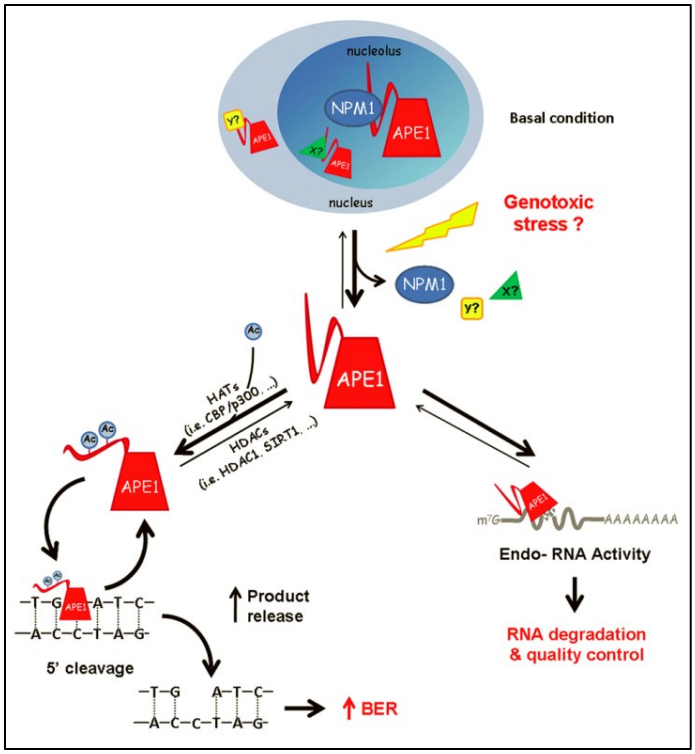

Fig. 10 – Proposed dynamic modulation of APE1 through interaction with NPM1, intracellular compartmentalization and PTMs. APE1 is mainly localized in the cell nucleoplasm; PTMs on the N-terminal domain (i.e. acetylation and ubiquitination) fine-tune the protein amount and activity, homeostatically maintaining genome stability. A fraction of the non-acetylated protein accumulates within nucleoli through the association with NPM1. Here, APE1 is possibly stored and exerts rRNA processing-related functions. Genotoxic stress may shift the equilibrium toward the acetylated form of APE1, which has lower affinity for RNA and NPM1, thus promoting its release from nucleoli and increasing its nucleoplasmic BER activity. Source: [91].

PTMs on the N-terminal region play a critical role in modulating the APE1 dynamics, as the charge status of this protein domain modulates the catalytic function of APE1 [91, 124], its nucleic acid binding activity [90] and its association with NPM1 (and, consequently, its nucleolar accumulation) [124]. Whether APE1 is retained within nucleoli to boost the nucleoplasmic DNA repair capacity upon release, or to maintain cellular proliferation through control of the ribosome processing, still remains unanswered.

Recent studies performed in our laboratory unveiled the potential implication of an aberrant APE1/NPM1 interaction in cancer onset and development. For the first time, we observed the occurrence of an abnormal APE1/NPM1 interaction in the cytoplasm of AML cells carrying the NPM1c+ mutation. The expression of the NPM1c+ form was associated with significant nuclear depletion of APE1, with increased sensitivity to genotoxins [186]. These observations lay the molecular basis to understand the good prognostic feature of NPM1c+ AMLs. As mentioned in the

previous chapters, both APE1 and NPM1 overexpression is a negative prognostic feature in solid tumors (e.g. ovarian and hepatocellular cancer). In collaboration with the Azienda Ospedaliera Universitaria of Udine we recently carried out a retrospective study on a cohort of 73 ovarian serous cancer specimens, and found that the expression profiles of APE1 and NPM1 were positively correlated in this carcinoma, with higher APE1/NPM1 expression in more aggressive tumors [188]. An increased APE1/NPM1 interaction was also associated with poor differentiation and augmented resistance to MMS in hepatic carcinoma cell lines (unpublished observations). These evidences suggest that an elevated APE1/NPM1 interaction might increase tumor aggressiveness and resistance to therapy. A comprehensive model emerging from the study of APE1, NPM1, and from the characterization of their interaction, is summarized in Fig. 11.

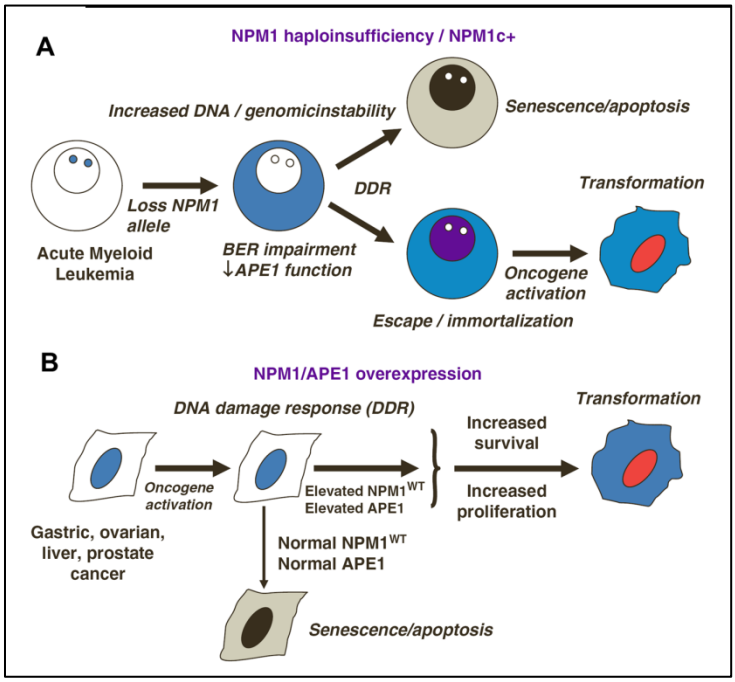

Fig. 11 – Schematic synopsis of the relative contribution of APE1 and NPM1 during tumorigenesis. A. Conditions of NPM1 haploinsufficiency and/or NPM1c+ expression characterize hematological malignancies. This situation can lead to BER dysregulation due to aberrant cytoplasmic APE1/NPM1 interaction, with intrinsic genomic instability caused by impaired APE1 and NPM1 function. Transformation is favored on this background and can be triggered by NPM1c+ expression itself. **B.** In solid tumors, the presence of elevated amounts of wild-type APE1 and NPM1 may facilitate oncogenic transformation by allowing DDR checkpoint evasion and by sustaining growth even under persistent DNA damage (e.g. during therapy). Source: [186].

The apparent involvement of the APE1/NPM1 interaction in cancer development and growth suggest that this protein-protein interaction might be a sensible target for anti-tumor therapy. Accordingly, we demonstrated that interfering with the APE1/NPM1 interaction HeLa cells abolishes APE1 accumulation in nucleoli and strongly impairs cell proliferation [124]. These observations highlight the translational relevance that novel compounds targeting the APE1/NPM1 association may have. As previously mentioned, APE1 is a ubiquitous protein and systemic administration of APE1 inhibitors of either the redox or the endonuclease activity may not be a suitable approach to cancer. Targeting the APE1/NPM1 interaction might be an interesting alternative approach to cancer treatment, as tumor cell that express higher level of both APE1 and NPM1 might be more sensitive to the inhibition of the interaction.

AIMS

The information gathered during the last fifteen years strongly suggest that both APE1 and NPM1 play an important role during cancer onset and progression; the presence of high levels of these proteins, moreover, is frequently a negative prognostic indicator and affects the response to anti-tumor therapy. The primary task of my PhD project was the development and characterization of novel low molecular weight compounds targeting the APE1/NPM1 interaction for translational purposes. The experiments that were carried out in this context led to a profound characterization of the functional relevance of the APE1/NPM1 association. These very same experiments, however, revealed that our knowledge on basic aspects of NPM1 and BER biology is still scanty. In particular, during my PhD project I realized that at least two fundamental questions did not find explanation in the existing literature:

1. Which is the involvement of NPM1 in the DDR? In particular, is there any link between NPM1 and the BER pathway beyond the control of the APE1 activity?
2. What is the purpose of the BER protein localization within nucleoli? Is the nucleolus merely a storage site, or is there a rationale behind the nucleolar accumulation of DNA repair factors?

In order to address these questions I systematically analyzed the BER pathway upon depletion of NPM1; moreover, by studying the effect of genotoxins known to induce a relocalization of NPM1 from nucleoli, I explored the consequences of nucleolar stress on the BER process.

Due to the limited amount of space, many of the data concerning the characterization of the APE1/NPM1 interaction, which have already been published, have been included in the introductory part of this thesis. The following chapter will describe the work undertaken during the last part of my PhD project which is, so far, submitted for publication. For the sake of clarity, this thesis has been divided into two sections. The first part ("*Targeting the APE1/NPM1 interaction*") focuses on the work carried out in order to develop and characterize small molecules targeting the APE1/NPM1 association. I describe the high-throughput screening developed in collaboration with the NIH Chemical Genomics Center (NCGC – Bethesda (MD), USA) and the efforts made in order to narrow the number of hits to three compounds that are able to disrupt the APE1/NPM1 in living cells, displaying interesting anti-tumor properties. The second part of the thesis ("*Investigating the role(s) of NPM1 during the DDR*"), instead, aims to clarify the role of NPM1 in the DDR, with particular emphasis on its involvement in BER. The experiments performed to pursue this second task also put forward a first tentative explanation for the role of BER proteins within nucleoli in tumor cells.

RESULTS

The data reported in this chapter are the subject of two articles recently submitted for publication:

- **Poletto M. et al., *"Inhibitors of the APE1/NPM1 interaction that display anti-tumor properties" (Mol Carcinogenesis, under revision)***
- **Poletto M. et al., *"Nucleophosmin modulates stability, activity and nucleolar accumulation of base excision repair proteins" (Mol Biol Cell, under revision)***

1. Targeting the APE1/NPM1 interaction

As elucidated in the introductive chapter, targeting the BER pathway, and in particular APE1, is a promising approach to cancer treatment. Aberrant sub-cellular localization, PTM pattern and expression levels of APE1 have been linked to tumor development and resistance to traditional therapeutic regimens. The interaction with NPM1, moreover, regulates several aspects of the APE1 biology, ranging from the nucleolar accumulation of APE1 to its AP-site incision activity on DNA and RNA.

The NPM1c+ AML model of aberrant APE1/NPM1 interaction shows that this molecular association is relevant in determining the tumor response to therapy [186]. Moreover, the impairment of the APE1/NPM1 interaction in tumor cell models strongly affects cell proliferation, suggesting that a functional molecular association between APE1 and NPM1 is pivotal for tumor cell growth and response to genotoxins [124]. These evidences imply that interfering with the APE1/NPM1 interaction might prove a relevant strategy to target tumor cell proliferation and/or their sensitivity to DNA damaging agents. In addition, targeting the APE1 interactome, rather than its enzymatic activities, might reveal more specific toward those cells which display increased APE1 and NPM1 expression levels. The recent observation of a positive correlation between the expression levels of APE1 and NPM1 in ovarian cancer specimens strongly supports this line of research [188].

1.1. An AlphaScreen®-based high-throughput screening for the identification of low molecular weight disruptors of the APE1/NPM1 interaction

In collaboration with the NIH Chemical Genomics Center (NCGC – Bethesda (MD), USA), we set up a quantitative high-throughput luminescence-based screening to detect small molecules able to interfere with the APE1/NPM1 interaction. The assay exploits the AlphaScreen® technology (the

principle of which is explained in Fig. 12A) using full-length recombinant GST-tagged APE1 and $His_{(6)}$-tagged NPM1.

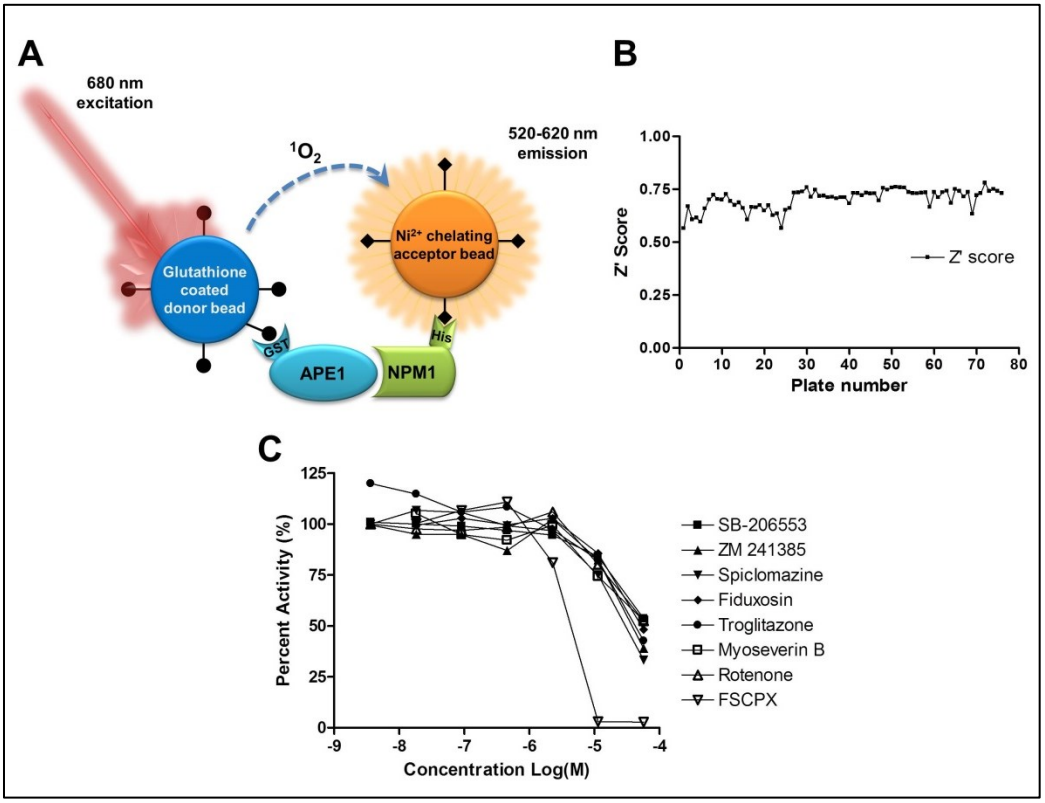

Fig. 12 – A high-throughput screening assay to detect APE1/NPM1 interaction inhibitors. A. Principle of the AlphaScreen® assay. The APE1/NPM1 interaction is detected, in solution, when a donor and an acceptor bead are brought in close proximity by the molecular association between GST-APE1 and $His_{(6)}$-NPM1. Upon excitation at 680 nm, the glutathione-coated donor beads release singlet oxygen ($^1O_2$), which is rapidly quenched by the aqueous milieu. If a Ni^{2+}-coated acceptor bead is within a range of 200 nm, the transfer culminates in light production at 520-620 nm. **B.** Schematic representation of the Z' score as measured throughout the screening; a stable score above 0.65 confirmed the high quality of the assay. **C.** Graphic overview of the dose-dependent activity for a subset of positive hits from the screening. The graph reports the concentration-dependent loss of APE1/NPM1 interaction signal for the indicated compounds, relative to the vehicle-treated samples. Molecules here reported are the ones further characterized in downstream assays.

Milligram amounts of recombinant proteins were expressed and purified to near homogeneity as described in the "*Experimental Methods*" section. The optimization of the assay was carried out by the NCGC team, which downscaled the reaction volume in order to increase the throughput of the assay, while minimizing reagent consumption. A pilot set of commercially available small molecule libraries (≈12,700 compounds in total) were screened at seven-concentration dilution series (3.7 nM to 57 μM) with an excellent Z' score (>0.65) that was maintained throughout the screening (Fig.

12B). Positive compounds were rescreened for confirmation and false positives were eliminated through a counterscreen assay measuring the AlphaScreen® signal in presence of a GST-$His_{(6)}$ conjugate which served as recognition moiety bridging both the donor and the acceptor beads. The screening led to the identification of 58 top hits that were selected on the basis of their dose-response curves, also manually removing molecules that were likely false positives (e.g. molecules with reactive groups, which could lead to modifications of the target proteins) (Fig. 12C). The screening assay also gave us some information on the potency of each compound, which was represented by an associated AC_{50} (Supplementary Table 1).

1.2. Selection of molecules able to impair the APE1/NPM1 interaction in living cells

Positive hits from the primary screening were subjected to a panel of orthogonal cell-based secondary validation assays. HeLa cells were used as a model to preliminarily test the cytotoxicity and the solubility of each compound in the culture medium. Individual toxicity of the molecules was tested through the MTS viability assay over a wide range of concentrations (0.1 – 100 μM) and time points (4 – 24 hours); whereas compound solubility was evaluated by assessing particle deposition through a phase contrast microscope. These information were exploited in the subsequent assays to reduce the likelihood of confounding effects.

The interaction with NPM1 is known to modulate the subcellular localization of APE1 [124, 186]; therefore, I decided to screen the molecules for their ability to induce a relocalization of APE1 upon cell treatment. HeLa cells were treated with test compounds in at least two different conditions (i.e. time and concentration) that affected cell viability less than 50% (as estimated through previous MTS assays) and the subcellular localization of APE1 was assessed through immuno-fluorescence. Treatment with a subset of the compounds affected differently the APE1 subcellular localization (Supplementary Table 1): while cell stimulation with some molecules (e.g. ZM 241385, troglitazone, ketoconazole) led to a reduction in the nucleolar accumulation of APE1, treatment with some others (e.g. fiduxosin, SB 206553, spiclomazine) elicited a relocalization of the protein to the cytoplasm (Fig. 13).

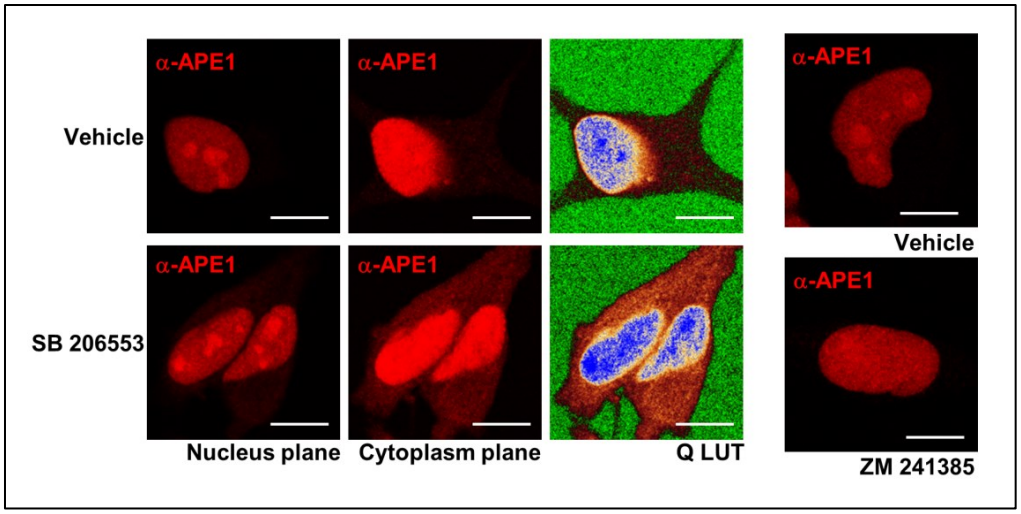

Fig. 13 – Immuno-fluorescence-based secondary screening on the putative APE1/NPM1 inhibitors. Representative immuno-fluorescence panels showing the APE1 relocalization induced in HeLa cells by some hits from the primary screening. *Left panel* – The increased cytoplasmic staining for APE1 induced by treatment with SB 206553 is visible on the cytoplasmic focal plane and using a quantitative color look-up table rendering (Q LUT). *Right panel* – Absence of APE1 nucleolar accumulation upon cell treatment with ZM 241385. Bars: 8 μm.

The molecules that induced a relocalization of APE1 were selected for further validation through a Proximity Ligation Assay (PLA). This assay couples the immuno-recognition of two targets (i.e. APE1 and NPM1) in fixed cells and a PCR-based amplification of the interaction signal, allowing the detection and quantitation of transient, as well as stable interactions, that appear as bright spots detectable through confocal microscopy [186, 201, 202]. The primary AlphaScreen® assay was carried out with N-terminally tagged proteins; in order to exclude any artifact arising from the presence of an N-terminal tag, I exploited an already available HeLa cell line stably expressing a C-terminally FLAG-tagged version of APE1 [124]. The presence of the tag, in this case, was functional to the PLA assay and was already shown not to interfere with the APE1/NPM1 association [186]. HeLa cells were incubated with the putative APE1/NPM1 inhibitors under conditions that induced a relocalization of APE1 and fixed immediately upon treatment. The extent of residual APE1/NPM1 interaction was thereby quantified through PLA (Fig. 14).

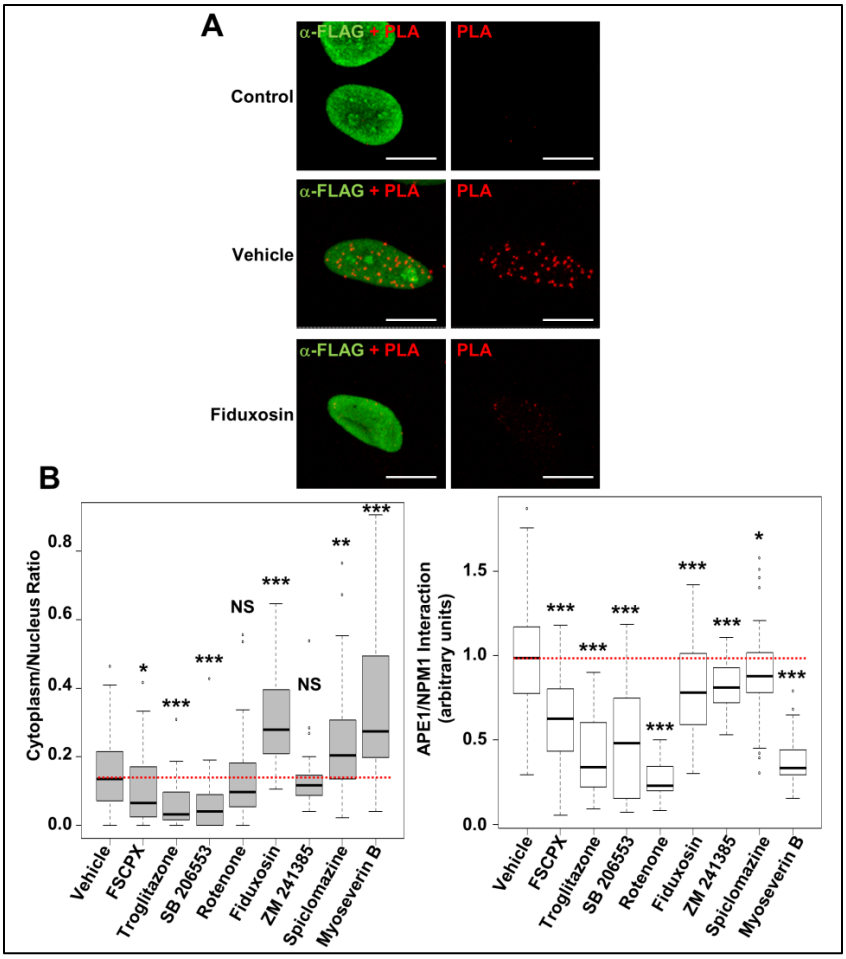

Fig. 14 – PLA validation of small molecules targeting the APE1/NPM1 interaction in living cells. HeLa cells were treated with the indicated APE1/NPM1 inhibitor and immediately fixed; PLA reactions were carried out and scored as described in the "*Experimental Methods*" section. **A.** Representative confocal micrographs showing a typical PLA result. The anti-FLAG staining (green) highlights APE1 and was used to individuate nuclei; the PLA signal is visible as red dots. In the control reaction the anti-NPM1 antibody was omitted. Fiduxosin-treated cells show a reduction in the PLA signal. Bars: 8 μm. **B.** The extent of APE1/NPM1 association upon treatment with a subset of inhibitors was measured through PLA, and the effect of the inhibitors on such interaction is reported as a boxplot graph. *Left panel* – Boxplot representation reporting the median cytoplasm-to-nucleus ratios of the amount of PLA interaction spots scored in HeLa cells upon treatment with the indicated APE1/NPM1 inhibitors. *Right panel* – The median number of interaction spots scored in vehicle-treated cells was used as reference and arbitrarily set to 1.0; the relative extent of APE1/NPM1 association upon inhibition of the interaction was calculated by scoring the PLA signals in the inhibitor-treated cells. Cell challenge with the indicated molecules determines a statistically significant reduction in the extent of cellular APE1/NPM1 interaction. Black marks represent the median value of the analyzed population; the red line indicates the median of the vehicle-treated cells, for easier identification of differences. The amount and the localization of the APE1/NPM1 interaction signals were assessed as described in the "*Experimental Methods*" section. N≥35, NS: not statistically significant, *: $p<0.05$, **: $p<0.01$, ***: $p<0.001$.

The secondary PLA-based validation screening led to the identification of eight compounds (i.e. FSCPX, troglitazone, SB 206553, ZM 241385, rotenone, spiclomazine, fiduxosin and myoseverin B) effectively able to interfere with the APE1/NPM1 interaction in living cells. In accordance with the preliminary immuno-fluorescence observations (Fig. 13 and Supplementary Table 1), a subset of compounds that induced a relocalization of APE1 to the cytoplasm was able to relocalize also part of the interaction spots to the cytoplasm (e.g. spiclomazine, fiduxosin). Other molecules, instead, did not show any variation in the distribution of the PLA signal, despite the observed relocalization of APE1 (e.g. SB 206553). At this point I decided to further restrict the panel of molecules under investigation excluding rotenone, a well-known respiratory chain poison and myoseverin B, a microtubule-binding molecule [203], because more likely to display off target effects.

1.3. Characterization of the molecular target of the top hits compounds

In order to understand whether the small molecules had preferential effect through APE1 or NPM1, I pursued two parallel strategies. On one side, I tested the effect of the APE1/NPM1 inhibitors on the APE1 redox activity in living cells; moreover, in collaboration with Dr. Daniela Marasco (University of Naples), the *in vitro* binding characteristics of the small molecules towards recombinant purified APE1 and NPM1 were investigated.

The effect of the APE1/NPM1 inhibitors on the APE1 redox function was assessed by exploiting a cell model developed by Cesaratto et al. [204]. Briefly, JHH6 hepatocellular carcinoma cells were transfected with a plasmid bearing a luciferase reporter which transcription is driven by an interleukin-8 (IL-8) promoter containing NF-κB binding sites. Cells were then challenged with tumor necrosis factor-α (TNF-α), which triggers the NF-κB-dependent IL-8 transcription through a mechanism involving the APE1 redox-mediated activation of NF-κB itself [204]. Any APE1/NPM1 inhibitor influencing the TNF-α-induced reporter transcription, therefore, could be inferred to affect the APE1 redox function.

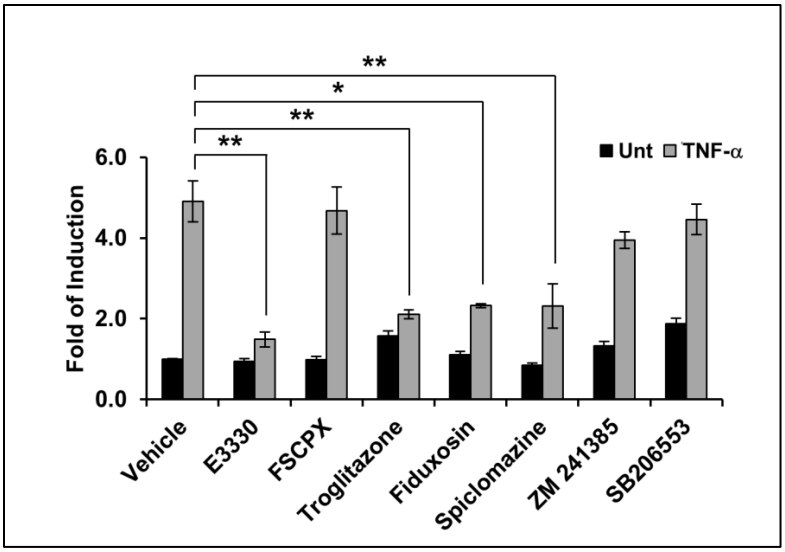

Fig. 15 – Evaluation of the effect of the APE1/NPM1 inhibitors on the APE1 redox function. Histogram showing the fold of reporter induction upon JHH6 cells stimulation with the indicated APE1/NPM1 inhibitors (10 μM) and subsequent challenge with TNF-α. E3330 (100 μM) was used as positive control for APE1 inhibition. Note that some inhibitors do not display any significant effect, while others efficiently impair the TNF-α-mediated reporter activation. The overall effect on the basal promoter activity is negligible. The histogram reports the mean ± SD from at least three independent experiments. *: $p<0.05$, **: $p<0.01$.

As described in Fig. 15, cell treatment with the APE1/NPM1 inhibitors had different effects on the APE1 redox activity. While some inhibitors (i.e. FSCPX, ZM 241385 and SB 206553) did not display any major effect on the TNF-α-induced reporter activation, others (i.e. troglitazone, fiduxosin, spiclomazine) efficiently blunted the NF-κB-mediated response, suggesting an inhibitory effect of these molecules on the APE1 redox function. Notably, troglitazone showed an inhibitory activity comparable to that of E3330 (a well characterized APE1 redox inhibitor used as positive control), even at tenfold lower concentration. These observations suggest that APE1, rather than NPM1, is the preferred binding partner for at least a subset of the APE1/NPM1 inhibitors.

In vitro binding assays carried out at the University of Naples were confirmative of these data. Purified recombinant APE1 or NPM1 were immobilized on a surface plasmon resonance (SPR) chip and each small molecule was tested for its protein binding activity. Although SPR experiments were limited by the poor solubility of the compounds in the aqueous running buffer, it is clear that the affinity of the APE1/NPM1 inhibitors is higher for APE1 than for NPM1 (Fig. 16).

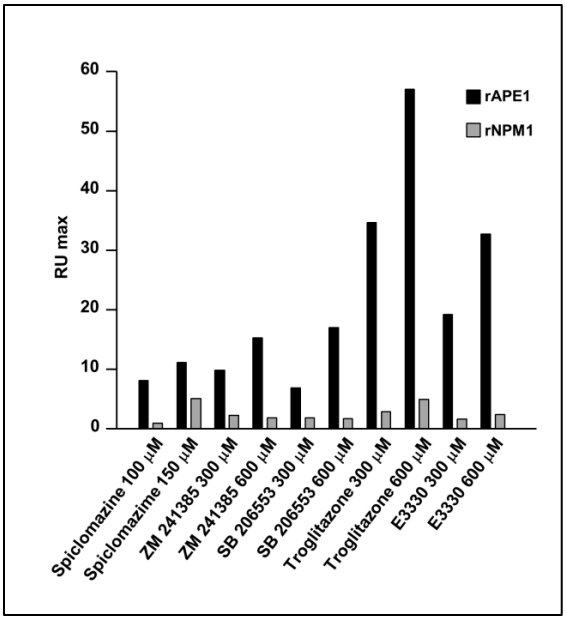

Fig. 16 – SPR binding experiments with the APE1/NPM1 inhibitors on recombinant purified APE1 and NPM1. Each protein was immobilized with similar efficiency on a SPR chip and the candidate small molecules were used as analytes. The histogram reports the protein-compound interaction efficiency for the indicated APE1/NPM1 inhibitors at two different concentrations. The affinity is expressed as maximal binding response adjusted for the compound molecular weight of each molecule. Note the good dose-response for APE1 and the poor binding towards NPM1 displayed by all the molecules. E3330 was used as positive control for APE1 binding.

Altogether, these observations suggest that the APE1/NPM1 inhibitors analyzed display diverse effects toward the APE1 redox function. Moreover, during the inhibition mechanism, the preferential binding partner is APE1, rather than NPM1.

1.4. Selected APE1/NPM1 inhibitors sensitize tumor cells to genotoxins and display anti-proliferative activity

In order to investigate the potential anti-tumor properties of the APE1/NPM1 inhibitors I assessed whether some of the molecules were able to sensitize tumor cells to different kinds of genotoxins. MMS, the radiomimetic drug bleomycin, and the PARP inhibitor PJ34 were chosen as genotoxic stimuli able to elicit a BER response [101, 205, 206].

As shown in Fig. 17 (panels A and B) cell exposure to either SB 206553 or spiclomazine sensitized HeLa cells (cervical cancer) to MMS-induced cell death. Combination of MMS with fiduxosin, ZM 241385 or FSCPX did not have any effect sensitizing effect (not shown). Furthermore, the interaction between SB 206553 and MMS was synergistic, as assessed through the combination index analysis [207].

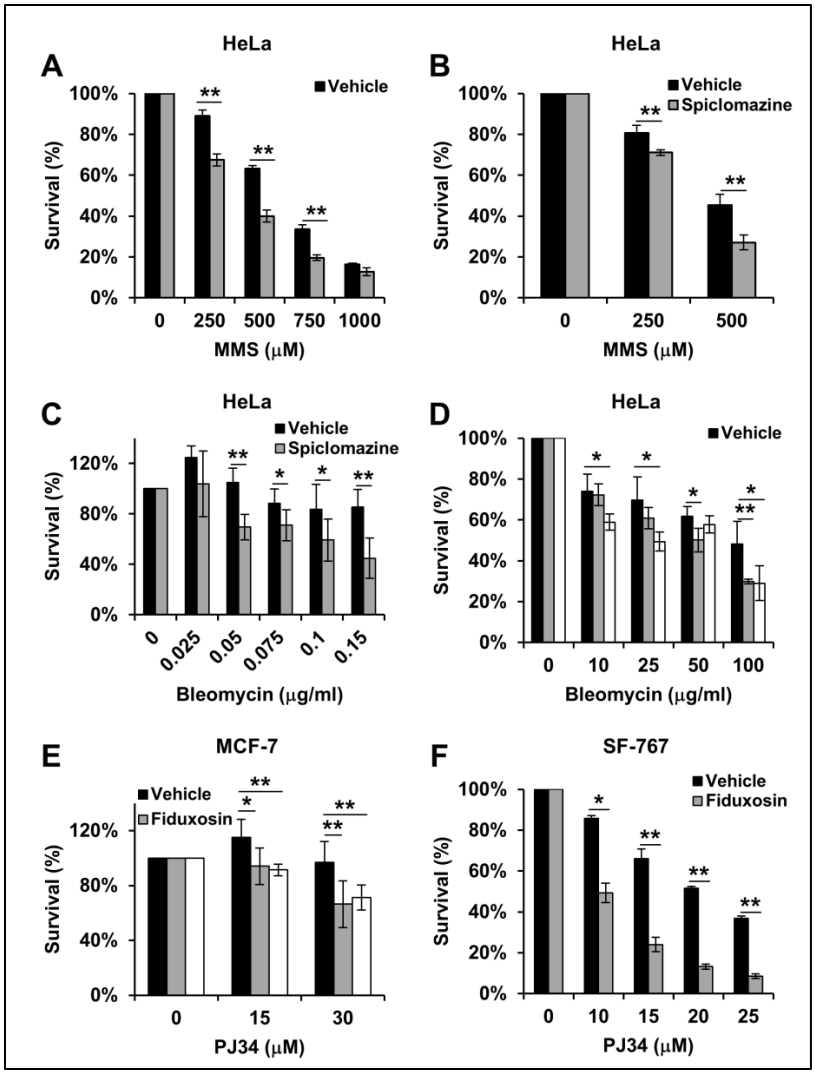

Fig. 17 – SB 206553, fiduxosin and spiclomazine differentially sensitize cells to MMS, bleomycin and PJ34. A-B. HeLa cells were pre-treated for 8 hours with 10 μM SB 206553 (**A**) or spiclomazine (**B**) and then challenged with the indicated amounts of MMS in presence of unchanged APE1/NPM1 inhibitor concentration for further 8 hours. Cell viability was evaluated by using the MTS assay. **C.** HeLa cells were co-treated for 1 hour with 10 μM spiclomazine in presence of increasing amounts of bleomycin. Immediately upon treatment, medium was replaced and cell viability was assessed through colony formation assay. **D.** HeLa cells were co-incubated for 1 hour with bleomycin and either fiduxosin or SB 206553. Cell viability was evaluated 48 hours later through cell counting. **E.** MCF-7 cells were co-incubated for 48 hours with PJ34 and either fiduxosin or SB 206553. **F.** SF-767 cells were co-treated for 48 hours with 10 μM fiduxosin in presence of the indicated amounts of PJ34. In panels **E** and **F** cell viability was assessed by using the MTS assay. The histograms report the mean ± SD from at least three independent experiments. *: $p<0.05$, **: $p<0.01$.

In a similar manner, a sensitizing activity of fiduxosin, spiclomazine and SB 206553 was observed when coupling these APE1/NPM1 inhibitors with bleomycin (Fig. 17, panels C and D).

Also in the case of the spiclomazine/bleomycin combination, the combination index analysis suggested the presence of a moderate synergism between these drugs. In addition, the cytotoxicity induced by the PARP inhibitor PJ34 was enhanced by SB 206553 and fiduxosin in both the glioblastoma-derived SF-767 cell line and the breast-cancer derived MCF-7 cell line (Fig. 17, panels E and F).

In summary, selected APE1/NPM1 inhibitors display interesting cell sensitizing effects when combined with DNA damaging drugs that trigger the BER activation. In order to investigate whether the molecules displayed any anti-proliferative activity as single agents, I measured the proliferation of HeLa cells upon acute or chronic exposure to the APE1/NPM1 inhibitors. Notably, cell treatment with fiduxosin and spiclomazine resulted in a dose-dependent impairment of the cell growth rate, both after short-term (24-72 hours) and long-term (10 days) treatment. SB 206553 had no significant effect on cellular proliferation (Fig. 18).

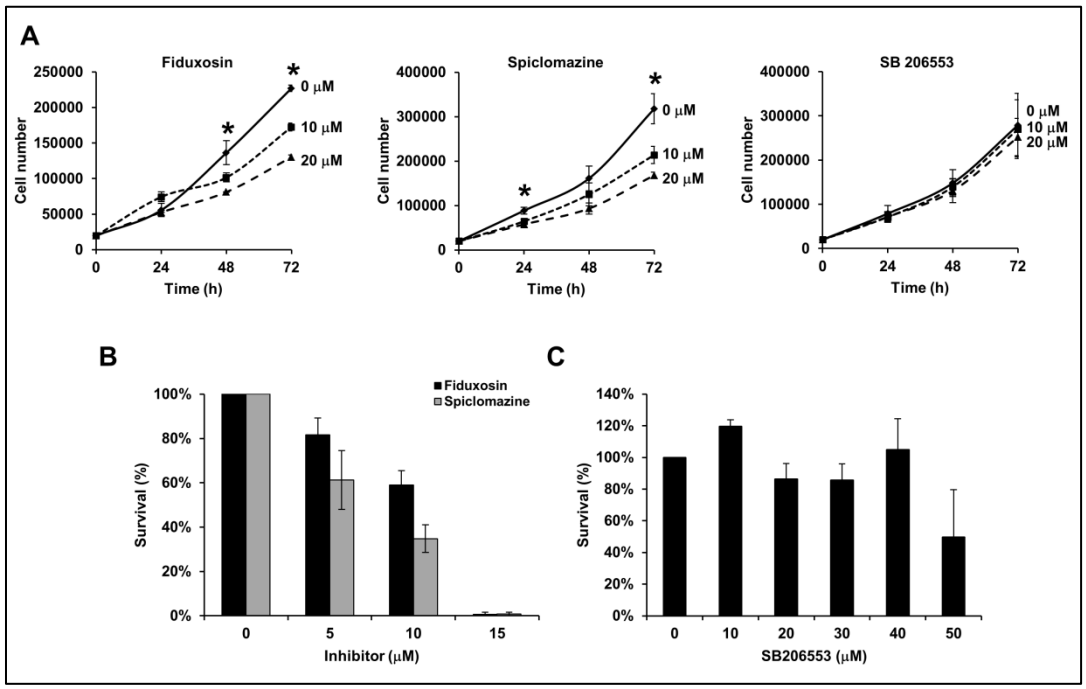

Fig. 18 – Fiduxosin and spiclomazine show anti-proliferative activity as single agents. A. HeLa cells were treated with vehicle (DMSO) or the indicated APE1/NPM1 inhibitor for 24, 48 or 72 hours. Cell proliferation was determined by cell counting in at least three independent experiments and is reported as representative growth curve from technical duplicates. *: $p<0.05$. **B-C.** HeLa cells were seeded at low density and allowed to form colonies for 10 days in presence of increasing concentrations of the indicated inhibitors. Survival is expressed as percentage of visible colonies assuming the vehicle-treated cells as a reference. Fiduxosin and spiclomazine (**B**), but not SB 206553 (**C**) display a dose-dependent anti-proliferative activity. The histograms report the mean ± SD from at least three independent experiments.

1.5. Investigating the mechanisms of action of the APE1/NPM1 inhibitors

The primary screening and the orthogonal validation assays narrowed the number of molecules under investigation to three interesting compounds (i.e. spiclomazine, SB 206553 and fiduxosin). Based on my data, these molecules are able to disrupt the APE1/NPM1 association in living cells and display interesting anti-tumor features, both as single-agents and in combination with different genotoxins (Table 1)

Inhibitor	Structure	Redox inhibition	Genotoxin			Anti-proliferative activity
			MMS	Bleomycin	PJ34	
Troglitazone	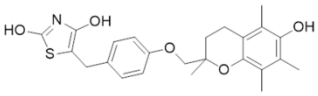	++	-	NA	-	NA
FSCPX	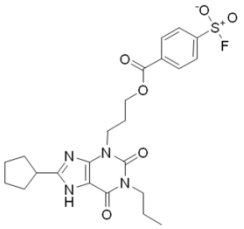	-	-	-	-	NA
ZM 241385	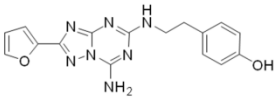	-	-	-	-	NA
Fiduxosin	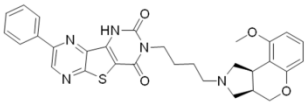	+	-	+	+	+
SB 206553	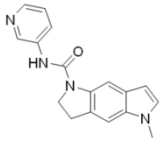	-	+	+	+	-
Spiclomazine	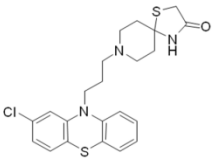	+	+	+	-	+

Table 1 – Characteristics of the positive hits from the secondary validation assays. For each molecule the table reports structure, effects on the APE1 redox function (where "++", "+" and "-" denote the strength of the phenotype as strong, mild or absent, respectively), presence/absence of sensitizing effect in combination with MMS, bleomycin or PJ-34, and presence of anti-proliferative activity. NA: not available.

The sensitization and anti-proliferative effects suggest that an inhibition of the APE1/NPM1 interaction may impair the function of at least one of the two interacting partners. In order to address this issue, I investigated the ribosome biogenesis dynamics and the DNA damage accumulation in treated HeLa cells, as biological processes that could be potentially affected by an impairment of the APE1/NPM1 association (see also the paragraph 2.4 "*APE1 is involved in the ribosome biogenesis process*").

I first assessed whether cell treatment with the APE1/NPM1 inhibitors induced any variation in the expression levels of the target proteins. None of the molecules tested led to downregulation of APE1 or NPM1 (Fig. 19A); moreover, NPM1 maintained its nucleolar localization over a 72 hours treatment with either spiclomazine or fiduxosin (Fig. 19B). Thus, it is possible to conclude that the inhibitory effect of fiduxosin, spiclomazine and SB 206553 on the APE1/NPM1 interaction was not provoked by a downregulation of the target proteins. Furthermore, at cytostatic spiclomazine and fiduxosin dosage, HeLa cells did not show any major nucleolar stress (as demonstrated by the integrity of nucleolar structures).

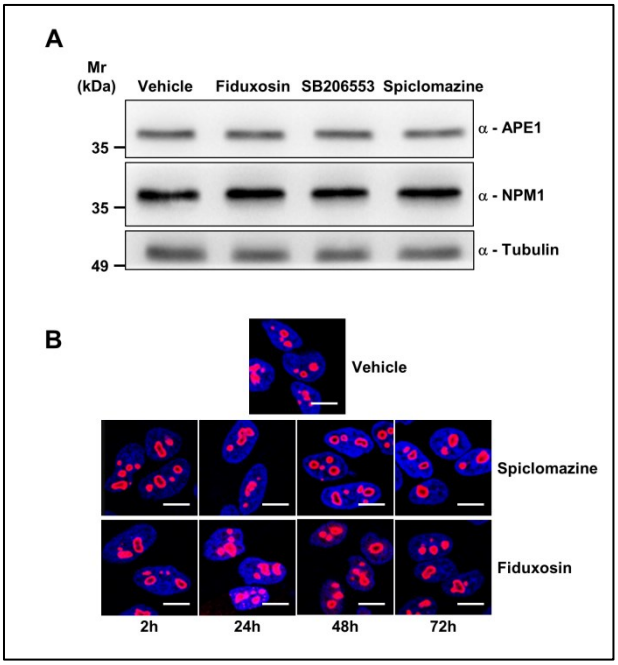

Fig. 19 – The APE1/NPM1 inhibitors do not induce modifications of APE1 or NPM1 expression, or nucleolar stress. A. HeLa cells were treated with the indicated molecules (10 μM for 16 hours) and the levels of APE1 and NPM1 were assessed through Western blotting on whole cell extracts (20 μg). Cell treatment under conditions leading to the disruption of the APE1/NPM1 association does not lead to modifications in the APE1 or NPM1 expression pattern. Tubulin was used as loading control. **B.** Representative immuno-fluorescence on HeLa cells treated with either spiclomazine or fiduxosin (20 μM) for the indicated time points. Staining with an anti-NPM1 antibody (red) shows the intactness of nucleolar structures. Nuclei were counterstained with TO-PRO-3, bars 16 μm.

In accordance with the absence of nucleolar disassembly upon fiduxosin or spiclomazine treatment, the ribosome processing profile of HeLa cells treated with the APE1/NPM1 inhibitors did not show any obvious alteration (Fig. 20). This indicates that the disruption of the APE1/NPM1 interaction was not associated with an impairment of the ribosome biogenesis and that other mechanisms might be responsible for the observed alteration of the cell proliferation rate.

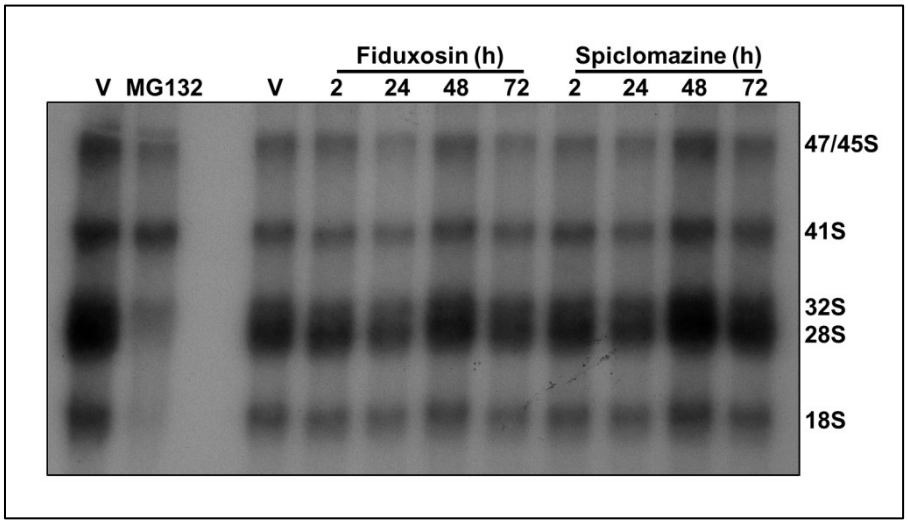

Fig. 20 – Treatment with the APE1/NPM1 inhibitors does not lead to ribosome maturation defects. HeLa cells were treated for the indicated time points with either fiduxosin or spiclomazine (20 μM). Cells underwent metabolic labeling and rRNA maturation kinetics was assessed as described in the "*Experimental Methods*" section. Major processing intermediates and ribosomal subunits are indicated on the right-hand side. The proteasome inhibitor MG132 (50 μM, 2 hours) was introduced as positive control [197] and, accordingly, leads to impairment in the late processing steps of rRNA maturation. Neither fiduxosin nor spiclomazine induce rRNA biogenesis defects. V: vehicle (DMSO).

I then tested whether cell treatment with the APE1/NPM1 targeting compounds led to DNA damage accumulation. Assessment of the AP-site content in genomic DNA indicated that HeLa cell treatment with spiclomazine or SB 206553 did not lead to any significant accumulation of abasic sites. Fiduxosin, conversely, induced a small increase in AP-sites; albeit statistically significant, the accumulation of damage was not comparable to that obtained using the known BER-eliciting compound MMS (Fig. 21A). Comet assays performed on HeLa cells confirmed that the APE1/NPM1 inhibitors did not induce any DNA damage accumulation even at higher dosage (Fig. 21B). These observations are consistent with the absence of effects of the small molecules on the APE1 AP-site incision activity measured *in vitro* using HeLa whole cell extracts (Fig. 21C).

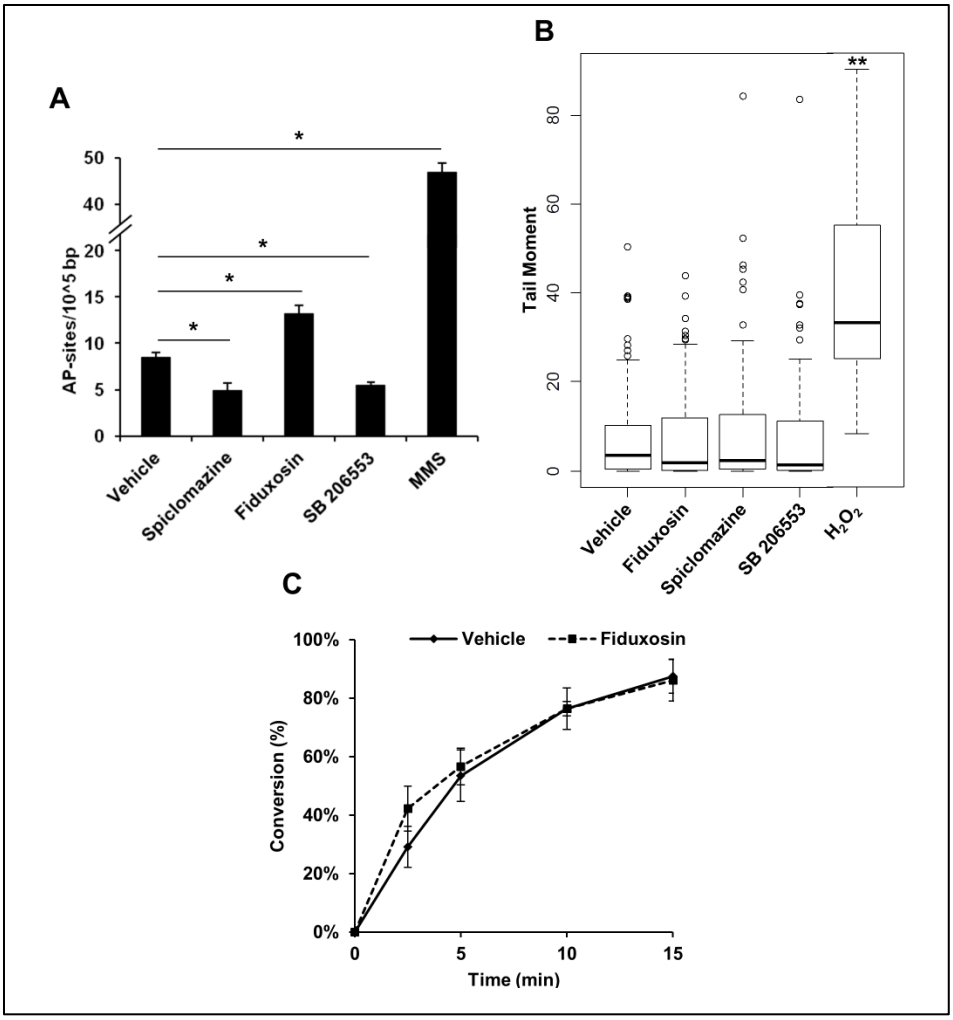

Fig. 21 – The APE1/NPM1 inhibitors do not induce any major accumulation of DNA damage in HeLa cells. A. HeLa cells were treated with fiduxosin or spiclomazine (10 μM, 48 hours), SB 206553 (20 μM, 16 hours), or MMS (250 μM, 16 hours) as positive control. AP-site accumulation in genomic DNA was measured as described in the "*Experimental Methods*" section. The histogram reports the mean ± SD from three measurements. *: $p<0.01$. **B.** Comet assay performed on HeLa cells treated with fiduxosin or spiclomazine (30 μM, 16 hours), SB 206553 (100 μM, 16 hours), or H_2O_2 (200 μM, 10 minutes) as positive control. The boxplot reports the median tail moment (black marks) for the analyzed cell population. $N\geq100$. **: $p<0.001$. **C.** Representative AP-site incision activity measurement on HeLa whole cell extracts (50 ng) pre-incubated with either vehicle (DMSO) or fiduxosin (5 μM). The APE1/NPM1 inhibitor shows no significant effect on the APE1 endonuclease function. The graph reports the mean ± SD from three independent assays.

Taken together, these data show that a subset of bioactive compounds, screened for their ability to impair the APE1/NPM1 interaction, display interesting anti-tumor properties (i.e. cell sensitization to genotoxins and anti-proliferative activity). The mechanism of action of the selected APE1/NPM1 inhibitors is, at present, poorly understood, as treated cells do not show any impairment

in the ribosome maturation process or evident accumulation of DNA damage. This suggests that the anti-proliferative and sensitizing effects are not related to a major disruption of the BER function of APE1 or of the NPM1 activity in ribosome processing.

The interesting anti-cancer properties of the APE1/NPM1 inhibitors certainly deserve further characterization; additional studies aimed at the improvement of these molecules and at the comprehension of their mechanism of action are therefore warranted.

2. Investigating the role(s) of NPM1 during the DDR

Despite the valuable insights emerging from the study of NPM1 KO models, the mechanisms underlying NPM1 function during the DDR are still poorly understood. It appears clear that NPM1 expression confers protection not only upon exogenous loads of DNA damage, but also under steady-state conditions. Our recent work suggested that NPM1 might be a novel modulator of the BER pathway, positively regulating the AP-site incision activity of APE1, possibly through mechanisms involving both protein-protein and protein-nucleic acids interaction [186]. Yet, the precise involvement of NPM1 during the overall BER processing remains unclear. Moreover, the DNA damage-induced relocalization of NPM1 from nucleoli, suggests a possible involvement of the protein during the DDR. It is not known, however, if NPM1 translocation has any impact on the BER capacity.

2.1. NPM1 depletion leads to BER protein upregulation

Earlier observations from our laboratory revealed the presence of higher APE1 protein amounts in NPM1/p53 double KO MEFs (hereafter referred to as $NPM1^{-/-}$) when compared to the isogenic single p53 KO control MEF cells ($NPM1^{+/+}$) [186]. In order to understand whether NPM1 could be further involved in the modulation of the BER pathway downstream APE1, I compared the protein and transcript expression profile of representative BER components in $NPM1^{+/+}$ and $NPM1^{-/-}$ cells. Western blotting analyses on MEF whole cell extracts revealed that BER protein levels were largely upregulated as a consequence of NPM1 depletion (Fig. 22, panels A and B). The increased BER protein expression, however, was not paralleled by a significantly augmented transcription rate of BER genes (Fig. 22C), suggesting that NPM1 effect is mediated post-transcriptionally. In this analysis Polβ was a notable exception, being upregulated both at the transcript and at the protein level.

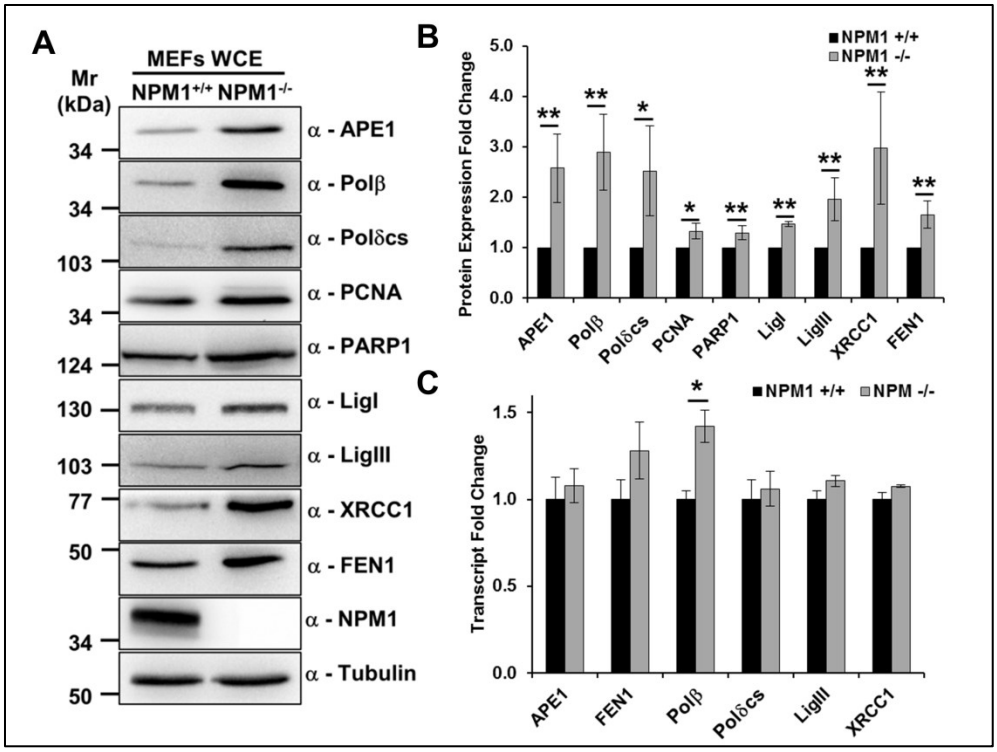

Fig. 22 – NPM1 depletion leads to BER protein upregulation. A. Representative Western blotting analysis on NPM1$^{+/+}$ and NPM1$^{-/-}$ MEF whole cell extracts (60 μg) showing increased BER protein amounts in the absence of NPM1. Proteins probed are indicated on the right hand-side, tubulin was used as loading control. **B.** Histogram reporting the average protein expression fold change in NPM1$^{-/-}$ cells, as measured through densitometric quantification of the Western blotting signals. **C.** Histogram showing the transcript fold change in NPM1$^{-/-}$ cells, as measured through Real-time PCR. Bars indicate the mean ± SD from at least three independent replicates. *: $p<0.05$, **: $p<0.01$, Polδcs: DNA polymerase δ catalytic subunit.

In order to rule out any confounding artifact, which may be caused by the intrinsic genetic instability exhibited by the NPM1$^{-/-}$ cells [194], I transiently depleted NPM1 in NPM1$^{+/+}$ cells and assessed the BER protein levels upon siRNA transfection. In accordance with my previous observations, siRNA-mediated knockdown of NPM1 recapitulated the BER expression phenotype for many of the proteins tested (Fig. 23).

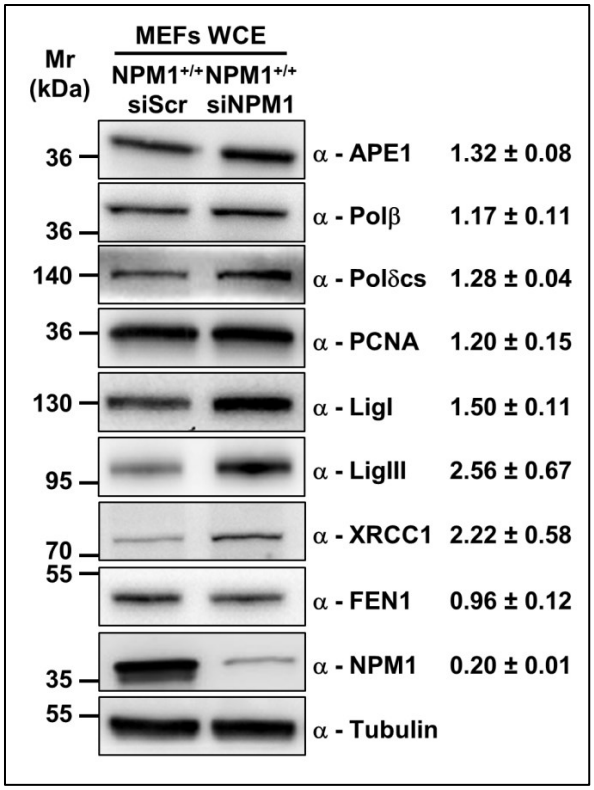

Fig. 23 – Transient downregulation of NPM1 induces BER protein stabilization in MEFs. Representative Western blotting analysis on $NPM^{+/+}$ whole cell extracts (50 μg) showing the increment of BER protein levels upon siRNA-mediated depletion of NPM1 (siNPM1). Proteins probed are indicated on the right hand-side, tubulin was used as loading control. The average protein expression fold change ± SD from at least three independent replicates is reported on the right hand-side. siScr: scrambled control siRNA.

Complete NPM1 KO requires p53 depletion in order to prevent triggering of apoptosis [194]; the link between NPM1 expression and BER protein stability was therefore further validated in human tumor cell lines bearing either active or inactive wild type p53 (i.e. HepG2 and HeLa, respectively). The experiments confirmed that NPM1 downregulation leads to an increased stabilization of BER proteins also in human cell lines, with variations in the degree of expression, likely reflecting cell-type specific differences (Fig. 24). The discrepancies observed in fold-induction when comparing the siRNA-mediated knockdown (Fig. 23 and Fig. 24) and the complete NPM1 KO (Fig. 22) are probably related to the residual amount of NPM1 (about 20%) upon depletion (see for instance FEN1, PCNA or LigI). Nonetheless, these data imply that NPM1 is a novel modulator of the BER protein stability.

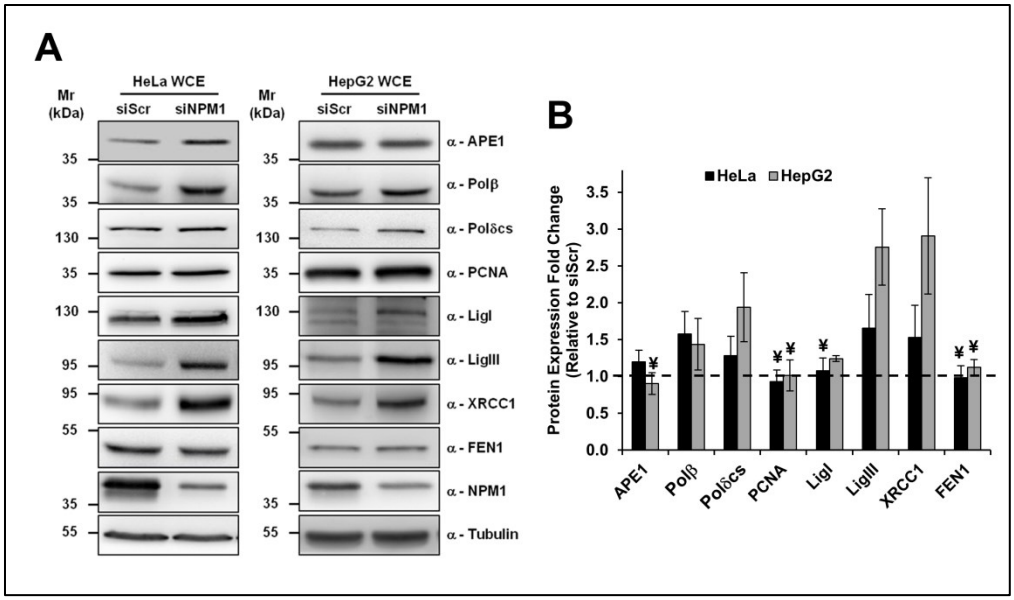

Fig. 24 – Downregulation of NPM1 induces BER protein stabilization in human cell lines bearing different p53 status. A. Representative Western blotting analyses on HeLa and HepG2 whole cell extracts (50 μg) upon treatment with scrambled (siScr) or NPM1-specific (siNPM1) siRNAs. Proteins probed are indicated on the right hand-side, tubulin was used as loading control. **B.** Histogram reporting average protein expression fold change in siNPM1-treated cells; signal from siScr-transfected cells was taken as reference. Bars indicate the mean ± SD from at least three independent replicates. ¥: not statistically significant ($p>0.05$).

2.2. NPM1 regulates BER protein localization and dynamics during nucleolar stress

NPM1 is considered a hub factor as it mediates the nucleolar retention of different proteins [19, 208], including $p14^{Arf}$ [162] and APE1 [75], at least in transformed cells. Given the BER dysregulation observed in $NPM1^{-/-}$ MEFs I checked whether NPM1 expression affected the subcellular localization of a subset of BER components. Strikingly, while in $NPM1^{+/+}$ cells a fraction of LigI, DNA polymerase δ catalytic subunit (Polδcs), FEN1 and APE1 revealed a nucleolar accumulation, the lack of NPM1 resulted in an impaired retention of these BER factors within nucleoli (Fig. 25A).

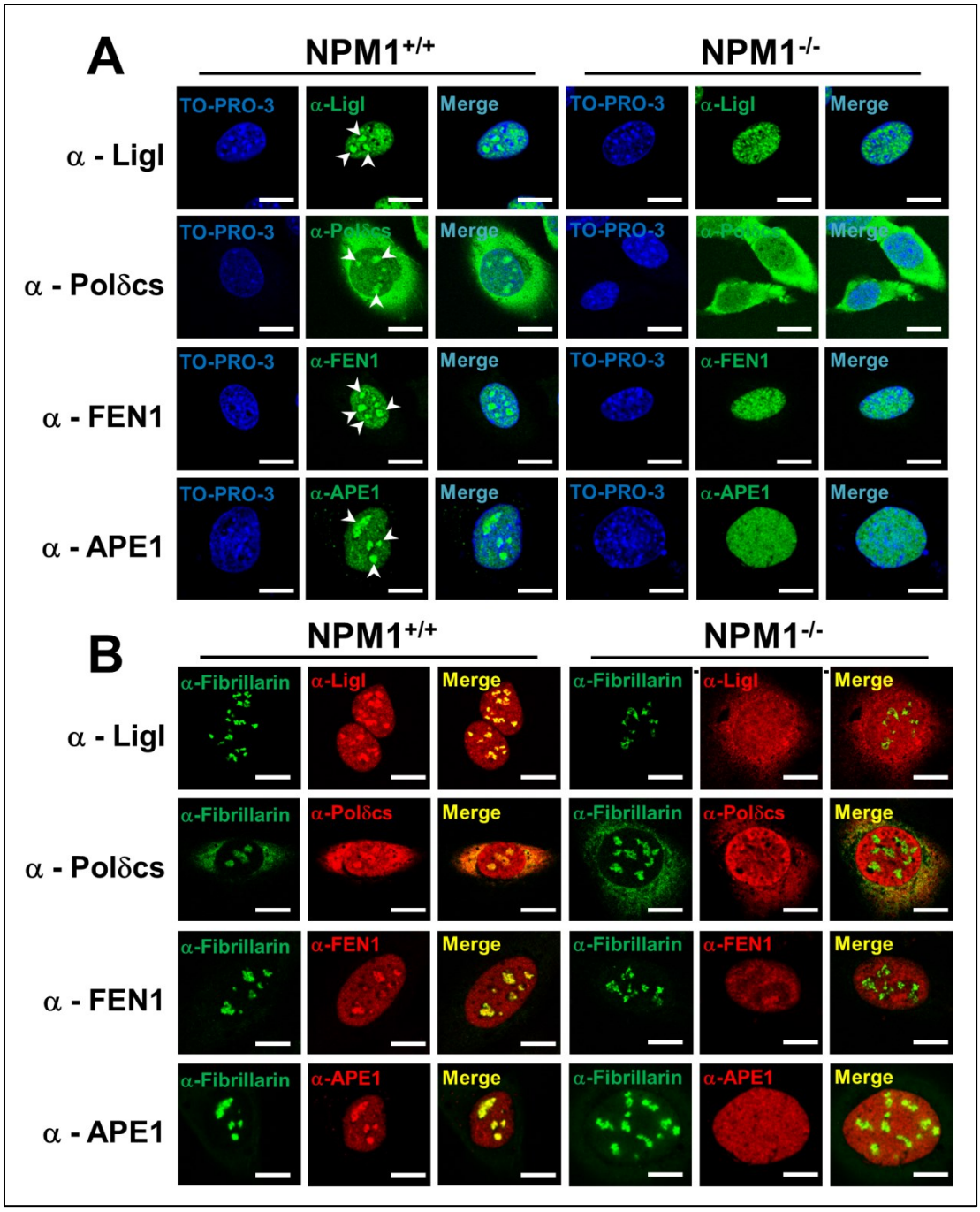

Fig. 25 – NPM1 promotes nucleolar accumulation of BER proteins. Representative immunofluorescence micrographs showing the differential subcellular localization of BER factors in NPM1$^{+/+}$ and NPM1$^{-/-}$ cells. **A.** Each protein analyzed shows nucleolar accumulation in NPM1$^{+/+}$ MEFs only (*white arrowheads*). Nuclei were counter-stained with TO-PRO-3. **B.** Fibrillarin shows the typical nucleolar staining pattern (green), whereas BER proteins (red) co-localize with fibrillarin only in NPM1-proficient cells (yellow). The BER protein analyzed in each experiment is indicated on the left-hand side. Bars: 16 μm.

Importantly, failure of BER proteins to accumulate within nucleoli was not determined by abnormalities in the nucleolar architecture of NPM1$^{-/-}$ cells, as already reported [162, 194] and confirmed by the ordinary nucleolar fibrillarin staining (Fig. 25B). The relevance of NPM1 expression for the correct nucleolar accumulation of BER proteins was confirmed by reconstitution experiments in NPM1$^{-/-}$ MEFs: these cells were transfected with a plasmid expressing a human FLAG-tagged NPM1 and restoration of nucleolar localization was observed for a subset of BER components (Fig. 26A and [186]).

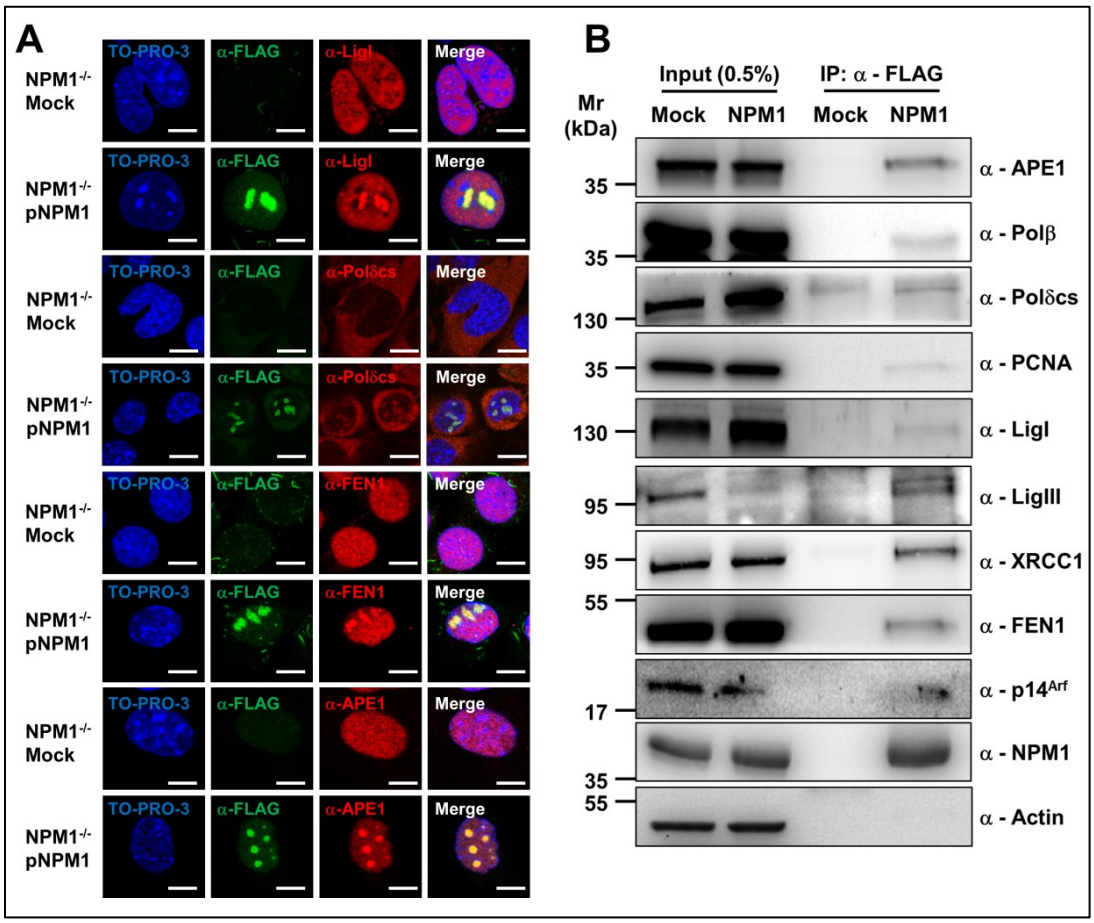

Fig. 26 – NPM1 co-purifies with BER protein complexes and is required for the nucleolar accumulation of a subset of BER components. A. NPM1$^{-/-}$ MEFs were transfected with either an empty vector (mock) or with a FLAG-tagged human NPM1-expressing plasmid (pNPM1). The representative immuno-fluorescence micrographs show the nucleolar accumulation of BER factors (red) only in NPM1-expressing cells (green). Nuclei were counter-stained with TO-PRO-3, bars 16 μm. **B.** HeLa cells were transfected with either an empty vector (mock) or FLAG-tagged NPM1 (NPM1) and immuno-precipitation was carried out with an anti-FLAG antibody. The immuno-purified material was subsequently subjected to Western blotting analyses, revealing an enrichment for several BER components. The antibodies used are indicated on the right-hand side.

In addition, co-immuno-precipitation experiments performed in HeLa cells confirmed that, under basal conditions, NPM1 can be co-purified with proteins belonging to the BER pathway (Fig. 26B). These data further suggest that NPM1 is essential for the accumulation of BER components within nucleoli.

Several studies verified that DNA damage induces reorganization of the nucleolar proteome, with a prevalent outflow from nucleoli (reviewed in [19]). NPM1 has been described as the main $p14^{Arf}$ interacting protein [209, 210] and the DNA damage-induced relocalization of both NPM1 and $p14^{Arf}$ is well documented [21, 59, 62, 197]. The redistribution of these proteins from nucleoli to the nucleoplasm is believed to boost the p53-mediated response [63]. I reasoned that if NPM1 was required for nucleolar accumulation of BER proteins, then a DNA damaging cue able to displace NPM1 from nucleoli would affect the localization of BER enzymes as well. Canonical BER-eliciting genotoxins (e.g. MMS, H_2O_2) did not affect the localization of NPM1 or APE1 (data not shown); conversely, as already reported [59, 211, 212], cell treatment with the DNA damaging agents cisplatin and daunorubicin, or the RNA polymerase I (Pol I) inhibitor actinomycin D led to a massive relocalization of NPM1 and $p14^{Arf}$ to the nucleoplasm. In accordance with the role of NPM1 in promoting the nucleolar accumulation of BER proteins, cell treatment with these compounds resulted in a complete nucleolar depletion of LigI, FEN1 and APE1 (Fig. 27 and not shown).

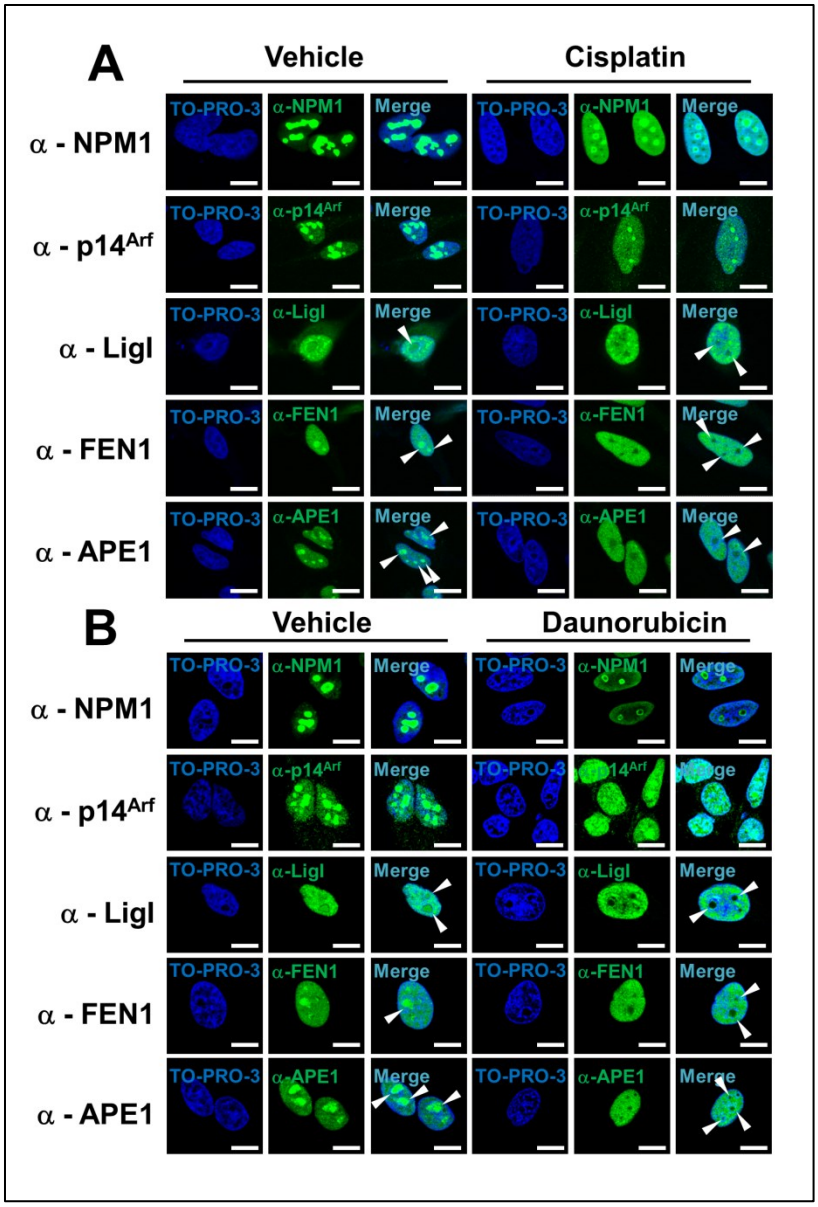

Fig. 27 – Cisplatin and daunorubicin induce a subcellular relocalization of NPM1, p14^{Arf} and BER enzymes. HeLa cells were treated with cisplatin (100 μM, 6 hours, **A**) or daunorubicin (1 μM, 2 hours, **B**), fixed and stained with the indicated antibodies. Representative immuno-fluorescence panels show the nucleoplasmic relocalization of NPM1 and p14^{Arf}; the concomitant depletion of LigI, FEN1 and APE1 from nucleoli is highlighted by white arrowheads. Nuclei were counter-stained with TO-PRO-3, bars 16 μm.

Taken together, these observations suggest that, in immortalized cells, NPM1 is responsible for the nucleolar accumulation of a subset of BER components; upon specific DNA damage or Pol I inhibition, NPM1, p14^{Arf} and BER enzymes are released from nucleoli and relocalize to the nucleoplasm.

2.3. Active redistribution of APE1 from nucleoli protects cells from cisplatin

Cisplatin treatment has been shown to induce APE1 expression in a lung cancer cell line; whereas depletion of APE1 sensitized the same cells to cisplatin-induced apoptosis [67]. Our and others' laboratories, moreover, observed interesting interrelations between cell sensitivity to cisplatin and BER capacity ([9, 13] and unpublished results). Given the observed link between BER protein localization and cisplatin, I decided to investigate thoroughly the functional significance of the BER protein nucleolar accumulation and cell response to cisplatin.

It is worth highlighting that, upon cisplatin treatment, the relocalization of $p14^{Arf}$ and BER proteins takes place in the absence of complete nucleolar breakdown, as still a moderate amount of NPM1 is retained within nucleoli (Fig. 27A, Fig. 28B). Under these conditions, however, nucleolar stress occurs in a measurable manner, as suggested by the formation of fibrillarin caps ([197] and Fig. 28A) and by the interruption of nucleolar transcription ([197] and Fig. 28C).

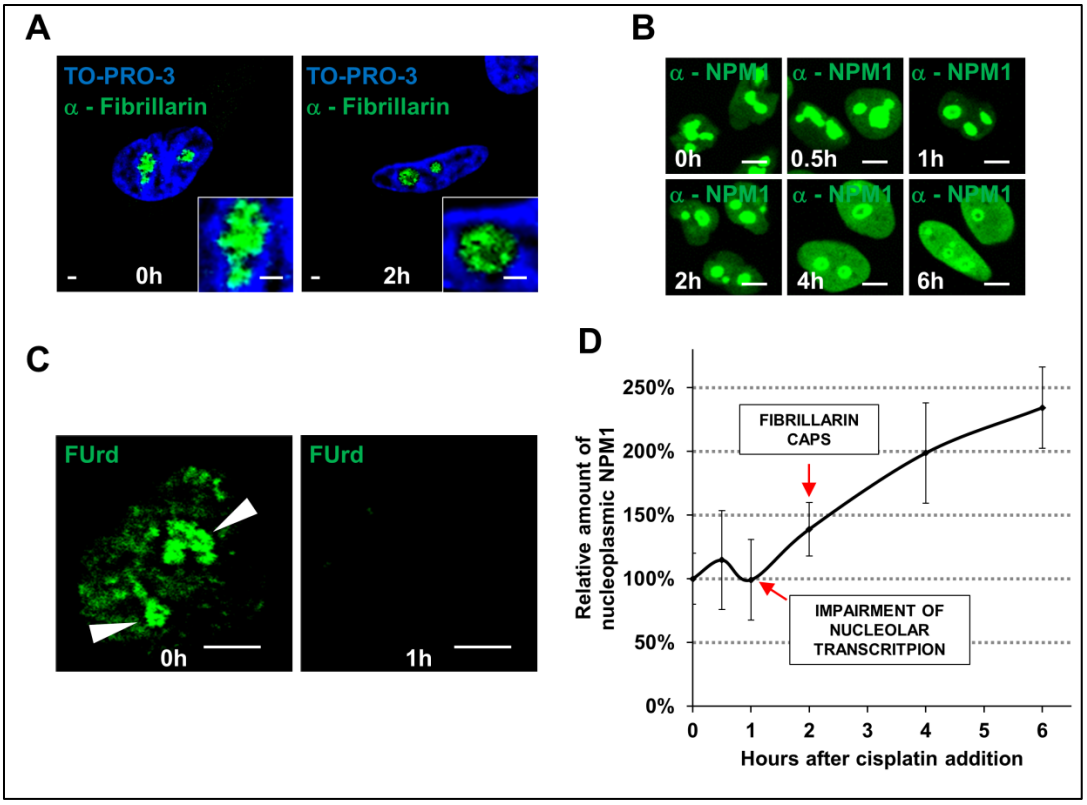

Fig. 28 – Cisplatin triggers nucleolar stress, which is followed by NPM1 relocalization. HeLa cells were treated with cisplatin (100 μM) and the effects on nucleolar function were monitored at different time points. **A.** Representative immuno-fluorescence showing the onset of nucleolar stress 2 hours after cisplatin addition, as evidenced by the appearance of perinucleolar fibrillarin caps (insets). Nuclei were counter-stained with TO-PRO-3, bars 1 μm. **B.** Representative immuno-staining for NPM1 reveals the nucleoplasmic translocation between 2 and 4 hours after cisplatin addition. Note that a significant amount of NPM1 still populates nucleoli after 6 hours. Bars 8 μm. **C.** Representative fluorouridine (FUrd) incorporation assay shows the absence of transcriptional activity within nucleoli one hour after cisplatin treatment. White arrowheads highlight the selective incorporation of FUrd in nucleolar compartments. Bars 4 μm. **D.** Graphical overview summarizing the timing of cisplatin effects. Impairment of nucleolar transcription occurs within 1 hour after cisplatin addition. Fibrillarin caps appear after 2 hours, when NPM1 starts to relocalize to the nucloeplasm. The amount of redistributed NPM1 was measured by analyzing the immuno-fluorescence presented in panel B through quantification of the mean nucleoplasmic NPM1 signal in randomly chosen cells (N≥20).

To exclude that the redistribution of BER proteins is merely a passive consequence of nucleolar disassembly, I analyzed the behavior of APE1, as representative enzyme of the pathway. Live cell imaging experiments exploiting an APE1-Dendra2 fusion construct [124, 213] revealed that APE1 and NPM1 relocalization are uncoupled, as the first protein reduces its nucleolar accumulation between 5 and 6 hours after cisplatin challenge (Fig. 29), whereas NPM1 redistribution to the nucleoplasm is already visible 2 hours after cell exposure to cisplatin (Fig. 28). As already observed

previously [124, 213] and confirmed by live cell imaging studies, the complete nucleolar emptying of APE1 induced by cisplatin (Fig. 27) is an artifact arising during the permeabilization procedures required for the immuno-fluorescence. In living cells, in fact, cisplatin is more likely to impair the nucleolar accumulation capacity of APE1 and other BER enzymes, rather than completely abolishing their nucleolar localization.

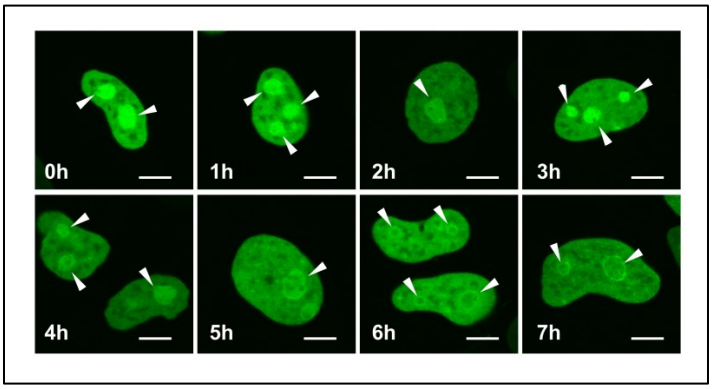

Fig. 29 – Cisplatin impairs the nucleolar accumulation capability of APE1 in a time-dependent manner. Live cell imaging analysis on HeLa cells transfected with the APE1-Dendra2 construct and treated with cisplatin show the time-dependent depletion of the protein from nucleoli (*white arrowheads*). The transition occurs between 5 and 6 hours after cisplatin addition. Bars 8 μm.

APE1 redistribution from nucleoli was further explored using two recently described acetylation mutants. APE1^{K4pleA}, where the lysine residues K27, K31, K32 and K35 are converted to alanine, generating a mutant protein endowed with higher AP-endonuclease activity that does not interact with NPM1, accumulates less efficiently within nucleoli and strongly impairs cell proliferation. In the second mutant (APE1^{K4pleR}) the same lysine residues are mutated to arginine, resulting in a protein refractory to acetylation, but not affecting its nucleolar accumulation, the cell growth rate or its ability to interact with NPM1 [124]. Remarkably, while cisplatin induced a relocalization of APE1^{WT} from nucleoli, the APE1^{K4pleR} mutant was incapable of such redistribution (Fig. 30A). Live cell imaging experiments confirmed the peculiar behavior of the APE1^{KpleR} mutant, showing a delayed redistribution of the protein in comparison with the wild type form. Importantly, expression of either APE1 mutant did not affect the cisplatin-induced relocalization of NPM1 (not shown), thus confirming that this phenomenon is directly linked to the APE1 mutation. These experiments indicate that, in addition to NPM1, other factors (e.g. rRNA) contribute to the nucleolar accumulation of APE1. Moreover, these evidences confirm that during cisplatin-induced nucleolar stress APE1 does not freely relocalize to the nucleoplasm as a consequence of nucleolar disassembly, nor the protein is simply towed to the nucleoplasm by NPM1. Some kind of PTM involving lysine

residues within the N-terminal domain of APE1 (e.g. acetylation [124] or ubiquitination [128, 129]) is seemingly required for its redistribution.

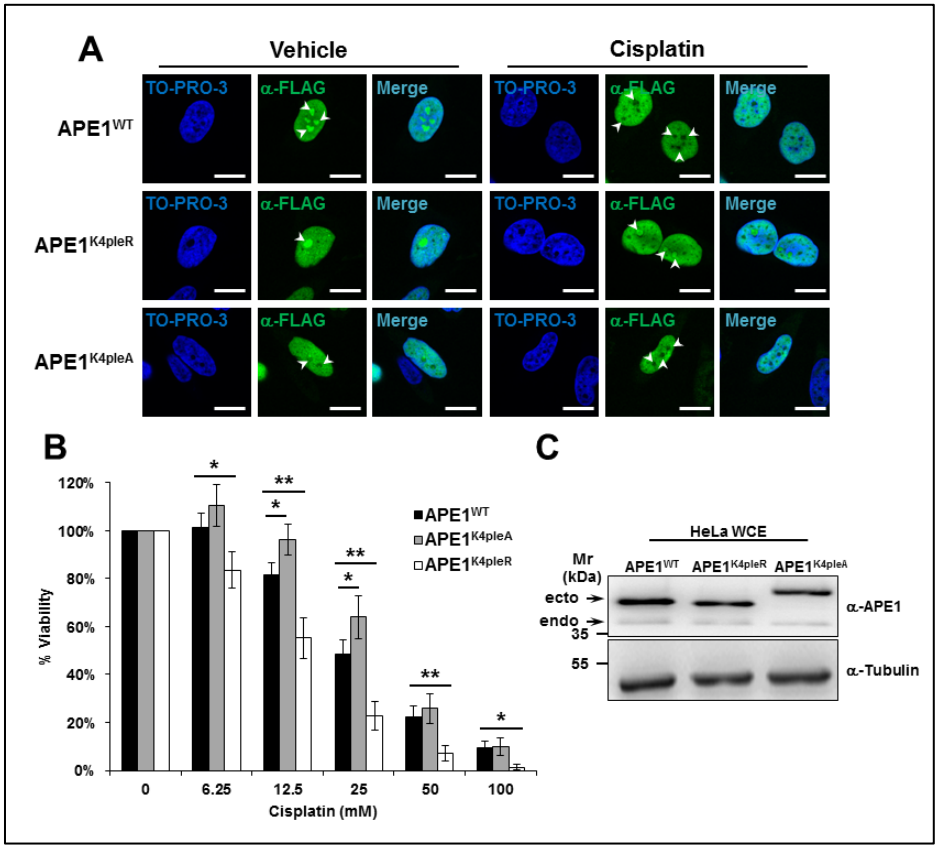

Fig. 30 – The redistribution of APE1 from nucleoli affects cell sensitivity to cisplatin. A. Representative immuno-fluorescence analysis on HeLa cells stably expressing FLAG-tagged APE1^{WT}, APE1^{K4pleA} or APE1^{K4pleR} and treated with cisplatin (100 μM, 6 hours). The treatment induces a relocalization of the APE1^{WT} form, but not of the APE1^{K4pleR} mutant (*white arrowheads*). The APE1^{K4pleA} form shows a nucleolar-excluded staining which is not affected by cisplatin. Nuclei were counter-stained with TO-PRO-3, bars 16 μm. **B.** MTS viability assay on HeLa cells stably expressing different APE1 forms upon depletion of the endogenous APE1 protein and challenged with increasing cisplatin concentrations for 24 hours. The APE1^{K4pleA} clone shows a resistant phenotype, while the APE1^{K4pleR} clone displays hypersensitivity. The histogram reports the mean viability ± SD from at least three independent replicates. *: $p<0.05$, **: $p<0.01$. **C.** Western blotting analysis on APE1-reconstituted HeLa cell clones showing the residual amount of endogenous APE1 (endo) and the comparable expression of the mutant, FLAG-tagged form (ecto). Tubulin was used as loading control.

In addition, viability assays showed that the ability of APE1 to redistribute from nucleoli affects cellular response to cisplatin. I exploited a previously characterized HeLa cell model that, through a doxycycline-dependent inducible expression of specific shRNAs, allows me to replace the endogenous form of APE1 with ectopically expressed siRNA-resistant wild-type or mutant forms

[124, 138]. As shown in Fig. 30, the APE1^{K4pleR}-expressing clone was hypersensitive to cisplatin treatment, indicating that the APE1 capacity to shuttle from nucleoli plays a critical role in dictating cisplatin cytotoxicity. Furthermore, the expression of the APE1^{KpleA} form was protective at lower doses of cisplatin (Fig. 30). Since inhibition of the APE1 catalytic activity in the APE1^{K4pleA}-expressing clone did not affect its resistance to cisplatin (Fig. 31), the observed protective effect might be ascribed to the lower proliferative capacity of these cells [124].

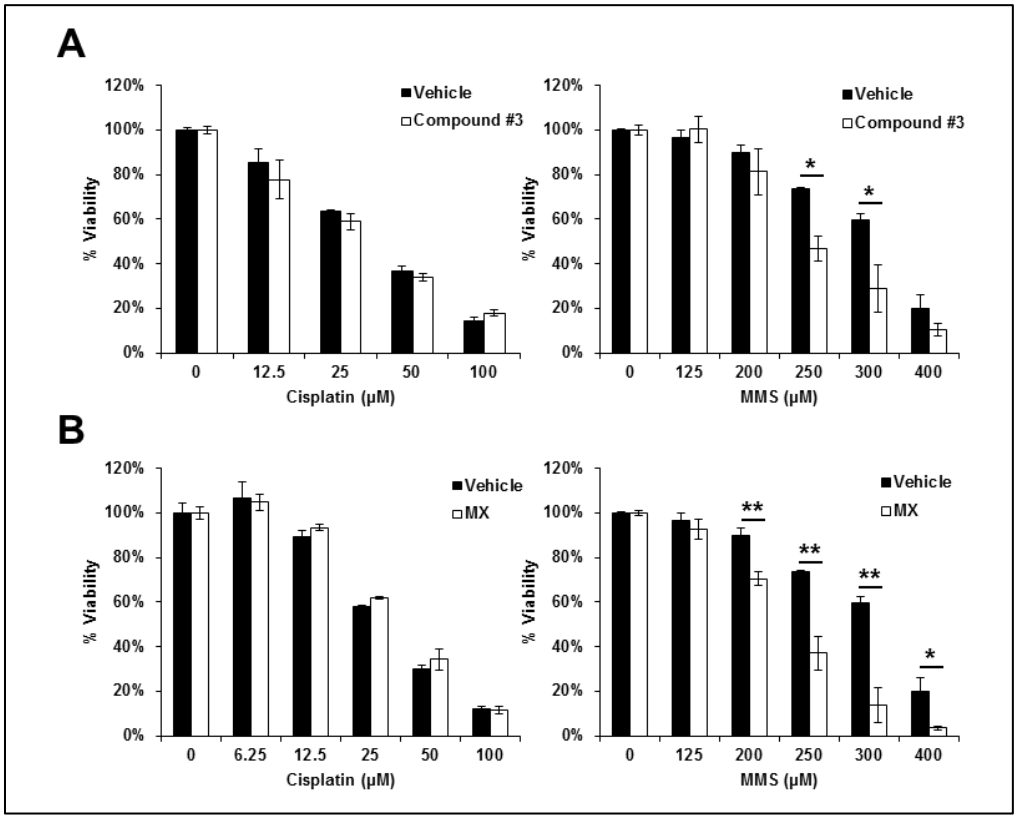

Fig. 31 – Inhibition of the APE1 catalytic activity in the APE1^{K4pleA}-expressing cells does not affect cell sensitivity to cisplatin. HeLa cells stably expressing the APE1^{KpleA} form were incubated with increasing cisplating concentrations for 24 hours, in presence of either methoxyamine (MX, 10 mM, **A**) or compound #3 (3.5 μM, **B**), to block the APE1 catalytic activity. MMS (24 hours) was used as positive control, to demonstrate the sensitizing activity of the APE1 inhibitors at the dosage tested. The histograms report the mean ± SD of three independent replicates. *: $p<0.05$, **: $p<0.01$.

In conclusion, these experiments point to an active role of APE1 redistribution (and possibly that of other BER proteins) upon cisplatin-induced nucleolar stress. The relocalization of APE1, in fact, does not appear to be a passive phenomenon, but rather a modulation involving PTMs of specific lysine residues seems to be required. Moreover, it is clear that interfering with cisplatin-induced BER protein relocalization has a major impact on cell response to this genotoxin.

2.4. APE1 is involved in the ribosome biogenesis process

The effect observed on the BER protein localization upon cisplatin, along with the concurrent impairment in the nucleolar transcription, point to a major role for the BER components in the maintenance of the ribosome biogenesis.

In order to gain further insights into the role of nucleolar BER enzymes, using again APE1 as a representative enzyme of the pathway I assessed the influence of APE1 depletion on the early ribosome biogenesis process. I transiently depleted cells of APE1 and measured the rRNA transcription rate through two complementary assays. First, I assessed the nucleolar incorporation of fluorouridine (FUrd), a fluorinated UTP analogue, into nascent rRNA transcripts [214, 215]. Notably, the depletion of APE1 resulted in a strong impairment in the nucleolar FUrd uptake (Fig. 32A, Fig. 32B). This observation was corroborated by metabolic [^{32}P]-orthophosphate labeling experiments, which confirmed the reduced synthesis rate of the 47S rRNA precursor in APE1-depleted cells (Fig. 32A, Fig. 32C). Altogether, these data demonstrate that the expression of APE1 is crucial for an efficient transcription of ribosomal genes.

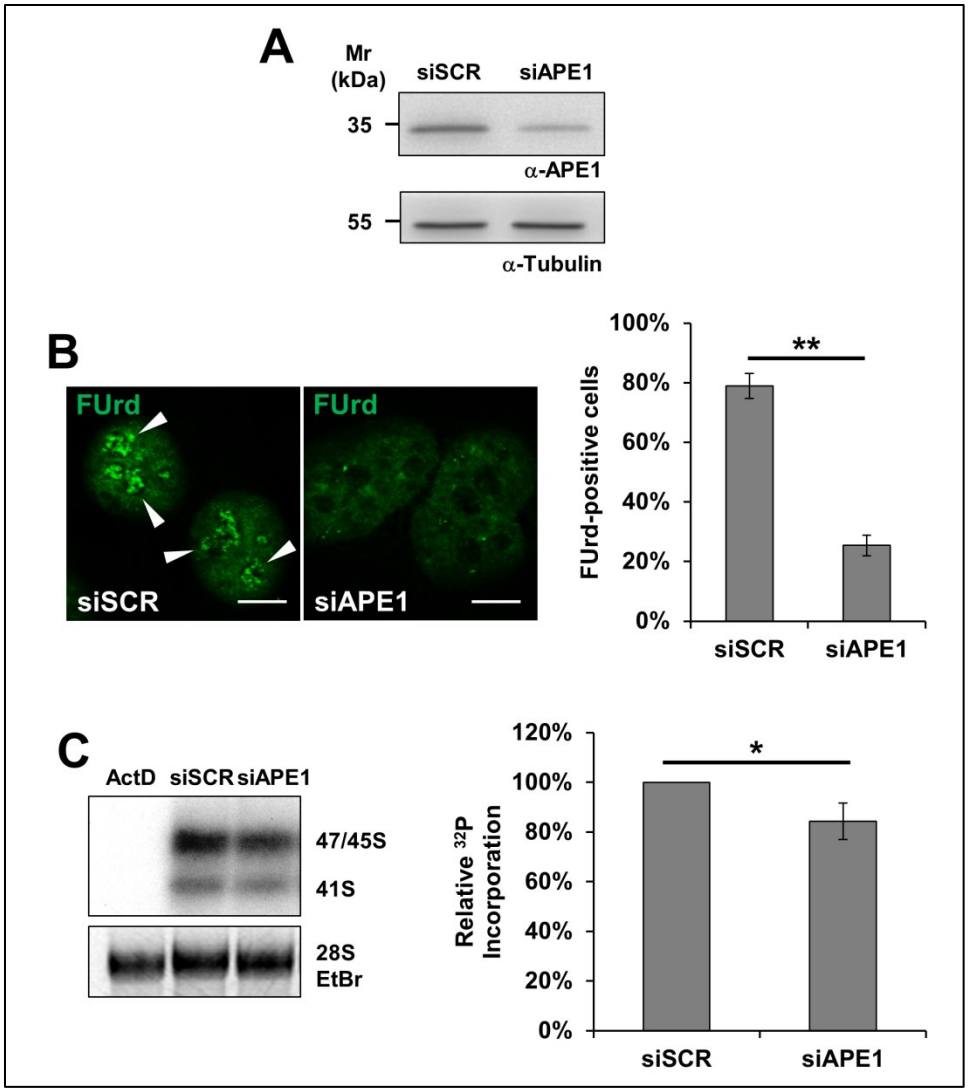

Fig. 32 – Depletion of APE1 leads to nucleolar impairment. A. Representative Western blotting analysis on HeLa cells treated with either a scrambled siRNA (siScr) or an APE1-specific siRNA (siAPE1) shows the efficiency of APE1 knockdown. Tubulin was used as loading control. **B.** Fluorouridine (FUrd) labeling of siScr- and siAPE1-treated HeLa cells. *Left panel* – representative immuno-fluorescence showing the preferential accumulation of FUrd within transcriptionally active nucleoli only in APE1-proficient cells (*white arrowheads*). Bars correspond to 8 μm. *Right panel* – histogram reporting the average FUrd nucleolar incorporation efficiency in siScr and siAPE1 cells. Values reported express the average amount of FUrd-positive cells ± SD from at least three independent experiments. **C.** [^{32}P]-phosphate metabolic labeling of nascent rRNA transcripts in HeLa cells treated with siScr, siAPE1 or actinomycin D (as positive control) reveals the nucleolar impairment in APE1-depleted cells. Cells were transfected with siRNAs and 48 hours later pulsed for 1 hour with [^{32}P]-orthophosphate, as described in the "*Experimental Methods*" section. *Left panel* – total RNA was extracted and the amount of labeled rRNA precursors was measured through autoradiography. Ethidium bromide staining was used as loading control. *Right panel* – histogram reporting the average [^{32}P]-phosphate incorporation into the 47S precursor in siScr and siAPE1 cells. Values reported express the mean incorporation ± SD from at least three independent experiments. siScr was used as reference sample. *: $p<0.01$, **: $p<0.001$.

I then checked whether the APE1 endonuclease activity of the protein might be involved in the modulation of the ribosome biogenesis process. To this aim I exploited the inhibitor "compound #3", which specifically targets the endonuclease activity of the protein [148], and I assessed the triggering of nucleolar stress phenotypes in HeLa cells. The onset of nucleolar stress upon APE1 inhibition was highlighted by the appearance of nucleolar fibrillarin caps (Fig. 33A); in addition, FUrd incorporation analyses revealed a reduction of the nucleolar activity in HeLa cells treated with compound #3 (Fig. 33B). Metabolic [^{32}P]-orthophosphate labeling, however, did not reveal any major impairment in the 47S precursor transcription, upon APE1 inhibition (Fig. 33C). Interestingly, on the other hand, I measured a reduced processing of mature rRNA species (Fig. 33, panels C and D). These data indicate that the APE1 endonuclease activity might be important for the correct processing of rRNA transcripts, rather than being involved in the transcription of the early 47S rRNA precursor.

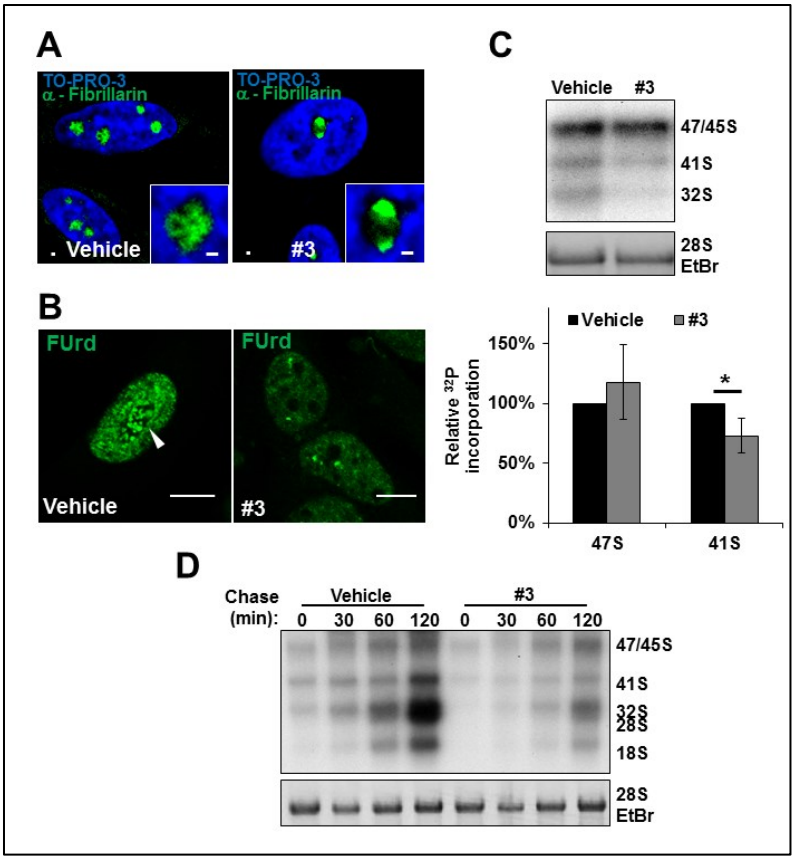

Fig. 33 – Inhibition of the APE1 endonuclease activity impairs ribosome biogenesis. HeLa cells were treated with compound #3 (1.75 μM, 24 hours) and nucleolar stress, rRNA transcription and processing were analyzed. **A.** Representative immuno-fluorescence panels and insets show the formation of fibrillarin caps upon inhibition of the APE1 endonuclease activity. Bars correspond to 1 μm, nuclei were counterstained with TO-PRO-3. **B.** Representative immuno-fluorescence showing the incorporation of fluorouridine (FUrd) within transcriptionally active nucleoli only in vehicle-treated cells (white arrowheads). Bars correspond to 8 μm. **C.** [^{32}P]-phosphate metabolic labeling of nascent rRNA transcripts does not show any significant impairment in the transcription of the 47S precursor, but reveals impairment in the processing of rRNA species following APE1 inhibition. *Top panel* –the amount of labeled rRNA precursors was measured through autoradiography, as described in the "*Experimental Methods*" section. Ethidium bromide staining was used as loading control. *Bottom panel* – histogram reporting the average [^{32}P]-phosphate incorporation into the 47S and 41S precursors in vehicle- or compound #3-treated cells. Values reported express the mean incorporation ± SD from three independent replicates. Vehicle-treated cells were used as reference sample, *: $p<0.05$. **D.** Analysis of the rRNA processing kinetics in HeLa cells upon [^{32}P]-phosphate metabolic labeling. The analysis was carried out as in panel C; after the [^{32}P]-orthophosphate pulse, cells were chased for the indicated time and intermediate rRNA species were analyzed on an agarose gel. The assay reveals a profound impairment in the rRNA processing kinetics upon inhibition of APE1.

These experiments, coupled with previous evidences [75], strongly suggest that the accumulation of APE1 and, possibly, of other BER enzymes within the nucleolus play an active role in the maintenance of the correct nucleolar function of the cell.

2.5. NPM1-mediated BER modulation is dependent on the activation of the p14^{Arf}/Mule axis

The experiments performed so far allowed me to demonstrate that NPM1 is a novel player in the BER pathway. NPM1 acts by promoting BER protein retention in nucleoli (Fig. 25); depletion of NPM1, moreover, stabilizes several BER components in a post-translational manner (Fig. 22, Fig. 23 and Fig. 24). In order to explain the mechanisms underlying this last observation, I investigated the interrelation between NPM1 and the p14^{Arf}/Mule axis, which has already been implicated in the modulation of BER protein stability [55].

NPM1 is known to regulate both the stability and the nucleolar accumulation of p14^{Arf}. This was demonstrated by monitoring the endogenous mouse p19^{Arf} ortholog in p53 KO MEFs [194] or through transfection of ectopic p14^{Arf} in human tumor cell lines [162]. Consistently with these reports, NPM1 depletion in HeLa cells decreased the stability of p14^{Arf} (Fig. 34A) and induced a nucleoplasmic translocation of the residual protein (Fig. 34B).

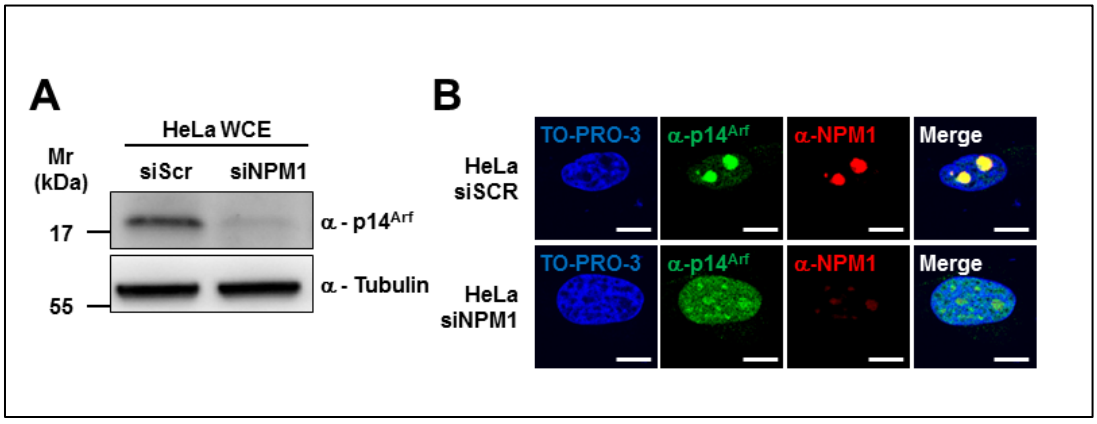

Fig. 34 – p14^{Arf} is unstable and undergoes nucleoplasmic relocalization upon NPM1 depletion. HeLa cells were transfected with either scrambled (siScr) or NPM1-specific (siNPM1) siRNAs and subjected to Western blotting and immuno-fluorescence analyses. **A.** Representative Western blotting on HeLa whole cell extracts (50 μg) highlights the decreased stability of p14^{Arf} after NPM1 downregulation. Tubulin was used as loading control. **B.** Representative immuno-fluorescence analysis on siNPM1-treated HeLa cells shows the nucleoplasmic redistribution of the residual p14^{Arf}. Note that the immuno-fluorescence images were acquired at constant microscope settings, and therefore the p14^{Arf} staining is saturated to allow for visualization of the downregulated p14^{Arf} protein in siNPM1-trated cells. Nuclei were counter-stained with TO-PRO-3, bars 16 μm.

The p14^{Arf} tumor suppressor has been reporter to inhibit the E3-ligase activity of Mule upon genotoxic stress [216]. I hypothesized that the chronic nucleoplasmic localization of p14^{Arf}, observed in NPM-depleted cells, could trigger the stabilization of BER proteins through constitutive inhibition of Mule. In agreement with this hypothesis, simultaneous depletion of either NPM1 and p14^{Arf}, or NPM1 and Mule, efficiently suppressed the upregulation of BER components observed when depleting NPM1 only (Fig. 35).

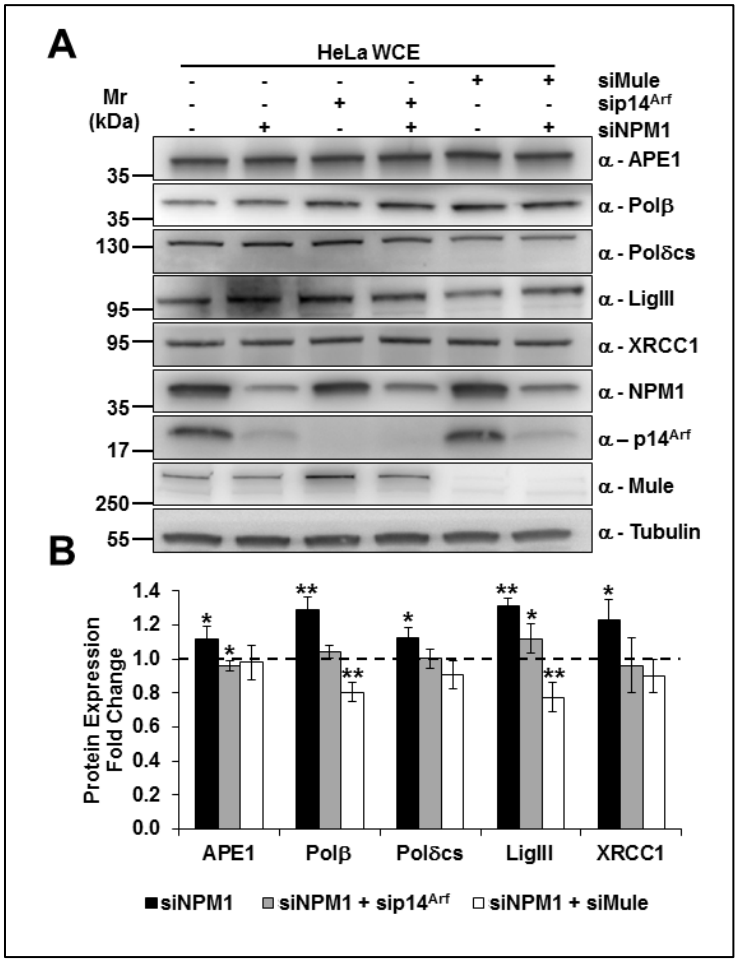

Fig. 35 – Interfering with the p14^{Arf}/Mule axis bluntens the BER stabilization effect obtained upon NPM1 depletion. HeLa cells were transiently depleted of NPM1, p14^{Arf} and Mule through specific siRNAs, as indicated. The expression levels of a subset of BER proteins was then assessed through Western blotting on whole cell extracts (50 μg) (**A**). **B.** Histogram reporting the quantitative protein expression fold change for siNPM1, siNPM1+sip14^{Arf} and siNPM1+siMule relative to control siRNAs (scrambled, sip14^{Arf} or siMule, respectively). The histogram shows the mean ± SD from at least three independent experiments. The statistical analysis was performed by comparing NPM1-depleted cells with their control counterparts (i.e. sScr, sip14^{Arf} and siMule, respectively). *: $p<0.05$, **: $p<0.01$.

The contribution of $p14^{Arf}$ to the NPM1-mediated control of the BER protein stability was further highlighted by knockdown studies on cell lines lacking detectable $p14^{Arf}$ (i.e. U2OS and SK-BR-3). In these cell lines the upregulation of BER components following depletion of NPM1 was partially abolished or reduced in order of magnitude (Fig. 36). A notable exception was represented by Polβ, but this phenotype might reflect a $p14^{Arf}$-independent regulation of the protein at the transcriptional level, as suggested by the previous Real-time PCR analysis (Fig. 22).

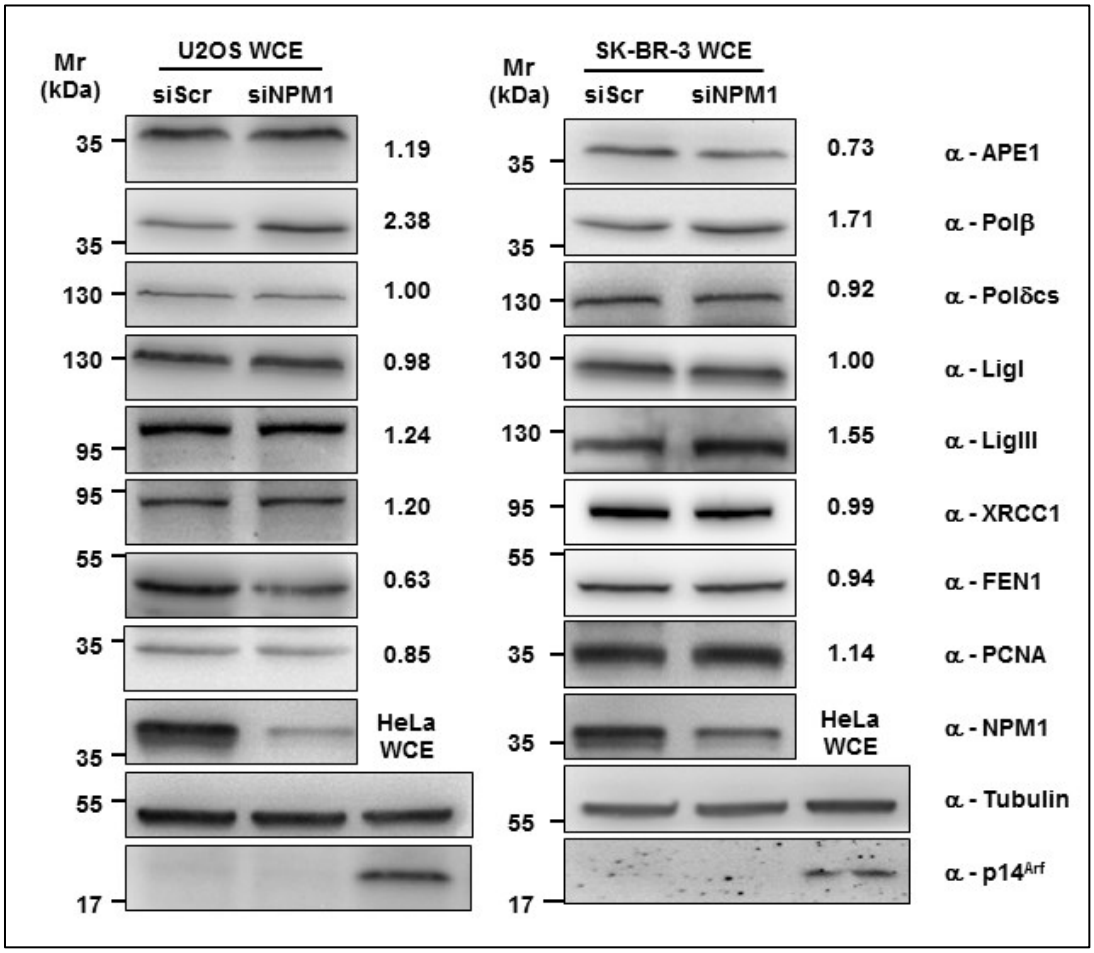

Fig. 36 – NPM1-mediated BER protein stabilization is partially impaired in cell lines lacking detectable $p14^{Arf}$. U2OS (**A**) or SK-BR-3 (**B**) cells were treated with either scrambled (siScr) or NPM1-specific (siNPM1) siRNAs and BER protein expression levels were assessed in whole cell exctracts (50 μg) using the indicated antibodies (*right-hand side*). The fold of protein induction upon NPM1 depletion is indicated for each protein analyzed. HeLa whole cell extract was used as positive control for $p14^{Arf}$ expression, while tubulin was used as loading control.

Additional immuno-fluorescence studies on NPM1-, p14^{Arf}- or Mule-depleted cells revealed a cross-modulation existing between these three factors, which dictates their subcellular localization. As previously demonstrated (Fig. 34), nucleolar localization of p14^{Arf} was promoted by NPM1, and, to a lesser extent, by Mule expression. NPM1 nucleoplasmic accumulation was increased when knocking down either p14^{Arf} or Mule, indicating that both proteins partially regulate NPM1 nucleolar retention. NPM1 down-regulation, moreover, resulted in the depletion of the nucleolar Mule pool, suggesting that Mule subcellular trafficking is, in turn, modulated by NPM1 (Fig. 37).

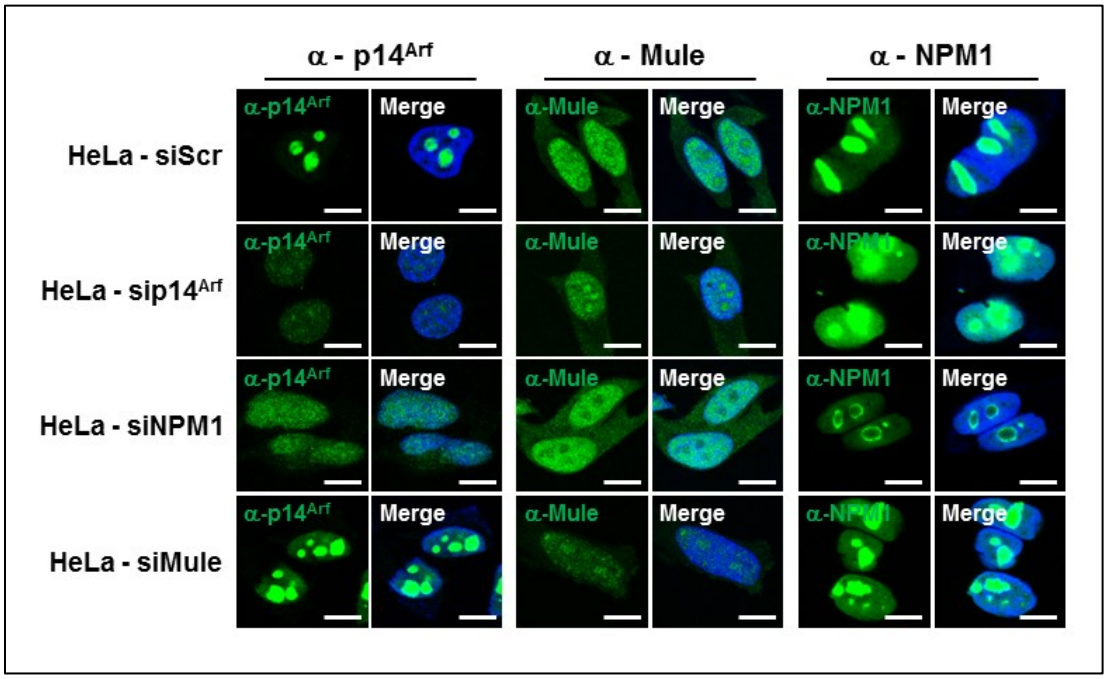

Fig. 37 – The subcellular localization of p14^{Arf}, Mule and NPM1 is modulated by an intricate cross-talk. Representative immuno-fluorescence experiments on HeLa cells treated with scrambled, p14^{Arf}-, NPM1- or Mule-targeting siRNAs (siScr, sip14^{Arf}, siNPM1 and siMule, respectively). Cells were probed with the antibodies indicated in the upper part of the figure. Note the increased p14^{Arf} nucleoplasmic localization upon NPM1 and Mule knockdown, the nucleolar depletion of Mule in NPM1-depleted cells, and the increased nucleoplasmic staining for NPM1 in p14^{Arf}- and Mule-depleted cells. Nuclei were counter-stained with TO-PRO-3, bars 16 μm.

2.6. BER capacity is positively modulated by NPM1

Despite the higher BER protein content, NPM1$^{-/-}$ MEFs have previously been shown to display increased susceptibility to BER-eliciting genotoxins [186]. We recently linked the augmented sensitivity to MMS, bleomycin and oxidizing agents to an impaired AP-site incision activity in NPM1$^{-/-}$ cell extracts [186]. Prompted by the observation that NPM1 depletion leads to a broad upregulation of the BER components, here I tested whether the enzymatic steps of the BER process downstream APE1 incision may be affected by NPM1 depletion. To this aim, I compared *in vitro* gap-filling, nick-ligation and flap-incision activities at equal amounts of NPM1$^{+/+}$ and NPM1$^{-/-}$ whole cell extracts (Fig. 38).

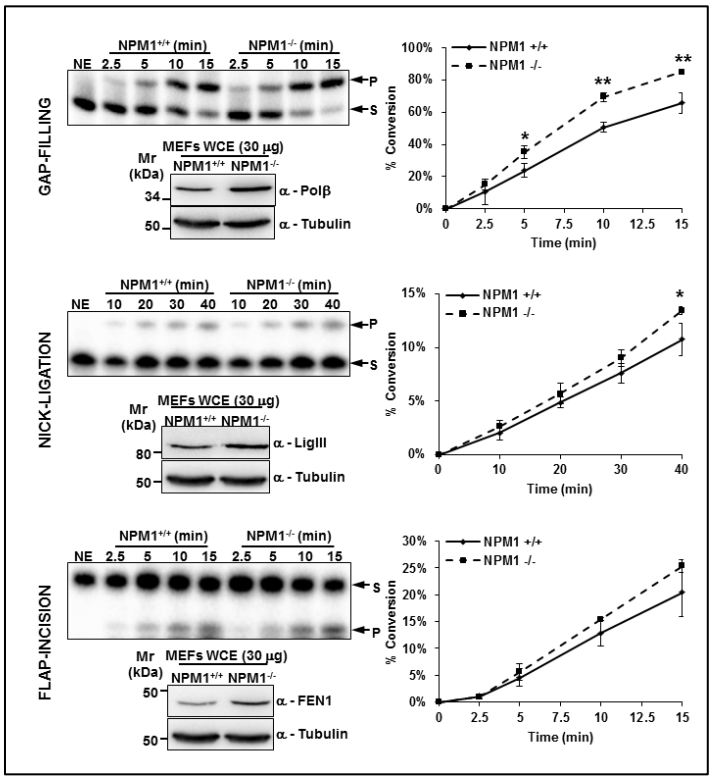

Fig. 38 – Comparison between NPM1$^{+/+}$ and NPM1$^{-/-}$ whole cell extracts show proficiency in gap-filling, but no significant difference in nick-ligation or flap-incision activities upon depletion of NPM1. BER enzymatic activities were meaured by using standard *in vitro* radioisotope-based assays, as indicated in the "*Experimental Methods*" section; equal amounts of MEF whole cell exctracts were compared in each reaction. BER activities were monitored in time-course reactions and, for every time point, the percentage of substrate (S) to product (P) conversion was calculated. Graphs on the right-hand side report the mean conversion ± SD from at least three independent replicates. For each BER activity a representative autoradiogram is reported, along with a Western blotting showing the different protein content among NPM1$^{+/+}$ and NPM1$^{-/-}$ cells. *: $p<0.05$, **: $p<0.01$.

As expected, the higher Polβ content was paralleled by a small, yet significant increased proficiency in gap-filling in NPM1$^{-/-}$ MEFs. Strikingly, despite the higher amount of LigIII and

FEN1, both the nick-ligation and the flap-incision activities in NPM1$^{+/+}$ and NPM1$^{-/-}$ cell extracts did not differ significantly (Fig. 38). The same repair activity results were obtained using whole cell extracts prepared by different methods (i.e. detergent vs. hypotonic extraction), suggesting that my measurements were not affected by differential protein extraction efficiency among the two cell lines (not shown).

In order to compare the BER enzymatic activities at equal protein content, I carried out the *in vitro* BER assays after precise normalization of the Polβ, LigIII and FEN1 levels in NPM1$^{+/+}$ and NPM1$^{-/-}$ whole cell extracts. This experimental setup highlighted a major impairment in each BER enzymatic step in the absence of NPM1, thus suggesting that NPM1 is a previously uncharacterized positive modulator of the BER process (Fig. 39).

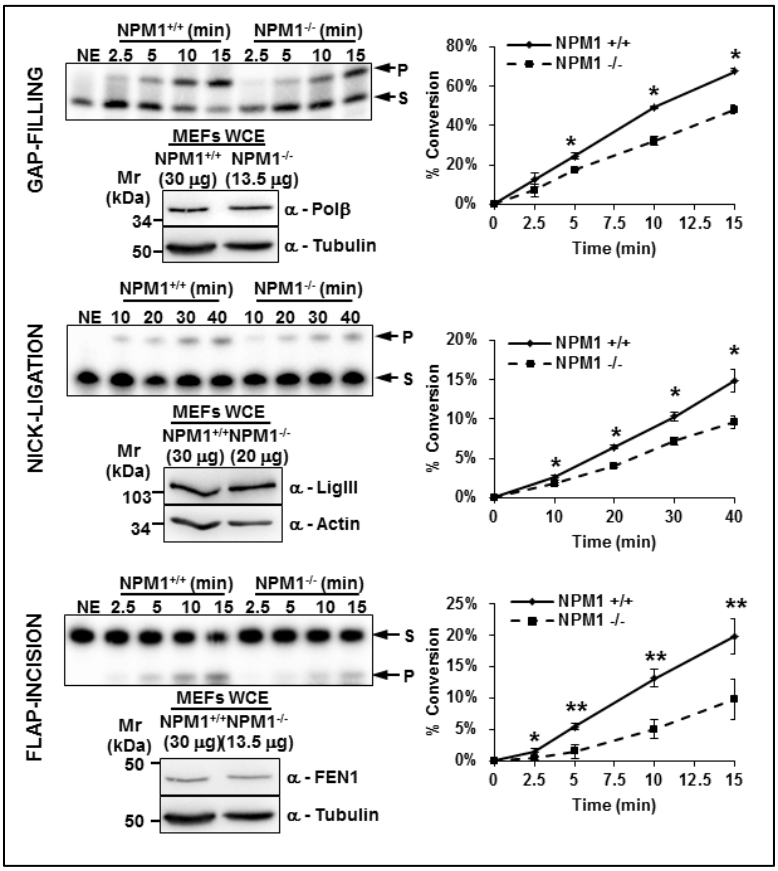

Fig. 39 – *In vitro* BER assays on NPM1$^{+/+}$ and NPM1$^{-/-}$ whole cell extracts at equal Polβ, LigIII and FEN1 content highlight the profound impairment in each BER step after depletion of NPM1. BER enzymatic activities were meaured as indicated in Fig. 38; MEF whole cell exctracts concentration was adjusted to compare equal protein amounts in each reaction. Graphs on the right-hand side report the mean percentage of substrate (S) to product (P) conversion ± SD from at least three independent replicates. For each BER activity a representative autoradiogram is reported, along with a Western blotting showing the comparable protein content in NPM1$^{+/+}$ and NPM1$^{-/-}$ extracts. *: p<0.05, **:p<0.001.

Despite the remarkable BER impairment in the absence of NPM1, under experimental conditions reflecting the protein expression pattern in living cells (i.e. without adjustment in whole cell extract amounts), I did not observe significant variations in the BER capacity (Fig. 38). Nonetheless, previous studies highlighted an increased sensitivity of $NPM1^{-/-}$ cells to BER-eliciting agents [186], along with the appearance of DDR markers in NPM1 KO embryos [194], as alluded to earlier. This indicates that the *in vitro* biochemical assays here reported do not entirely recapitulate the *in vivo* BER dynamics. To address this issue I developed a reporter-based assay suitable for the assessment of the overall BER capacity in living cells. A luciferase reporter-containing plasmid was heat-depurinated and transfected into living $NPM1^{+/+}$ or $NPM1^{-/-}$ MEFs and the luciferase activity was used as a direct measure of BER-mediated repair. As demonstrated by digestion with recombinant APE1, this treatment mainly generated AP-sites and SSBs with no detectable DSBs (Fig. 40B); thus, the plasmid obtained after heat-induced depurination is a substrate suitable to measure the overall cellular BER capacity, without confounding contributions from other DNA repair pathways.

Using this reporter-based assay I confirmed that, despite the increased BER protein expression, $NPM1^{-/-}$ cells have an impaired BER response (Fig. 40A), therefore explaining the augmented sensitivity to genotoxins. Consistently, NPM1 depletion in $NPM1^{+/+}$ MEFs recapitulated the $NPM1^{-/-}$ phenotype (Fig. 40 A and C); whereas reconstitution of $NPM1^{-/-}$ cells with recombinant human NPM1 rescued the BER deficiency (Fig. 40 A and C). Altogether, these results indicate that NPM1 is a novel positive modulator of the BER pathway both *in vitro* and *in vivo*.

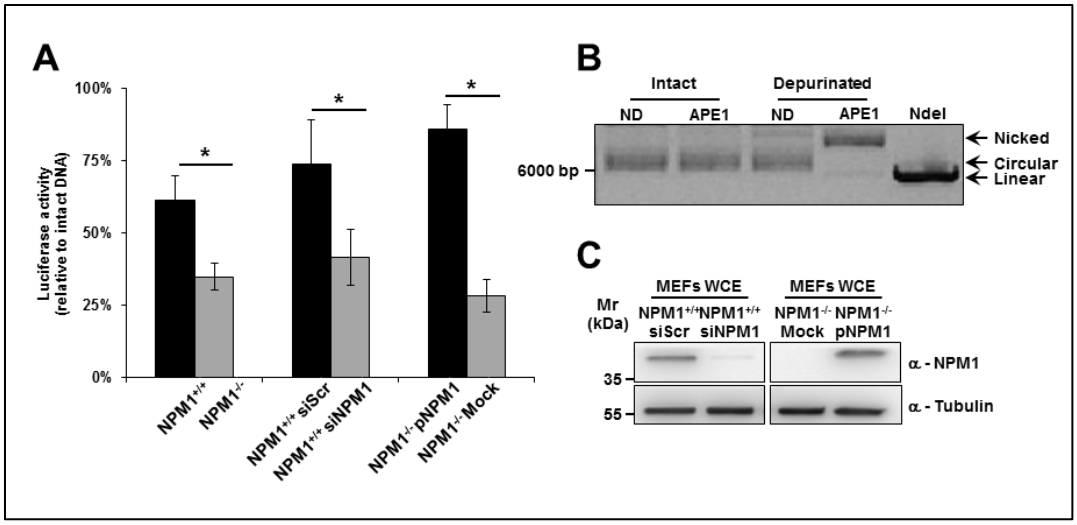

Fig. 40 – NPM1 depletion impairs the BER capacity *in vivo*. A. Reporter-based BER assays performed after transfection of a heat-depurinated luciferase plasmid reveal that NPM1$^{-/-}$ cells have an impaired repair capacity (*left bars*). siRNA-mediated depletion of NPM1 in NPM1$^{+/+}$ MEFs confirms this finding (*middle bars*); while transfection of human NPM1 in the NPM1$^{-/-}$ background rescues BER capacity (*right bars*). The histogram reports the mean luciferase activity (relative to that of intact DNA) ± SD from at least three independent replicates. *: $p<0.01$. **B.** Agarose gel analysis on the heat-depurinated reporter plasmid shows the formation of a small amount of spontaneously nicked DNA after depurination. Digestion of the damaged plasmid with recombinant APE1 results in the conversion of the plasmid into nicked and linear DNA, thus confirming the presence of AP-sites. A NdeI-linearized plasmid was used as marker to determine the migration of the linear vector. ND: not digested. **C.** Representative Western blotting analysis on MEF whole cell extracts from the experiment reported in panel A and showing the siRNA-mediated depletion of NPM1 (siNPM1) in NPM1$^{+/+}$ cells and the reconstitution of NPM1$^{-/-}$ cells (pNPM1).

2.7. Depletion of NPM1 does not significantly impair NHEJ- or HR-mediated DNA repair

As pointed out earlier, several evidences link NPM1 to DNA strand break-repair pathways [199, 200]. In the previous chapter I thoroughly analyzed the involvement of NPM1 in the BER-mediated DNA repair: the overall BER dysregulation in NPM1-depleted cells clearly explains the increased sensitivity of NPM1$^{-/-}$ cells to MMS, oxidizing agents, bleomycin and ionizing radiation ([186] and not shown). Some of the genotoxins used in previous studies, however, may also generate DSBs that are not directly targeted by the BER pathway. Therefore, in order to understand whether NPM1 has any significant relevance in the clearance of DNA strand breaks, I carried out a broad analysis to compare the DSB-repair capacity in NPM1$^{+/+}$ and NPM1$^{-/-}$ cells.

Western blotting analyses on NPM1-deficient MEFs revealed major variations in the expression levels of a small set of NHEJ components, with increased expression of the Ku70 antigen and of DNA ligase IV (LigIV), and reduction in the DNA-dependent protein kinase catalytic subunit (DNA-PKcs) amount (Fig. 41). Expression studies on a representative subset of HR factors, moreover, showed a significant upregulation of Rad51 in NPM1$^{-/-}$ cells (Fig. 41).

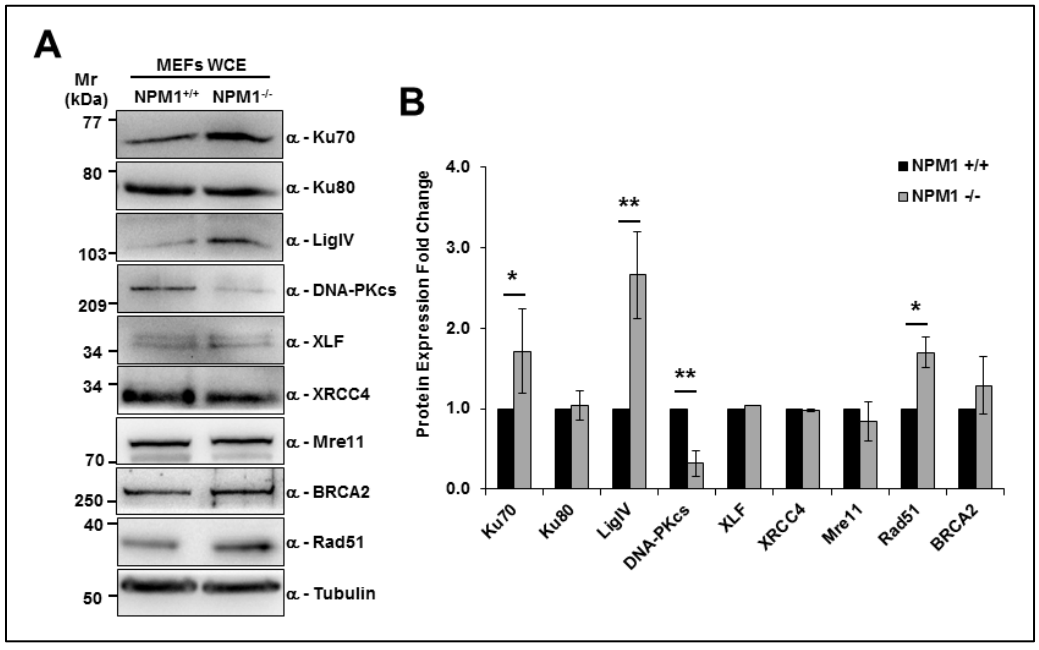

Fig. 41 – NPM1-depleted cells show upregulation of a subset of DSB-repair proteins. A. Representative Western blotting analysis on NPM1$^{+/+}$ and NPM1$^{-/-}$ MEFs whole cell extracts (60 μg) shows the variation in NHEJ and HR protein amounts in the absence of NPM1. Antibodies used are indicated on the right hand-side, tubulin was used as loading control. **B.** Histogram reporting the average protein expression fold change in NPM1$^{-/-}$ cells, as measured through densitometric quantification of the Western blotting signals. Bars indicate the mean ± SD from at least three independent replicates. *: $p<0.05$, **: $p<0.01$.

As already shown for the BER pathway, variation in DSB-repair protein levels may reflect a dysregulation in the DSB repair capacity of NPM1-deficient cells. In order to compare the NHEJ capacity of $NPM1^{+/+}$ and $NPM1^{-/-}$ MEFs, I carried out *in vitro* end-joining (EJ) assays using linear DNA substrates *ad hoc* generated through restriction of a plasmid DNA substrate. The *in vitro* EJ assays demonstrated that the ligation activity in whole cell extracts from $NPM1^{-/-}$ cells was significantly higher than $NPM1^{+/+}$ extracts toward DNA ends with cohesive overhangs (Fig. 42A). The ligation efficiency of blunt-ends did not show significant differences even if a trend toward higher activity of $NPM1^{-/-}$ lysates was still present (Fig. 42A).

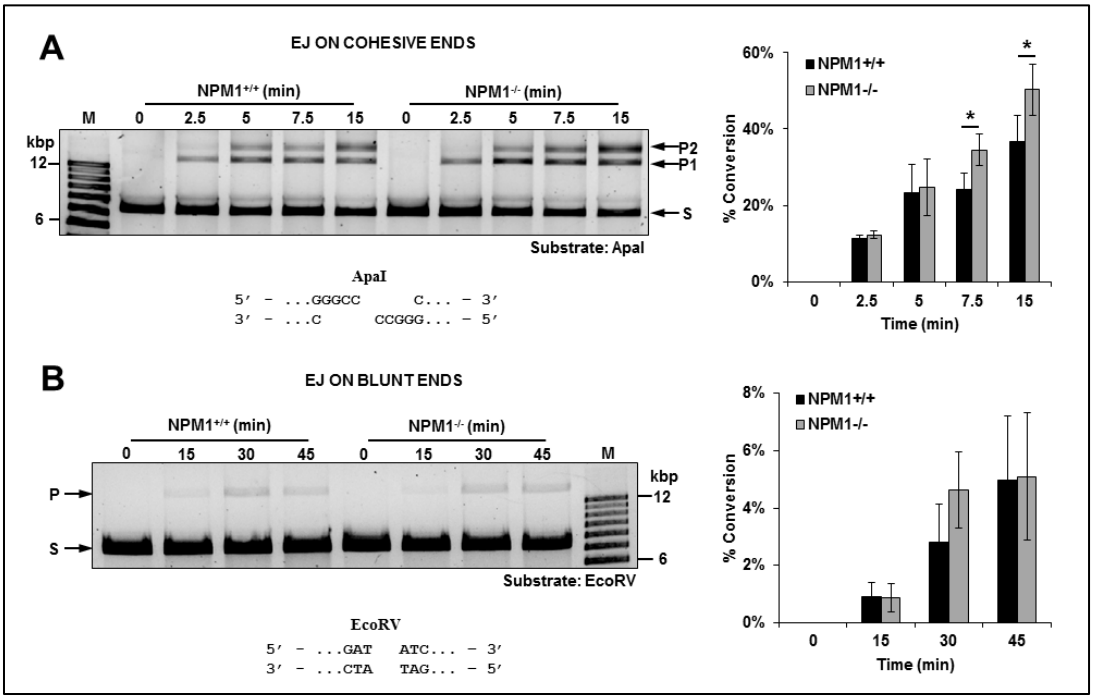

Fig. 42 – *In vitro* end-joining assays reveal a slight proficiency of $NPM1^{-/-}$ whole cell extracts. A. EJ assay on a linear DNA substrate with cohesive overhangs generated through restriction of a pmirGLO plasmid with the ApaI endonuclease. A representative gel shows the time-dependent conversion of the substrate (S) to oligomeric products (P1 and P2). The ApaI recognition sequence is also reported. **B.** EJ assay on a linear DNA substrate with blunt-ends generated through restriction of a pmirGLO plasmid with the EcoRV endonuclease. A representative gel shows the time-dependent conversion of the substrate (S) to a dimeric product (P). The EcoRV recognition sequence is reported below. The histograms (*right-hand side*) show the average percentage of substrate conversion ± SD from three independent experiments. *: $p<0.05$, M: DNA ladder.

Similar results were obtained using different enzymes, suggesting that the observed behavior is not linked to any sequence preference in the substrate.

I then assessed the *in vivo* DSB repair capacity of NPM1$^{+/+}$ and NPM1$^{-/-}$ cells exploiting a dual luciferase-containing pmirGLO plasmid. A single DSB was introduced within the vector by means of restriction endonucleases; the restriction site was carefully selected in order to repress the transcription of one selected reporter gene. MEF cells were subsequently transfected with the linear plasmid and the luciferase activity was measured to assess the EJ activity. Using different restriction enzymes I probed different biases in the DSB repair, such as the EJ activity on cohesive *vs.* blunt ends, or the overall *vs.* precise EJ capacity (Fig. 43).

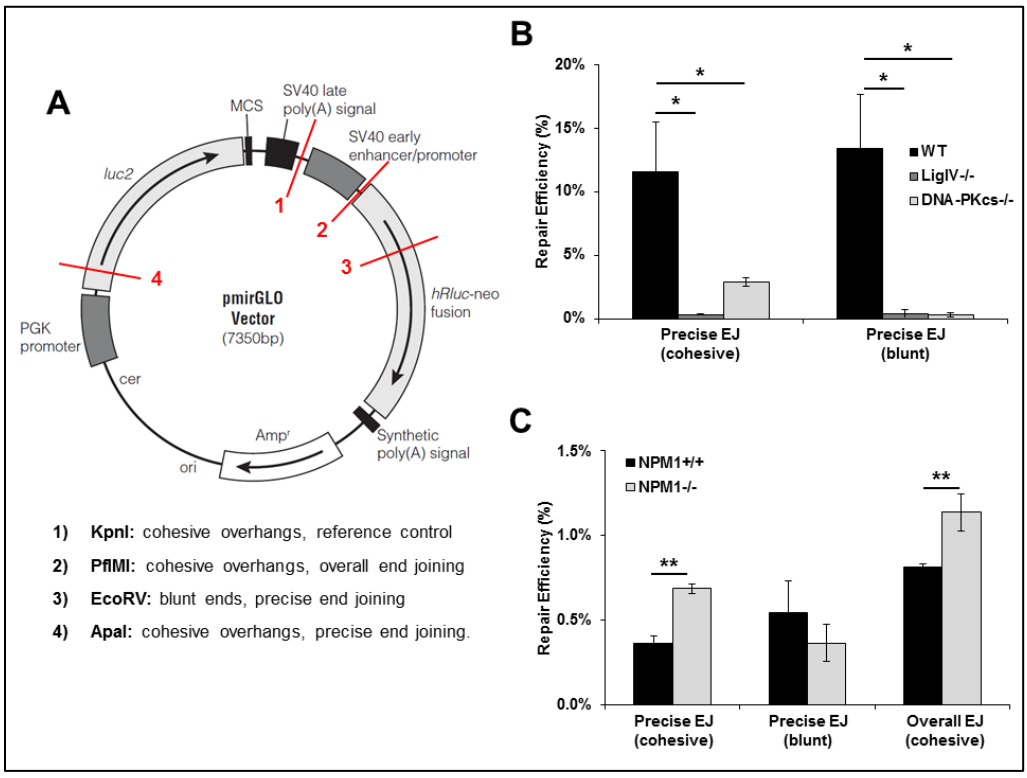

Fig. 43 – *In vivo* end-joining assays highlights the higher activity of NPM1$^{-/-}$ cells toward cohesive DNA ends. A. Schematic overview of the plasmid used in the assay with the restriction sites exploited to generate the substrate. The restriction endonucleases used are listed in the lower part of the panel, along with the characteristics of the substrate generated. KpnI-mediated restriction did not affect the activity of any reporter gene and was used to obtain a linear DNA substrate to be used as reference. PflMI was used to induce a DSB separating the SV40 promoter from the reporter gene and therefore allowing to monitor the overall EJ efficiency (as extensive editing at the DNA damage site is much more sustainable in a non coding region). *luc2*: firefly luciferase reporter; *hRluc*-neo fusion: humanized *Renilla* luciferase-neomycin resistance reporter cassette. **B.** *In vivo* EJ assay on control wild type (WT), LigIV$^{-/-}$ and DNA-PKcs$^{-/-}$ HCT116 cell lines highlights the assay performance and dependency on the presence of LigIV and, partially, on DNA-PKcs in the case of cohesive ends. The histogram reports the average repair efficiency ± SD from three technical replicates. *:p<0.05. **C.** *In vivo* EJ assay on NPM1$^{+/+}$ and NPM1$^{-/-}$ MEFs shows the proficiency of NPM1-depleted cells during cohesive end repair. The histogram reports the average repair efficiency ± SD from three independent replicates. **:p<0.01.

The *in vivo* EJ assays results were in accordance with the *in vitro* data (Fig. 42), highlighting a significantly increased EJ capacity for NPM1$^{-/-}$ cells over cohesive overhangs, regardless of the repair specificity (Fig. 43). These assays do not point to any significant difference in the EJ activity over blunt ended substrates. Reasonably, these data suggest that the presence of higher amounts of Ku70 and LigIV slightly improves the DNA EJ capacity of NPM1-deficient cell extracts.

Differently from other mammalian cells, the EJ capacity of MEFs is extremely low (compare the ligation efficiency in MEFs and human cell lines in Fig. 43) and the preferred DSB-repair pathway appears to be HR [217]. Therefore, in order to assess the HR-dependent DNA repair in NPM1-depleted MEFs, I challenged cells with the etoposide or bleomycin and measured the formation of Rad51 foci (Fig. 44). Being Rad51 a major component of the HR pathway involved in the homology search and pairing during the repair process, the dynamics of Rad51 foci clearance over the time allowed me to estimate the HR-dependent DSB repair.

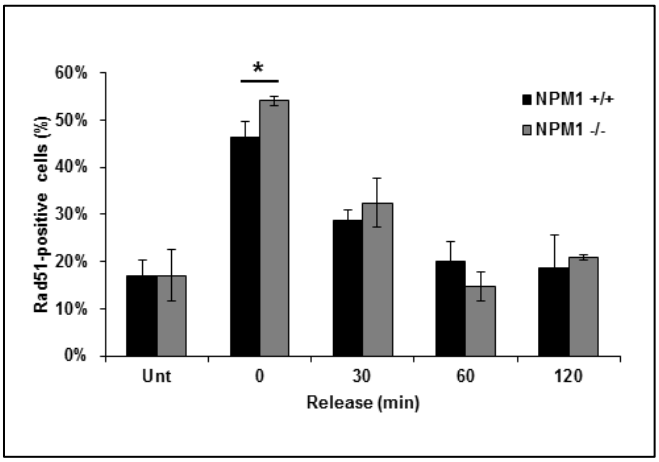

Fig. 44 – The HR pathway is not impaired in NPM1$^{-/-}$ cells. NPM1$^{+/+}$ and NPM1$^{-/-}$ MEFs were treated with etoposide (100 μM, 30 minutes) and Rad51 foci-positive cells were scored immediately (0) or after the indicated release time points. The histogram shows the mean percentage of Rad51-positive cells ± SD from three independent experiments. Unt: untreated; *: $p<0.05$.

The assessment of Rad51 foci formation showed a slightly increased susceptibility of NPM1$^{-/-}$ cells to etoposide (Fig. 44) and bleomycin (not shown), but similar DNA damage clearance kinetics. Consequently, despite the higher Rad51 expression levels in NPM1-depleted cells, it is possible to conclude that the HR pathway is not substantially affected by the absence of NPM1. These data are in agreement with comet assay analyses that did not reveal significant differences between NPM1$^{+/+}$ and NPM1$^{-/-}$ cells neither in the basal DNA damage content nor in the bleomycin-induced strand breaks repair (not shown).

DISCUSSION

The work described in this thesis broadens our comprehension of the BER mechanisms, presenting, on one side, the characterization of novel molecular entities targeting the interaction between a BER component and a non-canonical BER modulator. On the other hand, I carried out a wide analysis on the possible involvement of NPM1 in the DNA damage response, showing how a protein apparently unrelated to DNA repair may affect substantially the DDR.

The first part of this work led to the characterization of low molecular weight compounds targeting the APE1/NPM1 interaction. To the best of my knowledge, this is the first attempt to target the BER pathway through impairment of its protein-protein interaction network. The pilot-scale strategy set up during this project will be a useful starting point for the development of APE1/NPM1 inhibitors with increased potency and specificity. These molecules will likely provide novel translational tools and could be exploited to thoroughly characterize the biological relevance of the APE1/NPM1 association in the tumor biology.

A parallel and comprehensive analysis of the role(s) of NPM1 in the DDR revealed a tight link connecting NPM1 and the BER pathway. Analyses on the BER protein expression, localization and activity demonstrated that NPM1 is clearly a novel player in the BER response to DNA damage. The significance and the full implications of these findings, however, still remains to be elucidated, as it appears clear that canonical BER-eliciting stimuli are not able to induce NPM1 and BER protein relocalization. On the other hand, the observation of a link between cell response to cisplatin and NPM1/BER protein redistribution might open novel perspectives for a thorough comprehension of tumor resistance, explaining the involvement of the BER pathway in the scavenging of cisplatin-induced DNA damage.

1. The APE1/NPM1 interaction as a promising target for anti-tumor therapy

This thesis describes, for the first time, a pilot-scale screening aimed at the identification of low molecular weight compounds targeting the APE1/NPM1 association. In collaboration with the NCGC, we exploited the AlphaScreen® technology using full-length recombinant proteins and screened commercially available small molecule libraries in order to obtain putative disruptors of the APE1/NPM1 interaction. The hits from the screening underwent further prioritization through secondary cell-based orthogonal assays, and I obtained a set of compounds effectively able to interfere with the APE1/NPM1 association in living cells. The data available so far do not allow me to exclude the presence of *in vivo* off-target effects of the top-hit molecules, which are already known bioactive drugs. Through my proof of concept approach, however, I successfully demonstrated that the disruption of the APE1/NPM1 interaction can be achieved *via* structurally unrelated compounds under conditions of limited acute cytotoxicity, leading to interesting anti-tumor phenotypes. The APE1/NPM1 inhibitors, in fact, potentiate the cytotoxicity of clinically relevant genotoxins and show anti-proliferative activity as single agents in tumor cells of different histological origin (Fig. 17 and Fig. 18).

The mechanism of action of the APE1/NPM1 inhibitors has not been entirely characterized; however, as the protein-protein interaction is reported to involve the N-terminal domain of both proteins [75, 91], it is reasonable to speculate that the compounds might target the APE1 unstructured region or the NPM1 oligomerization domain. The change in the APE1 subcellular localization observed upon treatment with the compounds, indeed, suggests that the molecules might target the N-terminal domain of APE1, which is responsible for the nuclear accumulation of the protein [125] as well as for the interaction with NPM1 and rRNA [75, 90, 91]. SPR experiments (Fig. 16), and the negative effect of some molecules towards the APE1 redox activity (Fig. 15), would support a preference of the compounds for APE1 binding.

Curiously, among the screening hits was identified troglitazone, a PPARγ agonist with anti-diabetic properties, which was withdrawn from the market for its hepatotoxicity [218]. Troglitazone has previously been suggested to exert anti-inflammatory action through inhibition of the NF-κB pathway [219] and various reports have described interesting anti-tumor properties of the molecule [220, 221]. These observations might well be explained by the finding that troglitazone is a very potent inhibitor of the APE1/NF-κB axis (Fig. 15). A positive interaction between bleomycin and the antipsychotic phenothiazine trifluoperazine was also previously reported [222]; the APE1/NPM1 inhibitor spiclomazine is a member of the phenothiazine class of drugs and, consistently, I measure a

synergic effect between bleomycin and spiclomazine (Fig. 17). Albeit trifluoperazine has been suggested to impair the NHEJ process [222], an involvement of APE1 [101] or of the APE1/NPM1 interaction in the elimination of bleomycin-induced DNA damage could also explain the observed effects.

The sensitization effects measured when disrupting the APE1/NPM1 interaction in combination with MMS, bleomycin and PJ34 (Fig. 17) are not easily explained, as the endonuclease activity of APE1 is not directly impaired, *in vitro*, by the inhibitors (Fig. 21). Some of the molecules, however, induce relocalization of APE1 to the cytoplasm (Fig. 13 and Supplementary Table 1). It is therefore tempting to speculate that the sensitization observed toward genotoxins is driven by an impairment of the nuclear BER capacity, as already shown for NPM1c+ AML cells [186]. The measured effects might also reflect a possible role for the APE1/NPM1 association in the scavenging of DNA strand-breaks, as the genotoxins used in this study are likely to lead to the accumulation of SSBs and DSBs, in particular during the DNA replication process. Accordingly, NPM1 has been reported to associate with PARP1 and PARP2 [223], although the functional relevance of this interaction for DNA repair is still evanescent. Moreover, inhibition of the APE1 endonuclease activity was demonstrated to induce synthetic lethality in a DSB-repair deficient background [224]. It is conceivable, on the other hand, that non-canonical APE1 activities (e.g. RNA binding/cleavage, exonuclease, or RNaseH [95]) are involved in the response to the DNA damaging agents used in my experiments. Design of more selective APE1/NPM1 interaction inhibitors, therefore, will be useful to specifically characterize the relevance of this protein-protein interaction *in vivo*.

In conclusion, in the first part of this thesis I show that known bioactive molecules selected for their ability to displace the APE1/NPM1 association are endowed with previously uncharacterized anti-tumor properties. Potential targets of these inhibitors might be tumors that show upregulation of both APE1 and NPM1 levels and that might possibly rely on an increased APE1/NPM1 interaction for resistance and/or proliferation. As proposed in the introductory section, ovarian cancer, as well as hepatocarcinoma, might reveal sensible targets for the APE1/NPM1 inhibitors. Understanding the specificity of action of these molecules *in vivo* is clearly needed at this point. The improvement of these compounds, however, will lead to the development of new useful tools for the biological investigation of the APE1/NPM1 interaction under physiological and pathological conditions.

2. *NPM1 is a novel player in the BER*

The data presented in this thesis demonstrate that NPM1 is a novel multilevel modulator of the BER pathway. Previous work showed that NPM1 positively modulates the expression, the activity and the nucleolar accumulation of APE1 [186], but nothing was known about the relationship between NPM1 and the remainder of the BER pathway. My results suggest that NPM1 operates on the BER acting, at least at three different levels:

1) **NPM1 affects the stability of BER proteins.** Here I demonstrate that the lack of or reduced NPM1 expression results in the stabilization of several BER components (Figs. 22-24). The mechanisms underlying the BER protein upregulation still deserves further investigation; it appears clear, however, that BER stabilization following NPM1 depletion partially requires the functionality of the $p14^{Arf}$/Mule axis (Figs. 35 and 36). It is useful to underline that some of the expression changes that I observe are quantitatively small and may be indirect, in that increased expression of one BER protein may up-regulate another pathway component. The overall dysregulation of the protein expression levels, however, might play a significant role in reducing the coordination of the BER process, therefore affecting the repair capacity.

2) **NPM1 promotes the nucleolar accumulation of a subset of BER components.** The nucleolar localization of many DNA repair proteins is well established [19, 20] and several BER factors (including SMUG1 [76], aprataxin [225], APE1 [75, 186], FEN1 [77], PARP1/2 [223]) have been implicated in nucleolar functions that are possibly unrelated to their "canonical" DNA repair activity. Therefore, the novel discovery of the BER/replicative enzymes LigI and Polδcs within nucleoli was not unexpected. To the best of my knowledge, however, the prominent role of NPM1 in maintaining the nucleolar BER pool was never reported previously, if not for APE1 [75, 186] and PARP1/2 [223].

3) **NPM1 positively modulates the cellular BER capacity.** It has previously been shown by our group that NPM1 affects the APE1 endonuclease activity through direct protein-protein association [75, 91, 186]. In this thesis I demonstrate that NPM1 expression affects virtually each enzymatic step downstream the APE1 intervention in the BER process (Figs. 38 and 39). In addition, *in vivo* BER assays point to a significant dysregulation of the BER pathway dynamics upon NPM1 depletion (Fig. 40). A possible interpretation of these data could take into account the already documented chaperone activity of NPM1 [176]; by means of protein-protein or nucleic acid-protein contacts NPM1 could act as activator of the overall BER process. Nonetheless, attempts to restore the BER activity in $NPM1^{-/-}$ cell extracts using recombinant NPM1 *in vitro* were unsuccessful (not shown). Thus suggesting that PTMs either of, or induced by, NPM1 may be required for BER

modulation. Further studies aimed at elucidating the mechanisms underlying the NPM1-mediated BER activation are clearly needed at this point. Nevertheless, the BER impairment measured *in vivo* likely reflects a profound role for NPM1 in stimulating BER capacity. Additional analyses aimed at the elucidation of the NPM1 role in the DNA DSB-repair systems did not highlight any major effect of NPM1 depletion in the NHEJ and in the HR pathways (Figs. 42-44). Given the well-established responsiveness of NPM1 to UV-induced DNA damage [59, 195, 226] it would be probably worth to extend this analysis to other DNA repair pathways such as the NER.

3. BER and the nucleolus: speculations and perspectives on a brand new world

A peculiar aspect of my observations is the widespread relocalization of BER proteins from nucleoli upon DNA damage or after inhibition of Pol I-mediated transcription (Fig. 27). A point that still deserves extensive investigation is the effective role of BER components within nucleoli. It could be argued that nucleoli may act as mere storage depots for DNA repair proteins; under this assumption, my data would point to the BER protein redistribution as a means of increasing the nucleoplasmic DNA repair capacity. A possible contribution of the BER process to the direct elimination of the DNA damage induced by cisplatin was already suggested [10, 12], while daunorubicin, actinomycin D, and cisplatin itself have been reported to promote the accumulation of oxidative stress and strand-break markers [227-229]. Thus, the involvement of BER in the repair of DNA damage induced by these agents appears reasonable. There might be, however, some arguments against this hypothesis: first of all, the lack of any support of this model for canonical BER-eliciting compounds. Alkylating and oxidizing agents, in fact, have never been reported to induce NPM1 or BER protein translocation from nucleoli, nor have I been able to observe clear relocalization phenomena upon treatment with MMS or H_2O_2. In addition, crude estimates on nucleoli biochemically isolated from HeLa cells revealed that the BER protein content in these organelles is very low (ranging between 0.5% and 9%, depending on the protein, personal observations). A relocalization involving such a tiny amount of protein is unlikely to increase significantly the overall nucleoplasmic repair capacity. If we observe the problem from another perspective, however, the stress onset triggers a dramatic drop in the BER protein content within nucleoli, suggesting that the nucleolar BER capacity might be severely affected under these circumstances. As a matter of fact, nucleolar BER factors have been suggested to play a role in the rRNA quality control processes: the enzymatic activity of the SMUG1 glycosylase has been implicated in the rRNA quality check mechanisms [76], while nucleolar FEN1 was proposed to play a role in cell survival [77]. We showed that interfering with the nucleolar accumulation of APE1 results in growth defects [124], whereas depletion of APE1 leads to the accumulation of damaged rRNA species [75]. These phenotypes, however, were not accompanied by any obvious effect on the ribosome biogenesis, possibly reflecting a role for APE1 in the rRNA quality control process, rather than in rRNA synthesis [75]. The protracted (5-10 days) down-regulation of APE1 in those pioneering experiments, however, could have possibly triggered selection mechanisms that masked the early effects of APE1 depletion on the ribosome biogenesis. The short-term (48 h) depletion experiments presented in this thesis highlight a crucial role for APE1 in the early steps of the ribosome biogenesis process (Fig. 32). In this process,

the ribonuclease activity of the protein might be crucial for the elimination of damaged rRNA species; this observation, which deserves further investigation, would support the accumulation of oxidized rRNA species previously measured upon APE1 knockdown [75]. In addition, my data suggest that APE1's ability to redistribute from nucleoli also affects the cellular response to cisplatin (Fig. 30). Thus, it is conceivable that the relocalization of the BER proteins that I observe upon stimuli known to affect the cell cycle (e.g. cisplatin, daunorubicin, actinomycin D), but not to activate a canonical BER-mediated DNA repair, might contribute to the arrest of cell proliferation trough impairment of the rRNA synthesis. This hypothesis, which demands further investigation, would imply a leading role of nucleolar BER proteins in controlling cell proliferation.

As already pointed out, cisplatin is a widely used chemotherapeutic agent that generates a broad spectrum of lesions on DNA (and possibly RNA); platinum-based compounds are particularly used in combined chemo-radiation strategies. Intrinsic or acquired platinum resistance, however, is a major clinical problem, since alternative agents that circumvent cancer resistance do not currently exist [30]. It is commonly accepted that cisplatin-related adducts are eliminated by the NER pathway, nonetheless, recent findings suggest that BER might be at least partially involved in the removal of DNA lesions induced by crosslinking agents [10]. In addition, BER intervention on cisplatin-DNA adducts may significantly delay the removal of these lesions, competing with the NER pathway for the access to DNA [9]. An alternative explanation for the phenomena I observed takes into account a BER contribution to both the DNA repair and the nucleolar function. The presence of BER proteins within nucleoli might be necessary for rDNA/rRNA maintenance under unstressed conditions, ensuring correct transcription of the ribosomal genes and accurate processing of the rRNA. The reorganization of the nucleolar proteome observed upon cisplatin treatment might allow a cell cycle arrest through depletion of BER components from nucleoli, concurrently allowing NER factors to take over the repair of rDNA free of competing proteins. Interestingly, the importance of nucleolar BER proteins for cisplatin resistance is in accordance with a very recent report showing that 5-fluorouracil-induced rRNA biogenesis defects are dependent on DNA repair protein expression [14].

An additional link between BER protein relocalization and cell cycle arrest triggered by nucleolar stress is the $p14^{Arf}$ tumor suppressor. Under basal conditions, at least in cancer cells, the majority of $p41^{Arf}$ is associated with NPM1 in an inactive, nucleolar state [162, 209]. $p41^{Arf}$ is an established DNA damage sensor [59, 60, 230]: in tumor cells DNA damage promotes a transient subnuclear redistribution of $p41^{Arf}$ to the nucleoplasm, where it can boost the p53 response through interaction with at least two E3-ubiquitin ligases, namely Mdm2 [62, 63] and Mule [216]. My results strongly support the notion of the nucleolus as a stress sensor upstream p53. There are still conflicting reports concerning the effect of NPM1 on p53 activation following DNA damage. While elevated

levels of NPM1 following UV irradiation have been shown to suppress p53-mediated growth arrest, other reports point to a positive function of NPM1 on p53. These apparently contradictory observations suggest that NPM1 levels, together with the p41^{Arf} and p53 status of the cell, have to be taken into account [63]. The observation that NPM1 downregulation triggers p41^{Arf} redistribution, as happens under conditions of nucleolar stress, suggest that NPM1 act as a major sensing mechanism for the nucleolus.

Based on my findings, the dynamics following a nucleolar stress response and involving NPM1, p14^{Arf} and the BER pathway are compatible with the speculative model depicted in Fig. 45:

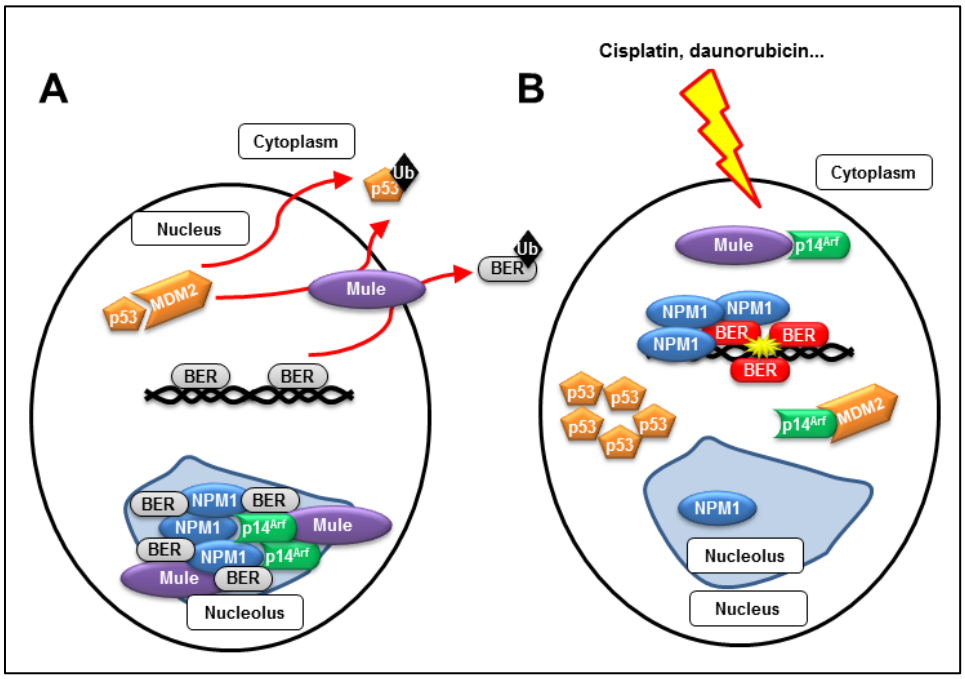

Fig. 45 – A model for BER modulation during nucleolar stress. A. Under unstressed conditions NPM1 localizes within nucleoli, promoting the accumulation of a subset of BER enzymes, along with the p14^{Arf} tumor suppressor and a sub-population of Mule. Basal BER capacity is maintained through constitutive Mule activity, while cell cycle progression is ensured by p53 destabilization and degradation. In this scenario, BER factors exert also nucleolus-specific functions that grant cellular proliferation. **B.** Upon triggering of nucleolar stress, relocalization of NPM1 p14^{Arf} and BER components occurs. This may lead to cell cycle delay through p14^{Arf}-mediated inhibition of Mule and MDM2 and consequent p53 stabilization. Cell cycle arrest is also enforced by BER protein redistribution from nucleoli. Simultaneously, BER capacity can be increased through NPM1-mediated stabilization of BER proteins and enhancement of enzymatic activity.

Under basal conditions NPM1 may function as a nucleolar gatekeeper, retaining a small subpopulation of BER proteins within nucleoli, along with the p14^{Arf} tumor suppressor. The nucleoplasmic BER capacity is homeostatically maintained through constitutive degradation of BER

factors exceeding the physiological threshold [54]. This mechanism limits the accumulation of DNA repair proteins, thus granting a steady state DNA repair level. The triggering of nucleolar stress leads to NPM1 release to the nucleoplasm, along with $p14^{Arf}$ and BER proteins. It is likely that this event fosters a p53-dependent cell cycle arrest that follows the p53 stabilization induced by NPM1- and $p14^{Arf}$-mediated sequestration of Mdm2 [160, 161, 231, 232]. The exit of BER proteins from nucleoli might contribute to the arrest of cell proliferation through impairment of the normal rRNA biogenesis process. Concurrently, $p14^{Arf}$ may help to increase the BER protein stability through inhibition of the Mule E3-ligase activity.

The signaling cascade following nucleolar stress should grant a cell cycle delay sufficient to carry out DNA repair; concurrently the NPM1-mediated activation of BER enzymes in the nucleoplasm could promote faster elimination of the DNA damage. The possible involvement of NPM1 in the modulation of other DSB-repair pathways is suggested by my experiments and by previous work [194, 199, 200], moreover, earlier observations highlighted how the rewiring of the nucleolar proteome upon DNA damage involves several DNA repair proteins belonging to different DNA repair pathways (reviewed in [19]). Therefore, the speculative model depicted in Fig. 45 might be also applicable to other DNA repair pathways, together with the BER.

It is worth pointing out that the proposed model may be important for tumor cells that are characterized by a nucleolar accumulation of $p14^{Arf}$. It has been suggested, in fact, that the localization of $p14^{Arf}$ in primary cells might not entirely recapitulate what observed in transformed cell models [60]. Nonetheless, the data presented in this thesis link for the first time the NPM1/$p14^{Arf}$ network and BER, providing a plausible explanation for the observed relocalization of DNA repair proteins from nucleoli upon nucleolar stress. Further comprehension of the precise functional significance of DNA repair protein within the nucleolus under basal conditions, however, deserves more extensive investigation.

EXPERIMENTAL METHODS

1. Recombinant protein expression and purification

For large scale production of recombinant proteins in *E. coli* I made use of a Bio-Flo110 (NewBrunswick) fermentor. GST-APE1 was expressed using a pGEX-3X vector, while $His_{(6)}$-NPM1 was expressed using a pET-15b [75, 91]. Purification of recombinant proteins was carried out essentially as described previously [75, 91], using an ÄKTA Purifier FPLC system (GE Healthcare) equipped with GSTrap™ FF and HisTrap™ HP chromatographic columns. Extensive dialysis was carried out to remove any trace of elution buffer and the quality of the purification was checked by Coomassie-stained SDS-PAGE.

2. AlphaScreen®-based high-throughput screening assay

The entire AlphaScreen®-based screening was optimized and carried out at the NIH Chemical Genomics Center (NCGC – Bethesda (MD), USA). Protein-protein interaction assessment for GST-APE1 and $His_{(6)}$Tag-NPM1 was carried out in 1,536-well plates screening the following libraries (number of compounds is indicated in parentheses): FDA Pharmaceutical Collections (2,816), MicroSource Spectrum collection (1,408), Tocris/TimTec (1,395), and bioactive compounds from Sigma Aldrich LOPAC1280 (1,280), FDA-Tocris-KU-DP (1,376), Prestwick (1,120), BU-GP-BioMol (1,302), Kinacore (2,037) and NCGC chemistry analogues. Briefly, 3 µl of GST-APE1 (125 nM final) was dispensed by BioRAPTR (Beckman Coulter) flying reagent dispenser, followed by addition of 23 nl of DMSO solution of compound library members achieved by a Kalypsys pintool [233]; after compound addition, 1 µl of $His_{(6)}$Tag-NPM1 (200 nM final) was dispensed and the assay plates were incubated for 20 minutes at room temperature. For detection, 1 µl of 20 µg/ml Glutathione donor/Ni^{2+} chelate acceptor AlphaScreen® bead mix was added. Plates were briefly centrifuged and incubated for 20 minutes at room temperature. The AlphaScreen® chemiluminescence signal was measured with an EnVision multilabel plate reader (PerkinElmer) equipped with a 1,536 Plate HTS AlphaScreen® aperture (80 ms excitation time, 240 ms measurement time). The signal was compared with that of DMSO-containing samples. Assay buffer consisted of 20 mM potassium phosphate pH 7.0, 50 mM NaCI, 5 mM $MgCI_2$, 0.01% Tween-20 and 2 mM DTT.

3. Cell culture and siRNA transfection

$p53^{-/-}$ ($NPM1^{+/+}$) and $p53^{-/-}$/$NPM1^{-/-}$ ($NPM1^{-/-}$) MEFs [194], HeLa, MCF-7, SF-767, HepG2, U2OS, and SK-BR-3 cells were grown in DMEM (GE Healthcare), JHH6 cells were cultured in William's Medium (Sigma) and HCT116 were cultured in McCoy's 5A Medium (Invitrogen). All media were supplemented with 10% fetal bovine serum (GE Healthcare), 100 U/ml penicillin, and 100 µg/ml streptomycin sulphate. HeLa cells reconstituted with mutant APE1 forms were grown as already indicated elsewhere [124].

For siRNA experiments 1 x 10^5 cells were seeded onto 6-well plates and transfected 24 hours later with 50 pmol of either a scrambled control siRNA or the target-specific siRNA by using the Oligofectamine™ Reagent (Invitrogen) as per manufacturer's indications. Mouse and human NPM1 siRNAs were from Thermo Scientific (ON-TARGETplus SMARTpool), $p14^{Arf}$ and Mule siRNAs were already described [58], while the oligonuclotide sequence used for APE1 was 5'-UACUCCAGUCGUACCAGACCU-3'. Cells were harvested 48 or 72 hours after transfection. Transient transfection procedures were carried out using the Lipofectamine®2000 Reagent (Invitrogen) as already described [186].

4. Chemical reagents and viability assays

Screening compounds were dissolved in DMSO as 10 mM stocks. MMS was from Sigma-Aldrich, bleomycin sulphate was from Santa Cruz Biotechnology and PJ34 (PARP Inhibitor VIII) was from Merck. Daunorubicin was from Bosche Scientific LLC, cisplatin was purchased from Sigma and freshly resuspended in dimethylformamide before every use.

Cell viability was assessed through the MTS ([3-(4,5-dimethylthiazol-2-yl)-5-(3-carboxymethoxyphenyl)-2-(4-sulfophenyl)-2H-tetrazolium, inner salt) assay (CellTiter 96® AQueous One Solution Cell Proliferation Assay – Promega) as per manufacturer's instructions. Briefly, 4-6 x 10^3 cells were seeded in 96-well plates and treated 24 hours later with the indicated compound; cell viability was measured at the indicated time points. Bleomycin cytotoxicity and cell proliferation were evaluated through cell counting experiments. In short, 3.2 x 10^4 cells were seeded into 12-well plates; 24 hours later cells were treated as indicated, medium was replaced and viability measured 48 hours later by a Trypan Blue exclusion assay or using a coulter counter (Beckman). For colony formation assays 2 x 10^2 HeLa cells were plated onto 6-well plates; 24 hours later cells were exposed to the selected compound(s) and cells were allowed to grow until formation of visible colonies (9-11

days) and stained as described earlier [75]. All the viability assays were performed in triplicate or quadruplicate and reproduced at least twice in independent experimental sessions.

5. *Immuno-fluorescence, Proximity Ligation Assay (PLA) and confocal microscopy*

For immuno-fluorescence analyses cells grown on glass coverslips were fixed with 4% paraformaldehyde for 20 min and extracted for 5 min in PBS/Triton X-100 0.1% at room temperature. Cells were saturated with 10% fetal bovine serum in TBS supplemented with 0.1% Tween 20 and incubated over night with primary antibodies. A complete list of the antibodies used can be found in the Supplementary Table 2. Rhodamine Red-, DyLight™549- or AlexaFluor®488-conjugated secondary antibodies (Jackson ImmunoResearch) were used for detection. Nuclei were counterstained with TO-PRO-3 (Invitrogen).

To monitor the interaction between APE1 and NPM1 in living cells, I used the in situ Proximity Ligation Assay kit (Olink Bioscience). HeLa cells stably expressing a FLAG-tagged form of APE1 [124] were seeded on glass slides, treated with the selected compounds and fixed/permeabilized immediately after the treatment as indicated above. Cells were incubated with a FITC-conjugated mouse anti-FLAG antibody for 3h at 37°C and then with a rabbit anti-NPM1 overnight at 4°C. PLA reactions were carried out following the manufacturer's instructions. Technical controls, represented by the omission of either the anti-NPM1 or the anti-FLAG primary antibodies, resulted in the complete loss of the PLA signal.

Fluorouridine (FUrd) incorporation to assess nucleolar transcription was monitored as described in [214, 215] with minor modifications. Briefly, cells were incubated with 2 mM FUrd (Sigma) in DMEM for 15 minutes at 37°C. Cells were then washed with ice-cold PBS and fixed with 4% paraformaldehyde for 10 minutes at room temperature. FUrd was visualized after cell permeabilization with 0.5% Triton X-100 for 5 minutes at room temperature and incubation with a monoclonal anti-BrdU antibody (Sigma) for 1 hour; cells were washed twice with PBS, and then stained for 1 hour with an AlexaFluor®488-conjugated anti-mouse secondary antibody (Jackson ImmunoResearch).

Cells were visualized through a Leica TCS SP laser-scanning confocal microscope (Leica Microsystems) equipped with a 488-nm argon laser, a 543-nm HeNe laser, and a 63X oil objective (HCX PL APO 63X Leica). Multi-color images were captured through sequential scanning.

Determination and scoring of PLA signals was performed by sectioning the whole cell height into six focal stacks, which were averaged and combined into a single image. This procedure allowed

me to detect the PLA signals present throughout the cell, regardless of their subcellular localization. At least 35 randomly selected cells per condition were analyzed following this procedure; PLA-spots present in each single cell were then scored using the BlobFinder software (Center for Image Analysis, Uppsala University, Uppsala, Sweden). The staining for FLAG-APE1 was used to identify cell nuclei, therefore allowing me to distinguish between nuclear and cytoplasmic interaction signals.

6. *In vivo assessment of the APE1 redox activity*

The APE1 redox activity was assessed as already described [204]. In brief, 1.1 x 10^4 JHH6 cells were seeded in 96-well plates, 24 hours later cells were co-transfected with 78.4 ng of pIL-8 (human IL-8 promoter – driven firefly luciferase reporter), 1.6 ng of pRL-CMV (*Renilla* reporter, as a reference for transfection efficiency) and 120 ng of pUC9 carrier plasmid, using the Lipofectamine®2000 Reagent (Invitrogen) as per manufacturer's instructions. One day after transfection cells were pre-treated with the selected APE1/NPM1 inhibitor (10 μM, 5 hours) or with E3330 (Sigma) (100 μM, 4 hours) in serum-free medium and subsequently challenged with 2000 U/ml TNF-α (Preprotech) for further 3 hours. The activity of luciferases was measured using the Dual-Glo® Luciferase Assay System (Promega).

7. *Surface Plasmon Resonance (SPR) Experiments*

SPR analyses were performed in collaboration with Dr. Daniela Marasco, at University of Naples, Italy. Real time binding assays were performed on a Biacore T-100 SPR instrument (GE Healthcare). Full length recombinant APE1 and NPM1 were bound at similar immobilization levels (2600 and 2800 RU, respectively) on a CM5 Biacore sensor chip in 10 mM sodium acetate, pH 5.5, by using the EDC/NHS chemistry, with a flow rate of 5 μl/min and an injection time of 7 min, as previously described [91]. Binding assays were carried out by injecting 100 μL of small molecule analyte, at 60 μl/min, in a running buffer composed of HBS (10 mM HEPES, 150 mM NaCl, 3 mM EDTA, pH 7.4), 0.1 mM TCEP and 10% DMSO. The BIAevaluation analysis package (version 4.1, GE Healthcare), was used to subtract the signal from the reference channel.

8. Preparation of cell extracts, Western blotting and co-immuno-precipitation

Whole cell extracts (WCE) and Western blotting analyses were performed as already described [75]. A complete list of the antibodies used can be found in the Supplementary Table 2. Protein concentration was determined by using the Protein Assay reagent (Bio-Rad) and images were acquired and quantified using a Chemidoc XRS video-densitometer.

Cell extracts for in vitro BER assays were prepared by resuspending cells in 50 mM Tris pH 7.4, 1 mM EDTA, 0.5 mM DTT, Protease Inhibitors Cocktail (Sigma), 1 mM PMSF; cell suspension was freeze-thawed and KCl was added to a final concentration of 222 mM. After 30 minutes on ice the cell lysate was cleared by centrifugation and supplemented with glycerol (10% final concentration) and stored at -80°C.

For co-immuno-precipitation assays cells were transfected with FLAG-tagged NPM1 and, 24 hours later, lysed in 50 mM Tris-HCl (pH 7.4), 150 mM NaCl, 1 mM EDTA, 1% Triton X-100 supplemented with protease inhibitor cocktail (Sigma), 0.5 mM PMSF, 1 mM NaF, and 1 mM Na_3VO_4 under gentle rocking for 20 minutes at 4°C. The cell extract was clarified by centrifugation and co-immuno-precipitation was carried out for 3 hours using the anti-FLAG M2 affinity gel (Sigma) as per manufacturer's indications. Co-immuno-precipitated material was eluted by incubation with 0.15 mg/ml FLAG peptide in Tris-buffered saline (TBS) and analyzed through Western blotting.

9. rRNA maturation kinetics

rRNA processing was monitored essentially as described by Burger and colleagues [197] with minor modifications. Briefly, 5 x 10^5 HeLa cells were incubated with the indicated inhibitors and metabolically labeled with [^{32}P]-orthophosphate (Perkin Elmer). For metabolic labeling cells were harvested by trypsinization and phosphate-depleted under rocking at 37°C for 1 hour in presence of unchanged drug concentrations, by incubation in phosphate-free DMEM (Invitrogen) supplemented with 10% dialyzed FBS. Medium was replaced with phosphate-free DMEM supplemented with 10% dialyzed FBS containing 15 μCi/ml [^{32}P]-orthophosphate and cells were labeled for 1 hour. Medium was again replaced with normal DMEM supplemented with 10% FBS in presence of unchanged drug concentrations and total RNA was isolated after 2 hours using the Trizol® Reagent (Invitrogen). RNA was separated on an agarose-formaldehyde gel loading the same amount of radioactivity per lane. Gels were vacuum-dried and subjected to autoradiography. To assess the 47S transcription rate RNA was isolated immediately after the [^{32}P]-orthophosphate pulse. Ethidium bromide staining of the 28S

specie was used as loading control. Actinomycin D (1 μg/ml) was used as positive control and was introduced for 1 hour during phosphate depletion.

10. DNA damage accumulation assays

Genomic DNA for AP-sites accumulation analysis was isolated from 1 x 10^6 HeLa cells by using the Get pureDNA Kit (Dojindo). AP-sites content was measured by using the DNA Damage Quantification Kit (Dojindo) as per manufacturer's indications. Briefly, 1 μg of genomic DNA was labeled with a biotinylated aldehyde reactive robe (ARP) at for 1 hour at 37°C and ARP-DNA was purified following the manufacturer's instructions. The amount of labeled ARP-DNA was then detected through a colorimetric reaction and eventually measured using a calibration curve provided with the kit.

Alkali comet assay was carried out essentially as described in [234]. Briefly, HeLa cells were exposed to the indicated concentrations of the APE1/NPM1 inhibitors and washed twice with ice-cold PBS. Approximately 3 x 10^3 cells were embedded in 0.5% low melting point agarose (Cambrex) in PBS and spread on microscope slides. Slides were placed in cold lysis solution (2.5 M NaCl, 100 mM EDTA, 10 mM Tris pH 10.0, 1% Triton X-100) for 1 hour at 4°C, and washed in cold 0.4 M Tris (pH 7.4). Next, the slides were incubated in alkali solution (300 mM NaOH, 1 mM EDTA, final pH 13.0) for 30 minutes at 4°C and then electrophoresed horizontally for 30 minutes at 25 V, 350 mA at 4°C. Slides were briefly neutralized with 0.4 M Tris (pH 7.4), stained with ethidium bromide (2 μg/ml) and viewed on a Ziess Axiovert 200 M fluorescent microscope (Zeiss). The analysis of the comet tail was carried out using the Comet Assay IV software (Perceptive Instruments) to determine the Olive tail moment. At least 100 cells per experimental condition were scored.

11. BER assays

The AP-incision activity in HeLa whole cell extracts was monitored as described earlier [235] with modifications. Briefly, HeLa cell extracts were prepared through lysis in 50 mM Tris-HCl pH 7.4, 150 mM NaCl, 1 mM EDTA, 1% Triton X-100, 0.5 mM PMSF and protease inhibitor cocktail (Sigma), for 20 minutes at 4°C and subsequent clarification; the supernatant was collected as whole cell extract. Enzymatic reactions were carried out using 50 ng of whole cell extract in a buffer containing 50 mM HEPES pH 7.5, 50 mM KCl, 1 mM MgCl2, and 1 mM DTT; the extract was pre-incubated for 15 minutes at 22°C with the selected inhibitor, reactions were started by adding 100 nM double stranded abasic DNA substrate (obtained by annealing of a 34F oligonucleotide 5'-

CTGCAGCTGATGCGCFGTACGGATCCCCGGGTAC-3', where F indicates a tetrahydrofuran residue, with a complementary 34G oligonucleotide 5'-GTACCCGGGGATCCGTACGGCGCATCAGCTGCAG-3') and incubated at 37°C for the indicated time. Reactions were halted by addition of formamide buffer (96% formamide, 10 mM EDTA with traces of bromophenol blue and xylene cyanol), separated onto a 20% denaturing polyacrylamide gel and stained with SYBR® Gold (Invitrogen) as per manufacturer's indications. The percentage of substrate converted to product was determined after background subtraction using standard phosphorimager analysis and the ImageQuant software.

In vitro WCE-based BER assays were carried out by using standard [^{32}P]-radiolabeled oligonucleotide substrates essentially as described in [235]. Briefly, all reactions were performed in the same reaction buffer (50 mM HEPES pH 7.5, 100 mM KCl, 10% glycerol, 1 mM DTT) at 37°C for the indicated time; oligonucleotide substrates were already described in [235, 236]. Flap-incision reactions were carried out using 1 μg of WCE; gap-filling reactions were carried out using 3 μg of WCE and nick-ligation assays were completed with 5 μg of WCE. Gap-filling reactions were supplemented with 0.5 mM dCTP, nick-ligation reactions were instead supplemented with 1 mM ATP. Reactions were stopped with 1 volume of formamide buffer and analyzed by electrophoresis on 15% denaturing polyacrylamide gels or 20% sequencing gels (for gap-filling reactions). The percentage of substrate converted to product was determined as above.

For reporter-based *in vivo* BER assays a pCMV/Luc plasmid was in vitro depurinated by incubation at 65°C for 40 minutes in 0.1 M sodium citrate and 0.5 M NaCl. DNA was ethanol-precipitated and resuspended in water for transfection. 1 x 10^4 cells were seeded onto 96 wells plates and transfected with 200 ng of either damaged or undamaged pCMV/Luc along with 8 ng of intact pCMV/RL (encoding for the *Renilla* luciferase, as a reference for transfection efficiency) using the Lipofectamine2000® Reagent (Invitrogen) as per manufacturer's indications. Luciferase activity was measured 8 hours after transfection by using the Dual-Glo® Luciferase Assay System (Promega); repair efficiency was expressed as percentage of luciferase signal normalized to the undamaged plasmid signal.

12. DSB-repair assays

In vitro NHEJ assays were performed using MEF whole cell extracts prepared as described in [237]. Briefly, cells were freeze-thawed and cell pellet was lysed for 10 minutes on ice in 45 mM HEPES-KOH pH 7.8, 0.4 M KCl, 1 mM EDTA, 0.2% Triton X-100, 0.1 mM DTT, 10% glycerol, protease inhibitors. After centrifugation at 20,000 x g for 10 minutes the supernatant was diluted four-

fold with 45 mM HEPES-KOH pH 7.8, 0.25 mM EDTA, 2% glycerol, 0.3 mg/ml BSA, aliquoted and stored at -80°C. NHEJ enzymatic assays were performed in a total volume of 10 µl in a reaction buffer containing 20 mM HEPES-KOH pH 7.5, 10 mM $MgCl_2$, 80 mM KCl, 1 mM ATP, and 1 mM DTT. Each reaction was carried out at 25°C using 2 µg of whole cell extract and 10 ng of plasmid DNA substrate. Reactions were halted by adding SDS (0.05%) and EDTA (50 mM), RNA and proteins were then removed by incubation with 0.5 mg/ml RNase A (10 minutes at 25°C) followed by 30 minutes at 37°C in presence of proteinase K (0.2 mg/ml). Samples were then resolved onto a 0.7% agarose gel and DNA was detected with SYBR® Gold staining.

For the reporter-based *in vivo* NHEJ assays a linear DNA substrate was generate through restriction or a dual luciferase-containing pmirGLO plasmid; after digestion, the restricted vector was separated by undigested forms and gel-purified. The day before transfection cells (6×10^3 MEFs or 2.5×10^4 HCT116) were plated onto 96-well plates and allowed to adhere for 24 hours; cells were then transfected with 150 ng of DNA substrate and luciferase activity was read 24 hours post-transfection. The presence of two reporter genes allowed me to calculate the repair capacity as the ratio between the luciferase activity of the cleaved reporter and the activity of the intact reporter. The intact reporter was here used as reference signal to normalize for transfection efficiency. A reference sample (i.e. the undamaged substrate, corresponding to 100% repair activity) was obtained through linearization of the pmirGLO plasmid with the KpnI restriction endonuclease, which did not damage any reporter in the vector.

Rad51 foci formation was assessed after cell treatment with etoposide (100 µM, 30 minutes) or bleomycin (100 µg/ml, 1 hour) and release for the indicated time points. Cells were stained with an α-Rad51 antibody and scored by manually counting cells containing more than three foci. At least 100 cells per condition were scored.

13. Real-time PCR

Real-time PCR analyses were performed as described [75], using a CFX96™ Real-Time PCR Detection System (BioRad). Primers sequences are listed in the Supplementary Table 3. FEN1 and XRCC1 primers sequences were from [238] and [239], respectively. Gene expression analysis was carried out using the CFX Manager™ Software (BioRad) and using *ACTB* and *GAPDH* as reference genes.

14. Statistical analyses

Statistical analyses were carried out by using the Student's t test available with the Microsoft Office Excel package. $p<0.05$ was considered as statistically significant.

REFERENCES

1. *Instability and decay of the primary structure of DNA.* **Lindahl T.** 1993, Nature., Vol. 362, pp. 709-715.

2. *Chemistry and biology of DNA repair.* **Schärer OD.** 2003, Angew Chem Int Ed Engl., Vol. 42, pp. 2946-2974.

3. *DNA repair mechanisms in dividing and non-dividing cells.* **Iyama T, Wilson DM 3rd.** 2013, DNA Repair (Amst)., Vol. 12, pp. 620-636.

4. *Implication of localization of human DNA repair enzyme O6-methylguanine-DNA methyltransferase at active transcription sites in transcription-repair coupling of the mutagenic O6-methylguanine lesion.* **Ali RB, Teo AK, Oh HK, Chuang LS, Ayi TC, Li BF.** 1998, Mol Cell Biol., Vol. 18, pp. 1660-1669.

5. **Kelley MR.** *DNA repair in cancer therapy.* Elsevier Inc., 2012. ISBN: 978-0-12-384999-1.

6. *Molecular mechanisms of mammalian global genome nucleotide excision repair.* **Gillet LC, Schärer OD.** 2006, Chem Rev., Vol. 106, pp. 253-276.

7. *The multifaceted mismatch-repair system.* **Jiricny J.** 2006, Nat Rev Mol Cell Biol., Vol. 7, pp. 335-346.

8. *Sensitivity and selectivity of the DNA damage sensor responsible for activating p53-dependent G1 arrest.* **Huang LC, Clarkin KC, Wahl GM.** 1996, Proc Natl Acad Sci USA., Vol. 93, pp. 4827-4832.

9. *Novel role of base excision repair in mediating cisplatin cytotoxicity.* **Kothandapani A, Dangeti VSMN, Brown AR, Banze LA, Wang XH, Sobol RW, Patrick SM.** 2011, J. Biol. Chem., Vol. 286, pp. 14564-14574.

10. *A novel link to base excision repair?* **Wilson DM 3rd, Seidman MM.** 2010, Trends Biochem Sci., Vol. 35, pp. 247-252.

11. *Passing the baton in base excision repair.* **Wilson SH, Kunkel TA.** 2000, Nat Struct Biol., Vol. 7, pp. 176-178.

12. *Evidence for base excision repair processing of DNA interstrand crosslinks.* **Kothandapani A, Patrick SM.** 2013, Mutat Res., Vols. 743-744, pp. 44-52.

13. *Epistatic role of base excision repair and mismatch repair pathways in mediating cisplatin cytotoxicity.* **Kothandapani A, Sawant A, Dangeti VS, Sobol RW, Patrick SM.** 2013, Nucleic Acids Res., Vol. 41, pp. 7332-7343.

14. *Base excision repair AP endonucleases and mismatch repair act together to induce checkpoint-mediated autophagy.* **Sengupta T, Torgersen ML, Kassahun H, Vellai T, Simonsen A, Nilsen H.** 2013, Nat Commun., p. 4:2578. doi: 10.1038/ncomms3674.

15. *ATM and ATR substrate analysis reveals extensive protein networks responsive to DNA damage.* **Matsuoka S, Ballif BA, Smogorzewska A, McDonald ER 3rd, Hurov KE, Luo J, Bakalarski CE, Zhao Z, Solimini N, Lerenthal Y, Shiloh Y, Gygi SP, Elledge SJ.** 2007, Science., Vol. 316, pp. 1160-1166.

16. *ATM-Dependent Downregulation of USP7/HAUSP by PPM1G Activates p53 Response to DNA Damage.* **Khoronenkova SV, Dianova II, Ternette N, Kessler BM,**

Parsons JL, Dianov GL. 2012, Mol Cell., Vol. 45, pp. 801-813.

17. *Basal Dynamics of p53 Reveal Transcriptionally Attenuated Pulses in Cycling Cells.* **Loewer A, Batchelor E, Gaglia G, Lahav G.** 2010, Cell, Vol. 142, pp. 89-100.

18. *Targeting checkpoint kinase 1 in cancer therapeutics.* **Tse AN, Carvajal R, Schwartz GK.** 2007, Clin Cancer Res., Vol. 13, pp. 1955-1960.

19. *Emerging Roles of the Nucleolus in Regulating the DNA Damage response: the non-canonical DNA repair enzyme APE1/Ref-1 as a paradigmatical example.* **Antoniali G, Lirussi L, Poletto M, Tell G.** 2014, Antioxid Redox Signal., Vol. 20, pp. 621-639.

20. *Quantitative proteomics and dynamic imaging of the nucleolus reveal distinct responses to UV and ionizing radiation.* **Moore HM, Bai B, Boisvert FM, Latonen L, Rantanen V, Simpson JC, Pepperkok R, Lamond AI, Laiho M.** 2011, Mol Cell Proteomics., Vol. 10. doi: 10.1074/mcp.M111.009241

21. *Disruption of the nucleolus mediates stabilization of p53 in response to DNA damage and other stresses.* **Rubbi CP, Milner J.** 2003, EMBO J., Vol. 22, pp. 6068-6077.

22. *Free radical-induced damage to DNA: mechanisms and measurement.* **Dizdaroglu M, Jaruga P, Birincioglu M, Rodriguez H.** 2002, Free Radic Biol Med., Vol. 32, pp. 1102-1115.

23. *Insertion of specific bases during DNA synthesis past the oxidation-damaged base 8-oxodG.* **Shibutani S, Takeshita M, Grollman AP.** 1991, Nature., Vol. 349, pp. 431-434.

24. *Transcriptional mutagenesis induced by 8-oxoguanine in mammalian cells.* **Brégeon D, Peignon PA, Sarasin A.** 2009, PLoS Genet., Vol. 5, p. e1000577.

25. *The mechanics of base excision repair, and its relationship to aging and disease.* **Wilson DM 3rd, Bohr VA.** 2007, DNA Repair (Amst)., Vol. 6, pp. 544-559.

26. *Early steps in the DNA base excision/single-strand interruption repair pathway in mammalian cells.* **Hegde ML, Hazra TK, Mitra S.** 2008, Cell Res., Vol. 18, pp. 27-47.

27. *A unified view of base excision repair: lesion-dependent protein complexes regulated by post-translational modification.* **Almeida KH, Sobol RW.** 2007, DNA Repair (Amst)., Vol. 6, pp. 695-711.

28. *Mammalian base excision repair: the forgotten archangel.* **Dianov GL, Hübscher U.** 2013, Nucleic Acids Res., Vol. 41, pp. 3483-3490.

29. *DNA glycosylases: in DNA repair and beyond.* **Jacobs AL, Schär P.** 2012, Chromosoma., Vol. 121, pp. 1-20.

30. *Targeting base excision repair to improve cancer therapies.* **Sharma RA, Dianov GL.** 2007, Mol Aspects Med., Vol. 28, pp. 345-374.

31. *Mammalian base excision repair and DNA polymerase beta.* **SH, Wilson.** 1998, Mutat Res., Vol. 407, pp. 203-215.

32. *AP endonuclease-independent DNA base excision repair in human cells.* **Wiederhold L, Leppard JB, Kedar P, Karimi-Busheri F, Rasouli-Nia A, Weinfeld M, Tomkinson AE, Izumi T, Prasad R, Wilson SH, Mitra S, Hazra TK.** 2004, Mol Cell., Vol. 15, pp. 209-220.

33. *Tyrosyl-DNA phosphodiesterase 1 (TDP1) repairs DNA damage induced by topoisomerases I and II and base alkylation in*

vertebrate cells. **Murai J, Huang SY, Das BB, Dexheimer TS, Takeda S, Pommier Y.** 2012, J Biol Chem., Vol. 287, pp. 12848-12857.

34. *Aprataxin, causative gene product for EAOH/AOA1, repairs DNA single-strand breaks with damaged 3'-phosphate and 3'-phosphoglycolate ends.* **Takahashi T, Tada M, Igarashi S, Koyama A, Date H, Yokoseki A, Shiga A, Yoshida Y, Tsuji S, Nishizawa M, Onodera O.** 2007, Nucleic Acids Res., Vol. 35, pp. 3797-3809.

35. *DNA polymerase beta promotes recruitment of DNA ligase III alpha-XRCC1 to sites of base excision repair.* **Parsons JL, Dianova II, Allinson SL, Dianov GL.** 2005, Biochemistry., Vol. 44, pp. 10613-10619.

36. *Proliferating cell nuclear antigen facilitates excision in long-patch base excision repair.* **Gary R, Kim K, Cornelius HL, Park MS, Matsumoto Y.** 1999, J Biol Chem., Vol. 274, pp. 4354-4363.

37. *Protein-protein interactions and posttranslational modifications in mammalian base excision repair.* **Fan J, Wilson DM 3rd.** 2005, Free Radic Biol Med., Vol. 38, pp. 1121-1138.

38. *Interaction between PCNA and DNA ligase I is critical for joining of Okazaki fragments and .* **Levin DS, McKenna AE, Motycka TA, Matsumoto Y, Tomkinson AE.** 2000, Curr Biol., Vol. 10, pp. 919-922.

39. *Orchestration of base excision repair by controlling the rates of enzymatic activities.* **Allinson SL, Sleeth KM, Matthewman GE, Dianov GL.** 2004, DNA Repair (Amst)., Vol. 3, pp. 23-31.

40. *Alternative nucleotide incision repair pathway for oxidative DNA damage.* **Ischenko AA, Saparbaev MK.** 2002, Nature., Vol. 415, pp. 183-187.

41. *Major oxidative products of cytosine are substrates for the nucleotide incision repair pathway.* **Daviet S, Couvé-Privat S, Gros L, Shinozuka K, Ide H, Saparbaev M, Ishchenko AA.** 2007, DNA Repair (Amst)., Vol. 6, pp. 8-18.

42. *Uracil in duplex DNA is a substrate for the nucleotide incision repair pathway in human cells.* **Prorok P, Alili D, Saint-Pierre C, Gasparutto D, Zharkov DO, Ishchenko AA, Tudek B, Saparbaev MK.** 2013, Proc Natl Acad Sci USA., Vol. 39, pp. E3695-3703. doi: 10.1073/pnas.1305624110.

43. *DNA polymerase beta expression differences in selected human tumors and cell lines.* **Srivastava DK, Husain I, Arteaga CL, Wilson SH.** 1999, Carcinogenesis., Vol. 20, pp. 1049-1054.

44. *Altered expression of the DNA repair protein, N-methylpurine-DNA glycosylase (MPG) in breast cancer.* **Cerda SR, Turk PW, Thor AD, Weitzman SA.** 1998, FEBS Lett., Vol. 431, pp. 12-18.

45. *Altered Expression of Ape1/ref-1 in Germ Cell Tumors and Overexpression in NT2 Cells Confers Resistance to Bleomycin and Radiation.* **Robertson KA, Bullock HA, Xu Y, Tritt R, Zimmerman E, Ulbright TM, Foster RS, Einhorn LH, Kelley MR.** 2001, Cancer Res., Vol. 61, pp. 2220-2225.

46. *Human AP endonuclease I (HAPI) protein expression in breast cancer correlates with lymph node status and angiogenesis.* **Kakolyris S, Kaklamanis L, Engels K, Fox SB, Taylor M, Hickson ID, Gatterl KC, Harris AL.** 1998, Br J Cancer., Vol. 77, pp. 1169-1173.

47. *APE1 overexpression in XRCC1-deficient cells complements the defective repair of oxidative single strand breaks but increases genomic instability.* **Sossou M, Flohr-Beckhaus C, Schulz I, Daboussi F,**

Epe B, Radicella JP. 2005, Nucleic Acids Res., Vol. 33, pp. 298-306.

48. *Overexpression of N-methylpurine-DNA glycosylase in Chinese hamster ovary cells renders them more sensitive to the production of chromosomal aberrations by methylating agents--a case of imbalanced DNA repair.* **Coquerelle T, Dosch J, Kaina B.** 1995, Mutat Res., Vol. 336, pp. 9-17.

49. *Overexpression of DNA polymerase beta in cell results in a mutator phenotype and a decreased sensitivity to anticancer drugs.* **Canitrot Y, Cazaux C, Fréchet M, Bouayadi K, Lesca C, Salles B, Hoffmann JS.** 1998, Proc Natl Acad Sci USA., Vol. 95, pp. 12586-12590.

50. *Deregulated DNA polymerase beta induces chromosome instability and tumorigenesis.* **Bergoglio V, Pillaire MJ, Lacroix-Triki M, Raynaud-Messina B, Canitrot Y, Bieth A, Garès M, Wright M, Delsol G, Loeb LA, Cazaux C, Hoffmann JS.** 2002, Cancer Res., Vol. 62, pp. 3511-3514.

51. *DNA damages processed by base excision repair: biological consequences.* **SS, Wallace.** 1994, Int J Radiat Biol., Vol. 66, pp. 579-589.

52. *Functions of disordered regions in mammalian early base excision repair proteins.* **Hegde ML, Hazra TK, Mitra S.** 2010, Cell Mol Life Sci., Vol. 67, pp. 3573-3587.

53. *Specific interaction of DNA polymerase beta and DNA ligase I in a multiprotein base excision repair complex from bovine testis.* **Prasad R, Singhal RK, Srivastava DK, Molina JT, Tomkinson AE, Wilson SH.** 1996, J Biol Chem., Vol. 271, pp. 16000-16007.

54. *Co-ordination of base excision repair and genome stability.* **Parsons JL, Dianov GL.** 2013, DNA Repair (Amst)., Vol. 12, pp. 326-333.

55. *The emerging role of Mule and ARF in the regulation of base excision repair.* **Khoronenkova SV, Dianov GL.** 2011, FEBS Lett., Vol. 585, pp. 2831-2835.

56. *USP47 Is a Deubiquitylating Enzyme that Regulates Base Excision Repair by Controlling Steady-State Levels of DNA Polymerase b.* **Parsons JL, Dianova II, Khoronenkova SV, Edelmann MJ, Kessler BM, Dianov GL.** 2011, Mol Cell., Vol. 41, pp. 609-615.

57. *CHIP-Mediated Degradation and DNA Damage-Dependent Stabilization Regulate Base Excision Repair Proteins.* **Parsons JL, Tait PS, Finch D, Dianova II, Allinson SL, Dianov GL.** 2008, Mol Cell., Vol. 29, pp. 477-487.

58. *Ubiquitin ligase ARF-BP1/Mule modulates base excision repair.* **Parsons JL, Tait PS, Finch D, Dianova II, Edelmann MJ, Khoronenkova SV, Kessler BM, Sharma RA, McKenna WG, Dianov GL.** 2009, EMBO J., Vol. 28, pp. 3207-3215.

59. *DNA damage disrupts the p14ARF-B23(nucleophosmin) interaction and triggers a transient subnuclear redistribution of p14ARF.* **Lee C, Smith BA, Bandyopadhyay K, Gjerset RA.** 2005, Cancer Res., Vol. 65, pp. 9834-9842.

60. *p14ARF is a component of the p53 response following ionizing irradiation of normal human fibroblasts.* **Khan S, Guevara C, Fujii G, Parry D.** 2004, Oncogene., Vol. 23, pp. 6040-6046.

61. *Regulation of p14ARF through subnuclear compartmentalization.* **Gjerset**

RA, Bandyopadhyay K. 2006, Cell Cycle., Vol. 5, pp. 686-690.

62. *Human p14(Arf): an exquisite sensor of morphological changes and of short-lived perturbations in cell cycle and in nucleolar function.* **David-Pfeuty T, Nouvian-Dooghe Y.** 2002, Oncogene., Vol. 21, pp. 6779-6790.

63. *DNA damage, p14ARF, nucleophosmin (NPM/B23), and cancer.* **RA, Gjerset.** 2006, J Mol Histol., Vol. 37, pp. 239-251.

64. *Estimating the effect of human base excision repair protein variants on the repair of oxidative DNA base damage.* **Sokhansanj BA, Wilson DM 3rd.** 2006, Cancer Epidemiol Biomarkers Prev., Vol. 15, pp. 1000-1008.

65. *Variation in base excision repair capacity.* **Wilson DM 3rd, Kim D, Berquist BR, Sigurdson AJ.** 2011, Mutat Res., Vol. 711, pp. 100-112.

66. *Impairment of APE1 function enhances cellular sensitivity to clinically relevant alkylators and antimetabolites.* **McNeill DR, Lam W, DeWeese TL, Cheng YC, Wilson DM 3rd.** 2009, Mol Cancer Res., Vol. 7, pp. 897-906.

67. *APE1 overexpression is associated with cisplatin resistance in non-small cell lung cancer and targeted inhibition of APE1 enhances the activity of cisplatin in A549 cells.* **Wang D, Xiang DB, Yang XQ, Chen LS, Li MX, Zhong ZY, Zhang YS.** 2009, Lung Cancer., Vol. 66, pp. 298-304.

68. *Functional characterization of Ape1 variants identified in the human population.* **Hadi MZ, Coleman MA, Fidelis K, Mohrenweiser HW, Wilson DM 3rd.** 2000, Nucleic Acids Res., Vol. 28, pp. 3871-3879.

69. *Common polymorphisms and somatic mutations in human base excision repair genes in ovarian and endometrial cancers.* **Pieretti M, Khattar NH, Smith SA.** 2001, Mutat Res., Vol. 432, pp. 53-59.

70. *Base Excision Repair: Contribution to Tumorigenesis and Target in Anticancer Treatment Paradigms.* **Illuzzi JL, Wilson III DM.** 2012, Curr Med Chem., Vol. 19, pp. 3922-3936.

71. *Directed proteomic analysis of the human nucleolus.* **Andersen JS, Lyon CE, Fox AH, Leung AK, Lam YW, Steen H, Mann M, Lamond AI.** 2002, Curr Biol., Vol. 12, pp. 1-11.

72. *The multifunctional nucleolus.* **Boisvert FM, van Koningsbruggen S, Navascués J, Lamond AI.** 2007, Nat Rev Mol Cell Biol., Vol. 8, pp. 574-585.

73. *Deciphering the human nucleolar proteome.* **Couté Y, Burgess JA, Diaz JJ, Chichester C, Lisacek F, Greco A, Sanchez JC.** 2006, Mass Spectrom Rev., Vol. 25, pp. 215-234.

74. *Functional proteomic analysis of human nucleolus.* **Scherl A, Couté Y, Déon C, Callé A, Kindbeiter K, Sanchez JC, Greco A, Hochstrasser D, Diaz JJ.** 2002, Mol Biol Cell., Vol. 13, pp. 4100-4109.

75. *APE1/Ref-1 Interacts with NPM1 within Nucleoli and Plays a Role in the rRNA Quality Control Process.* **Vascotto C, Fantini D, Romanello M, Cesaratto L, Deganuto M, Leonardi A, Radicella JP, Kelley MR, D'Ambrosio C, Scaloni A, Quadrifoglio F, Tell G.** 2009, Mol Cell Biol, Vol. 29, pp. 1834-1854.

76. *The human base excision repair enzyme SMUG1 directly interacts with DKC1 and contributes to RNA quality control.* **Jobert L, Skjeldam HK, Dalhus B, Galashevskaya A, Vågbø CB, Bjørås M, Nilsen H.** 2013, Mol Cell., Vol. 49, pp. 339-345.

77. *Nucleolar localization and dynamic roles of flap endonuclease 1 in ribosomal DNA replication and damage repair.* **Guo Z, Qian L, Liu R, Dai H, Zhou M, Zheng L, Shen B.** 2008, Mol Cell Biol., Vol. 28, pp. 4310-4319.

78. *Delocalization of nucleolar poly(ADP-ribose) polymerase-1 to the nucleoplasm and its novel link to cellular sensitivity to DNA damage.* **Rancourt A, Satoh MS.** 2009, DNA Repair (Amst)., Vol. 8, pp. 286-297.

79. *DNA ends alter the molecular composition and localization of Ku multicomponent complexes.* **Adelmant G, Calkins AS, Garg BK, Card JD, Askenazi M, Miron A, Sobhian B, Zhang Y, Nakatani Y, Silver PA, Iglehart JD, Marto JA, Lazaro JB.** 2012, Mol Cell Proteomics., Vol. 11, pp. 411-421.

80. *Cellular dynamics and modulation of WRN protein is DNA damage specific.* **Karmakar P, Bohr VA.** 2005, Mech Ageing Dev., Vol. 126, pp. 1146-1158.

81. *Mammalian DNA base excision repair proteins: their interactions and role in repair of oxidative DNA damage.* **Izumi T, Wiederhold LR, Roy G, Roy R, Jaiswal A, Bhakat KK, Mitra S, Hazra TK.** 2003, Toxicology., Vol. 193, pp. 43-65.

82. *The Intracellular Localization of APE1/Ref-1: More than a Passive Phenomenon?* **Tell G, Damante G, Caldwell D, Kelley MR.** 2005, Antioxid Redox Signal., Vol. 7, pp. 367-384.

83. *Cloning and expression of APE, the cDNA encoding the major human apurinic endonuclease: definition of a family of DNA repair enzymes.* **Demple B, Herman T, Chen DS.** 1991, Proc Natl Acad Sci USA., Vol. 88, pp. 11450-11454.

84. *Isolation of cDNA clones encoding a human apurinic/apyrimidinic endonuclease that corrects DNA repair and mutagenesis defects in E. coli xth (exonuclease III) mutants.* **Robson CN, Hickson ID.** 1991, Nucleic Acids Res., Vol. 19, pp. 5519-5523.

85. *Identification and characterization of Ref-1, a nuclear protein that facilitates AP-1 DNA-binding activity.* **Xanthoudakis S, Curran T.** 1992, EMBO J., Vol. 11, pp. 653-665.

86. *The redox/DNA repair protein, Ref-I, is essential for early embryonic development in mice.* **Xanthoudakis S, Smeyne RJ, Wallace JD, Curran T.** 1996, Proc Natl Acad Sci USA., Vol. 93, pp. 8919-8923.

87. *Heterozygosity for the mouse Apex gene results in phenotypes associated with oxidative stress.* **Meira LB, Devaraj S, Kisby GE, Burns DK, Daniel RL, Hammer RE, Grundy S, Jialal I, Friedberg EC.** 2001, Cancer Res., Vol. 61, pp. 5552-5557.

88. *Spontaneous mutagenesis is enhanced in Apex heterozygous mice.* **Huamani J, McMahan CA, Herbert DC, Reddick R, McCarrey JR, MacInnes MI, Chen DJ, Walter CA.** 2004, Mol Cell Biol., Vol. 24, pp. 8145-8153.

89. *The crystal structure of the human DNA repair endonuclease HAP1 suggests the recognition of extra-helical deoxyribose at DNA abasic sites.* **Gorman MA, Morera S, Rothwell DG, de La Fortelle E, Mol CD, Tainer JA, Hickson ID, Freemont PS.** 1997, EMBO J., Vol. 16, pp. 6548-6558.

90. *Role of the unstructured N-terminal domain of the hAPE1 (human apurinic/apyrimidinic endonuclease 1) in the modulation of its interaction with nucleic acids and NPM1 (nucleophosmin).* **Poletto M, Vascotto C, Scognamiglio PL, Lirussi L,**

Marasco D, Tell G. 2013, Biochem J., Vol. 452, pp. 545-557.

91. *Critical lysine residues within the overlooked N-terminal domain of human APE1 regulate its biological functions.* **Fantini D, Vascotto C, Marasco D, D'Ambrosio C, Romanello M, Vitagliano L, Pedone C, Poletto M, Cesaratto L, Quadrifoglio F, Scaloni A, Radicella JP, Tell G.** 2010, Nucleic Acids Res, Vol. 38, pp. 8239-8256.

92. *Two divalent metal ions in the active site of a new crystal form of human apurinic/apyrimidinic endonuclease, Ape1: implications for the catalytic mechanism.* **Beernink PT, Segelke BW, Hadi MZ, Erzberger JP, Wilson DM 3rd, Rupp B.** 2001, J Mol Biol., Vol. 307, pp. 1023-1034.

93. *The redox and DNA-repair activities of Ref-1 are encoded by nonoverlapping domains.* **Xanthoudakis S, Miao GG, Curran T.** 1994, Proc Natl Acad Sci USA., Vol. 91, pp. 23-27.

94. *Deletion analysis of human AP-endonuclease: minimum sequence required for the endonuclease activity.* **Izumi T, Mitra S.** 1998, Carcinogenesis., Vol. 19, pp. 525-527.

95. *Understanding different functions of mammalian AP endonuclease (APE1) as a promising tool for cancer treatment.* **Tell G, Fantini D, Quadrifoglio F.** 2010, Cell Mol Life Sci., Vol. 67, pp. 3589-3608.

96. *The many functions of APE1/Ref-1: not only a DNA repair enzyme.* **Tell G, Quadrifoglio F, Tiribelli C, Kelley MR.** 2009, Antioxid Redox Signal., Vol. 11, pp. 601-620.

97. *Site-directed mutagenesis of the human DNA repair enzyme HAP1: identification of residues important for AP endonuclease and RNase H activity.* **Barzilay G, Walker LJ, Robson CN, Hickson ID.** 1995, Nucleic Acids Res., Vol. 23, pp. 1544-1550.

98. *DNA-bound structures and mutants reveal abasic DNA binding by APE1 and DNA repair coordination.* **Mol CD, Izumi T, Mitra S, Tainer JA.** 2000, Nature., Vol. 403, pp. 451-456.

99. *A novel action of human apurinic/apyrimidinic endonuclease: excision of L-configuration deoxyribonucleoside analogs from the 3′ termini of DNA.* **Chou KM, Kukhanova M, Cheng YC.** 2000, J Biol Chem., Vol. 275, pp. 31009-31015.

100. *APE1 is the major 3′-phosphoglycolate activity in human cell extracts.* **Parsons JL, Dianova II, Dianov GL.** 2004, Nucleic Acids Res., Vol. 32, pp. 3531-3536.

101. *Distinct roles of Ape1 protein in the repair of DNA damage induced by ionizing radiation or bleomycin.* **Fung H, Demple B.** 2011, J Biol Chem., Vol. 286, pp. 4968-4977.

102. *Bleomycins: towards better therapeutics.* **Chen J, Stubbe J.** 2005, Nat Rev Cancer., Vol. 5, pp. 102-112.

103. *Insight into mechanisms of 3′-5′ exonuclease activity and removal of bulky 8,5′-cyclopurine adducts by apurinic/apyrimidinic endonucleases.* **Mazouzi A, Vigouroux A, Aikeshev B, Brooks PJ, Saparbaev MK, Morera S, Ishchenko AA.** 2013, Proc Natl Acad Sci USA., Vol. 110, pp. E3071-80. doi: 10.1073/pnas.1305281110.

104. *Genetic and biochemical characterization of human AP endonuclease 1 mutants deficient in nucleotide incision repair activity.* **Gelin A, Redrejo-Rodríguez M, Laval J, Fedorova OS, Saparbaev M, Ishchenko AA.** 2010, PLoS One., Vol. 5, p. e12241. doi: 10.1371/journal.pone.0012241.

105. *Human AP endonuclease 1 (APE1): from mechanistic insights to druggable target in cancer.* **Abbotts R, Madhusudan S.** 2010, Cancer Treat Rev., Vol. 36, pp. 425-435.

106. *Intrusion of a DNA repair protein in the RNome world: is this the beginning of a new era?* **Tell G, Wilson III DM, Lee CH.** 2010, Mol Cell Biol., Vol. 30, pp. 366-371.

107. *Characterization of the endoribonuclease active site of human apurinic/apyrimidinic endonuclease 1.* **Kim WC, Berquist BR, Chohan M, Uy C, Wilson III DM, Lee CH.** 2011, J Mol Biol., Vol. 411, pp. 960-971.

108. *Identification of Apurinic/apyrimidinic endonuclease 1 (APE1) as the endoribonuclease that cleaves c-myc mRNA.* **Barnes T, Kim WC, Mantha AK, Kim SE, Izumi T, Mitra S, Lee CH.** 2009, Nucleic Acids Res., Vol. 37, pp. 3946-3958.

109. *RNA-cleaving properties of human apurinic/apyrimidinic endonuclease 1 (APE1).* **Kim WC, King D, Lee CH.** 2010, Int J Biochem Mol Biol., Vol. 1, pp. 12-25.

110. *APE1/Ref-1 role in redox signaling: translational applications of targeting the redox function of the DNA repair/redox protein APE1/Ref-1.* **Kelley MR, Georgiadis MM, Fishel ML.** 2012, Curr Mol Pharmacol., Vol. 5, pp. 36-53.

111. *Evolution of the redox function in mammalian apurinic/apyrimidinic endonuclease.* **Georgiadis MM, Luo M, Gaur RK, Delaplane S, Li X, Kelley MR.** 2008, Mutat Res., Vol. 643, pp. 54-63.

112. *Inhibition of apurinic/apyrimidinic endonuclease I's redox activity revisited.* **Zhang J, Luo M, Marasco D, Logsdon D, LaFavers KA, Chen Q, Reed A, Kelley MR, Gross ML, Georgiadis MM.** 2013, Biochemistry., Vol. 52, pp. 2955-2966.

113. *Interactions of apurinic/apyrimidinic endonuclease with a redox inhibitor: evidence for an alternate conformation of the enzyme.* **Su D, Delaplane S, Luo M, Rempel DL, Vu B, Kelley MR, Gross ML, Georgiadis MM.** 2011, Biochemistry., Vol. 50, pp. 82-92.

114. *Identification of redox/repair protein Ref-1 as a potent activator of p53.* **Jayaraman L, Murthy KG, Zhu C, Curran T, Xanthoudakis S, Prives C.** 1997, Genes Dev., Vol. 11, pp. 558-570.

115. *Redox factor 1 (Ref-1) enhances specific DNA binding of p53 by promoting p53 tetramerization.* **Hanson S, Kim E, Deppert W.** 2005, Oncogene., Vol. 24, pp. 1641-1647.

116. *A redox factor protein, ref1, is involved in negative gene regulation by extracellular calcium.* **Okazaki T, Chung U, Nishishita T, Ebisu S, Usuda S, Mishiro S, Xanthoudakis S, Igarashi T, Ogata E.** 1994, J Biol Chem., Vol. 269, pp. 27855-27862.

117. *Implication of Ref-1 in the repression of renin gene transcription by intracellular calcium.* **Fuchs S, Philippe J, Corvol P, Pinet F.** 2003, J Hypertens., Vol. 21, pp. 327-335.

118. *Human AP-endonuclease 1 and hnRNP-L interact with a nCaRE-like repressor element in the AP-endonuclease 1 promoter.* **Kuninger DT, Izumi T, Papaconstantinou J, Mitra S.** 2002, Nucleic Acids Res., Vol. 30, pp. 823-829.

119. *SIRT1 gene expression upon genotoxic damage is regulated by APE1 through nCaRE promoter elements.* **Antoniali G, Lirussi L, D'Ambrosio C, Dal Piaz F, Vascotto C, Casarano E, Marasco D, Scaloni A, Fogolari F, Tell G.** 2013, Mol Biol Cell. [Epub ahead of print].

120. *Negative regulation of the major human AP-endonuclease, a multifunctional*

protein. **Izumi T, Henner WD, Mitra S.** 1996, Biochemistry., Vol. 35, pp. 14679-14683.

121. *XRCC1 coordinates the initial and late stages of DNA abasic site repair through protein-protein interactions.* **Vidal AE, Boiteux S, Hickson ID, Radicella JP.** 2001, EMBO J., Vol. 20, pp. 6530-6539.

122. *Probing conformational changes in Ape1 during the progression of Base Excision Repair.* **Yu E, Gaucher SP, Hadi MZ.** 2010, Biochemistry., Vol. 49, pp. 3786-3796.

123. *Human apurinic/apyrimidinic endonuclease is processive.* **Carey DC, Strauss PR.** 1999, Biochemistry., Vol. 38, pp. 16553-16560.

124. *Nucleolar accumulation of APE1 depends on charged lysine residues that undergo acetylation upon genotoxic stress and modulate its BER activity in cells.* **Lirussi L, Antoniali G, Vascotto C, D'Ambrosio C, Poletto M, Romanello M, Marasco D, Leone M, Quadrifoglio F, Bhakat KK, Scaloni A, Tell G.** 2012, Mol Biol Cell., Vol. 23, pp. 4079-4096.

125. *Analysis of nuclear transport signals in the human apurinic/apyrimidinic endonuclease (APE1/Ref1).* **Jackson EB, Theriot CA, Chattopadhyay R, Mitra S, Izumi T.** 2005, Nucleic Acids Res., Vol. 33, pp. 3303-3312.

126. *Human apurinic/apyrimidinic endonuclease 1.* **Li M, Wilson DM 3rd.** 2014, Antioxid Redox Signal., Vol. 20, pp. 678-707.

127. *Posttranslational modification of mammalian AP endonuclease (APE1).* **Busso CS, Lake MW, Izumi T.** 2010, Cell Mol Life Sci., Vol. 67, pp. 3609-3620.

128. *Ubiquitination of mammalian AP endonuclease (APE1) regulated by the p53-MDM2 signaling pathway.* **Busso CS, Iwakuma T, Izumi T.** 2009, Oncogene., Vol. 28, pp. 1616-1625.

129. *Ubiquitin ligase UBR3 regulates cellular levels of the essential DNA repair protein APE1 and is required for genome stability.* **Meisenberg C, Tait PS, Dianova II, Wright K, Edelmann MJ, Ternette N, Tasaki T, Kessler BM, Parsons JL, Tae Kwon Y, Dianov GL.** 2011, Nucleic Acids Res., Vol. 40, pp. 701-711.

130. *Cleaving the oxidative repair protein Ape1 enhances cell death mediated by granzyme A.* **Fan Z, Beresford PJ, Zhang D, Xu Z, Novina CD, Yoshida A, Pommier Y, Lieberman J.** 2003, Nat Immunol., Vol. 4, pp. 145-153.

131. *Human apurinic/apyrimidinic endonuclease (Ape1) and its N-terminal truncated form (AN34) are involved in DNA fragmentation during apoptosis.* **Yoshida A, Urasaki Y, Waltham M, Bergman AC, Pourquier P, Rothwell DG, Inuzuka M, Weinstein JN, Ueda T, Appella E, Hickson ID, Pommier Y.** 2003, J Biol Chem., Vol. 278, pp. 37768–37776.

132. *Granzyme K degrades the redox/DNA repair enzyme Ape1 to trigger oxidative stress of target cells leading to cytotoxicity.* **Guo Y, Chen J, Zhao T, Fan Z.** 2008, Mol Immunol., Vol. 45, pp. 2225-2235.

133. *Role of acetylated human AP-endonuclease (APE1/Ref-1) in regulation of the parathyroid hormone gene.* **Bhakat KK, Izumi T, Yang SH, Hazra TK, Mitra S.** 2003, EMBO J., Vol. 22, pp. 6299-6309.

134. *Acetylation on critical lysine residues of Apurinic/apyrimidinic endonuclease 1 (APE1) in triple negative breast cancers.* **Poletto M, Di Loreto C, Marasco D, Poletto E, Puglisi F, Damante G, Tell G.** 2012, Biochem Biophys Res Commun., Vol. 424, pp. 34-39.

135. *The multifunctional DNA repair/redox enzyme Ape1/Ref-1 promotes survival of neurons after oxidative stress.* **Vasko MR, Guo C, Kelley MR.** 2005, DNA Repair (Amst)., Vol. 4, pp. 367-379.

136. *Subcellular Localization of APE1/Ref-1 in Human Hepatocellular Carcinoma: Possible Prognostic Significance.* **Di Maso V, Avellini C, Crocè LS, Rosso N, Quadrifoglio F, Cesaratto L, Codarin E, Bedogni G, Beltrami CA, Tell G, Tiribelli C.** 2007, Mol. Med., Vols. 13, pp. 89-96.

137. *Two essential but distinct functions of the mammalian abasic endonuclease.* **Izumi T, Brown DB, Naidu CV, Bhakat KK, Macinnes MA, Saito H, Chen DJ, Mitra S.** 2005, Proc Natl Acad Sci USA., Vol. 102, pp. 5739-5743.

138. *Genome-wide analysis and proteomic studies reveal APE1/Ref-1 multifunctional role in mammalian cells.* **Vascotto C, Cesaratto L, Zeef LA, Deganuto M, D'Ambrosio C, Scaloni A, Romanello M, Damante G, Taglialatela G, Delneri D, Kelley MR, Mitra S, Quadrifoglio F, Tell G.** 2009, Proteomics., Vol. 9, pp. 1058-1074.

139. *A role for the human DNA repair enzyme HAP1 in cellular protection against DNA damaging agents and hypoxic stress.* **Walker LJ, Craig RB, Harris AL, Hickson ID.** 1994, Nucleic Acids Res., Vol. 22, pp. 4884-4889.

140. *Small molecule inhibitors of DNA repair nuclease activities of APE1.* **Wilson DM 3rd, Simeonov A.** 2010, Cell Mol Life Sci., Vol. 67, pp. 3621-3631.

141. *The Ape-1/Ref-1 redox antagonist E3330 inhibits the growth of tumor endothelium and endothelial progenitor cells: therapeutic implications in tumor angiogenesis.* **Zou GM, Karikari C, Kabe Y, Handa H, Anders RA, Maitra A.** 2009, J Cell Physiol., Vol. 219, pp. 209-218.

142. *High-performance affinity beads for identifying drug receptors.* **Shimizu N, Sugimoto K, Tang J, Nishi T, Sato I, Hiramoto M, Aizawa S, Hatakeyama M, Ohba R, Hatori H, Yoshikawa T, Suzuki F, Oomori A, Tanaka H, Kawaguchi H, Watanabe H, Handa H.** 2000, Nat Biotechnol., Vol. 18, pp. 877-881.

143. *Design and synthesis of novel quinone inhibitors targeted to the redox function of apurinic/apyrimidinic endonuclease 1/redox enhancing factor-1 (Ape1/ref-1).* **Nyland RL, Luo M, Kelley MR, Borch RF.** 2010, J Med Chem., Vol. 53, pp. 1200-1210.

144. *Functional analysis of novel analogues of E3330 that block the redox signaling activity of the multifunctional AP endonuclease/redox signaling enzyme APE1/Ref-1.* **Kelley MR, Luo M, Reed A, Su D, Delaplane S, Borch RF, Nyland RL 2nd, Gross ML, Georgiadis MM.** 2011, Antioxid Redox Signal., Vol. 14, pp. 1387-1401.

145. *Redox regulation of DNA repair: implications for human health and cancer therapeutic development.* **Luo M, He H, Kelley MR, Georgiadis MM.** 2010, Antioxid Redox Signal., Vol. 12, pp. 1247-1269.

146. *NMR studies reveal an unexpected binding site for a redox inhibitor of AP endonuclease 1.* **Manvilla BA, Wauchope O, Seley-Radtke KL, Drohat AC.** 2011, Biochemistry., Vol. 50, pp. 10540-10549.

147. *Diverse small molecule inhibitors of human apurinic/apyrimidinic endonuclease APE1 identified from a screen of a large public collection.* **Dorjsuren D, Kim D, Vyjayanti VN, Maloney DJ, Jadhav A, Wilson DM 3rd, Simeonov A.** 2012, PLoS One., Vol. 7, p. e47974. doi: 10.1371/journal.pone.0047974.

148. *Synthesis, biological evaluation, and structure-activity relationships of a novel class of apurinic/apyrimidinic endonuclease 1 inhibitors.* **Rai G, Vyjayanti VN, Dorjsuren D, Simeonov A, Jadhav A, Wilson DM 3rd, Maloney DJ.** 2012, J Med Chem., Vol. 55, pp. 3101-3112.

149. *Novel small-molecule inhibitor of apurinic/apyrimidinic endonuclease 1 blocks proliferation and reduces viability of glioblastoma cells.* **Bapat A, Glass LS, Luo M, Fishel ML, Long EC, Georgiadis MM, Kelley MR.** 2010, J Pharmacol Exp Ther., Vol. 334, pp. 988-998.

150. *Pharmacophore guided discovery of small-molecule human apurinic/apyrimidinic endonuclease 1 inhibitors.* **Zawahir Z, Dayam R, Deng J, Pereira C, Neamati N.** 2009, J Med Chem., Vol. 52, pp. 20-32.

151. *Therapeutic impact of methoxyamine: blocking repair of abasic sites in the base excision repair pathway.* **Liu L, Gerson SL.** 2004, Curr Opin Investig Drugs., Vol. 5, pp. 623-627.

152. *Processing in vitro of an abasic site reacted with methoxyamine: a new assay for the detection of abasic sites formed in vivo.* **Rosa S, Fortini P, Karran P, Bignami M, Dogliotti E.** 1991, Nucleic Acids Res., Vol. 19, pp. 5569-5574.

153. *"Numatrin," a nuclear matrix protein associated with induction of proliferation in B lymphocytes.* **Feuerstein N, Mond JJ.** 1987, J Biol Chem., Vol. 262, pp. 11389-11397.

154. *Intrinsically disordered regions of nucleophosmin/B23 regulate its RNA binding activity through their inter- and intra-molecular association.* **Hisaoka M, Nagata K, Okuwaki M.** 2014, Nucleic Acids Res., Vol. 42, pp. 1180-1195.

155. *Nucleophosmin and cancer.* **Grisendi S, Mecucci C, Falini B, Pandolfi PP.** 2006, Nat Rev Cancer., Vol. 7, pp. 493-505.

156. *The crystal structure of nucleoplasmin-core: implications for histone binding and nucleosome assembly.* **Dutta S, Akey IV, Dingwall C, Hartman KL, Laue T, Nolte RT, Head JF, Akey CW.** 2001, Mol Cell., Vol. 8, pp. 841-853.

157. *Crystal structure of human nucleophosmin-core reveals plasticity of the pentamer-pentamer interface.* **Lee HH, Kim HS, Kang JY, Lee BI, Ha JY, Yoon HJ, Lim SO, Jung G, Suh SW.** 2007, Proteins., Vol. 69, pp. 672-678.

158. *The structure and function of Xenopus NO38-core, a histone chaperone in the nucleolus.* **Namboodiri VM, Akey IV, Schmidt-Zachmann MS, Head JF, Akey CW.** 2004, Structure., Vol. 12, pp. 2149-2160.

159. *Essential role of the B23/NPM core domain in regulating ARF binding and B23 stability.* **Enomoto T, Lindström MS, Jin A, Ke H, Zhang Y.** 2006, J Biol Chem., Vol. 281, pp. 18463-18472.

160. *Nucleophosmin regulates the stability and transcriptional activity of p53.* **Colombo E, Marine JC, Danovi D, Falini B, Pelicci PG.** 2002, Nat Cell Biol., Vol. 4, pp. 529-533.

161. *Nucleolar protein NPM interacts with HDM2 and protects tumor suppressor protein p53 from HDM2-mediated degradation.* **Kurki S, Peltonen K, Latonen L, Kiviharju TM, Ojala PM, Meek D, Laiho M.** 2004, Cancer Cell., Vol. 5, pp. 465-475.

162. *Nucleophosmin (B23) targets ARF to nucleoli and inhibits its function.* **Korgaonkar C, Hagen J, Tompkins V, Frazier AA, Allamargot C, Quelle FW, Quelle DE.** 2005, Mol Cell Biol., Vol. 25, pp. 1258-1271.

163. *Acute myeloid leukemia carrying cytoplasmic/mutated nucleophosmin (NPMc + AML): biologic and clinical features.* **Falini B, Nicoletti I, Martelli MF, Mecucci C.** 2007, Blood., Vol. 109, pp. 874-885.

164. *Functional interplay between the DNA-damage-response kinase ATM and ARF tumour suppressor protein in human cancer.* **Velimezi G, Liontos M, Vougas K, Roumeliotis T, Bartkova J, Sideridou M, Dereli-Oz A, Kocylowski M, Pateras IS, Evangelou K, Kotsinas A, Orsolic I, Bursac S, Cokaric-Brdovcak M, Zoumpourlis V, Kletsas D, Papafotiou G, Klinakis A, Volarevic S, Gu W, Bartek J, Halazonetis TD, Gorgoulis VG.** 2013, Nat Cell Biol., Vol. 15, pp. 967-977.

165. *Structural consequences of nucleophosmin mutations in acute myeloid leukemia.* **Grummitt CG, Townsley FM, Johnson CM, Warren AJ, Bycroft M.** 2008, J Biol Chem., Vol. 283, pp. 23326-23332.

166. *Folding mechanism of the C-terminal domain of nucleophosmin: residual structure in the denatured state and its pathophysiological significance.* **Scaloni F, Gianni S, Federici L, Falini B, Brunori M.** 2009, FASEB J., Vol. 23, pp. 2360-2365.

167. *Nucleophosmin mutations alter its nucleolar localization by impairing G-quadruplex binding at ribosomal DNA.* **Chiarella S, De Cola A, Scaglione GL, Carletti E, Graziano V, Barcaroli D, Lo Sterzo C, Di Matteo A, Di Ilio C, Falini B, Arcovito A, De Laurenzi V, Federici L.** 2013, Nucleic Acids Res., Vol. 5, pp. 3228-3239.

168. *Major nucleolar proteins shuttle between nucleus and cytoplasm.* **Borer RA, Lehner CF, Eppenberger HM, Nigg EA.** 1989, Cell., Vol. 56, pp. 379-390.

169. *Preferential cleavage in pre-ribosomal RNA byprotein B23 endoribonuclease.* **Savkur RS, Olson MO.** 1998, Nucleic Acids Res., Vol. 26, pp. 4508-4515.

170. *NPM1/B23: A Multifunctional Chaperone in Ribosome Biogenesis and Chromatin Remodeling.* **Lindström MS.** 2011, Biochem Res Int., p. 2011:195209. doi: 10.1155/2011/195209.

171. *Nucleophosmin and its complex network: a possible therapeutic target in hematological diseases.* **Colombo E, Alcalay M, Pelicci PG.** 2011, Oncogene, Vol. 30, pp. 2595-2609.

172. *Role of mutual interactions in the chemical and thermal stability of nucleophosmin NPM1 domains.* **Marasco D, Ruggiero A, Vascotto C, Poletto M, Scognamiglio PL, Tell G, Vitagliano L.** 2013, Biochem Biophys Res Commun., Vol. 430, pp. 523-528.

173. *Structure of nucleophosmin DNA-binding domain and analysis of its complex with a G-quadruplex sequence from the c-MYC promoter.* **Gallo A, Lo Sterzo C, Mori M, Di Matteo A, Bertini I, Banci L, Brunori M, Federici L.** 2012, J Biol Chem., Vol. 287, pp. 26539-26548.

174. *G-quadruplex DNA recognition by nucleophosmin: new insights from protein dissection.* **Scognamiglio PL, Di Natale C, Leone M, Poletto M, Vitagliano L, Tell G, Marasco D.** *Submitted*.

175. *Nucleolar protein B23 has molecular chaperone activities.* **Szebeni A, Olson MO.** 1999, Protein Sci., Vol. 8, pp. 905-912.

176. *The multifunctional protein nucleophosmin (NPM1) is a human linker histone H1 chaperone.* **Gadad SS, Senapati P, Syed SH, Rajan RE, Shandilya J,**

Swaminathan V, Chatterjee S, Colombo E, Dimitrov S, Pelicci PG, Ranga U, Kundu TK. 2011, Biochemistry., Vol. 50, pp. 2780-2789.

177. *Transcription regulation of the rRNA gene by a multifunctional nucleolar protein, B23/nucleophosmin, through its histone chaperone activity.* **Murano K, Okuwaki M, Hisaoka M, Nagata K.** 2008, Mol Cell Biol., Vol. 28, pp. 3114-3126.

178. *Human histone chaperone nucleophosmin enhances acetylation-dependent chromatin transcription.* **Swaminathan V, Kishore AH, Febitha KK, Kundu TK.** 2005, Mol Cell Biol., Vol. 25, pp. 7534-7545.

179. *Acetylated NPM1 localizes in the nucleoplasm and regulates transcriptional activation of genes implicated in oral cancer manifestation.* **Shandilya J, Swaminathan V, Gadad SS, Choudhari R, Kodaganur GS, Kundu TK.** 2009, Mol Cell Biol., Vol. 29, pp. 5115-5127.

180. *Regulation of nucleolar chromatin by B23/nucleophosmin jointly depends upon its RNA binding activity and transcription factor UBF.* **Hisaoka M, Ueshima S, Murano K, Nagata K, Okuwaki M.** 2010, Mol Cell Biol., Vol. 30, pp. 4952-4964.

181. *Mutant nucleophosmin and cooperating pathways drive leukemia initiation and progression in mice.* **Vassiliou GS, Cooper JL, Rad R, Li J, Rice S, Uren A, Rad L, Ellis P, Andrews R, Banerjee R, Grove C, Wang W, Liu P, Wright P, Arends M, Allan Bradley.** 2011, Nat Genet., Vol. 43, pp. 470-475.

182. *Myeloid leukemia-associated nucleophosmin mutants perturb p53-dependent and independent activities of the Arf tumor suppressor protein.* **den Besten W, Kuo ML, Williams RT, Sherr CJ.** 2005, Cell Cycle., Vol. 4, pp. 1593-1598.

183. *Nucleophosmin and its AML-associated mutant regulate c-Myc turnover through Fbw7 gamma.* **Bonetti P, Davoli T, Sironi C, Amati B, Pelicci PG, Colombo E.** 2008, J Cell Biol., Vol. 182, pp. 19-26.

184. *Delocalization and destabilization of the Arf tumor suppressor by the leukemia-associated NPM mutant.* **Colombo E, Martinelli P, Zamponi R, Shing DC, Bonetti P, Luzi L, Volorio S, Bernard L, Pruneri G, Alcalay M, Pelicci PG.** 2006, Cancer Res., Vol. 66, pp. 3044-3050.

185. *A ribosomal protein L23-nucleophosmin circuit coordinates Mizl function with cell growth.* **Wanzel M, Russ AC, Kleine-Kohlbrecher D, Colombo E, Pelicci PG, Eilers M.** 2008, Nat Cell Biol., Vol. 10, pp. 1051-1061.

186. *Functional regulation of the Apurinic/apyrimidinic endonuclease APE1 by Nucleophosmin (NPM1): Impact on tumor biology.* **Vascotto C, Lirussi L, Poletto M, Tiribelli M, Damiani D, Fabbro D, Damante G, Demple B, Colombo E, Tell G.** 2013, Oncogene., doi: 10.1038/onc.2013.251. [Epub ahead of print]

187. *Increased expression of nucleophosmin/B23 in hepatocellular carcinoma and correlation with clinicopathological parameters.* **Yun JP, Miao J, Chen GG, Tian QH, Zhang CQ, Xiang J, Fu J, Lai PBS.** 2007, Br J Cancer., Vol. 96, pp. 477-484.

188. *Expression and prognostic significance of APE1/Ref1 and NPM1 proteins in high-grade ovarian serous cancer.* **Londero AP, Tell G, Marzinotto S, Orsaria M, Capodicasa V, Poletto M, Vascotto C, Mariuzzi L.** 2013, Am J Clin Pathol., *in press*.

189. *Nucleophosmin suppresses oncogene-induced apoptosis and senescence and enhances oncogenic cooperation in cells with genomic instability.* **Li J, Sejas DP, Burma S, Chen DJ, Pang Q.** 2007, Carcinogenesis., Vol. 28, pp. 1163-1170.

190. *Nucleophosmin interacts directly with c-Myc and controls c-Myc-induced hyperproliferation and transformation.* **Li Z, Boone D, Hann SR.** 2008, Proc Natl Acad Sci USA., Vol. 105, pp. 18794-18799.

191. *Nucleophosmin/B23 is a target of CDK2/cyclin E in centrosome duplication.* **Okuda M, Horn HF, Tarapore P, Tokuyama Y, Smulian AG, Chan PK, Knudsen ES, Hofmann IA, Snyder JD, Bove KE, Fukasawa K.** 2000, Cell., Vol. 103, pp. 127-140.

192. *Specific phosphorylation of nucleophosmin on Thr(199) by cyclin-dependent kinase 2-cyclin E and its role in centrosome duplication.* **Tokuyama Y, Horn HF, Kawamura K, Tarapore P, Fukasawa K.** 2001, J Biol Chem., Vol. 276, pp. 21529-21537.

193. *Role of nucleophosmin in embryonic development and tumorigenesis.* **Grisendi S, Bernardi R, Rossi M, Cheng K, Khandker L, Manova K, Pandolfi PP.** 2005, Nature., Vol. 437, pp. 147-153.

194. *Nucleophosmin is required for DNA integrity and p19Arf protein stability.* **Colombo E, Bonetti P, Lazzerini Denchi E, Martinelli P, Zamponi R, Marine JC, Helin K, Falini B, Pelicci PG.** 2005, Mol Cell Biol., Vol. 25, pp. 8874-8886.

195. *Involvement of nucleophosmin/B23 in the response of HeLa cells to UV irradiation.* **Wu MH, Chang JH, Chou CC, Yung BY.** 2002, Int J Cancer., Vol. 97, pp. 297-305.

196. *A proteomic approach to identify early molecular targets of oxidative stress in human epithelial lens cells.* **Paron I, D'Elia A, D'Ambrosio C, Scaloni A, D'Aurizio F, Prescott A, Damante G, Tell G.** 2004, Biochem J., Vol. 378, pp. 929-937.

197. *Chemotherapeutic drugs inhibit ribosome biogenesis at various levels.* **Burger K, Mühl B, Harasim T, Rohrmoser M, Malamoussi A, Orban M, Kellner M, Gruber-Eber A, Kremmer E, Hölzel M, Eick D.** 2010, J Biol Chem., Vol. 16, pp. 12416-12425.

198. *A novel interaction of nucleophosmin with BCL2-associated X protein regulating death evasion and drug sensitivity in human hepatoma cells.* **Lo SJ, Fan LC, Tsai YF, Lin KY, Huang HL, Wang TH, Liu H, Chen TC, Huang SF, Chang CJ, Lin YJ, Yung BY, Hsieh SY.** 2013, Hepatology., Vol. 57, pp. 1893-1905.

199. *Recruitment of phosphorylated NPM1 to sites of DNA damage through RNF8-dependent ubiquitin conjugates.* **Koike A, Nishikawa H, Wu W, Okada Y, Venkitaraman AR, Ohta T.** 2010, Cancer Res., Vol. 70, pp. 6746-6756.

200. *The novel chemical entity YTR107 inhibits recruitment of nucleophosmin to sites of DNA damage, suppressing repair of DNA double-strand breaks and enhancing radiosensitization.* **Sekhar KR, Reddy YT, Reddy PN, Crooks PA, Venkateswaran A, McDonald WH, Geng L, Sasi S, Van Der Waal RP, Roti JL, Salleng KJ, Rachakonda G, Freeman ML.** 2011, Clin Cancer Res., Vol. 17, pp. 6490-6499.

201. *Use of proximity ligation to screen for inhibitors of interactions between vascular endothelial growth factor A and its receptors.* **Gustafsdottir SM, Wennström S, Fredriksson S, Schallmeiner E, Hamilton**

AD, Sebti SM, Landegren U. 2008, Clin Chem., Vol. 54, pp. 1218-1225.

202. *High content screening for inhibitors of protein interactions and post-translational modifications in primary cells by proximity ligation.* **Leuchowius KJ, Jarvius M, Wickström M, Rickardson L, Landegren U, Larsson R, Söderberg O, Fryknäs M, Jarvius J.** 2010, Mol Cell Proteomics., Vol. 9, pp. 178-183.

203. *Myoseverin, a microtubule-binding molecule with novel cellular effects.* **Rosania GR, Chang YT, Perez O, Sutherlin D, Dong H, Lockhart DJ, Schultz PG.** 2000, Nat Biotechnol., Vol. 18, pp. 304-308.

204. *Correction: Specific Inhibition of the Redox Activity of Ape1/Ref-1 by E3330 Blocks Tnf-A-Induced Activation of Il-8 Production in Liver Cancer Cell Lines.* **Cesaratto L, Codarin E, Vascotto C, Leonardi A, Kelley MR, Tiribelli C, Tell G.** 2013, PLoS One., Vol. 8, pp. doi: 10.1371/annotation/a610ee5c-525c-4d3c-b6b7-a4cde7b8db54.

205. *BER, MGMT, and MMR in defense against alkylation-induced genotoxicity and apoptosis.* **Kaina B, Ochs K, Grösch S, Fritz G, Lips J, Tomicic M, Dunkern T, Christmann M.** 2001, Prog Nucleic Acid Res Mol Biol., Vol. 68, pp. 41-54.

206. *Treatment with the PARP-inhibitor PJ34 causes enhanced doxorubicin-mediated cell death in HeLa cells.* **Magan N, Isaacs RJ, Stowell KM.** 2012, Anticancer Drugs., Vol. 23, pp. 627-637.

207. *Theoretical basis, experimental design, and computerized simulation of synergism and antagonism in drug combination studies.* **TC, Chou.** 2006, Pharmacol Rev., Vol. 58, pp. 621-681.

208. *Nucleolar targeting: the hub of the matter.* **Emmott E, Hiscox JA.** 2009, EMBO Rep., Vol. 10, pp. 231-238.

209. *Physical and functional interactions of the Arf tumor suppressor protein with nucleophosmin/B23.* **Bertwistle D, Sugimoto M, Sherr CJ.** 2004, Mol Cell Biol., Vol. 24, pp. 985-996.

210. *Tumor suppressor ARF degrades B23, a nucleolar protein involved in ribosome biogenesis and cell proliferation.* **Itahana K, Bhat KP, Jin A, Itahana Y, Hawke D, Kobayashi R, Zhang Y.** 2003, Mol Cell., Vol. 12, pp. 1151-1164.

211. *Cyclosporin A and verapamil enhancement of daunorubicin-produced nucleolar protein B23 translocation in daunorubicin-resistant and -sensitive human and murine tumor cells.* **Sweet P, Chan PK, Slater LM.** 1989, Cancer Res., Vol. 49, pp. 677-680.

212. *Nucleolar protein B23 translocation after doxorubicin treatment in murine tumor cells.* **Chan PK, Aldrich MB, Yung BY.** 1987, Cancer Res., Vol. 47, pp. 3798-3801.

213. *Combining RNAi and in vivo confocal microscopy analysis of the photoconvertible fluorescent protein Dendra2 to study a DNA repair protein.* **Tell G, Di Piazza M, Kamocka MM, Vascotto C.** 2013, Biotechniques., Vol. 55, pp. 198-203.

214. *The ATM repair pathway inhibits RNA polymerase I transcription in response to chromosome breaks.* **Kruhlak M, Crouch EE, Orlov M, Montaño C, Gorski SA, Nussenzweig A, Misteli T, Phair RD, Casellas R.** 2007, Nature., Vol. 447, pp. 730-734.

215. *In vivo run-on assays to monitor nascent precursor RNA transcripts.* **Percipalle**

P, Louvet E. 2012, Methods Mol Biol., Vol. 809, pp. 519-533.

216. *ARF-BP1/Mule is a critical mediator of the ARF tumor suppressor.* **Chen D, Kon N, Li M, Zhang W, Qin J, Gu W.** 2005, Cell., Vol. 121, pp. 1071-1083.

217. *Homologous and non-homologous recombination differentially affect DNA damage repair in mice.* **Essers J, van Steeg H, de Wit J, Swagemakers SM, Vermeij M, Hoeijmakers JH, Kanaar R.** 2000, EMBO J., Vol. 19, pp. 1703-1710.

218. *Troglitazone, but not rosiglitazone, damages mitochondrial DNA and induces mitochondrial dysfunction and cell death in human hepatocytes.* **Rachek LI, Yuzefovych LV, Ledoux SP, Julie NL, Wilson GL.** 2009, Toxicol Appl Pharmacol., Vol. 240, pp. 348-354.

219. *Nuclear factor-kappaB suppressive and inhibitor-kappaB stimulatory effects of troglitazone in obese patients with type 2 diabetes: evidence of an antiinflammatory action?* **Aljada A, Garg R, Ghanim H, Mohanty P, Hamouda W, Assian E, Dandona P.** 2001, J Clin Endocrinol Metab., Vol. 86, pp. 3250-3256.

220. *Peroxisome proliferator-activated receptor gamma ligand troglitazone induces cell cycle arrest and apoptosis of hepatocellular carcinoma cell lines.* **Yoshizawa K, Cioca DP, Kawa S, Tanaka E, Kiyosawa K.** 2002, Cancer., Vol. 95, pp. 2243-2251.

221. *Troglitazone induces apoptosis via the p53 and Gadd45 pathway in vascular smooth muscle cells.* **Okura T, Nakamura M, Takata Y, Watanabe S, Kitami Y, Hiwada K.** 2000, Eur J Pharmacol., Vol. 407, pp. 227-235.

222. *The antipsychotic drug trifluoperazine inhibits DNA repair and sensitizes non–small cell lung carcinoma cells to DNA double-strand break–induced cell death.* **Polischouk AG, Holgersson A, Zong D, Stenerlow B, Karlsson HL, Moller L, Viktorsson K, Lewensohn R.** 2007, Mol Cancer Ther., Vol. 6, pp. 2303-2309.

223. *PARP-1 and PARP-2 interact with nucleophosmin/B23 and accumulate in transcriptionally active nucleoli.* **Meder VS, Boeglin M, de Murcia G, Schreiber V.** 2005, J Cell Sci., Vol. 118, pp. 211-222.

224. *Synthetic lethal targeting of DNA double-strand break repair deficient cells by human apurinic/apyrimidinic endonuclease inhibitors.* **Sultana R, McNeill DR, Abbotts R, Mohammed MZ, Zdzienicka MZ, Qutob H, Seedhouse C, Laughton CA, Fischer PM, Patel PM, Wilson III DM, Madhusudan S.** 2012, Int J Cancer., Vol. 131, pp. 2433-2444.

225. *Nucleolar localization of aprataxin is dependent on interaction with nucleolin and on active ribosomal DNA transcription.* **Becherel OJ, Gueven N, Birrell GW, Schreiber V, Suraweera A, Jakob B, Taucher-Scholz G, Lavin MF.** 2006, Hum Mol Genet., Vol. 15, pp. 2239-2249.

226. *Identification of nucleolin and nucleophosmin as genotoxic stress-responsive RNA-binding proteins.* **Yang C, Maiguel DA, Carrier F.** 2002, Nucleic Acids Res., Vol. 30, pp. 2251-2260.

227. *Induction of metallothionein by zinc protects from daunorubicin toxicity in rats.* **Ali MM, Frei E, Straub J, Breuer A, Wiessler M.** 2002, Toxicology., Vol. 179, pp. 85-93.

228. *Actinomycin D induces histone gamma-H2AX foci and complex formation of gamma-H2AX with Ku70 and nuclear DNA helicase II.* **Mischo HE, Hemmerich P,**

Grosse F, Zhang S. 2005, J Biol Chem., Vol. 280, pp. 9586-9594.

229. *Effect of naringin on the DNA damage induced by daunorubicin in mouse hepatocytes and cardiocytes.* **Cariño-Cortés R, Alvarez-González I, Martino-Roaro L, Madrigal-Bujaidar E.** 2010, Biol Pharm Bull., Vol. 33, pp. 697-701.

230. *Supramolecular complex formation between Rad6 and proteins of the p53 pathway during DNA damage-induced response.* **Lyakhovich A, Shekhar MP.** 2003, Mol Cell Biol., Vol. 23, pp. 2463-2475.

231. *The Ink4a tumor suppressor gene product, p19Arf, interacts with MDM2 and neutralizes MDM2's inhibition of p53.* **Pomerantz J, Schreiber-Agus N, Liégeois NJ, Silverman A, Alland L, Chin L, Potes J, Chen K, Orlow I, Lee HW, Cordon-Cardo C, DePinho RA.** 1998, Cell., Vol. 92, pp. 713-723.

232. *ARF promotes MDM2 degradation and stabilizes p53: ARF-INK4a locus deletion impairs both the Rb and p53 tumor suppression pathways.* **Zhang Y, Xiong Y, Yarbrough WG.** 1998, Cell., Vol. 92, pp. 725-734.

233. *Compound Management for Quantitative High-Throughput Screening.* **Yasgar A, Shinn P, Jadhav A, Auld D, Michael S, Zheng W, Austin CP, Inglese J, Simeonov A.** 2008, JALA Charlottesv Va., Vol. 13, pp. 79-89.

234. *A simple technique for quantitation of low levels of DNA damage in individual cells.* **Singh NP, McCoy MT, Tice RR, Schneider EL.** 1988, Exp. Cell Res., Vol. 175, pp. 184-191.

235. *Inhibition of Ape1 nuclease activity by lead, iron, and cadmium.* **McNeill DR, Narayana A, Wong HK, Wilson DM 3rd.** 2004, Environ Health Perspect., Vol. 112, pp. 799-804.

236. *Properties of and substrate determinants for the exonuclease activity of human apurinic endonuclease Ape1.* **Wilson DM 3rd.** 2003, J Mol Biol., Vol. 330, pp. 1027-1037.

237. *Inter-individual differences in repair of DNA base oxidation, measured in vitro with the comet assay.* **Collins AR, Dusinská M, Horváthová E, Munro E, Savio M, Stětina R.** 2001, Mutagenesis., Vol. 16, pp. 297-301.

238. *Kinetics of endogenous mouse FEN1 in base excision repair.* **Kleppa L, Mari PO, Larsen E, Lien GF, Godon C, Theil AF, Nesse GJ, Wiksen H, Vermeulen W, Giglia-Mari G, Klungland A.** 2012, Nucleic Acids Res., Vol. 40, pp. 9044-9059.

239. *XRCC1 suppresses somatic hypermutation and promotes alternative nonhomologous end joining in Igh genes.* **Saribasak H, Maul RW, Cao Z, McClure RL, Yang W, McNeill DR, Wilson DM 3rd, Gearhart PJ.** 2011, J Exp Med., Vol. 208, pp. 2209-2216.

APPENDIX

Supplementary Table 1 – Characteristics of the top hit molecules screened for their ability to inhibit the APE1/NPM1 interaction. For every compound analyzed the commercial or common name is indicated, as well as the AC_{50} measured during the primary screening, the conditions tested for the immuno-fluorescence assays, and the observed APE1 relocalization phenotype, if present. NA: not available, "-": no effect.

Compound ID	Common or commercial name	AC_{50} [μM]	Treatment conditions	Phenotype
NCGC00016600-01	Clofazimine	2.26	4.5 μM, 2 and 8h	-
NCGC00142391-04	Folic acid	2.67	100 and 500 μM, 4 and 16h	-
NCGC00025170-01	SU 4312	2.99	1 μM, 8 and 16h	-
NCGC00015447-04	FSCPX	3.16	10 μM, 8 and 16h	No nucleolar accumulation
NCGC00238831-01	NA	4.50	100 μM, 4 and 8h	-
NCGC00013628-01	Rolitetracycline	5.97	10 μM, 8 and 16h	-
NCGC00091268-01	Oxytetracycline	8.91	100 μM, 8 and 16h	-
NCGC00167776-01	NA	8.91	1 μM, 8 and 16h	-
NCGC00015478-02	GW 5074	9.47	10 μM, 2 and 8h	-
NCGC00165830-01	Myoseverin B	11.2	100 μM, 4 and 8h	No nucleolar accumulation
NCGC00025330-01	SB 408124	11.2	10 μM, 8 and 16h	-
NCGC00167819-01	NA	11.2	10 μM, 2 and 8h	-
NCGC00024246-05	Daunorubicinum	11.9	1 μM, 2h	No nucleolar accumulation
NCGC00025000-03	Ketoconazole	11.9	10 μM, 8 and 16h	No nucleolar accumulation
NCGC00017358-05	Rotenone	12.6	1 and 10 μM, 16h	No nucleolar accumulation
NCGC00240013-01	NA	12.6	10 μM, 8 and 16h	-
NCGC00016069-04	UK 14304	13.4	10 and 100 μM, 4-8-16h	-
NCGC00015747-06	Nicardipine	13.4	10 μM, 8 and 16h	-
NCGC00015280-03	C 8863	14.1	1 μM, 16h or 10 μM, 2h	-
NCGC00092382-02	GW405833	14.1	10 μM, 8 and 16h	-
NCGC00240145-01	NA	14.1	10 μM, 8 and 16h	-
NCGC00159457-02	Troglitazone	15.0	10 μM, 2-8-16h	No nucleolar accumulation
NCGC00159344-02	Carubicin	15.0	1 μM, 2h	No nucleolar accumulation
NCGC00167493-01	Manidipine	15.8	10 μM, 8 and 16h	-
NCGC00159958-01	NA	15.9	10 μM, 8 and 16h	Cyt. re-localization
NCGC00165892-01	NA	15.9	10 μM, 8 h	-
NCGC00159542-01	CGP 71683	15.9	10 μM, 2h	No nucleolar accumulation
NCGC00159584-01	NA	17.8	1 and 10 μM, 8h	-
NCGC00162178-02	Fiduxosin	17.8	10 μM, 8 and 16h	Cyt. re-localization
NCGC00090903-01	SASP	18.9	100 μM, 8 and 16h	-
NCGC00015392-04	DMCM	18.9	10 and 100 μM, 2h	-
NCGC00159758-01	NA	19.8	10 μM, 8 and 16h	-
NCGC00165880-01	NA	20.0	10 μM, 2 and 8h	-
NCGC00167835-01	NA	20.0	10 μM, 2 and 8h	-
NCGC00014648-01	Spiclomazine	21.2	10 μM, 2 and 4h	Cyt. re-localization
NCGC00024955-02	ZM 241385	21.2	10 μM, 8 and 16h	No nucleolar accumulation
NCGC00163174-01	N-(4-bromobenzyl)-5-methoxytryptamine	21.2	10 μM, 2 and 8h	-
NCGC00025014-01	(S)(+)-Niguldipine	21.2	10 μM, 2 and 8h	Cyt. re-localization
NCGC00015193-05	CGS-15943	21.2	10 μM, 8 and 16h	-
NCGC00161419-02	Trimetrexate glucuronate	22.4	100 μM, 2 and 8h	-
NCGC00094031-02	Ro 90-7501	22.4	100 μM, 8 and 16h	No nucleolar accumulation
NCGC00167826-01	NA	22.4	10 μM, 2 and 8h	-

NCGC00015823-13	Piroxicam	23.8	10 and 100 μM, 8h	-
NCGC00024650-01	BP 554 maleate	23.8	10 and 100 μM, 8h	-
NCGC00015917-02	SB 206553	23.8	10 μM, 8h or 100 μM, 2h	Cyt. re-localization
NCGC00025307-01	DMAQ-B1	23.8	1 and 10 μM, 8h	-
NCGC00025379-01	SR 33805 oxalate	23.8	10 μM, 2 and 8h	Cyt. re-localization
NCGC00025179-08	RU-486	25.1	10 μM, 8 and 16h	-
NCGC00093935-01	Flupirtine maleate	25.1	100 μM, 8 and 16h	-
NCGC00161030-01	NA	26.7	100 μM, 2h	-
NCGC00015155-03	Bepridil	26.7	10 μM, 8 and 16h	No nucleolar accumulation
NCGC00164547-01	Zafirlukast	26.7	10 μM, 2 and 4h	-
NCGC00015424-04	Fluspirilene	28.2	1 μM, 8 and 16h	-
NCGC00015300-05	Vanoxerine	28.2	1 μM, 8h	-
NCGC00024760-01	GF 109203X	29.9	10 μM, 2 and 4h	-
NCGC00074717-01	NA	29.9	100 μM, 2 and 8h	-
NCGC00166312-01	Closantel	31.6	1 μM, 2 and 8h	-
NCGC00015889-05	Raloxifene	31.6	10 μM, 2 and 8h	-

Supplementary Table 2 – List of the antibodies used in the Western blotting and immuno-fluorescence experiments. The LigI antibody was a kind gift from Prof. Alan Tomkinson (University of New Mexico).

Epitope	Clonality	Company
APE1	Polyclonal	Novus (NB 100-101)
NPM1	Monoclonal	Invitrogen (32-5200)
NPM1	Polyclonal	Abcam (ab15440)
LigIII	Monoclonal	SantaCruz (sc-135883)
XRCC1	Monoclonal	Thermo Scientific (MS-434-P0)
FEN1	Polyclonal	Abcam (ab17993)
PCNA	Monoclonal	SantaCruz (sc-56)
Polδcs	Monoclonal	Abcam (ab10362)
Polβ	Polyclonal	Abcam (ab26343)
$p14^{Arf}$	Polyclonal	Novus (NB200-111)
Mule	Polyclonal	Laboratories (A300-486A)
FLAG	Monoclonal	Sigma (F3165)
Fibrillarin	Monoclonal	SantaCruz (sc-166001)
Rad51	Polyclonal	Novus (H00005888-B01P)
LigIV	Polyclonal	Abcam (ab26039)
DNA-PKcs	Polyclonal	SantaCruz (sc-9051)
Ku70	Monoclonal	SantaCruz (sc-12729)
Mre11	Polyclonal	Novus (NB100-142)
BRCA2	Polyclonal	SantaCruz (sc-8326)

Supplementary Table 3 – Sequences of the primers used for the Real-time PCR experiments.

Transcript	Primer sequence (5' -> 3')
APE1	For: CGTCACAGCGATGCCAAAGC
	Rev: ATCTGGAGGGTCCTCGTACAGG
FEN1	For: ATTCGCTCTGCTCCGAACATTCCT
	Rev: TCAGCAATTAGTTTGGCAAGGCCG
Polβ	For: TGGACTCTGAGTACATTGCTA
	Rev: TGGCTGTTTGCTGGATTC
Polδcs	For: CGGCTACAACATTCAGAA
	Rev: GATTGGAAGGAGGAGTCA
LigIII	For: TTGTCTGCTACGAGAGTTC
	Rev: AATCTGCTTATCATTCAAGTTGT
XRCC1	For: AATGGCGAGGACCCGTATGC
	Rev: CACGTAGCGGATGAGCCTCC

ABBREVIATIONS

5'-dRP: 5'-deoxyribonucleotide-phosphate

8-oxo-dG: 7,8-dihydro-8-oxoguanine

AAG: N-alkyladenine DNA glycosylase

AML: acute myeloid leukemia

AP: apurinic/apyrimidinic (site)

APE1: apurinic/apyrimidinic endonuclease 1

APTX: aprataxin

ATM: ataxia telangiectasia mutated

ATR: ataxia telangiectasia and Rad3 related

BER: base excision repair

Compound #3: N-(3-(benzo[d]thiazol-2-yl)-6-isopropyl-4,5,6,7-tetrahydrothieno[2,3-c]pyridin-2-yl)acetamide

DDR: DNA damage response

DNA-PKcs: DNA-dependent protein kinase catalytic subunit

DSB: double-strand break

E3330: (2E)-3-[5-(2,3-dimethoxy-6-methyl 1,4-benzoquinoyl)] -2-nonyl-2-propenoic acid

EJ: end-joining

ExoIII: exonuclease III

FEN1: flap endonuclease 1

HR: homologous recombination

ICLs: interstrand crosslinks

IL-8: interleukin 8

IR: ionizing radiation

KO: knockout

LigI: DNA ligase I

LigIII: DNA ligase III

LigIV: DNA ligase IV

LP: long-patch

Mdm2: mouse double minute homolog 2

MEFs: mouse embryonic fibroblasts

MMR: mismatch repair

MMS: methyl methanesulfonate

MTS: [3-(4,5-dimethylthiazol-2-yl)-5-(3-carboxymethoxyphenyl)-2-(4-sulfophenyl)-2H-tetrazolium, inner salt

Mule: Mcl-1 ubiquitin ligase E3

MX: methoxyamine

nCaRE: negative calcium response elements

NF-κB: nuclear factor-κB

NIR: nucleotide incision repair

NER: nucleotide excision repair

NHEJ: nonhomologous end joining

NPM1: nucleophosmin

OGG1: 8-oxoguanine DNA glycosylase

$p14^{Arf}$: p14 alternative reading frame

PARP: poly(ADP-ribose) polymerase

PCNA: proliferating cell nuclear antigen

PNKP: polynucleotide kinase 3'-phosphatase

Pol I: RNA polymerase I

Polβ: DNA polymerase β

Polδcs: DNA polymerase δ catalytic subunit

PTMs: post-translational modifications

ROS: reactive oxygen species

rRNA: ribosomal RNA

SMUG1: single-strand-selective monofunctional uracil-DNA glycosylase 1

SP: short-patch

SSBR: single-strand break repair

SSBs: single-strand breaks

TDP1: tyrosyl-DNA phosphodiesterase 1

TNF-α: tumor necrosis factor-α

WCE: Whole cell exctract

XRCC1: X-ray repair cross-complementing 1

UNG: uracil-DNA glycosylase

zAPE1: zebrafish APE1

PAPERS PUBLISHED DURING THE Ph.D. COURSE

- **Poletto M.**, Di Loreto C., Marasco D., Poletto E., Damante G. and Tell G. *"Acetylation on critical lysine residues of apurinic/apyrimidinic endonuclease 1 (APE1) in triple negative breast cancers"* Biochem Biophys Res Commun. – (2012) 424(1):34-9.
- Lirussi L., Antoniali G., Vascotto C., D'Ambrosio C., **Poletto M.**, Romanello M., Marasco D., Leone M., Quadrifoglio F., Bhakat K., Scaloni A. and Tell G. "*Nucleolar accumulation of APE1 depends on charged lysine residues that undergo acetylation upon genotoxic stress and modulate its BER activity in cells*" Mol Biol Cell. – (2012) 23(20):4079-96.
- Marasco D., Ruggiero A., Vascotto C., **Poletto M.**, Scognamiglio P. L., Tell G. and Vitagliano L. "*Role of mutual interactions in the chemical and thermal stability of Nucleophosmin NPM1 domains*" Biochem Biophys Res Commun. – (2013) 430(2):523-8.
- **Poletto M.**, Vascotto C., Scognamiglio P. L., Marasco D. and Tell G. "*Role of the unstructured N-terminal domain of the hAPE1 (human apurinic/apyrimidinic endonuclease 1) in the modulation of its interaction with nucleic acids and NPM1 (nucleophosmin)*" Biochem J. – (2013) 452(3):545-57.
- Vascotto C., Lirussi L., **Poletto M.**, Tiribelli M., Damiani D., Fabbro D., Damante G., Demple B., Colombo E. and Tell G. "*Functional regulation of the apurinic/apyrimidinic endonuclease 1 by nucleophosmin: impact on tumor biology*" Oncogene. – (2013) Jul 8. doi: 10.1038/onc.2013.251. [Epub ahead of print].
- Londero A. P., Orsaria M., Tell G., Marzinotto S., Capodicasa V., **Poletto M.**, Vascotto C., Sacco C. and Mariuzzi L. "*Expression and prognostic significance of APE1/Ref1 and NPM1 proteins in high-grade ovarian serous cancer*" Am J Clin Pathol. – (2014) 141(3):404-14.
- Antoniali G., Lirussi L., **Poletto M.** and Tell G. *"Emerging roles of the nucleolus in regulating the DNA damage response: the non-canonical DNA repair enzyme APE1/Ref-1 as a paradigmatical example"* Antioxid Redox Signal. – (2014) 20(4):621-39. Review.
- Scognamiglio P. L., Di Natale C., Leone M., **Poletto M.**, Vitagliano L., Tell G. and Marasco D. "*G-quadruplex DNA recognition by nucleophosmin: New insights from protein dissection*" *(Biochim Biophys Acta, accepted for publication)*.

The work presented in this thesis is included in:

- **Poletto M.**, Dorjsuren D., Malfatti M.C., Scognamiglio P.L., Marasco D., Jadhav A., Maloney D.J., Wilson 3rd D.M., Simeonov A. and Tell G. *"Inhibitors of the APE1/NPM1 interaction that display anti-tumor properties" (Mol Carcingenesis, under revision).*
- **Poletto M.**, Lirussi L., Wilson D. M. 3rd and Tell G. *"Nucleophosmin (NPM1) modulates the stability and activity of DNA base excision repair proteins and is required for their nucleolar accumulation" (Mol Biol Cell, under revision).*

Biochemical and Biophysical Research Communications 424 (2012) 34–39

Contents lists available at SciVerse ScienceDirect

Biochemical and Biophysical Research Communications

journal homepage: www.elsevier.com/locate/ybbrc

Acetylation on critical lysine residues of Apurinic/apyrimidinic endonuclease 1 (APE1) in triple negative breast cancers

Mattia Poletto [a], Carla Di Loreto [a], Daniela Marasco [b,c], Elena Poletto [a], Fabio Puglisi [a], Giuseppe Damante [a], Gianluca Tell [a,*]

[a] Department of Medical and Biological Sciences, University of Udine, 33100 Udine, Italy
[b] Department of Biological Sciences, University of Naples "Federico II", 80134 Naples, Italy
[c] Institute of Biostructures and Bioimaging, National Research Council, 80134 Naples, Italy

ARTICLE INFO

Article history:
Received 2 June 2012
Available online 16 June 2012

Keywords:
Apurinic/apyrimidinic endonuclease/redox effector factor 1 (APE1/Ref-1)
Base excision repair (BER)
Acetylation
Triple negative breast cancer (TNBC)

ABSTRACT

Protein acetylation plays many roles within living cells, modulating metabolism, signaling and cell response to environmental stimuli, as well as having an impact on pathological conditions, such as cancer pathogenesis and progression. The Apurinic/apyrimidinic endonuclease APE1 is a vital protein that exerts many functions in mammalian cells, acting as a pivotal enzyme in the base excision repair (BER) pathway of DNA lesions, as transcriptional modulator and being also involved in RNA metabolism. As an eclectic and abundant protein, APE1 is extensively modulated through post-translational modifications, including acetylation. Many findings have linked APE1 to cancer development and onset of chemo- and radio-resistance. Here, we focus on APE1 acetylation pattern in triple negative breast cancer (TNBC). We describe the validation and characterization of a polyclonal antibody that is specific for the acetylation on lysine 35 of the protein. Finally, we use the new antibody to analyze the APE1 acetylation pattern on a cohort of TNBC specimens, exploiting immunohistochemistry. Our findings reveal a profound deregulation of APE1 acetylation status in TNBC, opening new perspectives for future improvements on treatment and prognosis of this molecular subtype of breast carcinomas.

1. Introduction

The complexity of the proteome extends far beyond the mere number of protein-coding genes: several mechanisms that act downstream transcription and translation greatly expand the plethora of functions that a single protein-coding sequence can achieve. Among these, post-translational modifications (PTMs) of proteins modulate nearly all processes within living cells. More than 200 different PTMs have been reported: from the covalent functionalization of proteins with relatively large modifiers (e.g. ubiquitin), to the alteration of target polypeptides with tiny chemical moieties (e.g. methylation or acetylation) [1]. Since its discovery in histones 40 years ago, lysine acetylation has been investigated as an essential PTM that act modulating histones-DNA interactions and, ultimately, chromatin accessibility. In the last decades, however, the significance of protein acetylation has increasingly become broader, as many groups have pointed out the importance of this PTM for several non-histone proteins [2]. Acetylation, in fact, has profound consequences on protein functions and regulates many physiological processes such as cellular metabolism, migration and signaling, as well as pathological conditions, such as cancer occurrence and progression [2,3].

The Apurinic/apyrimidinic endonuclease/redox effector factor-1 (APE1/Ref-1, hereafter APE1) is an essential and multifunctional protein, firstly discovered as central enzyme in the base excision repair (BER) pathway of DNA lesions [4,5]. APE1 acts as the main abasic endonuclease within mammalian cells, contributing to the maintenance of genomic stability against alkylative and oxidative DNA damage. As the acronym suggests, the protein has also been separately identified as a transcriptional modulator, able to activate a broad range of transcription factors through a redox-mediated mechanism. In addition to these "classical" functions, APE1 is involved in other cellular processes such as RNA metabolism and transcriptional repression through the binding of negative calcium response elements (nCaRE) sequences within gene promoters [6,7]. APE1 is an abundant protein (10^6–10^7 copies/cell) and is endowed with a relatively long half-life (approximately 8 h in HeLa cells), therefore, to cope with a rapidly changing environment, cells must rely on a fast way to modulate APE1 activities and localization.

Abbreviations: APE1, Apurinic/apyrimidinic endonuclease1; PTM, post-translational modification; nCaRE, negative calcium response elements; BER, base excision repair; TNBC, triple negative breast cancer; PARP, Poly(ADP-ribose) Polymerase; MMS, methyl-methanesulphonate.

* Corresponding author. Address: Department of Medical and Biological Sciences, University of Udine, P.le Kolbe 4, 33100 Udine, Italy. Fax: +39 0432 494301.
E-mail address: gianluca.tell@uniud.it (G. Tell).

0006-291X/$ - see front matter © 2012 Elsevier Inc. All rights reserved.
http://dx.doi.org/10.1016/j.bbrc.2012.06.039

Hence, it is not unexpected that the protein undergoes several PTMs including phosphorylation, ubiquitination, proteolysis, S-nitrosation and acetylation [4,8]. Several acetylation sites have been found within the APE1 poorly structured N-terminal region. In particular, acetylation/deacetylation on K^6 and K^7 has been linked to the modulation of several APE1 activities, including its affinity to the nCaRE sequences, the YB-1-mediated MDR1 gene activation and also the BER function of the protein, upon genotoxic insult [9–11]. Recent evidences from our laboratory, moreover, highlight the role of the lysine cluster between K^{27} and K^{35} in the modulation of APE1 functions. The acetylation status of these residues, in fact, appears to be modulated by genotoxic stress and likely influences the accessibility of K^6 and K^7 to lysine acetyl-transferases and deacetylases, suggesting the existence of a cross-talk between different acetylation hot-spots of the protein. The modification of lysines within the basic K^{27} to K^{35} cluster, has been also linked to a modulation of APE1 endonuclease activity, subcellular localization, nucleic acids binding affinity and protein–protein interaction [12] and (Lirussi et al., unpublished results). Moreover, acetylation of the K^{27} to K^{35} cluster induced by alkylating treatment with methyl-methanesulphonate (MMS), is associated with an increased DNA repair activity of APE1 which may account for the reduced sensitivity of some cancer cells to DNA damaging agents (Lirussi et al., unpublished results). As a central enzyme in the BER pathway, APE1 has in fact been linked to tumorigenesis and onset of chemo- and radio-resistance in several malignancies. In particular, aberrant APE1 localization and expression patterns, have been related to an increased tumor aggressiveness and recurrence, lymph node positivity and poor prognosis [13–16]. However, there are no data linking the acetylation status of APE1 and tumor progression.

In this paper, we investigated the status of APE1 acetylation, on the K^{27} to K^{35} cluster, in triple negative breast cancer (TNBC). We developed and characterized a polyclonal antibody specific for acetylated APE1 that we exploited to analyze, through immunohistochemistry, a cohort of TNBC specimens. Our data point to a profound deregulation of APE1 acetylation status in specific subtype of breast carcinoma and represent a descriptive starting point for future translational studies devoted to improve treatment and prognosis of this disease.

2. Materials and methods

2.1. Peptide synthesis and purification

Different APE1 peptide regions (Table 1) containing $K^{27}/K^{31}/K^{32}/K^{35}$ were chemically synthesized in the acetylated and non-acetylated form. Solid phase peptide synthesis was performed on an automated synthesizer Syro I (MultiSynTech), following Fmoc methodologies [17]. Peptides were purified by preparative RP-HPLC on a Shimadzu LC-8A, and analyzed through mass spectrometry. LC-ESI-Ion Trap (IT)-MS analysis was carried out on a Surveyor HPLC system connected to a LCQ DECA XP IT (Thermo Scientific).

Table 1
Sequences of the peptides used in this study.

Peptide name	Sequence[a]
25–38	^{25}KS**K**TAA**KK**ND**K**EAA^{38}
25–38^{27,31,32,35Ac}	^{25}KS**K**(Ac)TAA**K**(Ac)**K**(Ac)ND**K**(Ac)EAA^{38}
24–39	^{24}KKS**K**TAA**KK**ND**K**EAAG^{39}
24–39^{27,31,32,35Ac}	^{24}KKS**K**(Ac)TAA**K**(Ac)**K**(Ac)ND**K**(Ac)EAAG^{39}
14–38	^{14}GDELRTEPEAKKS**K**TAA**KK**ND**K**EAA^{38}
14–38^{27,31,32,35Ac}	^{14}GDELRTEPEAKKS**K**(Ac)TAA**K**(Ac)**K**(Ac)ND**K**(Ac)EAA^{38}
14–38^{31,32,35Ac}	^{14}GDELRTEPEAKKS**K**TAA**K**(Ac)**K**(Ac)ND**K**(Ac)EAA^{38}
14–38^{27,31,32Ac}	^{14}GDELRTEPEAKKS**K**(Ac)TAA**K**(Ac)**K**(Ac)ND**K**EAA^{38}
14–38^{35Ac}	^{14}GDELRTEPEAKKS**K**TAA**KK**ND**K**(Ac)EAA^{38}

[a] Numbers indicate the position of the peptide within APE1 amino acidic sequence. "Ac" denotes acetylated residues. $K^{27}/K^{31}/K^{32}/K^{35}$ are bolded.

2.2. Generation of polyclonal antibody specific for acetylated APE1

Based on the identified acetylation sites at $K^{27}/K^{31}/K^{32}/K^{35}$, we synthesized a peptide bearing the APE1 25–38 sequence and acetylated lysine residues, which was conjugated through the N-terminal CG dipeptide with keyhole limpet hemocyanin (KLH), i.e. KLH-CG^{25}KSK(Ac)TAAK(Ac)K(Ac)NDK(Ac)EAA^{38}. Polyclonal antibodies against this peptide were raised in rabbits following standard procedures (PRIMM).

2.3. In vitro acetylation of recombinant APE1

Recombinant full length APE1 mutants were previously described (Lirussi et al., unpublished results). Both recombinant proteins or APE1 peptides were non-enzymatically acetylated by incubation with 5 mM acetyl-CoA [18] and (Lirussi et al., unpublished results), in HAT buffer (50 mM Tris–HCl pH 8.0, 0.1 mM EDTA, 5% glycerol, 1 mM DTT) for 2 h at 30 °C. Reaction was stopped by adding Laemmli sample buffer and subjected to immunoblotting using the indicated antibodies. The acetylation of proteins and peptides was confirmed through MS analysis.

2.4. Cell culture, transfection and immuno-precipitation

Cell culture, transfection and immuno-precipitation have been performed by using already published methodologies [12].

2.5. Immuno-fluorescence and immunohistochemistry

Immuno-fluorescences with the anti-APE1$^{K27-35Ac}$ (PRIMM) have been carried out following previously described procedures [12]. Briefly, cells were paraformaldehyde-fixed for 20 min at RT and permeabilized for 5 min using a PBS, 0.5% (v/v) Triton X-100 solution. After saturation with 10% (v/v) foetal bovine serum (Euroclone) for 30 min, slides were incubated with the polyclonal anti-APE1$^{K27-35Ac}$ antibody (1:100 for 3 h at 37 °C), followed by a secondary anti-rabbit Dyt-Light549 conjugated (Jackson Immuno-Research). Microscope slides were visualized through a TCS SP laser-scanning confocal microscope (Leica).

Core biopsies of triple negative breast tumors were examined by immunohistochemistry. All tissues were formalin-fixed for 16–24 h. Five micrometers formalin-fixed paraffin-embedded tissue sections, mounted on Superfrost slides (Surgipath) were immunohistochemically stained by using the peroxidase/DAB Plus Dako REAL™ EnVision™ Detection System (Dako A/S). Antigen retrieval was performed in a water bath at 98 °C with 0.01 M citrate buffer, at pH 6.0 for 40 min. Endogenous peroxidase activity was blocked by incubation in the Peroxidase Block solution (Dako A/S) for 10 min. Primary mouse monoclonal anti-APE1 antibody [20] diluted 1:200 (optimum working dilution) and primary rabbit polyclonal anti-APE1$^{K27-35Ac}$ (PRIMM) antiserum diluted 1:100 were applied to each slide and incubated, respectively, for 60 min at room temperature and overnight at 4 °C. After washing, slides were incubated with the peroxidase/DAB Plus Dako REAL™ EnVision™ Detection System (Dako A/S) according to manufacturer's guidelines. For reaction visualization, 3-3 diaminobenzidine tetrahydrochloride was used as chromogen. The sections were counterstained with Mayer haematoxylin. Normal breast tissue sections were used as positive control, whereas negative control was performed by replacing the primary antibody with PBS. Controls were included in each staining run. Nuclear immunostaining was quantitatively evaluated by using light microscopy: the entire section was scanned at high-power magnification (400×) and the percentage of positive cells was scored.

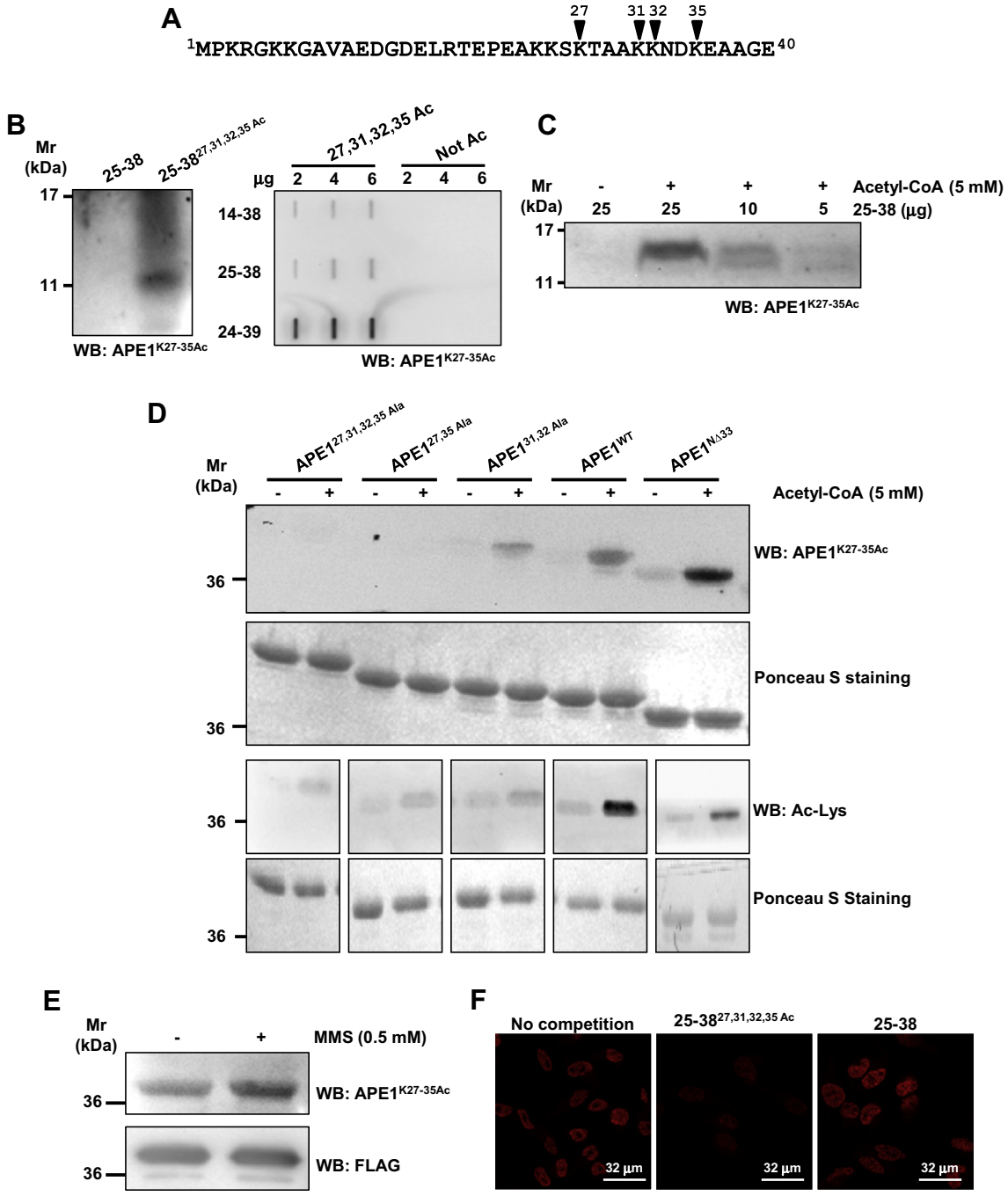

Fig. 1. The anti-APE1$^{K27-35Ac}$ antibody is specific for APE1 acetylation at $K^{27}/K^{31}/K^{32}/K^{35}$. (Panel A) Schematic view of the position of the acetyl-lysine residues in the primary sequence of APE1. Lysines residues targeted by the antibody are indicated by an arrowhead. (Panel B) Western blotting analyses on synthetic APE1 peptides. Left panel: 10 µg of chemically synthesized 25–38 or tetra-acetylated 25-38^{27,31,32,35Ac} were separated onto a discontinuous Tris-tricine SDS–PAGE and then subjected to immunoblotting. Right panel: the indicated amounts of BSA-conjugated 24–39 APE1 peptide, or unconjugated 14–38 and 25–38 APE1 peptides (either in their non-acetylated or tetra-acetylated forms) were slot-blotted on PVDF membrane and subjected to immunoblotting. (Panel C) Western blotting analysis on the *in vitro* acetylated 25–38 peptide; increasing amounts of the non-acetylated 25–38 peptide were *in vitro* acetylated as described in Section 2 and separated onto a discontinuous Tris-tricine SDS–PAGE prior to immunoblotting analysis. All Western blotting analyses were performed using the anti-APE1$^{K27-35Ac}$ antibody. (Panel D) The anti-APE1$^{K27-35Ac}$ antibody recognizes *in vitro* acetylated full length APE1. 2.5 µg of recombinant APE1 and its lysine to alanine mutants were *in vitro* acetylated as described in Section 2 and probed with either a commercial anti-Acetyl-lysine antibody (Millipore) or the anti-APE1$^{K27-35Ac}$ antibody. Ponceau-S staining was used as a loading control for normalization. (Panel E) The anti-APE1$^{K27-35Ac}$ antibody detects changes in the APE1 acetylation pattern upon MMS treatment. FLAG-APE1 was immuno-precipitated from HeLa cells treated for 4 h with MMS, as indicated, was probed using the anti-APE1$^{K27-35Ac}$ antibody. Anti-FLAG (Sigma) was used as loading control. (Panel F) Immuno-fluorescence on HeLa cells performed using either the anti-APE1$^{K27-35Ac}$ alone, or in presence of a 50-fold molar excess of 25–38^{27,31,32,35Ac} or 25–38 peptides. Images were captured maintaining fixed photomultiplier and laser parameters.

2.6. Western blotting analyses

Protein and peptides were separated onto 12% sodium dodecyl sulphate–polyacrylamide gel electrophoresis (SDS–PAGE) or onto a discontinuous Tris-tricine SDS–PAGE [19] and transferred to nitrocellulose or PVDF membranes (Perkin Elmer). Western blotting was carried out as already described [20], using 5% (w/v) bovine serum albumin (BSA) as blocking agent and revealed using ECL chemiluminescence procedure (GE Healthcare). Images were acquired through a ChemiDoc XRS video-densitometer (Bio-Rad).

2.7. Surface plasmon resonance (SPR)

The BIAcore 3000 SPR system for Real time binding assay and related reagents were from GE Healthcare. The polyclonal anti-APE1$^{K27-35Ac}$ antibody was immobilized at a concentration of 25 μg/mL in 10 mM acetate buffer pH 5.0 (flow rate 5 μL/min, time injection 7 min) on a CM5 Biacore sensor chip, using EDC/NHS chemistry following the manufacturer's instructions [21]. Residual reactive groups were deactivated by treatment with 1 M ethanolamine hydrochloride, pH 8.5. Reference channel was prepared by activating with EDC/NHS and deactivating with ethanolamine. Binding assays were carried out at 20 μL/min, with 4.5 min contact-time, APE1 peptides were diluted in running-buffer, HBS (10 mM HEPES, 150 mM NaCl, 3 mM EDTA, pH 7.4) 0.1 mM TCEP. Analyte injections of 90 μL were performed at the indicated concentrations. The BIAevaluation analysis package (v4.1, GE Healthcare) implemented by instrument software was used to subtract the signal of the reference channel and to evaluate kinetic and thermodynamic parameters of complexes.

3. Results and discussion

3.1. Specificity of anti-APE1$^{K27-35Ac}$ antibody

To gain new insights into the role of acetylation in the functional modulation of APE1, we developed a polyclonal antibody in rabbit. The antibody (hereafter referred to as anti-APE1$^{K27-35Ac}$) was developed to recognize the tetra-acetylated form of the APE1 N-terminal 27 to 35 lysines stretch (Fig. 1A). The anti-APE1$^{K27-35Ac}$ antibody specificity was tested both by Western blotting and slot blotting, using a panel of chemically synthesized APE1 25–38 or 24–39 peptides (Table 1) that were either acetylated during synthesis (Fig. 1B) or *in vitro* acetylated after synthesis (Fig. 1C). Immunoblotting analyses confirmed the ability of the antibody to discriminate the acetylated peptides from their non-acetylated counterparts. The ability of the anti-APE1$^{K27-35Ac}$ antibody to recognise APE1 acetylation within a full-length protein background was investigated using purified recombinant lysine to alanine APE1 mutants expressed in *Escherichia coli* (i.e. APE1^{WT}, the double mutants APE1^{27,35Ala} and APE1^{31,32Ala}, the quadruple mutant APE1^{27,31,32,35Ala} and the deletion mutant APE1$^{N\Delta33}$, that lacks the entire 1 to 33 N-terminal domain) (Lirussi et al., unpublished results). Recombinant proteins were *in vitro* acetylated using acetyl-CoA and subjected to Western blotting (Fig. 1D). Analyses revealed that the anti-APE1$^{K27-35Ac}$ is able to detect APE1 acetylation only in presence of an acetylatable (i.e. not mutated) lysine residue at position 35 (Fig. 1D – upper panel). The specificity of the anti-APE1$^{K27-35Ac}$ antibody was also compared to that of a commercial anti-Acetyl-lysine antibody (Millipore); this antibody is also able to discriminate between acetylated APE1 forms, though with a different pattern. In particular, all APE1 mutants are detected by the Acetyl-lysine antibody when in their acetylated form, in accordance with the broad specificity of the antibody and with the presence of other acetylatable residues within APE1 (e.g. K^6 and K^7) (Fig. 1D – lower panel). Altogether these data suggest that the anti-APE1$^{K27-35Ac}$ specifically recognizes APE1 acetylation within the 27 to 35 lysines stretch, with a particular affinity toward the acetylated K^{35} residue. This latter point is further highlighted by the strong signal obtained with the APE1$^{N\Delta33}$ deletion mutant, which conserves only K^{35}, that is possibly located in a more accessible position. To further validate the specificity of the anti-APE1$^{K27-35Ac}$ antibody, we used immuno-precipitated APE1 samples obtained from HeLa cells treated with MMS, to increase the acetylation status of the K^{27} to K^{35} cluster (Lirussi et al., unpublished results). Fig. 1E shows that the anti-APE1$^{K27-35Ac}$ efficiently detects changes in the acetylation pattern of the protein. We finally assessed the staining pattern of the antibody using immuno-fluorescence on HeLa cells: the selectivity of the staining was verified through competition studies using the acetylated 25–38 peptide (Fig. 1F).

Surface Plasmon resonance (SPR) biosensors are ideally suited for antibody characterization and quantitative immunoassay detection. Here, we exploited SPR to measure the affinity of the antibody for the acetyl-lysine residues within APE1 amino acids 27 to 35 (Fig. 2). To characterize the kinetic values for the anti-APE1$^{K27-35Ac}$ we employed different APE1 peptides as ligands (Table 1). SPR data confirmed what observed through Western blotting, showing that acetylated K^{35} is the preferential target site for immunorecognition, with a measured K_D in the sub-micromolar range (Table 2). Notably, the lack of acetylation on K^{35} only, results in a dramatic reduction in the antibody affinity for the cognate peptide (Fig. 2B, Table 2 and data not shown). Therefore, these analyses lead us to conclude that the developed antibody has major specificity toward the acetylated K^{35} residue of APE1.

3.2. Analysis of APE1 acetylation in triple negative breast Cancer

The APE1$^{K27-35Ac}$ antibody was used to study APE1 acetylation in a cohort of triple negative breast cancer (TNBC) specimens. This type of breast cancer comprises tumors that lack expression of estrogen receptor (ER), progesterone receptor (PR) and overexpression/gene amplification of epidermal growth factor receptor type 2 (HER2) [22]. TNBC account for approximately 15% of all invasive breast cancers and often show aggressive phenotypical characteristics, such as a high histologic grade [23,24]. To date, no specific molecular targets have been identified in TNBC and, accordingly, no specific targeted therapies have been developed [25]. Therefore, the prognosis of patients with TNBC is usually poorer than that of

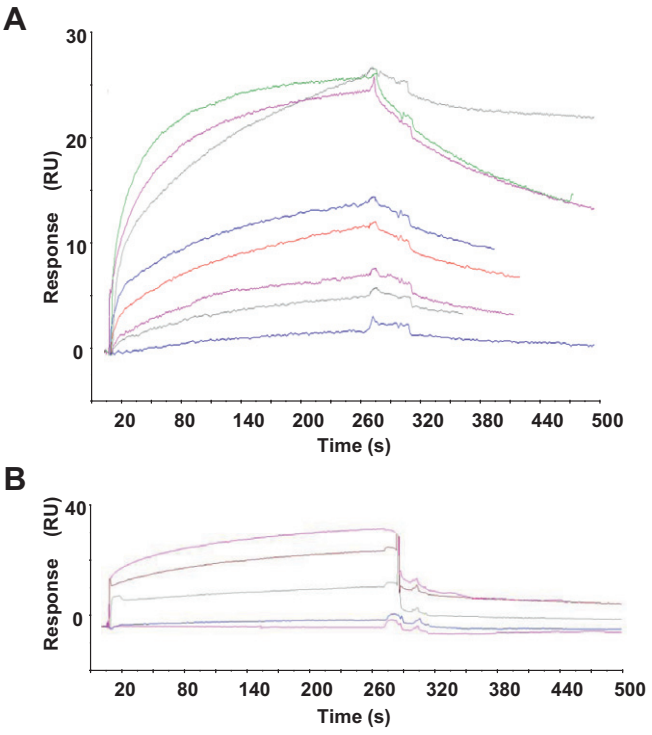

Fig. 2. The anti-APE1$^{K27-35Ac}$ antibody displays a major specificity for the acetylated lysine **35.** (Panel A) Representative overlay sensorgrams relative to a typical SPR experiment of immobilized anti-APE1$^{K27-35Ac}$ at a 2000RU level with either A the APE1 14–38^{27,31,32,35Ac} (5–800 nM) peptide or B the APE1 14-38^{27,31,32Ac} (0.1–1000 μM) peptide.

Table 2
Kinetic and thermodynamic parameters of anti-APE1$^{K27-35Ac}$ toward peptides described in Table 1.

Peptide	$K_a \times 10^4$ (Ms)	$K_d \times 10^{-3}$ (1/s)	K_D (M)
14–38	ND[a]	ND	$\sim 10^{-3}$
14–38^{35Ac}	2.39	6.52	$270 \pm 8 \times 10^{-9}$
14–38^{31,32,35Ac}	4.70	7.71	$164 \pm 3 \times 10^{-9}$
14–38^{27,31,32Ac}	ND	ND	$\sim 10^{-3}$
14–38^{27,31,32,35Ac}	3.62	5.10	$141 \pm 3 \times 10^{-9}$

[a] ND: Not Determined.

patients with other subtypes of breast cancer [26,27]. Various findings, however, indicate that a substantial diversity in biology, prognosis and treatment sensitivity can be observed among tumor defined as TNBC [28,29]. A cohort of 103 TNBC was investigated for levels of total APE1 and acetylated APE1 by using immunohistochemistry. Fig. 3 shows representative immunostainings and quantitation of positivity: overexpression of total APE1 was detected in TNBC compared to normal breast tissue, with 90% of tumor specimens showing an APE1 nuclear positivity higher than 80% (Fig. 3B). This result is in accordance with previous works that report a correlation between APE1 overexpression and tumor aggressiveness in a variety of cancers [4,6]. In contrast, immunostaining of acetylated APE1 was very heterogeneous among TNBC specimens: samples showing either low or high nuclear positivity were observed (T1 and T2, respectively, in Fig. 3A). The heterogeneity of APE1$^{K27-35Ac}$ immunostaining among TNBC is quantitatively captured in Fig. 3B. These data suggest that in TNBC, concomitantly with total APE1 overexpression, a specific deregulation of the acetylation status of this protein is occurring. APE1 deregulation in breast carcinoma (present data and [30]) may be linked to an impairment in its redox activity, being instrumental in altering estrogen-responsive gene expression in breast cancer cell lines [31].

Member of the Poly(ADP-ribose) Polymerase (PARP) family are central to specific DNA damage repair pathways, particularly the BER. PARP inhibition has been shown to enhance the cytotoxicity of agents that generate single-strand breaks in DNA, such as radiation and certain chemotherapy drugs (i.e. alkylating agents) [32]. In addition, PARP inhibitors may induce cell death through "synthetic lethality", if the DNA repair mechanisms that rescue BER-deficient cells are themselves impaired, as in BRCA-deficient breast cancers [32,33]. Because of the phenotypic similarities between some TNBC and most BRCA1-associated breast cancers, some have hypothesized that TNBC might also be sensitive to PARP inhibition [32]. Interestingly, it has been recently demonstrated that BRCA1 may be involved in regulation of the expression levels of DNA repair genes such as APE1, OGG1 and NTH1 [34]. Thus, APE1 represents an ideal candidate target for developing new therapeutic strategies for breast cancer treatment. In particular, deregulation of APE1 observed in breast cancer specimens might be exploited in order to induce synthetic lethality in tumors with defects in other DNA repair pathway, as recently pointed out [33]. Our observations, therefore, represent a descriptive starting point for future investigations; it would be interesting to understand

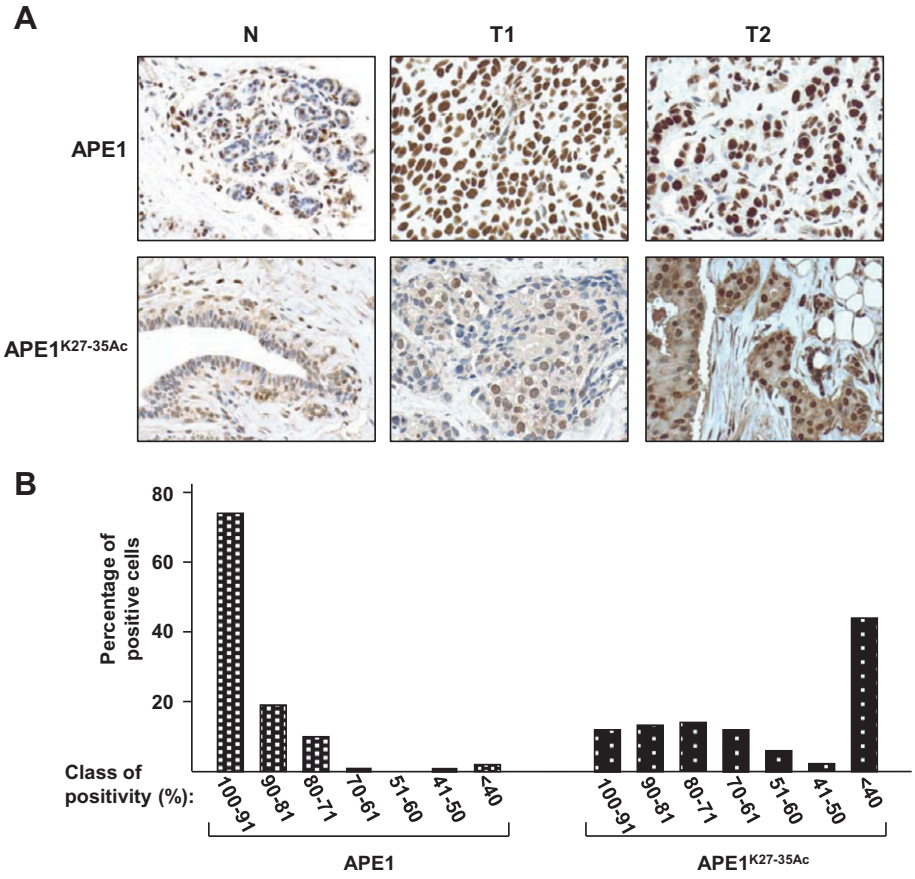

Fig. 3. Immunostaining of TNBC specimens for total APE1 and acetylated APE1. (Panel A) Representative cases of normal breast tissue (N) and TNBC (T1 and T2) stained with antibody against total (APE1) and acetylated (APE1$^{K27-35Ac}$) APE1. Positivity is indicated by the brown colour. (Panel B) Quantitative analysis of nuclear positivity for total APE1 and acetylated APE1. In x and y axes are indicated different classes of positivity and percentage of TNBC present within each class, respectively. APE1 or APE1$^{K27-35Ac}$ immunostaining is indicated below the respecting bars.

whether the deregulation of APE1 acetylation status is paralleled by an impairment of its functions, in order to design novel therapeutic approaches to breast carcinoma.

Conflict of Interest

Authors declare that they have no conflict of interest pending.

Acknowledgments

The authors thank Dr. Lisa Lirussi for technical help in some experiments. This work was supported by the Associazione Italiana per la Ricerca sul Cancro (IG10269) and Ministero dell'Istruzione, dell'Università e della Ricerca (FIRB_RBRN07BMCT and PRIN2008_CCPKRP_003 to G.T.).

References

[1] C.T. Walsh, S. Garneau-Tsodikova, G.J. Gatto, Protein posttranslational modifications: the chemistry of proteome diversifications, Angew. Chem. Int. Ed. Engl. 44 (2005) 7342–7372.
[2] X.J. Yang, E. Seto, Lysine acetylation: codified crosstalk with other posttranslational modifications, Mol. Cell 31 (2008) 449–461.
[3] P. Close, C. Creppe, M. Gillard, et al., The emerging role of lysine acetylation of non-nuclear proteins, Cell. Mol. Life Sci. 67 (2010) 1255–1264.
[4] G. Tell, G. Damante, D. Caldwell, et al., The intracellular localization of APE1/Ref-1: more than a passive phenomenon?, Antioxid Redox Signal. 7 (2005) 367–384.
[5] C. Vascotto, L. Cesaratto, L.A. Zeef, et al., Genome-wide analysis and proteomic studies reveal APE1/Ref-1 multifunctional role in mammalian cells, Proteomics 9 (2009) 1058–1074.
[6] G. Tell, D. Fantini, F. Quadrifoglio, Understanding different functions of mammalian AP endonuclease (APE1) as a promising tool for cancer treatment, Cell. Mol. Life Sci. 67 (2010) 3589–3608.
[7] G. Tell, D.M. Wilson 3rd, C.H. Lee, Intrusion of a DNA repair protein in the RNome world: is this the beginning of a new era?, Mol Cell. Biol. 30 (2010) 366–371.
[8] C.S. Busso, M.W. Lake, T. Izumi, Posttranslational modification of mammalian AP endonuclease (APE1), Cell. Mol. Life Sci. 67 (2010) 3609–3620.
[9] K.K. Bhakat, T. Izumi, S.H. Yang, et al., Role of acetylated human AP-endonuclease (APE1/Ref-1) in regulation of the parathyroid hormone gene, EMBO J. 22 (2003) 6299–6309.
[10] T. Yamamori, J. DeRicco, A. Naqvi, et al., SIRT1 deacetylates APE1 and regulates cellular base excision repair, Nucleic Acids Res. 38 (2010) 832–845.
[11] S. Sengupta, A.K. Mantha, S. Mitra, et al., Human AP endonuclease (APE1/Ref-1) and its acetylation regulate YB-1-p300 recruitment and RNA polymerase II loading in the drug-induced activation of multidrug resistance gene MDR1, Oncogene 30 (2011) 482–493.
[12] D. Fantini, C. Vascotto, D. Marasco, et al., Critical lysine residues within the overlooked N-terminal domain of human APE1 regulate its biological functions, Nucleic Acids Res. 38 (2010) 8239–8256.
[13] S. Kakolyris, L. Kaklamanis, K. Engels, et al., Human AP endonuclease I (HAPI) protein expression inbreast cancer correlates with lymph node status and angiogenesis, Br. J. Cancer 77 (1998) 1169–1173.
[14] K.A. Robertson, H.A. Bullock, Y. Xu, et al., Altered expression of Ape1/ref-1 in germ cell tumors and overexpression in NT2 cells confers resistance to bleomycin and radiation, Cancer Res. 61 (2001) 2220–2225.
[15] V. Di Maso, C. Avellini, L.S. Crocè, Subcellular localization of APE1/Ref-1 in human hepatocellular carcinoma: possible prognostic significance, Mol. Med. 13 (2007) 89–96.
[16] Q. Sheng, Y. Zhang, R. Wang, et al., Prognostic significance of APE1 cytoplasmic localization in human epithelial ovarian cancer, Med. Oncol. 29 (2012) 1265–1271.
[17] G.B. Fields, R.L. Noble, Solid phase peptide synthesis utilizing 9-fluorenylmethoxycarbonyl amino acids, Int. J. Pept. Protein Res. 35 (1990) 161–214.
[18] G.J. Garbutt, E.C. Abraham, Non-enzymatic acetylation of human hemoglobins, Biochim. Biophys. Acta 670 (1981) 190–194.
[19] H. Schägger, Tricine–SDS–PAGE, Nat. Protoc. 1 (2006) 16–22.
[20] C. Vascotto, D. Fantini, M. Romanello, et al., APE1/Ref-1 interacts with NPM1 within nucleoli and plays a role in the rRNA quality control process, Mol. Cell. Biol. 29 (2009) 1834–1854.
[21] B. Johnsson, S. Lofas, G. Lindquist, Immobilization of proteins to a carboxymethyldextran-modified gold surface for biospecific interaction analysis in surface plasmon resonance sensors, Anal. Biochem. 198 (1991) 268–277.
[22] W.D. Foulkes, I.E. Smith, J.S. Reis-Filho, Triple-negative breast cancer, N. Engl. J. Med. 363 (2010) 1938–1948.
[23] E.A. Rakha, J.S. Reis-Filho, I.O. Ellis, Basal-like breast cancer: a critical review, J. Clin. Oncol. 26 (2008) 2568–2581.
[24] J.S. Reis-Filho, A.N. Tutt, Triple negative tumours: a critical review, Histopathology 52 (2008) 108–118.
[25] C. Andreetta, A.M. Minisini, M. Miscoria, et al., First-line chemotherapy with or without biologic agents for metastatic breast cancer, Crit. Rev. Oncol. Hematol. 76 (2010) 99–111.
[26] C. Liedtke, C. Mazouni, K.R. Hess, et al., Response to neoadjuvant therapy and long-term survival in patients with triple-negative breast cancer, J. Clin. Oncol. 26 (2008) 1275–1281.
[27] R. Dent, M. Trudeau, K.I. Pritchard, et al., Triple-negative breast cancer: clinical features and patterns of recurrence, Clin. Cancer Res. 13 (2007) 4429–4434.
[28] C. Oakman, E. Moretti, G. Pacini, et al., Triple negative breast cancer: a heterogeneous subgroup defined by what it is not, Eur. J. Cancer 47 (Suppl 3) (2011) S370–S372.
[29] C.X. Ma, J. Luo, M.J. Ellis, Molecular profiling of triple negative breast cancer, Breast Dis. 32 (2010) 73–84.
[30] F. Puglisi, F. Barbone, G. Tell, et al., Prognostic role of Ape/Ref-1 subcellular expression in stage I-III breast carcinomas, Oncol. Rep. 9 (2002) 11–17.
[31] C.D. Curtis, D.L. Thorngren, Y.S. Ziegler, et al., Apurinic/apyrimidinic endonuclease 1 alters estrogen receptor activity and estrogen-responsive gene expression, Mol. Endocrinol. 23 (2009) 1346–1359.
[32] M.R. Kelley, DNA Repair In Cancer Therapy, first ed., Molecular Targets and Clinical Applications, Academic Press, 2012.
[33] R. Sultana, D.R. McNeill, R. Abbotts, et al., Synthetic lethal targeting of DNA double-strand break repair deficient cells by human apurinic/apyrimidinic endonuclease inhibitors, Int. J. Cancer (2012), http://dx.doi.org/10.1002/ijc.27512.
[34] T. Saha, M. Smulson, E.M. Rosen, BRCA1 regulation of base excision repair pathway, Cell Cycle 9 (2010) 2471–2472.

Nucleolar accumulation of APE1 depends on charged lysine residues that undergo acetylation upon genotoxic stress and modulate its BER activity in cells

Lisa Lirussi[a,*], Giulia Antoniali[a,*], Carlo Vascotto[a], Chiara D'Ambrosio[b], Mattia Poletto[a], Milena Romanello[a], Daniela Marasco[c,d], Marilisa Leone[d], Franco Quadrifoglio[a], Kishor K. Bhakat[e], Andrea Scaloni[b], and Gianluca Tell[a]

[a]Department of Medical and Biological Sciences, University of Udine, 33100 Udine, Italy; [b]Proteomics and Mass Spectrometry Laboratory, Istituto di Ricerche per il Sistema Produzione Animale in Ambiente Mediterraneo, National Research Council, 80147 Naples, Italy; [c]Department of Biological Sciences, University of Naples "Federico II," 80134 Naples, Italy; [d]Institute of Biostructures and Bioimaging, National Research Council, 80134 Naples, Italy; [e]Department of Biochemistry and Molecular Biology, University of Texas Medical Branch, Galveston, TX 77555

ABSTRACT **Apurinic/apyrimidinic endonuclease 1 (APE1) is the main abasic endonuclease in the base excision repair (BER) pathway of DNA lesions caused by oxidation/alkylation in mammalian cells; within nucleoli it interacts with nucleophosmin and rRNA through N-terminal Lys residues, some of which ($K^{27}/K^{31}/K^{32}/K^{35}$) may undergo acetylation in vivo. Here we study the functional role of these modifications during genotoxic damage and their in vivo relevance. We demonstrate that cells expressing a specific K-to-A multiple mutant are APE1 nucleolar deficient and are more resistant to genotoxic treatment than those expressing the wild type, although they show impaired proliferation. Of interest, we find that genotoxic treatment induces acetylation at these K residues. We also find that the charged status of $K^{27}/K^{31}/K^{32}/K^{35}$ modulates acetylation at K^{6}/K^{7} residues that are known to be involved in the coordination of BER activity through a mechanism regulated by the sirtuin 1 deacetylase. Of note, structural studies show that acetylation at $K^{27}/K^{31}/K^{32}/K^{35}$ may account for local conformational changes on APE1 protein structure. These results highlight the emerging role of acetylation of critical Lys residues in regulating APE1 functions. They also suggest the existence of cross-talk between different Lys residues of APE1 occurring upon genotoxic damage, which may modulate APE1 subnuclear distribution and enzymatic activity in vivo.**

Monitoring Editor
Karsten Weis
University of California, Berkeley

Received: Apr 17, 2012
Revised: Jul 25, 2012
Accepted: Aug 16, 2012

This article was published online ahead of print in MBoC in Press (http://www.molbiolcell.org/cgi/doi/10.1091/mbc.E12-04-0299) on August 23, 2012.

*These authors contributed equally to this work

The authors declare that they have no conflict of interests.

Address correspondence to: Gianluca Tell (gianluca.tell@uniud.it).

Abbreviations used: APE1/Ref-1, apurinic/apyrimidinic endonuclease/redox effector factor 1; BER, base excision repair; MMS, methyl methanesulfonate; MTS, 3-(4-5-dimethylthiazol-2-yl)-5-(3-carboxymethoxyphenyl)-2-(4-sulfophenyl)-2H-tetrazolium salt; NPM1, nucleophosmin 1; SIRT1, sirtuin 1; TBHP, *tert*-butyl hydroperoxide.

INTRODUCTION

Apurinic/apyrimidinic endonuclease 1/redox effector factor-1 (APE1) plays a central role in the maintenance of genome stability and redox signaling (Bapat *et al.*, 2009, 2010; Tell *et al.*, 2010a; Wilson and Simeonov, 2010). Through its C-terminal domain (residues 61–318), it acts as an essential enzyme in the base excision repair (BER) pathway of DNA damages caused by both endogenous and exogenous oxidizing/alkylating agents, including many chemotherapeutic drugs. In combination with thioredoxin (Ueno *et al.*, 1999; Seemann and Hainaut, 2005) and through its N-terminal domain (residues 1–127), it also functions as a regulatory redox agent to maintain cancer-related transcription factors (Egr-1, NF-κB, p53, HIF-1α, AP-1, and Pax proteins) in an active reduced state (Hirota *et al.*, 1997;

Supplemental Material can be found at:
http://www.molbiolcell.org/content/suppl/2012/08/20/mbc.E12-04-0299.DC1.html

Wei *et al.*, 2000; Ziel *et al.*, 2004; Gray *et al.*, 2005; Pines *et al.*, 2005; Tell *et al.*, 2005, 2010a). APE1 can also act as a transcriptional repressor through indirect binding to negative Ca^{2+}-response elements (nCaRE), which are regulated by K^6/K^7 acetylation (Bhakat *et al.*, 2003). Recently APE1 was demonstrated to bind/cleave abasic RNA (Vascotto *et al.*, 2009b; Fantini *et al.*, 2010; Tell *et al.*, 2010b) and to control *c-Myc* expression by cleaving its mRNA (Barnes *et al.*, 2009). These discoveries pointed to a new function of APE1 in regulating gene expression through posttranscriptional mechanisms and brought to light the fact that this protein is a possible target for anticancer therapy.

In this context, we showed that the first 35 amino acids in the nonstructured N-terminal domain of APE1 are required for a stable interaction with rRNA, nucleophosmin 1 (NPM1), and other proteins involved in ribosome biogenesis/RNA processing (Vascotto *et al.*, 2009b; Tell *et al.*, 2010b). In particular, K residues within the protein region spanning amino acids 24–35 are involved in the interaction of APE1 with both rRNA and NPM1 and also regulate its in vitro enzymatic activity (Fantini *et al.*, 2010). Of interest, some of these critical K residues, namely $K^{27}/K^{31}/K^{32}/K^{35}$, undergo in vivo acetylation. These results suggest that protein–protein interactions and/or posttranslational modifications (PTMs) involving the APE1 N-terminal domain may play important roles in vivo in coordinating and fine-tuning the protein's BER activity and functions on rRNA metabolism. Recently it was also demonstrated that APE1 K^6/K^7 may undergo acetylation during cell response to genotoxic treatment (Fantini *et al.*, 2008) and that the acetylation status of these K residues, controlled by the sirtuin 1 (SIRT1) deacetylase activity, should be important in modulating protein DNA-repair function by regulating the kinetics of its interaction with other enzymes involved in BER, for example, XRCC1 (Yamamori *et al.*, 2010).

APE1 is mainly a nuclear protein and is critical for controlling cellular proliferative rates (Fung and Demple, 2005; Izumi *et al.*, 2005; Vascotto *et al.*, 2009b). We also showed that a considerable amount of APE1 is accumulated within the nucleoli of different cell lines (Vascotto *et al.*, 2009b; Fantini *et al.*, 2010), but its role within this compartment is unknown. Cytoplasmic, mitochondrial, and endoplasmic reticulum localizations have also been ascertained (Tell *et al.*, 2001; Szczesny and Mitra, 2005; Chattopadhyay *et al.*, 2006; Grillo *et al.*, 2006; Mitra *et al.*, 2007). APE1 is an abundant and relatively stable protein in mammalian cells (Tell *et al.*, 2009, 2010a). Fine-tuning of the multiple APE1 functions may therefore depend on the modulation of its PTMs and, eventually, on its interactome. Although a functional role has been determined for some PTMs (K^6/K^7 acetylation and $K^{24}/K^{25}/K^{27}$ ubiquitination; Bhakat *et al.*, 2003; Fantini *et al.*, 2008; Busso *et al.*, 2009), the identity and importance of various interacting partners in modulating APE1 biological functions are still under investigation (Parlanti *et al.*, 2007; Busso *et al.*, 2009; Vascotto *et al.*, 2009b). APE1 may affect cell growth by directly acting on rRNA quality control mechanisms; in particular, APE1 interaction with NPM1 may affect its activity over rRNA molecules. However, many aspects of this new function are undefined (Vascotto *et al.*, 2009b; Tell *et al.*, 2010b).

In this study, we address the biological role of APE1 acetylation at $K^{27}/K^{31}/K^{32}/K^{35}$ and, in light of recent evidence showing the emerging function of the nucleolus as a central sensor of protein trafficking during DNA repair after genotoxic treatment (Nalabothula *et al.*, 2010), the role of the nucleolus itself on the APE1 protective function toward genotoxic damage. We used a reconstitution strategy with APE1 mutants in which the charged Lys residues were replaced by either Ala or Arg to mimic constitutive acetylated ($APE1^{K4pleA}$) and nonacetylatable ($APE1^{K4pleR}$) protein forms, respectively. These mutants are reintroduced into APE1-silenced cell clones to determine the role of these crucial amino acids during cell response to genotoxic treatment.

RESULTS

Positively charged $K^{27}/K^{31}/K^{32}/K^{35}$ residues are essential for APE1 nucleolar accumulation through stabilization of protein interaction with NPM1 and rRNA

We previously demonstrated that charged K residues, located within the unstructured APE1 N-terminal domain (i.e., $K^{24}/K^{25}/K^{27}/K^{31}/K^{32}$), are crucial for APE1 interaction with rRNA and NPM1 and for modulating its catalytic activity on abasic DNA through regulation of product binding. Of interest, some of these critical amino acids (i.e., $K^{27}/K^{31}/K^{32}$ in addition to K^{35}) may undergo in vivo acetylation under basal conditions (Fantini *et al.*, 2010). We hypothesized that the degree of positive charges, modified by acetylation at these residues, may modulate APE1's different functions through its redirection to different substrates and/or stimulation of its DNA-repair enzymatic activity (Fantini *et al.*, 2010). To address this issue, we inspected the role of the positively charged residues within the region 27–35 in modulating the interaction between APE1 and NPM1. Colocalization experiments in HeLa cells transiently transfected with either FLAG-tagged, wild-type APE1 ($APE1^{WT}$), a K-to-A mutant ($APE1^{K4pleA}$) in which the positive charges have been removed as in the case of constitutive acetylation, or a nonacetylatable K-to-R APE1 mutant ($APE1^{K4pleR}$) showed that $APE1^{K4pleA}$ mutant has a marked exclusion from the nucleoli apparent in all expressing cells (Figure 1A). Silencing of the endogenous APE1 protein did not alter either the ability of the $APE1^{WT}$ and $APE1^{K4pleR}$ proteins to accumulate within the nucleolar compartment or the inability of the $APE1^{K4pleA}$ to accumulate within the nucleolus (unpublished data). These data thus demonstrate that $APE1^{WT}$ and $APE1^{K4pleR}$ nucleolar accumulation is not the consequence of their overexpression.

To complement these observations and also to exclude a possible contribution of the FLAG tag used to generate recombinant ectopic proteins, we exploited a live-cell imaging system as suggested by Schnell *et al.* (2012). APE1 cDNA was cloned into a pDendra2 vector to express APE1 in fusion with the green photoconvertible fluorophore Dendra (Chudakov *et al.*, 2007). As reported in Figure 1B, the fluorophore alone is present in both the cytoplasm and the nuclear compartment, but it is completely excluded from the nucleoli, as demonstrated by quantitative fluorescence signal analyses. In contrast, whereas the expression of Dendra in fusion with $APE1^{WT}$ and $APE1^{K4pleR}$ results in an efficient accumulation of the protein within the nucleolar compartment, the Dendra-$APE1^{K4pleA}$ mutant displays a homogeneous nuclear distribution. This approach confirms immunofluorescence-based data on the reduced accumulation of FLAG-tagged $APE1^{K4pleA}$ within the nucleoli and supports the evidence that the nucleolar accumulation of APE1 protein does not depend on the protein abundance nor does it depend on the specific tag used to generate the ectopic recombinant proteins (see also Supplemental Figure S1).

We supported our immunofluorescence data with biochemical interaction experiments. Coimmunoprecipitation analysis showed that the $APE1^{K4pleA}$ mutant has a significantly reduced interaction with NPM1 (Figure 2A), in accordance with its impaired nucleolar accumulation. The altered electrophoretic mobility observed for the $APE1^{K4pleA}$ mutant (Figure 2A) was further confirmed by SDS–PAGE analysis of recombinant proteins expressed in *Escherichia coli* and purified by chromatography. The effect is likely due to alteration of its overall charge, since electrospray ionization mass spectrometry analysis confirmed the correctness of protein mass values, and the

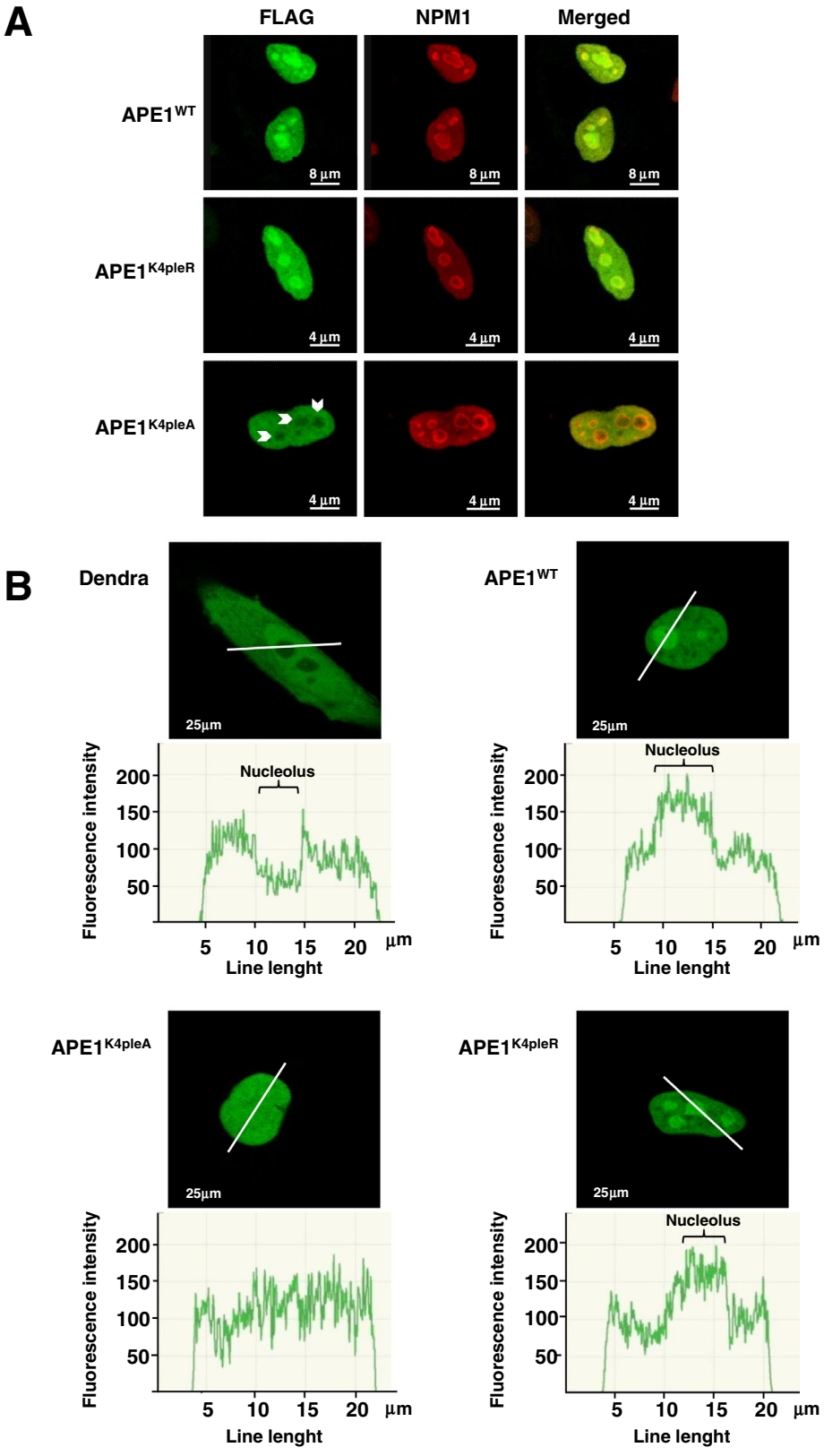

FIGURE 1: Positively charged $K^{27}/K^{31}/K^{32}/K^{35}$ residues are required for APE1 nucleolar accumulation. (A) Confocal microscopy of HeLa cells transfected with $APE1^{WT}$, $APE1^{K4pleA}$, or $APE1^{K4pleR}$ FLAG-tagged proteins and stained with antibodies against NPM1 (red) and ectopic FLAG-APE1 (green). Overlap of staining (yellow) demonstrated colocalization of the two proteins. Of note, the $APE1^{K4pleA}$ mutant was completely excluded from nucleoli (white arrowheads), whereas both $APE1^{WT}$ and the $APE1^{K4pleR}$ were accumulated within. Images are representative of 100% of transfected cells. (B) HeLa cells transfected with pDendra2-N empty vector or encoding APE1 (wild-type and mutants) in fusion with Dendra fluorophore were analyzed with a live confocal microscopy workstation. Cells transfected with empty vector (Dendra) showed diffuse green fluorescence within cytoplasm and nucleus, with exclusion of the nucleolar compartment. $APE1^{WT}$ and $APE1^{K4pleR}$ mutant mainly localized within the nuclear compartment and accumulated within nucleoli. In contrast, $APE1^{K4pleA}$ did not show any nucleolar accumulation. Images were captured by using the same settings (488-nm laser at 10% of intensity and PMT at 760 V). Fluorescence intensity analysis was carried out on a 25-µm-long line (white). Graphs represent the fluorescence intensity measured through a cross section of the nucleus and demonstrate an incremental fluorescence in corresponding nucleoli only in the case of $APE1^{WT}$ and $APE1^{K4pleR}$-Dendra fusion protein–expressing cells.

difference in their apparent mobility observed in SDS–PAGE was abolished when separating various mutants in urea-containing denaturing gels (Supplemental Figure S2 and unpublished data). It was also observed for other K-to-A mutants of APE1 (Fantini *et al.*, 2010). We then evaluated the contribution of the single K residues to the extent of APE1 nucleolar localization (Supplemental Figure S3) and the ability to interact with NPM1 (Figure 2B). Double mutants $APE1^{K27/35A}$, $APE1^{K31/32A}$, $APE1^{K27/35R}$, and $APE1^{K31/32R}$ and a deletion mutant lacking 33 amino acids at the protein N-terminus ($APE1^{N\Delta33}$) were compared with $APE1^{WT}$. Whereas $APE1^{WT}$, $APE1^{K27/35R}$, and $APE1^{K31/32R}$ displayed a nucleolar and nucleoplasmic staining, $APE1^{K27/35A}$ and $APE1^{K31/32A}$ showed two alternative stainings, exhibiting nucleolar/nucleoplasmic or only nucleoplasmic positivity, respectively (Supplemental Figure S3). Coimmunoprecipitation experiments (Figure 2B) were in accordance with immunofluorescence analyses and showed a substantial reduction of the interaction in the case of $APE1^{K4pleA}$ and $APE1^{N\Delta33}$ mutants and a moderate impairment for $APE1^{K27/35A}$ and $APE1^{K31/32A}$ mutants. Glutathione *S*-transferase (GST) pull-down assays with recombinant purified proteins confirmed that these results were due to effects on direct interaction between APE1 and NPM1 (Figure 2C). This confirmed previous hypotheses (Fantini *et al.*, 2010). We also checked the effect of the K-to-A mutation on the ability of APE1 to bind nucleolar rRNA (Vascotto *et al.*, 2009b). As expected, rRNA–chromatin immunoprecipitation (ChIP) analyses showed that K-to-A mutations significantly alter APE1 binding to

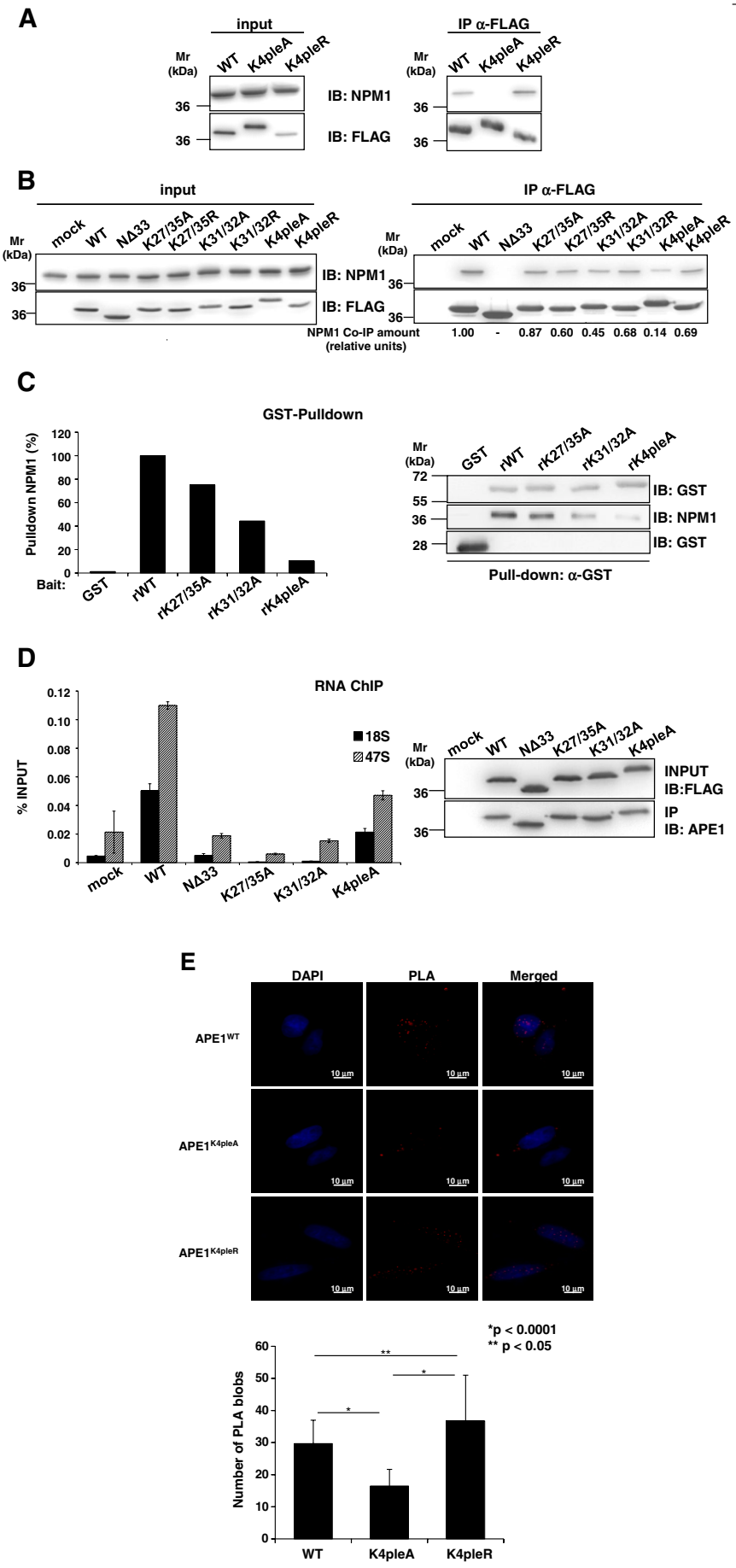

FIGURE 2: Positively charged $K^{27}/K^{31}/K^{32}/K^{35}$ residues are required for NPM1 interaction. (A) The $APE1^{K4pleA}$ mutant shows impaired interaction with NPM1. Coimmunoprecipitation (CoIP) analysis on HeLa cells transfected with $APE1^{WT}$, $APE1^{K4pleA}$, or $APE1^{K4pleR}$ FLAG-tagged proteins with endogenous NPM1. Western blot analysis was used to quantify the interaction among the different APE1 forms and NPM1 by using specific antibodies. IB, immunoblot. (B) $K^{27}/K^{31}/K^{32}/K^{35}$ residues are responsible for proper interaction of APE1 with NPM1. CoIP analysis on HeLa cells transfected with FLAG-tagged $APE1^{WT}$, $APE1^{N\Delta33}$, or the APE1 double ($APE1^{K27/35A}$, $APE1^{K31/32A}$, $APE1^{K27/35R}$, and $APE1^{K31/32R}$) or quadruple ($APE1^{K4pleA}$ and $APE1^{K4pleR}$) K-to-A or K-to-R mutants. Western blot analysis was performed on total cell extracts (left) and on immunoprecipitated material (right) with specific antibody for endogenous NPM1. Normalized coimmunoprecipitated amounts of NPM1 are indicated under each relative bar. Anti-FLAG staining was used as loading control. (C) Interaction of K-to-A APE1 mutants with NPM1 and rRNA. A 150-pmol amount of each bait GST-APE1 recombinant purified protein (rAPE1) was incubated with an equimolar amount of recombinant NPM1, as described in *Materials and Methods*. After GST pull-down, samples underwent Western blot analysis by using the indicated antibodies (right). NPM1 band intensities were normalized vs. those of GST-APE1 proteins, and the resulting values, expressed as percentage of bound with respect to $APE1^{WT}$, were plotted in the histogram (left). Each bar represents the mean of two independent experiments whose variation was <10%. (D) Interaction of K-to-A APE1 mutants with NPM1 and rRNA. After transfection of HeLa cells, total cell lysates were prepared as described in *Materials and Methods*, and an RNA-ChIP assay was performed to measure the rRNA-binding activity of the different APE1 mutants. Immunoprecipitated samples underwent either Western blot analysis (right) or RNA extraction and quantification by reverse transcription and quantitative PCR analysis, using 18S and 47S rRNA–specific primers. Data are presented as a fold percentage of the amount of total 18S or 47S rRNA with respect to the amount of immunoprecipitated FLAG-tagged APE1 protein, respectively. The resulting values are plotted in the histograms (left), showing the average values with SD of three independent experiments. (E) Nucleoplasmic interaction between APE1 and NPM1 is affected by K-to-A mutation on APE1. PLA technology was used to evaluate in vivo the effect of positively charged $K^{27}/K^{31}/K^{32}/K^{35}$ residues on APE1 interaction with NPM1 in the nuclear compartment. Stable HeLa clones expressing $APE1^{WT}$, $APE1^{K4pleA}$, or $APE1^{K4pleR}$ FLAG-tagged proteins were seeded on a glass coverslip, and PLA reaction was carried out using anti-FLAG and anti-NPM1 antibodies. 4′,6-Diamidino-2-phenylindole staining is used as a reference for the nuclei. The histogram represents the average number of PLA blobs scored for at least 30 cells per slide. Asterisks represent a significant difference between $APE1^{WT}$ and mutants.

rRNA molecules (Figure 2D) and that a partial removal of positive charges in the region 27–35 strongly affects the protein binding to rRNA molecules.

Interaction between APE1 and NPM1 may also occur in the nucleoplasmic compartment of cells. We measured the effect of the K-to-A mutation on the nucleoplasmic interaction of APE1 with NPM1 through proximity ligation assay (PLA) analysis, which allows in situ detection of two proteins that are at interacting distance of <40 nm (Weibrecht *et al.*, 2010). Data displayed in Figure 2E show that nucleoplasmic interaction between APE1 and NPM1 was significantly affected by the K-to-A mutation. Taken together, these data demonstrate that charged lysines within the 27–35 region are essential for APE1 maintenance within the nucleoli and for a proper/stable interaction of this protein with NPM1 or rRNA molecules. Moreover, our data suggest that APE1 must lose the positive charge at more than two K residues (among $K^{27}/K^{31}/K^{32}/K^{35}$) to get a significant reduction of the APE1/NPM1 interaction in the nucleus and loss of APE1 nucleolar accumulation.

Loss of APE1 nucleolar accumulation causes impairment of cell proliferation

APE1 protects cells against genotoxic damaging agents (Tell and Wilson, 2010). To clarify the biological relevance of the APE1 nucleolar accumulation, we estimated the effect of the expression of the nucleolar-deficient form of APE1 (i.e., $APE1^{K4pleA}$) on cell viability with respect to $APE1^{WT}$ and $APE1^{K4pleR}$ mutant. To test the effects of the mutant proteins and exclude the contribution of the endogenous one, we used inducible APE1-silenced (through small interfering RNA [siRNA] technology) HeLa cells, which were reconstituted with siRNA-resistant APE1 ectopic proteins in place of the endogenous one (Figure 3A; Vascotto *et al.*, 2009a). The levels of the ectopic proteins expressed by the different cell clones used for the following experiments were comparable to that of the wild-type endogenous one before silencing, as demonstrated by quantitative Western blot analysis (Supplemental Figure S4); the extent of the residual endogenous protein was <10%. Quantification of the nuclear amount of ectopic proteins after doxycycline treatment, demonstrated by Western blot analysis with a calibration curve, gave the following results (expressed as nanograms of APE1 per microgram of nuclear extract): 23.22 ± 6.04 for $APE1^{WT}$, 18.63 ± 4.84 for $APE1^{K4pleA}$, and 17.69 ±4.60 for $APE1^{K4pleR}$ (Supplemental Figure S4B). Therefore these cell lines represent a reliable system for testing our hypothesis. On the basis of previous data showing that nucleolar APE1 may act as a cleansing factor in rRNA quality control, possibly affecting cellular proliferation through an impairment of the overall protein synthesis machinery (Vascotto *et al.*, 2009b; Tell *et al.*, 2010b), we investigated the effect of the nucleolar-deficient form $APE1^{K4pleA}$ on cell proliferation rate under basal conditions. Of interest, by cell counting assays performed on reconstituted cell clones, we obtained proof that $APE1^{K4pleA}$ acts as a loss-of-function mutation in terms of cell proliferation, whereas $APE1^{K4pleR}$ behaves similarly to $APE1^{WT}$ (Figure 3B). These data, confirmed by using at least two different clones for each mutant cell line, suggest that nucleolar APE1 is required for appropriate control of cell proliferation, perhaps through its role in rRNA metabolism (Tell *et al.*, 2010b). Colony formation assays confirmed cell proliferation data (Figure 3C). However, although the cell number in each colony of $APE1^{K4pleR}$-expressing cells was always similar to that expressing $APE1^{WT}$, these cells grew in a more widespread manner, possibly due to an altered migrating phenotype and/or an intercellular adhesion pattern. These data were indicative that abolition of the acetylatable residues of APE1 at $K^{27}/K^{31}/K^{32}/K^{35}$ may significantly affect cell biology, even though it is also possible that the lower expression level of the $APE1^{K4pleR}$ (~76%) with respect to $APE1^{WT}$ may also have an effect on this phenotype.

Increased APE1 acetylation at $K^{27}/K^{31}/K^{32}/K^{35}$ residues upon genotoxic damage

APE1 acetylation at K^6/K^7 is known to be enhanced after genotoxic insult by methyl methanesulfonate (MMS) and it has been shown to play a role in modulating APE1 interaction with XRCC1, possibly coordinating different enzymatic steps in the BER pathway (Yamamori *et al.*, 2010). We therefore tested whether MMS treatment, which promotes generation of DNA damage specifically repaired through BER, may also induce APE1 acetylation at $K^{27}/K^{31}/K^{32}/K^{35}$ residues. Immunopurified APE1 samples from control and MMS-treated cells were separated by SDS–PAGE and excised bands and then analyzed by peptide mapping experiments. Semiquantitative nano–electrospray linear ion trap tandem mass spectrometry (nanoLC-ESI-LIT-MS/MS) analysis was performed on identical quantities of immunopurified $APE1^{WT}$-FLAG protein samples obtained from HeLa cells before and after MMS treatment (Supplemental Figure S5). In particular, we evaluated the amount of the peptides (15–33)Ac_3 and (15–35)Ac_4 in each APE1 endoprotease AspN digest and compared them to that of the nonmodified counterparts. Analysis was performed by extracting and integrating the corresponding nanoLC-ESI-LIT-MS peak areas equivalent to the assigned *m/z* values for the acetylated and nonacetylated peptides in the same total ion chromatogram. After MMS treatment, the amount of the peptide (15–33)Ac_3 was significantly increased, and the peptide (15–35)Ac_4 was almost doubled as compared with that of the nonmodified counterparts (Figure 4A). The MMS-induced acetylation on the aforementioned residues was further demonstrated by Western blotting using a commercial anti–Ac-Lys antibody on immunopurified proteins from HeLa cells transiently transfected with the FLAG-tagged $APE1^{WT}$ and the nonacetylatable $APE1^{K4pleR}$ forms. It is striking that a significant increase of APE1 acetylation was observed after MMS treatment but mainly for $APE1^{WT}$ rather than for $APE1^{K4pleR}$ (Supplemental Figure S6). These data show that, besides increasing the acetylation status of K^6/K^7 (see later discussion and Yamamori *et al.*, 2010), MMS treatment also promotes acetylation at $K^{27}/K^{31}/K^{32}/K^{35}$ residues. The mild increase of Lys acetylation level in the mutant $APE1^{K4pleR}$ may possibly be ascribed to K^6/K^7 acetylation (see later discussion).

We then investigated the cellular distribution pattern of acetylated APE1 at $K^{27}/K^{31}/K^{32}/K^{35}$ residues by using an ad hoc–developed antibody that specifically recognized the peptide 25–38 fully acetylated at $K^{27}/K^{31}/K^{32}/K^{35}$, hereafter referred to as anti-$APE1^{K27\text{-}35Ac}$ (Poletto *et al.*, 2012). This antibody was particularly efficient in recognizing acetylation at K^{35} with a measured affinity in the nanomolar range (196 nM for the tetra-acetylated stretch vs. 26,800 nM for the nonacetylated one, as assessed by surface plasmon resonance (SPR; Poletto *et al.*, 2012). Preincubation of the antibody with the acetylated and nonacetylated peptides confirmed the specificity of the antibody (Poletto *et al.*, 2012). The distribution pattern of $APE1^{WT}$, $APE1^{K4pleA}$, and $APE1^{K4pleR}$ was compared by using anti-FLAG and anti-$APE1^{K27\text{-}35Ac}$ antibodies. Of interest, staining with the anti-$APE1^{K27\text{-}35Ac}$ antibody gave a pattern quite similar (i.e., nucleolar exclusion) to that of the anti-FLAG antibody but only in the case of the $APE1^{K4pleA}$ mutant (Figure 4B). PLA was also carried out to demonstrate the in vivo occurrence of acetylation on endogenous APE1 by using either the anti-$APE1^{K27\text{-}35Ac}$ antibody alone (as a control) or together with an anti-APE1 antibody (Figure 4C). This assay clearly highlighted the proximity between the target of both

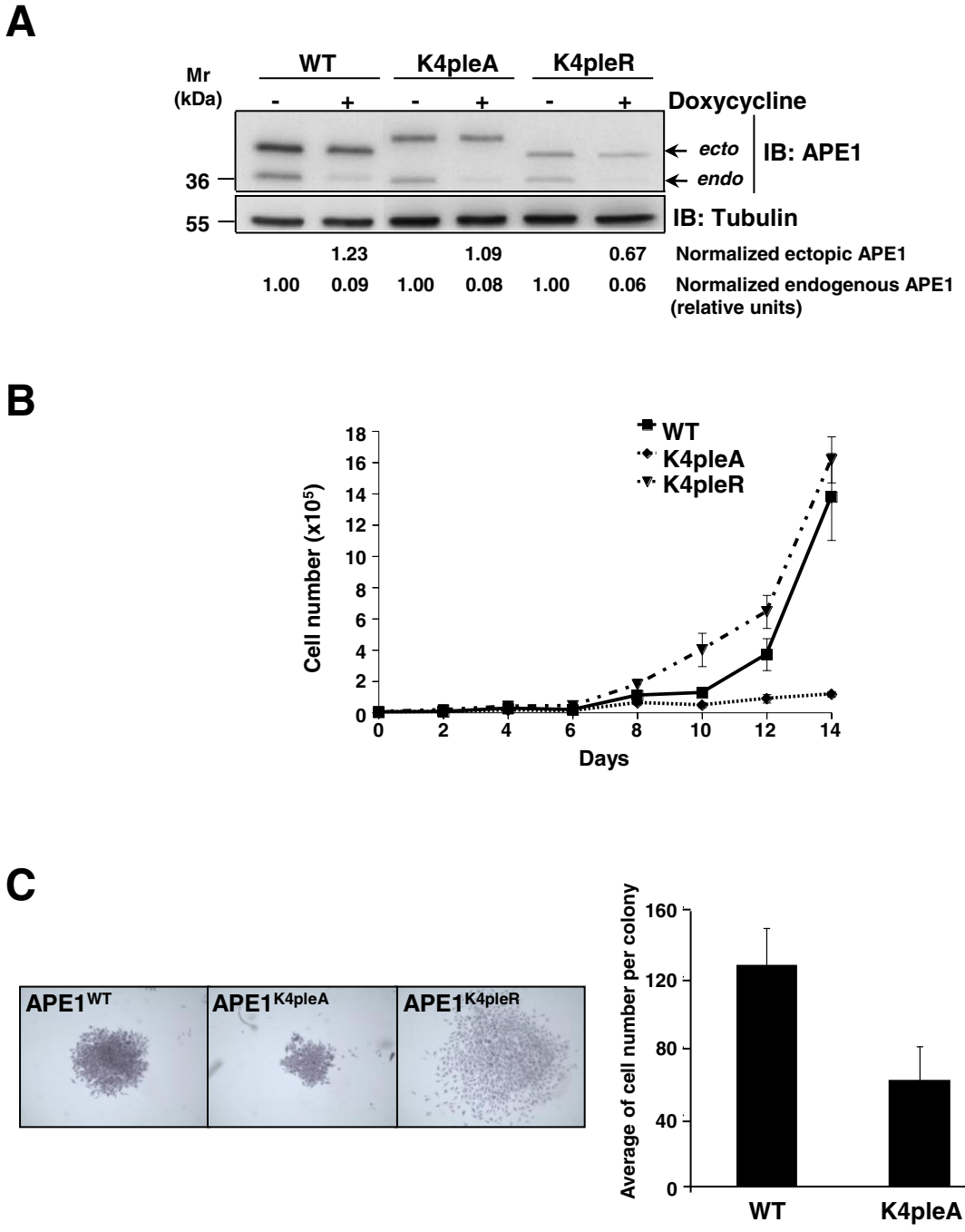

FIGURE 3: Expression of the nucleolus-deficient APE1 mutant causes impaired cell proliferation. (A) Generation of reconstituted cell lines expressing APE1^{K4pleA} and APE1^{K4pleR} mutants. HeLa cells were stably transfected with the inducible siRNA vectors and siRNA resistant APE1^{WT}, APE1^{K4pleA}, and APE1^{K4pleR}–expressing vectors, as previously described (Vascotto *et al.*, 2009a; Fantini *et al.*, 2010). Expression of ectopic APE1 forms without silencing and after the suppression of endogenous APE1 expression after 10 d of treatment with doxycycline (Doxy) was assayed by Western blotting on total cellular extracts with an anti-APE1 antibody. Normalized expression levels for each clone of ectopic and endogenous APE1 protein after the silencing are indicated under each relative band. β-Tubulin was used as loading control. (B) Cell proliferation assays for APE1-reconstituted cell lines. APE1-expressing cell clones were seeded in 60-mm Petri dishes. Growth was followed by measuring cell numbers at various times upon doxycycline treatment, as indicated. Cells were harvested at the indicated times, stained with trypan blue, and counted in triplicate. Data, expressed as cell number, are the mean ± SD of three independent experiments. (C) Colony formation assays for APE1-reconstituted cell lines. After 8 d of doxycycline treatment, 200 cells of APE1^{WT} and the indicated APE1 mutants were seeded in 60-mm Petri dishes and grown for 8 d in medium supplemented with doxycycline to promote endogenous APE1 silencing. Then cells were stained with crystal violet and images captured by using a Leica S8 microscope with 80× magnification. Data, expressed as number of cells per colony, are the mean ± SD of 10 colonies for each clone.

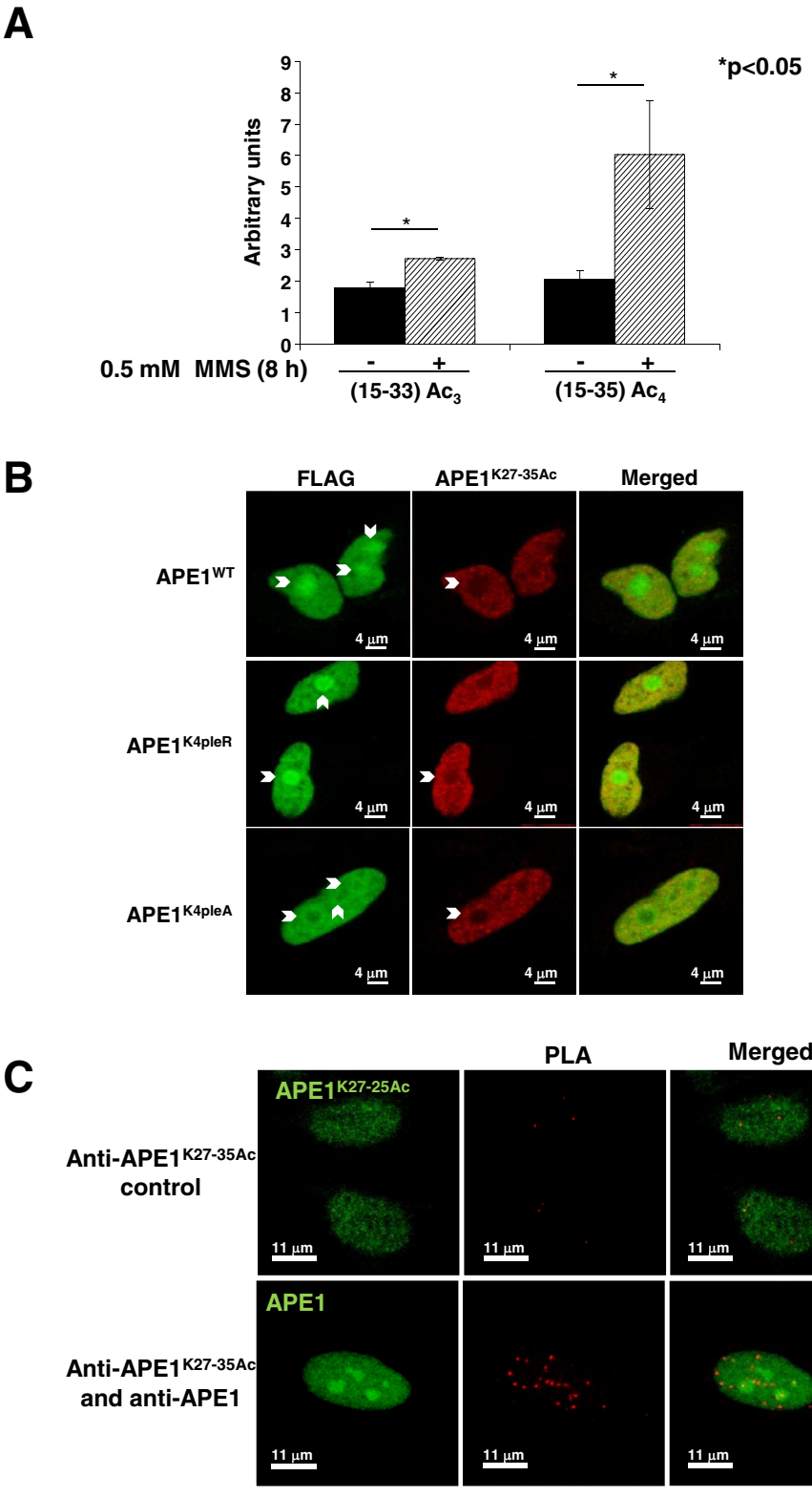

FIGURE 4: Genotoxic treatment promotes APE1 acetylation at $K^{27}/K^{31}/K^{32}/K^{35}$ residues. (A) Relative quantitative changes of APE1 acetylation at $K^{27}/K^{31}/K^{32}/K^{35}$ after MMS treatment. Mass spectrometry analysis of acetylated peptides present in the endoprotease AspN digest of FLAG-tagged $APE1^{WT}$ purified from HeLa cells (see *Materials and Methods* for details). Histograms indicate the relative amounts of the peptides (15–33)Ac_3 and (15–35)Ac_4 with respect to their nonmodified counterparts before and after MMS treatment. Identical ionization tendencies were assumed for each peptide pair. Each bar represents the mean of three independent experiments. (B) Acetylated APE1 at $K^{27}/K^{31}/K^{32}/K^{35}$ residues is present within cell nucleoplasm but is excluded from nucleoli. Confocal microscopy of HeLa cells transfected with $APE1^{WT}$, $APE1^{K4pleA}$, or $APE1^{K4pleR}$ FLAG-tagged proteins and stained with antibodies against endogenous $APE1^{K27–35Ac}$ (anti-$APE1^{K27–35Ac}$, red) and ectopic APE1 FLAG-tagged (green). Overlap of staining (yellow) demonstrated the codetection of the two protein forms. Images are representative of 100% of transfected cells. (C) APE1 acetylation at $K^{27}/K^{31}/K^{32}/K^{35}$ occurs in vivo. PLA signal obtained using the anti-$APE1^{K27–35Ac}$ antibody together with the anti-APE1 antibody on fixed HeLa cells. A technical control, using the anti-$APE1^{K27–35Ac}$ antibody alone, was introduced (top). Nuclei were counterstained using an Alexa Fluor 488–conjugated secondary anti-rabbit (recognizing the endogenous $APE1^{K27–35Ac}$, in the control reaction) or anti-mouse antibody (recognizing the endogenous APE1 protein in the PLA reaction; green).

antibodies, further suggesting that, in vivo, APE1 is acetylated at $K^{27}/K^{31}/K^{32}/K^{35}$ residues and that these acetylated forms are excluded from the nucleoli. Taken together, these data suggest that acetylation at these charged amino acids may control the nucleolar/nucleoplasmic distribution of APE1 within cells.

Removal of positively charged $K^{27}/K^{31}/K^{32}/K^{35}$ residues increases APE1 DNA-repair activity in vivo

We tested whether abolition of positive charges on acetylatable residues may affect the APE1 DNA repair function in cells, as previously demonstrated in vitro by using recombinant purified proteins bearing two different clusters of K-to-A mutation (i.e., on residues 24/25/27 and on residues 24/25/27/31/32; Fantini *et al.*, 2010). For this purpose we used nuclear extracts from reconstituted cell clones after precise normalization for the APE1 ectopic nuclear content with a titration curve (as shown in Supplemental Figure S4). This normalization for APE1 ectopic protein expression allowed comparison of the enzymatic activities of the different protein mutants in the nuclear fractions from each clone. Figure 5A shows that the AP-endonuclease activity of the $APE1^{K4pleA}$ mutant, measured through cleavage assays performed with nuclear extracts, was significantly increased with respect to $APE1^{WT}$-and $APE1^{K4pleR}$-expressing cells. Moreover, Figure 5B shows a lower amount of abasic DNA lesions accumulated after MMS treatment by the $APE1^{K4pleA}$- as compared with the $APE1^{WT}$-expressing cells. These results suggest that removal of positive charges at Lys 27–35, as exerted by acetylation, may result in a more enzymatically active protein.

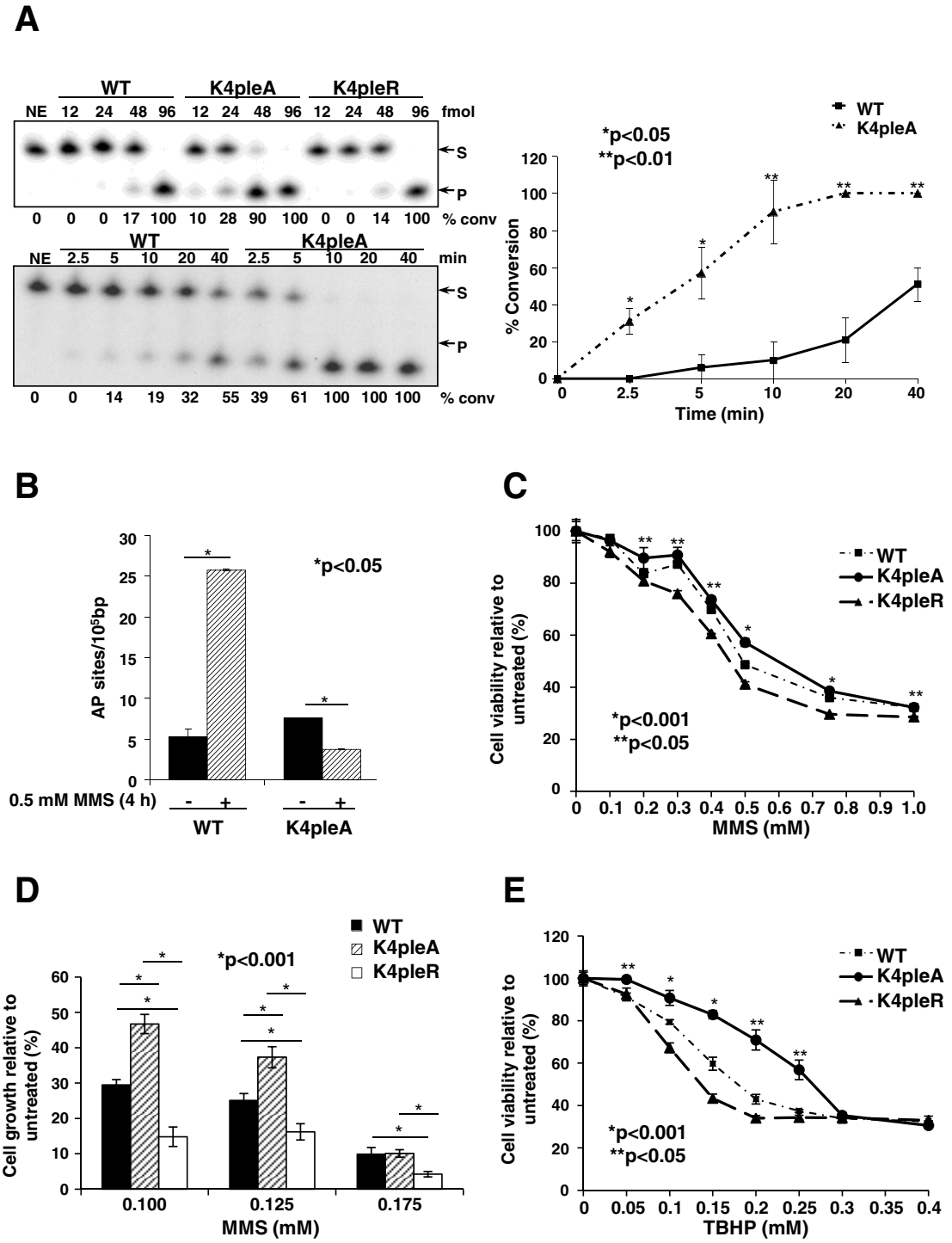

FIGURE 5: Abolition of positively charges $K^{27}/K^{31}/K^{32}/K^{35}$ residues increases APE1 DNA-repair activity. (A) Nuclear extracts from $APE1^{K4pleA}$ mutant present an increased AP endonuclease activity on abasic DNA. AP-site incision activity of the nuclear extracts from HeLa-reconstituted cell clones was tested using an AP endonuclease activity assay as described in *Material and Methods*. The nuclear APE1 content in each clone was precisely quantified through a titration curve obtained using purified recombinant APE1 (Supplemental Figure S4). Nuclear ectopic APE1 protein levels were then normalized between the different cell clones in order to compare their relative enzymatic activities. Top left, concentration-dependent conversion of an AP site–containing DNA substrate (S) to the incised product (P). A representative image of the denaturing polyacrylamide gel of the enzymatic reactions is shown. The amounts (femtomoles) of APE1 used in the reaction and the percentage of substrate converted into product, as determined by standard phosphorimager analysis, are indicated. NE, no cell extract control. Bottom left, time-dependent kinetics of APE1 (2.15 ng) endonuclease activity from nuclear extracts of the different reconstituted cell clones. The image of a representative gel analysis is shown (bottom). Right, graph depicting the time-course kinetics of APE1 from incision results shown on the left. Average values are plotted ± SD of three independent experiments. Asterisks represent a

Cell viability experiments, after MMS treatment, were carried out to verify the enzymatic data. Thus, the effect of $K^{27}/K^{31}/K^{32}/K^{35}$ mutation on cell viability after MMS treatment was measured by 3-(4-5-dimethylthiazol-2-yl)-5-(3-carboxymethoxyphenyl)-2-(4-sulfophenyl)-2H-tetrazolium salt (MTS) and clonogenic assays using the reconstituted cell clones. The MTS data (Figure 5C) showed that the $APE1^{K4pleA}$-mutant–expressing cells were significantly more resistant to MMS treatment than those expressing the nonacetylatable $APE1^{K4pleR}$ mutant. Of note, clonogenic assay experiments (Figure 5D) confirmed these results and highlighted the relevant acetylation occurring at the K residues, as demonstrated by the higher sensitivity of $APE1^{K4pleR}$-expressing cells after MMS treatment. We extended our observations on the protective function of the $APE1^{K4pleA}$ mutant by using *tert*-butyl-hydroperoxide (TBHP) as a reactive oxygen species (ROS) generator (Lazzé *et al.*, 2003). We recently demonstrated that APE1 knockdown sensitizes HeLa cells to TBHP treatment (Li *et al.*, 2012). Therefore we now measured the sensitivity of the different reconstituted cell clones to TBHP in a dose–response experiment (Figure 5E). As in the case of MMS treatment, expression of the $APE1^{K4pleA}$ mutant exerted a protective function with regard to TBHP treatment with respect to $APE1^{WT}$-expressing cells. Similarly to MMS treatment, the $APE1^{K4pleR}$-mutant–expressing clone evidenced even more sensitivity than the $APE1^{WT}$-expressing one. Taken together, these data show that acetylation at residues $K^{27}/K^{31}/K^{32}/K^{35}$ is associated with cell response to DNA damage and confers protection to genotoxic treatment. The increased activity of the $APE1^{K4pleA}$ mutant may explain its proficient protective effect in vivo against genotoxic treatment, even though further explanatory mechanisms, such as its altered protein association in the cell or its possible higher stability (Vascotto *et al.*, 2011), could also be invoked.

K^6/K^7 deacetylation by SIRT1 is modulated by the charged status of $K^{27}/K^{31}/K^{32}/K^{35}$residues

It was recently demonstrated that APE1 K^6/K^7 may undergo acetylation during cell response to genotoxic treatment (Fantini *et al.*, 2008; Yamamori *et al.*, 2010) and that modulation of the acetylation status of these residues through SIRT1 deacetylase activity is important for the regulation of APE1 DNA-repair function after MMS treatment (Yamamori *et al.*, 2010). However, the molecular mechanism regulating the SIRT1-mediated modification at these amino acids during MMS treatment is unknown. We thus checked whether the charged status of $K^{27}/K^{31}/K^{32}/K^{35}$ residues might play a role in modulating the acetylation status of K^6/K^7 through the contribution of SIRT1. First, we evaluated the effect of the modification at $K^{27}/K^{31}/K^{32}/K^{35}$ on the ability of SIRT1 to deacetylate K^6/K^7 in APE1. We found that recombinant purified APE1 protein is nonenzymatically acetylated after incubation with acetyl-CoA, as demonstrated for other proteins (Garbutt and Abraham, 1981). Thus, to obtain a significant amount of acetylated recombinant APE1 protein on K^6/K^7 residues, we treated purified recombinant rAPE1 obtained from *E. coli* with acetyl-CoA, as described in the Supplemental Information. Then we treated in vitro–acetylated $rAPE1^{WT}$, $rAPE1^{K4pleA}$, $rAPE1^{K27/35A,}$ or $rAPE1^{K31/32A}$ with purified recombinant SIRT1 protein and measured the acetylation level on K^6/K^7 through a specific antibody that recognizes only acetylation at these residues (Fantini *et al.*, 2008; Sengupta *et al.*, 2011). Of interest, although $APE1^{WT}$ was efficiently deacetylated by SIRT1 at K^6/K^7 (Figure 6A), the $APE1^{K4pleA}$ mutant did not show any deacetylation in this region; concomitant K-to-A substitutions at positions 27 and 35 ($APE1^{K27/35A}$ mutant) or at positions 31 and 32 ($APE1^{K31/32A}$ mutant) caused an intermediate effect.

We then verified the ability of SIRT1 to directly deacetylate APE1 at $K^{27}/K^{31}/K^{32}/K^{35}$ residues through in vitro deacetylation assays carried out on acetylated purified recombinant $rAPE1^{WT}$ or mutant proteins as substrates (Supplemental Figure S7). Protein acetylation level was monitored by using the anti-$APE1^{K27\text{-}35Ac}$ (Figure 6B). Incubation with recombinant-purified SIRT1 protein revealed a marked decrease in acetyl-APE1 signal but only when $APE1^{WT}$ was used. These data were corroborated by qualitative peptide mapping experiments on in vitro–acetylated $rAPE1^{WT}$ before and after incubation with SIRT1. This analysis demonstrated that SIRT1 was indeed able to deacetylate in vitro–acetylated $rAPE1^{WT}$ at least at $K^{25}/K^{27}/K^{32}$ residues (Supplemental Table S1).

The ability of SIRT1 to deacetylate in vitro APE1 at $K^{27}/K^{31}/K^{32}/K^{35}$ was also analyzed on APE1 (25–38) peptides (Figure 6C), which were chemically synthesized either in their nonacetylated or tetra-acetylated form at these K residues. These peptides were used in a competitive fluorescence-based assay in which a fluorogenic p53 acetylated peptide was used as SIRT1 substrate (Marcotte *et al.*, 2004). As expected, we observed a dose-dependent decrease in the

significant difference between $APE1^{WT}$ and $APE1^{K4pleA}$. (B) Accumulation of genomic abasic (AP) lesions after MMS treatment (0.5 mM, 4 h) of reconstituted cell clones with $APE1^{WT}$ and $APE1^{K4pleA}$ mutant as measured by an aldehyde-reactive probe. $APE1^{WT}$ and $APE1^{K4pleA}$-expressing HeLa cells were grown in medium supplemented with Doxy (10 d) to silence endogenous APE1 expression and were treated with 0.5 mM MMS for 4 h. Counting at the AP sites was performed by using the AP-site quantification kit, as described in *Materials and Methods*. In the histogram, data are expressed as number of AP sites per 10^5 base pairs and represent the mean ± SD of four independent experiments. Asterisks represent a significant difference between the two conditions (untreated and MMS-treated cells). (C) Effects of APE1 acetylation mutants on cell viability after MMS treatment in reconstituted cells. $APE1^{WT}$, $APE1^{K4pleA}$-, and $APE1^{K4pleR}$-expressing cells were grown in medium supplemented with Doxy to silence APE1 endogenous protein and treated with increasing concentrations of MMS for 8 h; the cytotoxic effect of this compound was determined by the MTS assay (see *Materials and Methods* for details). Each point, shown as percentage viability with respect to untreated clones, represents the mean ± SD of four observations, repeated in at least two independent assays. Asterisks represent a significant difference between $APE1^{K4pleA}$ and $APE1^{K4pleR}$ mutants. (D) Cell growth as measured by colony survival assay. One thousand cells of $APE1^{WT}$-, $APE1^{K4pleA}$-, and $APE1^{K4pleR}$-expressing clones treated with increasing concentrations of MMS for 8 h were seeded in Petri dishes and then treated with Doxy for 10 d to silence endogenous APE1. Data, expressed as the percentage of change with respect to untreated clones, are the mean ± SD of three independent experiments. (E) Effects of APE1 acetylation mutants on cell viability after TBHP treatment in $APE1^{WT}$-, $APE1^{K4pleA}$-, and $APE1^{K4pleR}$-expressing cells grown in medium supplemented with Doxy to silence APE1 endogenous protein. Cells were treated with increasing concentrations of TBHP for 6 h, and the cytotoxic effects were determined by the MTS assay. Each point, shown as percentage viability with respect to untreated clones, represents the mean ± SD of four observations, repeated in at least two independent assays. Asterisks represent a significant difference between $APE1^{K4pleA}$ and $APE1^{K4pleR}$ mutants.

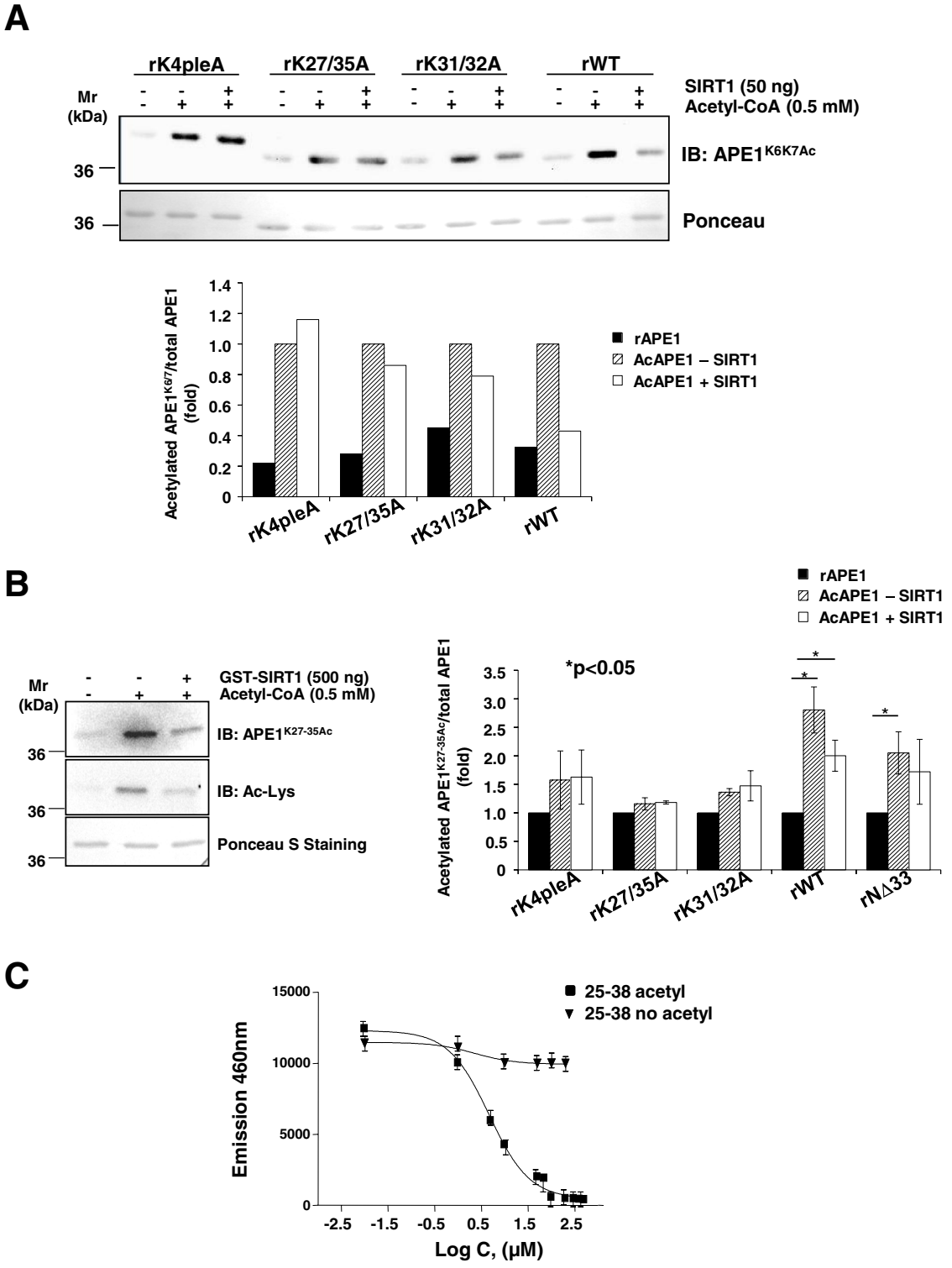

FIGURE 6: SIRT1 deacetylase activity on K^6/K^7 depends on the charged status of $K^{27}/K^{31}/K^{32}/K^{35}$ residues. (A) K^6/K^7 acetylation, modulated by SIRT1, depends on the charged status of $K^{27}/K^{31}/K^{32}/K^{35}$ residues. Western blot analysis on purified recombinant APE1 proteins in vitro acetylated with acetyl-CoA and then incubated in the presence/absence of recombinant GST-SIRT1, as indicated. The analysis was carried out using an antibody specific for acetylated K^6/K^7 APE1 (top). The histogram reports data obtained from densitometric quantification of the bands for each APE1 protein after normalization on Ponceau S staining (bottom). Data shown are the mean of two independent experimental sets whose variation was <10%. (B) SIRT1 deacetylates rAPE1 at $K^{27}/K^{31}/K^{32}/K^{35}$. Left, Western blot analysis on the in vitro–acetylated and deacetylated purified recombinant APE1, further subjected to MS analysis (Supplemental Table S1). $rAPE1^{WT}$ was incubated with 0.5 mM acetyl-CoA and then with recombinant SIRT1 protein, as shown. Samples were separated onto 10% SDS–PAGE, and Western blot analysis was performed by using the anti-$APE1^{K27-35Ac}$ antibody. Ponceau S staining was used as loading control. Right, the histogram shows the densitometric quantification of the

fluorescence signal by using different amounts of the tetra-acetylated peptide (25–38); the nonacetylated counterpart was used as a negative control substrate. Best data fitting was observed with a one-site competition equation, which provided an IC_{50} value of 4.6 ± 0.3 μM. These data support the conclusion that the acetylated APE1 region spanning amino acids 27–35 is a substrate for SIRT1 deacetylase activity. Taken together, these results demonstrate that SIRT1's ability to efficiently deacetylate APE1 at K^6/K^7 residues relies on the presence of positive charges at $K^{27}/K^{31}/K^{32}/K^{35}$. Moreover, SIRT1 is also able to bind and possibly deacetylate in vitro–acetylated APE1 $K^{27}/K^{31}/K^{32}/K^{35}$ residues.

Cross-talk between the charged state of $K^{27}/K^{31}/K^{32}/K^{35}$ and the acetylation status of K^6/K^7 residues through SIRT1

To understand whether SIRT1 activity on acetylated K^6/K^7 residues might be modulated in vivo by MMS as a function of the charged status of $K^{27}/K^{31}/K^{32}/K^{35}$, we performed coimmunoprecipitation experiments on transiently transfected HeLa cells. As shown in Figure 7A, an intact N-terminal domain is required for stable APE1 binding to SIRT1. The APE1/SIRT1 association was induced after MMS treatment and was abolished in the case of both $APE1^{N\Delta33}$ and $APE1^{K4pleA}$ mutants. Substitution of $K^{27}/K^{31}/K^{32}/K^{35}$ residues with nonacetylatable R residues was ineffective, suggesting that SIRT1 binding depends on the presence of positively charged amino acids spanning the APE1 region 27–35. Measurements of K^6/K^7 acetylation status with the specific antibody (performed on the same samples) clearly showed that, in agreement with the binding data, K^6/K^7 residues resulted in more acetylation both under basal and after MMS treatment but only in the case of the $APE1^{K4pleA}$ mutant. In addition, the acetylation status of $APE1^{WT}$ and $APE1^{K4pleR}$, both under basal conditions and after MMS treatment, was comparable (Figure 7B), supporting the existence of cross-talk between the charged status of $K^{27}/K^{31}/K^{32}/K^{35}$ and the acetylation level of K^6/K^7.

We then investigated the cross-talk between K^6/K^7 and $K^{27}/K^{31}/K^{32}/K^{35}$ acetylation status through siRNA experiments. HeLa cell lines stably expressing both endogenous APE1 and $APE1^{WT}$, $APE1^{K4pleA}$, and $APE1^{K4pleR}$ ectopic forms were silenced for SIRT1 expression as described in *Materials and Methods*. The acetylation level of K^6/K^7 was then measured through Western blotting. Data shown in Figure 7C demonstrate that the K^6/K^7 acetylation level of the ectopic APE1 forms was increased ~30–40% upon SIRT1 silencing but only in the case of $APE1^{WT}$- and $APE1^{K4pleR}$-expressing cells, whereas acetylation of K^6/K^7 of $APE1^{K4pleA}$ was <10%. As a control, the acetylation level of endogenous APE1 always increased (~60–70%) upon SIRT1 silencing in all the cell lines tested (unpublished data). Taken together, these data demonstrate that the acetylation/charged status of $K^{27}/K^{31}/K^{32}/K^{35}$ residues controls the stability of the SIRT1/APE1 complex, thus playing a role in the acetylation level of K^6/K^7.

Possible relevance of acetylation for APE1 subnuclear distribution and protein local conformation

The data suggest that a coordinated acetylation/deacetylation dynamic modulated by SIRT1 may occur within the cell nucleus and could be responsible for APE1 subnuclear trafficking. Thus, we examined the subnuclear distribution of SIRT1 on c-myc-SIRT1–transfected cells through immunofluorescence analysis. We found that transiently transfected c-myc-SIRT1 mainly localized in the nucleoplasmic compartment and was not found in the nucleoli (Figure 8A, left); quantification of the endogenous SIRT1 protein in biochemically purified nucleoli confirmed its absence from this subnuclear compartment (Figure 8A, right). Evaluation of the acetylation status of APE1 present in nucleolar or nucleoplasmic fractions under basal conditions showed that APE1 acetylated at K^6/K^7 is mainly present within the nucleoplasm but almost absent in the nucleolus (Figure 8B). Of note, these findings may have important implications for SIRT1-mediated deacetylation at K^6/K^7 and demonstrate the possibility that APE1 acetylation modulates the protein's subnuclear distribution and enzymatic functions, corroborating our previous work (Fantini *et al.*, 2010).

It is known that Lys acetylation may control local conformational stability of proteins, thus affecting their activity, subcellular distribution, and protein–protein interaction network. To examine the effect of acetylation on the local structure of the N-terminal APE1 region, we analyzed the conformational behavior of the protein portion of residues 14–38, which contain $K^{27}/K^{31}/K^{32}/K^{35}$ residues acetylatable in vivo. To this end, we chemically synthesized and purified four peptides bearing differential acetylation at positions 27, 31, 32, and 35 (Supplemental Table S2). To evaluate the effect of acetylation on peptide conformation, we undertook structural analysis of these peptides in solution by far-ultraviolet (UV) circular dichroism (CD) and nuclear magnetic resonance (NMR) spectroscopy. Figure 8C shows the overlay of CD spectra of APE1(14–38) and $APE1(14–38)^{K27/31/32/35Ac}$ in aqueous buffer, indicating a minimum at ~200 nm and a shoulder at ~220 nm. These features suggest the presence of mixed conformational states in which an unfolded state coexists with a certain helical content. The propensity of this domain to adopt helical conformation was also confirmed by trifluoroethanol (TFE) titration experiments (Supplemental Figure S8A). In particular, the CD spectrum of the tetra-acetylated peptide showed a minimum at 220 nm that was deeper than that of the nonacetylated counterpart, suggesting a role for the acetyl groups in determining structural changes in this protein region. An intermediate behavior was observed for the monoacetylated and triacetylated peptides, confirming the role of this K modification in modulating the conformation of the N-terminal APE1 region (unpublished data).

To further address this point, we carried out additional NMR experiments. In aqueous buffer, the one-dimensional (1D) spectra presented poor signal dispersion (Figure 8D, left), confirming a rather disordered state for both the tetra-acetylated and nonacetylated peptides. This observation was further strengthened by the analysis of two-dimensional (2D) [^{1}H, ^{1}H] total correlation spectroscopy (TOCSY) spectra (Griesinger *et al.*, 1988; Figure 8D, middle), and 2D [^{1}H, ^{1}H] rotating frame nuclear Overhauser effect spectroscopy (ROESY) spectra (Bax and Davis, 1985; Figure 8D, right). In the latter case, the presence of a restricted set of cross-peaks in the $_N$H-aliphatic side-chain proton correlation region made unfeasible the process of sequential resonance assignments, as often occurs for small, flexible

band intensities, after normalization to the nonacetylated APE1 form, of the in vitro–acetylated and deacetylated purified APE1 mutants. Data are the mean ± SD of three independent replicates. Asterisks represent a significant difference. (C) The acetylated APE1 25–38 peptide is a substrate of SIRT1 activity. Purified APE1 peptides (25–38) either in fully acetylated form at $K^{27}/K^{31}/K^{32}/K^{35}$ residues or not acetylated were analyzed as competitors in an in vitro deacetylase SIRT1 assay based on a fluorogenic acetylated peptide derived from p53 (region 379–382). Dose–response signals allowed an estimated IC_{50} value of 4.6 ± 0.3 μM of the acetylated APE1 25–38 region with respect to the p53 peptide.

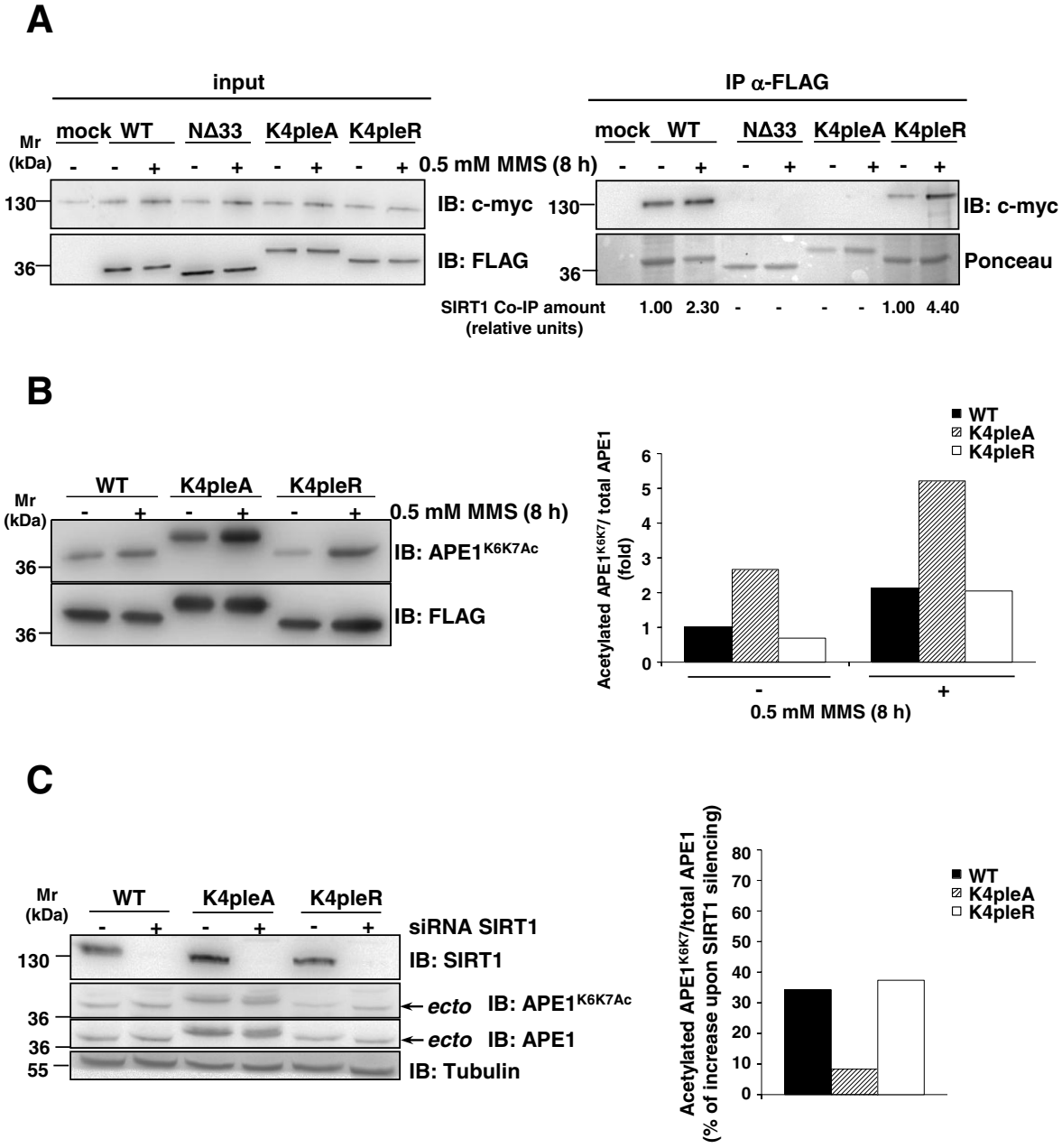

FIGURE 7: Cross-talk between the acetylation status of $K^{27}/K^{31}/K^{32}/K^{35}$ and K^6/K^7 residues through SIRT1. (A) Positive charges at $K^{27}/K^{31}/K^{32}/K^{35}$ residues strongly influence the stability of SIRT1 binding to APE1. Western blot analysis performed on total cell extracts (left) and on immunoprecipitated material (right) from HeLa cells cotransfected with c-myc–tagged SIRT1 and $APE1^{WT}$, $APE1^{N\Delta33}$, $APE1^{K4pleA}$, or $APE1^{K4pleR}$ FLAG-tagged proteins and treated with 0.5 mM MMS for 8 h. Coimmunoprecipitated amounts of SIRT1 normalized with respect to $APE1^{WT}$ or $APE1^{K4pleR}$, respectively, are indicated under each relative bar. Ponceau S staining was used as loading control. (B) Acetylation level of K^6/K^7 in $APE1^{K4pleA}$ mutant is higher than that of $APE1^{WT}$ both under basal conditions and after MMS treatment. Western blot analysis on CoIP material after MMS treatment from HeLa cells transfected with $APE1^{WT}$ and FLAG-tagged mutants is shown. The histogram indicates the relative amount of acetylated $APE1^{K6/K7}$ in the different clones obtained from the densitometric quantification of acetylated APE1 bands, normalized with respect to the amount of APE1 FLAG-tagged immunopurified protein. Data shown are the mean of two independent experimental sets whose variation was <10%. (C) SIRT1 siRNA knockdown increases APE1 K^6/K^7 acetylation. HeLa stable clones expressing $APE1^{WT}$, $APE1^{K4pleA}$, and $APE1^{K4pleR}$ were transfected with siRNA against SIRT1 protein or control siRNA. Western blot analysis was performed to detect differential amount of the acetylated K^6/K^7 APE1 after SIRT1 silencing. Arrows highlight bands of ectopic APE1 protein form; β-tubulin was used as a loading control. The histogram shows densitometric quantification of acetylated K^6/K^7 APE1 form. Data are expressed as percentage of induction of the acetylated K^6/K^7 APE1 after SIRT1 silencing after normalization for the total APE1 protein levels. Data shown are the mean of two independent experimental sets whose variation was <10%.

peptides that tumble very rapidly in solution. On the other hand, a detailed comparison of the 1D NMR data for the nonacetylated and tetra-acetylated APE1 peptides (Figure 8D, left) indicated that acetylation causes a small but clear improvement of spectral dispersion, which can be particularly appreciated in the $_N$H region (Figure 8D, top left). Moreover, the intensity of ROE cross-peaks is increased in the spectra of APE1(14-38)$^{K27/31/32/35Ac}$ peptide as compared with the nonmodified counterpart (Figure 8D, right). This evidence, together with small chemical shift changes, point toward the presence of more organized conformations for the tetra-acetylated peptide in aqueous solution, in agreement with CD data. Similar conclusions are drawn from the analysis of NMR data for APE1(14–38) and APE1(14–38)$^{K27/31/32/35Ac}$ peptides in phosphate:TFE solution (Supplemental Figure S8B), which suggested again the higher propensity of this domain in its acetylated form to adopt a more ordered conformation in contrast to the nonmodified counterpart. Also in this case, monoacetylated and triacetylated peptides showed an intermediate behavior (unpublished data). These data suggest that acetylation may account for local conformational changes on APE1 structure that may modulate its binding ability to different substrates.

DISCUSSION

APE1 is an unusually abundant DNA-repair protein in mammalian cells, with a wide nuclear distribution and an essential role in the BER pathway of DNA lesions (Tell and Wilson, 2010). We calculated that HeLa cells express ~4×10^7 molecules per cell (Supplemental Figure S4A), whereas other enzymes of the BER pathway, such as Pol β or XRCC1, are present at an extent of <1/10 (Demple and DeMott, 2002; Parsons *et al.*, 2008). Therefore APE1 involvement in preformed DNA-repair complexes may only partially explain the energy cost used to maintain such high protein concentration within the cells. Recently we found that APE1 may interact with rRNA and with proteins involved in RNA metabolism and is associated with nucleolar structures through its interaction with NPM1 (Vascotto *et al.*, 2009b; Tell *et al.*, 2010b). Interaction with rRNA and NPM1 strictly depends on the positive charge of K residues within the APE1 region 24–35 placed within the unstructured protein N-terminal domain, as demonstrated by the inability of the corresponding K-to-A mutants (resembling constitutive acetylation at these residues) to stably bind both rRNA and NPM1 (Fantini *et al.*, 2010). Of interest, some of these amino acids (i.e., $K^{27}/K^{31}/K^{32}/K^{35}$), which have been acquired during evolution, may undergo in vivo acetylation (Fantini *et al.*, 2010). We conjectured that, under physiological conditions, nonacetylated APE1 may be stored in the nucleolar compartment through its binding to NPM1 and rRNA, but the in vivo relevance of APE1 nucleolar accumulation was still unclear. This study was aimed at addressing this issue.

We also found that APE1^{K4pleA} binds poorly to NPM1 and rRNA in vivo and as a result is unable to accumulate within the nucleoli, whereas it is present in the nucleoplasm. Moreover, reconstitution of HeLa cells with this mutant gave improved protection from genotoxic damage induced by alkylating agents, such as MMS, and oxidative stress-generating compounds, such as TBHP, through increased DNA-repair activity. As expected for a regulated phenomenon such as the response to a genome insult, an in vivo–augmented acetylation at $K^{27}/K^{31}/K^{32}/K^{35}$ residues was observed during cell response to genotoxic damage. Furthermore, cross-talk involving the SIRT1 deacetylase occurred within cells between acetylation at $K^{27}/K^{31}/K^{32}/K^{35}$ and at K^6/K^7 residues. Therefore we hypothesized that genotoxic stress may shift the equilibrium between the nonacetylated and acetylated APE1 forms toward the latter, which would result in the most enzymatically active one on abasic DNA. This also corresponds to our previous data obtained in vitro with recombinant purified proteins (Fantini *et al.*, 2010). In many cases, the presence of the unstructured N-terminal domain of APE1 seemed essential for interaction of APE1 with different substrates (i.e., nucleic acids or proteins). Interaction also increased after histone deacetylase (HDAC) inhibition, which promotes APE1 acetylation at K^6/K^7 residues (Bhakat *et al.*, 2003; Yamamori *et al.*, 2010). This evidence strongly support the notion that this unstructured domain is responsible for the modulation of APE1's different functions through the recruitment of APE1 in different protein complexes by means of various amino acid side-chain modification events. From an evolutionary perspective, it can be hypothesized that mammalian APE1 activity was made adjustable (through PTMs and/or interaction with other proteins), or expanded toward other substrates, with the acquisition of a protein N-terminus containing positively charged residues, without major modifications on the enzyme catalytic site, which retained the "canonical" function toward abasic DNA. The existence of such an N-terminal extension in only mammals may suggest its evolutionary significance in the face of increased functional complexity. For the noncomplexed protein in solution, the intrinsic lack of a secondary structure associated with this domain can confer functional advantages to mammalian APE1, including the ability to bind to different protein targets (e.g., NPM1, XRCC1, CSB, RNA, etc.; Vidal *et al.*, 2001; Wong *et al.*, 2007; Vascotto *et al.*, 2009a; Tell *et al.*, 2010a), thus allowing efficient control over the thermodynamics in the binding process to different substrates. Because the protein's N-terminus is required for the stabilization of APE1 interaction with NPM1 or rRNA and for the control of the overall endonuclease activity (possibly decreasing the rate of product release once in the positively charged state; Fantini *et al.*, 2010; Figure 5), this region-specific multitasking function can provide a "trigger" for molecular regulation with important biological significance. This should be regarded, however, in light of BER coordination to prevent formation of harmful, unprotected DNA strand breaks. Therefore subcellular distribution of APE1 and its enzymatic activity seem to be finely tuned to demand and in a time-dependent manner through multiple interactions with various protein partners and the coordinated occurrence of different PTMs, such as acetylation and ubiquitination (Busso *et al.*, 2009, 2011). The observation that acetylation at $K^{27}/K^{31}/K^{32}/K^{35}$ residues may favor a transition toward a more organized conformation (Supplemental Figure S8) would support the notion that this modification may significantly modulate the interaction with several protein partners on a structural basis. In addition, acetylation at the mentioned K residues may profoundly affect APE1 protein stability, based on a recent report showing that the same K residues can be also polyubiquitinated by UBR3, targeting the protein for degradation by the proteasome (Meisenberg *et al.*, 2011). Given that acetylation competes with ubiquitination for the same K residues, it may represent the switch for controlling protein turnover rate. In this context, the acetylation at these residues that we observed during cell response to genotoxicants may stabilize protein half-life, thus preventing its degradation.

Few studies have reported on the effect of acetylation on the structure of small, ordered (Hughes and Waters, 2006; Liu and Duan, 2008) and disordered (Smet-Nocca *et al.*, 2010) peptides. Molecular dynamic simulations carried out on a peptide from the histone H3 N-terminal tail in the nonacetylated and doubly acetylated forms revealed that acetylation, although not appreciably disturbing the overall structure of the most-populated states, influenced peptide stability (Liu and Duan, 2008). The effect of acetylation at K residues on the conformational properties of small random-coil peptides from the histone H4 N-terminal tail and from nonhistone thymine DNA glycosylase indicated that acetylation had little effect on the

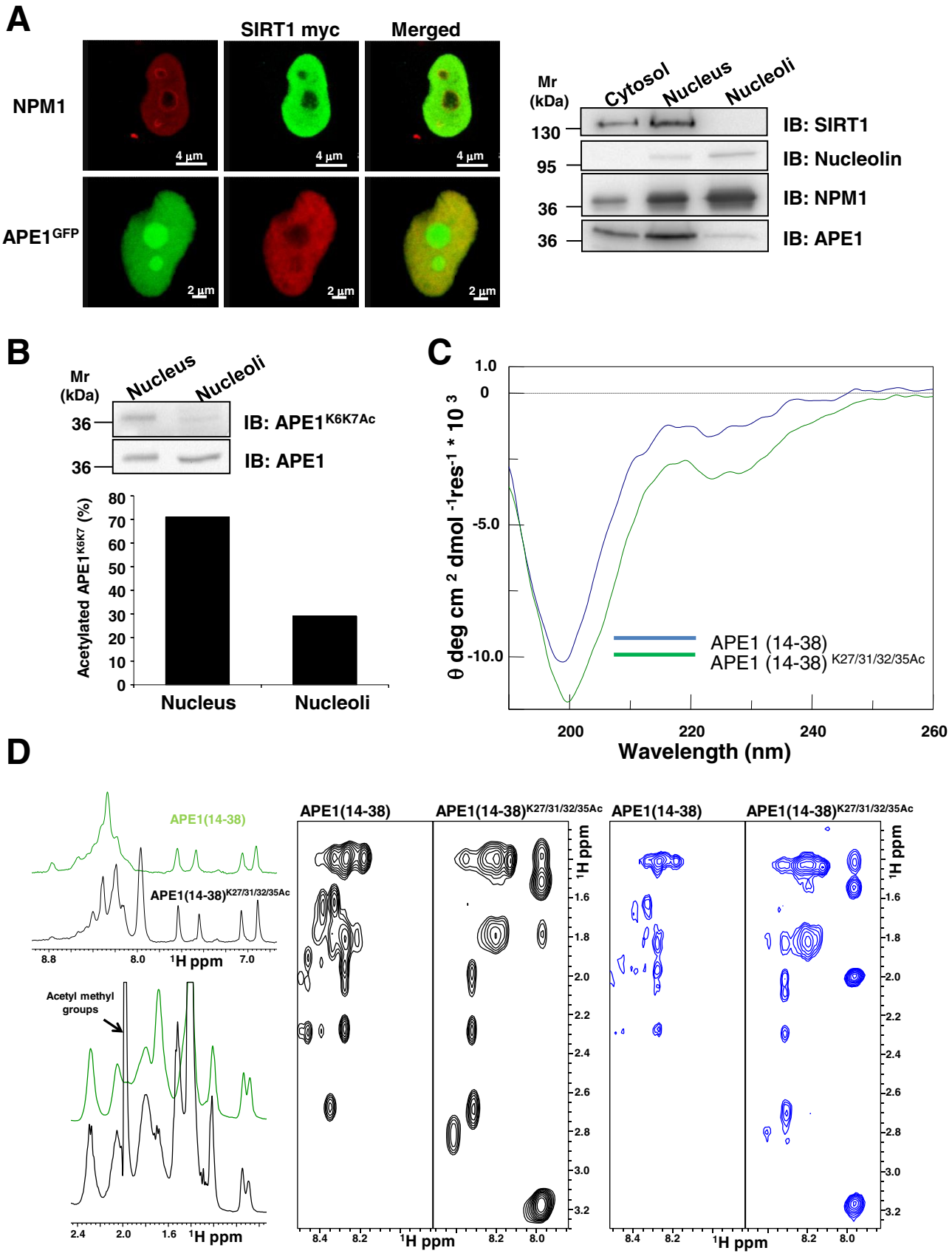

FIGURE 8: Nucleolar APE1 hypoacetylated on K^6/K^7 and conformational impact of acetylation at $K^{27}/K^{31}/K^{32}/K^{35}$ on APE1 local structure. (A) SIRT1 resides within the nucleoplasm of HeLa cells. Left, confocal microscopy of HeLa cells cotransfected with green fluorescent protein–fused APE1 ($APE1^{GFP}$) and c-myc-SIRT1 after fixing and staining with antibodies against NPM1 (red) and c-myc-SIRT1 (top, green; bottom, red). SIRT1, clearly excluded from nucleoli,

overall polypeptide structure, while inducing local conformational changes (Smet-Nocca *et al.*, 2010). In agreement with these studies, APE1(14–38) and APE1(14–38)$^{K27/31/32/35Ac}$ became disordered, as shown by the lack of ROE (Bax and Davis, 1985) cross-peak patterns, which are characteristic of ordered secondary structure elements. However, small differences in the NMR spectra (Figure 8 and Supplemental Figure S8), concerning both chemical shift values and signal intensities, seem to indicate that at least local conformational changes may occur following acetylation. We cannot ignore that these changes may be important for the interaction of APE1 with SIRT1 deacetylase and with NPM1; they highlight the role that the charged status of K residues within this region may play at the protein structural level. Based on our data, it can be speculated that full acetylation of $K^{27–35}$ may reduce SIRT1 binding to APE1, thus delaying its enzymatic activity on K^6/K^7. This mechanism could represent a way to coordinate the kinetics of the overall acetylation status of the protein. According to this hypothesis, SIRT1 should first deacetylate $K^{27–35Ac}$ before deacetylating K^6/K^{7Ac}. Our ability to identify APE1 peptides with varying amounts of acetylation on $K^{27–35}$ supports the existence of a dynamic equilibrium between multiple acetylated forms of the protein within cells and thus its functional regulatory role. Moreover, the presence of SIRT1, found exclusively in the nucleoplasm but not in the nucleoli (similar to the APE1 acetylated on $K^{27–35}$ and the reduced nucleolar presence of APE1 acetylated on K^6/K^7; Figure 8, A and B), suggests that acetylation of APE1 may force its exit from nucleoli to nucleoplasm, where it can be deacetylated by SIRT1. This model is further supported by the significantly reduced interaction of AcAPE1K^{27-35} with NPM1 (Figure 2). Further studies to identify the acetyltransferase able to acetylate APE1 within the nucleoli are in progress. Furthermore, this work supports findings by Yu *et al.* (2010), who demonstrated that these K residue conformational adjustments were concomitant with DNA binding and catalysis or with interaction with Pol β.

The nucleolar role of APE1 storage and regulation, as described here, may have profound biological consequences during cell response to stressor signals, especially in light of recent evidence pointing to the nucleolus as a central hub in DNA damage (Nalabothula *et al.*, 2010). Accordingly, the nucleolus seems responsible for actively transmitting signals to the molecular complex regulating p53 activity mediated by ARF–NPM1 interaction (Colombo *et al.*, 2002; Lee *et al.*, 2005; Nalabothula *et al.*, 2010), and thus it is involved in the maintenance of genome stability. A careful elucidation of the NPM1-ARF-p53 signaling networks and their involvement in the DNA-repair pathway coordinated by APE1 is an important subject for molecular carcinogenesis and deserves further study. This is also underway in our laboratory. Of note, data obtained in this work not only show that nucleoli may act as a storage site so that an appropriate amount of APE1 is readily available for maintenance of genome stability, but also emphasize that nucleolar accumulation of APE1 controls cell proliferation, possibly through its rRNA cleansing function. Compatible with this, APE1^{K4pleA}-expressing cells, under basal conditions, showed impairment in proliferation rate with respect to APE^{WT}-expressing ones (Figure 3). Therefore it can be speculated that nucleolar APE1 is responsible for functional activity of the nucleolus in ribosome biogenesis. APE1 release from the nucleoli after genotoxic treatment may constitute a signal to block active protein synthesis and allow activation of the proper DNA-repair mechanisms. Experiments are in progress along these lines to address this in light of the possibility that acetylation may control the APE1 trafficking from nucleoli to nucleoplasm.

In conclusion, our data shed light on novel molecular aspects highlighting the multifunctional nature of APE1 in regulating different biological outcomes and point to acetylation as an important mechanism for the fine-tuning of protein functions, subcellular distribution, and stability. They also emphasize the need for additional investigation of the APE1 N-terminal domain in order to understand the structural details of the regulatory mechanisms for this multifunctional protein. In addition, recent evidence on APE1 acetylation pattern in triple-negative breast cancer reveals that, concomitantly with total APE1 overexpression, a profound deregulation of APE1 acetylation status occurs under pathological conditions (Poletto *et al.*, 2012). This underscores the biological relevance of our findings and the need for future investigation.

MATERIALS AND METHODS

Inducible APE1 knockdown and generation of APE1 knock-in cell lines

Inducible silencing of endogenous APE1 and reconstitution with mutant proteins in HeLa cell clones was performed as described (Vascotto *et al.*, 2009a,b) and as reported in the Supplemental Information. For inducible shRNA experiments, doxycycline (1 μg/ml; Sigma-Aldrich, St. Louis, MO) was added to the cell culture medium, and cells were grown for 10 d. All biological data were reproduced in at least two different cell clones for each model.

Cell culture and transient transfection with plasmids or siRNA knockdown

HeLa cells were grown in DMEM (Invitrogen, Carlsbad, CA) supplemented with 10% fetal bovine serum (EuroClone, Milan, Italy), 100 U/ml penicillin, and 100 μg/ml streptomycin sulfate. One day

colocalizes with APE1 in the nucleoplasm. The inner part of nucleoli, marked in the granular zone by NPM1, is negative for SIRT1. Right, biochemical isolation of nucleoli confirms that SIRT1 localizes in the nucleoplasmic fraction and it is excluded from nucleoli, where nucleolin, NPM1, and APE1 reside (see *Materials and Methods* for details). Nucleolin was used as a positive control for nuclear and nucleolar compartment. (B) Acetylated K^6/K^7-containing APE1 is enriched within the nucleoplasmic compartment with respect to nucleoli. After normalization for total APE1 protein amount, the levels of acetylated APE1 in nucleolar and nucleoplasmic fractions were analyzed through Western blotting. APE1 acetylated at K^6/K^7 residues is predominately present within the nucleoplasmic fraction, whereas it is reduced in the nucleolar fraction. The histogram indicates the relative percentage amount of acetylated APE1 obtained from the densitometric quantification of acetylated APE1 bands normalized with respect to the amount of total APE1 in each fraction. Each bar represents the mean of two independent experiments whose variation was <10%. (C) CD spectra of the APE1(14–38) and APE1(14–38)$^{K27/31/32/35Ac}$ peptides in 10 mM phosphate buffer, pH 7. (D) Comparison of 1D (left), 2D [^{1}H, ^{1}H] TOCSY (middle), and 2D [^{1}H, ^{1}H] ROESY (right) spectra of APE1(14–38) and APE1(14–38)$^{K27/31/32/35Ac}$ peptides in 10 mM phosphate buffer, pH 7.0. Two different expansions of the proton 1D spectrum are shown; the region between 0.8 and 2.4 ppm, in the lower inset, contains signals from side-chain protons. Acetyl methyl groups originate a peak around 2 ppm, which can be clearly seen in the spectrum of the acetylated peptide; peaks of backbone and side-chain $_N$H atoms appear between 7.0 and 8.8 ppm in the upper inset. For 2D [^{1}H, ^{1}H] TOCSY and 2D [^{1}H, ^{1}H] ROESY experiments the H_N-aliphatic protons correlation region of the spectra are reported.

before transfection, cells were seeded in 10-cm plates at a density of 3.0×10^6 cells/plate. Cells were then transiently transfected with the indicated plasmids using the Lipofectamine 2000 reagent (Invitrogen), according to the manufacturer's instructions. Cells were harvested either 24 or 48 h after transfection, as indicated.

For SIRT1-knockdown experiments, HeLa clones were transfected with 150 nM siRNA siGENOME SMART pool or negative control siRNA 5′-CCAUGAGGUCAUGGUCUGdTdT-3′ (Dharmacon, Lafayette, CO), using Oligofectamine (Invitrogen). After 72 h the cells were harvested.

Preparation of total cell extracts and anti-FLAG coimmunoprecipitation

Preparation of total cell lysates and coimmunoprecipitation analyses were performed as described (Vascotto *et al.*, 2009a,b).

Determination of AP endonuclease activity and abasic site assay

Determination of APE1 AP endonuclease activity was performed using an oligonucleotide cleavage assay, as described previously (Vascotto *et al.*, 2009b) and detailed in the Supplemental Information.

Mass spectrometric analysis of APE1 acetylation

Characterization of APE1 acetylation was performed on the immunopurified protein obtained from APE1-FLAG–expressing HeLa cells (Vascotto *et al.*, 2009b). APE1 was resolved by SDS–PAGE; corresponding protein bands were excised, S-alkylated, and digested with endoprotease AspN (Fantini *et al.*, 2010). Digest aliquots were directly analyzed by nanoLC-ESI-LIT-MS/MS using an LTQ XL mass spectrometer (ThermoFisher Scientific, Waltham, MA) equipped with a Proxeon nanospray source connected to an Easy-nanoLC (ThermoFisher Scientific; Arena *et al.*, 2010; Scippa *et al.*, 2010), and analysis of APE1 acetylation was performed as described (D'Ambrosio *et al.*, 2006) and detailed in the Supplemental Information. A semiquantitative measurement of the amino acid modification was obtained by extracting and integrating nanoLC-ESI-LIT-MS peak areas corresponding to *m/z* values of the modified and nonmodified peptides in the same total ion chromatogram (Salzano *et al.*, 2011). Modification extent was then assayed by evaluating the peak area of the modified peptide with respect to that of the modified peptide plus that of the nonmodified peptide, assuming identical ionization properties for modified and nonmodified species. All these analyses were performed in triplicate.

Antibodies for immunofluorescence and immunoblotting

Antibodies used were anti-NPM1 monoclonal, anti-nucleolin monoclonal (Zymed, Invitrogen), anti-FLAG peroxidase-conjugated, anti-GST peroxidase-conjugated, anti-SIRT1 polyclonal (Abcam, Cambridge, MA), anti–c-myc (Santa Cruz Biotechnology, Santa Cruz, CA), and anti–β-tubulin monoclonal (Sigma-Aldrich). Anti-APE1 monoclonal (Vascotto *et al.*, 2009a) and anti-APE1^{K6K7Ac} (Bhakat *et al.*, 2003) were described previously. Anti-APE1$^{K27\text{-}35Ac}$ polyclonal antibody was generated by PRIMM (Milan, Italy; Poletto *et al.*, 2012).

Western blot analyses

For Western blot analyses, the indicated amounts of cell extracts were resolved in 12% SDS–PAGE and transferred to nitrocellulose membranes (Schleicher & Schuell BioScience, Dassel, Germany). Membranes were blocked with 5% (wt/vol) nonfat dry milk in phosphate-buffered saline (PBS) containing 0.1% (vol/vol) Tween 20 and probed with the indicated antibodies; blots were developed by using the ECL enhanced chemiluminescence procedure (GE Healthcare Piscataway, NJ) or Western Lightning Ultra (PerkinElmer, Waltham, MA). Normalization was performed by using a monoclonal anti-tubulin antibody (Sigma-Aldrich). Blots were quantified by using a Chemidoc XRS video densitometer (Bio-Rad, Hercules, CA).

Plasmids and expression of recombinant proteins

Expression and purification of recombinant proteins from *E. coli* were performed as previously described (Vascotto *et al.*, 2009b; Fantini *et al.*, 2010). Where recombinant proteins were used for in vitro assays, the acronym rAPE1 is used.

GST pull-down assay

A 150-pmol amount of either GST-tagged rAPE1^{WT} or mutant proteins was added to 15 μl of glutathione–Sepharose 4B beads (GE Healthcare), together with equimolar amounts of recombinant NPM1. Binding was performed in PBS, supplemented with 1 mM dithiothreitol (DTT) and 0.5 mM phenylmethylsulfonyl fluoride (PMSF) for 2 h, under rotation, at 4°C. Beads were washed three times with PBS, supplemented with 0.1% (vol/vol) Igepal CA-630 (Sigma-Aldrich), 1 mM DTT, and 0.5 mM PMSF and resuspended in Laemmli sample buffer for Western blot analysis.

DNA–RNA ChIP assays

DNA–RNA ChIP assays were carried out by using a modified version of a protocol described earlier (Gilbert *et al.*, 2000) and as detailed in the Supplemental Information.

Enzymatic fluorescence assays

To examine in vitro deacetylase activity on the acetylated APE1 region 25–38, we used the SIRT Fluorescent Activity Assay Kit (Biomol, Plymouth, PA). Optimizing manufacturer's instructions, we used white plates (OPTI PLATE; PerkinElmer) with 384 wells at reduced volume (total reaction volume, 20 μl). Purified peptides were incubated in 25 mM Tris-HCl, pH 8.0, 2.7 mM KCl, 137 mM NaCl, 1 mM $MgCl_2$, and 1 mg/ml bovine serum albumin containing the enzyme (0.04 U/μl) and 25 μM Fluor de Lys-p53 peptide substrate (Arg-His-Lys-Lys [Ac], from region 379–382 of human p53) in the presence/absence of 250 μM NAD^+ for 30 min at 37°C. Deacetylase activity was measured in arbitrary fluorescence units at 460 nm. Dose–response experiments were carried out by using a 0–500 μM range of peptide concentration. Data fitting was performed using the GraphPad Prism 4 software, version 4.02 (GraphPad, La Jolla, CA). Data were in triplicate/duplicate from three independent assays.

Immunofluorescence confocal and proximity ligation analyses

Immunofluorescence procedures and PLA were carried out as described earlier (Vascotto *et al.*, 2009b, 2011). To study the interaction between APE1 and NPM1 in vivo, we used the in situ Proximity Ligation Assay technology (Olink Bioscience, Uppsala, Sweden). After incubation with monoclonal anti-APE1 (1:50) or anti-FLAG antibody (1:200) for 3 h at 37°C, cells were incubated with polyclonal anti-NPM1 (1:200) overnight at 4°C. PLA was performed following manufacturer's instructions. Technical controls, represented by the omission of anti-NPM1 primary antibody, resulted in the complete loss of PLA signal. Cells were visualized through a Leica TCS SP laser-scanning confocal microscope (Leica Microsystems, Wetzlar, Germany). Determination of PLA signals was performed using BlobFinder software (Center for Image Analysis, Uppsala University, Uppsala, Sweden). PLA technology was also used to detect acetylated APE1 at $K^{27}/K^{31}/K^{32}/K^{35}$ residues. Cells were incubated with the

anti-APE1$^{K27–35Ac}$ rabbit-polyclonal antibody diluted 1:1500 and then with a mouse-monoclonal anti-APE1 antibody (1:27). PLA was subsequently carried out following manufacturer's instructions.

Confocal analyses of APE1-Dendra fusion protein through in vivo live imaging

For in vivo APE1-Dendra trafficking studies, HeLa cells were seated on glass-bottom Petri dishes (thickness #1.5; WillCo Wells, Amsterdam, Netherlands), transfected with APE1-Dendra constructs, and grown in the presence of DMEM without phenol red. A Leica TCS SP laser-scanning confocal microscope was equipped with a heating system (Incubator S) and a CO_2 controller (CTI Controller 3700 digital) to maintain cells in optimal growing conditions. Images were captured 24 h after transfection using a 63× oil fluorescence objective. For Dendra green fluorescence acquisition a 488-nm argon laser was regulated at 10% of power with PTM 750 V.

Cell viability, cell growth, and clonogenic assays

Cell viability was measured by using the MTS assay (Celltiter 96 Aqueous One solution cell proliferation assay; Promega, Madison, WI) on HeLa cells stably expressing APE1^{WT}, APE1^{K4pleA}, and APE1^{K4pleR} proteins grown in 96-well plates. After MMS (Sigma-Aldrich) treatment or TBHP (Sigma-Aldrich), the MTS solution was added to each well and the plates were incubated for 2 h. Absorbance was measured at 490 nm by using a multiwell plate reader. The values were standardized to wells containing media alone.

Cell growth assays were performed as described (Vascotto *et al.*, 2009a,b) and detailed in the Supplemental Information, and clonogenic assays were performed according to Plumb (1999) and essentially as described previously (Vascotto *et al.*, 2009a,b).

Circular dichroism spectroscopy

CD spectra were recorded on a Jasco J-810 spectropolarimeter (Jasco, Tokyo, Japan) at 25°C in the far-UV region from 190 to 260 nm. Each spectrum was obtained by averaging three scans, subtracting contributions from the corresponding blanks, and converting the signal to mean residue ellipticity in units of deg-cm^2 dmol^{-1} res^{-1}. Other experimental settings were 20 nm/min scan speed, 2.0 nm bandwidth, 0.2 nm resolution, 50 mdeg sensitivity, and 4 s response. Peptide concentration was kept at 100 μM, and a 0.1 cm path-length quartz cuvette was used. Spectra were acquired in 10 mM phosphate buffer, pH 7.0, containing various percentages of TFE.

NMR spectroscopy

NMR samples were prepared by dissolving APE1 peptides (1.5–2 mg) either in 600 μl of a 10 mM phosphate buffer, pH 7, containing 10% (vol/vol) D_2O or in a mixture of 10 mM phosphate buffer:2-2-2 trifluorethanol-d3 (98% deuterium; Armar Chemicals, Döttingen, Switzerland) 70:30 (vol/vol). The 2D [^{1}H, ^{1}H] TOCSY spectra (1024 × 256 total data points, 32 scans per t1 increment, 70 ms mixing time; Griesinger *et al.*, 1988) were recorded at 298 K on a Varian ^{UNITY}INOVA 600 spectrometer (Palo Alto, CA) equipped with a cold-probe. The 1D proton (128 scans and a relaxation delay of 1.5 s) and 2D [^{1}H, ^{1}H] ROESY (2048 × 256 total data points, 64 scans per t1 increment, 200 ms mixing time) spectra were acquired at 298 K on a Varian ^{UNITY}INOVA 400 spectrometer provided with *z*-axis pulsed-field gradients and a triple-resonance probe. Water signal was suppressed by means of either double pulsed field gradient selective echo techniques (Dalvit, 1998) or continuous wave irradiation. Varian software VNMRJ 1.1D was implemented for spectral processing. The programs MestRe-C2.3a (Universidade de Santiago de Compostela, Santiago de Compostela, Spain) and NEASY (Bartels *et al.*, 1995; www.nmr.ch) were used for analysis of 1D and 2D NMR data, respectively.

Statistical analyses

Statistical analyses were performed by using the Excel (Microsoft, Redmond, WA) data analysis program for Student's *t* test. $p < 0.05$ was considered as statistically significant.

ACKNOWLEDGMENTS

We thank Paolo Peruzzo for generation of mutant recombinant proteins, K. Irani for providing SIRT1-encoding plasmids, and Pablo Radicella for helpful comments on the manuscript. We also thank Julie Driscol for excellent help in editing the manuscript. This work was supported by the Associazione Italiana per la Ricerca sul Cancro (IG10269) and the Ministero dell'Istruzione, dell'Università e della Ricerca (FIRB_RBRN07BMCT and PRIN2008_CCPKRP_003 to G.T.; PRIN2008_CCPKRP_002 and FIRB2008_RBNE08YFN3_003 to A.S.). This work was also supported by a UICC Yamagiwa-Yoshida Memorial International Cancer Study Grant to G.T. and by the Regione Friulia Venezia Giulia for the Project MINA under the Programma per la Cooperazione Transfrontaliera Italia-Slovenia 2007–2013.

REFERENCES

Arena S, Renzone G, Novi G, Paffetti A, Bernardini G, Santucci A, Scaloni A (2010). Modern proteomic methodologies for the characterization of lactosylation protein targets in milk. Proteomics 10, 3414–3434.

Bapat A, Fishel ML, Kelley MR (2009). Going Ape as an approach to cancer therapeutics. Antioxid Redox Signal 11, 651–668.

Bapat A, Glass LS, Luo M, Fishel ML, Long EC, Georgiadis MM, Kelley MR (2010). Novel small-molecule inhibitor of apurinic/apyrimidinic endonuclease 1 blocks proliferation and reduces viability of glioblastoma cells. J Pharmacol Exp Ther 334, 988–998.

Barnes T, Kim WC, Mantha AK, Kim SE, Izumi T, Mitra S, Lee CH (2009). Identification of apurinic/apyrimidinic endonuclease 1 (APE1) as the endoribonuclease that cleaves c-myc mRNA. Nucleic Acids Res 37, 3946–3958.

Bartels C, Xia T, Billeter M, Gunthert P, Wüthrich K (1995). The program XEASY for computer-supported NMR spectral analysis of biological macromolecules. J Biomol NMR 6, 1–10.

Bax A, Davis DG (1985). Practical aspects of two-dimensional transverse NOE spectroscopy. J Magn Reson 63, 207–213.

Bhakat KK, Izumi T, Yang SH, Hazra TK, Mitra S (2003). Role of acetylated human AP-endonuclease (APE1/Ref-1) in regulation of the parathyroid hormone gene. EMBO J 1, 6299–6309.

Busso CS, Iwakuma T, Izumi T (2009). Ubiquitination of mammalian AP endonuclease (APE1) regulated by the p53-MDM2 signaling pathway. Oncogene 28, 1616–1625.

Busso CS, Wedgeworth CM, Izumi T (2011). Ubiquitination of human AP-endonuclease 1 (APE1) enhanced by T233E substitution and by CDK5. Nucleic Acids Res 39, 8017–8028.

Chattopadhyay R, Wiederhold L, Szczesny B, Boldogh I, Hazra TK, Izumi T, Mitra S (2006). Identification and characterization of mitochondrial abasic (AP)-endonuclease in mammalian cells. Nucleic Acids Res 34, 2067–2076.

Chudakov DM, Lukyanov S, Lukyanov KA (2007). Tracking intracellular protein movements using photoswitchable fluorescent protein PS-CFP2 and Dendra2. Nat Protoc 2, 2024–2032.

Colombo E, Marine JC, Danovi D, Falini B, Pelicci PG (2002). Nucleophosmin regulates the stability and transcriptional activity of p53. Nat Cell Biol 4, 529–533.

Dalvit C (1998). Efficient multiple-solvent suppression for the study of the interaction of organic solvents with biomolecules. J Biomol NMR 11, 437–444.

D'Ambrosio C, Arena S, Fulcoli G, Scheinfeld MH, Zhou D, D'Adamio L, Scaloni A (2006). Hyperphosphorylation of JNK-interacting protein 1, a protein associated with Alzheimer disease. Mol Cell Proteomics 5, 97–113.

Demple B, DeMott MS (2002). Dynamics and diversions in base excision DNA repair of oxidized abasic lesions. Oncogene 21, 8926–8934.

Fantini D *et al.* (2008). APE1/Ref-1 regulates PTEN expression mediated by Egr1. Free Radic Res 42, 20–29.

Fantini D *et al*. (2010). Critical lysine residues within the overlooked N-terminal domain of human APE1 regulate its biological functions. Nucleic Acids Res 38, 8239–8256.
Fung H, Demple B (2005). A vital role for APE1/Ref1 protein in repairing spontaneous DNA damage in human cells. Mol Cell 17, 463–470.
Garbutt GJ, Abraham EC (1981). Non-enzymatic acetylation of human hemoglobins. Biochim Biophys Acta 670, 190–194.
Gilbert SL, Pehrson JR, Sharp PA (2000). XIST RNA associates with specific regions of the inactive X chromatin. J Biol Chem 275, 36491–36494.
Gray MJ, Zhang J, Ellis LM, Semenza GL, Evans DB, Watowich SS, Gallick GE (2005). HIF-1alpha, STAT3, CBP/p300 and Ref-1/APE are components of a transcriptional complex that regulates Src-dependent hypoxia-induced expression of VEGF in pancreatic and prostate carcinomas. Oncogene 24, 3110–3120.
Griesinger C, Otting G, Wüthrich K, Ernst RR (1988). Clean TOCSY for 1H spin system identification in macromolecules. J Am Chem Soc 110, 7870–7872.
Grillo C, D'Ambrosio C, Scaloni A, Maceroni M, Merluzzi S, Turano C, Altieri F (2006). Cooperative activity of Ref-1/APE and ERp57 in reductive activation of transcription factors. Free Radic Biol Med 41, 1113–1123.
Hirota K, Matsui M, Iwata Z, Nishiyama A, Mori K, Yodoi J (1997). AP-1 transcriptional activity is regulated by a direct association between thioredoxin and Ref-1. Proc Natl Acad Sci USA 94, 3633–3638.
Hughes RM, (2006). Effects of lysine acetylation in a beta-hairpin peptide: comparison of an amide-pi and a cation-pi interaction. J Am Chem Soc 128, 13586–13591.
Izumi T, Brown DB, Naidu CV, Bhakat KK, Macinnes V, Saito H, Chen DJ, Mitra S (2005). Two essential but distinct functions of the mammalian abasic endonuclease. Proc Natl Acad Sci USA 102, 5739–5743.
Lazzé MC, Pizzala R, Savio M, Stivala LA, Prosperi E, Bianchi L (2003). Anthocyanins protect against DNA damage induced by tert-butyl-hydroperoxide in rat smooth muscle and hepatoma cells. Mutat Res 535, 103–115.
Lee C, Smith BA, Bandyopadhway K, Gjerset RA (2005). DNA damage disrupts the p14ARF-B23(nucleophosmin) interaction and triggers a transient subnuclear redistribution of p14ARF. Cancer Res 65, 9834–9842.
Li M, Vascotto C, Xu S, Dai N, Qing Y, Zhong Z, Tell G, Wang D (2012). Human AP endonuclease/redox factor APE1/ref-1modulates mitochondrial function after oxidative stress by regulating the transcriptional activity of NRF1. Free Radic Biol Med 53, 237–248.
Liu H, Duan Y (2008). Effects of posttranslational modifications on the structure and dynamics of histone H3 N-terminal Peptide. Biophys J 94, 4579–4585.
Marcotte PA, Richardson PL, Guo J, Barrett LW, Xu N, Gunasekera A, Glaser KB (2004). Fluorescence assay of SIRT protein deacetylases using an acetylated peptide substrate and a secondary trypsin reaction. Anal Biochem 332, 90–99.
Meisenberg C *et al*. (2011). Ubiquitin ligase UBR3 regulates cellular levels of the essential DNA repair protein APE1 and is required for genome stability. Nucleic Acids Res 40, 701–711.
Mitra S, Izumi T, Boldogh I, Bhakat KK, Chattopadhyay R, Szczesny B (2007). Intracellular trafficking and regulation of mammalian AP-endonuclease 1 (APE1), an essential DNA repair protein. DNA Repair 6, 461–469.
Nalabothula N, Indig FE, Carrier F (2010). The nucleolus takes control of protein trafficking under cellular stress. Mol Cell Pharmacol 2, 203–212.
Parlanti E, Locatelli G, Maga G, Dogliotti E (2007). Human base excision repair complex is physically associated to DNA replication and cell cycle regulatory proteins. Nucleic Acids Res 35, 1569–1577.
Parsons JL, Tait PS, Finch D, Dianova II, Allinson SL, Dianov GL (2008). CHIP-mediated degradation and DNA damage-dependent stabilization regulate base excision repair proteins. Mol Cell 29, 477–487.
Pines A, Bivi N, Romanello M, Damante G, Kelley MR, Adamson ED, D'Andrea P, Quadrifoglio F, Moro L, Tell G (2005). Cross-regulation between Egr-1 and APE/Ref-1 during early response to oxidative stress in the human osteoblastic HOBIT cell line: evidence for an autoregulatory loop. Free Radic Res 39, 269–281.
Poletto M, Loreto CD, Marasco D, Poletto E, Puglisi F, Damante G, Tell G (2012). Acetylation on critical lysine residues of apurinic/apyrimidinic endonuclease 1 (APE1) in triple negative breast cancers. Biochem Biophys Res Commun 424, 34–39.
Plumb JA (1999). Cell sensitivity assays: clonogenic assay. Methods Mol 28, 17–23.
Salzano AM, Renzone G, Scaloni A, Torreggiani A, Ferreri C, Chatgilialoglu C (2011). Human serum albumin modifications associated with reductive radical stress. Mol Biosyst 7, 889–898.
Schnell U, Dijk F, Sjollema KA, Giepmans BN (2012). Immunolabeling artifacts and the need for live-cell imaging. Nat Methods 9, 152–158.
Scippa GS, Rocco M, Ialicicco M, Trupiano D, Viscosi V, Di Michele M, Arena S, Chiatante D, Scaloni A (2010). The proteome of lentil (*Lens culinaris* Medik.) seeds: discriminating between landraces. Electrophoresis 31, 497–506.
Seemann S, Hainaut P (2005). Roles of thioredoxin reductase 1 and APE/Ref-1 in the control of basal p53 stability and activity. Oncogene 24, 3853–3863.
Sengupta S, Mantha AK, Mitra S, Bhakat KK (2011). Human AP endonuclease (APE1/Ref-1) and its acetylation regulate YB-1-p300 recruitment and RNA polymerase II loading in the drug-induced activation of multidrug resistance gene MDR1. Oncogene 30, 482–493.
Smet-Nocca C, Wieruszeski JM, Melnyk O, Benecke A (2010). NMR-based detection of acetylation sites in peptides. J Pept Sci 16, 414–423.
Szczesny B, Mitra S (2005). Effect of aging on intracellular distribution of abasic (AP) endonuclease 1 in the mouse liver. Mech Ageing Dev 126, 1071–1078.
Tell G, Crivellato E, Pines A, Paron I, Pucillo C, Manzini G, Bandiera A, Kelley MR, Di Loreto C, Damante G (2001). Mitochondrial localization of APE/Ref-1 in thyroid cells. Mutat Res 485, 143–152.
Tell G, Damante G, Caldwell D, Kelley MR (2005). The intracellular localization of APE1/Ref-1: more than a passive phenomenon. Antioxid Redox Signal 7, 367–384.
Tell G, Fantini D, Quadrifoglio F (2010a). Understanding different functions of mammalian AP endonuclease (APE1) as a promising tool for cancer treatment. Cell Mol Life Sci 67, 3589–3608.
Tell G, Quadrifoglio F, Tiribelli C, Kelley MR (2009). The many functions of APE1/Ref-1: not only a DNA-repair enzyme. Antioxid Redox Signal 11, 601–620.
Tell G, Wilson DM 3rd (2010). Targeting DNA repair proteins for cancer treatment. Cell Mol Life Sci 67, 3569–3572.
Tell G, Wilson DM 3rd, Lee CH (2010b). Intrusion of a DNA repair protein in the RNome world: is this the beginning of a new era. Mol Cell Biol 30, 366–371.
Ueno M, Masutani H, Arai RJ, Yamauchi A, Hirota K, Sakai T, Inamoto T, Yamaoka Y, Yodoi J, Nikaido T (1999). Thioredoxin-dependent redox regulation of p53-mediated p21 activation. J Biol Chem 274, 35809–35815.
Vascotto C *et al*. (2011). Knock-in reconstitution studies reveal an unexpected role of Cys-65 in regulating APE1/Ref-1 subcellular trafficking and function. Mol Biol Cell 22, 3887–3901.
Vascotto C *et al*. (2009a). Genome-wide analysis and proteomic studies reveal APE1/Ref-1 multifunctional role in mammalian cells. Proteomics 9, 1058–1074.
Vascotto C *et al*. (2009b). APE1/Ref-1 interacts with NPM1 within nucleoli and plays a role in the rRNA quality control process. Mol Cell Biol 29, 1834–1854.
Vidal AE, Boiteux S, Hickson ID, Radicella JP (2001). XRCC1 coordinates the initial and late stages of DNA abasic site repair through protein-protein interactions. EMBO J 20, 6530–6539.
Wei SJ, Botero A, Hirota K, Bradbury CM, Markovina S, Laszlo A, Spitz DR, Goswami PC, Yodoi J, Gius D (2000). Thioredoxin nuclear translocation and interaction with redox factor-1 activates the activator protein-1 transcription factor in response to ionizing radiation. Cancer Res 60, 6688–6695.
Weibrecht I, Leuchowius KJ, Clausson CM, Conze T, Jarvius M, Howell WM, Kamali-Moghaddam M, Söderberg O (2010). Proximity ligation assays: a recent addition to the proteomics toolbox. Expert Rev Proteomics 7, 401–409.
Wilson DM 3rd, (2010). Small molecule inhibitors of DNA repair nuclease activities of APE1. Cell Mol Life Sci 67, 3621–3631.
Wong HK, Muftuoglu M, Beck G, Imam SZ, Bohr VA, Wilson DM 3rd (2007). Cockayne syndrome B protein stimulates apurinic endonuclease 1 activity and protects against agents that introduce base excision repair intermediates. Nucleic Acids Res 35, 4103–4113.
Yacoub A, Kelley MR, Deutsch WA (1997). The DNA repair activity of human redox/repair protein APE/Ref-1 is inactivated by phosphorylation. Cancer Res 57, 5457–5459.
Yamamori T, DeRicco J, Naqvi A, Hoffman TA, Mattagajasingh I, Kasuno K, Jung SB, Kim CS, Irani K (2010). SIRT1 deacetylates APE1 and regulates cellular base excision repair. Nucleic Acids Res 38, 832–845.
Yu E, Gaucher SP, Hadi MZ (2010). Probing conformational changes in Ape1 during the progression of base excision repair. Biochemistry 49, 3786–3796.
Ziel KA, Campbell CC, Wilson GL, Gillespie MN (2004). Ref-1/Ape is critical for formation of the hypoxia-inducible transcriptional complex on the hypoxic response element of the rat pulmonary artery endothelial cell VEGF gene. FASEB J 18, 986–988.

Biochemical and Biophysical Research Communications 430 (2013) 523–528

Contents lists available at SciVerse ScienceDirect

Biochemical and Biophysical Research Communications

journal homepage: www.elsevier.com/locate/ybbrc

Role of mutual interactions in the chemical and thermal stability of nucleophosmin NPM1 domains

Daniela Marasco [a,b,*], Alessia Ruggiero [a], Carlo Vascotto [c], Mattia Poletto [c], Pasqualina Liana Scognamiglio [a,b], Gianluca Tell [c], Luigi Vitagliano [a,*]

[a] Institute of Biostructures and Bioimaging, CNR via Mezzocannone 16, I-80134 Napoli, Italy
[b] Department of Biological Sciences, University "Federico II" of Naples, Via Mezzocannone 16, 80134 Naples, Italy
[c] Department of Medical and Biological Sciences, University of Udine, 33100 Udine, Italy

ARTICLE INFO

Article history:
Received 13 November 2012
Available online 8 December 2012

Keywords:
Structure–stability relationships
Acute myeloid leukemia
Protein denaturation
Protein secondary structure content

ABSTRACT

Nucleophosmin (NPM1) is a key factor involved in fundamental biological processes. Mutations involving the NPM1 gene are the most frequent molecular alterations in acute myeloid leukemia. Here we report a biophysical characterization of NPM1 and of its domains in order to gain insights into the role that inter-domain interactions plays in the protein stabilization. Thermal denaturation analyses show that the N-terminal domain is endowed with an exceptional thermal stability, as it does not unfold in the investigated temperature range (20–105 °C). This finding is corroborated by chemical denaturation experiments showing that this domain is not significantly affected by the addition of 8 M urea. These results are consistent with the chaperone function of NPM1. In line with literature data, the other folded domain of the NPM1, a 3-helix bundle domain located at the C-terminus, shows a lower stability. Interestingly, the chemical and thermal stability of this latter domain, which embeds natural mutations related to acute myeloid leukemia, is influenced by the presence of other regions of the protein. Small but significant stabilizations of the C-terminal 3-helix bundle are provided by the adjacent unfolded fragment as well as by the rest of the protein.

1. Introduction

The large majority of proteins are multidomain proteins, as a result of complex gene duplication events [1]. In these proteins, each domain may fulfill its own function independently, or may operate in a concerted manner with its neighbors. For practical reason, most of biochemical and structural studies are concentrated on the analysis of individual domains. Therefore, the mutual influence of individual domains in determining the functional properties of multidomain proteins is an open question in many cases.

Nucleophosmin (NPM1), also known as nucleolar phosphoprotein B23 or numatrin, is a multidomain protein that is implicated in many fundamental biological processes [2,3]. Physiologically, NPM1, despite its nucleolar localization, shuttles constantly across nucleolar, nucleoplasmic and cytoplasmic compartments. This shuttling activity of NPM1 is critical for most of its functions, including regulation of ribosome biogenesis and control of centrosome duplication. Deregulation of NPM1 is implicated in the pathogenesis of several human malignancies. Indeed, NPM1 has been described both as an oncogene and as a tumor suppressor depending on the cell type [4–6]. It is important to note that mutations involving the NPM1 gene are the most frequent molecular alteration in acute myeloid leukemia (AML) accounting for about 60% of cases (i.e. one-third of adult AML) [7].

From the molecular point of view, NPM1 has a modular structure (Fig. 1). The analysis of the protein sequence shows the presence of distinct domains [8]. The N-terminal domain ($NPM1_{N\text{-}Ter}$ residues 1–117) is the oligomerization domain, that plays a crucial role in the molecular chaperone activity of the protein [2]. The high resolution three-dimensional structure of this domain shows that the $NPM1_{N\text{-}Ter}$ pentamer is formed by monomers that fold into an eight-stranded β-barrel with a jellyroll topology [9]. The analysis of the crystal packing has also suggested that $NPM1_{N\text{-}Ter}$ has a propensity to form decamers through the association of two distinct pentamers [9]. These NPM1 oligomers are the structural units that engage in interaction with several proteins including protamines, protamine-like type proteins, APE1/Ref-1, etc. [10,11].

Abbreviations: AML, acute myeloid leukemia; NPM1, Nucleophosmin; NPM1_fl, full length Nucleophosmin; $NPM1_{N\text{-}Ter}$, residues 1–117 of NPM1; $NPM1_{C\text{-}Ter108}$, residues 188–294 of NPM1; $NPM1_{C\text{-}Ter53}$, residues 243–294 of NPM1; $NPM1_{C\text{-}Ter70}$, residues 226–294 of NPM1; $Pep_{225\text{–}243}$, residues 225–243 of NPM1.

* Corresponding authors.
E-mail addresses: daniela.marasco@unina.it (D. Marasco), luigi.vitagliano@unina.it (L. Vitagliano).

0006-291X/$ - see front matter © 2012 Elsevier Inc. All rights reserved.
http://dx.doi.org/10.1016/j.bbrc.2012.12.002

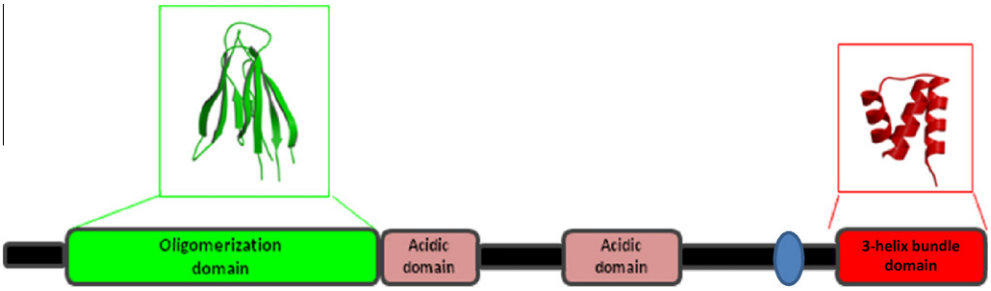

Fig. 1. Schematic organization of NPM1 domains. Models of the folded domains at the N- (residues 9–117) and the C-terminal (residues 243–294) of the protein are reported in the insets. The DNA binding region recently identified by Federici et al. is shown in cyan [13].

The C-terminal region of the protein contains the structural elements responsible for RNA/DNA recognition. NMR investigations have shown that the last 53 C-terminal residues ($NPM1_{C\text{-}Ter53}$) fold in a 3-helix bundle [12]. Interestingly, mutagenesis studies, carried out on the protein region containing last 70 C-terminal residues ($NPM1_{C\text{-}Ter70}$), have shown that the high affinity of NPM1 for DNA is due to the region proceeding the 3-helix bundle (residues 225–243) [13], although it has been recently demonstrated that no direct interaction is established by this fragment with the DNA [14]. The central portion of NPM1 is characterized by the presence of two acid domains (residues 119–133 and 161–188). Finally, the protein contains two nuclear export and two nuclear localization signals.

It is important to note that the interest for this protein is not only dictated by its multiple biological functions. In recent years, this protein, and in particular its C-terminal region $NPM1_{C\text{-}Ter53}$, has been a valuable subject for understanding basic questions related to protein folding and stability [15,16]. In this scenario, we here report an analysis of the thermal and chemical stability of NPM1 full length and some of its domains. Present analyses demonstrate that the N-terminal domain $NPM1_{N\text{-}Ter}$ is endowed with an uncommon thermal stability. Moreover, the completely different secondary structure content of the folded N- and C-terminal domains and the presence of Trp residues exclusively in the C-terminal region of the protein have provided the opportunity to selectively analyze the folding state of different NPM1 domains, and, specifically, to evaluate the stability of the 3-helix bundle in different contexts. Our analysis suggests that the stability of this motif, that embeds mutation sites related to AML, is affected by the rest of the protein.

2. Materials and methods

2.1. Preparation of recombinant NPM1, $NPM1_{N\text{-}Ter}$, and $NPM1_{C\text{-}Ter108}$

NPM1 full-length (NPM1_fl residues 1–294), $NPM1_{N\text{-}Ter}$ (residues 1–117), and $NPM1_{C\text{-}Ter108}$ (residues 188–294) constructs were expressed and purified as HisTag-fusion proteins in *Escherichia coli* BL21(DE3) following or adapting the procedure previously described [11]. The quality of purification was checked by coomassie-stained SDS–polyacrylamide gel electrophoresis (PAGE) analysis. Extensive dialysis against PBS was performed to remove any trace of imidazole from the purified proteins.

2.2. Chemical synthesis of the fragment 225–243 ($Pep_{225–243}$)

The fragment 225–243 (QESFKKQEKTPKTPKGPSS) embedding the K229–K230 motifs, that are essential for the high affinity DNA binding by NPM1, was chemically synthesized. Reagents for peptide synthesis (Fmoc-protected amino acids and resins, activation and deprotection reagents) were from Novabiochem (Laufelfingen, Switzerland) and InBios (Napoli, Italy). Solvents for peptide synthesis and HPLC analyses were from Romil (Dublin, Ireland); reversed phase columns for peptide analysis and the LC–MS system were from ThermoFisher (Milan, Italy). Solid phase peptide syntheses were performed on a fully automated multichannel peptide synthesizer Syro I (Multisynthech, Germany). Preparative RP-HPLC were carried out on a Shimadzu LC-8A, equipped with a SPD-M10 AV detector and with a Phenomenex C18 Jupiter column (50 × 22 mm ID; 10 μm). LC–MS analyses were carried out on a LCQ DECA XP Ion Trap mass spectrometer equipped with a OPTON ESI source, operating at 4.2 kV needle voltage and 320 °C with a complete Surveyor HPLC system, comprised of MS pump, an autosampler and a photo diode array (PDA). Narrow bore 50 × 2 mm C18 BioBasic LC–MS columns were used for these analyses.

The peptide was synthesized employing the solid phase method on a 50 μmol scale following standard Fmoc strategies [17]. Crude product was purified by RP-HPLC applying a linear gradient of 0.1% TFA CH3CN in 0.1% TFA water from 5% to 65% over 12 min using a semi-preparative 2.2 × 5 cm C18 column at a flow rate of 20 mL/min. Peptide purity and identity were confirmed by LC–MS and once purified it was lyophilized and stored at −20 °C until use.

2.3. CD spectroscopy and thermal denaturation

Far-UV CD spectra were recorded on a Jasco J-810 spectropolarimeter (JASCO Corp) in the wavelength interval 195–260 nm. For each spectrum the signal was converted to mean residue ellipticity in units of deg cm^2 $dmol^{-1}$ res^{-1}.

Experiments were performed employing protein concentrations of 16 μM in 50 mM phosphate buffer at pH 7.0, 1 mM DTT using a 0.1 cm path-length quartz cuvette. $Pep_{225–243}$ at 100 μM concentration was tested using the same buffer and identical instrumental experimental conditions.

Thermal denaturation experiments were performed by following the CD signal at 214 nm for $NPM1_{N\text{-}Ter}$ and at 222 nm for NPM1_fl and $NPM1_{C\text{-}Ter108}$.

Data were collected at 0.2 nm resolution, 20 nm/min scan speed, 1.0 nm bandwidth and 4 s response. A Peltier temperature controller was used to set up the temperature of the sample.

2.4. Chemically induced denaturation

A buffer solution containing 50 mM of sodium phosphate (pH 7.0) 1 mM DTT was used in chemical denaturation experiments. Urea was purchased from Sigma and further purified by recrystallization from ethanol/water (1:1) mixtures. Stock solutions of urea were mixed with protein solutions to give a constant final value of the protein concentration (8 μM). The final concentration of denaturant was in the range 0.0–8.0 M. Each sample was incubated overnight. Longer incubation times led to identical spectroscopic signals.

Table 1
Thermodinamic parameters of urea-induced denaturation of NPM1 and of its truncated forms.

	NPM1_fl	$NPM1_{C\text{-}Ter108}$	$NPM1_{C\text{-}Ter70}$*	$NPM1_{C\text{-}Ter53}$*
m Value (kcal mol^{-1} M^{-1})	0.66 ± 0.04	0.99 ± 0.03	0.93 ± 0.16	0.787 ± 0.07
ΔG (kcal mol^{-1})	2.77	3.76	3.49	2.02

* Values are taken from Ref. [13].

Chemical denaturation profiles as a function of urea concentration were followed by fluorescence spectroscopy investigations that were carried out at 25 °C. In order to follow the signal of the Trp residues located in the C-terminal domain, spectra for NPM1_fl and $NPM1_{C\text{-}Ter108}$ were recorded upon excitation at 295 nm. On the other hand, for $NPM1_{N\text{-}Ter,}$ which does not contain Trp residues, an excitation at 280 nm was employed. Spectra were recorded in the 300–400 nm wavelength range using a Varian Cary Eclipse spectrofluorimeter. The determination of the *m* values reported in Table 1 was performed by using the linear extrapolation method (LEM) as described by Pace [18]. ΔG was calculated as $mC_{1/2}$, where $C_{1/2}$ is the concentration of the denaturant at the denaturation midpoint.

3. Results and discussion

3.1. NPM1 overall structure: insights from secondary structure prediction and circular dichroism studies

Previous literature studies have highlighted the modular domain organization of NPM1. Two structured domains at the N- and the C-terminus have been identified. Interestingly these domains are characterized by different types of secondary structure elements (Fig. 1). Indeed, the N-terminal folded domain (∼residues 1–117) assumes essentially a β-structure [9], whereas the C-terminal folded domain (residues 243–294) forms a well defined right handed 3-helix bundle [12].

In order to check the presence of additional structured domains within the protein, we performed a secondary structure prediction session on NPM1 sequence by using the PSIPRED server (http://bioinf.cs.ucl.ac.uk/psipred/). As shown in Fig. S1, the program predicts the occurrence of several β-strands in the 15–120 region of the protein, in agreement with the structural data reported on the N-terminal oligomerization domain. In line with previous observations [13], the server provides a convincing prediction of helical regions that form the C-terminal bundle. These findings proved the reliability of the prediction method employed in this analysis. As shown in Fig. S1, PSIPRED also predicts that the central region of the protein is essentially unfolded, as only minor and sporadic secondary structure elements with a low level of confidence are detected. No secondary structure elements is detected in the region 225–243 (QESFKKQEKTPKTPKGPSS) preceding the three helix bundle, which contains the motif responsible for the high affinity DNA binding. The analysis of the circular dichroism spectrum of $Pep_{225\text{–}243}$ confirms that this fragments is intrinsically unfolded since it presents a single minimum below 200 nm (Fig. 2A). This observation is in line with the very recent finding that this region is disordered in the NMR structure of $NPM1_{C\text{-}Ter70}$ [14].

The circular dichroism spectrum of the full-length protein NPM1_fl registered at 20 °C in the far-UV exhibits a rather sharp minimum centered at 205 nm and a broader one at 222 nm (Fig. 2B). These features are indicative of the presence of both α and β secondary structure elements. A quantitative estimation of the secondary structure content, performed by using the software distributed with the Jasco-810 spectropolarimeter, suggests that the α-helix and the β-sheet contents are 14% and 34%, respectively.

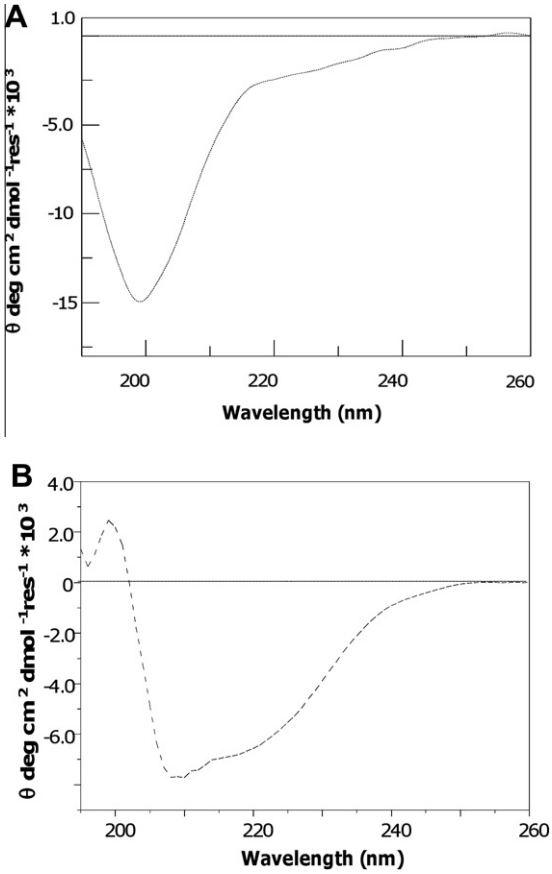

Fig. 2. CD spectra registered at 20 °C of the synthetic $Pep_{225\text{–}243}$ (A) and NPM1_fl (B) in 50 mM phosphate buffer 50 mM (pH = 7).

These values are in line with those derived from the crystallographic structures of the N- and C-terminal domains and by assuming that the central region is unfolded. Under this hypothesis, the number of residues in α-helix and in β-sheet is 45 and 75, respectively. Taking into account the total number of the residues in the protein (294) the α-helix and the β-sheet content is 15% and 26%.

Altogether these results corroborate the notion that the modular structure of NPM1 is characterized by regions endowed with distinct structural properties. Indeed, an unfolded central region separates two folded domains displaying different secondary structure elements. This feature has been here exploited to follow the behavior of a single domain in the context of the entire protein.

3.2. The N-terminal domain of NPM1 is endowed with a remarkable structural stability

In line with literature crystallographic data, the CD spectrum of NPM1 N-terminal domain (residues 1–117 and hereafter denoted as $NPM1_{N\text{-}Ter}$), characterized by the presence of a single minimum at 214 nm, is suggestive of domain assuming a β structure (Fig. 3). The analysis of $NPM1_{N\text{-}Ter}$ CD spectra as a function of temperature clearly indicates that the protein is stable over a wide range of temperatures. Indeed, no significant variations of the spectra are detected in the interval 20–90 °C (Fig. 3A). Moreover, the signal at the minimum (214 nm) does not display any significant variation up to 105 °C (Fig. 3A). The remarkable thermal stability of this domain is in line with the chaperone function of NPM1. Indeed, previous literature studies have unveiled the ability of this protein to protect several proteins from aggregation and to preserve their activity at high temperatures.

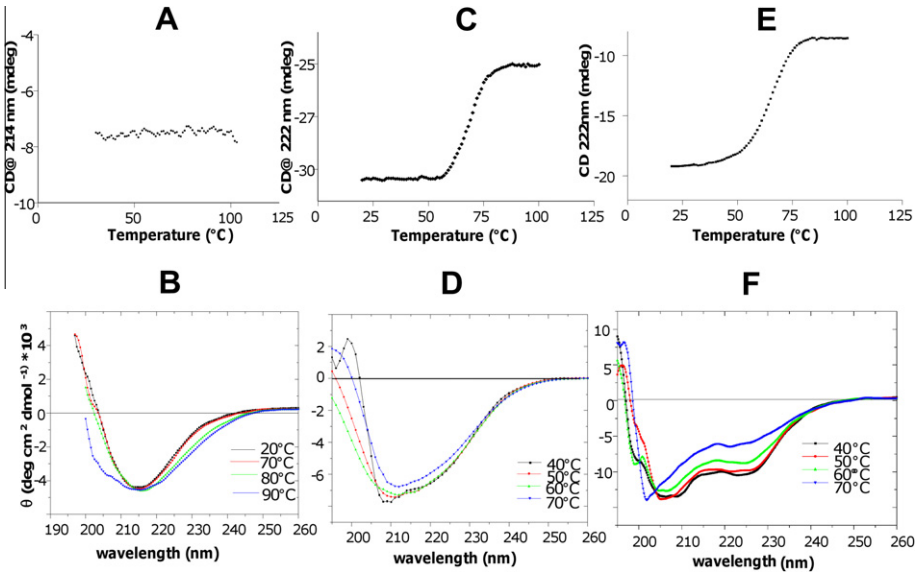

Fig. 3. Thermally induced denaturation of NPM1$_{N\text{-}Ter}$, NPM1_fl, NPM1$_{C\text{-}Ter108}$, in the presence of 50 mM sodium phosphate buffer (pH 7.0) and 1 mM DTT. Panels (A, C, and E) report the evolution of the CD signal as function of temperature for NPM1$_{N\text{-}Ter}$, NPM1_fl, NPM1$_{C\text{-}Ter108}$, respectively. Panels (B, D, and F) report the overlay of CD spectra recorded at different temperatures for NPM1$_{N\text{-}Ter}$, NPM1_fl, NPM1$_{C\text{-}Ter108}$, respectively.

3.3. Thermal stability of full-length NPM1and NPM1$_{C\text{-}Ter108}$

The dependence of NPM1_fl CD spectra with temperature is reported in Fig. 3C. A clear transition is detected at 68.3 °C. Interestingly, the protein presents a significant level of residual secondary structure upon heating (Fig. 3D). Taking into account the high thermal stability of NPM1$_{N\text{-}Ter}$, these data may be interpreted by assuming that the observed transition corresponds to the unfolding of the C-terminal domain of the protein. Literature data carried out on the isolated C-terminal 3-helix bundle NPM1$_{C\text{-}Ter53}$, under the same experimental conditions here employed to characterize the full-length protein, indicate an unfolding temperature below 60 °C (see Fig. 2 of Ref. [16]). Altogether, these observations suggest that the 3-helix bundle is stabilized in the protein context by approximately 10 °C. To identify the structural determinant of this stabilization, we performed thermal denaturation analysis on a domain containing the last 108 C-terminal residues (NPM1$_{C\text{-}Ter108}$) that follows the second acidic region of the protein. Therefore, NPM1$_{C\text{-}Ter108}$ includes, in addition to the 3-helix bundle, residues 223–245 implicated in the high affinity binding of DNA as well as the fragment 188–222. As shown in Fig. 3E, NPM1$_{C\text{-}Ter108}$ presents a Tm of 64.3 °C, a value that is intermediate between those displayed by NPM1$_{C\text{-}Ter53}$ and NPM1_fl. This finding indicates that the presence of both the fragment 188–243 and the N-terminal regions of the protein induce a stabilization of the C-terminal 3-helix bundle.

3.4. Chemical stability of NPM1$_{N\text{-}Ter}$, NPM1_fl, and NPM1$_{C\text{-}Ter108}$

The chemical stability of NPM1 domains was checked by using urea as denaturant. For NPM1$_{N\text{-}Ter}$, upon the addition of urea, spectra were recorded after an excitation at 280 nm to measure the fluorescence signal of the three Tyr residues located in this domain (positions 17, 29, and 67). These denaturation experiments confirmed the uncommon stability of the NPM1$_{N\text{-}Ter}$ domain highlighted by the thermal analyses. Indeed, as shown in Fig. 4A and B, no significant variation of the fluorescence signal was detected after the addition of the denaturant. Moreover, the maximum of the fluorescence signal, located at ~310 nm, suggests that the three Tyr residues are buried in the entire range of urea concentration tested (0–8 M).

The particular distribution of Trp residues, that are exclusively located in the C-terminal region of the protein (positions 288 and 290), allows the evaluation of the folding state of the C-terminal domain in different contexts. Indeed, *ad hoc* excitation of Trp residues (using a radiation with a 295 nm wavelength) could provide information about their local environments independently from the presence of other protein domains. As shown in Fig. 4C, both the intensity and the wavelength of the peak of the fluorescence signal exhibited by NPM1_fl are strongly affected by the addition of the denaturant. The comparison of the spectra of samples containing the protein incubated with either 0 or 8 M urea shows a clear increase of the peak intensity and a shift of its wavelength to higher values. The shift of the wavelength of the maximum from 325 to 355 nm is indicative of a process in which the initially buried Trp residues are fully exposed after the addition of 8 M urea. The analysis of the progression of the increase of the peak intensity upon denaturant addition shows that denaturation midpoint ($C_{1/2}$) occurs at [urea] = 4.2 M (Fig. 4D).

In analogous experiments (Fig. 4E and F), the $C_{1/2}$ exhibited by NPM1$_{C\text{-}Ter108}$ against urea denaturation is 3.8 M. This value is virtually coincident with that found for NPM1$_{C\text{-}Ter70}$ in experiments carried out by following the CD signal at 222 nm [13]. On the other hand, literature data show that NPM1$_{C\text{-}Ter53}$ presents a much lower value for $[urea]_{1/2}$ 2.6 M.

Taken together these findings show that the presence of the fragment 225–243 and the N-terminal regions significantly stabilizes the terminal 3-helix bundle also against chemical denaturants. The similar stability exhibited by NPM1$_{C\text{-}Ter70}$ and NPM1$_{C\text{-}Ter108}$ suggests that the fragment 188–225 does not provide any further contribution to the 3-helix bundle stability.

The similarity of the denaturation process of NPM1$_{C\text{-}Ter108}$ and NPM1$_{C\text{-}Ter70}$ is also confirmed by the analysis of the *m* values and ΔG values reported in Table 1 Notably, NPM1_fl presents a lower *m* value when compared to the truncated forms. Since the *m* value is related to the change in solvent accessible surface area upon denaturation, this observation suggests that the other regions of the protein (the N-terminal domains and/or the central acidic region) influences the denaturated state of the C-terminal domain.

In conclusion, present investigations show that the individual domains of NPM1 are endowed with different stabilities. Indeed, the N-terminal domain is endowed with an extraordinary stability

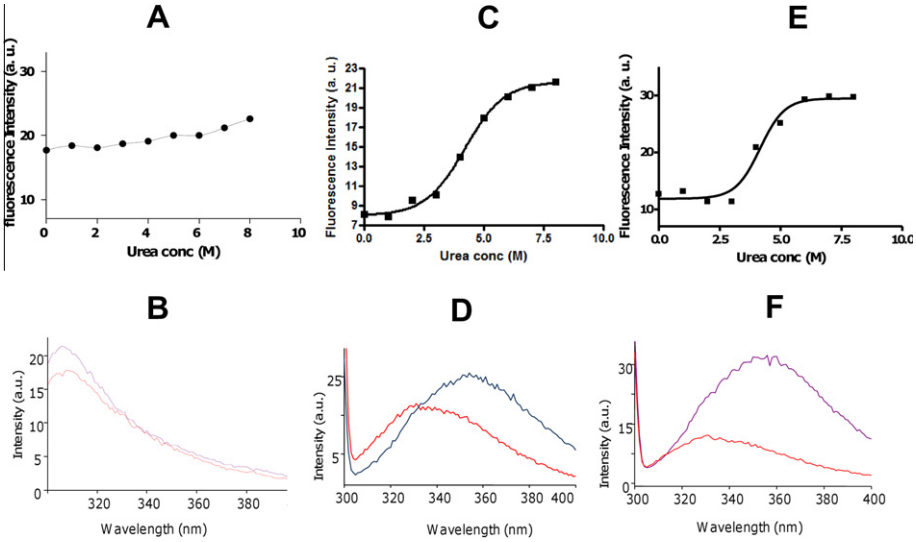

Fig. 4. Effect of urea incubation for for $NPM1_{N\text{-}Ter}$, NPM1_fl, $NPM1_{C\text{-}Ter108}$, followed at pH 7.0 and 25 °C in the presence of 50 mM sodium phosphate buffer (pH 7.0) and 1 mM DTT. (A) Tyr fluorescence upon excitation at 280 nm after the treatment with urea in the concentration range 0–8 M for $NPM1_{N\text{-}Ter}$. (B) Overlay of fluorescence spectra at of $NPM1_{N\text{-}Ter}$ sample untreated (red) or incubated with 8 M urea (blue). Panels (C and E) Trp fluorescence upon excitation at 295 nm after the treatment with urea in the concentration range for NPM1_fl and $NPM1_{C\text{-}Ter108}$, respectively. (D and F) Overlay of the fluorescence spectra at of the protein sample untreated (red) or incubated with 8 M urea (blue) for NPM1_fl, and $NPM1_{C\text{-}Ter108}$, respectively. (For interpretation of the references to color in this figure legend, the reader is referred to the web version of this article.)

against both urea and temperature. These observations are in line with the chaperone role of this domain highlighted by literature reports [3,19,20]. On the other hand, present and literature data indicate that the C-terminal 3-helix bundle, which embeds natural mutations causing severe human diseases, undergoes thermal transitions in the temperature range 55–70 °C, depending on the presence of additional protein regions in the investigated constructs. Particularly significant is the increase of the thermal stability of this domain likely due to the presence of the proximal fragment 225–243. Although present data show that this latter region is intrinsically unfolded and that this fragment is disordered in $NPM1_{C\text{-}Ter70}$ [14], it confers an extra stability to the bundle of about 8 °C. The presence of the remaining regions of the protein confers further stability to the C-terminal domain. Similar results have been obtained by performing chemical denaturation experiments. Present results suggest that the effects of natural mutations linked to severe diseases located in NPM1 C-terminal domain should be evaluated in vitro by considering the entire protein or at least the C-terminal fragment 225–294. On more general basis, the common practice of dissecting multi-domain proteins into small fragments may, in some circumstances, be an oversimplification that can lead to artifactual interpretations of the results.

Acknowledgments

This work was financially supported by MIUR (FIRB RBRN07BMCT) and by AIRC (IG10269) to G.T. The authors thank Giuseppe Perretta for skilful technical assistance.

Appendix A. Supplementary data

Supplementary data associated with this article can be found, in the online version, at http://dx.doi.org/10.1016/j.bbrc.2012.12.002.

References

[1] G. Apic, J. Gough, S.A. Teichmann, Domain combinations in archaeal, eubacterial and eukaryotic proteomes, Journal of Molecular Biology 310 (2001) 311–325.

[2] M. Okuwaki, The structure and functions of NPM1/Nucleophsmin/B23, a multifunctional nucleolar acidic protein, Journal of Biochemistry 143 (2008) 441–448.

[3] L.J. Frehlick, J.M. Eirin-Lopez, J. Ausio, New insights into the nucleophosmin/nucleoplasmin family of nuclear chaperones, BioEssays: news and reviews in molecular, Cellular and Developmental Biology 29 (2007) 49–59.

[4] M.J. Lim, X.W. Wang, Nucleophosmin and human cancer, Cancer Detection and Prevention 30 (2006) 481–490.

[5] S. Grisendi, C. Mecucci, B. Falini, P.P. Pandolfi, Nucleophosmin and cancer, Nature Reviews Cancer 6 (2006) 493–505.

[6] S. Grisendi, R. Bernardi, M. Rossi, K. Cheng, L. Khandker, K. Manova, P.P. Pandolfi, Role of nucleophosmin in embryonic development and tumorigenesis, Nature 437 (2005) 147–153.

[7] B. Falini, I. Gionfriddo, F. Cecchetti, S. Ballanti, V. Pettirossi, M.P. Martelli, Acute myeloid leukemia with mutated nucleophosmin (NPM1): any hope for a targeted therapy?, Blood Reviews 25 (2011) 247–254

[8] K. Hingorani, A. Szebeni, M.O. Olson, Mapping the functional domains of nucleolar protein B23, The Journal of Biological Chemistry 275 (2000) 24451–24457.

[9] H.H. Lee, H.S. Kim, J.Y. Kang, B.I. Lee, J.Y. Ha, H.J. Yoon, S.O. Lim, G. Jung, S.W. Suh, Crystal structure of human nucleophosmin-core reveals plasticity of the pentamer–pentamer interface, Proteins 69 (2007) 672–678.

[10] D. Fantini, C. Vascotto, D. Marasco, C. D'Ambrosio, M. Romanello, L. Vitagliano, C. Pedone, M. Poletto, L. Cesaratto, F. Quadrifoglio, A. Scaloni, J.P. Radicella, G. Tell, Critical lysine residues within the overlooked N-terminal domain of human APE1 regulate its biological functions, Nucleic Acids Research 38 (2010) 8239–8256.

[11] C. Vascotto, D. Fantini, M. Romanello, L. Cesaratto, M. Deganuto, A. Leonardi, J.P. Radicella, M.R. Kelley, C. D'Ambrosio, A. Scaloni, F. Quadrifoglio, G. Tell, APE1/Ref-1 interacts with NPM1 within nucleoli and plays a role in the rRNA quality control process, Molecular and Cellular Biology 29 (2009) 1834–1854.

[12] C.G. Grummitt, F.M. Townsley, C.M. Johnson, A.J. Warren, M. Bycroft, Structural consequences of nucleophosmin mutations in acute myeloid leukemia, The Journal of Biological Chemistry 283 (2008) 23326–23332.

[13] L. Federici, A. Arcovito, G.L. Scaglione, F. Scaloni, C. Lo Sterzo, A. Di Matteo, B. Falini, B. Giardina, M. Brunori, Nucleophosmin C-terminal leukemia-associated domain interacts with G-rich quadruplex forming DNA, The Journal of Biological Chemistry 285 (2010) 37138–37149.

[14] A. Gallo, C. Lo Sterzo, M. Mori, A. Di Matteo, I. Bertini, L. Banci, M. Brunori, L. Federici, Structure of nucleophosmin DNA-binding domain and analysis of its complex with a G-quadruplex sequence from the c-MYC promoter, The Journal of Biological Chemistry (2012).

[15] F. Scaloni, L. Federici, M. Brunori, S. Gianni, Deciphering the folding transition state structure and denatured state properties of nucleophosmin C-terminal domain, Proceedings of the National Academy of Sciences of the United States of America 107 (2010) 5447–5452.

[16] F. Scaloni, S. Gianni, L. Federici, B. Falini, M. Brunori, Folding mechanism of the C-terminal domain of nucleophosmin: residual structure in the denatured state and its pathophysiological significance, FASEB Journal: Official

Publication of the Federation of American Societies for Experimental Biology 23 (2009) 2360–2365.
[17] G.B. Fields, R.L. Noble, Solid phase peptide synthesis utilizing 9-fluorenylmethoxycarbonyl amino acids, International Journal of Peptide and Protein Research 35 (1990) 161–214.
[18] C.N. Pace, K.L. Shaw, Linear extrapolation method of analyzing solvent denaturation curves, Proteins (Suppl. 4) (2000) 1–7.
[19] M. Okuwaki, K. Matsumoto, M. Tsujimoto, K. Nagata, Function of nucleophosmin/B23, a nucleolar acidic protein, as a histone chaperone, Fatigue of Engineering Materials and Structures Letters 506 (2001) 272–276.
[20] A. Szebeni, M.O. Olson, Nucleolar protein B23 has molecular chaperone activities, Protein Science: A Publication of the Protein Society 8 (1999) 905–912.

Biochem. J. (2013) **452**, 545–557 (Printed in Great Britain) doi:10.1042/BJ20121277

Role of the unstructured N-terminal domain of the hAPE1 (human apurinic/apyrimidinic endonuclease 1) in the modulation of its interaction with nucleic acids and NPM1 (nucleophosmin)

Mattia POLETTO*, Carlo VASCOTTO*, Pasqualina L. SCOGNAMIGLIO†‡, Lisa LIRUSSI*, Daniela MARASCO†‡ and Gianluca TELL*[1]

*Department of Medical and Biological Sciences, University of Udine, 33100 Udine, Italy, †Department of Pharmacy, CIRPEB (Centro Interuniversitario di Ricerca sui Peptidi Bioattivi), University of Naples 'Federico II', 80134 Naples, Italy, and ‡Institute of Biostructures and Bioimaging CNR, 80134 Naples, Italy

The hAPE1 (human apurinic/apyrimidinic endonuclease 1) is an essential enzyme, being the main abasic endonuclease in higher eukaryotes. However, there is strong evidence to show that hAPE1 can directly bind specific gene promoters, thus modulating their transcriptional activity, even in the absence of specific DNA damage. Recent findings, moreover, suggest a role for hAPE1 in RNA processing, which is modulated by the interaction with NPM1 (nucleophosmin). Independent domains account for many activities of hAPE1; however, whereas the endonuclease and the redox-active portions of the protein are well characterized, a better understanding of the role of the unstructured N-terminal region is needed. In the present study, we characterized the requirements for the interaction of hAPE1 with NPM1 and undamaged nucleic acids. We show that DNA/RNA secondary structure has an impact on hAPE1 binding in the absence of damage. Biochemical studies, using the isolated N-terminal region of the protein, reveal that the hAPE1 N-terminal domain represents an evolutionary gain of function, since its composition affects the protein's stability and ability to interact with both nucleic acids and NPM1. Although required, however, this region is not sufficient itself to stably interact with DNA or NPM1.

Key words: apurinic/apyrimidinic endonuclease 1 (APE1), nucleophosmin (NPM1), protein–DNA interaction, protein–protein interaction, phylogenesis.

INTRODUCTION

The hAPE1 [human APE1 (apurinic/apyrimidinic endonuclease 1)] is an essential and multifaceted protein involved in the DNA BER (base excision repair) pathway and in the regulation of gene expression, acting both as a redox co-activator for several transcription factors and as a transcriptional repressor on nCaRE (negative calcium response elements)-containing promoters [1–3]. These biological activities are located in two distinct, but partially overlapping, regions. The conserved C-terminal portion (residues 61–318) is responsible for the enzymatic activity on abasic DNA, whereas the N-terminal domain (residues 1–127) is mainly devoted to the redox co-activating function towards different transcription factors such as Egr1 (early growth response 1), NF-κB (nuclear factor κB) and p53 [4,5]. The mechanisms of hAPE1 binding and recognition of its canonical substrate, the abasic site containing DNA, have been thoroughly investigated by several laboratories [6–8]. However, the notion that hAPE1 is constitutively bound to undamaged nucleic acids is getting stronger. Examples include the interaction of the protein with genomic regions, such as the nCaRE sequences [2] or the *MDR1* (multidrug resistance protein 1) gene promoter [9], and the reported association of hAPE1 with undamaged RNA [10]. Acquisition of particular secondary structures (i.e. bulges, hairpins, cruciforms, quadruplex etc.) by nucleic acids and their regulatory roles *in vivo* are a well-known paradigm in molecular biology. A previous study has carefully explored the interaction between hAPE1 and undamaged nucleic acids [11]; nonetheless, potential impacts of the secondary structure of the nucleic acid on the binding affinity of hAPE1 have never been investigated.

In the last few years, an unexpected involvement of hAPE1 in RNA metabolism has been unveiled: the protein is accumulated within nucleoli through interaction with NPM1 (nucleophosmin; also known as nucleolar phosphoprotein B23) and rRNA and affects cell growth by directly acting on the RNA quality control mechanisms [10,12,13]. Notably, the N-terminal domain of hAPE1 (the first 43 residues) plays a pivotal role in this non-canonical function of the protein, serving as an adaptable device for protein–protein interactions and modulating its enzymatic activity on abasic DNA, as well as its binding to RNA molecules. Although many studies have thoroughly characterized the structure of the hAPE1 C-terminal globular domain, only a few have addressed the role of its N-terminal extension, perhaps as a consequence of its intrinsic disordered folding [14–16]. A basic cluster of lysine residues located within this region (Lys^{25}–Lys^{35}) controls the binding affinity of hAPE1 for both NPM1 and nucleic acids. Furthermore, several strands of evidence suggest that the different functions of hAPE1 might be rapidly modulated *in vivo* by post-translational modifications on its N-terminal domain, such as ubiquitination, acetylation and proteolysis [2,17–21]. Interestingly, whereas the C-terminal portion of the protein shares extensive similarity with most of its orthologue counterparts, from *Escherichia coli* to mammals, its N-terminal extension is considerably less conserved. The importance of this protein region in modulating the many activities of hAPE1 suggests that the N-terminal domain may be a recent acquisition during evolution

Abbreviations used: APE1, apurinic/apyrimidinic endonuclease 1; BER, base excision repair; DSP, dithiobis(succinimidyl propionate); DTT, dithiothreitol; FBS, fetal bovine serum; GST, glutathione transferase; hAPE1, human APE1; MAT, metal-affinity tag; nCaRE: negative calcium response elements; NPM1, nucleophosmin; PLA, proximity ligation assay; RU, response unit; SPR, surface plasmon resonance; zAPE1, zebrafish APE1.

[1] To whom correspondence should be addressed (email gianluca.tell@uniud.it).

[17], as already suggested for other BER proteins [22]. Aberrant hAPE1 expression and localization patterns have been linked to neurodegeneration and cancer; therefore, many groups are currently directing their efforts to develop specific small-molecule modulators of the different activities of the protein [23].

In the present study, we systematically characterized the functional properties of the hAPE1 N-terminal domain, exploring its nucleic acid-binding properties and its role in hAPE1–NPM1 interaction. In an effort to better characterize the features guiding the binding of hAPE1 to undamaged nucleic acids, we used a combined approach based on SPR (surface plasmon resonance), EMSA analyses and GST (glutathione transferase) pull-down experiments. The results of the present study show that the affinity of hAPE1 for nucleic acids is enhanced by certain structural elements and that the nucleic acid-binding activity of hAPE1 is promoted by the N-terminal extension of the protein. This region, although necessary for both the stabilization of the hAPE1–nucleic acids and hAPE1–NPM1 interactions, shows only a weak affinity for DNA or NPM1 when isolated from the hAPE1 globular domain. Finally, exploiting a 'domain swapping' approach, we demonstrate that lysine residues located within the N-terminal domain of hAPE1 represent a phylogenetic gain of function for the protein, since the composition of this domain influences the stability of the protein and its ability to interact with both nucleic acids and NPM1. Altogether, these data highlight the role for the hAPE1 N-terminal region in modulating the many functions of this pleiotropic protein. Further structural analyses on this overlooked extension of the protein would be therefore worthwhile in order to fully understand the substrate specificity of hAPE1 and to design new anti-cancer drugs targeting this protein.

EXPERIMENTAL

Cell culture and transient transfection experiments

HeLa cells were grown in DMEM (Dulbecco's modified Eagle's medium) supplemented with 10 % FBS (fetal bovine serum), 100 units/ml penicillin and 10 mg/ml streptomycin sulfate. At 1 day before transfection, cells were seeded in 10-cm plates at a density of 3×10^6 cells/plate. Cells were then transiently transfected with 6 μg of either pcDNA5.1 (empty vector) or pcDNA5.1-hAPE1 (full-length or amino acids 1–49) plasmids per dish using the Lipofectamine™ 2000 Reagent (Invitrogen) according to the manufacturer's instructions. Cells were harvested at 24 h after transfection.

Multiple sequence alignments

For the multiple sequence alignments full-length hAPE1 orthologous metazoan sequences (human, *Pan troglodytes*, *Macaca mulatta*, *Equus caballus*, *Mus musculus*, *Rattus norvegicus*, *Canis lupus familiaris*, *Sus scrofa*, *Bos taurus*, *Ornithorhyncus anatinus*, *Salmo salar*, *Gasterosteus aculeatus*, *Danio rerio*, *Xenopus tropicalis and Xenopus laevis*) were retrieved from the RefSeq protein database using the BLAST algorithm (http://blast.ncbi.nlm.nih.gov/Blast.cgi) and aligned using the ClustalW2 program with default parameters (http://www.ebi.ac.uk/Tools/msa/clustalw2/).

Western blotting analyses

The protein samples were electrophoresed by SDS/PAGE (10–18 % gels) or discontinuous Tris/Tricine SDS/PAGE [24]. Proteins were then transferred on to nitrocellulose membranes (PerkinElmer), developed as described previously [12] using an ECL (enhanced chemiluminescence) procedure (GE Healthcare) and then quantified by using a ChemiDoc XRS video-densitometer (Bio-Rad Laboratories).

Plasmids and expression of recombinant proteins

The constructs pGEX-3X-hAPE1 and pGEX-3X-zAPE1, encoding for the GST-fused hAPE1 and zAPE1 (zebrafish APE1) full-length proteins respectively, were provided by Dr Mark R. Kelley (Indiana University, Indianapolis, IN, U.S.A.). The plasmid encoding for full-length GST–NPM1 was provided by Dr P.G. Pelicci (European Institute of Oncology, Milan, Italy). The pTAC-MAT/hAPE1 and the pETM-20/zAPE1 constructs, encoding for C-terminal-tagged MAT (metal-affinity tag)–hAPE1 and His_6–zAPE1 respectively, were generated by subcloning. All proteins were expressed in *E. coli* BL21(DE3) cells, induced with 1 mM IPTG (isopropyl β-D-thiogalactopyranoside) and then purified on an ÄKTA Purifier FPLC system (GE Healthcare) by using a GSTrap HP column (GE Healthcare) for the GST-tagged proteins, or a HisTrap HP column (GE Healthcare) for the His_6- and MAT-tagged proteins. The quality of purification was checked by SDS/PAGE analysis. Extensive dialysis against PBS was performed to remove any trace of imidazole from the HisTrap-purified proteins. Accurate quantification of all recombinant proteins was performed by colorimetric Bradford assays (Bio-Rad Laboratories) and confirmed by SDS/PAGE and Western blotting analysis. To remove the GST tag, GST–hAPE1 was further hydrolysed with Factor X_a as described previously [17]. The zAPE1 K27 'swapping mutant' and the hAPE1 NΔ43 and zAPE1 NΔ36 deletion mutants, as well as the hAPE1 1–48 and 1–49 constructs, were generated using the QuikChange Mutagenesis kit (Stratagene) and the respective full-length constructs as templates, following the manufacturer's instructions and using standard subcloning procedures.

GST pull-down assays with RNA or NPM1 and co-immunoprecipitation

The indicated amount of GST-tagged protein was mixed, together with the prey protein or 10 μg of total RNA, with 10 μl of glutathione–Sepharose 4B beads (GE Healthcare). RNA was extracted using the TRIzol® Reagent (Invitrogen). Binding was performed in PBS supplemented with 5 mM DTT (dithiothreitol) and 0.5 mM PMSF for 2 h under rotation at 4 °C. The beads were washed three times with washing buffer [PBS supplemented with 0.1 % Igepal CA-630 (Sigma), 5 mM DTT and 0.5 mM PMSF]. Beads were then resuspended in Laemmli sample buffer for Western blotting analyses or in TRIzol® Reagent for RNA extraction and rRNA quantification. The levels of 28S and 18S rRNA transcripts were determined as described previously [17] by using the iScript cDNA synthesis kit (Bio-Rad Laboratories) according to the manufacturer's instructions. Quantitative PCR was then performed in an iQ5 multicolour real-time PCR detection system (Bio-Rad Laboratories) according to the manufacturer's protocol. GST-tagged proteins were detected with an HRP (horseradish peroxidase)-conjugated anti-GST antibody (Sigma), whereas the prey proteins were detected using the indicated antibodies. Co-immunoprecipitation analyses were performed as described previously [12].

DSP [dithiobis(succinimidyl propionate)] cross-linking

The indicated amounts of recombinant NPM1 and hAPE1 (either full-length or the amino acids 1–48 peptide), were allowed to

interact at 37 °C for 15 min in a total volume of 10 μl; DSP (2 μg in DMSO) was added and cross-linking was carried out for 30 min at room temperature (22 °C). The reactions were quenched by adding 0.5 volumes of ice-cold 0.4 M ammonium acetate and incubating on ice for 10 min. Non-reducing Laemmli sample buffer was immediately added and the samples were separated by SDS/PAGE (8 % gel).

Immunofluorescence confocal analyses and PLA (proximity ligation assay)

Immunofluorescence was carried out as described previously [12]. FLAG-tagged 1–49 hAPE1 was labelled using an anti-FLAG antibody and stained with a secondary anti-mouse Alexa Fluor™ 488-conjugated antibody (Jackson ImmunoResearch). Nuclei were counterstained with DAPI (4′,6-diamidino-2-phenylindole). For the PLA analyses we used the Duolink II® reagent kit (Olink Bioscience); cells were fixed in 4 % (w/v) paraformaldehyde, permeabilized with 0.25 % PBS-Triton (PBS with Triton X-100) and saturated with 10 % (v/v) FBS. Slides were incubated with primary antibodies (mouse anti-FLAG, 1:100 dilution and rabbit anti-NPM1, 1:200 dilution) and then reactions were carried out following the manufacturer's instructions. Microscope slides were mounted and visualized through a Leica TCS SP laser-scanning confocal microscope.

hAPE1–nucleic acid binding through EMSA

hAPE1 binding to nucleic acids was assessed as described previously [1] with some modifications. Briefly, in order to reduce unspecific binding and to obtain more defined bound complexes, recombinant proteins or peptides were incubated at 37 °C with 250 pmol of unlabelled poly(dT) for 15 min and then 2.5 pmol of ^{32}P-labelled probe was added. The reactions were then incubated for further 15 min and separated by native PAGE (6–10 % gel) at 150 V for 4 h.

Southwestern assays

Bait proteins were separated using a pre-cast SDS/PAGE (Bio-Rad Laboratories), electrotransferred on to a nitrocellulose membrane and subsequently denatured and renatured by washing six times in 1:1 serial dilutions of 6 M guanidinium/HCl in EMSA buffer [40 mM Hepes (pH 8.0), 50 mM KCl, 2 mM EDTA, 10 % (v/v) glycerol and 1 mM DTT]. The membrane was then saturated in 5 % (w/v) BSA in EMSA buffer and incubated with 50 pmol of the indicated ^{32}P-labelled DNA probe at 37 °C, washed in EMSA buffer to remove unspecific bound probe and finally subjected to autoradiography.

SPR

Real-time binding assays were performed on a Biacore T-100 SPR instrument (GE Healthcare). Streptavidin was immobilized on to a research-grade CM5 sensor chip using amine-coupling chemistry. The immobilization steps were carried out at a flow rate of 10 μl/min in Hepes buffer {20 mM Hepes, 150 mM NaCl, 3.4 mM EDTA, 0.005 % P20 surfactant and 0.1 mM TCEP [tris-(2-carboxyethyl)phosphine]}. All surfaces were simultaneously activated for 30 s with a mixture of NHS (*N*-hydroxysuccinimide; 0.05 M) and EDC [*N*-ethyl-*N*′-(3-dimethylaminopropyl)carbodiimide; 0.2 M]. Streptavidin was injected at a concentration of 20 μg/ml in 10 mM sodium acetate (pH 4.5) for 1 min. Ethanolamine (1 M, pH 8.5) was injected for 7 min to saturate the remaining activated groups. An average of 5000 RU (response units) of streptavidin was immobilized on each flow cell. Biotinylated oligonucleotides were injected at a concentration of 500 nM until the desired level of immobilization was achieved (average value of 300 RU). Proteins were serially diluted in running buffer (80 nM–2.0 μM) and injected at 20 °C at a flow rate of 60 μl/min for 1 min. Disruption of any complex that remained bound after a 5-min dissociation was achieved using a 30 s injection of 1 M NaCl at 100 μl/min. When the experimental data met the quality criteria, the kinetic parameters were estimated assuming a 1:1 binding model and using version 4.1 Evaluation Software (GE Healthcare). Conversely, an affinity steady-state model was applied to fit the RU_{max} data compared with the protein concentrations and fitting was performed with GraphPad Prism v4.00 [17].

CD

Far-UV CD spectra were recorded on a Jasco J-810 spectropolarimeter (JASCO) in a 195–260 nm interval. Experiments were performed employing a protein concentration of 5 μM in 10 mM phosphate buffer (pH 7.0), supplemented with 1 mM DTT and using a 0.1 cm path-length cuvette. Thermal denaturation profiles were obtained by measuring the temperature dependence of the signal at 225 nm in the 20–100 °C range with a resolution of 0.5 °C and 1.0-nm bandwidth. A Peltier temperature controller was used to set up the temperature of the sample with the heating rate set to 1 °C/min. Data were collected at a 0.2-nm resolution, 20 nm/min scan speed and a 4 s response and were reported as the unfolded fraction against the temperature.

Statistical analyses

Statistical analyses were performed by using the Microsoft Excel data analysis software for Student's *t* test analysis. $P < 0.05$ was considered statistically significant.

RESULTS AND DISCUSSION

The binding affinity of hAPE1 for undamaged nucleic acids is dependent on their secondary structure

Several studies have thoroughly characterized hAPE1 structure and its enzymatic activities on abasic DNA, examining its substrate specificity and recognition mechanisms [7,11,25–28]. However, when considering undamaged structured nucleic acids, the knowledge of hAPE1 substrate selectivity is still scarce. In the present study we sought to determine whether some particular structural features were favoured by hAPE1 when binding to nucleic acids. Hence, we used a biophysical approach exploiting the SPR technique to quantitatively measure the binding affinity of hAPE1 for intact oligonucleotides [29,30]. We compared the binding affinity of recombinant purified full-length hAPE1 toward different single-stranded DNA probes, either intrinsically lacking secondary structure (i.e. 34dT), or having a stem and loop-like folding (e.g. Stem10 and Stem20) as predicted by bioinformatics analyses (Figure 1A and Table 1). The results of the SPR experiments (representative sensorgrams in Figure 1B and Supplementary Figure S1C at http://www.biochemj.org/bj/452/bj4520545add.htm) are summarized in Table 2. As already observed by Beloglazova et al. [11], an increased length in the stem region of the oligonucleotides augmented the affinity of hAPE1 for undamaged DNA (compare the Stem10 and the Stem20 sequences). This observation was confirmed by direct EMSA experiments (Figure 1C) and by competition EMSA

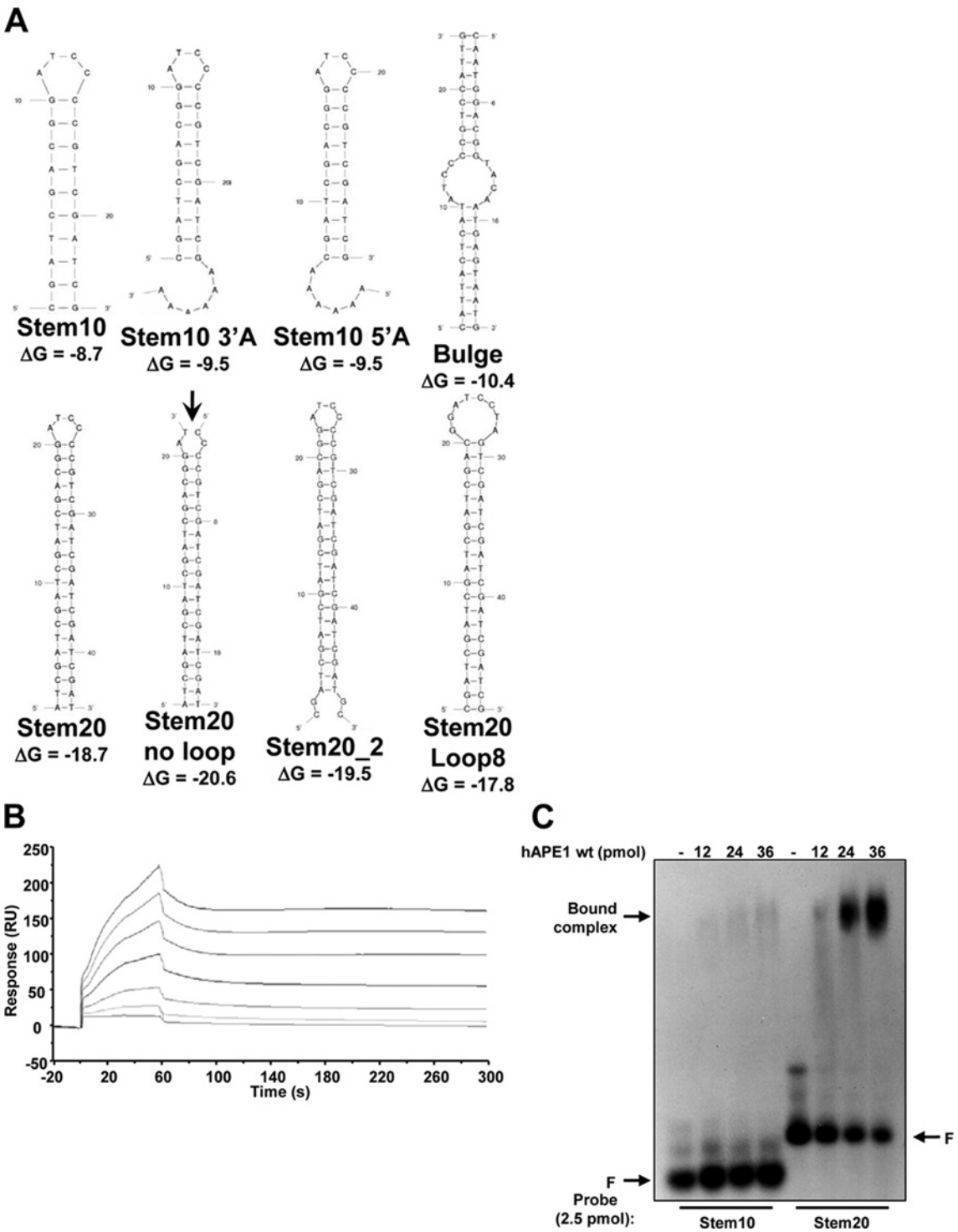

Figure 1 The secondary structure of the substrate determines the binding selectivity of hAPE1

(**A**) The predicted structures for the oligonucleotides used in the present study. Calculations were performed using either the Mfold web server (http://mfold.rna.albany.edu/?q=mfold) or the DINAMelt web server (http://mfold.rna.albany.edu/?q=DINAMelt). The calculated minimum free energy for folding (ΔG) at 37 °C and 50 mM Na^+ is also reported. The arrow indicates the absence of loop in the Stem20 no loop probe. (**B**) Representative overlay sensorgrams relative to a typical SPR experiment for the binding of hAPE1 to immobilized Biot-Stem20. The kinetic parameters were measured injecting purified recombinant hAPE1 solutions at increasing concentrations (i.e. 87.5, 175, 350, 700, 1050, 1400 and 1750 nM). The K_d values were estimated for each concentration using the BIAevaluation v.4.1 software. (**C**) Positive effect of the stem length on ability of hAPE1 to bind undamaged DNA as evaluated through EMSA using the Stem10 and Stem20 oligonucleotides (Table 1). For each reaction the indicated amount of purified recombinant hAPE1 was used. The results confirm a different binding capacity of hAPE1 towards double-stranded oligonucleotides of different lengths. The arrow indicates the hAPE1–DNA complexes, whereas F denotes the position of the free oligonucleotide probe. wt, wild-type.

Table 1 Oligonucleotide sequences used in the present study

The underlined nucleotides denote the position of the predicted loops.

Name	Sequence
34dT	5′-TTTTTTTTTTTTTTTTTTTTTTTTTTTTTTTTTT-3′
Stem10	5′-CGATCGACGGATCCCCGTCGATCG-3′
Stem10 3′ A	5′-CGATCGACGGATCCCCGTCGATCGAAAAAA-3′
Stem10 5′ A	5′-AAAAAACGATCGACGGATCCCCGTCGATCG-3′
Stem20	5′-ATCGATCGATCGATCGACGGATCCCCGTCGATCGATCGATCGAT-3′
Stem20 no loop	Forward, 5′-ATCGATCGATCGATCGACGGAT-3′ and reverse, 5′-CCCCGTCGATCGATCGATCGAT-3′
Stem20_2	5′-CGATCGATCGATCGATCGACGGATCCCCGTCGATCGATCGATCGATGC-3′
Stem20 Loop8	5′-CGATCGATCGATCGATCGACGGATCCTAGTCGATCGATCGATCGATCG-3′
Bulge	Forward, 5′-CATTACTCATATCCCCGTCCATTG-3′ and reverse, 5′-CAATGGACGGTACAATGAGTAATG-3′
nCaRE_B2	Forward, 5′-TTTTTGAGACGGAGTTTCGCTCTTG-3′ and reverse, 5′-CAAGAGCGAAACTCCGTCTCAAAAA-3′

Table 2 Dissociation constants and kinetic parameters for the interaction of full-length hAPE1 with different undamaged oligonucleotides

Data reported were obtained through SPR analyses using hAPE1 as analyte on the indicated biotinylated oligonucleotide ligands. The kinetic parameters highlight the importance of secondary structure for the recognition of undamaged nucleic acids by hAPE1.

Ligand	k_{on} ($M^{-1} \cdot s^{-1} \times 10^5$)	k_{off} (s^{-1})	K_d (μM)
34dT	0.004	0.112	308 ± 3.00
Stem10	0.270	0.020	1.03 ± 0.02
Stem20	0.292	0.007	0.25 ± 0.01
Stem20 no loop	0.068	0.024	4.06 ± 0.01
Stem10 3′A	0.060	0.240	6.20 ± 0.01
Stem10 5′A	0.059	0.059	2.11 ± 0.03
Stem20_2	0.284	0.007	0.25 ± 0.01
Stem20 Loop8	0.061	0.004	0.74 ± 0.02
Bulge	0.834	0.019	0.23 ± 0.02
nCaRE_B2	0.270	0.105	3.90 ± 0.80

experiments demonstrating the poor competitive ability of the Stem10 toward the Stem20 oligonucleotide (results not shown). The effect of the presence of an intact loop structure on the stability of the protein–DNA complex then was investigated by comparing the affinities of the Stem20 and the Stem20 no loop sequences. Notably, hAPE1 showed a reduced affinity toward the ligand without a loop (approximately 16-fold, Table 2). Accordingly, EMSA experiments confirmed these findings, showing a more stable hAPE1–DNA complex in the presence of an intact loop (Supplementary Figures S1A and S1B). Furthermore, competitive EMSA assays demonstrated that the Stem20 probe was a more efficient competitor if compared with the Stem20 no loop (results not shown). Binding affinities were also negatively affected by the presence of an unstructured nucleotide stretch either 3′ or 5′ to the double-stranded stem region (compare Stem10 3′A and Stem10 5′A with the Stem10 sequence). Experimental data allowed us to speculate that the steric hindrance of a free poly(A) tail on the double-stranded region bound by hAPE1 might accelerate the dissociation rate, if protruding from the 3′-side. When using the same stem length the size of the loop region affected the binding: the expansion from 4 to 8 nucleotides reduced the affinity of hAPE1 approximately 3-fold (compare the Stem20_2 and the Stem20 Loop8 sequence). The difference in K_d value can be accounted for by a reduction in the association rate, suggesting that hAPE1 preferentially approaches the DNA molecules from the loop side as the stem side remains invariant between the two oligonucleotides. A lower stability of the stem region in the Stem20 Loop8 sequence could also reflect the decreased binding affinity; bioinformatic predictions, however, do not suggest any major difference in the unfolding free energy of the two molecules (Figure 1A). We finally investigated whether the position of the unstructured region might affect the binding capacity of hAPE1 (compare Bulge, Stem20 and Stem20_2). Despite the differences in both the dissociation and the association rates, the overall affinity of hAPE1 for the oligonucleotides remained unchanged, suggesting that a local denaturation of the double helix, rather than its location within the double-stranded region, is a feature that enhances binding of hAPE1 to undamaged DNA. To compare our measurements on synthetic oligonucleotides with a physiologically relevant undamaged DNA substrate, we investigated the binding properties of hAPE1 towards an nCaRE duplex sequence, namely nCaRE_B2 (G. Antoniali, L. Lirussi, C. D'Ambrosio, F. Dal Piaz, C. Vascotto, D. Marasco, A. Scaloni, F. Fogolari and G. Tell, unpublished work). This sequence displayed a K_d value akin to that of the unstructured Stem20 no loop sequence (Table 2). It is worth pointing out that our *in vitro* assays, performed with the isolated purified recombinant protein, might underestimate the real affinity of hAPE1 for this sequence, since interactions with other protein partners [e.g. Ku70/80 and hnRNPL (heterogeneous nuclear ribonucleoprotein L)] significantly increase the protein–DNA complex stability, as already demonstrated previously (G. Antoniali, L. Lirussi, C. D'Ambrosio, F. Dal Piaz, C. Vascotto, D. Marasco, A. Scaloni, F. Fogolari and G. Tell, unpublished work) [31].

EMSA analyses were also performed on RNA substrates to test whether the nature of the sugar backbone might affect the binding activity of hAPE1 toward structured nucleic acids. The results obtained confirmed that the structural requirements for hAPE1 binding to undamaged substrates are not influenced by the composition of the sugar backbone (results not shown). These observations suggest that hAPE1 shows no apparent preference for DNA or RNA substrates, as long as the nucleic acid is undamaged and is endowed with a secondary structure. The results of the present study are in agreement with experimental data from other laboratories that have estimated K_d values for the interaction of hAPE1 with structured RNA that is similar to our values for DNA ($\sim$0.9 μM) [32]. It must be noted, however, that these experiments do not allow the exclusion of the existence of a differential affinity of hAPE1 for abasic site-containing DNA or RNA molecules, as has been suggested by others [12,26].

In summary, hAPE1 binding to undamaged nucleic acids appears to be strongly affected by the presence of secondary structural elements. In particular, the presence of a double-stranded region is a primary element required for hAPE1 binding. The occurrence of a single-stranded local distortion, moreover, greatly enhances the interaction with nucleic acids. These factors are corroborated by studies reporting a significant reduction in the APE activity of the protein on single-stranded unstructured (or poorly structured) substrates (e.g. [7]). The requirement of a double-stranded DNA region is conceivable, on the basis of the observation that hAPE1 contacts both of the DNA strands [27,28]. The presence of a loop or a bulge within a double-stranded stem could mimic a local denaturation region that resembles a baseless spot, hence explaining the increased affinity for loop-containing structures displayed *in vitro* by hAPE1.

The N-terminal domain contributes to nucleic acid-binding by hAPE1

We have shown previously that the N-terminal 33 amino acids of hAPE1 is able itself to bind RNA oligonucleotides in solution [17]. Sequence alignment analyses, performed on different metazoan

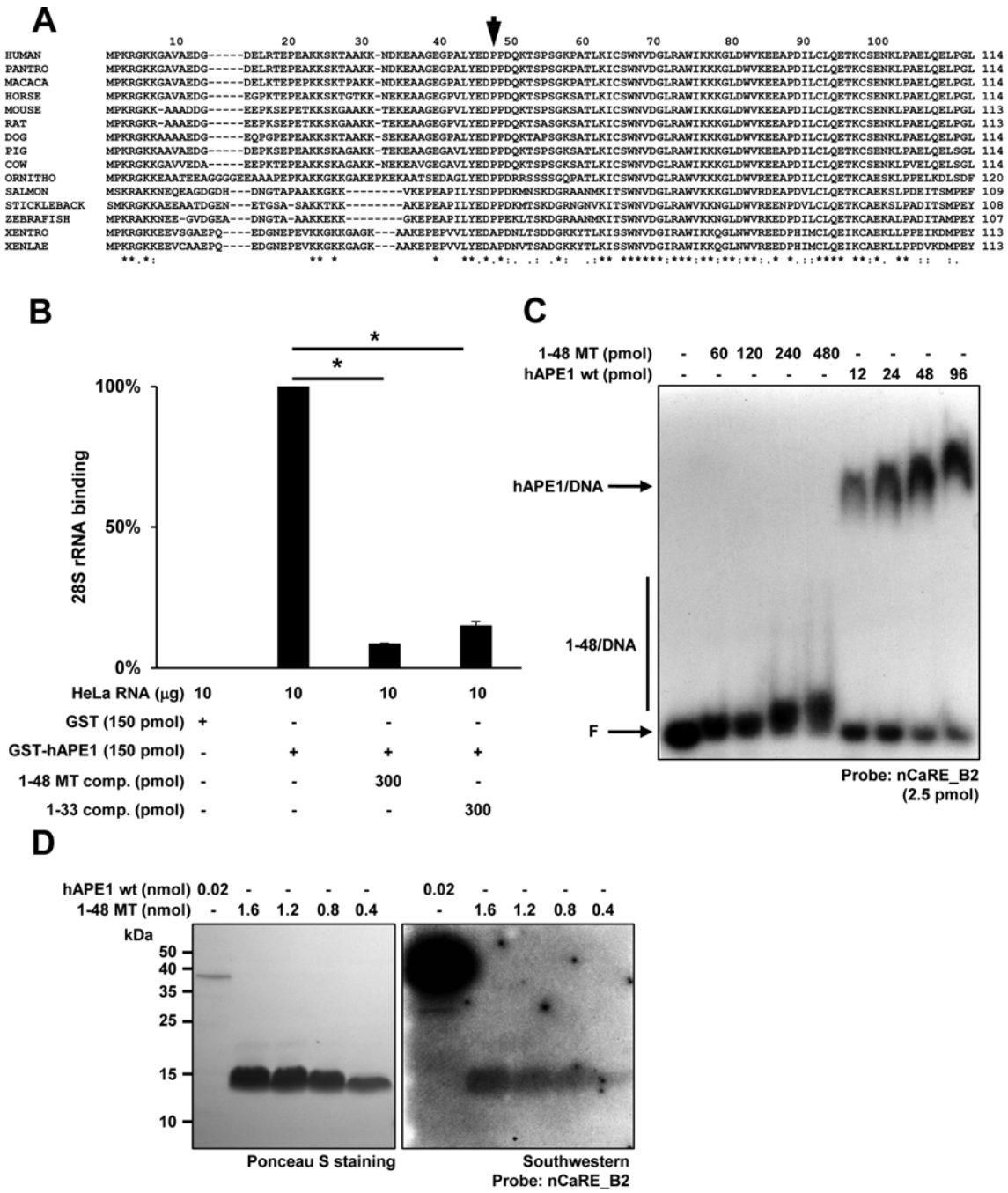

Figure 2 The isolated N-terminal region of hAPE1 interacts weakly with nucleic acids

(**A**) Multiple sequence alignment between full-length APE1 protein sequences from 15 different metazoan species. Only the N-terminal region of the alignment is reported. The arrow indicates the beginning of the high-similarity region within the C-terminal globular domain; whereas the N-terminal part of the sequences is significantly less conserved. (**B**) The isolated recombinant 1–48 hAPE1 N-terminal peptide is able to compete (comp.) with the full-length protein for RNA binding. The binding ability of the peptide was evaluated through competition RNA pull down using GST-tagged full-length hAPE1 as the bait and whole HeLa RNA as the prey in the presence of the indicated competitor. To quantify the amount of residual hAPE1-bound rRNA the pulled-down RNA was then retrotranscribed and 28S or 18S rRNAs were amplified by real-time PCR. The affinity for the 18S rRNA was similar to that shown for the 28S (results not shown). The competition activity of the 1–48 hAPE1 peptide was also confirmed using an untagged synthetic 1–33 hAPE1 peptide. The histogram shows the relative affinity to rRNA with respect to the GST–hAPE1 sample. The error bars represent the S.D. ($n = 3$). *$P < 0.05$. (**C**) EMSA dose–response analysis showing that the 1–48 peptide binds undamaged DNA with a low affinity when compared with the full-length hAPE1 protein. For each reaction the indicated amount of purified recombinant protein was used. F denotes the position of the free oligonucleotide probe. (**D**) Southwestern blot assay showing a dose–response binding of the nCaRE_B2 duplex to the 1–48 peptide. The indicated amounts of protein or peptide were separated by SDS/PAGE, electrotransferred on to nitrocellulose membranes (left-hand panel) and probed with ^{32}P-labelled nCaRE_B2 (right-hand panel). Note the difference in binding affinity between the full-length hAPE1 protein and the isolated peptide. MT, Mat; wt, wild-type.

species, highlight that the phylogenetic conservation of the amino acid sequence among APE1 proteins from different organisms starts at position 48 in the human protein, and is significantly lower in the region spanning amino acids 1–48 (Figure 2A). In order to better clarify the relevance of the non-conserved N-terminal domain in modulating the binding ability of hAPE1 to nucleic

acids, we cloned and expressed in *E. coli* cells the 1–48 amino acid region of hAPE1 in fusion with a C-terminal MAT (Supplementary Figures S2A and S2B at http://www.biochemj.org/bj/452/bj4520545add.htm) and evaluated the binding properties of the recombinant purified peptide toward different substrates, including DNA and RNA. We indirectly estimated the rRNA-binding activity of the peptide exploiting a GST pull-down competition strategy. In these experiments, the full-length GST–hAPE1 was used as the bait and total HeLa RNA as the prey, while either the recombinant purified 1–48 peptide or its synthetic untagged 1–33 counterpart were used as soluble competitors. The data obtained revealed that both soluble peptides were able to compete with full-length hAPE1 for rRNA binding, independently of the presence of a tag (Figure 2B).

In order to compare the nucleic acid-binding activity of the 1–48 peptide and that of the full-length hAPE1 protein, we used EMSA analyses. Under our experimental conditions we observed a low-affinity binding activity for the hAPE1 N-terminal peptide towards the nCaREB_2 duplex sequence (Figure 2C and Supplementary Figure S2C). Although at a reduced affinity, however, the interaction with DNA was specific, as demonstrated by both Southwestern assays (Figure 2D and Supplementary Figure S2D) and Western blotting performed after the EMSA analysis (Supplementary Figure S2E). These results, along with the notion that the N-terminal 1–33 amino acid portion of hAPE1 is absolutely required for the stable interaction of the protein with nucleic acids [12,17], suggest that this lysine-rich region might act by stabilizing the association of hAPE1 with nucleic acids through electrostatic interactions, whereas the remaining C-terminal domain accounts for the specific binding to DNA/RNA. Our data support a two-step model to describe the mechanism through which hAPE1 contacts nucleic acids. The unstructured N-terminal domain would be required for the preliminary low-affinity binding process in search of the proper lesion to be repaired, as suggested for other DNA-binding proteins [33]. Recognition of a local distortion (or an abasic site) involves and is stabilized by a higher-affinity binding event. The whole hAPE1 molecule would, at this point, become necessary for the recognition of the structured nucleic acid region. Intriguingly, this model nicely fits previous hypothesis proposed by Masuda et al. [34] more than a decade ago.

The N-terminal domain of hAPE1 is necessary, but not sufficient, for a stable binding to NPM1

In our previous work, we demonstrated that the N-terminal 1–33 amino acid domain of hAPE1, besides being essential for stabilizing its binding to nucleic acids, is also required for a stable interaction with NPM1 [12] and that lysine residues spanning the region 27–35 of hAPE1 are directly involved in stabilizing this interaction [17]. However, we did not check whether the N-terminal domain of hAPE1 was able to directly bind to NPM1 itself. In an effort to better characterize the protein–protein interaction features of the hAPE1 N-terminal domain and its relative contribution to the overall binding, we analysed the ability of the 1–48 peptide to directly interact with NPM1. We expressed both the full-length hAPE1 and the 1–48 peptide in fusion with a MAT. The recombinant proteins were affinity purified and tested for their binding ability toward GST-tagged NPM1 through GST pull-down assays (Figure 3A). Although the full-length hAPE1 protein was able to directly interact with NPM1 (Figure 3A, left-hand panel), we failed to detect any stable peptide–NPM1 association *in vitro* (Figure 3A, right-hand panel), even under less stringent binding conditions (results not shown). This negative result prompted us to hypothesize that, if present, any peptide–NPM1 association could be too weak to be detected through a direct pull-down assay. We confirmed this hypothesis through a competition GST pull-down assay, in which the 1–48 peptide was used to squelch the binding occurring between the full-length hAPE1 and GST–NPM1 (Figure 3B). The peptide, as well as an untagged full-length hAPE1, was able to displace the association between the MAT-tagged hAPE1 and GST–NPM1. However, whereas the competitor untagged hAPE1 was also efficiently recovered in the pulled-down fraction, the competitor 1–48 peptide was not. This indicates that the peptide was able to mask the hAPE1-binding site on NPM1, thus competing with the hAPE1–NPM1 association, although its interaction with the protein was too weak to be maintained during the washing steps. The observed competition effect could also be interpreted by assuming a masking effect of the peptide on the full-length hAPE1 N-terminal region, however, to the best of our knowledge, no oligomerization ability has ever been described for hAPE1.

To definitely prove the ability of the N-terminal peptide to directly associate with NPM1, we performed an *in vitro* stabilization of the complex exploiting the bifunctional cross-linker DSP (Figure 3C). As expected, treatment of NPM1 alone with DSP resulted in the stabilization of slow migrating oligomers, as documented previously [35]. Moreover, the full-length hAPE1 protein and its N-terminal peptide were detected as slow migrating signals only in the presence of both NPM1 and DSP, indicating a direct association for both with NPM1. The lower affinity of the 1–48 peptide toward NPM1, in comparison with that of the full-length protein, indicates that the C-terminal domain of hAPE1 contributes to the stabilization of the protein–protein interaction.

To evaluate whether the interaction between the hAPE1 N-terminal extension and NPM1 also occurs *in vivo*, we created a HeLa cell line expressing a FLAG-tagged 1–49 hAPE1 peptide upon treatment with doxycycline, as already described previously [36]. As assessed using Western blotting, the peptide expression increased after the addition of doxycycline to the culture medium (Figure 4A, upper panel). Interestingly, the ectopically expressed peptide showed a peculiar localization pattern, being cytoplasmic and nuclear, but excluded from nucleoli (Figure 4A, lower panel), in contrast with the nuclear/nucleolar accumulation observed for the wild-type protein both under basal conditions [12,21] and when ectopically expressed (Figure 4A, lower panel). This result confirms that the C-terminal domain of hAPE1 contributes to the nucleolar accumulation of the protein within cells, despite the fact that the N-terminal domain retains the nuclear localization signal of the protein [37]. This phenomenon may be explained by the relevance that the C-terminal domain has in stabilizing both rRNA and NPM1 binding. By exploiting this cell model, we performed co-immunoprecipitation experiments and demonstrated the occurrence of a molecular interaction between NPM1 and the isolated hAPE1 N-terminal peptide. However, the FLAG-tagged 1–49 peptide was only able to co-precipitate NPM1 poorly when compared with the full-length protein (Figure 4B). This result parallels our *in vitro* results with recombinant purified proteins and confirms that the unstructured N-terminal region of hAPE1 does indeed interact with NPM1, albeit with a lower affinity in the absence of the remaining C-terminal domain. We further confirmed the presence of an interaction occurring between the FLAG-tagged 1–49 hAPE1 peptide and endogenous NPM1 using a PLA [21], which allows the quantification of physical proximity between molecules at a distance lower than 40 nm (Supplementary Figure S3A at http://www.biochemj.org/bj/452/bj4520545add.htm) [38]. The PLA signal was present in the nucleoplasmic compartment only in the presence of both the anti-FLAG and the anti-NPM1 antibodies,

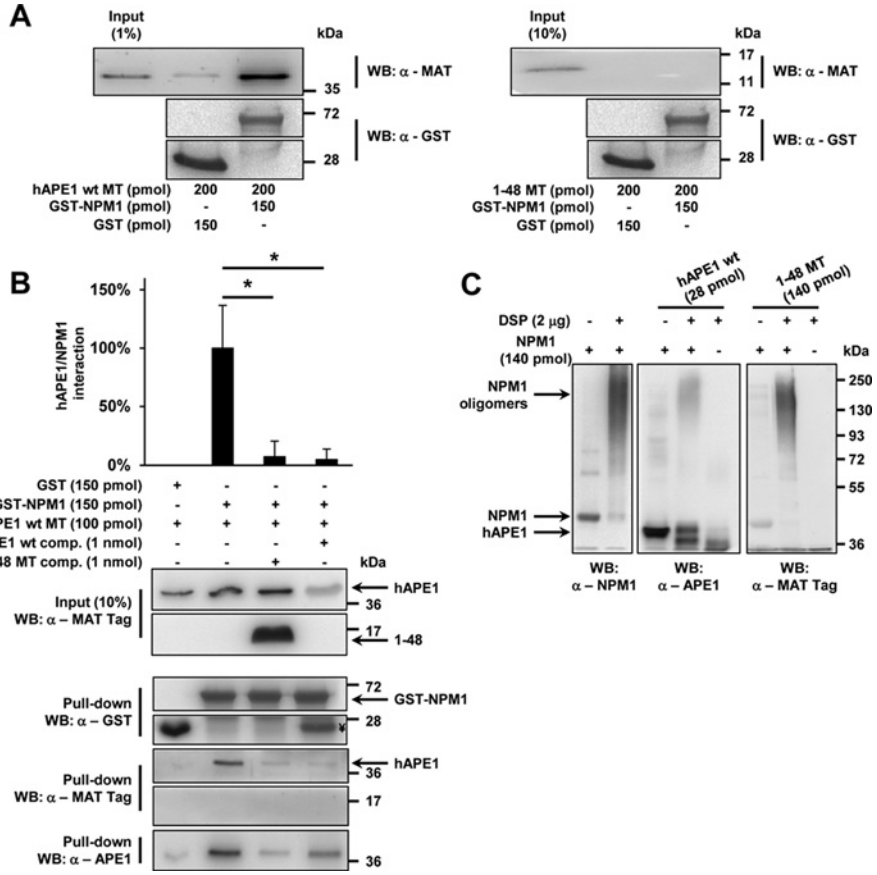

Figure 3 The unstructured N-terminal domain of hAPE1 is required, but not sufficient, for stable binding to NPM1 *in vitro*

(**A**) A representative GST pull-down experiment showing the absence of a stable interaction, *in vitro*, between recombinant GST-tagged NPM1 (bait) and the MAT-tagged 1–48 hAPE1 N-terminal peptide (prey) (right-hand panel). The same assay using full-length MAT-tagged hAPE1 is reported as a positive control (left-hand panel). The assay was performed as described in the Experimental section using the indicated amounts of recombinant proteins. (**B**) The recombinant 1–48 hAPE1 peptide is able to compete, *in vitro*, with the full-length hAPE1 protein for the binding to NPM1. Competition GST pull down using GST–NPM1 as the bait and MAT-tagged full-length hAPE1 as the prey. The hAPE1–NPM1 interaction was evaluated in the presence of a 10-fold excess competitor (comp.; i.e. untagged full-length hAPE1 as a positive control or MAT-tagged 1–48 peptide). The extent of interaction was assessed using an anti-MAT antibody to recognize the pulled down hAPE1 prey. The competing untagged hAPE1 was visualized using an anti-APE1 antibody. The histogram shows the average of three independent experiments with the error bars representing the S.D. $^*P < 0.05$. ¥, Residual GST contaminant in the untagged hAPE1 preparation. (**C**) The low-affinity binding between the N-terminal recombinant hAPE1 peptide and NPM1 is stabilized by *in vitro* cross-linking. Recombinant purified NPM1 was incubated alone or together with either the 1–48 peptide or full-length hAPE1 as indicated. The bifunctional cross-linker DSP was also added where indicated. The presence of high-molecular-mass complexes was assessed by Western blotting using an anti-NPM1, an anti-APE1 or an anti-MAT antibody. The formation of high-molecular-mass complexes in the presence of DSP denotes the ability of the 1–48 peptide to interact weakly with NPM1. MT, Mat; WB, Western blot; wt, wild-type.

being absent when using either the anti-FLAG or the anti-NPM1 alone. This demonstrates the existence of an interaction between the isolated hAPE1 N-terminal domain and endogenous NPM1 only in the nucleoplasmic compartment. We also measured, using PLA, the extent of endogenous hAPE1–NPM1 interaction in the presence or absence of expression of the 1–49 peptide. In this case, the expression of the N-terminal region resulted in a poor, but statistically significant, competing effect (about 10 % loss in interaction, Figure 4C). Altogether, these results confirm that the unstructured hAPE1 N-terminal domain alone is required, but not sufficient, for a stable binding of hAPE1 to NPM1 both *in vitro* and *in vivo*. Notably, several studies have demonstrated that hAPE1, targeted by granzymes A and K, undergoes proteolysis in living cells and its truncation products (hAPE1 NΔ31 or 35) have been proposed to take part in the apoptotic process [18,39,40]. In light of the results of the present paper, it may be tempting to speculate that the N-terminal proteolytic products (the 1–31 or 1–35 peptides) might also exert an active regulatory function within cell, for example by competing with the full-length protein for binding to nucleic acids or protein partners, such as NPM1, XRCC1 (X-ray repair complementing defective repair in Chinese hamster cells) [41], DNA polymerase β [42] or CSB (Cockayne syndrome B) [43] and thus possibly acting as decoy peptide.

The evolutionarily acquired N-terminal domain of hAPE1 influences the stability and the binding properties of the protein

Given the importance of the unstructured N-terminal region of hAPE1 in tuning many of the protein's functions, the poor evolutionary conservation of this domain appears remarkable. hAPE1 belongs to the exonuclease III family of endonucleases, being 27 % identical with the archetype *E. coli* ExoIII (*xth*) [14]. Although the C-terminal domain of the human protein is conserved from prokaryotes to mammals, the N-terminal portion of hAPE1, comprising the redox domain, is not [17,44]. Metazoan hAPE1 orthologues, in fact, share a unique basic N-terminal extension that heavily affects the isoelectric point of the whole protein. Interestingly, the overall positive charges number within this basic region increased during evolution (from nine in fishes

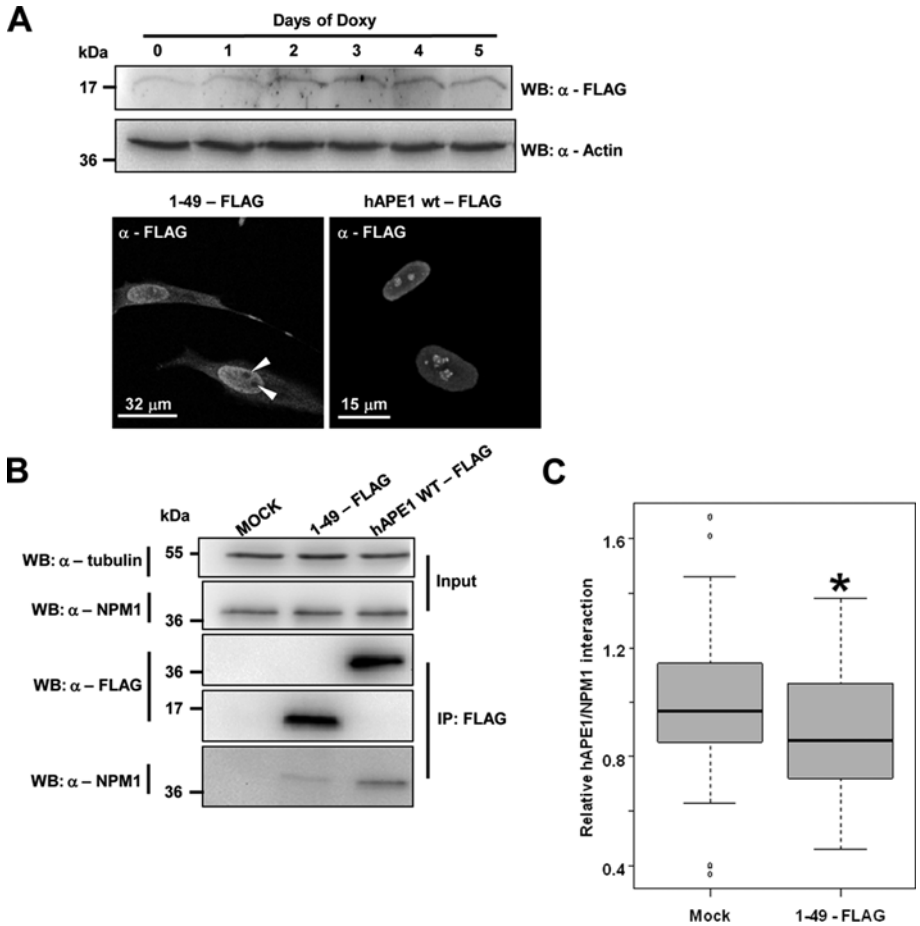

Figure 4 The hAPE1 N-terminal peptide interacts weakly with endogenous NPM1 in HeLa cells

(**A**) Upper panels, Western blotting analysis of the expression kinetics of the FLAG-tagged 1–49 hAPE1 peptide following the doxycycline treatment of HeLa. The peptide expression is induced after 2 days of treatment. Lower panel, immunofluorescence confocal analysis on HeLa cells after 5 days of doxycycline treatment shows the lack of nucleolar accumulation of the 1–49 peptide (white arrowheads), in contrast with the nucleolar positivity shown by the full-length hAPE1. (**B**) The recombinant 1–49 peptide binds poorly to endogenous NPM1 *in vivo*. NPM1 co-immunoprecipitation carried out using HeLa cells transfected either with an empty vector (mock) or a FLAG–full-length hAPE1- or a FLAG–1–49-expressing vector as shown. The amount of immunoprecipitated NPM1 was evaluated using Western blotting with an anti-NPM1 antibody. (**C**) The competition effect of the 1–49 hAPE1 peptide on endogenous hAPE1–NPM1 interaction. The extent of endogenous hAPE1–NPM1 interaction was measured by PLA of HeLa cells either expressing the 1–49 hAPE1 peptide or mock transfected. The hAPE1–NPM1 association was estimated by scoring the interaction signals in transfected cells. Peptide expression resulted in a significant competing effect, leading to a 10% reduction in hAPE1–NPM1 interaction. The boxplot shows the relative amount of hAPE1–NPM1 interaction in 1–49-expressing cells with respect to the mock-transfected cells $\pm$ S.D. ($n = 70$). *$P < 0.05$. IP, immuoprecipitation; WB, Western blot; wt, wild-type.

to 11 in mammals; Figure 2A; [17]), this event has possibly been paralleled by an improved ability of APE1 to cope with a progressively complex cellular environment.

Our recent work showed that the DNA-binding activity of hAPE1 is substantially higher than that of the orthologous protein from a phylogenetically distant organism, such as zebrafish (zAPE1) [17]. In the present study, we hypothesized that evolutionarily acquired amino acids within the N-terminal domain of the protein could account for the increased binding properties of hAPE1 towards both nucleic acids and NPM1. As a proof of concept, we performed interaction experiments with recombinant purified hAPE1 and zAPE1 enzymes. Initially, through GST pull-down experiments, we confirmed that zAPE1 has a lower binding activity towards both NPM1 (Figure 5A) and rRNA (Figure 5B). We then used insertional mutagenesis to generate a mutant recombinant zAPE1 protein (namely, zAPE1 K27) bearing, after Glu^{26}, a lysine residue followed by a TAA (threonine–alanine–alanine) spacer spanning amino acids 28–30, in order to mimic the local charge density and distribution present within the wild-type hAPE1 N-terminal 24–35 region (Figure 5C). Interestingly, the theoretical isoelectric point, calculated for the whole unstructured N-terminal domain, is identical in both the wild-type human protein and the zAPE1 K27 mutant (Table 3).

The NPM1-binding activity of the purified recombinant proteins was then analysed using GST pull down with equimolar amounts of each protein (Figure 5D and Supplementary Figure S4A at http://www.biochemj.org/bj/452/bj4520545add.htm). The data obtained indicate that, whereas the wild-type zAPE1 is less able to interact with NPM1 than hAPE1, the full NPM1-binding activity of the 'swapping mutant' is clearly restored. Notably, both the hAPE1 NΔ43 and the zAPE1 NΔ36 deletion mutants, lacking the entire N-terminal extension, showed neglectable interaction ability. Although recognizing the limitations of this approach when evaluating the binding of zAPE1 to a human NPM1 protein (even though both human and zebrafish NPM1 share extensive similarity and have a nearly identical pI value), our 'domain swapping' approach supports the notion that the reduction in binding affinity might be a consequence of a decreased

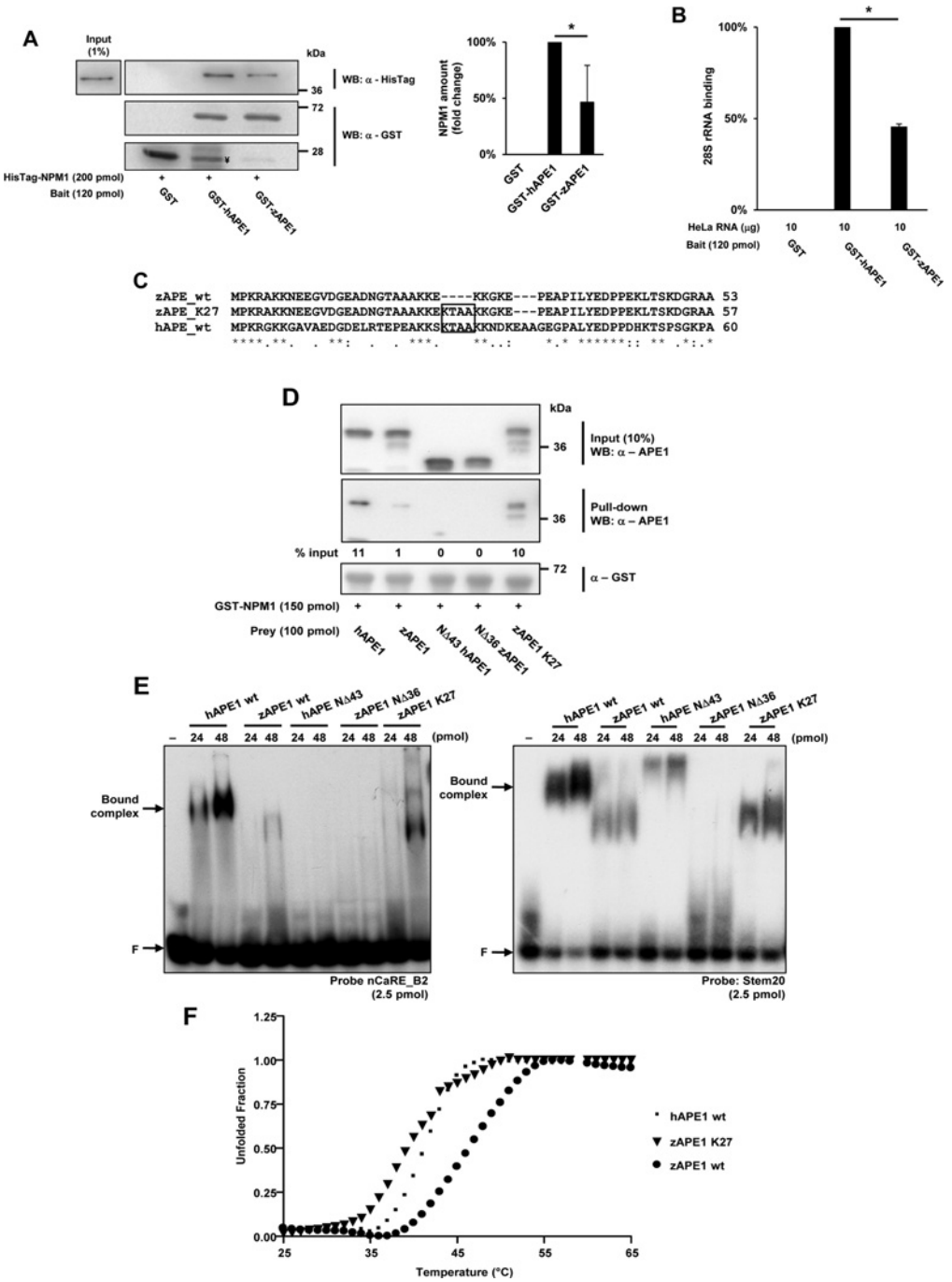

Figure 5 The amino acidic composition of the N-terminal region enhances the affinity of the human APE1 protein for nucleic acids and NPM1

(**A**) zAPE1 has a lower affinity than hAPE1 for NPM1. GST pull-down assay using equimolar amounts of recombinant GST-tagged hAPE1 or zAPE1 as baits and His-tagged NPM1 as the prey. The amount of pulled-down NPM1 was quantified through densitometric analysis (right-hand panel). The histogram show the results from three independent experiments with the error bars representing the S.D. ($n = 3$), $^*P < 0.05$. ¥, Residual GST contaminant in the GST–hAPE1 preparation. (**B**) zAPE1 has lower affinity than hAPE1 for rRNA. The APE1–RNA-binding capacity was evaluated through RNA pull down using GST-tagged full-length hAPE1 or zAPE1 as the bait and whole HeLa RNA as the prey. To quantify the amount of residual hAPE1-bound rRNA the pulled-down RNA was then retrotranscribed and 28S or 18S rRNAs were amplified by real-time PCR. The affinity for the 18S rRNA was similar to what shown for the 28S (results not shown). The histogram reports the relative affinity to rRNA with respect to the GST–hAPE1 sample. Error bars represent the S.D. ($n = 3$). $^*P < 0.001$. (**C**) Multiple sequence alignment of the N-terminal region of wild-type hAPE1, zAPE1 and the mutant zAPE1 K27. The four-amino-acid insertion mutation in zAPE1 K27 is boxed. (**D**) The NPM1-binding affinity of the 'domain swapping' mutant measured using GST pull down. GST-tagged NPM1 was used as the bait, whereas wild-type or mutant APE1 proteins were used as preys. The amount of pulled-down preys was assessed by Western blotting using an anti-APE1 antibody and is shown as the percentage of input prey. Whereas wild-type zAPE1 and the deletion mutants NΔ43 hAPE1 and NΔ36 zAPE1 show a loss of function phenotype, the NPM1-binding capacity of the zAPE1 K27 mutant is restored. (**E**) Binding affinity of the 'domain swapping' mutant for the nCaRE_B2 (left-hand panel) or the Stem20 (right-hand panel) oligonucleotides as measured using EMSA. The nucleic acid-binding activity of the proteins reflects what was observed using SPR (Table 4): the wild-type zAPE1 protein and the deletion mutants NΔ43 hAPE1 and NΔ36 zAPE1 show a reduced binding ability, whereas the zAPE1 K27 mutant displays a gain of function. F, the position of the free oligonucleotide probe. Arrows indicate the bound complex. (**F**) Overlay of thermal melting profiles for recombinant hAPE1, zAPE1 and zAPE1 K27 in the 25–65 °C range shown as the unfolded fraction against temperature, measured by CD at 222 nm. The difference in thermal stability observed between the wild-type hAPE1 and zAPE1 is clearly restored by the N-terminal insertions in the zAPE1 K27 mutant. WB, Western blot; wt, wild-type.

Table 3 Predicted biophysical characteristics of the recombinant proteins used in the present study

The table reports the theoretical molecular masses and isoelectric points calculated using the Expasy pI/Mw tool (http://web.expasy.org/compute_pi/). The pI value of the N-terminal region was calculated restricting the analysis to the human Ala[43] or the homologue Ile[36] in fish. Note the identical pI values between the wild-type (wt) hAPE1 and the zAPE1 K27 N-terminal extensions. N/A, not available.

Protein	Molecular mass	Isoelectric point (whole protein)	Isoelectric point (N-terminal)
hAPE1 wt	35564	8.33	9.10
zAPE1 wt	34881	5.77	8.04
hAPE1 NΔ43	31217	7.59	N/A
zAPE1 NΔ36	31207	5.54	N/A
zAPE1 K27	35252	5.96	9.10

Table 4 Dissociation constants and kinetic parameters for the interaction of the mutated APE1 proteins with the Stem20 and nCaRE_B2 oligonucleotides

Results were obtained using SPR analyses using different APE1 mutants as analytes on the indicated biotinylated oligonucleotide ligands. The affinity values for the nCaRE_B2 sequence were determined through Langmuir isotherm fitting (see the text for details). wt, wild-type.

	Stem20			nCaRE_B2
Protein	k_{on} ($M^{-1} \cdot s^{-1} \times 10^5$)	k_{off} (s^{-1})	K_d (μM)	K_d (μM)
zAPE1 wt	0.174	0.053	3.28 ± 0.07	5.7 ± 0.2
zAPE1 NΔ36	0.232	0.530	23.0 ± 0.5	No binding
hAPE1 NΔ43	0.841	0.733	10.3 ± 0.3	No binding
zAPE1 K27	0.419	0.067	1.60 ± 0.02	2.4 ± 0.9

number of positive charges within the N-terminal region of zAPE1.

A similar functional rescue for the zAPE1 K27 mutant was also observed when analysing the DNA-binding activity of the proteins (Figure 5E). EMSA experiments carried out with either a nCaRE_B2 duplex (Figure 5E, left-hand panel) or the Stem20 sequence (Figure 5E, right-hand panel) revealed a reduced binding activity for wild-type zAPE1 and both the hAPE1 NΔ43 and the zAPE1 NΔ36 deletion mutants, with a restored functionality in the case of the zAPE1 K27 protein. EMSA analyses showed clear differences in the electrophoretic mobility of the hAPE1 and zAPE1 in complex with the nucleic acid substrates, suggesting the existence of possible conformational differences between the two recombinant proteins when bound to the cognate DNA. The formation of a DNA–protein complex between the hAPE1 NΔ43 mutant and the Stem20 substrate (Figure 5E, right-hand panel), but not with the nCaRE_B2 DNA, is probably owing to the presence of a highly stable stem-loop structure within the Stem20 sequence, absent in the case of the nCaRE_B2 duplex (also see the SPR data below). This observation again supports the concept that the C-terminal domain of hAPE1 may account for the high-affinity binding to structured nucleic acid substrates. Moreover, the complete lack of nucleic acid-binding activity observed for the hAPE1 NΔ33 mutant [12,17] suggests that the acidic residues in the 33–42 region might have a negative effect on the overall nucleic acid-binding capacity of the protein.

In order to corroborate these findings, we carried out SPR experiments on zAPE1 and its mutants (Table 4) using both the Stem20 and nCaRE_B2 sequences, which showed different affinities for hAPE1 (Table 2). Interestingly, both the association and dissociation rate constants could be determined when the Stem20 was used as ligand; whereas, they were too high to be determined with the nCaRE_B2 (in this case affinities were determined through Langmuir isotherm fitting; Supplementary Figure S4B). These results further point to the relevance of the presence of a stable stem-loop secondary structure within the oligonucleotide for a robust APE1–nucleic acid interaction. This result is corroborated by the presence of a detectable binding activity of the N-terminal truncated proteins (hAPE1 NΔ43 and zAPE1 NΔ36) only for the stem-loop substrate (i.e. Stem20). Similarly to what was observed in the EMSA experiments (Figure 5E) with both DNA substrates, the measured K_d values were higher for zAPE1 than for hAPE1 (for the kinetic parameters with the human protein see Table 2). The zAPE1 K27 mutant, in turn, displayed an intermediate behaviour, confirming the restored binding activity of the 'swapping mutant' (Table 4).

In order to correlate the solution stability with binding ability, we performed CD analyses on wild-type, mutant and truncated APE1 proteins. The crystal structures of two vertebrate redox-inactive enzymes C65A hAPE1 and zAPE1, in their N-terminally truncated variants (C65A 40–318 hAPE1 and 33–310 zAPE1), revealed no substantial differences in the structural organization of the globular region of APE1 [44]. This was confirmed by our analyses as the CD spectra of all our proteins exhibited minima at 225 and 208 nm, typical of α-helices and β-strands (results not shown). This indicates that, as expected, the C-terminal globular region of the protein predominantly accounts for the folded portion of the APE1 proteins. Thermal denaturation experiments were carried out to investigate protein stability: the sigmoidal profile of folded fraction against temperature (Figure 5F) shows that the unfolding process was fully co-operative for all of the proteins tested. By comparing the T_m values, however, an influence of the N-terminal extension on protein stability could be highlighted. Indeed, whereas hAPE1 has a T_m value of 41.5 °C, the T_m value measured for zAPE1 was 46.5 °C. Interestingly, the mutations and insertions in the zAPE1 K27 mutant effectively reduced the stability of the protein, since the measured T_m value (39.5 °C) was closer to that of hAPE1 (Figure 5F). These results suggest a direct correlation between the ability to recognize different oligonucleotides or protein substrates and the flexibility of the N-terminal region of APE1. Moreover, these data also support the hypothesis that the altered mobility observed in the EMSA experiments between hAPE1 and zAPE1 bound to the cognate DNA sequences (Figure 5E) might be ascribed to substantial conformational differences in the two protein–DNA complexes. Similar CD analyses carried out on both the hAPE1 NΔ43 and the zAPE1 NΔ36 deletion mutants indicated that the differences in thermal stability between human and zebrafish proteins are already present in their globular portions (the T_m values were 44 °C and 50.5 °C respectively), despite the similar structural organization (Supplementary Figure S4C).

Taken together, these results indicate that the amino acid composition and the local charge distribution within the N-terminal domain of hAPE1 are responsible for its evolutionarily acquired binding properties towards both nucleic acids and NPM1 and have an impact on the flexibility of the N-terminal region of APE1. Therefore the results of the present study point to the insertion of human Lys[27], as well as the proper charge distribution, as central steps in the phylogenesis of this protein. From a phylogenic perspective, the acquisition of additional lysine residues could have provided the human protein with novel ways to fine-tune its different activities by the means of new 'hot spots'

that can undergo acetylation or ubiquitination [17,19–21] and regulate substrate accessibility, on the basis of protein plasticity in solution. In conclusion, in light of the results of the present study and others [17,21,42,45], we suggest that the hAPE1 unstructured N-terminal domain might represent a flexible device that has been selected during evolution to specifically modulate the nucleic acid- and NPM1-binding functions of the protein. It would be interesting to explore novel pharmacological strategies aiming at the functional modulation of the protein using small molecules and/or peptides that target its N-terminal region.

AUTHOR CONTRIBUTION

Mattia Poletto, Daniela Marasco and Gianluca Tell provided substantial contributions to conception and design of the study, substantial contributions to acquisition of data or to analysis and interpretation of data, drafting the article or revising it critically for important intellectual content, and approved the final version. Carlo Vascotto and Lisa Lirussi provided substantial contributions to acquisition of data or to analysis and interpretation of data. Pasqualina Scognamiglio provided substantial contributions to conception and design, and substantial contributions to acquisition of data or to analysis and interpretation of data.

ACKNOWLEDGEMENTS

We thank Dr Mengxia Li and Professor Franco Quadrifoglio for critically reading the paper prior to submission and for their helpful comments and input and Professor A. Zagari and Dr V. Granata of CEINGE-NAPOLI (Naples, Italy) for their helpful discussion on the SPR experiments.

FUNDING

This work was supported the Associazione Italiana per la Ricerca sul Cancro (AIRC) [grant number IG10269] and the Ministero dell'Istruzione, dell'Università e della Ricerca (MIUR) [grant numbers FIRB_RBRN07BMCT and PRIN2008_CCPKRP_003 (to G.T.)]

REFERENCES

1 Fung, H. and Demple, B. (2005) A vital role for Ape1/Ref1 protein in repairing spontaneous DNA damage in human cells. Mol. Cell **17**, 463–470
2 Bhakat, K. K., Izumi, T., Yang, S. H., Hazra, T. K. and Mitra, S. (2003) Role of acetylated human AP-endonuclease (APE1/Ref-1) in regulation of the parathyroid hormone gene. EMBO J. **1**, 6299–6309
3 Vascotto, C., Cesaratto, L., Zeef, L. A., Deganuto, M., D'Ambrosio, C., Scaloni, A., Romanello, M., Damante, G., Taglialatela, G., Delneri, D. et al. (2009) Genome-wide analysis and proteomic studies reveal APE1/Ref-1 multifunctional role in mammalian cells. Proteomics **9**, 1058–1074
4 Tell, G., Damante, G., Caldwell, D. and Kelley, M. R. (2005) The intracellular localization of APE1/Ref-1: more than a passive phenomenon? Antioxid. Redox Signaling **7**, 367–384
5 Xanthoudakis, S., Miao, G. G. and Curran, T. (1994) The redox and DNA-repair activities of Ref-1 are encoded by nonoverlapping domains. Proc. Natl. Acad. Sci. U.S.A. **91**, 23–27
6 Erzberger, J. P., Barsky, D., Schärer, O. D., Colvin, M. E. and Wilson, III, D. M. (1998) Elements in abasic site recognition by the major human and *Escherichia coli* apurinic/apyrimidinic endonucleases. Nucleic Acids Res. **26**, 2771–2778
7 Fan, J., Matsumoto, Y. and Wilson, III, D. M. (2006) Nucleotide sequence and DNA secondary structure, as well as replication protein A, modulate the single-stranded abasic endonuclease activity of APE1. J. Biol. Chem. **281**, 3889–3898
8 Marenstein, D. R., Wilson, III, D. M. and Teebor, G. W. (2004) Human AP endonuclease (APE1) demonstrates endonucleolytic activity against AP sites in single-stranded DNA. DNA Repair **3**, 527–533
9 Sengupta, S., Mantha, A. K., Mitra, S. and Bhakat, K. K. (2011) Human AP endonuclease (APE1/Ref-1) and its acetylation regulate YB-1-p300 recruitment and RNA polymerase II loading in the drug-induced activation of multidrug resistance gene *MDR1*. Oncogene **30**, 482–493
10 Tell, G., Wilson, III, D. M. and Lee, C. H. (2010) Intrusion of a DNA repair protein in the RNome world: is this the beginning of a new era? Mol. Cell. Biol., **30**, 366–371
11 Beloglazova, N. G., Kirpota, O. O., Starostin, K. V., Ishchenko, A. A., Yamkovoy, V. I., Zharkov, D. O., Douglas, K. T. and Nevinsky, G. A. (2004) Thermodynamic, kinetic and structural basis for recognition and repair of abasic sites in DNA by apurinic/apyrimidinic endonuclease from human placenta. Nucleic Acids Res. **32**, 5134–5146
12 Vascotto, C., Fantini, D., Romanello, M., Cesaratto, L., Deganuto, M., Leonardi, A., Radicella, J. P., Kelley, M. R., D'Ambrosio, C., Scaloni, A. et al. (2009) APE1/Ref-1 interacts with NPM1 within nucleoli and plays a role in the rRNA quality control process. Mol. Cell. Biol. **29**, 1834–1854
13 Barnes, T., Kim, W. C., Mantha, A. K., Kim, S. E., Izumi, T., Mitra, S. and Lee, C. H. (2009) Identification of apurinic/apyrimidinic endonuclease 1 (APE1) as the endoribonuclease that cleaves c-myc mRNA. Nucleic Acids Res. **37**, 3946–3958
14 Gorman, M. A., Morera, S., Rothwell, D. G., de La Fortelle, E., Mol, C. D., Tainer, J. A., Hickson, I. D. and Freemont, P. S. (1997) The crystal structure of the human DNA repair endonuclease HAP1 suggests the recognition of extra-helical deoxyribose at DNA abasic sites. EMBO J. **16**, 6548–6558
15 Beernink, P. T., Segelke, B. W., Hadi, M. Z., Erzberger, J. P., Wilson, III, D. M. and Rupp, B. (2001) Two divalent metal ions in the active site of a new crystal form of human apurinic/apyrimidinic endonuclease, Ape1: implications for the catalytic mechanism. J. Mol. Biol. **307**, 1023–1034
16 Strauss, P. R. and Holt, C. M. (1998) Domain mapping of human apurinic/apyrimidinic endonuclease. Structural and functional evidence for a disordered amino terminus and a tight globular carboxyl domain. J. Biol. Chem. **273**, 14435–14441
17 Fantini, D., Vascotto, C., Marasco, D., D'Ambrosio, C., Romanello, M., Vitagliano, L., Pedone, C., Poletto, M., Cesaratto, L., Quadrifoglio, F. et al. (2010) Critical lysine residues within the overlooked N-terminal domain of human APE1 regulate its biological functions. Nucleic Acids Res. **38**, 8239–8256
18 Fan, Z., Beresford, P. J., Zhang, D., Xu, Z., Novina, C. D., Yoshida, A., Pommier, Y. and Lieberman, J. (2003) Cleaving the oxidative repair protein Ape1 enhances cell death mediated by granzyme A. Nat. Immunol. **4**, 145–153
19 Busso, C. S., Iwakuma, T. and Izumi, T. (2009) Ubiquitination of mammalian AP endonuclease (APE1) regulated by the p53–MDM2 signaling pathway. Oncogene **28**, 1616–1625
20 Meisenberg, C., Tait, P. S., Dianova, I. I., Wright, K., Edelmann, M. J., Ternette, N., Tasaki, T., Kessler, B. M., Parsons, J. L., Tae Kwon, Y. and Dianov, G. L. (2011) Ubiquitin ligase UBR3 regulates cellular levels of the essential DNA repair protein APE1 and is required for genome stability. Nucleic Acids Res. **40**, 701–711
21 Lirussi, L., Antoniali, G., Vascotto, C., D'Ambrosio, C., Poletto, M., Romanello, M., Marasco, D., Leone, M., Quadrifoglio, F., Bhakat, K. K. et al. (2012) Nucleolar accumulation of APE1 depends on charged lysine residues that undergo acetylation upon genotoxic stress and modulate its BER activity in cells. Mol. Biol. Cell **23**, 4079–4096
22 Hedge, M. L., Izumi, T. and Mitra, S. (2012) Oxidized base damage and single-strand break repairin mammalian genomes: role of disordered regions and posttranslational modifications in early enzymes. Prog. Mol. Biol. Transl. Sci. **110**, 123–153
23 Tell, G., Fantini, D. and Quadrifoglio, F. (2010) Understanding different functions of mammalian AP endonuclease (APE1) as a promising tool for cancer treatment. Cell. Mol. Life Sci. **67**, 3589–3608
24 Schägger, H. (2006) Tricine-SDS-PAGE. Nat. Protoc. **1**, 16–22
25 Nguyen, L. H., Barsky, D., Erzberger, J. P. and Wilson, III, D. M. (2000) Mapping the protein–DNA interface and the metal-binding site of the major human apurinic/apyrimidinic endonuclease. J. Mol. Biol. **298**, 447–459
26 Berquist, B. R., McNeill, D. R. and Wilson, III, D. M. (2008) Characterization of abasic endonuclease activity of human Ape1 on alternative substrates, as well as effects of ATP and sequence context on AP site incision. J. Mol. Biol. **379**, 17–27
27 Mol, C. D., Izumi, T., Mitra, S. and Tainer, J. A. (2000) DNA-bound structures and mutants reveal abasic DNA binding by APE1 and DNA repair coordination. Nature **403**, 451–456
28 Wilson, III, D. M., Takeshita, M. and Demple, B. (1997) Abasic site binding by the human apurinic endonuclease, Ape, and determination of the DNA contact sites. Nucleic Acids Res. **25**, 933–939
29 Katsamba, P. S., Park, S. and Laird-Offringa, I. A. (2002) Kinetic studies of RNA–protein interactions using surface plasmon resonance. Methods **26**, 95–104
30 Law, M. J., Rice, A. J., Lin, P. and Laird-Offringa, I. A. (2006) The role of RNA structure in the interaction of U1A protein with U1 hairpin II RNA. RNA **12**, 1168–1178
31 Izumi, T., Henner, W. D. and Mitra, S. (1996) Negative regulation of the major human AP-endonuclease, a multifunctional protein. Biochemistry **35**, 14679–14683
32 Kim, W. C., Berquist, B. R., Chohan, M., Uy, C., Wilson, III, D. M. and Lee, C. H. (2011) Characterization of the endoribonuclease active site of human apurinic/apyrimidinic endonuclease 1. J. Mol. Biol. **411**, 960–971
33 Vuzman, D. and Levy, Y. (2012) Intrinsically disordered regions as affinity tuners in protein–DNA interactions. Mol. Biosyst. **8**, 47–57

34 Masuda, Y., Bennett, R. A. O. and Demple, B. (1998) Dynamics of the interaction of human apurinic endonuclease (Ape1) with its substrate and product. J. Biol. Chem. **273**, 30352–30359
35 Yung, B. Y. and Chan, P. K. (1987) Identification and characterization of a hexameric form of nucleolar phosphoprotein B23. Biochim. Biophys. Acta **925**, 74–82
36 Vascotto, C., Bisetto, E., Li, M., Zeef, L. A., D'Ambrosio, C., Domenis, R., Comelli, M., Delneri, D., Scaloni, A., Altieri, F. et al. (2011) Knock-in reconstitution studies reveal an unexpected role of Cys^{65} in regulating APE1/Ref-1 subcellular trafficking and function. Mol. Biol. Cell **22**, 3887–3901
37 Jackson, E. B., Theriot, C. A., Chattopadhyay, R., Mitra, S. and Izumi, T. (2005) Analysis of nuclear transport signals in the human apurinic/apyrimidinic endonuclease (APE1/Ref1). Nucleic Acids Res. **33**, 3303–3312
38 Weibrecht, I., Leuchowius, K. J., Clausson, C. M., Conze, T., Jarvius, M., Howell, W. M., Kamali-Moghaddam, M. and Söderberg, O. (2010) Proximity ligation assays: a recent addition to the proteomics toolbox. Expert Rev. Proteomics **7**, 401–409
39 Yoshida, A., Urasaki, Y., Waltham, M., Bergman, A. C., Pourquier, P., Rothwell, D. G., Inuzuka, M., Weinstein, J. N., Ueda, T., Appella, E. et al. (2003) Human apurinic/apyrimidinic endonuclease (Ape1) and its N-terminal truncated form (AN34) are involved in DNA fragmentation during apoptosis. J. Biol. Chem. **278**, 37768–37776
40 Guo, Y., Chen, J., Zhao, T. and Fan, Z. (2008) Granzyme K degrades the redox/DNA repair enzyme Ape1 to trigger oxidative stress of target cells leading to cytotoxicity. Mol. Immunol. **45**, 2225–2235
41 Vidal, A. E., Boiteux, S., Hickson, I. D. and Radicella, J. P. (2001) XRCC1 coordinates the initial and late stages of DNA abasic site repair through protein–protein interactions. EMBO J. **20**, 6530–6539
42 Yu, E., Gaucher, S. P. and Hadi, M. Z. (2010) Probing conformational changes in Ape1 during the progression of base excision repair. Biochemistry **49**, 3786–3796
43 Wong, H. K., Muftuoglu, M., Beck, G., Imam, S. Z., Bohr, V. A. and Wilson, III, D. M. (2007) Cockayne syndrome B protein stimulates apurinic endonuclease 1 activity and protects against agents that introduce base excision repair intermediates. Nucleic Acids Res. **35**, 4103–4113
44 Georgiadis, M. M., Luo, M., Gaur, R. K., Delaplane, S., Li, X. and Kelley, M. R. (2008) Evolution of the redox function in mammalian apurinic/apyrimidinic endonuclease. Mutat. Res. **643**, 54–63
45 Yamamori, T., DeRicco, J., Naqvi, A., Hoffman, T. A., Mattagajasingh, I., Kasuno, K., Jung, S. B., Kim, C. S. and Irani, K. (2010) SIRT1 deacetylates APE1 and regulates cellular base excision repair. Nucleic Acids Res. **38**, 832–845

Received 14 August 2012/28 March 2013; accepted 2 April 2013
Published as BJ Immediate Publication 2 April 2013, doi:10.1042/BJ20121277

Oncogene (2013), 1–12

www.nature.com/onc

ORIGINAL ARTICLE

Functional regulation of the apurinic/apyrimidinic endonuclease 1 by nucleophosmin: impact on tumor biology

C Vascotto[1], L Lirussi[1], M Poletto[1], M Tiribelli[2], D Damiani[2], D Fabbro[1], G Damante[1], B Demple[3], E Colombo[4] and G Tell[1]

Nucleophosmin 1 (NPM1) is a nucleolar protein involved in ribosome biogenesis, stress responses and maintaining genome stability. One-third of acute myeloid leukemias (AMLs) are associated with aberrant localization of NPM1 to the cytoplasm (NPM1c+). This mutation is critical during leukemogenesis and constitutes a good prognostic factor for chemotherapy. At present, there is no clear molecular basis for the role of NPM1 in DNA repair and the tumorigenic process. We found that the nuclear apurinic/apyrimidinic endonuclease 1 (APE1), a core enzyme in base excision DNA repair (BER) of DNA lesions, specifically interacts with NPM1 within nucleoli and the nucleoplasm. Cytoplasmic accumulation of APE1 is associated with cancers including, as we show, NPM1c+ AML. Here we show that NPM1 stimulates APE1 BER activity in cells. We provide evidence that expression of the NPM1c+ variant causes cytoplasmic accumulation of APE1 in: (i) a heterologous cell system (HeLa cells); (ii) the myeloid cell line OCI/AML3 stably expressing NPM1c+; and (iii) primary lymphoblasts of NPM1c+ AML patients. Consistent with impaired APE1 localization, OCI/AML3 cells and blasts of AML patients have impaired BER activity. Cytoplasmic APE1 in NPM1c+ myeloid cells is truncated due to proteolysis. Thus, the good prognostic response of NPM1c+ AML to chemotherapy may result from the cytoplasmic relocalization of APE1 and the consequent BER deficiency. NPM1 thus has an indirect but significant role in BER *in vivo* that may also be important for NPM1c+ tumorigenesis.

Oncogene (2013) **0,** 000–000. doi:10.1038/onc.2013.251

Keywords: APE1/Ref-1; NPM1; acute myeloid leukemia; base excision repair

INTRODUCTION

The nucleolar protein nucleophosmin 1 (NPM1) is implicated in a variety of cellular processes including ribosome biogenesis and centrosome duplication, and NPM1 is frequently altered in some cancers.[1] NPM1 physically interacts with p53 and is believed to regulate this tumor-suppressor protein, thus contributing to maintenance of genome integrity.[2,3] However, a direct involvement of NPM1 in DNA repair has not been demonstrated.

NPM1 mutations are the most frequently known gene alterations in cytogenetically normal acute myeloid leukemia (AML) patients and are considered as positive prognostic factors.[4] The NPM1 mutations identified so far in cytogenetically normal AML patients generate a new nuclear export signal while also disrupting the nucleolar localization signal (Supplementary Figure S1), which relocalizes mutated NPM1 to the cytoplasm (NPM1c+).[5,6] A formal *in vivo* demonstration that mutant NPM1c+ is endowed with oncogenic potential has been recently presented.[7] A plausible hypothesis is that NPM1c+ causes abnormal cytoplasmic localization of important NPM1-interacting proteins that impairs their functions.[1,8–15] All NPM1c+ AMLs are characterized by haploinsufficient expression, with only one NPM1 allele affected by the mutation. NPM1c+ is dominant by forming mixed oligomers with wild-type (WT) NPM1 and moving it to the cytoplasm. The presence of the NPM1c+ mutation is a favorable marker for relapse-free and overall survival in AML with a normal karyotype, and for complete remission after chemotherapy using DNA-damaging compounds (that is, daunorubicin, cytarabine and so on).

Interestingly, overexpression of WT NPM1 has been described in a number of solid malignancies such as hepatic, gastric, ovarian and prostate cancers.[1,16] In those cases, it has been suggested that increased amounts of NPM1 could limit the DNA-damage response to help effect cellular transformation. However, molecular support for this hypothesis is still lacking.

We recently demonstrated that NPM1 physically interacts with apurinic/apyrimidinic endonuclease 1/redox effector factor 1 (APE1/Ref-1) within nucleoli and in the nucleoplasm of tumor cells.[17] APE1 has a crucial role in the maintenance of genome stability, in redox signaling and other processes,[18] and it is a promising target for augmenting chemotherapy.[18,19] APE1 is the main apurinic/apyrimidinic (AP) endonuclease in mammalian cells and a multifunctional protein. APE1 is an essential enzyme in the base excision DNA repair (BER) pathway for DNA damage caused by both endogenous and exogenous oxidizing or alkylating agents, including chemotherapeutic drugs.[20–23] APE1 can also act as a redox-regulatory protein, maintaining cancer-related transcription factors (Egr-1, NF-κB, p53, HIF-1α, AP-1 and Pax proteins) in an active reduced state,[18,24–28] and it may act as a transcriptional repressor.[29] APE1 binds and cleaves abasic sites in RNA[17,30,31] and can control *c-Myc* expression by nicking its mRNA.[32] In this context, we have shown that the first 35 amino acids of APE1 are required for a stable interaction with NPM1 and other proteins involved in ribosome biogenesis/RNA processing,[17] and for APE1 stable binding to RNA.[30,33] The direct interaction with NPM1 stimulates the enzymatic activity of APE1 on abasic

[1]Department of Medical and Biological Sciences, University of Udine, Udine, Italy; [2]Department of Experimental and Clinical Medical Sciences, University of Udine, Udine, Italy; [3]Department of Pharmacological Sciences, Stony Brook University School of Medicine, Stony Brook, NY, USA and [4]Department of Medicine, Surgery and Dentistry, University of Milan, Milan, Italy. Correspondence: Professor G Tell, Department of Medical and Biological Sciences, University of Udine, Piazzale Kolbe 4, 33100 Udine, Italy
E-mail: gianluca.tell@uniud.it
Received 27 June 2012; revised 24 April 2013; accepted 19 May 2013

DNA *in vitro*,[17,30] although the *in vivo* effects were not known. This work presented here is aimed at filling this gap.

RESULTS

NPM1$^{-/-}$ cells are more sensitive than control cells to DNA damages repaired through the BER pathway

We earlier demonstrated that NPM1 stimulates the APE1 endonuclease activity *in vitro* by means of protein–protein interaction.[17,30] Our data clearly showed that, although the K_m of APE1 for the abasic substrate is not significantly affected by the presence of NPM1, its catalytic activity is increased almost 10-fold in the presence of a two-fold excess of NPM1 recombinant protein. As product release by APE1 appears to be rate-limiting,[34,35] these observations suggest that interaction with NPM1 increases the speed of this reaction step. To evaluate the role of the APE1/NPM1 interaction *in vivo*, we tested the effect of NPM1 absence on the BER capacity exploiting a NPM1$^{-/-}$ cell model developed on the p53$^{-/-}$ background for immortalization.[36]

First, we checked whether NPM1 expression affected the amount of APE1 protein and its subcellular localization. APE1 and NPM1 protein levels were evaluated by immunoblot analysis of nuclear and cytoplasmic fractions of p53$^{-/-}$ mouse embryonic fibroblasts (MEFs) with NPM1$^{+/+}$ or NPM1$^{-/-}$ alleles[36] (Figure 1a left and Supplementary Figure S2). Quantification of the immunoblots (Figure 1a right and Supplementary Figure S3) showed that NPM1$^{-/-}$ cells had about 40% more nuclear APE1

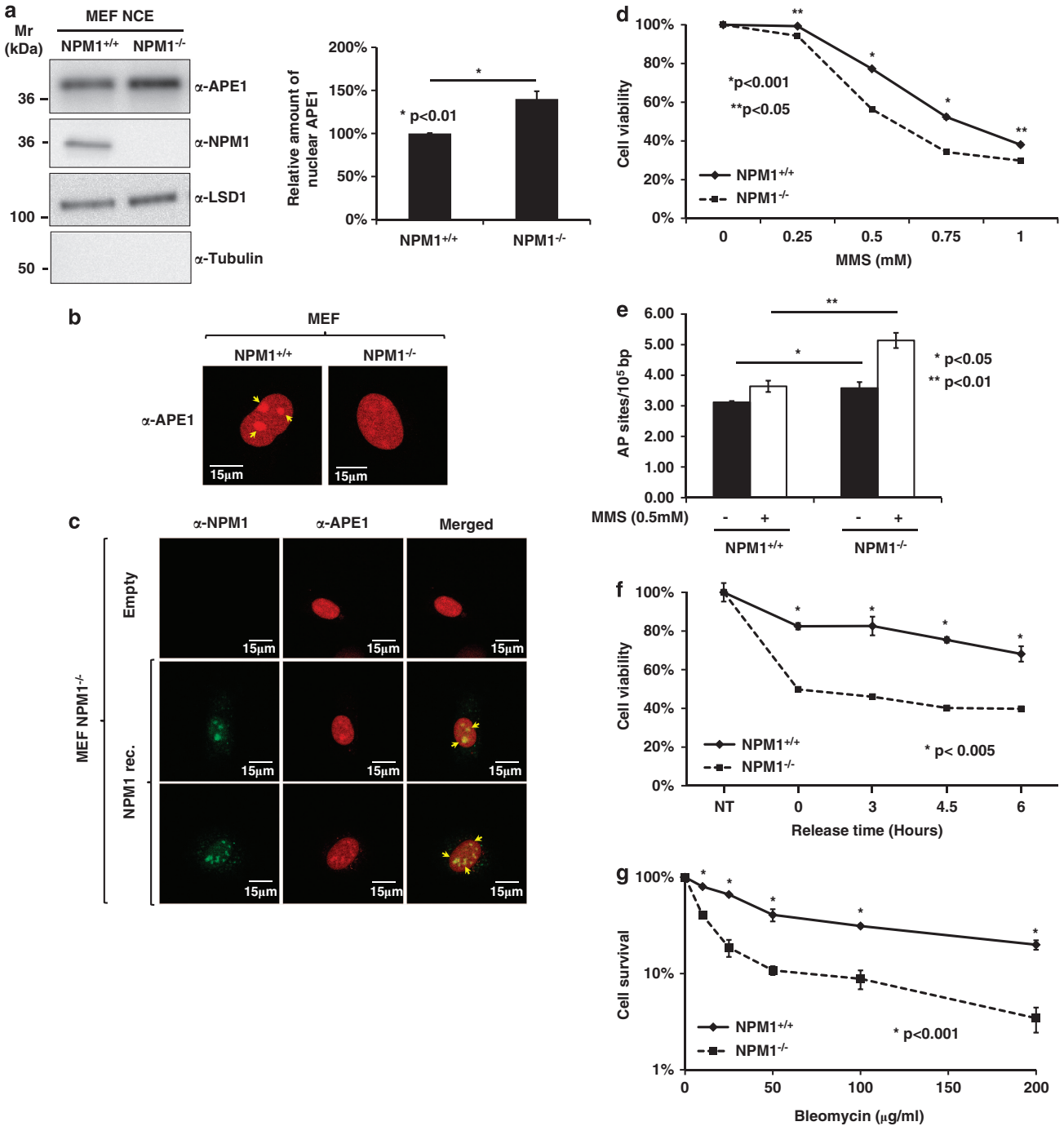

than cells expressing WT NPM1 protein. This increased content was associated with a slightly increased APE1 transcription, as measured by quantitative PCR analysis (not shown). Immunofluorescence (IF) analysis (Figure 1b) showed that, in NPM1$^{+/+}$ cells, APE1 localization was nuclear with a strong accumulation in nucleolar structures, as previously shown for some tumor cell lines.[17] In contrast, in NPM1$^{-/-}$ cells, APE1 did not accumulate within nucleoli, although nucleolar structures are still intact in these cells (data not shown).[36] Reexpression of NPM1 in MEF-NPM1$^{-/-}$ cells promoted APE1 nucleolar accumulation (Figure 1c and Supplementary Figure S4), demonstrating that interaction with NPM1 is essential for APE1 nucleolar distribution. Moreover, recent data from our laboratory also showed that expression of an APE1 mutant not able to interact with NPM1 was unable to accumulate within nucleoli, demonstrating that a functional interaction with NPM1 is required for physical accumulation of APE1 within nucleoli.[37]

To test the functional relevance of NPM1 in BER, we next assayed the sensitivity of the NPM1$^{-/-}$ cells to different genotoxic treatments known to cause DNA lesions that are repaired through the BER pathway.[38] First, we used methyl methanesulfonate (MMS), which is a monofunctional methylating agent causing lesions repaired predominantly by BER pathway.[39] Cell viability experiments showed that NPM1$^{-/-}$ cells were significantly more sensitive than NPM1$^{+/+}$ cells to MMS (Figure 1d). We then evaluated the ability of the MEFs to efficiently remove AP sites from the DNA of MMS-treated cells. As shown in Figure 1e, NPM1$^{-/-}$ cells retained a significantly higher level of AP sites following MMS treatment than did NPM1$^{+/+}$ cells. Notably, this difference was also apparent under basal conditions, further pointing to an impairment in the AP-site incision step within the BER pathway in NPM1$^{-/-}$ cells.

BER removes also damages caused by reactive oxygen species, such as oxidized bases (for example, 8-oxoG). Thus, we performed cell viability experiments with acute doses of H_2O_2 as genotoxic agent, combined with treatment of the cells with methoxyamine, an inhibitor of APE1-dependent repair.[40] Data reported in Supplementary Figure S5A clearly showed that NPM1$^{-/-}$ cells were significantly more sensitive to this treatment than NPM1$^{+/+}$ cells. To confirm this result with an alternative oxidizing agent, we used $KBrO_3$, a carcinogenic agent known to induce predominantly 8-oxoG lesions on DNA after reduction of the bromate by cellular thiols, such as glutathione, or reduced cysteines.[41] As displayed in Figure 1f, treatment with $KBrO_3$, NPM1$^{-/-}$ cells were significantly less viable than control cells at all the release time points.

We also determined the sensitivity of NPM1$^{-/-}$ cells to the radiomimetic bleomycin (BLM), as still another DNA-damaging agent that requires BER intervention.[42] BLM, which targets both single-stranded DNA and double-stranded DNA, as well as RNA molecules, causes formation of 4-oxidized AP sites or 3′-phosphoglycolate products that account for the majority of the BLM-induced DNA lesions.[42,43] Cell viability was measured on MEFs after a 1-h treatment with increasing doses of BLM, followed by 48 h of recovery. Data reported in Figure 1g and Supplementary Figure S5B clearly confirmed the protective function exerted by NPM1 against BLM treatment. Notably, the differential sensitivity of the two isogenic cell lines was not apparent when using the poly (ADP-ribose) polymerase-inhibitor PJ34 (Supplementary Figure S6A) or upon ultraviolet-C irradiation, which promotes DNA damages repaired through NER (Supplementary Figure S6B). Comet assay analysis performed under basal condition (data not shown) did not reveal any significant difference between the steady-state level of DNA damage of the two isogenic cell lines. The latter observations suggest that, if any, only a marginal involvement of the other pathways, besides BER, may account for the observed effects on cell viability exerted by the genotoxicants used in this study, which, besides AP sites, may cause DNA-strand breaks.

Collectively, these data indicate that NPM1 is essential for cell protection from different genotoxic treatments that elicit a BER response.

The lower APE1 BER activity of NPM1$^{-/-}$ cells is rescued by NPM1 reconstitution

To define the BER defect accompanying NPM1 deficiency, we measured the APE1 enzymatic activity in nuclear extracts from the two MEF cell lines. Endonuclease assays showed that despite the higher expression levels of APE1 protein in NPM1$^{-/-}$ cells, their AP endonuclease activity did not significantly differ from that of the control cells (Figure 2a). Treatment of the two cell lines with two different APE1 inhibitors (that is, methoxyamine[39] and compound 3[44]) alone demonstrated that NPM1$^{-/-}$ cells were significantly more sensitive to AP endonuclease activity inhibition, confirming the hypothesis that APE1 functional activity, under genotoxic conditions, strictly depends on NPM1 expression

Figure 1. Absence of NPM1 is associated to a higher sensitivity of cells to genotoxic treatments causing DNA lesions repaired through BER. (**a**) Left: representative western blotting analysis of MEF-NPM1$^{+/+}$ and NPM1$^{-/-}$ nuclear extracts of three independent subfractionation experiments. Nuclear cell extracts of 5 μg of the two cell lines were analyzed through western blotting for the expression of APE1 and NPM1 content. Lysine demethylase (LSD1) was used as nuclear marker and loading control, whereas tubulin was used to evaluate cytoplasmic contaminations. Right: relative percentages of chemiluminescence intensity of APE1 signals are reported in the histogram showing a significant increase of APE1 nuclear expression in NPM1$^{-/-}$ clone (40 ± 9%) with respect to NPM1$^{+/+}$ cells. Histograms, showing the amount of APE1 nuclear protein, represent the mean ± s.d. values of three independent experiments. (**b**) APE1 subcellular localization was detected through confocal analysis on MEF-NPM1$^{+/+}$ and NPM1$^{-/-}$ cells using a specific monoclonal α-APE1 antibody and a secondary antibody α-mouse conjugated with Rhodamine-Red. Yellow arrows indicate APE1 accumulation within nucleoli. A diffused nuclear staining without nucleolar accumulation could be observed in the NPM1$^{-/-}$ cells. (**c**) Confocal analysis of APE1/NPM1 colocalization in MEF-NPM1$^{-/-}$ after reexpression of NPM1. NPM1$^{-/-}$ cells transfected with the empty vector (Empty) showed a uniform nuclear staining for APE1 (red). On the contrary, NPM1$^{-/-}$ cells transfected with pCMV5.1 vector expressing NPM1 in fusion with a C-term FLAG (NPM1 rec.) show APE1 accumulation within nucleolar structure and colocalization with NPM1 (yellow arrows). (**d**) MTS assay was used to evaluate cell viability of MEF-NPM1$^{+/+}$ and NPM1$^{-/-}$ cells after treatment with increasing amounts of MMS for 8 h. Absence of NPM1 negatively affects cell viability making NPM1$^{-/-}$ cells more sensitive to genotoxic damages. Mean ± s.d. values are the result of three independent experiments. (**e**) The amount of abasic (AP) sites was measured in MEF-NPM1$^{+/+}$ and NPM1$^{-/-}$ cells under basal conditions and after treatment with 0.5 mM of MMS for 4 h. NPM1$^{-/-}$ cells display a significantly higher amount of AP sites if compared with NPM1$^{+/+}$ cells. Treatment with an alkylating agent leads to the accumulation of AP sites in NPM1$^{-/-}$ cells (5.14 ± 0.25/10^5 bp) if compared with NPM1$^{+/+}$ cells (3.58 ± 0.20/10^5 bp). Mean ± s.d. values are the result of three independent experiments. (**f**) MTS assay was used to evaluate cell viability of MEF-NPM1$^{+/+}$ and NPM1$^{-/-}$ cells. After Potassium bromate (40 mM for 30 min) treatment, cells were allowed to recover for the indicated periods of time. Absence of NPM1 negatively affects cell viability, making NPM1$^{-/-}$ cells more sensitive to genotoxic damages. Mean ± s.d. values are the result of three independent experiments. (**g**) Trypan blue cell counting was used to measure cytotoxicity of BLM in MEF cells. Mean ± s.d. values are the result of three independent experiments.

(Figures 2b and c). We circumstantiated these findings by measuring the endonuclease activity of APE1, using nuclear extracts of MEF cells after normalization for APE1 content. Consistent with our previous *in vitro* findings,[17] APE1 endonuclease activity in NPM1$^{-/-}$ extracts was significantly lower than that from NPM1$^{+/+}$ cells (Figure 2d). Thus, the

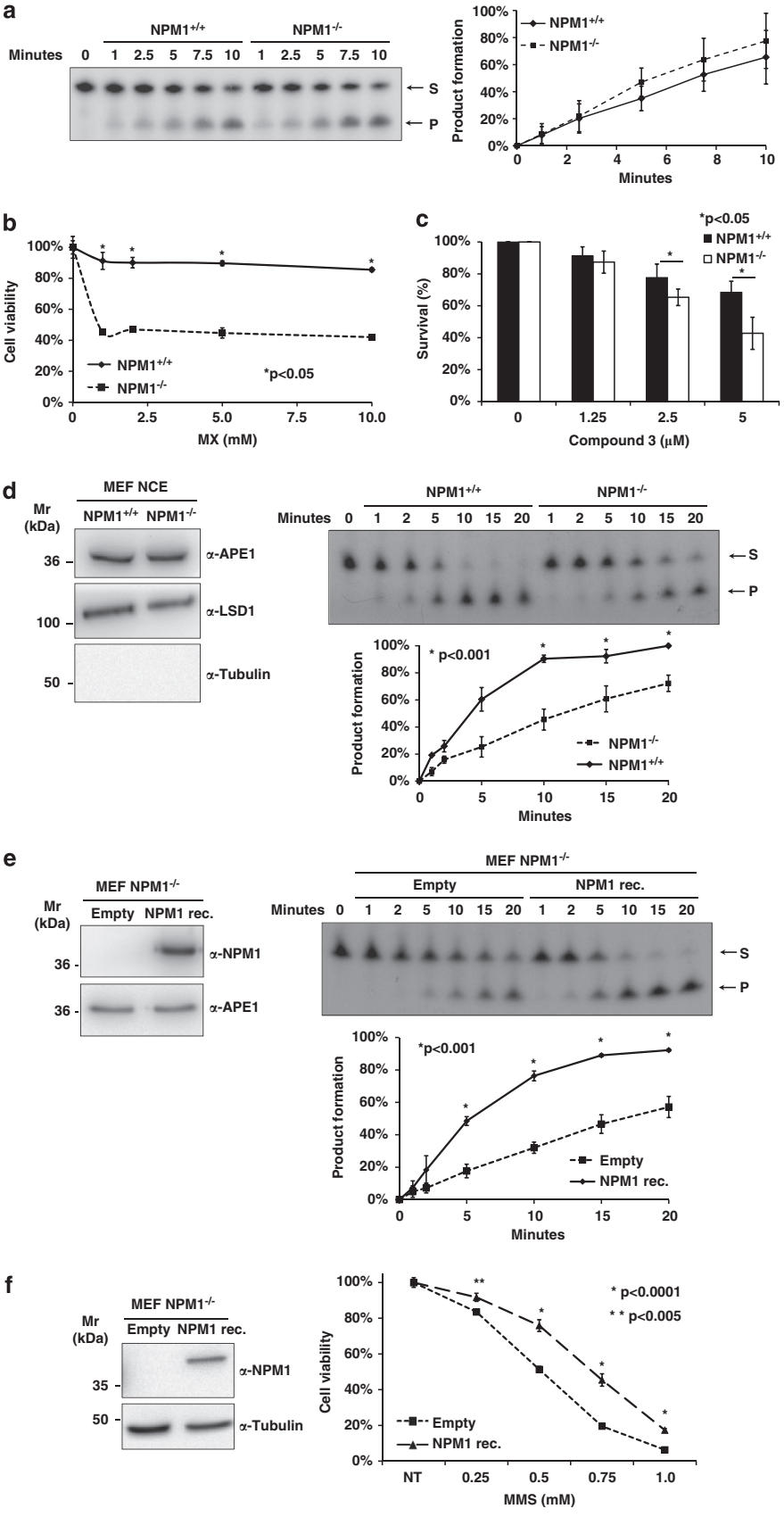

increased APE1 nuclear content observed in NPM1$^{-/-}$ cells could reflect a compensatory mechanism to maintain overall BER activity that still remains insufficient to efficiently correct genotoxic damage. To confirm that the APE1 defect observed in NPM1$^{-/-}$ cells was due to NPM1 loss, rather than some other effect of the knockout gene, we restored NPM1 in the NPM1$^{-/-}$ cell lines by ectopic expression of the WT protein from a plasmid vector and measured the AP endonuclease activity in these cells (Figure 2e). The results showed that NPM1 reexpression in NPM1$^{-/-}$ cells increased their AP endonuclease activity when compared with control cells transfected with the empty expression vector. We biologically circumstantiated these biochemical data, by performing cell viability experiments in stable cell lines reexpressing the WT NPM1 protein in the NPM1$^{-/-}$ background. Data reported in Figure 2f confirmed the hypothesis made, clearly showing that reexpression of NPM1 significantly reduced the sensitivity of NPM1$^{-/-}$ cells to genotoxic treatment.

Collectively, our data demonstrate that NPM1 is a novel indirect effector of BER by regulating APE1 localization and activity *in vivo*.

Ectopic expression of the NPM1c+ AML protein causes increased cytoplasmic APE1 localization in HeLa cells

We examined the oncological relevance of our findings by testing the effect of the NPM1c+ mutation on BER, and by studying the effect of NPM1c+ on the APE1–NPM1 interaction. To address the latter, we assessed the extent of APE1–NPM1 interaction using the proximity ligation assay (PLA).[45] HeLa cells expressing the NPM1c+mutant protein showed relocalization of NPM1 to the cytoplasmic compartment of the protein. As expected, the control WT protein presented its typical nucleolar staining (Figure 3a). The specificity of the PLA analysis was tested by comparing the ability of NPM1 to interact with APE1^{WT}, or with an APE1$^{N\Delta33}$-deletion mutant that has lower affinity for NPM1.[17] Specificity was clearly demonstrated (Supplementary Figure S7 and Supplementary Movies) by the presence of nuclear and nucleolar PLA spots only when APE1^{WT} was expressed. When the APE1$^{N\Delta33}$ protein was instead expressed, the PLA signals were reduced in number and relocalized to the cytoplasmic compartment in accordance with APE1$^{N\Delta33}$ pancellular localization. We then tested the ability of the NPM1c+[46] mutant protein to interact with Flag-tagged APE1 protein. In control cells (NPM1^{WT}), the APE1–NPM1 interaction occurred primarily in the nucleolar and nucleoplasmic compartments, whereas the interaction with NPM1c+ protein was mostly apparent in the cytoplasmic compartment (Figure 3b). Quantification of these results, through scoring of the PLA signals, showed that the NPM1c+ mutation significantly reduced the APE1–NPM1 association within the nuclei of transfected cells, leading to a significant increase of the APE1–NPM1 interaction within the cytoplasmic compartment. Accordingly, only in the case of cells expressing the NPM1c+mutant protein, the APE1 staining was extranuclear, consistent with the PLA signal distribution (Figures 3b and c). These observations indicate the existence of a direct correlation between expression of the NPM1c+ protein and the presence of APE1 in the cytoplasm.

NPM1c+ expression is associated with altered APE1 protein stability in both AML cell lines and blasts from AML patients

We assessed the biochemical relevance of the APE1 cytoplasmic relocalization due to NPM1c+ expression in the myeloid cell line OCI/AML3, which stably expresses a NPM1c+mutant protein.[47] We analyzed the distribution of APE1 using IF and by quantification of the nuclear and cytoplasmic levels of APE1 in subcellular fractions of OCI/AML3 and control OCI/AML2 cell lines through western blot analysis. The mRNA expression levels of APE1 were similar between the two cell lines, as demonstrated by quantitative PCR analyses (data not shown). IF analysis showed that NPM1c+ expression was associated with APE1 accumulation in the cytoplasmic compartment of OCI/AML3 cells (Figure 4a). Immunoblot analysis indicated that a significant amount of truncated APE1 protein could be detected in the whole and in the cytoplasmic extracts of OCI/AML3 cell line (Figure 4b). Strikingly, accumulation of this truncated protein form was also apparent in blasts from AML patients (Figure 4c), confirming the biological relevance of this observation. Several groups have demonstrated that APE1 is targeted by granzymes A and K, to generate truncation products (APE1$^{N\Delta31\text{-}35}$) that functionally inactivate APE1 in DNA repair and to take part in apoptosis.[48–50] We have also recently shown that expression of non-cleavable proficient form of APE1 protein protects cells from genotoxic stresses,[51] thus confirming that the N-terminal deletion of the protein causes its functional impairment *in vivo*. This truncated protein corresponded to the APE1$^{N\Delta33}$ truncation derivative already described,[48–50] but was due to a specific proteolytic activity, independent of granzyme A protein, which is not expressed in these cell lines (Lirussi *et al.*, in preparation).

Figure 2. Absence of NPM1 negatively affects APE1 endonuclease activity. (**a**) The same amount of whole-cell extracts (600 ng) from MEF-NPM1$^{+/+}$ and NPM1$^{-/-}$ was used to evaluate APE1's endonuclease activity in the two cell lines. A representative image shows the conversion of the substrate (S) to product (P) operated by APE1. In the diagram on the right, the mean ± s.d. values of the densitometric analyses of three independent experiments are reported. (**b**) MTS assay was used to evaluate cell viability of MEF-NPM1$^{+/+}$ and NPM1$^{-/-}$ cells after treatment with increasing amount of methoxyamine (MX) for 24 h. Absence of NPM1 negatively affects cell viability, making NPM1$^{-/-}$ cells more sensitive to the damage. Mean ± s.d. values are the result of three independent experiments. (**c**) WST-8 assay was used to evaluate the sensitization of MEF-NPM1$^{+/+}$ and NPM1$^{-/-}$ cells to the inhibition of the APE1 endonuclease activity. Cells were incubated with the indicated amounts of the APE1-inhibitor compound 3, and viability was measured 24 h later. Mean ± s.d. values are the result of three independent experiments. (**d**) Left: on the basis of western blotting analysis of MEF-NPM1$^{+/+}$ and NPM1$^{-/-}$ cells reported in Figure 1a, normalized amount of nuclear cell extract (NCE) was loaded onto SDS–PAGE to obtain equal amounts of APE1. Immunoblot analysis confirmed the presence of the same amount of APE1 protein in the nuclear extracts of the two cell lines. LSD1 was used as nuclear marker, whereas tubulin was used to evaluate cytoplasmic contaminations. Right: normalized amount of NCE from both cell lines was used to evaluate APE1 endonuclease activity. A representative image shows the conversion of the substrate (S) to product (P) operated by APE1. In the diagram below are reported the mean ± s.d. values of the densitometric analysis of three independent experiments. (**e**) Left: MEF-NPM1$^{-/-}$ cells were transiently transfected with pCMV5.1 vector expressing NPM1 in fusion with a C-term FLAG (NPM1 rec.) or the empty vector (Empty) as control. Total cell extracts of 7.5 μg from Empty and NPM1-transfected cells were separated onto SDS–PAGE, and western blotting analysis was performed using α-NPM1 and α-APE1 antibodies. Right: cell extracts of 50 ng from Empty and NPM1-reconstituted MEF-NPM1$^{-/-}$ cells were used to evaluate APE1 endonuclease activity. The representative image reported shows the conversion of the substrate (S) to product (P) by the endonuclease activity of APE1. In the diagram below are reported the mean ± s.d. values of the densitometric analyses of three independent experiments. (**f**) Left: MEF-NPM1$^{-/-}$ cells were stably transfected with p3X-FLAG-CMV vector expressing NPM1 in fusion with a C-term FLAG (NPM1) or the empty vector (Empty) as control. Total cell extracts of 7.5 μg of each clone were separated onto SDS–PAGE, and western blotting analysis was performed using α-NPM1 and α-tubulin antibodies. Right: MTS assay was used to evaluate cell viability of MEF-NPM1$^{-/-}$ cells reconstituted with NPM1 after treatment with increasing amounts of MMS for 8 h. Reexpression of NPM1 rescues cell viability, making NPM1$^{-/-}$ reconstituted cells less sensitive to genotoxic damages. Mean ± s.d. values are the result of three independent experiments.

Though total APE1 protein levels were comparable between OCI/AML3 and OCI/AML2 control cells, NPM1c+ expressing cells, having almost 50% less WT NPM1 protein, have lower APE1 nuclear content (Figure 4b). AP endonuclease assays performed with nuclear extracts of the two cell lines confirmed that OCI/AML3 cells have a significantly reduced APE1 DNA incision

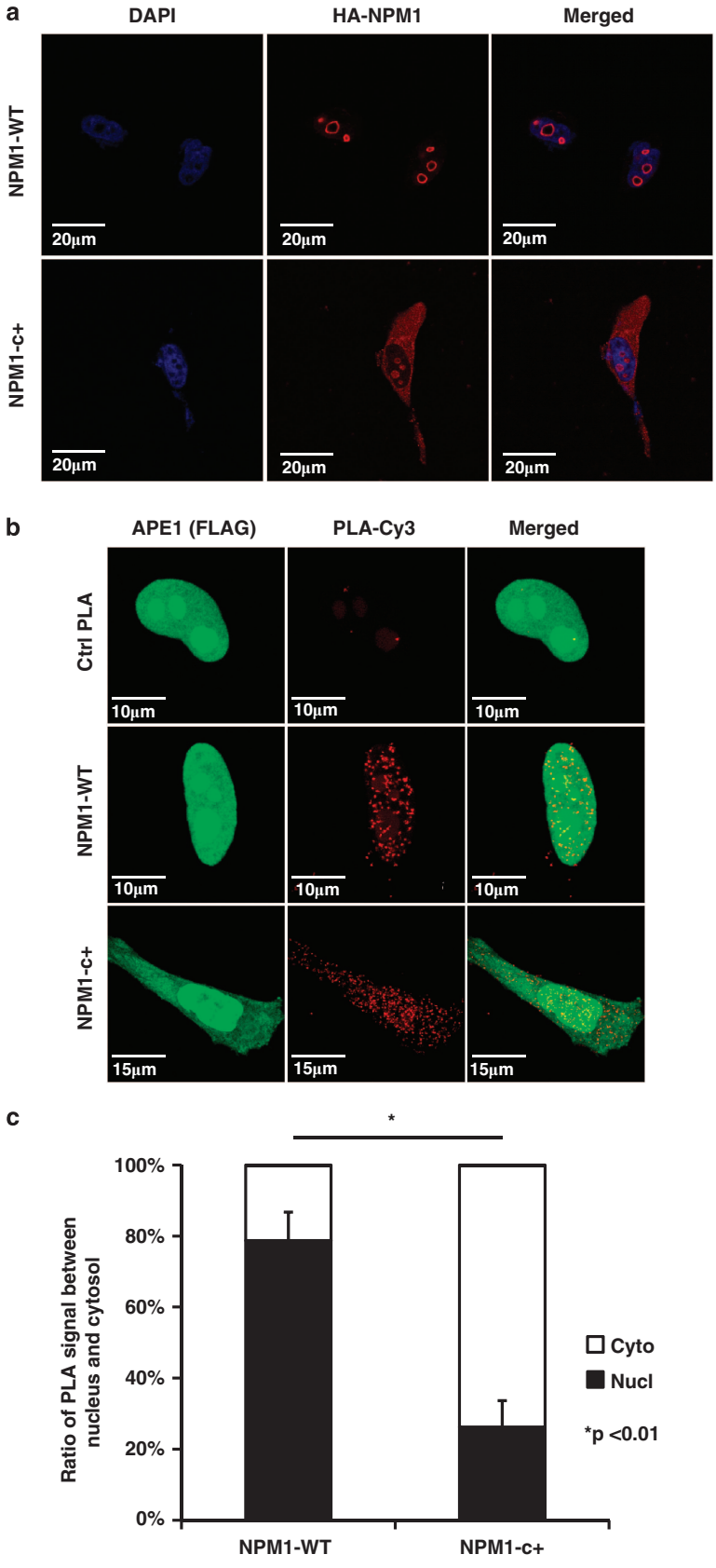

activity (Figure 4d). We then evaluated the ability of the AML cells to efficiently remove AP sites from the DNA of MMS-treated cells. As shown in Figure 4e, OCI/AML3 cells retained a significantly higher level of AP sites both under basal conditions and following MMS treatment than did OCI/AML2 cells. Cell-viability experiments were in agreement with these observations showing that OCI/AML3 cells were significantly more sensitive to MMS treatment than OCI/AML2 cells (Figure 4f).

To provide additional mechanistic insights into the role of APE1 delocalization in NPM1c+ cells and to prove which of the APE1 known functions (that is, DNA repair or redox) are affected by NPM1c+ expression accounting for the higher sensitivity of OCI/AML3 cells to genotoxicants, we performed sensitization experiments to MMS treatment with specific APE1 inhibitors. Methoxyamine, as an APE1 DNA-repair inhibitor, and the well-known E3330 redox inhibitor[52] were used for this purpose. Data obtained (Supplementary Fig S8) show that treatment with the DNA-repair inhibitor, but not with the E3330 redox inhibitor, sensitizes OCI/AML2 cells to MMS treatment and phenocopies the response of the NMP1c+ expressing cells. Moreover, this experiment demonstrates that the functional impairment of the APE1 DNA repair in NPM1c+ cells does not further increase the sensitivity of NPM1c+ cells to genotoxic damage.

Altogether, these data allow to conclude that APE1 functional suppression by NPM1c+ induced relocalization is important for regulating cellular sensitivity to DNA damage in NPM1c+ cells.

Blasts from AML patients, expressing the NPM1c+ mutant protein, have increased cytoplasmic APE1–NPM1 interaction and show impaired BER activity

We tested whether the altered interaction between APE1 and NPM1c+ observed upon ectopic expression of the mutant protein in cell lines also occurs in blasts from AML patients constitutively expressing the NPM1c+ protein. IF and PLA analyses (Figures 5a and b) clearly showed that the NPM1c+ mutations leads to a reduction of the APE1/NPM1 interaction in nuclei, coupled to a strong increase of the APE1/NPM1 association in the cytoplasms of AML blasts. This phenotype is associated with the relocalization of APE1 protein to the cytoplasm, as previously observed in a heterologous cell system (Figure 3b).

To evaluate the physiological relevance of the altered interaction between APE1 and NPM1c+, we compared the sensitivity of blasts from AML patients expressing either the WT or the c+ form of NPM1 with that of healthy donors to DNA-alkylation damage induced by MMS. Cell-viability experiments demonstrated that blasts from AML patients expressing the NPM1c+ form were significantly more sensitive to MMS than healthy control cells and AML-WT NPM1 blasts (Figure 5c). These data support the conclusion that alteration of APE1 distribution due to the NPM1c+ mutation has a significant impact on the BER activity *in vivo* and has a functional relevance in AML pathogenesis.

DISCUSSION

Here we demonstrated that NPM1 has an indirect but significant role in BER through functional regulation of the APE1 endonuclease activity. This observation is the first evidence highlighting a clear function of NPM1 in DNA repair, and these new results provide a possible alternative explanation for a role of NPM1 in the maintenance of genomic stability in addition to its known effect on p53 stability.[2,3] It has been recently shown that homologous recombination-impaired BRCA-deficient cells are hypersensitive to poly (ADP-ribose) polymerase inhibitors that block repair of single-strand breaks, a subpathway of BER. Interestingly, NPM1 functionally interacts with BRCA2 having a role in centrosome duplication.[53] Therefore, it could be speculated that the differential sensitivity of NPM1$^{-/-}$ cells to genotoxicants used in this study could be ascribed to an impaired ability of these cells to repair DNA-strand breaks. However, our data showing no differential sensitivity to poly (ADP-ribose) polymerase inhibitors, together with a similar efficiency of repair of strand breaks (as measured through comet assays) by the two isogenic cell lines, would exclude this hypothesis, leaving BER impairment as the main process affected by the loss of NPM1 expression. Moreover, our findings may illuminate the prompt response to chemotherapy of AML expressing the NPM1c+ mutation. Our data support the hypothesis that some biological effects of NPM1c+ may be exerted through impaired functions of important NPM1-interacting proteins caused by their abnormal cytoplasmic localization.[1,8–13]

APE1 subcellular distribution within different cell types is mainly nuclear and critically controls the cellular proliferation rate,[54–56] however, in some tumors APE1 can be cytoplasmic or nuclear/cytoplasmic.[18,28] Increased expression of APE1 is associated with different tumorigenic processes.[28] In particular, a higher expression of APE1, with consequently increased BER activity, has been described in several cancer types,[28] where it correlates with a higher tumor aggressiveness and is associated with chemoresistance.[18] Extranuclear APE1 has a role within mitochondria in repairing mitochondrial DNA damage[57–59] and in controlling the intracellular reactive oxygen species production through inhibition of Rac1.[60,61] However, a possible causal role of an increased APE1 expression in tumorigenesis, as well as the mechanisms responsible for the unusual APE1 accumulation in the cytoplasmic compartment, has never been investigated in detail.

The observations reported herein provide a molecular explanation for the delocalization of APE1 to the cytoplasm observed in AML tumors associated with NPM1c+. Because APE1 interacts with many different partners involved in RNA metabolism,[17,31,37] the occurrence of extranuclear APE1 localization may be explained on the basis of altered expression levels of its protein partners that may undergo delocalization, as is the case of NPM1c+ itself. Alternatively, increased expression of APE1 cytoplasmic partners, rather than mutations occurring in APE1 itself, may directly affect the distribution of the protein. Notably, no polymorphisms

Figure 3. NPM1 mutation alters APE1 localization in HeLa cells. (**a**) Representative confocal microscopy images of HeLa cells transiently transfected with pcDNA-HA vectors expressing WT NPM1 or the NPM1c+ mutant. Twenty-four hours after transfection cells were fixed and stained with a primary antibody α-HA-Tag and a secondary antibody α-rabbit conjugated with Rhodamine Red. In cells expressing WT NPM1, the ectopic HA-tagged protein localizes, as expected, only within the granular component of nucleoli. On the contrary, cells expressing NPM1c+ mutant show also strong cytoplasm positivity. (**b**) PLA technology was used on HeLa cells to quantify the occurrence of *in vivo* interaction between APE1 and NPM1. Cells were transiently transfected with APE1-FLAG and NPM1-HA-WT or the NPM1c+ mutant. Confocal microscopy analysis highlights the presence of distinct fluorescent red dots (PLA signals), indicating the occurrence of *in vivo* interaction between APE1-FLAG and NPM1-HA, whereas green fluorescence shows APE1-FLAG-tagged protein localization. PLA control is represented by cells incubated only with α-FLAG antibody. In cells transfected with WT NPM1, APE1 accumulates within the nucleus where also PLA signals are mostly present. In NPM1c+ expressing cells, a diffused cytoplasmic APE1 staining could be observed along with the relocalization of PLA signal. (**c**) *Blob Finder* software was used to quantify the relative distribution of PLA signals between nucleus and cytoplasm of cells transfected with WT NPM1 or NPM1c+ mutant. In NPM1c+ expressing cells, most of the interaction between APE1 and NPM1 occurs within the cytoplasm (nuclear: 26 ± 7%), whereas in WT NPM1 cells, PLA signal is predominantly nuclear (nuclear: 79 ± 8%). Reported results are the mean of 30 cells for each condition.

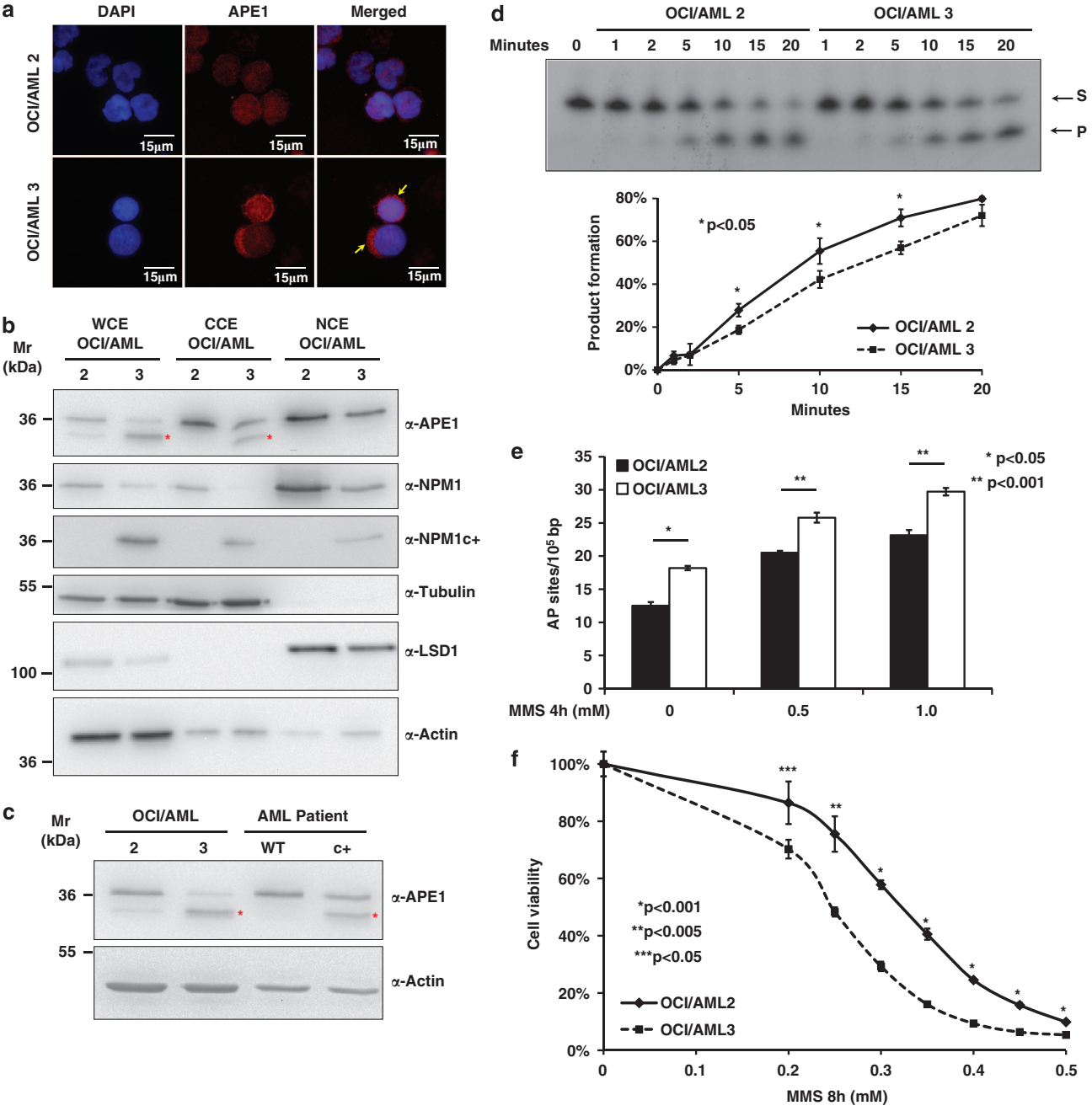

Figure 4. NPM1c+ mutation alters APE1 subcellular localization and affects its endonuclease activity in OCI/AML3 cell line. (**a**) Representative images of fluorescence microscopy analysis of APE1 on OCI/AML2 (WT NPM1) and OCI/AML3 (NPM1c+) cell lines. A total of 2×10^4 cells were centrifuged onto glass slides using a cytospin, and IF was performed as reported in Materials and Methods section. A secondary α-mouse Rhodamine Red-conjugated antibody was used to visualize APE1. Nuclei are stained with 4′,6-diamidino-2-phenylindole. A predominant cytoplasmic positivity of APE1 could be observed in OCI/AML3 cells only, linking NPM1c+ mutation with APE1 cytoplasmic relocalization. (**b**) In all, 10 μg of total cell extract (WCE), 10 μg of cytoplasmic cell extract (CCE) and 5 μg of nuclear cell extract (NCE) of OCI/AML2 and 3 were separated onto SDS–PAGE, immunoblotted and analyzed for their content of APE1 and NPM1 (WT and c+). NPM1c+ protein was detected with a specific antibody recognizing only the NPM1c+ mutant form.[47] Western blotting analysis showed the presence of truncated APE1 protein (*) only in the whole and cytoplasmic extracts from OCI/AML3 cell line. Actin was used as loading control, whereas tubulin and LSD1 were used as markers of cytoplasmic and nuclear fraction enrichment, respectively. (**c**) Total cell extracts of 10 μg from OCI/AML2 and 3 and of blast from AML patients expressing WT NPM and NPM1c+ mutant were separated onto SDS–PAGE, immunoblotted and analyzed for their APE1 content. The expression of NPM1c+ mutant form is associated with the presence of truncated APE1 protein (*) in extracts from both the OCI/AML3 cell line and blasts from a patient carrying this mutation. Actin was used as loading control. (**d**) OCI/AML2 and OCI/AML3 nuclear cell extracts of 50 ng were used to evaluate the APE1 endonuclease activity. A representative image shows the conversion of the substrate (S) to product (P) operated by APE1. OCI/AML3 cells show lower AP-incision activity, in accordance with the decreased nuclear APE1 content. The diagram below reports the mean ± s.d. values obtained from the densitometric analysis of three independent experiments. (**e**) The amount of abasic (AP) sites was measured in OCI/AML2 and OCI/AML3 cells under basal conditions and after treatment with 0.5 and 1 mM MMS for 4 h. OCI/AML3 cells display a significantly higher amount of AP sites if compared with OCI/AML2 cells. Mean ± s.d. values are the result of three independent experiments. (**f**) CellTiter-Glo Luminescent Cell Viability assay was used to evaluate the sensitization of OCI/AML2 and OCI/AML3 cells to MMS. Cells were incubated with the indicated amounts of MMS for 8 h. Expression of NPM1c+ negatively affects cell viability. Mean ± s.d. values are the result of three independent experiments.

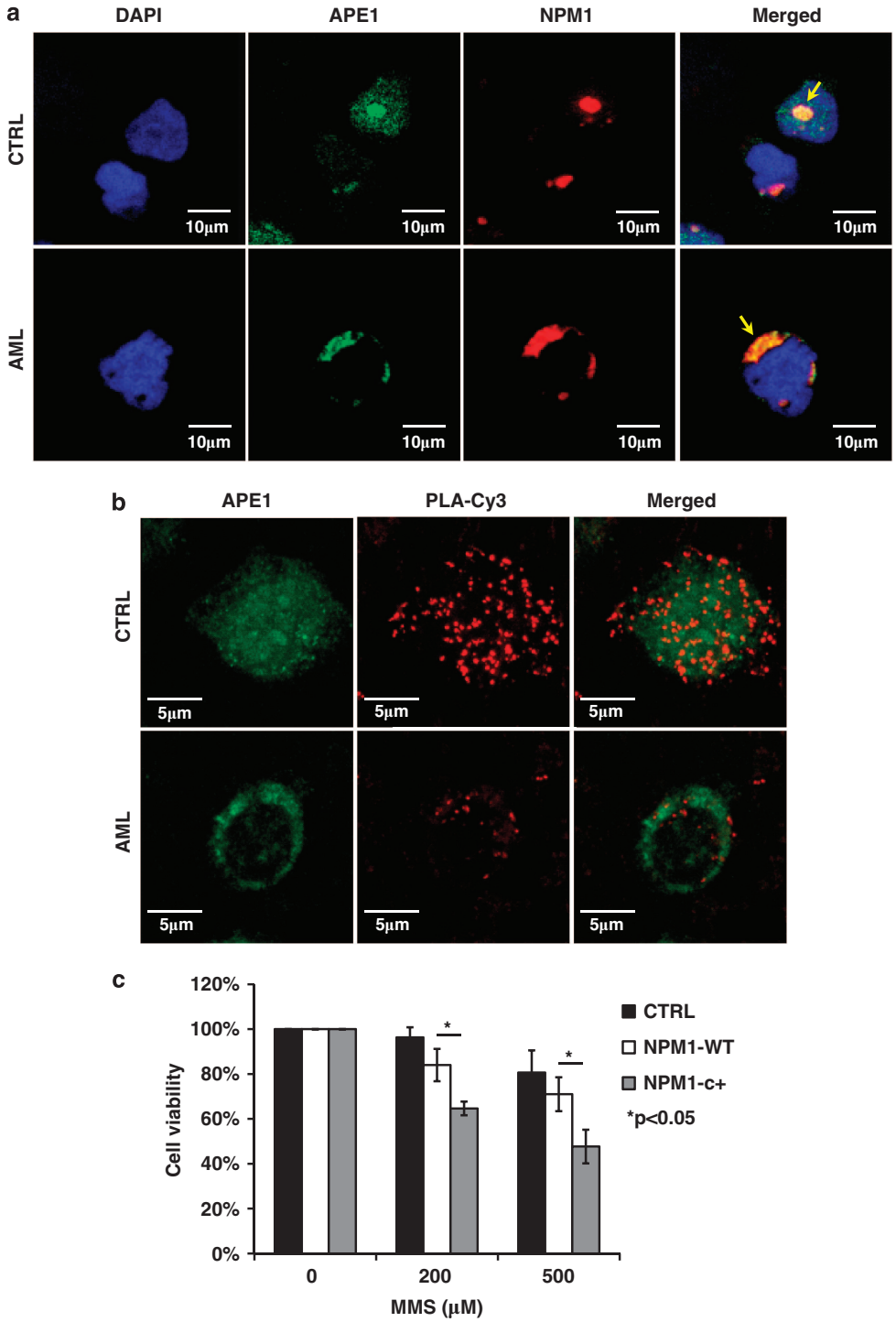

Figure 5. NPM1 mutation alters APE1 localization, reducing cell resistance to genotoxic damage in blasts from AML patients. (**a**) Representative images of fluorescence microscopy analysis of APE1 and NPM1 on blasts from AML patients (AML) carrying NPM1c+ mutation and healthy donors (CTRL). A total of 2×10^4 cells were centrifuged onto glass slides using a cytospin, and IF analyses were performed as reported in Materials and Methods section. A secondary α-mouse-Alexa Fluor 488-conjugated antibody was used to visualize APE1 (green), and a secondary α-rabbit-Rhodamine-conjugated antibody was used to visualize NPM1 (red). Nuclei are stained with 4′,6-diamidino-2-phenylindole. In merged images, yellow arrows indicate the occurrence of colocalization between APE1 and NPM1. In control cells, NPM1 accumulates within nucleoli while being mainly excluded from this subcellular compartment in blasts from AML patients, which show a predominant cytoplasmic positivity. Accordingly, APE1 delocalizes from nucleus to cytoplasm in blasts from AML patients. (**b**) Representative images of PLA analysis to evaluate the interaction between APE1 and NPM1 on blasts from AML patients (AML) carrying NPM1c+ mutation and healthy donors (CTRL). A total of 2.5×10^4 cells were centrifuged onto glass slides using a cytospin, and PLA was performed as reported in Materials and Methods section. APE1 (green) accumulates within the nucleus in control cells while being mainly excluded from this subcellular compartment in blasts from AML patients. In accordance, also PLA signal delocalizes from nucleus to cytoplasm in blasts from AML patients. (**c**) Cell viability of blasts from healthy donors (CTRL, $n = 3$), AML patients expressing WT NPM1 (NPM1-WT, $n = 3$) or the NPM1c+ mutant form (NPM1c+, $n = 4$) after 4 h of treatment with the indicated doses of MMS was measured through the MTS assay. AML cells expressing the NPM1-c+ are more sensitive to the alkylating agent than blasts from healthy donors and AML patients expressing the NPM1-WT form. Mean ± s.d. values are the result of three independent experiments.

occurring on the known bipartite NLS of APE1 have been described so far, nor alternative splicing forms have been found that could explain the cytoplasmic accumulation of APE1 in tumors. As the majority of the polymorphisms described in literature involve residues not responsible for either the DNA repair or the redox functions of the protein, but rather changes that often fall within the N domain involved in protein–protein interactions and protein stability,[33,62] a reasonable explanation for the delocalization of the protein observed in tumors may be ascribed to alterations of a complex network of interactions affecting, in turn, APE1 functional status. Here, we showed that in OCI/AML3 cells expressing the NPM1c+ allele, as well as in blasts from AML patients, APE1 protein is destabilized (Figures 4b and c). It can be inferred that, similarly to the case of $p19^{Arf}$, the physiological function of NPM1 is to ensure the proper localization of APE1 and to protect it from degradation, being possible that NPM1 protein may function as a chaperone for APE1, allowing its correct folding.

Our model (Figure 6a) is in accordance and further extends a previous one[1] trying to explain the relative contribution (direct or indirect) of NPM1 expression to cellular transformation. Our model takes into account the evidence that tumors of hematopoietic origin, such as AML, are associated with WT NPM1 deficiency, whereas a number of solid tumors (that is, gastric, hepatic and ovarian) show increased expression of WT NPM1. In the first case, the contribution of a NPM1 mutation is causally linked to the transformation process. Indeed, reduced nuclear NPM1 levels, as a consequence of the mutation of one WT allele, may lead to genomic instability due to BER impairment, and thus to an increased cellular burden of DNA damage. Therefore, the impaired DNA-damage response may block cell proliferation inefficiently, such that some cells would escape the checkpoint and establish an immortalized clone prone to further oncogenic transformation. Alternatively (Figure 6b), elevated WT NPM1 expression levels would contribute to the generation of permissive condition for oncogenic transformation. In that case, the presence of high NPM1 levels may limit DNA damage and promote the DNA-damage response (due to increased BER), associated with oncogenic stress signals in a normal cell, and therefore may support cell survival and eventually transformation. This model could also involve the APE1 protein in two ways: through an impaired BER response and the resulting genetic instability; and through the establishment of conditions permissive for transformation. Our evidence suggests that defects in the APE1–NPM1 interaction can be associated with the genomic instability observed in tumors, which supports the concept that interfering with this interaction may sensitize cancer cells to chemotherapy and radiotherapy.

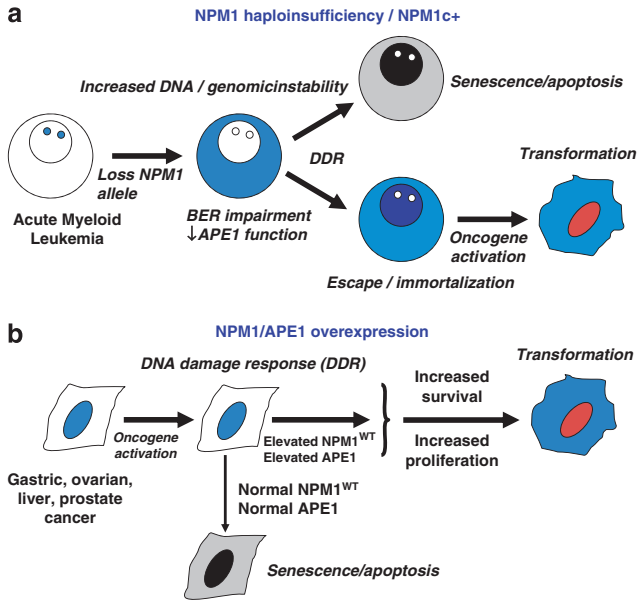

Figure 6. Relative contribution of NPM1/APE1 expression to cellular transformation: a model for APE1 role in tumorigenesis? (**a**) Reduced NPM1 levels due to loss of one WT allele leads to genomic instability through impairment of BER and increased DNA damage. As a consequence, the DNA-damage response blocks cellular proliferation. Few cells may escape the block and establish an immortalized clone prone to be transformed by oncogene activation. (**b**) Oncogene activation in a normal cell leads to unscheduled DNA replication and DNA damage. Cellular checkpoints are activated favoring apoptosis or senescence as response to uncontrolled proliferative signals. The presence of high NPM1/APE1 levels may limit DNA damage and DNA-damage response, and therefore support cell survival and eventually transformation. This model also includes APE1 protein both in the first case as having a causative role in the transformation process itself and in the second case, in which NPM1 and APE1 expression levels are simultaneously elevated, generating a permissive condition for transformation.

MATERIALS AND METHODS

Cell lines and materials

HeLa, MEF $p53^{-/-}$/$NPM1^{+/+}$ ($NPM1^{+/+}$)[36] and MEF $p53^{-/-}$/$NPM1^{-/-}$ ($NPM1^{-/-}$)[36] cell lines were grown in Dulbecco's modified Eagle's medium (Euroclone, Milan, Italy) supplemented with 10% fetal bovine serum (Euroclone), 100 U/ml penicillin and 10 μg/ml streptomycin sulfate. OCI/AML2 and 3 cells were grown in alpha-MEM (Euroclone) supplemented with 20% fetal bovine serum, 100 U/ml penicillin and 10 μg/ml streptomycin sulfate. Leukemic cells were obtained from the bone marrow of patients with acute leukemia during diagnostic procedures. Mononuclear cells were separated on a Ficoll–Hystopaque 1077 (Sigma Aldrich, Milan, Italy) density gradient, then were washed twice in phosphate-buffered saline, checked for viability by using the trypan blue exclusion test and suspended in phosphate-buffered saline. Presence of mutations in the *NPM1* gene was detected as previously described.[63] Blast from patients were grown in RPMI (Invitrogen, Monza, Italy) supplemented with 20% fetal bovine serum. Stable cell lines reexpressing WT NPM1 in the $NPM1^{-/-}$ background were obtained as previously described.[17] All chemical reagents were supplied from Sigma Aldrich unless otherwise specified.

Cell-viability analyses

Cell viability was measured by using the MTS assay (Promega, Milan, Italy) on MEF cells (5×10^3 cells) and blasts from patients (60×10^3 cells) grown in 96-well plates. Cells were plated, and after MMS, $KBrO_3$ or acute H_2O_2 treatment, 20 μl of MTS solution was added to each well and plates were incubated for 2 h at 37 °C. Absorbance (at 490 nm) was measured by using a multiwell plate reader. The values were standardized to wells containing media alone. Cytotoxicity induced by BLM was evaluated using a trypan blue exclusion assay. A total of 4×10^4 cells per well were plated in six-well plates, treated for 60 min with reported amounts of BLM and then grown for 2 additional days in fresh media. Cell viability for OCI/AML cell lines (2.5×10^4 cells) was measured by CellTiter-Glo Luminescent Cell Viability Assay (Promega) according to the manufacturer's protocol. Cells were incubated with the indicated doses of MMS for 8 h at 37 °C in agitation. Luminescent signals were measured using the Turner BioSystems Luminometer (Promega). Cell survival upon inhibition of APE1 AP endonuclease activity was measured with the WST-8 assay. MEF cells were seeded onto 96-well plates (6×10^3 cells) and allowed to adhere for 24 h. MEFs were then incubated with the indicated amounts of compound 3 (*N*-(3-(benzo[*d*]thiazol-2-yl)-6-isopropyl-4,5,6,7-tetrahydrothieno[2,3-*c*]pyridin-2-yl)acetamide),[44] and viability was measured 24 h later using the CCK-8 Kit (Dojindo, Munich, Germany) as per the manufacturer's instructions.

Plasmid preparation

The construct pcDNA3-HA-NPM1c+ was generated by using the Quickchange II XL Mutagenesis kit (Stratagene, Milan, Italy) and the pcDNA3-HA-NPM1-WT as template following the manufacturer's instructions. Direct sequencing was performed in order to verify the sequence accuracy. WT NPM1 and NPM1c+ cDNA were also subcloned in pCMV5.1-FLAG and p3X-FLAG-CMV vectors for reconstitution experiments on MEF-$NPM1^{-/-}$ cells.

AP-sites measurements

Genomic DNA was isolated from 2×10^6 cells by using the DNAzol Reagent (Invitrogen), and then concentration and purity were determined spectrophotometrically. Samples of 0.1 mg/ml of genomic DNA were analyzed to quantify abasic damage in chromosomal DNA using the DNA Damage Quantification Kit (Dojindo) according to the manufacturer's instructions.

IF and PLA analysis

For IF analysis on HeLa and MEFs, cells were grown on glass coverslips, whereas blasts and OCI/AML 2 and 3 cells were centrifuged onto glass slides using a cytospin. Then, cells were fixed with 4% (wt/vol) paraformaldehyde for 20 min at room temperature and permeabilized for 5 min with phosphate-buffered saline–0.25% (vol/vol) Triton X-100. Cells were incubated for 30 min with 10% fetal bovine serum in TBS–0.1% (vol/vol) Tween 20 (blocking solution) to block unspecific binding of the antibodies. Cells were then incubated with primary antibodies diluted in blocking solutions: monoclonal-α-APE1 (diluted 1:50, 3 h, 37 °C), polyclonal α-NPM1 (diluted 1:200, overnight, 4 °C), monoclonal α-FLAG-FITC-conjugated (diluted 1:100, 3 h, 37 °C) and polyclonal α-HA (diluted 1:500, overnight, 4 °C). Then cells were washed three times for 5 min each with TBS–0.1% (vol/vol) Tween 20 (Washing Solution) and incubated with secondary antibody: α-mouse or α-rabbit Rhodamine Red-conjugated or Alexa Fluor 488-conjugated (diluted 1:200, 2 h, 25 °C) (Jackson Immuno, West Grove, PA, USA). After washing three times, coverslips were mounted on microscope slides with a mounting media containing 4′,6-diamidino-2-phenylindole and an anti-fade reagent. For PLA analysis on blasts from patient's primary antibody α-APE1 was previously labeled with the Zenon α-Mouse IgG Labeling Kit (Invitrogen) using the Alexa Fluor 488 according to the manufacturer's instructions.

To study the interaction of APE1 with NPM1 *in vivo*, we used the *in situ* PLA technology (Olink Bioscience, Uppsala, Sweden). After incubation with monoclonal α-APE1 (1:50) or α-FLAG antibody (1:100) for 3 h at 37 °C, cells were incubated with polyclonal α-NPM1 (1:200) or polyclonal α-HA antibody (Sigma-Aldrich) (1:500) overnight at 4 °C. PLA was performed following the manufacturer's instructions and as previously reported.[36] Technical controls, represented by the omission of α-NPM1/α-HA primary antibody, resulted in the complete loss of PLA signal. Images were captured through a confocal microscope, and quantification of PLA signal was performed using the *Blob Finder* software (Center for Image Analysis, Uppsala University).

Cells were visualized through a Leica TCS SP laser-scanning confocal microscope (Leica Microsystems, Milan, Italy) or a DMB6000B inverted microscope equipped with a DFC300FX digital camera (Leica Microsystems).

Preparation of cell extracts and protein quantification

Cell extracts were prepared as already described in Vascotto *et al.*[17] and as reported in Supplementary Information.

Cell transfection and western blotting analyses

Plasmids were prepared and used for transfection and western blotting analysis, as already described in Fantini *et al.*[30] and as reported in Supplementary Information.

Incision assays on abasic double-stranded DNA

APE1 endonuclease activity was evaluated as already described[17] and as reported in Supplementary Information.

Statistical analysis

Statistical analysis on biological data was performed using the Microsoft Excel data analysis program for Student's *t*-test analysis.

ABBREVIATIONS

AML, acute myeloid leukemia; APE1/Ref-1, apurinic/apyrimidinic endonuclease 1/redox effector factor 1; BER, base excision DNA repair; NPM1, nucleophosmin 1.

CONFLICT OF INTEREST

The authors declare no conflict of interest.

ACKNOWLEDGEMENTS

We greatly thank the National Center for Advancing Translational Sciences (NCATS) and Dr David M Wilson III for providing the APE1 specific inhibitor (compound 3). We also thank Dr Malgorzata M Kamocka from the Indiana University School of Medicine, Department of Medicine, Division of Nephrology, Indiana Center for Biological Microscopy, Indianapolis, IN, USA. for her helpful suggestions during IF analyses, Dr Laura Cesaratto for cell-viability assays and Sofia Tell for kind support. This work was supported by grants from: AIRC (IG10269) and MIUR (FIRB_RBRN07BMCT and PRIN2008_CCPKRP_003) to GT. This work has been also supported by a UICC Yamagiwa-Yoshida Memorial International Cancer Study Grant to GT.

REFERENCES

1 Colombo E, Alcalay M, Pelicci PG. Nucleophosmin and its complex network: a possible therapeutic target in hematological diseases. *Oncogene* 2011; **30**: 2595–2609.
2 Colombo E, Marine JC, Danovi D, Falini B, Pelicci PG. Nucleophosmin regulates the stability and transcriptional activity of p53. *Nat Cell Biol* 2002; **4**: 529–533.
3 Lee C, Smith BA, Bandyopadhyay K, Gjerset RA. DNA damage disrupts the p14ARF-B23 (nucleophosmin) interaction and triggers a transient subnuclear redistribution of p14ARF. *Cancer Res* 2005; **65**: 9834–9842.
4 Mrózek K, Marcucci G, Paschka P, Whitman SP, Bloomfield CD. Clinical relevance of mutations and gene-expression changes in adult acute myeloid leukemia with normal cytogenetics: are we ready for a prognostically prioritized molecular classification? *Blood* 2007; **109**: 431–448.
5 Falini B, Bolli N, Shan J, Martelli MP, Liso A, Pucciarini A *et al.* Both carboxy-terminus NES motif and mutated tryptophan(s) are crucial for aberrant nuclear export of nucleophosmin leukemic mutants in NPMc+ AML. *Blood* 2006; **107**: 4514–4523.
6 Pianta A, Fabbro D, Damiani D, Tiribelli M, Fanin R, Franzoni A *et al.* Two novel NPM1 mutations in a therapy-responder AML patient. *Hematol Oncol* 2010; **28**: 151–155.
7 Vassiliou GS, Cooper JL, Rad R, Li J, Rice S, Uren A *et al.* Mutant nucleophosmin and cooperating pathways drive leukemia initiation and progression in mice. *Nat Genet* 2011; **43**: 470–475.
8 den Besten W, Kuo ML, Williams RT, Sherr CJ. Myeloid leukemia-associated nucleophosmin mutants perturb p53-dependent and independent activities of the Arf tumor suppressor protein. *Cell Cycle* 2005; **4**: 1593–1598.
9 Colombo E, Martinelli P, Zamponi R, Shing DC, Bonetti P, Luzi L *et al.* Delocalization and destabilization of the Arf tumor suppressor by the leukemia-associated NPM mutant. *Cancer Res* 2006; **66**: 3044–3050.
10 Bonetti P, Davoli T, Sironi C, Amati B, Pelicci PG, Colombo E. Nucleophosmin and its AML-associated mutant regulate c-Myc turnover through Fbw7 gamma. *J Cell Biol* 2008; **182**: 19–26.
11 Cilloni D, Messa F, Rosso V, Arruga F, Defilippi I, Carturan S *et al.* Increase sensitivity to chemotherapeutical agents and cytoplasmatic interaction between NPM leukemic mutant and NF-kappaB in AML carrying NPM1 mutations. *Leukemia* 2008; **22**: 1234–1240.
12 Gurumurthy M, Tan CH, Ng R, Zeiger L, Lau J, Lee J *et al.* Nucleophosmin interacts with HEXIM1 and regulates RNA polymerase II transcription. *J Mol Biol* 2008; **378**: 302–317.
13 Wanzel M, Russ AC, Kleine-Kohlbrecher D, Colombo E, Pelicci PG, Eilers M. A ribosomal protein L23-nucleophosmin circuit coordinates Mizl function with cell growth. *Nat Cell Biol* 2008; **10**: 1051–1061.
14 Falini B, Nicoletti I, Martelli MF, Mecucci C. Acute myeloid leukemia carrying cytoplasmic/mutated nucleophosmin (NPMc+ AML): biologic and clinical features. *Blood* 2007; **109**: 874–885.
15 Falini B, Martelli MP, Bolli N, Sportoletti P, Liso A, Tiacci E *et al.* Acute myeloid leukemia with mutated nucleophosmin (NPM1): is it a distinct entity? *Blood* 2011; **117**: 1109–1120.
16 Londero AP, Orsaria M, Tell G, Marzinotto S, Capodicasa V, Poletto M *et al.* Expression and prognostic significance of APE1/Ref1 and NPM1 proteins in ovarian serous cancer; submitted.
17 Vascotto C, Fantini D, Romanello M, Cesaratto L, Deganuto M, Leonardi A *et al.* APE1/Ref-1 interacts with NPM1 within nucleoli and plays a role in the rRNA quality control process. *Mol Cell Biol* 2009; **29**: 1834–1854.
18 Tell G, Fantini D, Quadrifoglio F. Understanding different functions of mammalian AP endonuclease (APE1) as a promising tool for cancer treatment. *Cell Mol Life Sci* 2010; **67**: 3589–3608.
19 Wilson 3rd DM, Simeonov A. Small molecule inhibitors of DNA repair nuclease activities of APE1. *Cell Mol Life Sci* 2010; **67**: 3621–3631.
20 Xanthoudakis S, Curran T. Identification and characterization of Ref-1, a nuclear protein that facilitates AP-1 DNA-binding activity. *EMBO J* 1992; **11**: 653–665.

21 Xanthoudakis S, Miao GG, Curran T. The redox and DNA-repair activities of Ref-1 are encoded by nonoverlapping domains. *Proc Natl Acad Sci USA* 1994; **91**: 23–27.
22 Ueno M, Masutani H, Arai RJ, Yamauchi A, Hirota K, Sakai T *et al.* Thioredoxin-dependent redox regulation of p53-mediated p21 activation. *J Biol Chem* 1999; **274**: 35809–35815.
23 Seemann S, Hainaut P. Roles of thioredoxin reductase 1 and APE/Ref-1 in the control of basal p53 stability and activity. *Oncogene* 2005; **24**: 3853–3863.
24 Hirota K, Matsui M, Iwata Z, Nishiyama A, Mori K, Yodoi J. AP-1 transcriptional activity is regulated by a direct association between thioredoxin and Ref-1. *Proc Natl Acad Sci USA* 1997; **94**: 3633–3638.
25 Wei SJ, Botero A, Hirota K, Bradbury CM, Markovina S, Laszlo A *et al.* Thioredoxin nuclear translocation and interaction with redox factor-1 activates the activator protein-1 transcription factor in response to ionizing radiation. *Cancer Res* 2000; **60**: 6688–6695.
26 Ziel KA, Campbell CC, Wilson GL, Gillespie MN. Ref-1/Ape is critical for formation of the hypoxia-inducible transcriptional complex on the hypoxic response element of the rat pulmonary artery endothelial cell VEGF gene. *FASEB J* 2004; **18**: 986–988.
27 Gray MJ, Zhang J, Ellis LM, Semenza GL, Evans DB, Watowich SS *et al.* HIF-1alpha, STAT3, CBP/p300 and Ref-1/APE are components of a transcriptional complex that regulates Src-dependent hypoxia-induced expression of VEGF in pancreatic and prostate carcinomas. *Oncogene* 2005; **24**: 3110–3120.
28 Tell G, Damante G, Caldwell D, Kelley MR. The intracellular localization of APE1/Ref-1: more than a passive phenomenon? *Antioxid Redox Signal* 2005; **7**: 367–384.
29 Bhakat KK, Izumi T, Yang SH, Hazra TK, Mitra S. Role of acetylated human AP-endonuclease (APE1/Ref-1). in regulation of the parathyroid hormone gene. *EMBO J* 2003; **22**: 6299–6309.
30 Fantini D, Vascotto C, Marasco D, D'Ambrosio C, Romanello M, Vitagliano L *et al.* Critical lysine residues within the overlooked N-terminal domain of human APE1 regulate its biological functions. *Nucleic Acids Res* 2010; **38**: 8239–8256.
31 Tell G, Wilson 3rd DM, Lee CH. Intrusion of a DNA repair protein in the RNome world: is this the beginning of a new era? *Mol Cell Biol* 2010; **30**: 366–371.
32 Barnes T, Kim WC, Mantha AK, Kim SE, Izumi T, Mitra S *et al.* Identification of apurinic/apyrimidinic endonuclease 1 (APE1) as the endoribonuclease that cleaves c-myc mRNA. *Nucleic Acids Res* 2009; **37**: 3946–3958.
33 Poletto M, Vascotto C, Scognamiglio PL, Lirussi L, Marasco D, Tell G. Role of the unstructured N-terminal domain of the human apurinic/apyrimidinic endonuclease 1 (hAPE1) in the modulation of its interaction with nucleic acids and nucleophosmin (NPM1). *Biochem J* 2013; **452**: 545–557.
34 Mol CD, Izumi T, Mitra S, Tainer JA. DNA-bound structures and mutants reveal abasic DNA binding by APE1 and DNA repair coordination (corrected). *Nature* 2000; **403**: 451–456.
35 Masuda Y, Bennett RA, Demple B. Dynamics of the interaction of human apurinic endonuclease (Ape1) with its substrate and product. *J Biol Chem* 1998; **273**: 30352–30359.
36 Colombo E, Bonetti P, Lazzerini Denchi E, Martinelli P, Zamponi R, Marine JC *et al.* Nucleophosmin is required for DNA integrity and p19Arf protein stability. *Mol Cell Biol* 2005; **25**: 8874–8886.
37 Lirussi L, Antoniali G, Vascotto C, D'Ambrosio C, Poletto M, Romanello M *et al.* Nucleolar accumulation of APE1 depends on charged lysine residues that undergo acetylation upon genotoxic stress and modulate its BER activity in cells. *Mol Biol Cell* 2012; **23**: 4079–4096.
38 Svilar D, Goellner EM, Almeida KH, Sobol RW. Base excision repair and lesion-dependent subpathways for repair of oxidative DNA damage. *Antioxid Redox Signal* 2011; **14**: 2491–2507.
39 Kaina B, Ochs K, Grosch S, Fritz G, Lips J, Tomicic M *et al.* BER, MGMT, and MMR in defense against alkylation-induced genotoxicity and apoptosis. *Prog Nucleic Acid Res Mol Biol* 2001; **68**: 41–54.
40 Jiang Y, Guo C, Fishel ML, Wang ZY, Vasko MR, Kelley MR. Role of APE1 in differentiated neuroblastoma SH-SY5Y cells in response to oxidative stress: use of APE1 small molecule inhibitors to delineate APE1 functions. *DNA Repair (Amst)* 2009; **8**: 1273–1282.
41 Ballmair D, Epe B. DNA damage by bromate: mechanism and consequences. *Toxicology* 2006; **221**: 166–171.
42 Chen J, Stubbe J. Bleomycins: towards better therapeutics. *Nat Rev Cancer* 2005; **5**: 102–112.
43 Fung H, Demple B. Distinct roles of Ape1 protein in the repair of DNA damage induced by ionizing radiation or bleomycin. *J Biol Chem* 2011; **286**: 4968–4977.
44 Rai G, Vyjayanti VN, Dorjsuren D, Simeonov A, Jadhav A, Wilson 3rd DM *et al.* Synthesis, biological evaluation, and structure-activity relationships of a novel class of apurinic/apyrimidinic endonuclease 1 inhibitors. *J Med Chem* 2012; **55**: 3101–3112.
45 Weibrecht I, Leuchowius KJ, Clausson CM, Conze T, Jarvius M, Howell WM *et al.* Proximity ligation assays: a recent addition to the proteomics toolbox. *Expert Rev Proteomics* 2010; **7**: 401–409.
46 Falini B, Mecucci C, Tiacci E, Alcalay M, Rosati R, Pasqualucci L *et al.* GIMEMA Acute Leukemia Working Party. Cytoplasmic nucleophosmin in acute myelogenous leukemia with a normal karyotype. *N Engl J Med* 2005; **352**: 254–266Erratum in: *N Engl J Med* 2005; **352**: 740.
47 Quentmeier H, Martelli MP, Dirks WG, Bolli N, Liso A, Macleod RA *et al.* Cell line OCI/AML3 bears exon-12 NPM gene mutation-A and cytoplasmic expression of nucleophosmin. *Leukemia* 2005; **19**: 1760–1767.
48 Yoshida A, Urasaki Y, Waltham M, Bergman AC, Pourquier P, Rothwell DG *et al.* Human apurinic/apyrimidinic endonuclease (Ape1) and its N-terminal truncated form (AN34) are involved in DNA fragmentation during apoptosis. *J Biol Chem* 2003; **278**: 37768–37776.
49 Fan Z, Beresford PJ, Zhang D, Xu Z, Novina CD, Yoshida A *et al.* Cleaving the oxidative repair protein Ape1 enhances cell death mediated by granzyme A. *Nat Immunol* 2003; **4**: 145–153.
50 Guo Y, Chen J, Zhao T, Fan Z. Granzyme K degrades the redox/DNA repair enzyme Ape1 to trigger oxidative stress of target cells leading to cytotoxicity. *Mol Immunol* 2008; **45**: 2225–2235.
51 Vascotto C, Bisetto E, Li M, Zeef LA, D'Ambrosio C, Domenis R *et al.* Knock-in reconstitution studies reveal an unexpected role of Cys-65 in regulating APE1/Ref-1 subcellular trafficking and function. *Mol Biol Cell* 2011; **22**: 3887–3901.
52 Kelley MR, Luo M, Reed A, Su D, Delaplane S, Borch RF *et al.* Functional analysis of novel analogues of E3330 that block the redox signaling activity of the multifunctional AP endonuclease/redox signaling enzyme APE1/Ref-1. *Antioxid Redox Signal* 2011; **14**: 1387–1401.
53 Wang HF, Takenaka K, Nakanishi A, Miki Y. BRCA2 and nucleophosmin coregulate centrosome amplification and form a complex with the Rho effector kinase ROCK2. *Cancer Res* 2011; **71**: 68–77.
54 Fung H, Demple B. A vital role for APE1/Ref1 protein in repairing spontaneous DNA damage in human cells. *Mol. Cell* 2005; **17**: 463–470.
55 He T, Weintraub NL, Goswami PC, Chatterjee P, Flaherty DM, Domann FE *et al.* Redox factor-1 contributes to the regulation of progression from G0/G1 to S by PDGF in vascular smooth muscle cells. *Am J Physiol Heart Circ Physiol* 2003; **285**: H804–H812.
56 Izumi T, Brown DB, Naidu CV, Bhakat KK, Macinnes MA, Saito H *et al.* Two essential but distinct functions of the mammalian abasic endonuclease. *Proc Natl Acad Sci USA* 2005; **102**: 5739–5743.
57 Szczesny B, Tann AW, Longley MJ, Copeland WC, Mitra S. Long patch base excision repair in mammalian mitochondrial genomes. *J Biol Chem* 2008; **283**: 26349–26356.
58 Szczesny B, Tann AW, Mitra S. Age- and tissue-specific changes in mitochondrial and nuclear DNA base excision repair activity in mice: Susceptibility of skeletal muscles to oxidative injury. *Mech Ageing Dev* 2010; **131**: 330–337.
59 Tell G, Crivellato E, Pines A, Paron I, Pucillo C, Manzini G *et al.* Mitochondrial localization of APE/Ref-1 in thyroid cells. *Mutat Res* 2001; **485**: 143–152.
60 Angkeow P, Deshpande SS, Qi B, Liu YX, Park YC, Jeon BH *et al.* Redox factor-1: an extra-nuclear role in the regulation of endothelial oxidative stress and apoptosis. *Cell Death Differ* 2002; **9**: 717–725.
61 Ozaki M, Suzuki S, Irani K. Redox factor-1/APE suppresses oxidative stress by inhibiting the rac1 GTPase. *FASEB J* 2002; **16**: 889–890.
62 Yu ET, Hadi MZ. Bioinformatic processing to identify single nucleotide polymorphism that potentially affect Ape1 function. *Mutat Res* 2011; **722**: 140–146.
63 Pitiot AS, Santamaría I, García-Suárez O, Centeno I, Astudillo A, Rayón C *et al.* A new type of NPM1 gene mutation in AML leading to a C-terminal truncated protein. *Leukemia* 2007; **21**: 1564–1566.

Supplementary Information accompanies this paper on the Oncogene website (http://www.nature.com/onc)

CME/SAM

Expression and Prognostic Significance of APE1/Ref-1 and NPM1 Proteins in High-Grade Ovarian Serous Cancer

Ambrogio P. Londero, MD,[1] Maria Orsaria, MD,[2] Gianluca Tell, MSc,[2] Stefania Marzinotto, MSc,[2] Valentina Capodicasa, MD, PhD,[1] Mattia Poletto, MSc,[2] Carlo Vascotto, PhD,[2] Cosimo Sacco, MD,[3] and Laura Mariuzzi, MD[2]

From the [1]Deparment of Experimental Clinical and Medical Science, Clinic of Obstetrics and Gynecology, University of Udine, Udine, Italy; [2]Department of Medical and Biological Sciences, University of Udine, Udine, Italy; and [3]Clinic of Oncology, University Hospital of Udine, Udine, Italy.

Key Words: APE1/Ref-1; NPM1; Survival; Prognostic factors; Ovarian cancer

DOI: 10.1309/AJCPIDKDLSGE26CX

ABSTRACT

Objectives: *To correlate the expression profile of human apurinic endonuclease/redox factor 1 (APE1/Ref-1) with that of nucleolar/nucleoplasmic protein nucleophosmin 1 (NPM1) in association with the aggressiveness and progression of high-grade ovarian serous cancer.*

Methods: *Retrospective study analyzing a tissue microarray of 73 women affected by high-grade ovarian serous cancer. Protein expression was assessed by immunohistochemistry on primary tumor masses and synchronous peritoneal metastases if present.*

Results: *APE1/Ref-1 and NPM1 showed a significant correlation in ovarian serous cancer. Patients with a poorer outcome showed a significant overexpression of nuclear NPM1 protein. A Cox proportional hazards multivariate regression model revealed NPM1 expression to be independently significant for overall survival in high-grade ovarian serous cancers after correcting for stage, age, cytoreduction completeness, and platinum resistance.*

Conclusions: *APE1/Ref-1 interacts with NPM1 to control the DNA damage repair system, and it is likely that this interaction plays a defining role in high-grade ovarian serous carcinoma. A high NPM1 immunohistochemical expression was independently correlated with a shorter survival period and thus appears to be an important prognostic factor.*

Upon completion of this activity you will be able to:

- describe the roles of apurinic endonuclease/redox factor 1 (APE1/Ref-1) and nucleolar/nucleoplasmic protein nucleophosmin 1 (NPM1) in the DNA base excision repair pathway.
- describe APE1/Ref-1 and NPM1 interaction in ovarian high-grade serous cancer.
- predict overall survival of ovarian serous cancer based on low vs high expression of NPM1.

The ASCP is accredited by the Accreditation Council for Continuing Medical Education to provide continuing medical education for physicians. The ASCP designates this journal-based CME activity for a maximum of 1 *AMA PRA Category 1 Credit*™ per article. Physicians should claim only the credit commensurate with the extent of their participation in the activity. This activity qualifies as an American Board of Pathology Maintenance of Certification Part II Self-Assessment Module.

The authors of this article and the planning committee members and staff have no relevant financial relationships with commercial interests to disclose.

Questions appear on p 000. Exam is located at www.ascp.org/ajcpcme.

Ovarian cancer occurs relatively rarely (accounting for 3.1% of female cancers in our region of Italy), but it is a leading cause of death among gynecologic malignancies as a result of three key tensions: the advanced stage of the tumor at diagnosis, the high frequency of recurrences, and its highly chemoresistant nature. Despite an improvement in survival in the past years—due to a more effective combination of surgery and empirically optimized cytotoxic drugs—the overall cure rate remains low.[1] A hallmark of high-grade serous carcinoma is defective homologous DNA repair. The newest breakthrough in treatment is poly adenosine diphosphate ribose polymerase inhibitors,[2] which suppress the ability of cells to repair single-strand DNA breaks, leading to cell death (for tumor cells that lack homologous repair capability). The use of alternative DNA repair inhibitors as a therapeutic

strategy presents an interesting avenue for exploration, and the study of the DNA repair system in ovarian cancer is the first step in this direction.

DNA repair mechanisms appear to play out both in the development and chemoresistance of ovarian cancer.[1,3] In this article, we focus on the immunohistochemical expression of two proteins involved in DNA repair mechanisms: human apurinic endonuclease/redox factor 1 (APE1/Ref-1) and nucleolar/nucleoplasmic protein nucleophosmin 1 (NPM1).

The DNA base excision repair (BER) pathway repairs DNA damage caused by various agents, including chemotherapeutics such as bleomycins, cisplatin, alkylating agents, and ionizing radiations, generating abasic (AP) sites.[4-8] APE1/Ref-1 is the main apurinic/apyrimidinic endonuclease in mammalian cells and catalyzes the removal of the abasic site, a rate-limiting step in BER.[9] It does this by hydrolyzing the 5′ phosphodiester bond of the AP site to generate a DNA intermediate that contains a single-strand break with 3′-hydroxyl and deoxy-ribose-5′-phosphate (5′-dRp) termini. However, APE1/Ref-1 can generate a 3′-hydroxyl terminus in other ways: through its 3′-5′ exonuclease activity, APE1/Ref-1 can remove a 3′-phospho-a,b-unsaturated aldehyde, formed by complex glycosylases and by radiation.[4] APE1/Ref-1 can also remove a 3′ terminal phosphate (through its 3′ phosphatase activity), produced by glycosylases NEIL1 and NEIL2.[9] As such, the APE1/Ref-1 enzyme has a key responsibility for the incision of AP sites and the generation of a 3′-OH, a primer for Pol-b.[4] Upregulation of this ubiquitous and essential protein is at the core of chemoresistance in several tumors, such as hepatic, prostate, and ovarian cancers; accordingly, the protein is attracting attention since it offers a promising target for combination cancer therapy.[4,10]

While APE1/Ref-1 essentiality is attributed to its specific role in BER,[11] it has a secondary independent cellular function as a redox factor, coactivating several transcription factors involved in cancer promotion and progression, such as nuclear factor (NF)–κB. It thus plays a causative role in a range of inflammatory processes.[11,12] Several recent advances have centered on the development of new APE1/Ref-1 inhibitors that interfere with either the DNA repair function or the redox activity of the protein.[4,10] However, since it is hard to separate the roles played by each different APE1/Ref-1 function in tumor chemoresistance and identify how a specific inhibitor would discriminate between untransformed and neoplastic cells, these methods potentially present some functional limitations.

NPM1 is an abundant protein that resides specifically within the granular region of the nucleolus. It is involved in a variety of cellular processes, including centrosome duplication, maintenance of the genome integrity, and ribosome biogenesis.[13] It also has a chaperone activity regulated by phosphorylation[14] and an endoribonuclease activity at a specific site of the spacer region between the 5.8S and the 28S ribosomal RNAs (rRNAs).[15] Notably, it has recently been demonstrated that the role of NPM1 in centrosome duplication is triggered by its interaction with *BRCA2*, a gene with germline mutations that are known to be linked to a predisposition to ovarian cancer.[16]

Recent studies have discovered and characterized the molecular interaction between NPM1 and APE1/Ref-1, which modulates a new function of APE1/Ref-1 in rRNA metabolism.[17,18] This interaction involves Lys27/31/32/35 residues of APE1/Ref-1 and the oligomerization domain of NPM1. Observations prove that NPM1 has a significant stimulatory effect on APE1/Ref-1 DNA repair activity in BER and that without this interaction, the proliferation of tumor cell lines is affected, thus providing a new means through which APE1/Ref-1 can affect cell growth and gene expression in cancer cells. Accordingly, NPM1–/– cells impair BER and react more sensitively to alkylating agents.[19] These findings suggest that an aberrant APE1/Ref-1–NPM1 functional interaction can be linked with the genomic instability of cancers and imply that interfering with the APE1/Ref-1–NPM1 dynamic might allow for improved sensitization of patients to chemotherapy.

Ovarian cancer, as well as hepatocellular carcinoma, is characterized by altered expression and subcellular distribution of APE1/Ref-1 in relation to normal tissue,[20,21] with hepatocellular carcinoma also showing increased NPM1 expression levels.[22] Data are not, however, currently available concerning either the expression of NPM1 in ovarian cancer or a possible association between APE1/Ref-1 and NPM1 expression levels and cancer progression. This study was aimed at filling in this gap. APE1/Ref-1 localization is eminently nuclear, while in these tumors, it can be cytoplasmic and nuclear/cytoplasmic. Elevated levels of APE1/Ref-1 have been linked to chemotherapy resistance, poor prognosis, and survival[11,20] and are related to a higher repair activity, suggesting that BER may account for the onset of chemoresistance.[23-25]

In this study, by assessing a cohort comprising 73 patients affected by high-grade ovarian serous carcinoma, we correlated the expression profile of APE1/Ref-1 with that of NPM1 in association with the aggressiveness and progression of the tumor.

Materials and Methods

Patients and Specimens

From the registry of the Pathology Department of the University Hospital of Udine, Udine, Italy, a total of 105 patients who had a pathologic diagnosis of ovarian serous carcinoma between January 2003 and July 2008 were identified.

DOI: 10.1309/AJCPIDKDLSGE26CX

We focused solely on cases involving primary interventions with a diagnosis of high-grade ovarian serous carcinoma and excluded patients who underwent chemotherapy before surgery. This retrospective study was conducted in accord with the code of ethics of the 1975 Declaration of Helsinki. The histopathologic grading of these cases was evaluated using the Malpica system[26] (low and high grade), and we decided to include in this study only high-grade ovarian serous carcinoma, in accordance with literature that considers low- and high-grade serous carcinomas as two different types of carcinoma.[27] This resulted in a total population of 73 patients. Excluded cases consisted of 20 patients with intraperitoneal recurrences, three who underwent neoadjuvant therapy after laparoscopic staging but before primary surgery, and nine affected by low-grade ovarian serous cancer. All cases were classified into stages according to the International Federation of Gynecology and Obstetrics (FIGO) staging system[28] (stages I, II, III, and IV) and the TNM classification of malignant tumors for ovarian cancer.[29] Other information, such as clinical history and treatment of each patient, was gathered from clinical files. Data collected included age at intervention, date and radicality of intervention, contingent assumption of any hormonal or nonhormonal therapy, parity, gravidity, last menses before intervention, and information on clinical follow-up activities up to January 2011. In archived clinical records, follow-up information consisted of data collected during medical examination (unexplained weight loss, presence of ascites), diagnostic imaging (ultrasound, computed tomography [CT], or positron emission tomography–fludeoxyglucose/CT), blood tests (increase of serum CA125), and second-look surgery. We also made detailed notes about any first-line chemotherapy. During the study period, patients were treated with either single-agent chemotherapy (carboplatin) or platinum-based combination chemotherapy (carboplatin and paclitaxel) **Table 1**. Patients with FIGO stage IA or IB with low-grade tumors were not treated with adjuvant chemotherapy (National Comprehensive Cancer Network guidelines, http://www.nccn.org/professionals/physician_gls/f_guidelines.asp). Platinum resistance was defined as disease progression during first-line chemotherapy or relapse within 6 months after treatment.[30]

Table 1
Population Description[a]

Characteristic	Value
Age at intervention, mean (SD), y	63.6 (12.2)
Menopausal status (n = 73)	56 (77)
Family history of cancer (n = 73)	11 (15)
Adjuvant chemotherapy (n = 73)	70 (96)
Survival after intervention, median (IQR), mo	39 (22-57)
Death from cancer (n = 73)	43 (59)
FIGO staging (n = 73)	
IA	7 (9)
IB	0
IC	4 (6)
IIA	3 (4)
IIB	4 (6)
IIC	6 (8)
IIIA	7 (9)
IIIB	14 (19)
IIIC	26 (36)
IV	2 (3)
Cytoreduction among stage FIGO III (n = 47)	
Complete	39 (83)
Incomplete	8 (17)
First-line chemotherapy (n = 73)	
Carboplatin monotherapy	9 (12)
Carboplatin combination therapy	61 (84)
No chemotherapy	3 (4)
Five-year overall survival, % (95% CI)	
FIGO I-II	42 (24-75)
FIGO III-IV	31 (20-49)

CI, confidence interval; FIGO, International Federation of Gynecology and Obstetrics; IQR, interquartile range.
[a] Data are presented as number (%) unless otherwise indicated.

Preparation of Tissue Microarray Slides

The tissue microarray (TMA) technique allows us to simultaneously analyze multiple formalin-fixed, paraffin-embedded tissues. H&E-stained sections were carefully examined to select representative regions from each selected donor block. TMAs were created using a Beecher (Sun Prairie, WI) tissue microarrayer, and a cylindrical, thin-walled needle (inner diameter of 1.5 mm) was used for coring tissues and transferring cored samples into array cavities in the recipient block. A total of 73 blocks were available, and for each block, we performed two core biopsies representing the primary carcinoma (which involved one or both ovaries) and the metastasis, where a specimen was available. From the recipient block, we obtained 4-µm-thick transverse sections.

For antigen retrieval and deparaffinization, slides were heated for 20 minutes at 98°C in Target Retrieval Solution (low pH, K8005; DAKO, Glostrup, Denmark) with PT-link (DAKO). The slides were then incubated at room temperature in hydrogen peroxide (H_2O_2) for 10 minutes to block endogenous peroxidase activity. The sections were rinsed in phosphate-buffered saline and then incubated in a wet chamber at room temperature for 1 hour with the following primary antibodies: monoclonal APE1/Ref-1 (diluted 1:300; Novus Biologicals, Cambridge, England)[18] and NPM1 (diluted 1:200; Invitrogen Life Technologies, Milan, Italy). A DAKO REAL EnVision Rabbit/Mouse (K5007) was used as a second antibody. Horseradish peroxidase activity was detected using DAKO REAL 3,3′-diaminobenzidine + chromogen (K5007) as substrate for three minutes in accordance with the manufacturer's instructions. Sections were counterstained with hematoxylin with a cover slip. Sections incubated with nonimmune rabbit serum instead of the primary antibody were used as negative controls.

DOI: 10.1309/AJCPIDKDLSGE26CX

Semiquantitative analysis of the immunohistochemical staining was performed independently by two pathologists (M.O. and L.M.), and the staining was semiquantitatively evaluated to produce an H-score (the product of the actual percentage of positive-stained cells and intensity score—evaluated as 3 = strong, 2 = moderate, and 1 = weak—giving a possible range of 0-300). In case of discrepancies, the pathologists together reviewed the specimen and gave a final shared score. In case of disagreement, they reviewed the case with a third pathologist.

Statistical Analysis

Data were analyzed using R (version 2.14.1, R Foundation for Statistical Computing, Vienna, Austria), and $P < .05$ was considered significant. For all proteins analyzed, the staining was investigated in terms of percentage of positive cells and H-score. Normality of variables was tested with the Kolmogorov-Smirnov test. Nonparametric data were presented with the median value and the interquartile range (IQR), whereas parametric data were described with the mean value and its standard deviation. The Kruskal-Wallis test and the one-way analysis of variance for continuous variables were used for the variance analysis where appropriate. For comparison of multiple categorical variables, the χ^2 test was used. For bivariate analysis, the following statistical tests were applied: the Wilcoxon test, *t* test, Spearman ρ, and Kendall τ for continuous variables and the χ^2 and Fisher exact tests for categorical variables. In this work except where otherwise specified, the H-score of the primary ovarian tumor was used for survival analysis. Overall survival was analyzed using Kaplan-Meier curves and with a log-rank test being performed to test for trends. In the Kaplan-Meier survival analysis, we divided our population into two sets: one where the studied proteins were expressed at a level higher than the median value of the distribution and the other in which the expression was lower. Last, we performed Cox proportional hazards univariate and multivariate regression analysis. All potentially influencing factors and their interactions were accommodated in a single statistical model, except when the interaction term was nonsignificant (in which case, we analyzed the no-interaction model). All *P* values presented also have been adjusted for multiple comparisons using the Holm-Bonferroni correction.

Results

Description of the Population

In Table 1, we present the characteristics of our population. Twelve percent received single-agent carboplatin chemotherapy as their first-line treatment; 84% underwent carboplatin combination chemotherapy. The remaining 4% received no chemotherapy (FIGO IA or IB). On the basis of our retrospective analysis, we found that nine patients were platinum resistant at first-line chemotherapy. We also noted that all patients who had platinum resistance were classed as FIGO stage III or higher. We therefore experienced a 12% prevalence of platinum resistance among the total population and an 18% prevalence for the subpopulation of patients at FIGO stage III and higher.

APE1/Ref-1, NPM1 Protein Expression, and Overall Survival

We found APE1/Ref-1 and NPM1 proteins to be expressed in the nucleus of high-grade ovarian serous cancer cells with median (IQR) H-scores, respectively, of 100 (20-133) and 10 (0-77) **Image 1A**, **Image 1B**, **Image 1C**, and **Image 1D**. Both primary ovarian mass and peritoneal metastasis expressed these two proteins in a comparable manner. We recorded median (IQR) APE1/Ref-1 H-scores of 100 (20-133) in the primary ovarian cancer and 80 (40-130) in peritoneal locations ($P = .442$). Similarly, the median (IQR) NPM1 H-score was 10 (0-77) in the primary ovarian location and 8 (0-80) in the peritoneal metastasis (again, the difference was not significant; $P = .765$). Furthermore, APE1/Ref-1 and NPM1 H-scores in our specimens displayed a significant positive correlation, with a ρ of 0.39 (95% confidence interval [CI], 0.19-0.56; $P < .05$) **Image 1E**. All nine patients with platinum resistance presented a significantly higher nuclear APE1/Ref-1 H-score (190; IQR, 190-195) than did platinum-sensitive patients (120; IQR, 74-142) ($P < .05$). Moreover, the NPM1 H-score was nonsignificantly higher in platinum-resistant patients (median [IQR], 90 [80-100]) than in platinum-sensitive patients (52 [20-100]) ($P = .300$).

We then focused specifically on the set of patients who expressed NPM1 or APE1/Ref-1 at levels higher than the median value of the distribution (data not shown), and we noted differences in overall survival, which we detail below **Figure 1A** and **Figure 1B** ($P < .05$).

A significantly decreased overall survival rate in the group of women expressing NPM1 at levels higher than the median value of the distribution in the ovarian primary tumor ($P < .05$) was found (as shown in Figure 1B). We also observed a significant decreased survival rate among women with a nuclear expression of APE1/Ref-1 higher than the median value of the distribution (see Figure 1A). However, this significant difference was not confirmed in the multivariate model, as shown below **Table 2**. Furthermore, the five-year overall survival rate was 51% (95% CI, 36%-71%) for patients with an NPM1 H-score lower than the median value of the distribution, while for patients expressing NPM1 at levels higher than the median, the same rate was 17% (95% CI, 7%-40%) ($P < .05$). In **Image 2**, we present

DOI: 10.1309/AJCPIDKDLSGE26CX

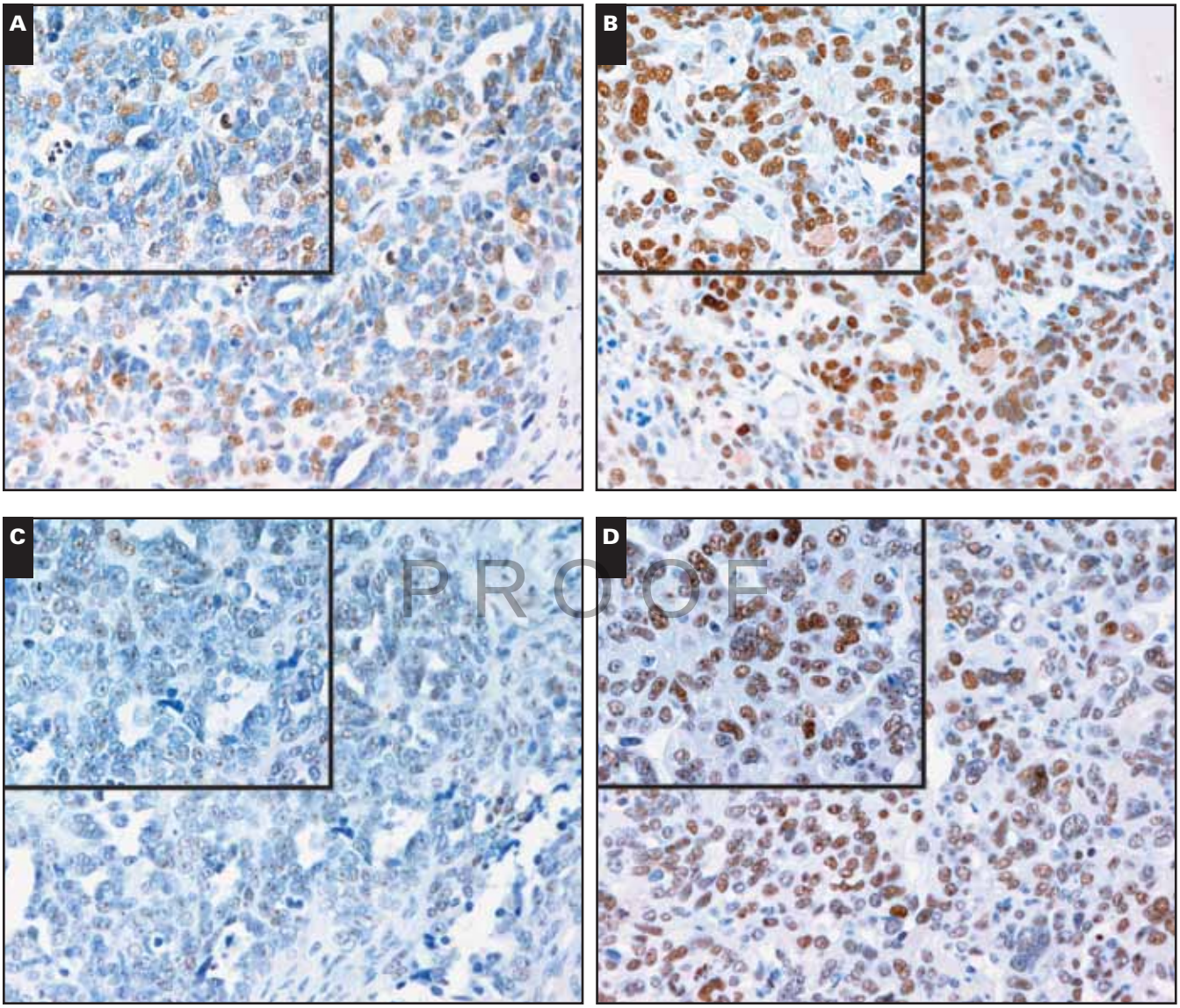

Image 1 Human apurinic endonuclease/redox factor 1 (APE1/Ref-1) and nucleolar/nucleoplasmic protein nucleophosmin 1 (NPM1) expression in ovarian serous cancer and correlation between APE1/Ref-1 and NPM1 expression. We show one case with a high APE1/Ref-1 and NPM1 H-score (case 1, **A** and **C**) and one case with a low APE1/Ref-1 and NPM1 H-score (case 2, **B** and **D**). **A**, APE1/Ref-1 expression shown by immunohistochemistry in high-grade ovarian serous cancer (high H-score = above the 50th percentile of the distribution). APE1/Ref-1 staining was observed in the tumor cell nucleus (×200; inset, ×400). **B**, APE1/Ref-1 expression shown by immunohistochemistry in high-grade ovarian serous cancer (low H-score = under the 50th percentile of the distribution) (×200; inset, ×400). **C**, NPM1 expression shown by immunohistochemistry in high-grade ovarian serous cancer (high H-score = above the 50th percentile of the distribution). NPM1 staining was observed in the tumor cell nucleus and nucleoli (×200; inset, ×400). **D**, NPM1 expression shown by immunohistochemistry in high-grade ovarian serous cancer (low H-score = under the 50th percentile of the distribution) (×200; inset, ×400). **E**, Correlation between human APE1/Ref-1 and NPM1 H-score values (least squares line and Pearson test).

DOI: 10.1309/AJCPIDKDLSGE26CX

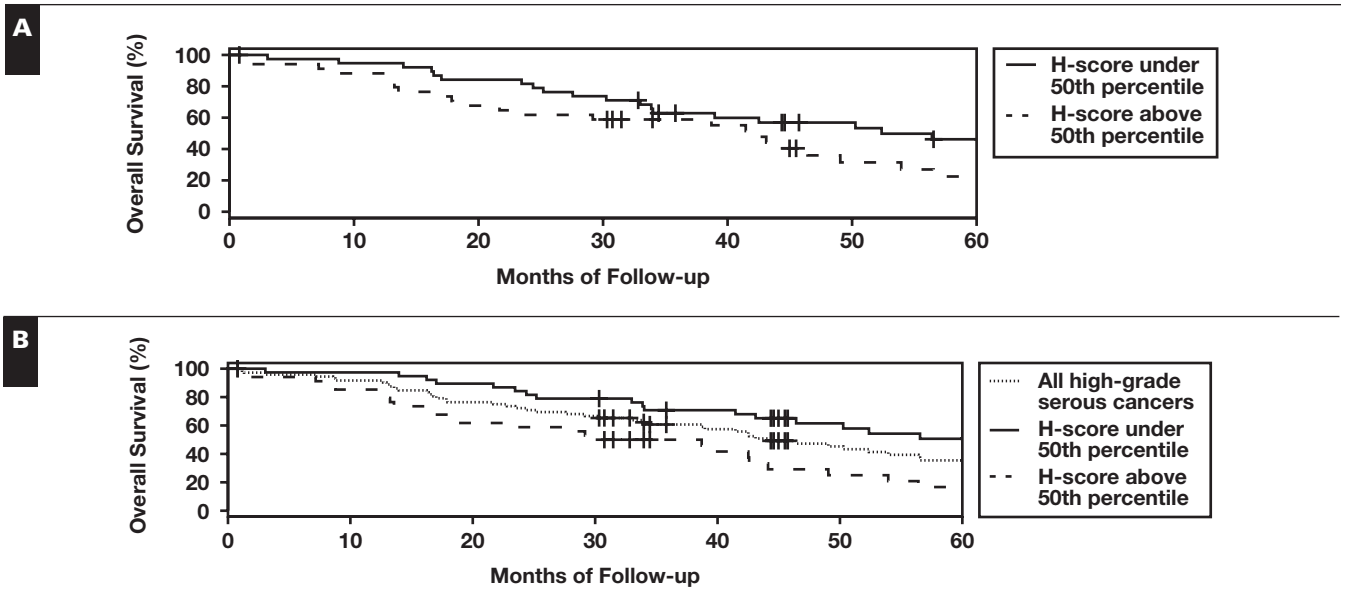

Figure 1 Kaplan-Meier curves of overall survival and human apurinic endonuclease/redox factor 1 (APE1/Ref-1) or nucleolar/nucleoplasmic protein nucleophosmin 1 (NPM1) expression in high-grade ovarian serous cancer (*P* values refer to log-rank test). **A**, Nuclear H-score of APE1/Ref1 above the 50th percentile of the distribution (H-score >100, dashed line) showed a significantly lower survival than the subgroup with H-scores under the 50th percentile of the distribution (solid line). APE1/Ref-1 nuclear staining, $P = .042$. **B**, Women with a nuclear NPM1 H-score above the 50th percentile of the distribution (H-score >10, dashed line) showed a significantly lower survival than the subgroup with H-scores under the 50th percentile of the distribution (solid line). NPM1 nuclear staining, $P = .001$.

Table 2
Cox Proportional Hazards Regression Models in High-Grade Cancers

	Univariate		Multivariate		
Characteristic	**HR (95% CI)**	***P* Value**	**HR (95% CI)**	***P* Value**	***P* Value[a]**
APE1/Ref-1 H-score >100[b]	1.86 (1.01-3.40)	<.05	1.74 (0.88-3.41)	.110	.148
NPM1 H-score >10[b]	2.65 (1.42-4.95)	<.05	2.98 (1.46-6.08)	<.05	<.05
Age at intervention	1.01 (0.98-1.03)	.584	1.03 (1.0-1.06)	.074	.148
FIGO III-IV	1.6 (1.06-2.42)	<.05	1.65 (1.02-2.67)	<.05	.127
Complete cytoreduction	0.43 (0.21-0.85)	<.05	0.41 (0.20-0.83)	<.05	.055
Platinum resistance	4.87 (2.19-10.83)	<.05	9.07 (3.61-22.76)	<.05	<.05

APE1/Ref-1, human apurinic endonuclease/redox factor 1; CI, confidence interval; FIGO, International Federation of Gynecology and Obstetrics; HR, hazard ratio; NPM1, nucleophosmin 1.
[a] Holm-Bonferroni correction.
[b] H-score value higher than the median of the distribution.

more details about H-score distribution and show that with increasing NPM1 H-score, it will decrease the chance of survival (Image 2A).

We performed Cox proportional hazards univariate and multivariate regression analysis for our population of high-grade ovarian serous cancers, analyzing the two studied proteins in context with the main variables known to affect survival (Table 2). Our results demonstrated that high NPM1 H-score values were associated with a higher probability of death than were low H-score values ($P < .05$) in both univariate and multivariate analysis when we corrected for FIGO staging, age at intervention, complete surgical cytoreduction at first intervention, and platinum resistance at first-line chemotherapy (Table 2).

We then looked in detail at FIGO stages in high-grade serous carcinomas and the significant impact that high nuclear NPM1 H-scores had on survival **Figure 2A** and **Figure 2B**. There was no significant difference in NPM1 H-score values between the FIGO stages (Figure 2B). In addition, there was a clear division among high-grade ovarian serous cancers for patients at FIGO stages III to IV: those with low NPM1 nuclear expression had a significantly longer overall survival period than those with a high NPM1 expression ($P < .05$) (Figure 2A). Only in 66% of cases with peritoneal metastases was

DOI: 10.1309/AJCPIDKDLSGE26CX

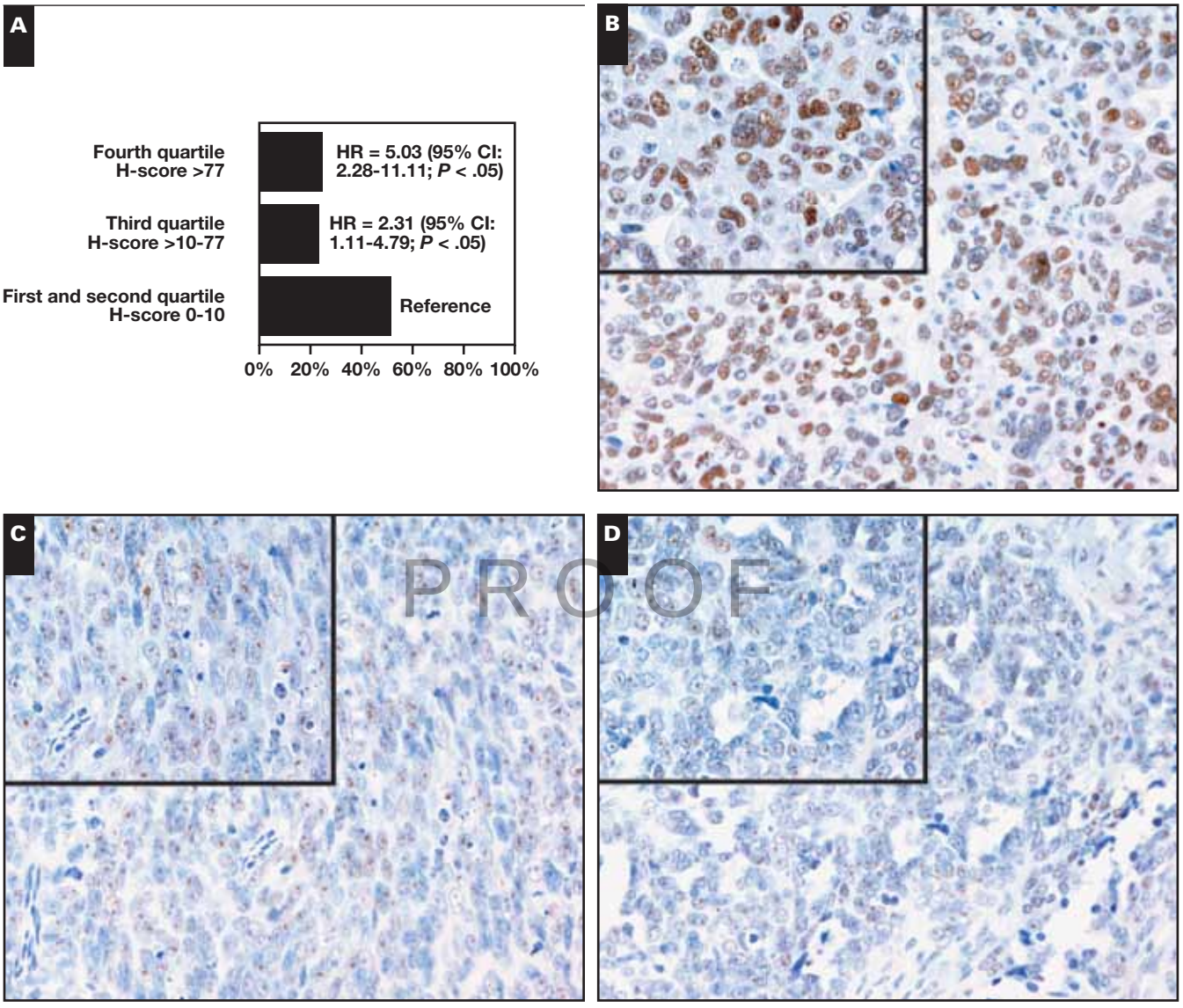

Image 2 Nucleolar/nucleoplasmic protein nucleophosmin 1 (NPM1) and human apurinic endonuclease/redox factor 1 (APE1/Ref-1) expression in ovarian serous cancer. **A**, NPM1 H-score distribution and Cox proportional hazards analysis. We found an increased hazard ratio (HR) in cases with an H-score in the third or fourth quartile of the distribution, with a greater risk of reduced survival in the fourth quartile of the distribution compared with the third quartile. **B-D**, Some examples of NPM1 H-score distribution. **B**, NPM1 expression shown by immunohistochemistry in high-grade ovarian serous cancer (fourth quartile of the distribution H-score >77). NPM1 staining was observed in the tumor cell nucleus and nucleoli (×200; inset, ×400). **C**, NPM1 expression shown by immunohistochemistry in high-grade ovarian serous cancer (third quartile of the distribution H-score >10-77) (×200; inset, ×400). **D**, NPM1 expression shown by immunohistochemistry in high-grade ovarian serous cancer (first to second quartiles of the distribution H-score 0-10) (×200; inset, ×400).

a tissue sample of peritoneal spread present in our archives. Anyway, we also found the NPM1 H-score of peritoneal metastases to be correlated with survival. In fact, an NPM1 H-score higher than the median value of the distribution had a hazard ratio (HR) of 1.88 (95% CI, 0.85-4.15; $P = .117$) and the NPM1 H-score higher than the third quartile value of the distribution had an HR of 3.73 (95% CI, 1.37-10.15; $P < .05$). Delving deeper, we found that among women at FIGO stages III to IV, those who expressed low nuclear NPM1 had a five-year overall survival rate of 48% (95% CI, 31%-76%), while those in the subgroup with high levels experienced a five-year overall survival rate of just 15% (5%-41%) ($P < .05$). We observed the same general pattern in overall survival again for patients at FIGO stages I to II in high-grade ovarian serous cancers, but in these cases, our findings were without statistical significance.

DOI: 10.1309/AJCPIDKDLSGE26CX

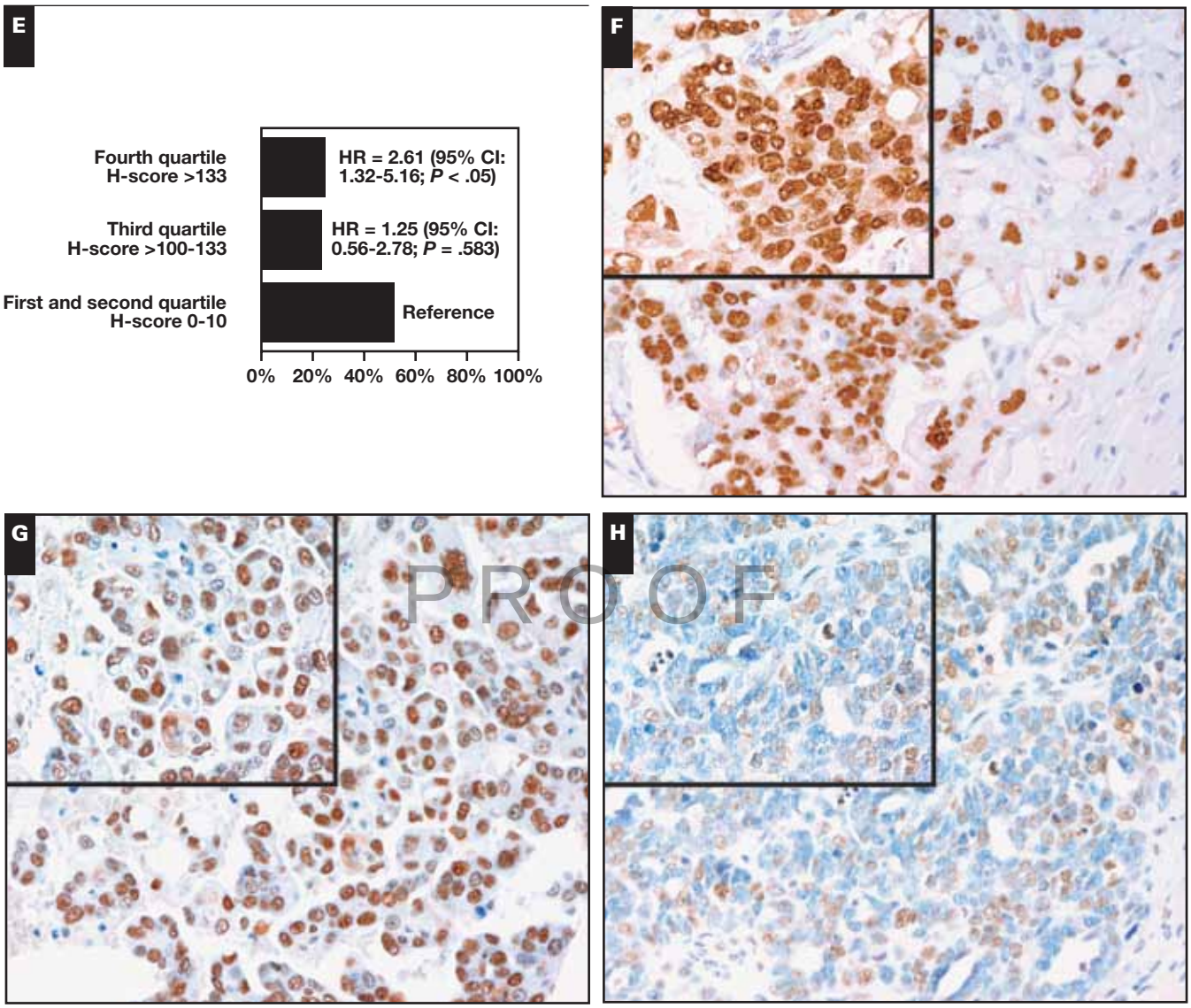

Image 2 (cont) **E**, APE1/Ref-1 H-score distribution and Cox proportional hazards analysis. We found an increased HR in cases with an H-score in the fourth quartile of the distribution. **F-H**, Some examples of APE1/Ref-1 H-score distribution. **F**, APE1/Ref-1 expression shown by immunohistochemistry in high-grade ovarian serous cancer (fourth quartile of the distribution H-score >133). APE1/Ref-1 staining was observed in the tumor cell nucleus (×200; inset, ×400). **G**, APE1/Ref-1 expression shown by immunohistochemistry in high-grade ovarian serous cancer (third quartile of the distribution H-score >100-133) (×200; inset, ×400). **H**, APE1/Ref-1 expression shown by immunohistochemistry in high-grade ovarian serous cancer (first to second quartiles of the distribution H-score 0-100) (×200; inset, ×400).

Discussion

Our study revealed a link between an overexpression of nuclear NPM1 protein and poor outcomes for women diagnosed with high-grade ovarian serous cancer. Interestingly, we found a significant positive correlation between APE1/Ref-1 and NPM1 H-scores, possibly lending support to the emerging hypothesis that the DNA repair function of these two proteins may contribute to a patient's chemoresistance. The relative contribution of NPM1 overexpression to cancer progression may be due to its role in generating a permissive condition for further oncogenic transformation, with its indirect stimulatory effect on APE1/Ref-1 being a key dynamic.[19,31,32] High NPM1 levels may both limit damage to DNA and promote DNA repair (due to increased BER), associated with oncogenic stressor signals activation in a normal cell, so that it may support, in association with an increased APE1/Ref-1 expression level, cell survival as the cancer develops. Our evidence suggests that APE1/Ref-1–NPM1 proteins are linked to cancer aggressiveness, which supports the concept that interfering with the APE1/

DOI: 10.1309/AJCPIDKDLSGE26CX

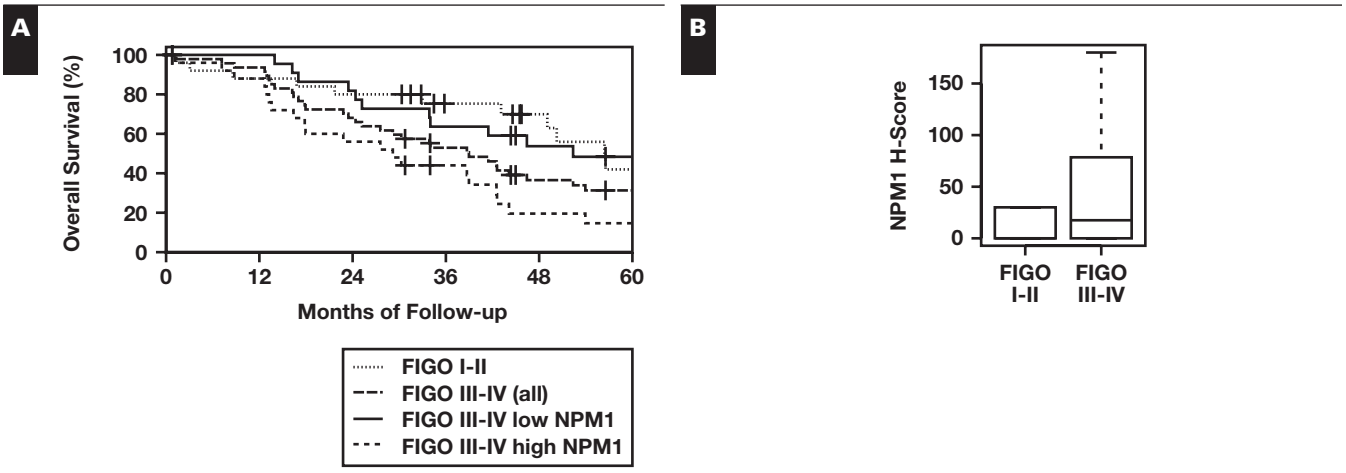

Figure 2 Kaplan-Meier curves of overall survival, International Federation of Gynecology and Obstetrics (FIGO) staging in high-grade ovarian serous cancer, and nucleolar/nucleoplasmic protein nucleophosmin 1 (NPM1) expression in high-grade ovarian serous cancer. **A**, Stage III to IV and NPM1 expression in high-grade ovarian serous cancer: looking at NPM1 expression among the stage III to IV cases (dot-dash line), we identified two subgroups. The subgroup of women with a nuclear NPM1 H-score above the 50th percentile of the distribution (H-score >10, dashed line) showed a significantly lower survival than the subgroup with H-scores under the 50th percentile of the distribution (solid line) ($P < .05$, log-rank test). **B**, NPM1 H-score in stages I to II and III to IV in high-grade ovarian serous cancer ($P = .151$, Wilcoxon test).

Ref-1–NPM1 interaction might enable improved sensitization of cancer cells to chemotherapy and radiotherapy. Corroborating this hypothesis, we found a higher nuclear expression of APE1/Ref-1 in platinum-resistant cancers than in platinum-sensitive ones.

In this article, we have not inspected which of the known APE1/Ref-1 functions are associated with NPM1 overexpression. It is plausible that both BER and rRNA activities may be involved, thus affecting cell proliferation and cell survival. Work along these lines is currently ongoing.

The APE1/Ref-1 interactome network is gaining significance in the research field for understanding ovarian cancer development. This has recently been underlined by the discovery that another known protein binding partner (ERp57)[33] plays an important role in chemoresistance mechanisms in ovarian cancer by modulating the attachment of microtubules to chromosomes following paclitaxel treatment. An interaction with the NPM1 protein is also involved.[34,35]

The main limitation of this study is its retrospective design. This prevented us from accurately assessing cases of disease-free survival and from building a true picture of chemotherapy effectiveness that accounted for the emergence of tumor chemoresistance during the follow-up period. Another limitation was the retrospective application of platinum resistance definitions at first-line chemotherapy. The definition we used likely underestimates the real prevalence in our population—to illustrate, platinum resistance rates in the existing literature for FIGO stage III or higher sit at about 30%.[36] Conversely, the strong correlation between high nuclear NPM1 H-scores and shortened survival periods, which to our knowledge has been evidenced in ovarian cancer for the first time, is a key strength of our study. Data presented herein could influence the clinical management (prognosis determination) and planning of future therapies with respect to drug development and testing on ovarian cancer by presenting new avenues for exploration. Our study also benefitted from a relatively long follow-up period (from a minimum of three years to a maximum of eight years) and from the statistical power gained by analyzing a large number of affected women in the TMA model.

To conclude, we have presented the first study linking NPM1 expression and its prognostic role in overall survival for high-grade ovarian serous carcinoma. Our preliminary data demonstrate that the level of NPM1 expression in the primary tumor and peritoneal metastases influences survival and strongly suggests that its interaction with APE1/Ref-1 plays an important role in ovarian cancer. In particular, the NPM1 immunohistochemical assay would allow specialists to more accurately define a prognosis for patients with high-grade ovarian serous carcinoma.

Address reprint requests to Dr Londero: Dept. of Experimental Clinical and Medical Science, Clinic of Obstetrics and Gynecology, University of Udine, Piazzale SM della Misericordia, 15–33100 Udine, Italy; ambrogio.londero@gmail.com.

This work was supported by grants from the Associazione Italiana per la Ricerca sul Cancro (IG10269) and Ministero Istruzione Università e Ricerca (FIRB_RBRN07BMCT and

DOI: 10.1309/AJCPIDKDLSGE26CX

PRIN2008_CCPKRP_003) to G.T. This study had also financial support from the University of Udine.

This study was presented at Società Italiana di Anatomia Patologica e Citopatologia Diagnostica—Divisione Italiana della International Academy of Pathology; October 25-27, 2012; Florence, Italy.

Acknowledgments: We are grateful to Eilidh P. J. McIntosh for her suggestions on the style and grammatical correctness of our English. We are grateful to Matteo De Luca and Federico Todaro for the technical assistance. We are also grateful to Diego Marchesoni, MD, Carlo Alberto Beltrami, MD, Giuliano Fabiani, MD, and Monica Della Martina, MD, for their help and suggestions.

References

1. Bast RC Jr, Hennessy B, Mills GB. The biology of ovarian cancer: new opportunities for translation. *Nat Rev Cancer*. 2009;9:415-428.
2. Ratner ES, Sartorelli AC, Lin ZP. Poly (ADP-ribose) polymerase inhibitors: on the horizon of tailored and personalized therapies for epithelial ovarian cancer. *Curr Opin Oncol*. 2012;24:564-571.
3. Alvero AB, Chen R, Fu HH, et al. Molecular phenotyping of human ovarian cancer stem cells unravels the mechanisms for repair and chemoresistance. *Cell Cycle*. 2009;8:158-166.
4. Wilson DM III, Simeonov A. Small molecule inhibitors of DNA repair nuclease activities of APE1. *Cell Mol Life Sci*. 2010;67:3621-3631.
5. Kothandapani A, Dangeti VSMN, Brown AR, et al. Novel role of base excision repair in mediating cisplatin cytotoxicity. *J Biol Chem*. 2011;286:14564-14574.
6. Sengupta S, Mantha AK, Mitra S, et al. Human AP endonuclease (APE1/Ref-1) and its acetylation regulate YB-1-p300 recruitment and RNA polymerase II loading in the drug-induced activation of multidrug resistance gene MDR1. *Oncogene*. 2011;30:482-493.
7. Arora S, Kothandapani A, Tillison K, et al. Downregulation of XPF-ERCC1 enhances cisplatin efficacy in cancer cells. *DNA Repair (Amst)*. 2010;9:745-753.
8. Wu HH, Cheng YW, Chang JT, et al. Subcellular localization of apurinic endonuclease 1 promotes lung tumor aggressiveness via NF-kappaB activation. *Oncogene*. 2010;29:4330-4340.
9. Tell G, Fantini D, Quadrifoglio F. Understanding different functions of mammalian AP endonuclease (APE1) as a promising tool for cancer treatment. *Cell Mol Life Sci*. 2010;67:3589-3608.
10. Kelley MR, Georgiadis MM, Fishel ML. APE1/Ref-1 role in redox signaling: translational applications of targeting the redox function of the DNA repair/redox protein APE1/Ref-1. *Curr Mol Pharmacol*. 2012;5:36-53.
11. Tell G, Damante G, Caldwell D, et al. The intracellular localization of APE1/Ref-1: more than a passive phenomenon? *Antioxid Redox Signal*. 2005;7:367-384.
12. Xanthoudakis S, Miao GG, Curran T. The redox and DNA-repair activities of Ref-1 are encoded by nonoverlapping domains. *Proc Natl Acad Sci U S A*. 1994;91:23-27.
13. Frehlick LJ, Eirín-López JM, Ausió J. New insights into the nucleophosmin/nucleoplasmin family of nuclear chaperones. *Bioessays*. 2007;29:49-59.
14. Szebeni A, Hingorani K, Negi S, et al. Role of protein kinase CK2 phosphorylation in the molecular chaperone activity of nucleolar protein b23. *J Biol Chem*. 2003;278:9107-9115.
15. Savkur RS, Olson MO. Preferential cleavage in pre-ribosomal RNA byprotein B23 endoribonuclease. *Nucleic Acids Res*. 1998;26:4508-4515.
16. Wang HF, Takenaka K, Nakanishi A, et al. BRCA2 and nucleophosmin coregulate centrosome amplification and form a complex with the Rho effector kinase ROCK2. *Cancer Res*. 2011;71:68-77.
17. Tell G, Wilson DM III, Lee CH. Intrusion of a DNA repair protein in the RNome world: is this the beginning of a new era? *Mol Cell Biol*. 2010;30:366-371.
18. Vascotto C, Fantini D, Romanello M, et al. APE1/Ref-1 interacts with NPM1 within nucleoli and plays a role in the rRNA quality control process. *Mol Cell Biol*. 2009;29:1834-1854.
19. Vascotto C, Lirussi L, Poletto M, et al. Functional regulation of the apurinic/apyrimidinic endonuclease 1 by nucleophosmin: impact on tumor biology. *Oncogene*. 2013. doi:10.1038/onc.2013.251.
20. Di Maso V, Avellini C, Crocè LS, et al. Subcellular localization of APE1/Ref-1 in human hepatocellular carcinoma: possible prognostic significance. *Mol Med*. 2007;13:89-96.
21. Kakolyris S, Kaklamanis L, Giatromanolaki A, et al. Expression and subcellular localization of human AP endonuclease 1 (HAP1/Ref-1) protein: a basis for its role in human disease. *Histopathology*. 1998;33:561-569.
22. Yun JP, Miao J, Chen GG, et al. Increased expression of nucleophosmin/B23 in hepatocellular carcinoma and correlation with clinicopathological parameters. *Br J Cancer*. 2007;96:477-484.
23. Bobola MS, Blank A, Berger MS, et al. Apurinic/apyrimidinic endonuclease activity is elevated in human adult gliomas. *Clin Cancer Res*. 2001;7:3510-3518.
24. Robertson KA, Bullock HA, Xu Y, et al. Altered expression of Ape1/Ref-1 in germ cell tumors and overexpression in NT2 cells confers resistance to bleomycin and radiation. *Cancer Res*. 2001;61:2220-2225.
25. Rossi O, Carrozzino F, Cappelli E, et al. Analysis of repair of abasic sites in early onset breast cancer patients. *Int J Cancer*. 2000;85:21-26.
26. Malpica A, Deavers MT, Lu K, et al. Grading ovarian serous carcinoma using a two-tier system. *Am J Surg Pathol*. 2004;28:496-504.
27. Vang R, Shih IM, Kurman RJ. Ovarian low-grade and high-grade serous carcinoma: pathogenesis, clinicopathologic and molecular biologic features, and diagnostic problems. *Adv Anat Pathol*. 2009;16:267-282.
28. Heintz APM, Odicino F, Maisonneuve P, et al. Carcinoma of the ovary: FIGO 26th Annual Report on the Results of Treatment in Gynecological Cancer. *Int J Gynaecol Obstet*. 2006;95(suppl 1):S161-S192.
29. Gospodarowicz M, Wittekind C, Sobin L, et al. *TNM Classification of Malignant Tumours*. 7th ed. New York, NY: Wiley-Blackwell; 2009.
30. Al-Attar A, Gossage L, Fareed KR, et al. Human apurinic/apyrimidinic endonuclease (APE1) is a prognostic factor in ovarian, gastro-oesophageal and pancreatico-biliary cancers. *Br J Cancer*. 2010;102:704-709.
31. Fantini D, Vascotto C, Marasco D, et al. Critical lysine residues within the overlooked N-terminal domain of human APE1 regulate its biological functions. *Nucleic Acids Res*. 2010;38:8239-8256.

DOI: 10.1309/AJCPIDKDLSGE26CX

32. Vascotto C, Cesaratto L, Zeef LAH, et al. Genome-wide analysis and proteomic studies reveal APE1/Ref-1 multifunctional role in mammalian cells. *Proteomics*. 2009;9:1058-1074.
33. Vascotto C, Bisetto E, Li M, et al. Knock-in reconstitution studies reveal an unexpected role of Cys-65 in regulating APE1/Ref-1 subcellular trafficking and function. *Mol Biol Cell*. 2011;22:3887-3901.
34. Cicchillitti L, Di Michele M, Urbani A, et al. Comparative proteomic analysis of paclitaxel sensitive A2780 epithelial ovarian cancer cell line and its resistant counterpart A2780TC1 by 2D-DIGE: the role of ERp57. *J Proteome Res*. 2009;8:1902-1912.
35. Cicchillitti L, Della Corte A, Di Michele M, et al. Characterisation of a multimeric protein complex associated with ERp57 within the nucleus in paclitaxel-sensitive and -resistant epithelial ovarian cancer cells: the involvement of specific conformational states of beta-actin. *Int J Oncol*. 2010;37:445-454.
36. McGuire WP, Hoskins WJ, Brady MF, et al. Cyclophosphamide and cisplatin compared with paclitaxel and cisplatin in patients with stage III and stage IV ovarian cancer. *N Engl J Med*. 1996;334:1-6.

DOI: 10.1309/AJCPIDKDLSGE26CX

ANTIOXIDANTS & REDOX SIGNALING
Volume 20, Number 4, 2014

DOI: 10.1089/ars.2013.5491

Discoveries

FORUM REVIEW ARTICLE

Emerging Roles of the Nucleolus in Regulating the DNA Damage Response: The Noncanonical DNA Repair Enzyme APE1/Ref-1 as a Paradigmatical Example

Giulia Antoniali,* Lisa Lirussi,* Mattia Poletto,* and Gianluca Tell

Abstract

Significance: An emerging concept in DNA repair mechanisms is the evidence that some key enzymes, besides their role in the maintenance of genome stability, display also unexpected noncanonical functions associated with RNA metabolism in specific subcellular districts (*e.g.,* nucleoli). During the evolution of these key enzymes, the acquisition of unfolded domains significantly amplified the possibility to interact with different partners and substrates, possibly explaining their phylogenetic gain of functions. ***Recent Advances:*** After nucleolar stress or DNA damage, many DNA repair proteins can freely relocalize from nucleoli to the nucleoplasm. This process may represent a surveillance mechanism to monitor the synthesis and correct assembly of ribosomal units affecting cell cycle progression or inducing p53-mediated apoptosis or senescence. ***Critical Issues:*** A paradigm for this kind of regulation is represented by some enzymes of the DNA base excision repair (BER) pathway, such as apurinic/apyrimidinic endonuclease 1 (APE1). In this review, the role of the nucleolus and the noncanonical functions of the APE1 protein are discussed in light of their possible implications in human pathologies. ***Future Directions:*** A productive cross-talk between DNA repair enzymes and proteins involved in RNA metabolism seems reasonable as the nucleolus is emerging as a dynamic functional hub that coordinates cell growth arrest and DNA repair mechanisms. These findings will drive further analyses on other BER proteins and might imply that nucleic acid processing enzymes are more versatile than originally thought having evolved DNA-targeted functions after a previous life in the early RNA world. *Antioxid. Redox Signal.* 20, 621–639.

Overview on RNA Oxidative Damages, a Glimpse on Human Pathologies

An emerging body of evidence links DNA repair proteins to specific aspects of RNA metabolism associated with quality control processes toward damaged RNA molecules (*e.g.,* oxidized or abasic RNA) (Fig. 1). Due to its intrinsic nature (*i.e.,* mostly single-stranded and with bases not protected by hydrogen bonding or binding to specific proteins) and to its relatively higher amount, RNA may be more susceptible to oxidative insults than DNA (107). Not only 8-hydroxyguanosine (8-OHG) but also 5-hydroxycytidine, 5-hydroxyuridine, and 8-hydroxyadenosine have been identified in oxidized RNA (160). While oxidative damage to DNA is essentially repaired through the base excision repair (BER) pathway, no evidences of similar repair processes have been described for RNA molecules, even though some BER proteins recently entered the arena of the RNome world (138). If not repaired, damage to RNA molecules may lead to ribosomal dysfunctions and erroneous translation; thus, significantly affecting the overall protein synthesis mechanism (38, 135). Moreover, RNA damage has been shown to cause cell cycle arrest and cell death with or without the contribution of p53 and inhibition of protein synthesis (11). Oxidative RNA modifications can occur not only in protein-coding RNAs, but also in noncoding RNAs that recently have been revealed to

Department of Medical and Biological Sciences, University of Udine, Udine, Italy.
*These authors equally contributed to this work.

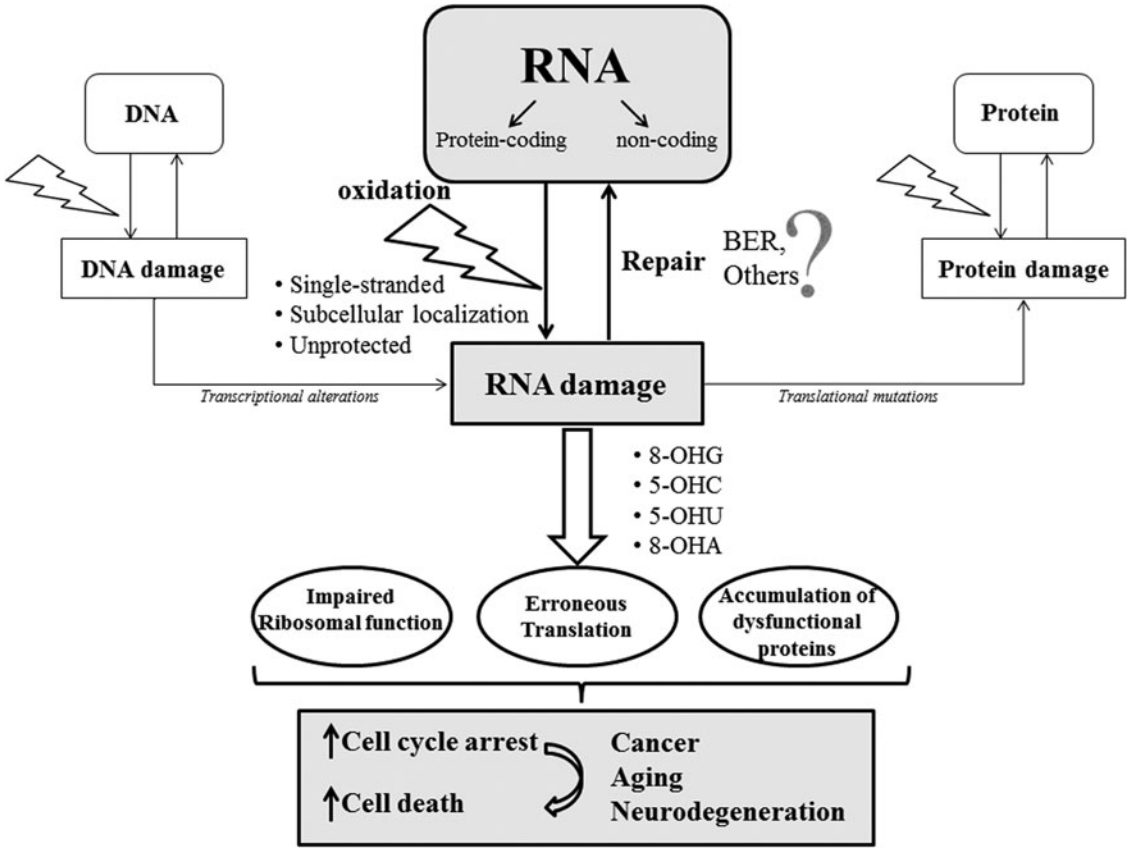

FIG. 1. Potential consequences of unrepaired RNA damage. RNA intrinsic nature renders it more susceptible to damage, such as oxidation. The molecular and surveillance mechanisms that cope with RNA damage are still poorly understood. If unrepaired, aberrant RNA may give rise to translation of defective and toxic protein aggregates that eventually leads to cell cycle arrest and consequently to cell death. These molecular processes have been associated with cancer onset, aging, and neurodegeneration.

contribute to the complexity of the mammalian brain (109). It has been hypothesized that RNA oxidation, causing aberrant expression of microRNAs and proteins, may initiate inappropriate cell fate pathways. Such sublethal damage to cells, while less toxic than genomic mutations and not inheritable, might be associated with underlying mechanisms of degeneration, such as age-associated neurodegeneration.

Currently, little is known about how cells may cope with damaged RNA, either modified or oxidized, but it is clear that such RNA can impair protein synthesis; thus, affecting cell function and viability. Therefore, specific surveillance mechanisms are needed to remove damaged molecules from the RNA pool to guarantee the biological integrity of cells. The idea that quality control mechanisms might exist to repair RNA was put forward after the identification of the biochemical activities of the mammalian AlkB homologs. In particular, it was discovered that AlkB (from *Escherichia coli*) and the human homolog hABH3, besides being able to directly reverse alkylation damage on DNA bases, were able to demethylate damaged bases on RNA; thus, playing a key role in the repair of specific RNA lesions (1, 111). While repair mechanisms have been demonstrated for alkylated RNA, the existence of such cleansing activities has not yet been identified for oxidatively damaged RNA. However, their existence appears unlikely, in the absence of direct reversal strategies, due to the lack of a template for accurate repair, as happens in the case of double-stranded DNA. The observation that under oxidative stress RNA modifications can occur up to a 10–20-fold higher extent than DNA (88), raises the question of how oxidized RNA may be specifically removed or repaired. The recent findings by Berquist *et al.* (12), Barnes *et al.* (7), and Vascotto *et al.* (149) highlight a novel "moonlighting" role for the repair apurinic/apyrimidinic (AP) endonuclease 1 (APE1) in RNA metabolism, both as a possible "cleansing" factor for damaged abasic RNA and as a regulator of *c-myc* gene expression through mRNA decay. In agreement with this hypothesis, a significant reduction in the protein synthesis rate occurs upon silencing of APE1 expression (149). Enzymatic (*e.g.*, by specific N-ribohydrolases, including the toxin ricin) (126), besides spontaneous (91), generation of abasic sites occurs upon ribosomal RNA (rRNA) oxidation. A role for the Y box binding protein 1 (YB-1) in recognizing 8-OHG sites has also been hypothesized (56), but no specific enzymatic mechanisms that can remove the oxidized base have been described yet. The accumulation of the 8-OHG substrates, which occurs upon silencing of APE1 expression (149), may thus, be explained under the assumption that enzymatic removal of oxidized RNA bases represents the limiting step in the process. According to this model, as already hypothesized for DNA substrates, APE1 could act through stimulation of a yet unknown glycosylase activity, by allowing a faster turnover (152). The APE1 interaction with RNA and with proteins

involved in ribosome assembly (*i.e.,* RSSA, RLA0) and RNA maturation (*i.e.,* PRP19) within the cytoplasm (149), could also represent a molecular proof of concept for the "extranuclear" functions of this noncanonical DNA repair enzyme. The RNA-mediated association with some of the APE1 protein partners would reinforce the view of APE1 as an essential factor in the RNA quality control process and may also explain the cytoplasmic accumulation of APE1 observed in a number of tumoral cell types (136, 137). An age-associated increase in oxidative nucleic acids damage, predominantly to RNA, has been recently highlighted in neurons from human and rodent brains; this phenomenon may play a fundamental role in the development of age-associated neurodegeneration (109). Oxidative damage to RNA molecules, both coding for proteins (mRNA) or performing translation (rRNA and tRNA), has been recently associated with the occurrence of neurodegenerative diseases, such as Alzheimer's disease (AD), Parkinson disease (PD), dementia with Lewy bodies, and amyotrophic lateral sclerosis (107) and its impact in cancer development cannot be excluded, at present (11). Remarkably, studies performed on either human samples or experimental models, show that RNA oxidation is a characteristic of aging neurons. Its prominent occurrence in vulnerable neurons at early stage of age-associated neurodegenerative disorders indicates that RNA oxidation actively contributes to the development of the degeneration. Therefore, all the hypotheses concerning the involvement of APE1 in the development of such pathologies should be re-interpreted in light of these findings. The role played by APE1 in RNA-related processes needs further investigations, since its ability to recognize and cleave the RNA abasic sites (12, 42, 89, 138, 149) is compatible with a leading role in the early stages of the RNA quality control process. Additional studies aiming at the understanding the mechanisms related to oxidative RNA damage processing and their consequences may provide significant insights into the pathogenesis of neurodegenerative disorders, leading to improvements in the current therapeutic strategies.

The vast majority of cellular RNA is transcribed, assembled, and processed within nucleoli. These subcellular compartments appear to be perfect sensors for cellular stress, as they integrate RNA damage and growth control with signals to the DNA repair machineries. The following paragraphs will describe the emerging dynamics roles of this organelle in regulating the trafficking of DNA repair proteins during genotoxic damage.

Structure, Composition, and Classical Functions of the Nucleolus

The nucleolus is considered the ribosome factory of eukaryotic cells (18, 62) in which synthesis, maturation, and processing of rRNA, as well as assembly of rRNA with ribosomal proteins (RPs) take place (62) (Fig. 2). This membraneless organelle is considered a dynamic structure (4, 84), where protein complexes are continuously exchanged with the nucleoplasm. Its classical tripartite organization has been dissected using electron microscopy and reflects the different steps of ribosomal biogenesis (130): (i) the fibrillar center, where the RNA polymerase I (Pol I) transcription starts; (ii) the dense fibrillar component, where the initial stages of pre-rRNA processing occur and (iii) the granular component involved in the late processing steps (62). Transcription of the ribosomal DNA (rDNA) repeats generates a 47S pre-rRNA precursor that is further cleaved and processed into 28S, 18S, and 5.8S rRNAs and concomitantly assembled into large and small ribosomal subunits together with the 5S rRNA molecules (18, 32a). These complex series of events is controlled, in yeast, by roughly 150 small nucleolar RNAs (snoRNAs) and two large ribonucleoprotein complexes, named small subunit processosome (for the 40S ribosomal subunit) and large subunit processosome (for the 60S ribosomal subunit) (130). Two types of nucleotide modifications (2′-*O*-methylation and pseudouridylation) are introduced during the maturation process by snoRNAs belonging to the box C/D or box H/ACA families and mediate endonucleolytic cleavages of pre-RNAs (130, 32a). In addition, ribosomal gene transcription is regulated through the modulation of the transcriptional apparatus and epigenetic silencing (131). Large and small mature ribosome particles are independently exported to the cytoplasm through an exportin 1 (CRM1) and Ran-GTP-dependent mechanism: export of 60S subunit requires the exchange of complexes Noc1-Noc2 by Noc3-Noc2 (102) and the association with the adaptor shuttling protein NMD3 (142), whereas the 40S needs the heterodimer Noc4p/Nop14p (103). The work by Hinsby *et al.* exploited a machine learning-based predictor of nuclear export signals to analyze the late stage pre-40S complex, suggesting a role also for the human homolog of yeast DIM2p in the targeting and translocation of the late 40S to the cytoplasm (63).

The organization, the number, and the size of nucleoli in each cell is directly linked to the nucleolar activity (*i.e.,* Pol I transcription rate), which, in turn, depends on cell growth and metabolism (20). Generally, highly proliferating cells present many small nucleoli (62, 130). Ribosomal biosynthesis is a highly energy- and resources-consuming process (134); this explains why this process is tightly regulated by changes in cell proliferation, growth rates, and metabolic activities. Nucleoli constantly integrate different signaling events, maintaining the ribosomal subunit pool required to properly support protein synthesis during cell growth and division (18).

Biosynthesis of ribosomes is a very efficient process, since it has been estimated that 14,000 new ribosomal subunits can be synthesized every minute in an exponentially growing cell (125). The process has to be fine-tuned and several evidences indicate that ubiquitin and ubiquitin-like proteins-based regulatory circuits may control different stages of ribosome formation (129). Lam *et al.* (83) demonstrated that the levels of unassembled RPs within nucleoli exceed the required RP:rRNA ratio and identified an ubiquitin-proteasome-mediated mechanism, that monitors and degrades this excess (115). Ribosomal structural proteins are imported from the cytoplasm in supra-stoichiometric complexes and exported in the form of assembled ribosomal subunits; this ensures that RPs are never rate-limiting for the ribosomal assembly (83). The excess of protein undergoes ubiquitylation and degradation in the nucleoplasm through the proteasome system (114, 129), indicating that mammalian cells produce large amount of these proteins and degrade those that are not assembled with rRNA.

"Dynamic Trafficking:" Keywords of the Nucleolar Physiology

The nucleolus appears as a very dynamic organelle and different types of rearrangements involve this subnuclear

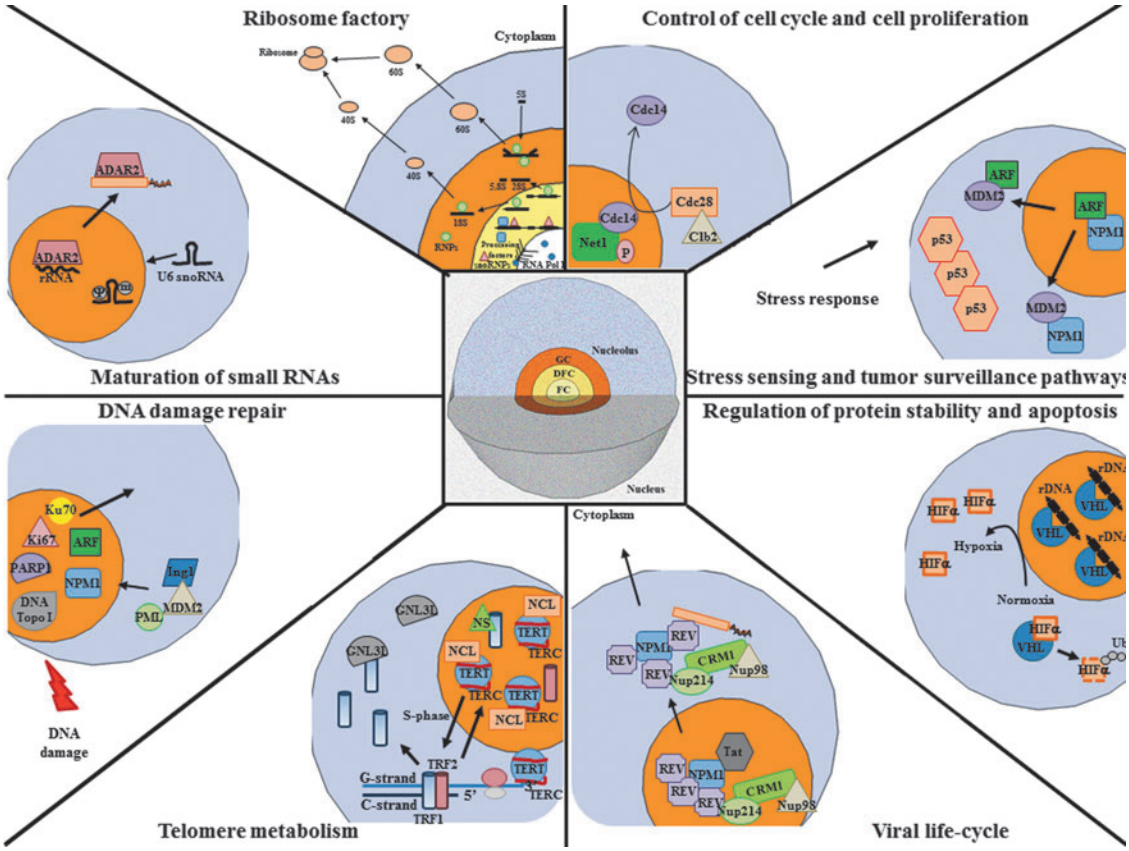

FIG. 2. The nucleolus, a multifunctional domain. The unveiling of the "nucleolome" allowed the understanding of the complexity of the nucleolus, firstly described only as a ribosome factory. The multifunctionality of the nucleolus includes different noncanonical functions as the control of cell proliferation and cell growth, regulation of protein stability, stress and DDR, telomere metabolism, maturation of small RNAs, and control of viral life-cycle. An illustrative mechanism for each function is summarized. MDM2, mouse double minute 2 homolog; ARF, p14 alternative reading frame; ADAR2, double-stranded RNA-specific adenosine deaminase 2; NS, nucleostemin; VHL, von Hippel-Lindau protein; HIF, hypoxia-inducible factor; ING1, inhibitor of growth family protein, member 1; PML, promyelocytic leukemia protein; DNA Topo I, DNA topoisomerase I; TERC, telomerase RNA component; TERT, telomerase reverse transcriptase; GNL3L, guanine nucleotide binding protein-like 3 (nucleolar)-like; TRF, telomeric repeat-binding factor 2; REV, regulator of expression of virion protein; Tat, trans-activator of transcription; Ub, ubiquitin; DDR, DNA damage response. To see this illustration in color, the reader is referred to the web version of this article at www.liebertpub.com/ars

district. First, the ribosome assembly is a vectorial process, in which the ribosomal particles move away from their biogenesis sites. The second dynamic aspect is represented by the constant flux of proteins from the nucleoli to the nucleoplasm. Lastly, nucleolar components present scheduled reorganization every cell cycle, with assembly and disassembly steps required for the redistribution of nucleolar components between the two daughter cells (110).

The cyclic reorganization observed during cell cycle involves the nucleolus as a whole, as this organelle assembles at the end of each mitosis to remain functionally active until the beginning of the next one (4, 62). The nucleolar disassembly observed during mitosis is linked to rDNA transcriptional repression induced by CDK1-cyclin B-directed phosphorylation of components of the rDNA transcription machinery (130). Conversely, the formation of functional nucleoli at the exit of mitosis is not uniquely controlled by the resumption of rDNA transcription, but by a two-steps process regulated by cyclin-dependent kinases that connects the resumption of rDNA transcription and the restoration of rRNA processing (130). During late telophase, nucleoli form around the nucleolar organization regions, which are chromosomal domains where rDNAs, clustered in head-to-tail arrays (62, 84), are transcribed. This sub-nuclear compartmentalization allows the cells to locally concentrate all the factors required for the ribosomal biogenesis (18, 20).

The Way to Move: Visitors *Versus* Resident Nucleolar Proteins

Differently from nuclear localization signals (NLSs), nucleolar localization sequences (NoLSs) are not well characterized and no clear consensus sequences have been described yet (115, 130). NoLSs identified so far are rich in basic residues (*e.g.*, Arg and Lys) (40), but also Trp residues were described to play a functional role for the nucleolar localization of nucleophosmin 1 (NPM1) (108a). Since the mass per unit nucleolar volume is only twofold higher compared with the nucleoplasm, all diffusing macromolecules should theoretically be able to enter nucleoli: it is now clear that the residence time of nucleolar proteins depends on their relative affinity for preanchored complexes present within the nucleolus itself

(114, 115). The ability of different proteins to localize within the nucleolus has been linked to the stable interaction with anchored resident proteins, such as NPM1 or nucleolin (NCL), that may act as carriers, or as a retention scaffolds, supporting the idea that the residence time of proteins within the nucleolar compartment is strongly related to their specific interactions in a process known as "nucleolar sequestration" (40, 115, 130). Though all the molecules resident in the nucleoplasm may, in principle, enter into nucleoli, only those with an affinity for nucleolar resident proteins, are retained for longer times (110). For this reason some authors suggested the concept of "retention signal" in place of "targeting signal" for the nucleoli (121). Since the residence time is quite short and most of the nucleolar proteins shuttle from nucleoli to nucleoplasm and vice versa, the interaction of visitor proteins with anchored nucleolar residents has to be reversible (110, 115). Current models show that proteins and RNAs continuously flow and freely diffuse through the nuclear space (131): the average residence time for most nucleolar proteins within nucleoli is estimated to be only a few tens of seconds. Thus, nucleolus appears as a steady state structure with its component in a dynamic equilibrium with the surrounding nucleoplasm (121). However, in spite of this continual exchange of molecules between these two compartments, nucleolar domains are maintained because the number of retained proteins is higher than the amount of molecules that are released from the same domain (32a). Resident factors, able to connect and bind multiple protein partners, are considered as "hub proteins" and might be responsible for the nucleolar localization of the vast majority of visitor proteins in the absence of RNA–protein interactions. Each hub protein may have different recognition requirements; thus, possibly explaining the occurrence of different NoLSs. Two typical examples of hub proteins are NCL and NPM1, which contain disordered regions involved in protein–RNA interactions (40).

Recently, an additional protein retention mechanism based on GTP-driven cycles has been identified for nucleostemin (121). The GTP-GDP exchange mechanism is not the only intracellular signal able to move nucleolar proteins: stimuli as the hydrogen ion were already described by Mekhail *et al.* (98), who demonstrated how the nucleolar sequestration of the von Hippel-Lindau protein after a pH change promotes the stabilization of the hypoxia-inducible factor, triggering a general cell response to hypoxic conditions (115).

New Concepts in the Nucleolus Physiology: Beyond the Ribosome Factory

In the 60s, after the identification of the localization of ribosomal genes, the main function of the nucleolus was nicely summarized as "an organelle formed by the act of building a ribosome" (63). In the last decades, thanks to the development of technologies, such as protocols for the isolation of large amounts of nucleoli and the improvement of high-throughput mass-spectrometry-based proteomic approaches, several proteomic analyses were undertaken, unveiling the "nucleolome" (4, 5, 18, 32a, 125). Over 4500 proteins were described to localize within nucleoli and both bibliographic and bioinformatics analyses allowed to classify eight major functional groups (RPs, ribosome biogenesis, chromatin structure, mRNA metabolism, translation, chaperones, fibrous proteins, and others [see Fig. 3 for further details]) (3, 18, 32a, 108). Characterization of the nucleolar proteome under different stress conditions (*e.g.*, actinomycin D) further underlined the complexity of the nucleolome dynamics (5).

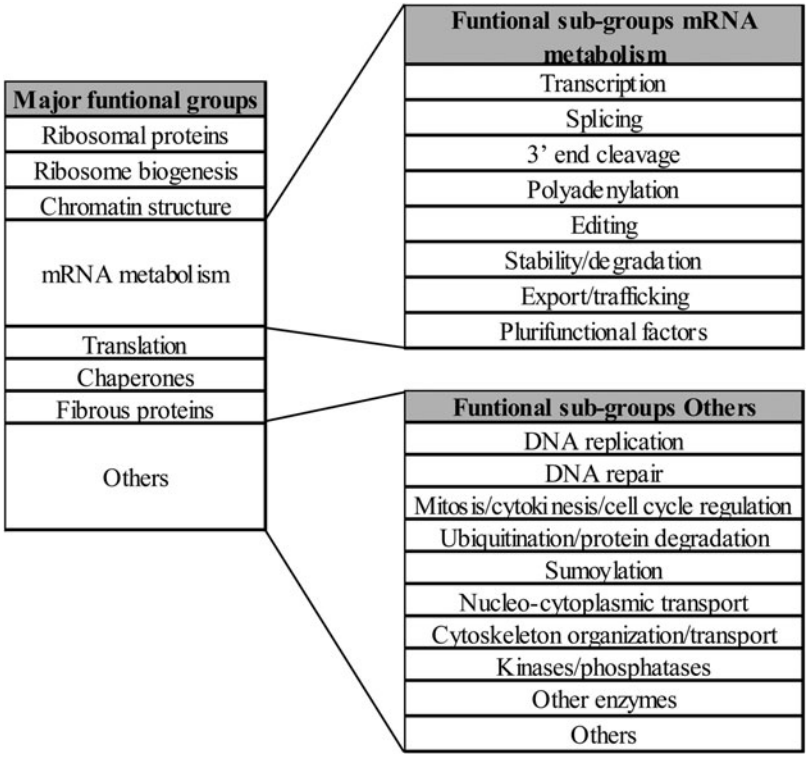

FIG. 3. Classification of functional groups and subgroups for the "nucleolome."

The nucleolome includes proteins related to cell cycle regulation, DNA damage and pre-mRNA processing (84), suggesting that this organelle may act as a multitasking district, being more than a simple ribosome factory (18, 62, 63, 84, 125). These particular multifunctional features are possibly related to the presence of many different nucleolar proteins endowed with multiple roles (*e.g.,* NCL and Nopp140) (90a). Nucleolar proteins unrelated to ribosome assembly mostly contain an RNA-binding motif or have a chaperone function and are able to shuttle between the nucleolus and the nucleoplasm (90a). It is currently known that nucleoli carry out many nonribosomal activities, such as: control of cell cycle and proliferation (62, 63, 130), stress sensing (18, 21, 64, 96, 108, 124, 139), tumor surveillance, DNA damage repair (18, 41, 84), regulation of protein stability and apoptosis, telomere metabolism (18), maturation of small RNAs, including tRNAs and small nuclear RNAs, maturation of the spliceosome and of the signal recognition particle (63, 115, 121), and also control of viral lifecycle (62, 71), acting in several ways as a sequestration core facility (Fig. 2) (21, 40, 63).

The assumption that a protein acts and executes its functions where it is more abundant is invalid for some nucleolar components: a high protein concentration in a given cellular compartment might not correspond to a quantitative signal for its activity (114). A clear example is represented by the many DNA repair proteins that reside within nucleoli (see Table 1 for more details), which in this instance, appear to act as storage sites (see below). After nucleolar stress or DNA damage, these proteins can relocalize to the nucleoplasm. The nucleolar stress response may therefore, act as a mechanism of surveillance monitoring the synthesis and the correct assembly of ribosomal units: it may halt the cell cycle progression until enough functional ribosomes are built or it may induce p53-mediated apoptosis or senescence (134). This represents an elegant and efficient way to coordinate arrest of cell growth and induction of DNA repair by controlling only the subcellular distribution of proteins.

Linking Nucleolar Physiology to Human Diseases

Several reports highlighted the presence of a layer of heterochromatin, called perinucleolar compartment (PNC), at the nucleolar periphery. The PNC is associated with specific DNA loci and it is enriched in RNA-binding proteins and RNA polymerase III transcripts (62, 114). These discoid-shaped caps are usually found in mammalian transformed cells, tumor-derived cell lines, and tumor biopsies, accounting for a possible connection between PNC and tumor initiation and progression (114). Despite the apparent link between cancer and PNC, the exact role of these nucleolar subdomains has not been identified yet.

Nucleoli are closely linked to cellular homeostasis and human health (62): rapidly proliferating cells, such as cancer cells, usually present a strong upregulation of genes involved in the ribosomal biogenesis. This phenomenon accounts for the presence of several prominent nucleoli that are a typical cytological feature of neoplastic cells (129). Morphological and functional changes associated with cancer usually correlate with quantitative and qualitative differences in the ribosome biosynthesis rate (62) and are a consequence of the increased metabolic needs of the cell (105). This could indicate that the nucleolus undergoes an adaptive response upon cellular transformation; on the other hand, the increased rate of ribosome biogenesis might be actively involved in, and contribute to, tumorigenesis (105). More recently, the accumulation of chemically modified ribosomes upon oxidative stress (*e.g.,* bearing 8-OHG modifications, or cross-linked rRNA-RPs complexes) is emerging as a contributing factor in the progression of neurodegenerative diseases, such as AD and PD (62). In addition, a novel link between nucleolar damage and neurodegeneration has recently been established through the association of PD with nucleolar integrity. These interesting findings also establish the existence of a direct signaling axis connecting the ribosomal synthesis rate and oxidative stress (122). Under this perspective, the deep understanding of changes related to tumor progression and the composition and dynamics of the nucleolome might be important to clarify the mechanisms of tumorigenesis and for designing new therapeutic strategies.

Dynamics of DNA Repair Proteins During Genotoxic Damage: Nucleolus and RNA Binding

Cellular life is continuously threatened by stressful conditions, such as viral infections, oncogenic activations, temperature shocks, and genotoxic damage, which must be immediately dealt with by the cell to maintain its homeostasis. DNA damage typically involves the storage sites of the genetic material, such as nucleus and mitochondria. Depending on the origin of the genotoxin (exogenous *vs.* endogenous), its nature (physical *vs.* chemical) or its uptake mechanisms, differential burden of damage can be accumulated both in nuclear and in mitochondrial DNA. Upon genotoxic insults a dynamic redistribution of DNA repair proteins to the site of damage is frequently observed; this phenomenon leads to the accumulation of DNA repair factors, often into spatially restricted foci. Relocalization events usually occur through cytoplasmic-mitochondrial, cytoplasmic-nucleoplasmic, and nucleolar-nucleoplasmic shuttling regulated by post-translational modifications (PTMs) and triggered by the damage itself (51).

Why nature selected such a time-consuming process involving reorganization of cell proteome upon DNA damage, instead of constitutively accumulating each DNA repair factor within the proper target compartment? Is there any functional relationship between RNA metabolism and the DNA damage response (DDR), which may involve an active site of RNA production, such as the nucleolus? These legitimate questions are still a matter of debate; however, based on existing data at least four possible explanations, not mutually exclusive, appear reliable: (i) the concentration, under physiological levels of DNA damage, of high amounts of DNA repair proteins in specific subcellular regions might be deleterious for nucleic acids integrity. Many repair proteins, in fact, are endowed with DNA trimming or modifying activities. Examples include APE1 or the DNA polymerase β (Polβ); overexpression of these proteins has already been shown to promote genomic instability, possibly due to the lack of coordination of their enzymatic activities (26); (ii) repair factors may exert more than one specific function that cannot be directly linked to their DNA repair activity. This situation is nicely exemplified by the APE1 protein, which nucleolar localization is necessary for cellular proliferation (see below), or by proteins, such as the Werner syndrome helicase (WRN), or the flap

Table 1. DNA Repair Protein Composition in the Nucleolus

Protein name	Putative role inside the nucleolus	Role(s) outside the nucleolus	Genotoxic stress leading to protein relocalization		References
			Imported	Exported	
APE1	RNA processing	AP endonuclease		Actinomycin D	(5, 149)
ATM		DNA damage signaling			(106)
ATR		DNA damage signaling			(106)
BLM	rDNA transcription	DNA helicase		Camptothecin	(5, 120, 163)
BRCA1/BARD1		E3 Ligase involved in HR		IR	(53)
CSB		Core NER factor			(99)
DNA-PK catalytic subunit		Kinase involved in NHEJ		UV, cisplatin	(36, 106)
FEN1	Resolution of stalled replication forks	Structure-specific nuclease		UV	(54)
ILF2 and ILF3		dsRNA binding proteins interacting with Ku70/80 and DNA-PK		UV	(106)
Ku70/80		DSB recognition in the NHEJ pathway		UV, cisplatin, IR, Actinomycin D, mitomycin C, hydroxyurea, doxorubicin	(2, 36, 106)
LigIII		DNA ligase involved in the BER pathway and in the SSB repair		UV, IR	(106)
MRE11		Nuclease involved in DSB repair			(5, 108)
MSH6		MMR factor		MNNG	(95)
Mus81	rDNA repair	Structure-specific endonuclease			(48)
OGG1		DNA glycosylase	Ro19-8022 + light (405 nm), $KBrO_3$		(25, 99)
p53		Multifunctional tumor suppressor, auxiliary roles in NER and BER		UV	(123, 139)
PARP1 and PARP2		DNA damage signaling and transcriptional modulation		Actinomycin D, H_2O_2, MMS, camptothecin, UV	(5, 97, 106)
PCNA		Sliding clamp involved in DNA repair and replication			(161)
PNK		DNA end trimming kinase/phosphatase			(5, 63)
Polβ		DNA polymerase involved in the BER pathway			(63)
Rad9B	rDNA repair	Poorly understood	UV, Actinomycin D		(117)
Rad17		DNA repair and replication modulator		UV, IR, MMS, adriamycin	(28)
Rad50		Part of the MRN complex			(5)
Rad52	rDNA repair	DSB responsive protein			(32)
RECQL4		DNA helicase	H_2O_2, streptonigrin		(156)
RNF8	Modulation of ribosome biogenesis	E3 ligase involved in HR		IR	(53)
RPA		Single-strand DNA binding protein involved in DNA repair and replication			(108)
Slx1-Slx4 complex	rDNA repair	Structure-specific endonuclease			(32)
SMUG1	rRNA quality control	DNA glycosylase			(73)
SSRP1		Structure-specific protein binding to cisplatin-DNA adducts		Cisplatin	(36)
TDP1		Tyrosyl DNA phosphodiesterase		Camptothecin	(8)
TOPBP1		DNA repair and replication modulator			(106)
Topo I		DNA topoisomerase		UV, camptothecin	(22, 93, 104)
Top2a and Top2b		DNA topoisomerases			(5)
WRN	rDNA transcription	DNA helicase implicated in BER and recombination		UV, IR, MMC, MMS, bleomycin, camptothecin, etoposide, cisplatin	(5, 16, 36, 75, 94)
XPC		Core NER factor	Ro19-8022 + light (405 nm)		(99)
XPG	rDNA transcription	NER endonuclease		UV	(112)
XRCC1		Scaffold protein in the BER pathway		Camptothecin	(5, 63, 120)

APE1, apurinic/apyrimidinic endonuclease 1; ATM, ataxia telangiectasia mutated; ATR, ataxia telangiectasia and Rad3-related; BER, base excision repair; DSB, double-strand break; FEN1, flap endonuclease 1; HR, homologous recombination; IR, ionizing radiation; NER, nucleotide excision repair; NHEJ, nonhomologous end joining; OGG1, 8-OHG DNA glycosylase; PARP, poly [ADP-ribose] polymerase; PCNA, proliferating cell nuclear antigen; Polβ, DNA polymerase β; rDNA, ribosomal DNA; rRNA, ribosomal RNA; RPA, replication protein A; SSB, single-strand break; WRN, Werner syndrome helicase; XRCC1, X-ray repair cross-complementing protein 1.

endonuclease 1 (FEN1) (54), that are required for the active transcription of ribosomal genes in the nucleolus. All these factors promptly relocalize to the nucleoplasm to exert their DNA repair function upon UV irradiation; (iii) while a lower steady-state amount of DNA repair enzymes is sufficient to grant a basal level of genome stability maintenance, it is likely that genotoxin-induced protein accumulation mechanisms have evolved, to cope with sustained DNA damage. Thus, increasing the local concentration of DNA repair factors may be a simple and fast way to amplify the local DNA repair capacity; (iv) disruption of the nucleolar structure, often observed occurring upon DNA damage, may halt rRNA production; thus, leading to a block of the protein synthesis machinery and allowing proper DNA repair. This may represent an efficient coupling mechanism involving nucleolus dynamics, RNA-binding, and DNA repair, which allows synchronization of DDR and arrest of cellular growth.

While many examples of proteome dynamics have been reported to occur during DDR, this review will focus on the relocalization of nucleolar proteins; for detailed information concerning general subcellular reorganization, please refer to Tembe and Henderson (139) and references therein.

The Nucleolus as DNA Damage Sensor and Storage Facility for DNA Repair Proteins

As already mentioned, recent proteomic analyses have pointed at the nucleolus as a mediator of the cell cycle regulation, tumor suppressing or protumorigenic activities, and DDR (5, 17, 63, 108). The presence of rRNA and hub proteins, such as NCL and NPM1 is likely the critical factor for the nucleolar accumulation of many proteins not uniquely related to ribosome biogenesis (27, 40). Among these, many DNA repair factors have been shown to localize within the nucleolus (Table 1), which acts as a stress response organelle and responds, in a unique damage-specific manner, to different cellular stresses (5, 17, 30, 106). During a stress response a broad reorganization of the nucleolar proteome occurs; interestingly, the vast majority of nucleolar proteins migrate toward the nucleoplasm and not vice versa, indicating that the nucleolus may act as a reservoir able to release critical factors upon DNA damage (108, 139). Very few proteins have been reported to migrate to the nucleolus during the stress response. Among these ING1 and PML, which are thought to participate in triggering of apoptosis and in cell cycle arrest, respectively (139). Intriguingly, chaperones, such as Hsc70 are targeted to the nucleolus after the stress response, possibly to restore the nucleolar function during the cellular recovery from stress. Typically, during the response to DNA damage or transcriptional inhibition, one of the first events is represented by the interruption of the ribosomal synthesis (108). This mechanism likely represents a cellular strategy to maintain homeostasis, indeed, as already pointed out, the ribosomal biogenesis is a rather expensive energy-consuming process (20). The impairment of rRNA transcription and processing is often, but not always, associated with nucleolar disintegration and condensation phenomena that lead to the formation of caps and necklace-like structures (20, 106). An extensive analysis of the effects of chemotherapeutic drugs on ribosome biogenesis and nucleolar integrity has recently been carried out by Burger *et al.* (23). For a broader list of responses to different stress stimuli, please refer to Boulon *et al.* (20). Along with the inhibition of ribosomal biogenesis, massive reorganization occurs, with a rapid outflow of "nucleolar effectors", such as $p14^{Arf}$, NCL, and NPM1, which slow down or arrest the cell-cycle in both p53-dependent and independent manners (20, 31, 34, 49, 86). Concurrently, also DNA repair factors stored within nucleoli and frequently bound to NCL and NPM1 are released into the nucleoplasm; the transient arrest of the cell-cycle progression possibly facilitates the DNA repair process. Only after resolution of DNA damage, rRNA synthesis is restored, as suggested by the inverse correlation existing between the rDNA transcription rate and γ-H2AX foci number (80). Notably, many nucleolar effectors also play a role within the nucleoplasm: beside the contribution to the modulation of the cell-cycle, several reports have pointed out that NCL or NPM1 may directly participate in the DDR. For instance, NCL has been shown to tune proliferating cell nuclear antigen (PCNA) activity in the nucleotide excision repair (NER) pathway (161), while NPM1 has been involved in the BER modulation (see below). Interestingly, both these proteins display strand annealing activity *in vitro* (19, 55) and have been identified as stress-responsive RNA-binding proteins, suggesting that upon genotoxic damage these factors may modulate DNA, as well as RNA repair or cleansing (162). More importantly, emerging evidences further highlight the importance of nucleolar hub proteins in human pathology. The link between NPM1 and oncogenesis, for example, is a well-established paradigm (31, 52, 151) and we recently demonstrated that in acute myeloid leukemia bearing NPM1 mutations, the cytoplasmic de-localization of the mutant NPM1c+ leads to extensive BER impairment due to APE1 nuclear deprivation (150). This evidence denotes how the deregulation of an important nucleolar factor might impact on the overall cellular dynamics and not only on the ribosome biogenesis, supporting the view of the nucleolus as a multifunctional and versatile organelle. Recent evidences from Lewinska *et al.* showed that, in yeast, the nucleolus acts as stress sensor also for oxidative stress. Their work linked the nucleolar exit of the Pol I-specific transcription factor Rrn3p, to the response to oxidation, suggesting that oxidative damage is indeed a cellular stress that is sensed from the nucleolus leading to arrest of the ribosome transcription (87). Interestingly, diethyl maleate-induced oxidative stress has been demonstrated to modulate also the whole nuclear export system through impairment of the CRM1-mediated nuclear export, coupled to relocalization of the nuclear pore component Nup98 to the nucleolus (33). Altogether, these observations underline the role of the nucleolus as stress sensor, further confirming the validity of the aforementioned model involving arrest of ribosome biogenesis, followed by nucleoplasmic and nucleolar proteome rewiring.

The damage-specificity of the nucleolar response is clearly depicted by the differential response to diverse DNA damaging stimuli: DNA repair factors undergo selective mobilization upon specific genotoxic conditions (Table 1). UV and ionizing radiation (IR), for instance, elicit markedly differential responses in terms of nucleolar proteome reorganization. Whereas UV stress is characterized by fast and persistent (hours), fluctuations of nucleolar nonhomologous end joining (NHEJ) proteins, IR lead to quicker (minutes), but less persistent responses, which are more limited, in terms of magnitude (106). The dynamic reorganization of nucleolar proteins upon DNA damage has been nicely described by

Adelmant *et al.*, who showed that microinjection of sheared DNA, to mimic the presence of strand breaks, leads to the rearrangement of Ku complexes. Intriguingly, in the absence of DNA damage, Ku associates with rRNA- and RP-containing complexes; a DDR onset elicits the exit of Ku from nucleoli and the modification of its interactome (2). This process likely represents a general response mechanism, where the nucleolus acts as a sensitive "antenna" for stress and DNA damage and as central hub for the coordination of the cellular response to stress conditions. The ability to undergo highly dynamic and selective reorganization allow for prompt release of DNA repair factors that are stored within this organelle. An essential question still remains to be answered: which is the triggering event that begins the signaling cascade linking DNA damage to the early nucleolar response? PTMs are usually a quick way to rewire the cellular proteome. APE1 and WRN translocation from the nucleolus is for instance triggered by acetylation (16, 89); on the contrary, FEN1 has been shown to migrate to the nucleoplasm upon UV irradiation in a phosphorylation-dependent manner. Remarkably, mutations that mimic or impair the UV-induced FEN1 phosphorylation, cause UV sensitivity (54), suggesting that DNA damage-induced protein translocation is essential for a correct DDR. Griffiths *et al.* pointed to SUMOylation as the major PTM targeting DNA glycosylases in yeast (51); this PTM has also been implicated in the modulation of rDNA repair through export of the rDNA double-strand breaks (DSBs) to the nucleoplasm by the homologous recombination (HR) machinery (39). In addition, the nucleolus has been reported to contain several DNA damage sensors (*e.g.*, the ataxia telangiectasia mutated [ATM], the ataxia telangiectasia and Rad3-related [ATR], and p53) (5, 123) and it has been demonstrated that, upon DNA damage induction, Pol I-mediated transcription is blocked in an ATM-dependent manner, and not by the DNA damage itself. Interestingly, through microirradiation studies, Kruhlak *et al.* showed that transcription of rDNA is transiently arrested only in damaged nucleoli, whereas the neighboring ones maintain normal transcriptional activity (80). Moreover, Rubbi and Milner, have elegantly shown that nucleolar disruption, rather than DNA damage, may lead to p53 stabilization, suggesting that the nucleolus may constitutively promote p53 degradation, unless DNA damage occurs (124). It would be interesting to understand if and how the extra-nucleolar DNA damage is ultimately signaled to the nucleolus and which is the event that triggers the nucleolar segregation.

The Paradigmatic Example of the APE1/NPM1 Interaction

APE1 is a typical example of DNA repair protein activated during the nucleolar stress response. APE1 is a multifunctional and essential factor in mammals that was identified about 20 years ago as the major AP-endonuclease in the BER pathway, as well as a redox coactivator of transcription factors (37, 157). The recent observation that APE1 is able to bind and cleave RNA highlighted previously unsuspected roles for the protein (77, 138). We found indeed that this protein associates with NPM1 in the nucleolus, where it may have a functional role as RNA cleansing factor. This hypothesis is corroborated by studies performed with inducible HeLa APE1 knock down cell lines, which showed how APE1 depletion leads to a widespread accumulation of unrepaired oxidized RNA species (*i.e.*, 8-OHG) upon oxidative stress. Notably, under unstressed conditions, APE1 knock down cells display impaired translation ability, lower protein content and overall cell growth impairment (149). These evidences point to a major contribution for APE1 as cellular scavenger of damaged RNA species. The nucleolar storage of APE1 is mediated by the interaction of the flexible and evolutionarily acquired N-terminal extension of the protein with both rRNA and NPM1 (42, 89, 116). However, the protein does not constitutively accumulate in the nucleoli; in fact, upon Pol I inhibition with actinomycin D, APE1 shuttles to the nucleoplasm (149). The evidence that treatment with the E3330 redox inhibitor (45) causes APE1 nucleolar exit and its accumulation to the nucleoplasm (147) suggests that the redox status of APE1 may play a significant role in controlling its subcellular trafficking. Interestingly, the APE1/NPM1 association is also impaired during oxidative stress (149), suggesting that the protein may be released from the nucleolus during stress conditions, possibly to operate within the BER pathway. In accordance with this observation, we delineated a complex regulatory pattern of NPM1 on APE1 endonuclease activities: NPM1 acts as an inhibitor of the APE1 ribonuclease function, but as an activator of the AP-endonuclease function on DNA (149, 150). This model suggests that when APE1 resides within the nucleolus, its activity is mainly focused on the rRNA quality control machinery, possibly modulated by NPM1. Whereas, during the DDR, the simultaneous outflow of APE1 and NPM1 to the nucleoplasm, leads to the activation of the APE1 AP-endonuclease function (Fig. 4). In agreement with this view, many reports point to the involvement of NPM1 in different aspects of the DDR, yet, the exact contribution(s) of this protein to the stress response is currently elusive (31, 79, 127). It is worth pointing out that the lack of NPM1 has been proved to sensitize cells to genotoxins that elicit a BER response and that APE1 catalytic activity is impaired in NPM1 knock out cells (150). These elements suggest that NPM1 plays a direct role in the BER modulation, which is still poorly understood. As discussed in the previous section of this review, the key event that triggers the APE1 release from nucleoli upon genotoxic stress is still a matter of debate. It is known that the APE1/NPM1 interaction is modulated by acetylation on the N-terminal domain of APE1 (42, 89). Acetylation of this protein region is induced upon genotoxic stress (89, 128); it is therefore, likely that, once again, stress-induced PTMs drive APE1 shuttling to the nucleoplasm in response to DNA damage. In an effort to characterize the response of APE1 to genotoxic stress, we generated a quadruple lysine to alanine substitution that mimics constitutive APE1 acetylation. As anticipated, the inability of this mutant to interact with NPM1 leads to nucleolar exclusion of the APE1 mutant. Interestingly, the lack of APE1 nucleolar accumulation causes a severe impairment of cellular proliferation, indicating that the presence of APE1 within nucleoli is required to ensure a proper cellular growth rate (89). These aspects of the APE1 biology still deserve thorough investigation and fascinatingly open novel perspectives for antitumor therapy, as targeting the APE1/NPM1 interaction may prove effective in counteracting cellular proliferation.

The APE1 protein is commonly renowned as DNA repair protein and only recently it has been identified as an enzyme active on abasic RNA molecules, unveiling its noncanonical function. Perhaps earlier examples of this versatility of function in dealing with genotoxic damage were described for the RP S3, both in *Drosophila* and humans. Specifically, S3 has

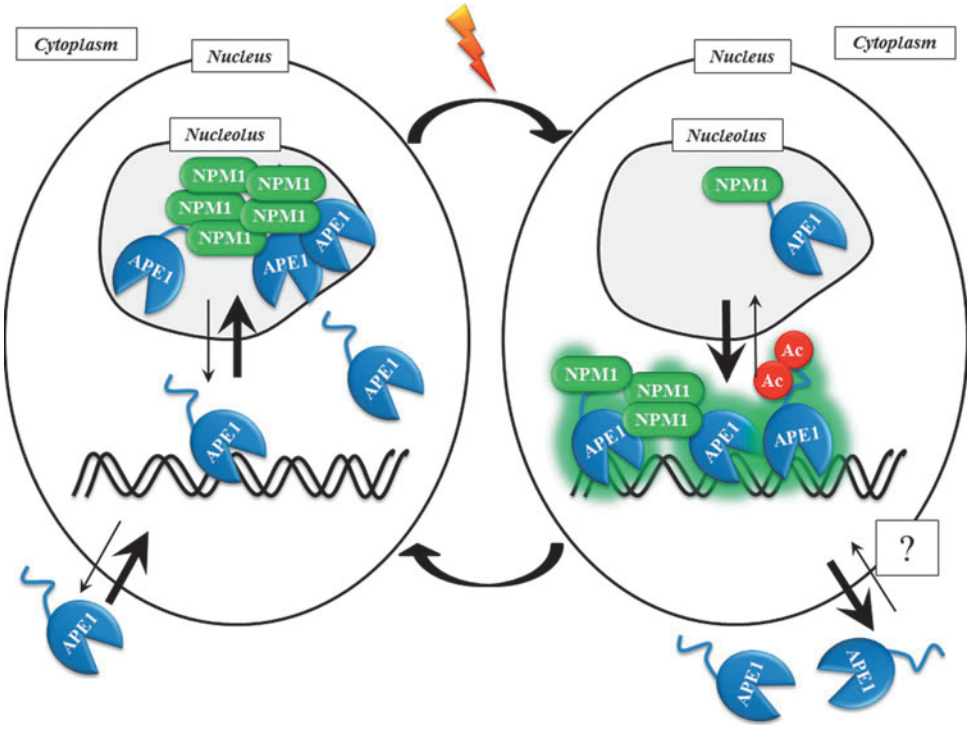

FIG. 4. Dynamic turnover of the APE1/NPM1 complex in response to cellular stress. Under basal conditions (left) the cellular APE1 pool is dynamically distributed throughout the cell, with prevalent accumulation in the nucleus and nucleoli. This accounts for the maintenance of a basal DNA repair capacity (both nuclear and mitochondrial), redox-mediated transcriptional modulation, cell proliferation, and RNA cleansing activity. Upon genotoxic stress and/or arrest of Pol I transcription (right) the dynamic equilibrium of APE1 localization is tipped towards a nucleoplasmic accumulation of the protein (149). The APE1 relocalization is likely mediated by simultaneous migration of NPM1 outside the nucleolus and hyperacetylation of the N-terminal region of APE1 itself (90). This situation ensures a potentiated DNA repair response, as both the nucleoplasmic APE1/NPM1 association and its acetylation have been linked to increased catalytic activity of the protein. The absence of APE1 from nucleoli, moreover, might favor a temporary arrest of cellular proliferation, useful to allow for more efficient DNA repair. If the DNA damage is sustained, it is likely a redistribution of a pool of APE1 to the cytoplasm. This phenomenon should boost the mitochondrial BER and possibly contribute to the cellular RNA cleansing capacity. APE1, apurinic/apyrimidinic endonuclease 1; BER, base excision repair; NPM1, nucleophosmin 1; Pol I, RNA polymerase I. To see this illustration in color, the reader is referred to the web version of this article at www.liebertpub.com/ars

been found to protect cells from genotoxic stress through: (i) its DNase activity on abasic sites in *Drosophila* (155); (ii) its ability to stimulate, the activity of the uracil-DNA glycosylase hUNG in human cells (78); (iii) its ability to bind with high affinity the oxidative lesion 8-OHG in humans (60) and (iv) its functional interaction, always in human cells, with other well-known DNA repair proteins, such as the 8-OHG DNA glycosylase (OGG1) and APE1 (61). Recent findings are increasingly pointing to the involvement of noncanonical proteins (57) and even of noncoding RNA molecules (46) in the DDR, adding more layers of complexity to this mechanism. An intriguing emerging evidence is that the association of DNA repair proteins to noncanonical binding partners (*i.e.*, RNA and RNA-binding proteins) is mainly driven by the presence of unfolded protein domains acquired during phylogenesis, which may be responsible for novel gain of function activities.

Relevance of the Unfolded Domains in BER Proteins: The Missing Link for a Phylogenetic Gain of Function?

Until recently, BER was considered the simplest among the DNA repair pathways since an *in vitro* reconstituted nuclear BER required only four or five core enzymes. However, recent studies have revealed that BER is much more complex, involving a network of distinct and integrated cell cycle- and genome-specific sub-pathways in which numerous noncanonical proteins take part (58, 59). Notably, many of these proteins are involved in RNA-metabolism processes. Actually, several noncanonical factors have been demonstrated to participate BER, even though their *in vivo* functions are yet to be fully unraveled. The list of non-BER proteins includes for instance: YB-1 [which has been shown to interact with the endonuclease VIII-like 2 (NEIL2) glycosylase (35), the endonuclease III-like glycosylase (NTH1) and APE1 (29)], NEIL2 [which was also found to interact with the RNA-binding protein hnRNP-U (6)], HMGB1 [which has been implicated in single-strand break (SSB) repair involving Polβ (90)] and the tumor suppressor p53, which was also shown to play a role in DNA damage repair through direct binding to APE1 and Polβ (168). The list of these non-BER proteins is still growing, supporting the notion that BER *in vivo* is far more complex than the simple model that we can reconstitute *in vitro*. In particular, the characterization of the BER interactome identified multiprotein complexes; thus, suggesting that complete

repair occurs through the action of BER complexes formed by core proteins and noncanonical factors (BERosomes) (59). The previous and simplistic view of the BER mechanism, based on the analysis of cocrystal structures of substrate-bound proteins, proposed a pathway consisting of sequential steps in which individual repair enzymes carry out reactions independently. In contrast with this original concept, recent discoveries showed that early BER enzymes stably interact with most of the downstream repair components. The initial view of BER as a "hand-off" or "passing the baton" process has been revisited by Hegde *et al.* who introduced, rather, a new paradigm in which the dynamic interplay of highly coordinated interactions between different BER proteins would increase the efficiency and the versatility of the process.

It has been observed that frequently those machines whose operations must be tuned rapidly in response to specific and diverse cellular needs, present components that are not fully structured. Such "malleable machines" (47), conversely to rigid entities, might presumably better respond to different conditions, for instance by promoting conformational rearrangements and facilitating multiple targets recognition. Structural analyses exploiting both experimental and modeling approaches have indeed evidenced the presence of disordered segments preferentially localized at the N- or C-terminus of different mammalian DNA repair proteins, a peculiar feature which is absent in their bacterial prototypes. These observations thus, suggest that, during evolution, higher organisms have acquired these binding domains to regulate multiprotein interactions and to improve pathways (*e.g.,* BER) efficiency, in an increasingly oxidizing environment. Long disordered segments are a common feature observed in a large percentage of proteins; being prevalent especially among proteins involved in vital processes, such as transcription, translation, signal transduction, and protein phosphorylation (47, 145). Such unstructured regions may provide versatility in recognizing multiple targets, promoting communication with many proteins in response to environmental changes; thus, expanding the capacities of ordered complexes and representing a powerful strategy selected by nature to quickly explore a vast interaction space with unique thermodynamic advantages (132). Disordered regions were shown to be prevalent in DNA binding proteins, particularly in those involved in targeted sequence binding (*e.g.,* repair proteins and transcription factors) (143, 153). Disordered prediction tools (PONDR and PrDOS) have been used to compare the secondary structure of human and bacterial early BER proteins (59). These analyses showed that mammalian DNA glycosylases are endowed with unique nonconserved extensions at their N- or C-termini, which are absent in their homologs in lower organisms (58). The human NEIL1 glycosylase, for instance, contains an extended disordered region spanning about 100 residues at the C-terminus, absent in the *E. coli* Nei-like protein. Similar comparisons between the human DNA glycosylases hNTH1, the MutY homolog (hMYH), and their *E. coli* prototypes (*i.e.,* endonuclease III and MutY, respectively), indicate that both hNTH1 and hMYH have extended disordered tails at the N-terminus that are absent in the *E. coli* enzymes (66, 140). Likewise, the N-terminal disordered region present in the human APE1 is absent in exonuclease III (Xth), its *E. coli* ortholog. The size range of the unstructured extensions is about 50–100 residues. In the case of human APE1 it consists of ~65 residues, being mostly disordered (59).

These disordered regions, due to their structural flexibility and plasticity have been shown to provide BER proteins with functional advantages and appear to be essential for their biological functions, including damage sensing (153), protein–protein interactions, repair regulation *via* PTMs and containing NLSs (118). Furthermore, the presence of disordered segments only in eukaryotic proteins, with the highest degree of disorder in mammals, suggests their evolutionary acquisition and well correlates with the increase in regulatory complexity observed in higher organisms.

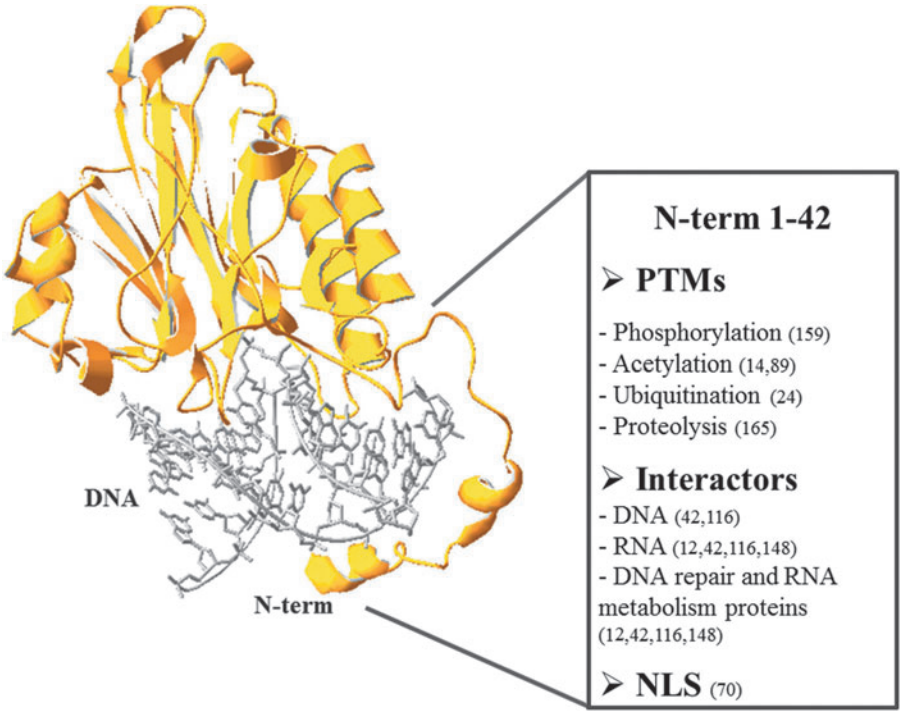

FIG. 5. Schematic representation of multiple regulatory functions of the APE1 disordered N-terminal region. APE1 crystal structure (yellow) bound to abasic DNA (grey) is from the pdb (1DEW) and displayed using the PDBV software. The deposited APE1 crystal structure was obtained using a truncated APE1 form (residues 40–318); missing residues have been manually added. The unstructured N-terminal portion of APE1 (residues 1–42) is essential for APE1 biological functions being site of PTMs, target of many interactions and, including the NLS. NLS, nuclear localization signal; PTMs, post-translational modifications. To see this illustration in color, the reader is referred to the web version of this article at www.liebertpub.com/ars

Among the BER enzymes, APE1 offers a paradigmatic example of how a disordered tail can endow a protein with unique activities. The first crystallographic structure of the human APE1 in complex with DNA was obtained using a truncated protein lacking the first 35 amino acids and reveled that this protein consists of two symmetric alpha/beta fold with a significant structural similarity to both bovine DNase I and its *E. coli* homologue Xth (50). A crystal structure of the full-length protein has also been reported, but again, the N-terminal region was unresolved (10). Three functionally independent domains can be distinguished within the APE1 protein (Fig. 5): (i) the first 33–35 amino acid region consists of a structurally disordered segment (133) essential for the interaction with other proteins (148, 149) and harboring sites for PTMs (14, 24, 70, 89, 159, 165, 166) and RNA interaction (89); (ii) the redox domain is located in a region between amino acids 35 and 127; and (iii) the DNA repair domain, which spans the C-terminal domain of the protein from about residue 61 onwards (42, 68). Whereas the APE1 C-terminal domain involved in AP endonuclease activity is conserved from bacteria to humans, the N-terminal region is unique to mammals suggesting a recent acquisition during evolution.

Remarkably, this peculiar region also accounts for noncanonical activities that have been ascribed to APE1, including its role in RNA metabolism (42, 89, 116, 138, 148, 149). Over the past two decades, knowledge of the biological functions, mechanisms of action, interactions, and regulation of the APE1 protein has increased exponentially. In particular, it has become apparent that APE1 participates in multiple cellular processes not only confined to the maintenance of genome stability, in accordance with the current general view that many DNA repair enzymes may exert miscellaneous activities, being implicated, for example, in different steps of gene regulation (74, 113). As already mentioned, RNA decay and processing events require a wide spectrum of proteins, including RNA helicases, polymerases and, above all, exoribonucleases and endoribonucleases. For many years, it has been assumed that eukaryotes RNA cleavage relies mostly on the action of exoribonucleases, in contrast with prokaryotes, where RNA decay is mainly mediated by endoribonucleolytic processes (82, 101). In recent years, the unexpected implication of numerous endoribonucleases in the RNA turnover in eukaryotes significantly contributed to a change of perspective on the eukaryotic RNA metabolism (141). APE1 is among the several examples of recently identified enzymes whose endoribonucleolytic activity has been found to associate with the regulation of RNA stability. Evidence of its RNase H-like activity was first suggested by Barzilay *et al.* who demonstrated that APE1 is able to bind with relatively low affinity undamaged single- and double-stranded RNA molecules, albeit not exhibiting unspecific nuclease activity (9). Later on, it has been discovered that APE1 possesses the ability to cleave AP sites within single-stranded RNA molecules and that the nucleic acid secondary structure significantly influences the APE1 incision activity (12). Despite these first *in vitro* suggestions of APE1 biological relevance in the removal of AP-site-containing RNA, the unequivocal demonstration of APE1 involvement in RNA processing was brought only few years later. Very recently, in fact, Barnes *et al.* identified APE1 as the major endonuclease associated with polysomes and capable of cleaving the coding region determinant of the *c-myc* mRNA; thus, influencing *c-myc* half-life in cells (7). Surprisingly, recent biochemical studies performed using recombinant APE1 demonstrated that the APE1 endoribonuclease function is not limited to *c-myc* mRNA, but it may potentially influence the biogenesis and hence, the stability of other transcripts, including also miRNAs (77). These works demonstrated that APE1-mediated RNA cleavage occurred, *in vitro*, at single-stranded or weakly paired regions, preferentially 3′ of pyrimidines at UA, UG, and CA sites. This latter finding, in particular, led to hypothesize the possible involvement of APE1 in mRNA splicing events, since CA repeats are renowned as potent splicing modulators (15). Furthermore, the *in vivo* involvement of APE1 in RNA metabolic pathways was further corroborated by the observation of the APE1 association, through its N-terminal domain, with rRNA and the ribosome processing protein NPM1 within nucleoli (149). Furthermore, APE1 has been shown to interact with factors involved in the splicing process, such as the heterogeneous nuclear ribonucleoprotein L (81) [which is a key regulator of splicing that binds CA repeats with high affinity (65)], YB-1 (29, 119), as well as with proteins involved in the ribosome assembly and RNA maturation within cytoplasm (149).

So far, many studies have characterized the involvement of the APE1 C-terminal domain in RNA metabolism, demonstrating that the APE1 endoribonuclease activity and its nuclease function on DNA share the same active site (76). However, few groups have investigated the role of the unstructured N-terminal extension, possibly as a consequence of its disordered nature. A recent work published form our group systematically characterized the binding properties of the APE1 N-terminal disordered region towards nucleic acids and NPM1. We demonstrated that the N-terminus, in particular acquired Lys residues therein located, appear to be essential for the stabilization of both protein–protein and nucleic acids–protein interactions, as well as influencing the thermal stability of the protein. These evidences clearly support the notion that this unstructured domain might represent an evolutionary gain function necessary for mammals to cope with a progressively complex cellular environment (116).

In light of these recent findings and taking into account also previous reports on the pivotal role of APE1 disordered N-terminal region, we speculate that the targeting of this unfolded protein domain could be a valuable tool to interfere with the different APE1 functions *in vivo*.

Relevance of the Unstructured Domain of BER Proteins for Designing Novel Anticancer Strategies

BER proteins have been broadly explored as targets for cancer therapy (67); in particular, current approaches to cancer treatment report more effective results when specific DNA repair inhibitors are used in combination with DNA damaging drugs. The foremost rationale of the combined therapy is that impairment of BER enzymes is likely to sensitize cancer cells to chemotherapeutic agents. Druggable BER targets for cancer treatment include: FEN1, Polβ, APE1, and the poly [ADP-ribose] polymerase 1 (PARP1); while targeting of DNA glycosylases results inefficacious because of the functional redundancy of this class of enzymes (58).

In the last decade, remarkable attention has been posed on the development of PARP1 and APE1 inhibitors. The APE1 relevance for cell survival is demonstrated by the fact that

knocking out the APE1 gene induces either apoptosis in differentiated cells (69) or developmental failure during embryogenesis (158). Accumulating evidences have indicated that deregulation of APE1 in both expression and subcellular localization is indeed associated with different tumorigenic processes: APE1 upregulation or dysregulated expression has been described in a variety of cancers, including prostate, pancreatic, ovarian, cervical, germ cell, rhabdomyosarcoma, and colon (43, 92). Furthermore, it has been reported that elevated APE1 levels and anomalous intracellular localization are also typically correlated with aggressive proliferation and increased resistance to chemotherapeutic drugs and IR, implying that APE1 enhances repair and survival of tumor cells (92). Therefore, considering that APE1 expression appears to be linked to chemoresistance and taking into account that several studies have shown that decreasing APE1 levels may lead to cell growth arrest and to an increased cellular sensitivity to DNA damaging agents (44, 45, 85, 154), APE1 represents a promising target for pharmacological treatment. A description of all the APE1-targeting molecules currently under investigation is beyond the focus of this review, for an exhaustive review on APE1 inhibitors, the reader is redirected to (146). All the APE1 small-molecule inhibitors developed so far were designed to target specific APE1 functions, namely the DNA repair or the redox activity of the protein. It is however, still a matter of debate whether the enhanced sensitivity to cytotoxic agents observed upon APE1 inhibition is solely related to the loss of DNA repair activity, or is also linked to the loss of its transcriptional regulatory function, or both. Despite the efforts aimed at determining the relative importance of the attenuation of the APE1's repair or transcriptional functions, all currently available APE1 inhibitors display limited specificity for cancer cells. Therefore, exploration of novel opportunities for APE1 targeting is obviously a path that deserves further consideration. Based on several observations attesting the critical role of disordered segments in many BER enzyme functions, we propose that the N-terminal unstructured portion of the APE1 protein could be considered as a new potential target for cancer therapy. Classical pharmacological strategies usually target structured regions of proteins; however, considering the biological relevance of intrinsically disordered proteins, the ability to interfere with their interactions opens enormous potentials for drug discovery. Actually, there is a continuous progress in the development of small molecules directed against disordered protein regions; several low molecular weight compounds are effective in the specific inhibition of molecular interactions based on intrinsically disordered domains. For example, small molecules binding the disordered regions of *c-myc*, Aβ, EWS-Fli1 have recently been discovered (100, 144). Although the binding of a small molecule to a disordered region/protein may appear counterintuitive due to the intrinsic poor selectivity, this may also be considered a major advantage because it would facilitate the screening of initial compounds, which affinity and specificity could be successively improved through standard molecular optimization procedures.

In conclusion, we suggest that it would be interesting to investigate novel pharmacological approaches aimed at interfering with the APE1 N-terminal region in light of its important role in the coordination of many different functions of the protein, both in DNA repair and RNA metabolism.

Conclusions and Speculations

Different independent studies provided *in vitro* and *in vivo* evidence that many DNA repair proteins, particularly in the BER pathway (*e.g.,* APE1), are involved in RNA metabolism. Interestingly, many of these proteins are also part of the nucleolar proteome where they bind specific carrier proteins (*e.g.,* NPM1, NCL) and rRNA. Upon genotoxic stress, many DNA repair proteins exit from nucleoli and switch their interactome network from proteins involved in RNA metabolism to DNA repair complexes. Although still in the early phases, these findings have raised many questions and speculations concerning the role of these proteins, including APE1 as a paradigmatic example, in RNA metabolism. For instance:

1. Why should a protein involved in DNA repair play a role in RNA metabolism? One possible explanation is that this duality would preserve genetic stability not only through the DNA repair activity, but also through the ability to cleanse damaged RNA that may otherwise be inaccurately translated, or degrade unwanted foreign RNA (*e.g.,* viral RNA).
2. Do the redox function of APE1 and its role in RNA metabolism represent two sides of the same coin devoted to modulate gene expression through transcriptional and post-transcriptional mechanisms? Modulation of APE1 subcellular distribution through its redox status may represent an elegant, specific, and energetically economic mechanism to tune gene expression upon genotoxic stress conditions.
3. Is APE1 an ancient protein with a newly identified and yet unappreciated role? The current information regarding the primary amino acid sequence of APE1 across species seems to suggest a phylogenetic "gain-of-function" and hence, support this hypothesis. However, further experimental and bioinformatics studies of APE1 orthologs may reveal additional insights into this question.
4. Suppressing the amount of APE1 has proven effective in sensitizing cancer cells to chemotherapeutic agents. This finding has led to the proposal that selective inhibition of the APE1 DNA repair activity is an attractive avenue for the development of novel anticancer therapies. Similarly, one can envision targeting the non-DNA repair functions of APE1, namely its RNA-repair and/or RNA-cleavage activities, as novel approaches for the treatment of cancer or neurological disorders. Nonetheless, such therapeutic aims still need further studies to increase our understanding of the role of APE1 in its noncanonical functions.

In closing, a productive cross-talk between DNA repair enzymes and proteins involved in RNA metabolism seems reasonable and nucleolus is emerging as a dynamic functional hub that coordinates cell growth arrest and DNA repair mechanisms. These findings will drive further analysis of other BER proteins, such as FEN1, and might imply that nucleic acid processing enzymes are more versatile than originally thought and may have evolved DNA-targeted functions after a prior life in the early RNA world. The observation of cytoplasmic localization for canonical DNA repair proteins, such as APE1, simply beyond their mitochondrial targeting, may therefore, suggest much more than just an "abnormal" distribution pattern.

Acknowledgments

We regret the omission of many important references due to space limitations. This work was supported by grants from: AIRC (IG10269) and MIUR (FIRB_RBRN07BMCT) to G.T.

References

1. Aas PA, Otterlei M, Falnes PO, Vågbø CB, Skorpen F, Akbari M, Sundheim O, Bjørås M, Slupphaug G, Seeberg E, and Krokan HE. Human and bacterial oxidative demethylases repair alkylation damage in both RNA and DNA. *Nature* 421: 859–863, 2003.
2. Adelmant G, Calkins AS, Garg BK, Card JD, Askenazi M, Miron A, Sobhian B, Zhang Y, Nakatani Y, Silver PA, Iglehart JD, Marto JA, and Lazaro J. DNA ends alter the molecular composition and localization of Ku multicomponent complexes. *Mol Cell Proteomics* 11: 411–421, 2012.
3. Ahmad Y, Boisvert FM, Gregor P, Cobley A, and Lamond AI. NOPdb: Nucleolar Proteome Database—2008 update. *Nucleic Acids Res* 37: D181–D184, 2009.
4. Andersen JS, Lyon CE, Fox AH, Leung AK, Lam YW, Steen H, Mann M, and Lamond AI. Directed proteomic analysis of the human nucleolus. *Curr Biol* 12: 1–11, 2002.
5. Andersen JS, Lam YW, Leung AKL, Ong S, Lyon CE, Lamond AI, and Mann M. Nucleolar proteome dynamics. *Nature* 433: 77–83, 2005.
6. Banerjee D, Mandal SM, Das A, Hegde ML, Das S, Bhakat KK, Boldogh I, Sarkar PS, Mitra S, and Hazra TK. Preferential repair of oxidized base damage in the transcribed genes of mammalian cells. *J Biol Chem* 286: 6006–6016, 2011.
7. Barnes T, Kim W, Mantha AK, Kim S, Izumi T, Mitra S, and Lee CH. Identification of Apurinic/apyrimidinic endonuclease 1 (APE1) as the endoribonuclease that cleaves c-myc mRNA. *Nucleic Acids Res* 37: 3946–3958, 2009.
8. Barthelmes HU, Habermeyer M, Christensen MO, Mielke C, Interthal H, Pouliot JJ, Boege F, and Marko D. TDP1 overexpression in human cells counteracts DNA damage mediated by topoisomerases I and II. *J Biol Chem* 279: 55618–55625, 2004.
9. Barzilay G, Walker LJ, Robson CN, and Hickson ID. Site-directed mutagenesis of the human DNA repair enzyme HAP1: identification of residues important for AP endonuclease and RNase H activity. *Nucleic Acids Res* 23: 1544–1550, 1995.
10. Beernink PT, Segelke BW, Hadi MZ, Erzberger JP, Wilson DM, and Rupp B. Two divalent metal ions in the active site of a new crystal form of human apurinic/apyrimidinic endonuclease, Ape1: implications for the catalytic mechanism. *J Mol Biol* 307: 1023–1034, 2001.
11. Bellacosa A and Moss EG. RNA repair: damage control. *Curr Biol* 13: R482–R484, 2003.
12. Berquist BR, McNeill DR, and Wilson DM. Characterization of abasic endonuclease activity of human Ape1 on alternative substrates, as well as effects of ATP and sequence context on AP site incision. *J Mol Biol* 379: 17–27, 2008.
13. This reference has been deleted.
14. Bhakat KK, Izumi T, Yang S, Hazra TK, and Mitra S. Role of acetylated human AP-endonuclease (APE1/Ref-1) in regulation of the parathyroid hormone gene. *EMBO J* 22: 6299–6309, 2003.
15. Black DL. Mechanisms of alternative pre-messenger RNA splicing. *Annu Rev Biochem* 72: 291–336, 2003.
16. Blander G, Zalle N, Daniely Y, Taplick J, Gray MD, and Oren M. DNA damage-induced translocation of the Werner helicase is regulated by acetylation. *J Biol Chem* 277: 50934–50940, 2002.
17. Boisvert F, Lam YW, Lamont D, and Lamond AI. A quantitative proteomics analysis of subcellular proteome localization and changes induced by DNA damage. *Mol Cell Proteomics* 9: 457–470, 2010.
18. Boisvert F, van Koningsbruggen S, Navascues J, and Lamond AI. The multifunctional Nucleolus. *Nat Rev Mol Cell Biol* 8: 574–585, 2007.
19. Borggrefe T, Wabl M, Akhmedov AT, and Jessberger R. A B-cell-specific DNA recombination complex. *J Biol Chem* 273: 17025–17035, 1998.
20. Boulon S, Westman BJ, Hutten S, Boisvert F, and Lamond AI. The nucleolus under stress. *Mol Cell* 40: 216–227, 2010.
21. Boyd MT, Vlatkovic N, and Rubbi CP. The nucleolus directly regulates p53 export and degradation. *J Cell Biol* 194: 689–703, 2011.
22. Buckwalter CA, Lin AH, Tanizawa A, Pommier YG, Cheng YC, and Kaufmann SH. RNA synthesis inhibitors alter the subnuclear distribution of DNA topoisomerase I. *Cancer Res* 56: 1674–1681, 1996.
23. Burger K, Mühl B, Harasim T, Rohrmoser M, Malamoussi A, Orban M, Kellner M, Gruber-Eber A, Kremmer E, Hölzel M, and Eick D. Chemotherapeutic drugs inhibit ribosome biogenesis at various levels. *J Biol Chem* 285: 12416–12425, 2010.
24. Busso CS, Iwakuma T, and Izumi T. Ubiquitination of mammalian AP endonuclease (APE1) regulated by the p53-MDM2 signaling pathway. *Oncogene* 28: 1616–1625, 2009.
25. Campalans A, Amouroux R, Bravard A, Epe B, and Radicella JP. UVA irradiation induces relocalisation of the DNA repair protein hOGG1 to nuclear speckles. *J Cell Sci* 120: 23–32, 2007.
26. Canitrot Y, Cazaux C, Fréchet M, Bouayadi K, Lesca C, Salles B, and Hoffmann JS. Overexpression of DNA polymerase beta in cell results in a mutator phenotype and a decreased sensitivity to anticancer drugs. *Proc Natl Acad Sci USA* 95: 12586–12590, 1998.
27. Carmo-Fonseca M, Mendes-Soares L, and Campos I. To be or not to be in the nucleolus. *Nat Cell Biol* 2: E107–E112, 2000.
28. Chang MS, Sasaki H, Campbell MS, Kraeft SK, Sutherland R, Yang CY, Liu Y, Auclair D, Hao L, Sonoda H, Ferland LH, and Chen LB. HRad17 colocalizes with NHP2L1 in the nucleolus and redistributes after UV irradiation. *J Biol Chem* 274: 36544–36549, 1999.
29. Chattopadhyay R, Das S, Maiti AK, Boldogh I, Xie J, Hazra TK, Kohno K, Mitra S, and Bhakat KK. Regulatory role of human AP-endonuclease (APE1/Ref-1) in YB-1-mediated activation of the multidrug resistance gene MDR1. *Mol Cell Biol* 28: 7066–7080, 2008.
30. Cohen AA, Geva-Zatorsky N, Eden E, Frenkel-Morgenstern M, Issaeva I, Sigal A, Milo R, Cohen-Saidon C, Liron Y, Kam Z, Cohen L, Danon T, Perzov N, and Alon U. Dynamic proteomics of individual cancer cells in response to a drug. *Science* 322: 1511–1516, 2008.
31. Colombo E, Alcalay M, and Pelicci PG. Nucleophosmin and its complex network: a possible therapeutic target in hematological diseases. *Oncogene* 30: 2595–2609, 2011.
32. Coulon S, Noguchi E, Noguchi C, Du L, Nakamura TM, and Russell P. Rad22Rad52-dependent repair of ribosomal DNA repeats cleaved by Slx1-Slx4 endonuclease. *Mol Biol Cell* 17: 2081–2090, 2006.

32a. Couté Y, Burgess JA, Diaz JJ, Chichester C, Lisacek F, Greco A, and Sanchez JC. Deciphering the human nucleolar proteome. *Mass Spectrom Rev* 25: 215–234, 2006.

33. Crampton N, Kodiha M, Shrivastava S, Umar R, and Stochaj U. Oxidative stress inhibits nuclear protein export by multiple mechanisms that target FG nucleoporins and Crm1. *Mol Biol Cell* 20: 5106–5116, 2009.
34. Daniely Y, Dimitrova DD, and Borowiec JA. Stress-dependent nucleolin mobilization mediated by p53-nucleolin complex formation. *Mol Cell Biol* 22: 6014–6022, 2002.
35. Das S, Chattopadhyay R, Bhakat KK, Boldogh I, Kohno K, Prasad R, Wilson SH, and Hazra TK. Stimulation of NEIL2-mediated oxidized base excision repair via YB-1 interaction during oxidative stress. *J Biol Chem* 282: 28474–28484, 2007.
36. Dejmek J, Iglehart JD, and Lazaro J. DNA-dependent protein kinase (DNA-PK)-dependent cisplatin-induced loss of nucleolar facilitator of chromatin transcription (FACT) and regulation of cisplatin sensitivity by DNA-PK and FACT. *Mol Cancer Res* 7: 581–591, 2009.
37. Demple B, Herman T, and Chen DS. Cloning and expression of APE, the cDNA encoding the major human apurinic endonuclease: definition of a family of DNA repair enzymes. *Proc Natl Acad Sci USA* 88: 11450–11454, 1991.
38. Ding Q, Markesbery WR, Chen Q, Li F, and Keller JN. Ribosome dysfunction is an early event in Alzheimer's disease. *J Neurosci* 25: 9171–9175, 2005.
39. Eckert-Boulet N and Lisby M. Regulation of rDNA stability by sumoylation. *DNA Repair (Amst)* 8: 507–516, 2009.
40. Emmott E and Hiscox JA. Nucleolar targeting: the hub of the matter. *EMBO Rep* 10: 231–238, 2009.
41. Essers J, Vermeulen W, and Houtsmuller AB. DNA damage repair: anytime, anywhere?. *Curr Opin Cell Biol* 18: 240–246, 2006.
42. Fantini D, Vascotto C, Marasco D, D'Ambrosio C, Romanello M, Vitagliano L, Pedone C, Poletto M, Cesaratto L, Quadrifoglio F, Scaloni A, Radicella JP, and Tell G. Critical lysine residues within the overlooked N-terminal domain of human APE1 regulate its biological functions. *Nucleic Acids Res* 38: 8239–8256, 2010.
43. Fishel ML and Kelley MR. The DNA base excision repair protein Ape1/Ref-1 as a therapeutic and chemopreventive target. *Mol Aspects Med* 28: 375–395, 2007.
44. Fishel ML, He Y, Reed AM, Chin-Sinex H, Hutchins GD, Mendonca MS, and Kelley MR. Knockdown of the DNA repair and redox signaling protein Ape1/Ref-1 blocks ovarian cancer cell and tumor growth. *DNA Repair (Amst)* 7: 177–186, 2008.
45. Fishel ML, He Y, Smith ML, and Kelley MR. Manipulation of base excision repair to sensitize ovarian cancer cells to alkylating agent temozolomide. *Clin Cancer Res* 13: 260–267, 2007.
46. Francia S, Michelini F, Saxena A, Tang D, de Hoon M, Anelli V, Mione M, Carninci P, and d'Adda di Fagagna F. Site-specific DICER and DROSHA RNA products control the DNA-damage response. *Nature* 488: 231–235, 2012.
47. Fuxreiter M, Tompa P, Simon I, Uversky VN, Hansen JC, and Asturias FJ. Malleable machines take shape in eukaryotic transcriptional regulation. *Nat Chem Biol* 4: 728–737, 2008.
48. Gao H, Chen X, and McGowan CH. Mus81 endonuclease localizes to nucleoli and to regions of DNA damage in human S-phase cells. *Mol Biol Cell* 14: 4826–4834, 2003.
49. Gjerset RA and Bandyopadhyay K. Regulation of p14ARF through subnuclear compartmentalization. *Cell Cycle* 5: 686–690, 2006.
50. Gorman MA, Morera S, Rothwell DG, de La Fortelle E, Mol CD, Tainer JA, Hickson ID, and Freemont PS. The crystal structure of the human DNA repair endonuclease HAP1 suggests the recognition of extra-helical deoxyribose at DNA abasic sites. *EMBO J* 16: 6548–6558, 1997.
51. Griffiths LM, Swartzlander D, Meadows KL, Wilkinson KD, Corbett AH, and Doetsch PW. Dynamic compartmentalization of base excision repair proteins in response to nuclear and mitochondrial oxidative stress. *Mol Cell Biol* 29: 794–807, 2009.
52. Grisendi S, Mecucci C, Falini B, and Pandolfi PP. Nucleophosmin and cancer. *Nat Rev Cancer* 6: 493–505, 2006.
53. Guerra-Rebollo M, Mateo F, Franke K, Huen MSY, Lopitz-Otsoa F, Rodríguez MS, Plans V, and Thomson TM. Nucleolar exit of RNF8 and BRCA1 in response to DNA damage. *Exp Cell Res* 318: 2365–2376, 2012.
54. Guo Z, Qian L, Liu R, Dai H, Zhou M, Zheng L, and Shen B. Nucleolar localization and dynamic roles of flap endonuclease 1 in ribosomal DNA replication and damage repair. *Mol Cell Biol* 28: 4310–4319, 2008.
55. Hanakahi LA, Bu Z, and Maizels N. The C-terminal domain of nucleolin accelerates nucleic acid annealing. *Biochemistry* 39: 15493–15499, 2000.
56. Hayakawa H, Uchiumi T, Fukuda T, Ashizuka M, Kohno K, Kuwano M, and Sekiguchi M. Binding capacity of human YB-1 protein for RNA containing 8-oxoguanine. *Biochemistry* 41: 12739–12744, 2002.
57. Hegde ML, Banerjee S, Hegde PM, Bellot LJ, Hazra TK, Boldogh I, and Mitra S. Enhancement of NEIL1 protein-initiated oxidized DNA base excision repair by heterogeneous nuclear ribonucleoprotein U (hnRNP-U) via direct interaction. *J Biol Chem* 287: 34202–34211, 2012.
58. Hegde ML, Hazra TK, and Mitra S. Early steps in the DNA base excision/single-strand interruption repair pathway in mammalian cells. *Cell Res* 18: 27–47, 2008.
59. Hegde ML, Hazra TK, and Mitra S. Functions of disordered regions in mammalian early base excision repair proteins. *Cell Mol Life Sci* 67: 3573–3587, 2010.
60. Hegde V, Wang M, and Deutsch WA. Characterization of human ribosomal protein S3 binding to 7,8-dihydro-8-oxoguanine and abasic sites by surface plasmon resonance. *DNA Repair (Amst)* 3: 121–126, 2004.
61. Hegde V, Wang M, and Deutsch WA. Human ribosomal protein S3 interacts with DNA base excision repair proteins hAPE/Ref-1 and hOGG1. *Biochemistry* 43: 14211–14217, 2004.
62. Herandez-Verdun D, Roussel P, Thiry M, Sirri V, and Lafontaine DLJ. The nucleolus: structure/function relationship in RNA metabolism. *Wiley Interdiscip Rev RNA* 1: 415–431, 2010.
63. Hinsby AM, Kiemer L, Karlberg EO, Lage K, Fausbøll A, Juncker AS, Andersen JS, Mann M, and Brunak S. A wiring of the human nucleolus. *Mol Cell* 22: 285–295, 2006.
64. Horn HF and Vousden KH. Cancer: Guarding the guardian? *Nature* 427: 110–111, 2004.
65. Hung L, Heiner M, Hui J, Schreiner S, Benes V, and Bindereif A. Diverse roles of hnRNP L in mammalian mRNA processing: a combined microarray and RNAi analysis. *RNA* 14: 284–296, 2008.
66. Ikeda S, Biswas T, Roy R, Izumi T, Boldogh I, Kurosky A, Sarker AH, Seki S, and Mitra S. Purification and characterization of human NTH1, a homolog of *Escherichia coli* endonuclease III. Direct identification of Lys-212 as the active nucleophilic residue. *J Biol Chem* 273: 21585–21593, 1998.
67. Illuzzi JL and Wilson DM. Base excision repair: contribution to tumorigenesis and target in anticancer treatment paradigms. *Curr Med Chem* 19: 3922–3936, 2012.

68. Izumi T and Mitra S. Deletion analysis of human AP-endonuclease: minimum sequence required for the endonuclease activity. *Carcinogenesis* 19: 525–527, 1998.
69. Izumi T, Brown DB, Naidu CV, Bhakat KK, Macinnes MA, Saito H, Chen DJ, and Mitra S. Two essential but distinct functions of the mammalian abasic endonuclease. *Proc Natl Acad Sci USA* 102: 5739–5743, 2005.
70. Jackson EB, Theriot CA, Chattopadhyay R, Mitra S, and Izumi T. Analysis of nuclear transport signals in the human apurinic/apyrimidinic endonuclease (APE1/Ref1). *Nucleic Acids Res* 33: 3303–3312, 2005.
71. Jarboui MA, Bidoia C, Woods E, Roe B, Wynne K, Elia G, Hall WW, and Guatier VW. Nucleolar protein trafficking in response to HIV-1 Tat: rewiring the nucleolus. *PLoS One* 7: e48702, 2012.
72. This reference has been deleted.
73. Jobert L, Skjeldam HK, Dalhus B, Galashevskaya A, Vagbo CB, Bjoras M, and Nilsen H. The human base excision repair enzyme SMUG1 directly interacts with DKC1 and contributes to RNA quality control. *Mol Cell* 49: 339–345, 2013.
74. Ju B, Solum D, Song EJ, Lee K, Rose DW, Glass CK, and Rosenfeld MG. Activating the PARP-1 sensor component of the groucho/TLE1 corepressor complex mediates a CaMKinase IIdelta-dependent neurogenic gene activation pathway. *Cell* 119: 815–829, 2004.
75. Karmakar P and Bohr VA. Cellular dynamics and modulation of WRN protein is DNA damage specific. *Mech Ageing Dev* 126: 1146–1158, 2005.
76. Kim W, Berquist BR, Chohan M, Uy C, Wilson DM3, and Lee CH. Characterization of the endoribonuclease active site of human apurinic/apyrimidinic endonuclease 1. *J Mol Biol* 411: 960–971, 2011.
77. Kim W, King D, and Lee CH. RNA-cleaving properties of human apurinic/apyrimidinic endonuclease 1 (APE1). *Int J Biochem Mol Biol* 1: 12–25, 2010.
78. Ko SI, Park J, Park MJ, Kim J, Kang L, and Han YS. Human ribosomal protein S3 (hRpS3) interacts with uracil-DNA glycosylase (hUNG) and stimulates its glycosylase activity. *Mutat Res* 648: 54–64, 2008.
79. Koike A, Nishikawa H, Wu W, Okada Y, Venkitaraman AR, and Ohta T. Recruitment of phosphorylated NPM1 to sites of DNA damage through RNF8-dependent ubiquitin conjugates. *Cancer Res* 70: 6746–6756, 2010.
80. Kruhlak M, Crouch EE, Orlov M, Montaño C, Gorski SA, Nussenzweig A, Misteli T, Phair RD, and Casellas R. The ATM repair pathway inhibits RNA polymerase I transcription in response to chromosome breaks. *Nature* 447: 730–734, 2007.
81. Kuninger DT, Izumi T, Papaconstantinou J, and Mitra S. Human AP-endonuclease 1 and hnRNP-L interact with a nCaRE-like repressor element in the AP-endonuclease 1 promoter. *Nucleic Acids Res* 30: 823–829, 2002.
82. Kushner SR. mRNA decay in prokaryotes and eukaryotes: different approaches to a similar problem. *IUBMB Life* 56: 585–594, 2004.
83. Lam YW, Lamond AI, Mann M, and Andersen JS. Analysis of nucleolar protein dynamics reveals the nuclear degradation of ribosomal proteins. *Curr Biol* 17: 749–760, 2007.
84. Lam YW, Trinkle-Mulcahy L, and Lamond AI. The nucleolus. *J Cell Sci* 118: 1335–1337, 2005.
85. Lau JP, Weatherdon KL, Skalski V, and Hedley DW. Effects of gemcitabine on APE/ref-1 endonuclease activity in pancreatic cancer cells, and the therapeutic potential of antisense oligonucleotides. *Br J Cancer* 91: 1166–1173, 2004.
86. Lee C, Smith BA, Bandyopadhyay K, and Gjerset RA. DNA damage disrupts the p14ARF-B23(nucleophosmin) interaction and triggers a transient subnuclear redistribution of p14ARF. *Cancer Res* 65: 9834–9842, 2005.
87. Lewinska A, Wnuk M, Grzelak A, and Bartosz G. Nucleolus as an oxidative stress sensor in the yeast *Saccharomyces cerevisiae*. *Redox Rep* 15: 87–96, 2010.
88. Li Z, Wu J, and Deleo CJ. RNA damage and surveillance under oxidative stress. *IUBMB Life* 58: 581–588, 2006.
89. Lirussi L, Antoniali G, Vascotto C, D'Ambrosio C, Poletto M, Romanello M, Marasco D, Leone M, Quadrifoglio F, Bhakat KK, Scaloni A, and Tell G. Nucleolar accumulation of APE1 depends on charged lysine residues that undergo acetylation upon genotoxic stress and modulate its BER activity in cells. *Mol Biol Cell* 23: 4079–4096, 2012.
90. Liu Y, Prasad R, and Wilson SH. HMGB1: roles in base excision repair and related function. *Biochim Biophys Acta* 1799: 119–130, 2010.

90a. Lo SJ, Lee CC, and Lai HJ. The nucleolus: reviewing oldies to have new understandings. *Cell Res* 16: 530–538, 2006.

91. Loeb LA and Preston BD. Mutagenesis by apurinic/apyrimidinic sites. *Annu Rev Genet* 20: 201–230, 1986.
92. Luo M, He H, Kelley MR, and Georgiadis MM. Redox regulation of DNA repair: implications for human health and cancer therapeutic development. *Antioxid Redox Signal* 12: 1247–1269, 2010.
93. Mao Y, Mehl IR, and Muller MT. Subnuclear distribution of topoisomerase I is linked to ongoing transcription and p53 status. *Proc Natl Acad Sci USA* 99: 1235–1240, 2002.
94. Marciniak RA, Lombard DB, Johnson FB, and Guarente L. Nucleolar localization of the Werner syndrome protein in human cells. *Proc Natl Acad Sci USA* 95: 6887–6892, 1998.
95. Mastrocola AS and Heinen CD. Nuclear reorganization of DNA mismatch repair proteins in response to DNA damage. *DNA Repair (Amst)* 9: 120–133, 2010.
96. Mayer C and Grummt I. Cellular stress and nucleolar function. *Cell Cycle* 4: 1036–1038, 2005.
97. Meder VS, Boeglin M, de Murcia G, and Schreiber V. PARP-1 and PARP-2 interact with nucleophosmin/B23 and accumulate in transcriptionally active nucleoli. *J Cell Sci* 118: 211–222, 2005.
98. Mekhail K, Gunaratnam L, Bonicalz M, and Lee S. HIF activation by pH-dependent nucleolar sequestration of VHL. *Nat Cell Biol* 6: 642–647, 2004.
99. Menoni KH, Hoeijmakers JH, and Vermeulen W. Nucleotide excision repair-initiating proteins bind to oxidative DNA lesions *in vivo*. *J Cell Biol* 199: 1037–1046, 2012.
100. Metallo SJ. Intrinsically disordered proteins are potential drug targets. *Curr Opin Chem Biol* 14: 481–488, 2010.
101. Meyer S, Temme C, and Wahle E. Messenger RNA turnover in eukaryotes: pathways and enzymes. *Crit Rev Biochem Mol Biol* 39: 197–216, 2004.
102. Milkereit P, Gadal O, Podtelejnikov A, Trumtel S, Gas N, Petfalski E, Tollervey D, Mann M, Hurt E, and Tschochner H. Maturation and intranuclear transport of pre-ribosomes requires Noc proteins. *Cell* 105: 499–509, 2001.
103. Milkereit P, Strauss D, Bassler J, Gadal O, Kuhn H, Schutz S, Gas N, Lechner J, Hurt E, and Tschochner H. A Noc complex specifically involved in the formation and nuclear export of ribosomal 40 S subunits. *J Biol Chem* 278: 4072–4081, 2003.
104. Mo X and Dynan WS. Subnuclear localization of Ku protein: functional association with RNA polymerase II elongation sites. *Mol Cell Biol* 22: 8088–8099, 2002.

105. Montanaro L, Trerè D, and Derenzini M. Nucleolus, ribosomes, and cancer. *Am J Pathol* 173: 301–310, 2008.
106. Moore HM, Bai B, Boisvert F, Latonen L, Rantanen V, Simpson JC, Pepperkok R, Lamond AI, and Laiho M. Quantitative proteomics and dynamic imaging of the nucleolus reveal distinct responses to UV and ionizing radiation. *Mol Cell Proteomics* 10: M111.009241, 2011.
107. Moreira PI, Nunomura A, Nakamura M, Takeda A, Shenk JC, Aliev G, Smith MA, and Perry G. Nucleic acid oxidation in Alzheimer disease. *Free Radic Biol Med* 44: 1493–1505, 2008.
108. Nalabothula N, Indig FE, and Carrier F. The nucleolus takes control of protein trafficking under cellular stress. *Mol Cell Pharmacol* 2: 203–212, 2010.
108a. Nishimura Y, Ohkubo T, Furuichi Y, and Umekawa H. Tryptophans 286 and 288 in the C-terminal region of protein B23.1 are important for its nucleolar localization. *Biosci Biotechnol Biochem* 66: 2239–2242, 2002.
109. Nunomura A, Moreira PI, Castellani RJ, Lee H, Zhu X, Smith MA, and Perry G. Oxidative damage to RNA in aging and neurodegenerative disorders. *Neurotox Res* 22: 231–248, 2012.
110. Olson MO and Dundr M. The moving parts of the nucleolus. *Histochem Cell Biol* 123: 203–216, 2005.
111. Ougland R, Zhang C, Liiv A, Johansen RF, Seeberg E, Hou Y, Remme J, and Falnes PØ. AlkB restores the biological function of mRNA and tRNA inactivated by chemical methylation. *Mol Cell* 16: 107–116, 2004.
112. Park MS, Knauf JA, Pendergrass SH, Coulon CH, Strniste GF, Marrone BL, and MacInnes MA. Ultraviolet-induced movement of the human DNA repair protein, Xeroderma pigmentosum type G, in the nucleus. *Proc Natl Acad Sci USA* 93: 8368–8373, 1996.
113. Pavri R, Lewis B, Kim T, Dilworth FJ, Erdjument-Bromage H, Tempst P, de Murcia G, Evans R, Chambon P, and Reinberg D. PARP-1 determines specificity in a retinoid signaling pathway via direct modulation of mediator. *Mol Cell* 18: 83–96, 2005.
114. Pederson T. The nucleolus. *Cold Spring Harbor Perspect Biol* 3: 1–15, 2011.
115. Pederson T and Tsai RY. In search of nonribosomal nucleolar protein function and regulation. *J Cell Biol* 184: 771–776, 2009.
116. Poletto M, Vascotto C, Scognamiglio PL, Lirussi L, Marasco D, and Tell G. Role of the unstructured N-terminal domain of the human apurinic/apyrimidinic endonuclease 1 (hAPE1) in the modulation of its interaction with nucleic acids and nucleophosmin (NPM1). *Biochem J* 452: 545–557, 2013.
117. Pérez-Castro AJ and Freire R. Rad9B responds to nucleolar stress through ATR and JNK signalling, and delays the G1-S transition. *J Cell Sci* 125: 1152–1164, 2012.
118. Radivojac P, Iakoucheva LM, Oldfield CJ, Obradovic Z, Uversky VN, and Dunker AK. Intrinsic disorder and functional proteomics. *Biophys J* 92: 1439–1456, 2007.
119. Raffetseder U, Frye B, Rauen T, Jürchott K, Royer H, Jansen PL, and Mertens PR. Splicing factor SRp30c interaction with Y-box protein-1 confers nuclear YB-1 shuttling and alternative splice site selection. *J Biol Chem* 278: 18241–18248, 2003.
120. Rancourt A and Satoh MS. Delocalization of nucleolar poly(ADP-ribose) polymerase-1 to the nucleoplasm and its novel link to cellular sensitivity to DNA damage. *DNA Repair (Amst)* 8: 286–297, 2009.
121. Raska I, Shaw PJ, and Cmarko D. Structure and function of the nucleolus in the spotlight. *Curr Opin Cell Biol* 18: 325–334, 2006.
122. Rieker C, Engblom D, Kreiner G, Domanskyi A, Schober A, Stotz S, Neumann M, Yuan X, Grummt I, Schütz G, and Parlato R. Nucleolar disruption in dopaminergic neurons leads to oxidative damage and parkinsonism through repression of mammalian target of rapamycin signaling. *J Neurosci* 31: 453–460, 2011.
123. Rubbi CP and Milner J. Non-activated p53 co-localizes with sites of transcription within both the nucleoplasm and the nucleolus. *Oncogene* 19: 85–96, 2000.
124. Rubbi CP and Milner J. Disruption of the nucleolus mediates stabilization of p53 in response to DNA damage and other stresses. *EMBO J* 22: 6068–6077, 2003.
125. Scherl A, Couté Y, Déon C, Callé A, Kindbeiter K, Sanchez J, Greco A, Hochstrasser D, and Diaz J. Functional proteomic analysis of human nucleolus. *Mol Biol Cell* 13: 4100–4109, 2002.
126. Schramm VL. Enzymatic N-riboside scission in RNA and RNA precursors. *Curr Opin Chem Biol* 1: 323–331, 1997.
127. Sekhar KR, Reddy YT, Reddy PN, Crooks PA, Venkateswaran A, McDonald WH, Geng L, Sasi S, Van Der Waal RP, Roti JLR, Salleng KJ, Rachakonda G, and Freeman ML. The novel chemical entity YTR107 inhibits recruitment of nucleophosmin to sites of DNA damage, suppressing repair of DNA double-strand breaks and enhancing radiosensitization. *Clin Cancer Res* 17: 6490–6499, 2011.
128. Sengupta S, Mantha AK, Mitra S, and Bhakat KK. Human AP endonuclease (APE1/Ref-1) and its acetylation regulate YB-1-p300 recruitment and RNA polymerase II loading in the drug-induced activation of multidrug resistance gene MDR1. *Oncogene* 30: 482–493, 2011.
129. Shcherbik N and Pestov DG. Ubiquitin and ubiquitin-like proteins in the nucleolus: multitasking tools for a ribosome factory. *Genes Cancer* 1: 681–689, 2010.
130. Sirri V, Urcuqui-Inchima S, Roussel P, and Hernandez-Verdun D. Nucleolus: the fascinating nuclear body. *Histochem Cell Biol* 129: 13–31, 2008.
131. Stark LA and Taliansky M. Old and new faces of the nucleolus. Workshop on the Nucleolus and Disease. *EMBO Rep* 10: 35–40, 2009.
132. Stein A, Pache RA, Bernadó P, Pons M, and Aloy P. Dynamic interactions of proteins in complex networks: a more structured view. *FEBS J* 276: 5390–5405, 2009.
133. Strauss PR and Holt CM. Domain mapping of human apurinic/apyrimidinic endonuclease. Structural and functional evidence for a disordered amino terminus and a tight globular carboxyl domain. *J Biol Chem* 273: 14435–14441, 1998.
134. Suzuki A, Kogo R, Kawahara K, Sasaki M, Nishio M, Maehama T, Sasaki T, Mimori K, and Mori M. A new PICTure of nucleolar stress. *Cancer Sci* 103: 632–637, 2012.
135. Tanaka M, Chock PB, and Stadtman ER. Oxidized messenger RNA induces translation errors. *Proc Natl Acad Sci USA* 104: 66–71, 2007.
136. Tell G, Damante G, Caldwell D, and Kelley MR. The intracellular localization of APE1/Ref-1: more than a passive phenomenon? *Antioxid Redox Signal* 7: 367–384, 2005.
137. Tell G, Quadrifoglio F, Tiribelli C, and Kelley MR. The many functions of APE1/Ref-1: not only a DNA repair enzyme. *Antioxid Redox Signal* 11: 601–620, 2009.
138. Tell G, Wilson DM, and Lee CH. Intrusion of a DNA repair protein in the RNome world: is this the beginning of a new era? *Mol Cell Biol* 30: 366–371, 2010.

139. Tembe V and Henderson BR. Protein trafficking in response to DNA damage. *Cell Signal* 19: 1113–1120, 2007.
140. Thayer MM, Ahern H, Xing D, Cunningham RP, and Tainer JA. Novel DNA binding motifs in the DNA repair enzyme endonuclease III crystal structure. *EMBO J* 14: 4108–4120, 1995.
141. Tomecki R and Dziembowski A. Novel endoribonucleases as central players in various pathways of eukaryotic RNA metabolism. *RNA* 16: 1692–1724, 2010.
142. Trotta C, Lund E, Kahan L, Johnson A, and Dahlberg J. Coordinated nuclear export of 60S ribosomal subunits and NMD3 in vertebrates. *EMBO J* 22: 2841–2851, 2003.
143. Tóth-Petróczy A, Simon I, Fuxreiter M, and Levy Y. Disordered tails of homeodomains facilitate DNA recognition by providing a trade-off between folding and specific binding. *J Am Chem Soc* 131: 15084–15085, 2009.
144. Uversky VN. Intrinsically disordered proteins and novel strategies for drug discovery. *Expert Opin Drug Discov* 7: 475–488, 2012.
145. Uversky VN, Oldfield CJ, and Dunker AK. Showing your ID: intrinsic disorder as an ID for recognition, regulation and cell signaling. *J Mol Recognit* 18: 343–384, 2005.
146. Vascotto C and Fishel ML. Blockade of base excision repair: inhibition of small lesions results in big consequences to cancer cells. In: *DNA Repair in Cancer Therapy*, edited by Kelley MR. San Diego, CA: Academic Press, 2012, pp. 29–53.
147. Vascotto C, Bisetto E, Li M, Zeef LAH, D'Ambrosio C, Domenis R, Comelli M, Delneri D, Scaloni A, Altieri F, Mavelli I, Quadrifoglio F, Kelley MR, and Tell G. Knock-in reconstitution studies reveal an unexpected role of Cys-65 in regulating APE1/Ref-1 subcellular trafficking and function. *Mol Biol Cell* 22: 3887–3901, 2011.
148. Vascotto C, Cesaratto L, Zeef LAH, Deganuto M, D'Ambrosio C, Scaloni A, Romanello M, Damante G, Taglialatela G, Delneri D, Kelley MR, Mitra S, Quadrifoglio F, and Tell G. Genome-wide analysis and proteomic studies reveal APE1/Ref-1 multifunctional role in mammalian cells. *Proteomics* 9: 1058–1074, 2009.
149. Vascotto C, Fantini D, Romanello M, Cesaratto L, Deganuto M, Leonardi A, Radicella P, Kelley M, D'Ambrosio C, Scaloni A, Quadrifoglio F, and Tell G. APE1/Ref-1 interacts with NPM1 within Nucleoli and plays a role in the rRNA quality control process. *Mol Cell Biol* 29: 1834–1854, 2009.
150. Vascotto C, Lirussi L, Poletto M, Tiribelli M, Damiani D, Fabbro D, Damante G, Demple B, Colombo E, and Tell G. Functional regulation of the apurinic/apyrimidinic endonuclease APE1 by nucleophosmin (NPM1): impact on tumor biology. *Oncogene* (in press); doi:10.1038/onc.2013.251
151. Vassiliou GS, Cooper JL, Rad R, Li J, Rice S, Uren A, Rad L, Ellis P, Andrews R, Banerjee R, Grove C, Wang W, Liu P, Wright P, Arends M, and Bradley A. Mutant nucleophosmin and cooperating pathways drive leukemia initiation and progression in mice. *Nat Genet* 43: 470–475, 2011.
152. Vidal AE, Hickson ID, Boiteux S, and Radicella JP. Mechanism of stimulation of the DNA glycosylase activity of hOGG1 by the major human AP endonuclease: bypass of the AP lyase activity step. *Nucleic Acids Res* 29: 1285–1292, 2001.
153. Vuzman D, Azia A, and Levy Y. Searching DNA via a "Monkey Bar" mechanism: the significance of disordered tails. *J Mol Biol* 396: 674–684, 2010.
154. Wang D, Luo M, and Kelley MR. Human apurinic endonuclease 1 (APE1) expression and prognostic significance in osteosarcoma: enhanced sensitivity of osteosarcoma to DNA damaging agents using silencing RNA APE1 expression inhibition. *Mol Cancer Ther* 3: 679–686, 2004.
155. Wilson DM3, Deutsch WA, and Kelley MR. Drosophila ribosomal protein S3 contains an activity that cleaves DNA at apurinic/apyrimidinic sites. *J Biol Chem* 269: 25359–25364, 1994.
156. Woo LL, Futami K, Shimamoto A, Furuichi Y, and Frank KM. The Rothmund-Thomson gene product RECQL4 localizes to the nucleolus in response to oxidative stress. *Exp Cell Res* 312: 3443–3457, 2006.
157. Xanthoudakis S and Curran T. Identification and characterization of Ref-1, a nuclear protein that facilitates AP-1 DNA-binding activity. *EMBO J* 11: 653–665, 1992.
158. Xanthoudakis S, Smeyne RJ, Wallace JD, and Curran T. The redox/DNA repair protein, Ref-1, is essential for early embryonic development in mice. *Proc Natl Acad Sci USA* 93: 8919–8923, 1996.
159. Yacoub A, Kelley MR, and Deutsch WA. The DNA repair activity of human redox/repair protein APE/Ref-1 is inactivated by phosphorylation. *Cancer Res* 57: 5457–5459, 1997.
160. Yanagawa H, Ogawa Y, and Ueno M. Redox ribonucleosides. Isolation and characterization of 5-hydroxyuridine, 8-hydroxyguanosine, and 8-hydroxyadenosine from Torula yeast RNA. *J Biol Chem* 267: 13320–13326, 1992.
161. Yang C, Kim MS, Chakravarty D, Indig FE, and Carrier F. Nucleolin binds to the proliferating cell nuclear antigen and inhibits nucleotide excision repair. *Mol Cell Pharmacol* 1: 130–137, 2009.
162. Yang C, Maiguel DA, and Carrier F. Identification of nucleolin and nucleophosmin as genotoxic stress-responsive RNA-binding proteins. *Nucleic Acids Res* 30: 2251–2260, 2002.
163. Yankiwski V, Marciniak RA, Guarente L, and Neff NF. Nuclear structure in normal and Bloom syndrome cells. *Proc Natl Acad Sci USA* 97: 5214–5219, 2000.
164. This reference has been deleted.
165. Yoshida A, Pourquier P, and Pommier Y. Purification and characterization of a Mg2+-dependent endonuclease (AN34) from etoposide-treated human leukemia HL-60 cells undergoing apoptosis. *Cancer Res* 58: 2576–2582, 1998.
166. Yoshida A, Urasaki Y, Waltham M, Bergman A, Pourquier P, Rothwell DG, Inuzuka M, Weinstein JN, Ueda T, Appella E, Hickson ID, and Pommier Y. Human apurinic/apyrimidinic endonuclease (Ape1) and its N-terminal truncated form (AN34) are involved in DNA fragmentation during apoptosis. *J Biol Chem* 278: 37768–37776, 2003.
167. This reference has been deleted.
168. Zhou J, Ahn J, Wilson SH, and Prives C. A role for p53 in base excision repair. *EMBO J* 20: 914–923, 2001.

Address correspondence to:
Prof. Gianluca Tell
Department of Medical and Biological Sciences
University of Udine
P.Le M. Kolbe 4
Udine 33100
Italy

E-mail: gianluca.tell@uniud.it

Date of first submission to ARS Central, July 8, 2013; date of acceptance, July 22, 2013.

Abbreviations Used

8-OHG = 8-hydroxyguanosine
AD = Alzheimer's disease
AP = apurinic/apyrimidinic
APE1 = apurinic/apyrimidinic endonuclease 1
ATM = ataxia telangiectasia mutated
ATR = ataxia telangiectasia and Rad3-related
BER = base excision repair
CRM1 = exportin 1
DDR = DNA damage response
DSB = double-strand break
FEN1 = flap endonuclease 1
hMYH = human MutY glycosylase homolog
HR = homologous recombination
IR = ionizing radiation
NCL = nucleolin
NEIL2 = endonuclease VIII-like 2
NER = nucleotide excision repair
NHEJ = nonhomologous end joining
NLS = nuclear localization signal
NPM1 = nucleophosmin 1
NoLS = nucleolar localization sequence
NTH1 = endonuclease III-like glycosylase
OGG1 = 8-OHG DNA glycosylase
PARP1 = poly [ADP-ribose] polymerase 1
PCNA = proliferating cell nuclear antigen
PD = Parkinson disease
PNC = perinucleolar compartment
Polβ = DNA polymerase β
Pol I = RNA polymerase I
PTMs = post-translational modifications
rDNA = ribosomal DNA
rRNA = ribosomal RNA
RP = ribosomal protein
RPA = replication protein A
snoRNA = small nucleolar RNA
SSB = single-strand break
WRN = Werner syndrome helicase
XRCC1 = X-ray repair cross-complementing protein 1
Xth = exonuclease III
YB-1 = Y box binding protein 1

Biochimica et Biophysica Acta xxx (2014) xxx–xxx

Contents lists available at ScienceDirect

Biochimica et Biophysica Acta

journal homepage: www.elsevier.com/locate/bbagen

G-quadruplex DNA recognition by nucleophosmin: New insights from protein dissection

Q1 Pasqualina Liana Scognamiglio [a,c,1], Concetta Di Natale [a,c,1], Marilisa Leone [d,b], Mattia Poletto [e], Luigi Vitagliano [d], Gianluca Tell [e], Daniela Marasco [a,b,*]

Q6
[a] Department of Pharmacy, University of Naples "Federico II", DFM-Scarl, 80134 Naples, Italy
[b] CIRPEB: Centro Interuniversitario di Ricerca sui Peptidi Bioattivi, University of Naples "Federico II", DFM-Scarl, 80134 Naples, Italy
[c] Istituto Italiano di Tecnologia (IIT), 80125 Naples, Italy
[d] Institute of Biostructures and Bioimaging, CNR, 80134 Naples, Italy
[e] Department of Medical and Biological Sciences, University of Udine, 33100 Udine, Italy

ARTICLE INFO

Article history:
Received 16 December 2013
Received in revised form 13 February 2014
Accepted 18 February 2014
Available online xxxx

Keywords:
Disordered protein region
Surface Plasmon Resonance
Helical stability

ABSTRACT

Q7

Background: Nucleophosmin (NPM1, B23) is a multifunctional protein that is involved in a variety of fundamental biological processes. NPM1/B23 deregulation is implicated in the pathogenesis of several human malignancies. This protein exerts its functions through the interaction with a multiplicity of biological partners. Very recently it is has been shown that NPM1/B23 specifically recognizes DNA G-quadruplexes through its C-terminal region.
Methods: Through a rational dissection approach of protein here we show that the intrinsically unfolded regions of NPM1/B23 significantly contribute to the binding of c-MYC G-quadruplex motif. Interestingly, the analysis of the ability of distinct NPM1/B23 fragments to bind this quadruplex led to the identifications of distinct NPM1/B23-based peptides that individually present a high affinity for this motif.
Results: These results suggest that the tight binding of NPM1/B23 to the G-quadruplex is achieved through the cooperation of both folded and unfolded regions that are individually able to bind it. The dissection of NPM1/B23 also unveils that its H1 helix is intrinsically endowed with an unusual thermal stability.
Conclusions: These findings have implications for the unfolding mechanism of NPM1/B23, for the G-quadruplex affinity of the different NPM1/B23 isoforms and for the design of peptide-based molecules able to interact with this DNA motif.

1. Introduction

Nucleophosmin (NPM1, also known as B23, No38 and numatrin) is an abundant multifunctional protein, initially identified as a phosphoprotein, which is present in high quantities in the granular region of nucleoli [1,2]. NPM1/B23 is, however, capable of shuttling between nucleus and cytoplasm [3]. NPM1/B23 plays a plethora of functions including the regulation of ribosome biogenesis, chromatin remodeling, DNA replication, recombination, transcription, repair and the control of centrosome duplication [4,5]. This protein has been found overexpressed in tumors of different histological origins, including gastric, ovarian, bladder and prostate carcinomas and in various hematological malignancies [6–9]. Notably, NPM1/B23 has been identified as the most frequently mutated gene in acute myeloid leukemia (AML) patients, accounting for approximately 30% of cases [10–14].

NPM1/B23 belongs to the nucleophosmin/nucleoplasmin family of proteins [15]. Three distinct isoforms of the protein have been reported to be expressed in human cells. B23.1, the longest and the most abundant, is also the best characterized isoform. B23.2 and B23.3 are splicing variants that lack the C-terminal 35 amino-acids and a 29 amino-acid stretch (residues 195–223) in the basic region, respectively [16].

Structural characterizations of B23.1 have shown that the protein is endowed with a modular structure (Fig. 1). The N-terminal domain extends for approximately 100 residues and displays an eight-stranded

Abbreviations: TIS, Triisopropylsilane; TFA, Trifluoroacetic acid; DMF, Dimethylformamide; DCM, Dichloromethane; HBTU, 1-H-Benzotriazolium, 1-[bis(dimethylamino)methylene]-hexafluorophosphate(1-), 3 oxide; HOBt, N-hydroxybenzotriazole; DIEA, Di-isopropylethylamine; Fmoc, Fluorenylmethoxycarbonyl; TCEP, Tris(2-Carboxyethyl) phosphine; HPLC, High Performance Liquid Chromatography; LC–MS, Liquid Chromatography–Mass Spectrometry; EDC, 1-Ethyl-3-[3-dimethylaminopropyl]carbodiimide hydrochloride; NHS, N-hydroxysuccinimide; NOESY, Nuclear Overhauser Enhancement Spectroscopy; RMSD, Root Mean Square Deviation; TOCSY, Total Correlation Spectroscopy; C_53 NPM1, NPM1 242–294; C_70 NPM1, NPM1 225–294; C_107 NPM1, NPM1 188–294

* Corresponding author at: Department of Pharmacy, University "Federico II", Via Mezzocannone, 16, 80134 Naples, Italy. Tel.: +39 081 2532043; fax: +39 081 2534574.
E-mail address: daniela.marasco@unina.it (D. Marasco).
[1] These are co-first authors.

http://dx.doi.org/10.1016/j.bbagen.2014.02.017
0304-4165/

A

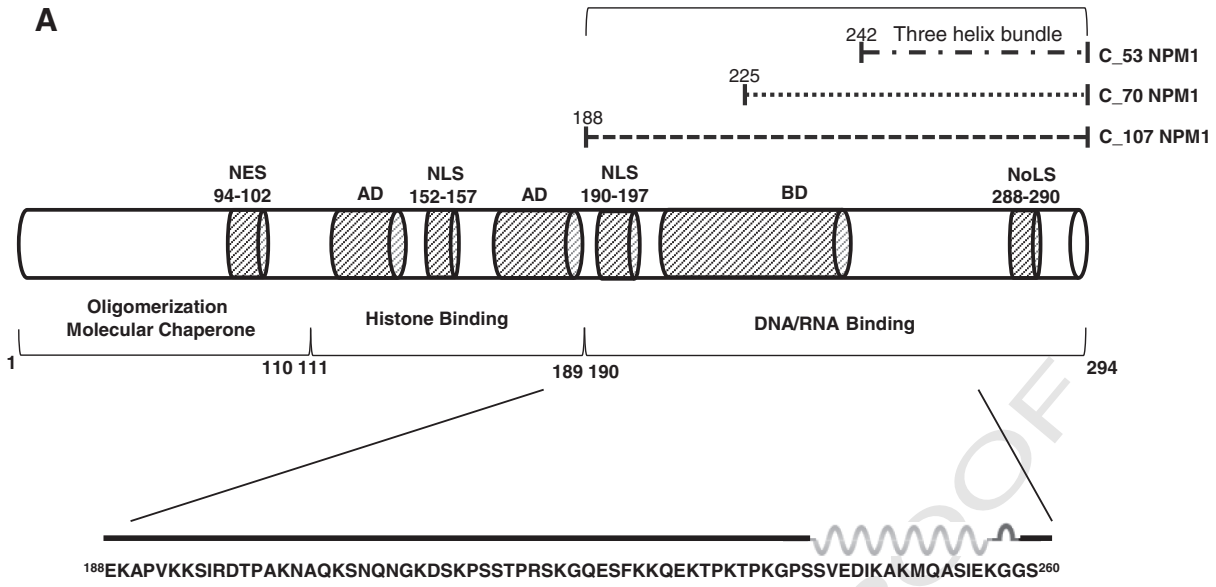

B

188-225	EKAPVKKSIRDTPAKNAQKSNQNGKDSKPSSTPRSKGQ
225-243	QESFKKQEKTPKTPKGPSS
242-259 B23.1	SSVEDIKAKMQASIEKGG
242-259 B23.2	SSVEDIKAKMQASIEKAH
259-277 B23.1	GSLPKVEAKFINYVKNCFR

Fig. 1. Schematic representation of NPM1 protein. (A) The modular structure of NPM1, functional, structural domains and primary structure of C_107NPM1 are pointed out and (B) primary sequences of C_107NPM1-based peptides were analyzed in this study.

beta-barrel fold. Five N-terminal domains oligomerize to form a crown-shaped pentamer [17]. Two or more of these pentamers may associate to form decamers or higher oligomeric species [18]. The central portion of NPM1 is characterized by the presence of two acid domains (residues 119–133 and 161–188) and a basic region (residues 198–239). The C-terminal domain (CTD) of B23.1 forms a globular structure consisting of a three helix bundle. The destabilization of this structural unit abolishes the nucleolar localization of the protein [19]. The C-terminal region of the protein has also been the subject of a number of intriguing investigations aimed at unveiling its folding mechanism [20–23]. Despite the structural heterogeneity of the different regions of the protein, recent biophysical studies have highlighted their mutual stabilization upon treatments with temperature or chemical denaturants [21,24].

The analysis of the NPM1/B23 sequence also shows that the protein shuttling abilities between intracellular compartments rely on several signaling sequences: i) a NES (nuclear export) motif with two leucines in the N-terminal domain, ii) NLSs (nuclear localization) between the two acidic stretches and, iii) a NoLS (nucleolar localization) with aromatic-rich residues at the C-terminal domain [20]. NPM1/B23 exerts its functions essentially through interactions with a variety of biological partners. NPM1 interactions with other proteins (e.g. p53, p14arf, Fbw7γ, APE-1) [25–29], ribosomal proteins RPL5, RPS9, RPL23, HIV proteins REV TAT) [30] are generally mediated by the N-terminal domain, whereas the C-terminal moiety regulates the binding of DNA/RNA.

NPM1 was shown to bind both DNA and RNA oligonucleotides, with a preference for single stranded structures with respect to those double-stranded, independently of the sequence [31,32].

Recently, it is has been shown that the C-terminus of NPM1 is able to specifically recognize G-quadruplex DNA motifs [33,34]. This finding is of great interest since these motifs are attractive targets for tumor treatment for their selective localization on promoters of several oncogenes and on telomeric regions [34,35]. In particular, it has been demonstrated that the NPM1 C-terminal domain recognizes in vitro a well-characterized G-quadruplex forming sequence present at the NHEIII region of the c-MYC oncogene promoter [33]. This promoter region adopts a G-quadruplex structure both in vitro and in vivo, regulating up to 90% of the total c-MYC transcriptional rate [36]. NMR studies have shown that this G-quadruplex is recognized by NPM1 primarily by residues belonging to the helices H1 and H2 of the three-helix bundle. Nevertheless, mutagenesis analyses have shown that a fundamental contribution to the G-quadruplex binding is provided by the residues Lys 229 and Lys 230 [34]. Intriguingly, the region embedding these residues is disordered in the NMR structure of the complex. Attempts to explain these puzzling findings were based on the observation that the presence of an unstructured segment adjacent to the interacting domain could provide a larger platform for long-range electrostatic interactions or transient physical contacts [34].

In order to gain further insights into this intricate recognition mechanism, here we evaluated the ability of individual fragments of NPM1 to bind this G-quadruplex. Interestingly, the dissection of NPM1 led to the identification of distinct protein segments that present high affinity for this motif. The structural characterization of these fragments provides new clues about the folding/unfolding process of the triple helix bundle motif. Moreover, present findings delineate strategies for the development of peptide-based entities for targeting the c-MYC G-quadruplex.

Please cite this article as: P.L. Scognamiglio, et al., G-quadruplex DNA recognition by nucleophosmin: New insights from protein dissection, Biochim. Biophys. Acta (2014), http://dx.doi.org/10.1016/j.bbagen.2014.02.017

2. Material and methods

2.1. Preparation of recombinant C_107 NPM1

C_107 NPM1 (residues 188–294) constructs were expressed and purified as HisTag-fusion proteins in *Escherichia coli* BL21 (DE3) following or adapting the procedure previously described [37]. The quality of purification was checked by Coomassie-stained SDS-polyacrylamide gel electrophoresis (PAGE) analysis. Extensive dialysis against PBS was performed to remove any trace of imidazole from the purified proteins.

2.2. G-quadruplex

Oligonucleotide TGGGGAGGGTGGGGAGGGTGGGGAAGG biotinylated at the 5′-end used in this study was purchased from PRIMM s.r.l (Milan, Italy) and purified by HPLC. For annealing, as already reported, in 20 mM Hepes, pH 7.0, with 100 mM NaCl, oligo was heated to 95 °C for 15 min and slowly cooled down at RT, overnight.

2.3. Surface Plasmon Resonance

The interactions between biotinylated c-MYC G-quadruplex with purified C_107 NPM1, and peptides NPM1 188–225, 225–243, 242–259 and 242–259_B23.2, were all measured using the SPR technique and BIAcore T-100, 3000 (GE Healthcare Milano, Italy). Biotinylated c-MYC G-quadruplex was immobilized on a sensor chip SA, pre-coated with streptavidin (GE Healthcare Milano, Italy). The capturing procedure on the biosensor surface was performed as reported in [38]. Running buffer was Hepes-buffered saline-EP, which contains 10 mM Hepes, pH 7.4, 0.15 M NaCl, 3 mM EDTA, 0.005% (v/v) surfactant P20. Analytes were dissolved in running buffer, and binding experiments were performed at 25 °C with a flow rate of 20 μL/min. The association phase (k_{on}) was followed for 180 s, whereas the dissociation phase (k_{off}) was followed for 300 s. The complete dissociation of active complex formed was achieved by addition of 1 M NaCl, for 60 s before each new cycle start. The reference chip sensorgrams were opportunely subtracted to sample sensorgrams. When experimental data met quality criteria, kinetic parameters were estimated assuming a 1:1 binding model and using version 4.1 Evaluation Software (GE Healthcare), and it was so only for C_107 NPM1. Conversely, for C_107 NPM1 derived peptides the fit of the equilibrium values for the SPR response vs. the ligand concentration was employed and performed with GraphPad Prism v4.00 [39] using the one-site binding equation.

2.4. Peptide synthesis

Reagents for peptide synthesis (Fmoc-protected amino acids and resins, activation and deprotection reagents) were from Novabiochem (Läufelfingen, Switzerland) and InBios (Napoli, Italy). Solvents for peptide synthesis and HPLC analyses were from Romil (Dublin, Ireland); reversed phase columns for peptide analysis and the LC–MS system were from ThermoFisher (Milan, Italy). Solid phase peptide syntheses were performed on a fully automated multichannel peptide synthesizer Syro I (Multisynthech, Germany). Preparative RP-HPLC was carried out on a Shimadzu LC-8A, equipped with a SPD-M10 AV detector and with a Phenomenex C18 Jupiter column (50 × 22 mm ID; 10 μm). LC–MS analyses were carried out on a LCQ DECA XP Ion Trap mass spectrometer equipped with a OPTON ESI source, operating at 4.2 kV needle voltage and 320 °C with a complete Surveyor HPLC system, comprised of MS pump, an autosampler and a photo diode array (PDA). Narrow bore 50 × 2 mm C18 BioBasic LC–MS columns were used for these analyses.

The peptides 188–225, 225–243, 242–259, 242–259_B23.2, and 259–277 were synthesized employing the solid phase method on a 50 μmol scale following standard Fmoc strategies [40]. Rink-amide resin (substitution 0.5 mmol/g) was used as solid support. Activation of amino acids was achieved using HBTU/HOBt/DIEA (1:1:2), whereas Fmoc deprotection was carried out using a 20% (v/v) piperidine solution in DMF. All couplings were performed for 15 min and deprotections for 10 min and at the end of peptide chain assembly peptides were acetylated at their N-termini. Peptides were removed from the resin by treatment with a TFA:TIS:H2O (90:5:5, v/v/v) mixture for 90 min at room temperature; then crude peptides were precipitated in cold ether, dissolved in a water/acetonitrile (1:1, v/v) mixture and lyophilized.

Products were purified by RP-HPLC applying a linear gradient of 0.1% TFA CH_3CN in 0.1% TFA water from 5% to 65% over 12 min using a semi-preparative 2.2 × 5 cm C18 column at a flow rate of 20 mL/min. Peptides and purity and identity were confirmed by LC–MS. Purified peptides were lyophilized and stored at −20 °C until use.

2.5. Circular dichroism (CD) spectroscopy

CD spectra were recorded on a Jasco J-810 spectropolarimeter (JASCO Corp, Milan, Italy). CD spectra were registered at 25 °C in the far UV region from 190 to 260 nm. Each spectrum was obtained averaging three scans, subtracting contributions from corresponding blanks and converting the signal to mean residue ellipticity in units of $deg*cm^2*dmol^{-1}*res^{-1}$. Other experimental settings were: 20 nm/min scan speed, 2.0 nm band width, 0.2 nm resolution, 50 mdeg sensitivity, and 4 s response. The concentration of peptides was kept at 10×10^{-5} M and a 0.1 cm path-length quartz cuvette was used. Spectra were acquired in 10 mM phosphate buffer at pH 7.0.

Thermal denaturation profiles were obtained by measuring the temperature dependence of the ellipticity at 220 nm in the 293–363 K range with a resolution of 0.5 °C and 1.0 nm bandwidth. The heating rate was 1 K/min and the response at 16 s with a Peltier temperature controller.

A buffer solution containing 10 mM of sodium phosphate was used in chemical denaturation experiments. Urea was purchased from Sigma and further purified by recrystallization from ethanol/water (1:1) mixtures. Stock solutions of urea were mixed with peptide solutions to give a constant final value of the peptide concentration (100 μM). The final concentration of denaturant was in the range 0.0–8.0 M. Each sample was incubated overnight. Longer incubation times led to identical spectroscopic signals.

2.6. NMR experiment

NMR analysis was performed for 242–259 and 242–259_B23.2. NMR samples consisted of peptides (242–259: 1 mg; 242–259_B23.2: 0.8 mg) dissolved in 600 μL of 10 mM sodium phosphate buffer pH = 7.2; samples contain 5% (v/v) D_2O (99.8% d, Armar Scientific, Switzerland). Most NMR spectra were recorded at 298 K on a Varian Unity INOVA 600 MHz spectrometer provided with a cold probe. The process of proton resonance assignment was conducted by following a standard protocol which relies on comparison of 2D[^{1}H, ^{1}H] TOCSY (Total Correlation Spectroscopy) [41] (70 ms mixing time) and NOESY (Nuclear Overhauser Enhancement Spectroscopy) [42] (200 and 300 ms mixing times) spectra. Chemical shifts were referenced with respect to internal TSP (trimethylsilyl-3-propionic acid sodium salt-d4, 99% d, Armar Scientific, Switzerland) (see Appendix Tables A1, A2 for 242–259_B23.1, 242–259_B23.2, respectively).

1D spectra were recorded with a relaxation delay of 1 s and 32–64 scans. 2D experiments were generally acquired with 32–64 scans, 128–256 FIDs in t_1, 1024 or 2048 data points in t_2.

Water suppression was achieved with the DPFGSE (Double Pulsed Field Gradient Selective Echo) [43] sequence. Spectra were processed with VNMRJ 1.1D (Varian by Agilent Technologies, Italy) and analyzed with the NEASY [44] program that is included in the CARA (Computer Aided Resonance Assignment) software package (http://www.nmr.ch/). Analysis of Hα chemical shifts and deviations from random coil values

Please cite this article as: P.L. Scognamiglio, et al., G-quadruplex DNA recognition by nucleophosmin: New insights from protein dissection, Biochim. Biophys. Acta (2014), http://dx.doi.org/10.1016/j.bbagen.2014.02.017

were estimated with NmrView [45,46] by using the database by Wishart et al. for peptide random coil chemical shift values [47].

For the 242–259 peptide additional NMR spectra (1D [^{1}H] and 2D [^{1}H, ^{1}H] TOCSY (70 ms)) were recorded on a Varian Unity INOVA 400 MHz spectrometer at the following temperatures: 298, 303, 308, 313, 318, 323, and 333 K.

Peptide structure calculations were performed with CYANA [48] (version 2.1). Distance constraints for structure calculations were gained from NOESY experiments (300 ms mixing time). Angular constraints were generated with the GRIDSEARCH module of CYANA. Calculations generally started from 100 random conformers; the 20 structures with the best CYANA target functions (i.e. the lowest values) were inspected with MOLMOL [49].

3. Results

3.1. C_107 NPM1/B23.1 binds c-MYC G-quadruplex with high affinity

Previous investigations have shown that the binding affinity of NPM1 toward the c-MYC G-quadruplex depends on the length of the C-terminal region considered. Indeed, the C_53 NPM1 fragment of the protein (residues 242–294), which exclusively includes the three-helix bundle motif, binds the quadruplex with a K_D of 82 μM. The affinity increases (K_D = 1.9 μM) if an 18-residue stretch of the basic region is added to C_53 to generate C_70 NPM1 (residues 225–294) [33]. Since we have recently shown that the region 188–225 has stabilizing effects on C_70 NPM1, we evaluated the effect of this extension of the C-terminal region on G-quadruplex recognition. In particular, the affinity of C_107 NPM1 (residues 188–294) toward c-MYC G-quadruplex sequence was measured by SPR. A biotinylated oligonucleotide sequence was efficiently immobilized on SA-chip (averaged immobilization level 300 RU) and C_107 NPM1 was employed as analyte (concentration range 0.1–10 μM). Dose–response sensorgrams (Fig. 2) revealed that C_107 NPM1 avidly binds c-MYC G-quadruplex; the association rate appeared to be rapid (ka = 8.09 * 10^4 M^{-1} s^{-1}) whereas the dissociation was slow (kd = 0.0266 s^{-1}), thus providing a K_D value of 0.328 μM (Table 1). This finding clearly indicates that C_107 NPM1 presents a higher affinity for the G-quadruplex compared to C_70 and C_53 NPM1. Therefore, in addition to the region 225–241 [33], the region 188–224 also contributes to the complex formation.

3.2. Dissecting the C-terminal region of B23.1 and B23.2

The progressive increase of the affinity for the G-quadruplex upon the addition of extra-fragments on the N-terminal side of the three helix bundle motif, prompted us to dissect the C-terminal region of NPM1 in individual fragments to evaluate their intrinsic structural preferences and their DNA binding ability. Taking into account present and previous findings, the following fragments of NPM1/B23.1 were considered: 188–225, 225–243 (both belonging to the basic region), 242–259 (Helix 1), and 259–277 (Helix 2). For the region 242–259, a variant corresponding to the C-terminal end of B23.2 (242–259_B23.2) was also investigated (Fig. 1).

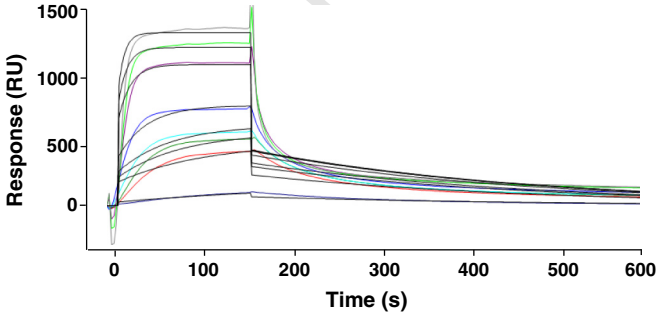

Fig. 2. Binding of C_107 NPM1 with c-MYC G-quadruplex through SPR. Overlay of sensorgrams for the interaction between biotinylated at 5′ c-MYC G-quadruplex sequence immobilized on a SA (streptavidin) sensor chip and C_107 NPM1 (as analyte). Experimental curves (colored lines) related to different concentrations of analyte (0.1, 0.5, 0,8 1, 2, 5, 7, 10 μM) were fitted according to a single exponential binding model with 1:1 stoichiometry (gray lines).

Table 1
Dissociation constants for the interaction of NPM1 regions with c-MYC G-quadruplex.

Ligand	K_D (μM)
C_70 NPM1	1.9 ± 0.1*
C_53 NPM1	82 ± 15*
C_107 NPM1	0.328 ± 0.003
188–225 NPM1	18 ± 5
225–243 NPM1	54 ± 15
242–259 NPM1	275 ± 43

* [33].

3.2.1. Intrinsic structural preferences of fragments of B23.1 and B23.2 C-terminal region

All peptides reported in Fig. 1 were chemically synthesized with good yields by SPPS, using Fmoc methodologies as N-terminal acetylated and C-terminal amidated derivatives and purified by RP-HPLC (see Materials and methods for further details). Their identity and purity (averaged purity > 97%) were assessed by LC–MS (data not shown).

To evaluate the impact of structural preferences of these fragments on their ability to bind c-MYC G-quadruplex, all peptides were characterized by far-UV circular dichroism (CD) and NMR spectroscopies. It is worth mentioning that the intrinsic tendency to aggregate and precipitate of the peptide 259–277 (corresponding to H2) prevented accurate structure and binding analyses.

The CD analysis shows a different structural behavior of the peptides used.

NPM1 188–225 (Fig. 3A) and 225–243 [21] CD spectra show typical random coil profiles presenting only one minimum at around 200 nm, as expected. On the other hand the two variants corresponding to the region 242–259 (242–259_B23.1 and 242–259_B23.2) showed spectra with bands at 190, 205, and 222 nm suggestive of the presence of α-helical conformation (Figs. 3B and A1). This conformation appeared stable within 4 h. Indeed the overlay of CD spectra registered within this time-lapse did not show any variation in the position and intensity of the bands.

In this framework, to gain deeper insights into the structure of the H1 region once separated from protein context, we performed NMR studies on both 242–259 variants.

For 242–259 in phosphate buffer, proton resonance assignments were obtained by comparison of 2D [^{1}H,^{1}H] TOCSY [41] and NOESY experiments [42] (Fig. 4A). Chemical shift deviations from random coil values [47] (Fig. 5a) were then evaluated and indicated a propensity for the peptide to form a helix in the region between Glu245 and Met251 (estimated helical content: 38.9%). The tendency of the peptide to adopt a helical conformation was further verified by NOE pattern [50] (Fig. 4B). Here, several contacts indicative of helices, mainly $H_N i$–$H_N(i+1)$; $H_\alpha i$–$H_N(i+2)$; $H_\alpha i$–$H_N(i+3)$; and $H_\alpha i$–$H_\beta(i+3)$, were observed in the segment encompassing residues Val244–Lys250. However, these NOEs coexist with rather strong sequential contacts of the type $H_\alpha i$–$H_N(i+1)$ that are, instead, hallmarks of extended and/or random coil conformations and suggest a certain degree of disorder for the peptide in solution.

To get additional informations, we carried out complete structural calculations. The analysis of the NMR ensemble of structures (Fig. 5B), carried out with the software MOLMOL [49], revealed the presence, in

Please cite this article as: P.L. Scognamiglio, et al., G-quadruplex DNA recognition by nucleophosmin: New insights from protein dissection, Biochim. Biophys. Acta (2014), http://dx.doi.org/10.1016/j.bbagen.2014.02.017

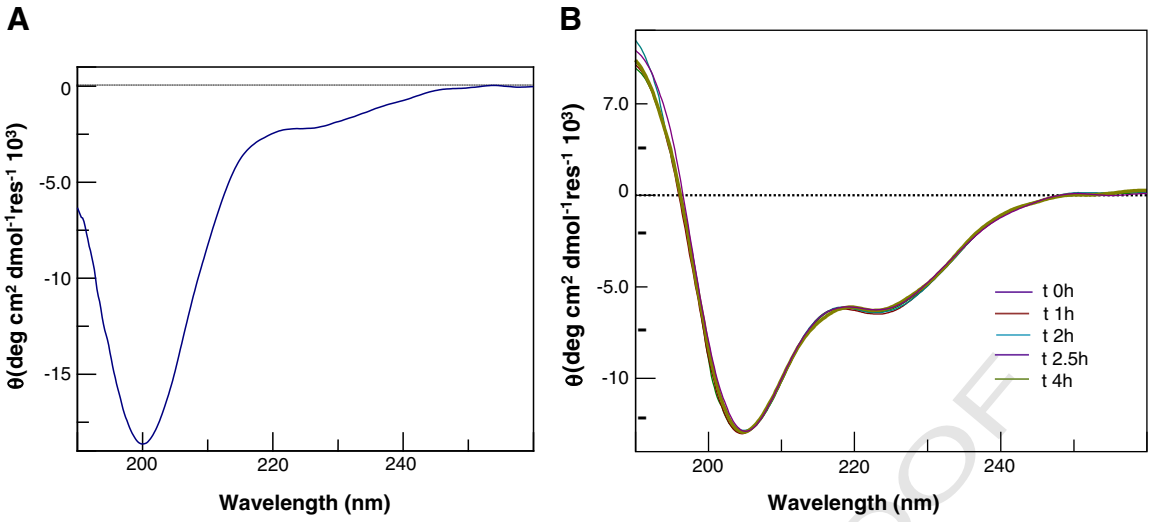

Fig. 3. Circular dichroism studies of C_107NPM1-based peptides. CD spectra of NPM1 (A) 188–225 and (B) 242–259, for the latter the overlay of spectra recorded at different times (0–4 h) is reported, and they were registered at 293 K in 10 mM phosphate buffer, pH 7.2.

most of the conformers, of a disordered pseudo-helical segment in between Val244 and Met251, composed of a turn of 3.10 helix (Val244–Ile247), and of a bend from Ile247 to Met251. This analysis clearly indicates that the C-terminal end is flexible.

NMR conformational analyses were carried out for 242–259_B23.2 in similar experimental conditions. Recorded 2D [^{1}H, ^{1}H] TOCSY and NOESY spectra (Fig. A2) allowed to assign proton resonances also for this peptide. The NMR parameters, i.e. chemical shift deviations from random coil values (Fig. 5g) and NOE pattern (Fig. A3), indicate a similar helix propensity and conformational behavior as 242–259 in the region between Val244 and Ala249. Despite the two amino-acid substitutions occurring at the very end of the two peptides (Fig. 1), the C-terminus of both 242–259 and 242–259_B23.2 is disordered.

3.2.2. The helical fragments 242–259 of B23.1 and B23.2 are endowed with a remarkable stability

The analysis of the thermal and chemical stabilities of 242–259 and 242–259_B23.2 unveils some unexpected features. Spectra collected over the temperature range 293 to 371 K indicate a marginal decrease of the CD signal (Fig. 6A). This experiment indicates that this sequence retains a significant amount of the helical structure at a very high temperature, even if a slight variation of ellipticity at 222 nm in the range 333–371 K (inset of Fig. 6A) suggests that a decrease of total helical content occurs. This thermal stability is very unusual for short peptides and has been occasionally reported for peptides with unnatural constrains [51].

These observations prompted us to perform additional NMR studies to better characterize the influence of higher temperatures on 242–259

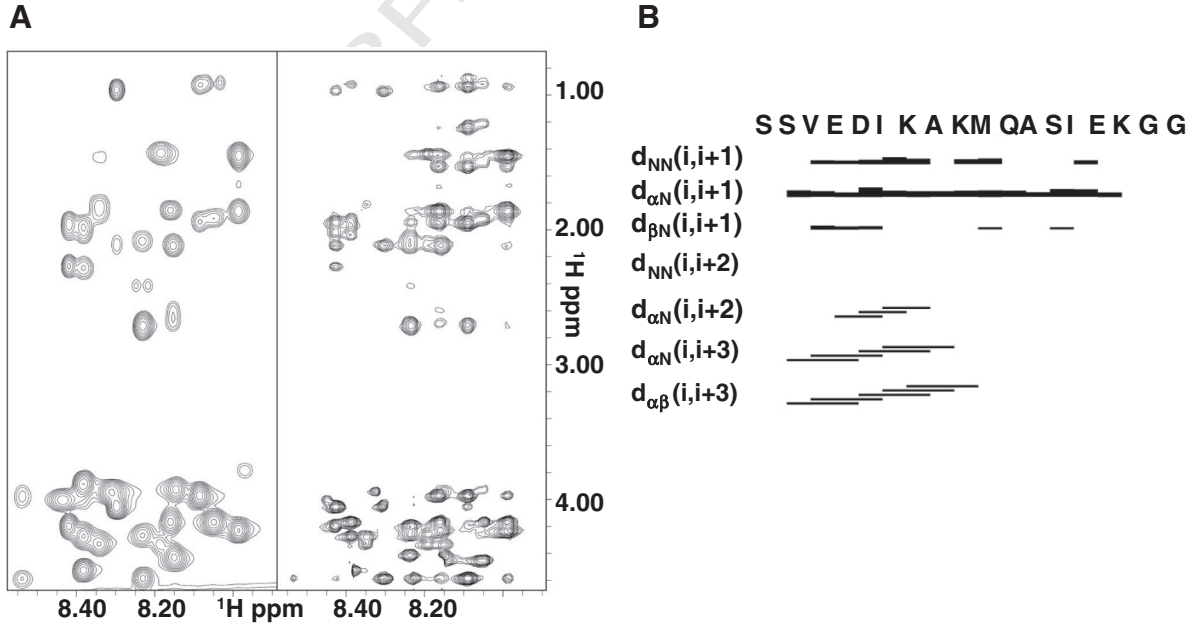

Fig. 4. NMR analysis of NPM1 242–259 B23.1 peptide. (A) 2D [^{1}H, ^{1}H] TOCSY (70 ms mixing time) (left panel) and 2D [^{1}H, ^{1}H] NOESY (300 ms mixing time) (right panel), the HN-aliphatic proton correlation region is shown. (B) NOE intensity diagrams for NPM1 242–259 B23.1. The amino acid sequence is reported on the top of diagram with the one letter code. A NOE connectivity between the Hx and Hy protons in the i and i + z residue respectively is indicated with "*d*xy(i, i + z)". The thickness of the bars reflects the corresponding NOE intensity. The software CYANA [48] was used to generate the NOE diagram.

Please cite this article as: P.L. Scognamiglio, et al., G-quadruplex DNA recognition by nucleophosmin: New insights from protein dissection, Biochim. Biophys. Acta (2014), http://dx.doi.org/10.1016/j.bbagen.2014.02.017

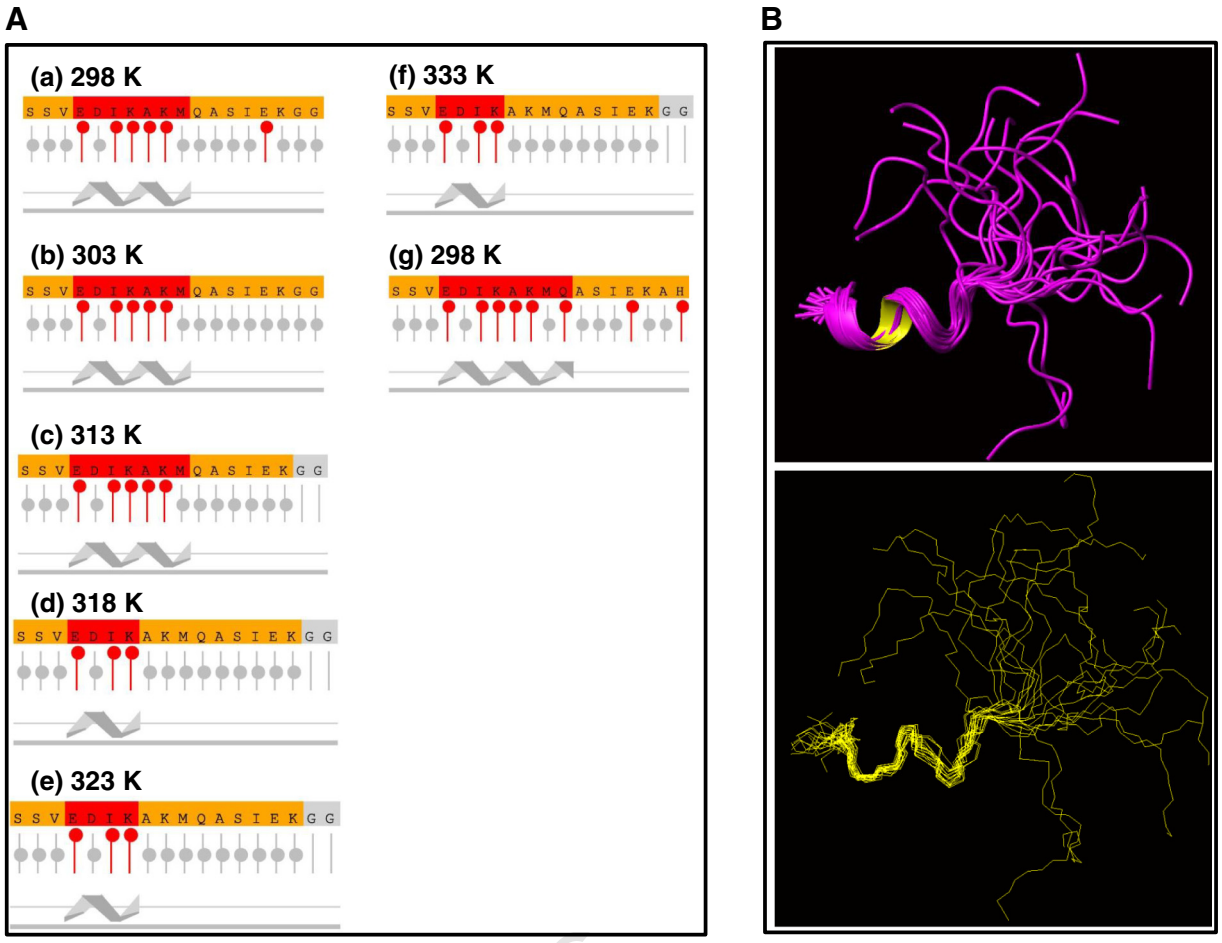

Fig. 5. Correlation between NMR chemical shifts and secondary structure content. Panel A) Hα chemical shift deviations from random coil values (CSD) for NPM1 242–259 B23.1 at (a) 298, (b) 303, (c) 313, (e) 318, (e) 323 and (f) 333 K. (g) Hα chemical shift deviations for NPM1 242–259 B23.2 at 298 K. Graphs were generated with the software NmrView [45] by using as reference random coil chemical shift values proposed by Wishart et al. [47]. In each panel red circles indicate residues with CSD values characteristic of helical secondary structure elements, whereas gray circles represent intermediate deviations equal or close to zero indicative of a residue in a random coil configuration. Peptide regions predicted to be helical are highlighted by the ribbon drawing on the bottom of each panel and corresponding residues are colored red on the amino acid sequence reported on the top. For the NPM1 242–259 B23.1 peptide the last two C-terminal glycines were excluded from the chemical shift analysis in the temperature range 313–333 K, as represented by a line lacking a circle in panels from (c) to (f), due to signal overlaps caused by the increase in temperature. NMR solution structure of NPM1 242–259 B23.1 peptide, Panel B): Superposition on the backbone atoms (residues 242–252) of twenty NPM1 242–259 B23.1 structures (RMSD: 0.96 Å). The ribbon and line representations are shown in the upper and lower panels respectively. The final structure calculation included 74 distance constraints: 30 intra-residues, 28 short- and 16 medium-range and 83 angle constraints. The software MOLMOL [49] has been implemented to generate the figure.

conformation (Fig. 6B). Proton Hα chemical shift changes were monitored as a function of the temperature (298–333 K) and chemical shift deviations from random coil values were estimated to indicate possible changes in the overall helical content. NMR signals that are mainly influenced by temperature are those belonging to H_N protons that become progressively broad and totally disappear at 333 K (Fig. 6B), minor changes are evident and affect the side chain aliphatic protons as well (Fig. A4a, b).

The broadening of H_N lines (Fig. 6B) indicates that by raising the temperature, H_N amide protons become gradually more exposed to the solvent, possibly because a partial unfolding of the pseudo-helical structure takes place. In details, for 242–259 when increasing the temperature the helical content drops from 38.9% to 22.2% (according to CD results) and a residual helical structure is likely to persist between Glu245 and Lys248, as estimated from chemical shift deviations of Hα protons from random coil values (Fig. 5f).

The analysis of the chemical stability of 242–259 was checked by using urea as chaotropic reagent. As shown in Fig. 6C–D, the intensity of the CD signal measured at 222 nm was significantly affected by the addition of even low amounts of the denaturant. Nevertheless, the analysis of the progression of the decrease of the CD signal intensity shows that a significant degree of secondary structure is retained even upon the addition of urea, 8 M. Similar trends were observed for the urea-induced chemical denaturation of 242–259_B23.2 (data not shown).

3.2.3. Fragments of B23.1 and B23.2 C-terminal region are individually able to bind the c-MYC G-quadruplex

The ability of C_107 NPM1-based peptides to bind G-quadruplex was checked by using SPR direct binding assays. These experiments were carried out in the same way of those involving the C_107 NPM1 by using biotinylated c-MYC G-quadruplex as a ligand and the peptides as analytes.

All the C_107 NPM1 regions showed detectable binding to c-MYC G-quadruplex (Table 1). The overlay of the sensorgrams corresponding to the peptide NPM1 188–225 (Fig. 7A–B) showed a clear dose–response binding, in the concentration range of 5–450 μM, and the estimation of K_D value was 18 ± 5 μM, while the affinity of NPM1 225–243 was three-fold lower, since experiments performed in a larger concentration range (10–1000 μM) provided a K_D value of 54 ± 15 μM (Fig. 7C–D). The sequence corresponding to H1 was analyzed in a similar concentration range (50–1200 μM) and data fitting provided a further fifteen-fold higher K_D value of 275 ± 43 μM (Fig. 7E–F). Other variants of NPM1

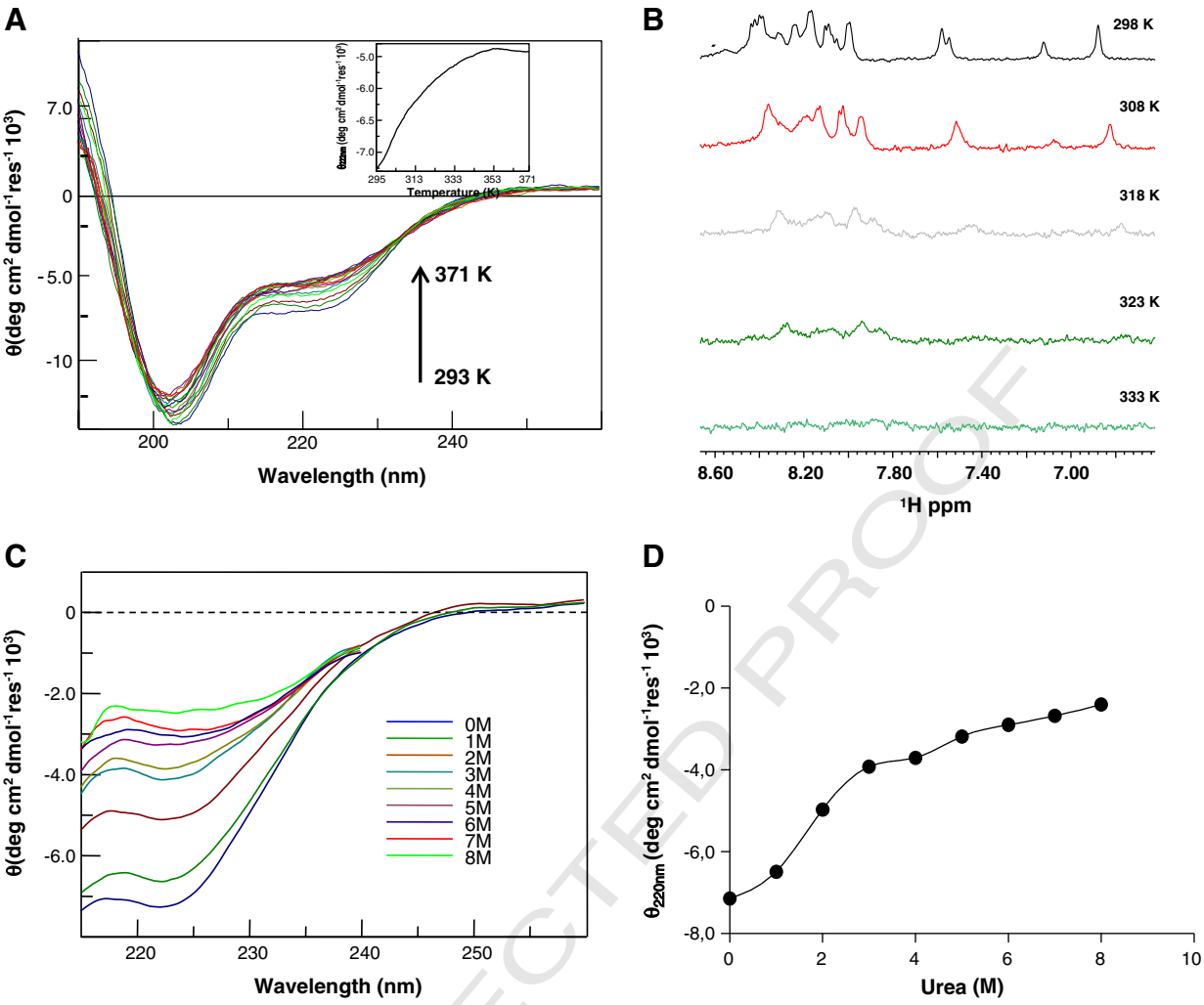

Q4 **Fig. 6.** Analysis of the stability of NPM1 242–259 B23.1 peptide. Overlay of CD spectra registered at (A) different temperatures in the range 293–371 K, as inset of the dependence of ellipticity at 222 nm versus temperature is reported, (C) increasing urea concentrations in the range 0–8 M. In the latter experiment CD spectra were registered in the range 215–260 nm since at lower wavelengths the presence of urea causes too high signal-to-noise ratio; (B) 1D [^{1}H] spectra of NPM1 242–259 B23.1 recorded at different temperatures. In detail, in the re-
Q5 ported expansion – from 6.80 to 8.60 ppm – signals arising from backbone and side chain H_N protons can be observed in (D) interpolation of experimental ellipticity at 222 nm versus urea concentration.

242–259 exhibited similar values of K_D toward c-MYC G-quadruplex (Fig. A5). The presence of different residues in the C-terminal region did not substantially affect the binding capacities of H1 variants.

4. Discussion

The involvement of NPM1/B23 in a variety of distinct biological processes is a direct consequence of its ability to establish intermolecular partnerships. The promiscuity of the protein is favored by its modular structure, in which structured domains alternate with disordered regions. Despite the importance of the NPM1/B23 interactions in physiological and pathological conditions, their biophysical and structural characterization is still incomplete. Very recently, it has been shown that the binding of G-quadruplex DNA by NPM1/B23 is important for the nucleolar localization of the protein [52]. The inability of leukemic NPM1/B23 variant to establish this interaction leads to the aberrant cytoplasmic localization of the protein.

Present findings demonstrate that the C-terminal region of the protein is able to bind the c-MYC G-quadruplex with a sub-micromolar affinity. The comparison of these results with previous literature data indicates that the progressive inclusion of portions of the basic region increases the binding affinity of NPM1/B23 for the G-quadruplex sequence. Intriguingly, the inclusion of these regions had also stabilizing effects on the thermal and chemical stabilities of the terminal three helix bundle motif [21,24].

The dissection of NPM1/B23 demonstrates that several fragments of the protein are intrinsically able to bind the G-quadruplex with high affinity. Present data also indicate that, in addition to the unfolded region 225–242, another intrinsically disordered fragment of the protein (residues 188–225) significantly contributes to the binding of the G-quadruplex. Therefore, the tight binding of NPM1/B23 to the G-quadruplex is achieved through the cooperation of both folded and unfolded regions that are individually able to bind it. As mentioned in the Introduction, in the NMR structure of the complex between NPM1 C_70 and the c-MYC G-quadruplex direct interactions with the DNA were established only by the three helix bundle motif [34]. Indeed, the region 225–242 remains flexible without forming any permanent contact with the G-quadruplex. On the other hand, here we show that both regions 188–225 and 225–243 of NPM1/B23 are indeed able to directly bind the G-quadruplex. These apparently contrasting results may be reconciled by assuming that the three helix bundle motif and the disordered basic regions recognize the same regions of the G-quadruplex. In this scenario, the intrinsically disordered regions may play a dual role in the G-quadruplex binding. Taking advantage of the great flexibility, they could efficiently anchor the DNA in the initial stage of the recognition process. Subsequently, after the binding of the G-quadruplex to

Please cite this article as: P.L. Scognamiglio, et al., G-quadruplex DNA recognition by nucleophosmin: New insights from protein dissection, Biochim. Biophys. Acta (2014), http://dx.doi.org/10.1016/j.bbagen.2014.02.017

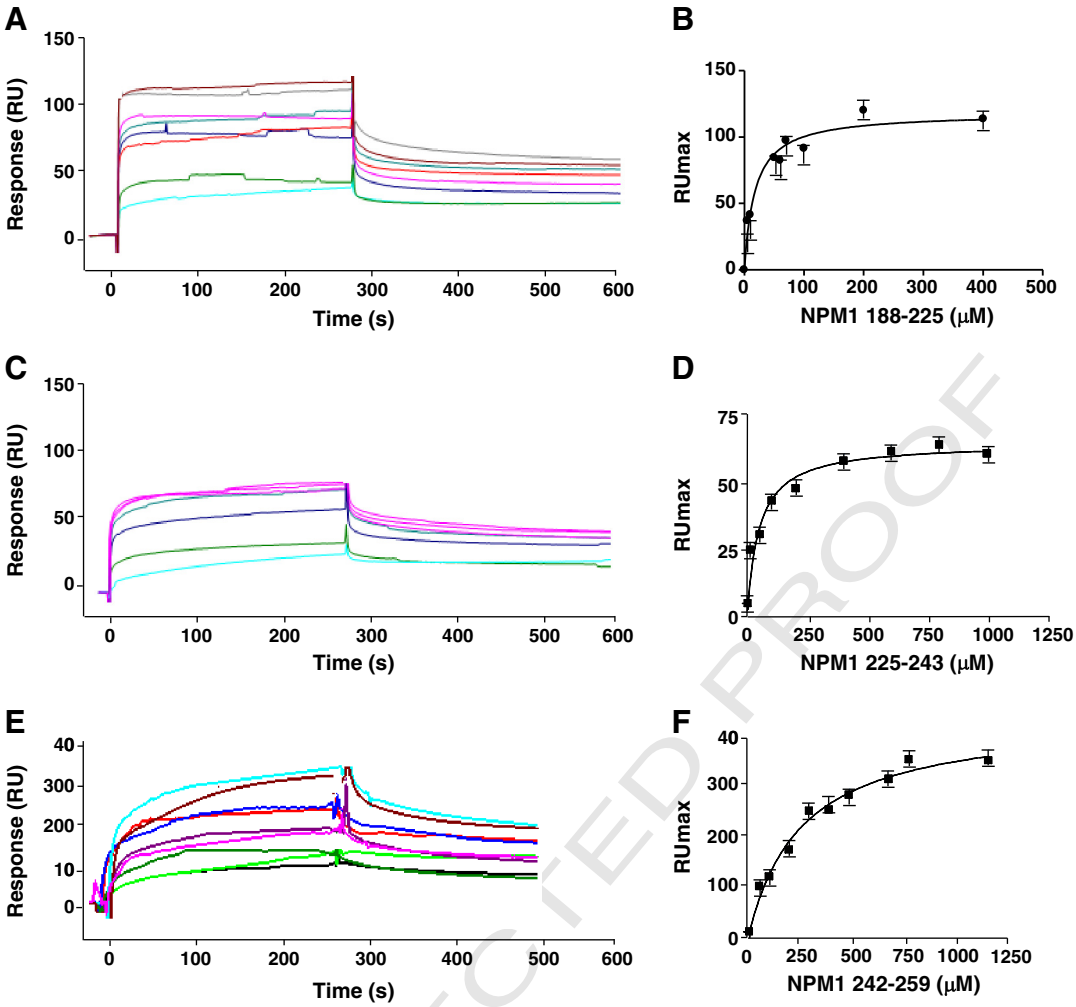

Fig. 7. Binding of C_107NPM1 derived peptides to c-MYC G-quadruplex through SPR. Overlay of sensorgrams for the interaction between biotinylated at 5′ c-MYC G-quadruplex sequence immobilized on a SA (streptavidin) sensor chip and C_107 NPM1 derived peptides. NPM1 (A) 188–225 (C) 225–243, and (E) 242–259 experimental curves that represent different concentrations of analyte and were fitted according to a single exponential binding model with 1:1 stoichiometry, (B), (D), and (F), respectively.

the three helix binding motif, the positively charges of these basic regions may generate a long-range favorable electrostatic environment, as previously suggested [34]. The ability of analyzed peptides to bind c-MYC G-quadruplex represents a solid ground for designing new molecules able to interact with this DNA motif.

The present findings also suggest a reduced G-quadruplex affinity for the two splicing variants B23.2 and B23.3. In particular, a reduced affinity of B23.3 is likely due to the lack of the basic region 195–223 in this isoform. Moreover, the truncation of the C-terminus of the three helix bundle motif to the helix H1 in B23.2 is also expected to strongly decrease the affinity for the G-quadruplex, since we show here that this helix exhibits a significantly reduced affinity, when compared to the whole domain. These suggestions are in line with the results independently obtained by Okuwaki and coworkers, who very recently analyzed the binding of the different NPM1/B23 isoforms and truncated forms to RNA [53]. However, very recently, it has been demonstrated, through ITC analysis, that the affinity of the full-length NPM1 for the same G-quadruplex is 3.8 μM [54] that is a value closer to that one obtained for the C_70 NPM1 than that for the C_107 NPM1. In the case of full-length NPM1 the electrostatic interactions established between the basic domain and the preceding acidic unstructured domains could influence G-quadruplex recognition.

The dissection of NPM1/B23 and the biophysical characterization of the resulting fragments also unveil that the H1 helix of both B23.1 and B23.2 is intrinsically endowed with an unusual thermal stability. A combined CD and NMR analyses show that the N-terminal region of H1 assumes a helical conformation, despite the intrinsic flexibility of the peptides. Indeed, the NMR analysis shows that the segment from Glu245 to Met251 clearly exhibits a tendency to adopt an ordered helical structure. CD and NMR data both indicate that this short helical segment is rather stable upon temperature increase. Evidence of this structure is detected in the entire temperature range (293–371 K for CD and 298–333 K for NMR) explored by using the two techniques. This thermal stability is very unusual for a short peptide that has been derived from a protein sequence. Similar high stabilities have rather been reported, only in few cases, for peptides whose sequences have been ad-hoc designed [51,55]. These unexpected results hold interesting implications for NPM1/B23 folding/unfolding process. In the last years, the folding pathway of several constructs of the NPM1 C-terminal region has been characterized in detail [21–24]. These studies have highlighted the presence of residual structure in the denatured state of the protein [56]. In particular, biophysical characterizations have detected a "native-like" structure that is retained in the denatured state of the wild-type protein, involving the helices H2–H3 of the three helix bundle motif. It has been shown that the presence of these native-like features in the NPM1/B23 denatured state accelerates the folding process. Moreover, it has been suggested that the identification and the characterization of these native-like features may be a way to design new molecules that could restore the native fold in pathological mutants. The intrinsic stability of the H1 helix provides support to the

Please cite this article as: P.L. Scognamiglio, et al., G-quadruplex DNA recognition by nucleophosmin: New insights from protein dissection, Biochim. Biophys. Acta (2014), http://dx.doi.org/10.1016/j.bbagen.2014.02.017

view that the denatured state retains some native-like structural properties, although in previous analyses this helix was considered to be unfolded. Of particular interest, in this context, is the observation that Trp290 interacts in the native fold with the intrinsically folded N-terminal region of H1. In line with the previous suggestions, this observation may be exploited in future studies for designing molecules able to stabilize the fold of the domain and to restore the protein function in NPM1/B23 mutants.

5. Conclusions

In conclusion this study unveils structural and functional determinants of the interaction between G-quadruplex DNA and NPM1, by analyzing the contribution of single protein regions in DNA recognition mechanism. Through a rational fragmentation approach results clearly indicate a crucial and direct role exerted by IDRs in DNA recognition, speculating a synergic action of IDRs along with H1 region in formation of the complex with G-quadruplex in which the flexible basic fragments primarily allow to accommodate DNA structures. This study shed new light for the design of small molecules and/or peptides able to stabilize G-quadruplex/NPM1complex which could help the research in the field of AML disease.

Acknowledgements

This work was funded in part by the MIUR Ricerca e Competitività 2007–2013 #PON 01_2388. The authors are grateful to Luca De Luca and Dr Giuseppe Perretta for the technical assistance, and Prof A. Zagari and Dr V. Granata of CEINGE – NAPOLI for their helpful discussion on SPR experiments.

Appendix A. Supplementary data

Supplementary data to this article can be found online at http://dx.doi.org/10.1016/j.bbagen.2014.02.017.

References

[1] Y.J. Kang, M.O. Olson, C. Jones, H. Busch, Nucleolar phosphoproteins of normal rat liver and Novikoff hepatoma ascites cells, Cancer Res. 35 (1975) 1470–1475.
[2] M. Okuwaki, K. Matsumoto, M. Tsujimoto, K. Nagata, Function of nucleophosmin/B23, a nucleolar acidic protein, as a histone chaperone, FEBS Lett. 506 (2001) 272–276.
[3] R.A. Borer, C.F. Lehner, H.M. Eppenberger, E.A. Nigg, Major nucleolar proteins shuttle between nucleus and cytoplasm, Cell 56 (1989) 379–390.
[4] M. Okuwaki, A. Iwamatsu, M. Tsujimoto, K. Nagata, Identification of nucleophosmin/B23, an acidic nucleolar protein, as a stimulatory factor for in vitro replication of adenovirus DNA complexed with viral basic core proteins, J. Mol. Biol. 311 (2001) 41–55.
[5] M.S. Lindstrom, NPM1/B23: a multifunctional chaperone in ribosome biogenesis and chromatin remodeling, Biochem. Res. Int. (2011) 195209 (16 pp.).
[6] L.B. Maggi Jr., M. Kuchenruether, D.Y. Dadey, R.M. Schwope, S. Grisendi, R.R. Townsend, P.P. Pandolfi, J.D. Weber, Nucleophosmin serves as a rate-limiting nuclear export chaperone for the mammalian ribosome, Mol. Cell. Biol. 28 (2008) 7050–7065.
[7] E. Colombo, M. Alcalay, P.G. Pelicci, Nucleophosmin and its complex network: a possible therapeutic target in hematological diseases, Oncogene 30 (2011) 2595–2609.
[8] J.P. Yun, J. Miao, G.G. Chen, Q.H. Tian, C.Q. Zhang, J. Xiang, J. Fu, P.B. Lai, Increased expression of nucleophosmin/B23 in hepatocellular carcinoma and correlation with clinicopathological parameters, Br. J. Cancer 96 (2007) 477–484.
[9] S. Grisendi, C. Mecucci, B. Falini, P.P. Pandolfi, Nucleophosmin and cancer, Nat. Rev. Cancer 6 (2006) 493–505.
[10] R. Balusu, W. Fiskus, R. Rao, D.G. Chong, S. Nalluri, U. Mudunuru, H. Ma, L. Chen, S. Venkannagari, K. Ha, S. Abhyankar, C. Williams, J. McGuirk, H.J. Khoury, C. Ustun, K.N. Bhalla, Targeting levels or oligomerization of nucleophosmin 1 induces differentiation and loss of survival of human AML cells with mutant NPM1, Blood 118 (2011) 3096–3106.
[11] B. Falini, I. Nicoletti, N. Bolli, M.P. Martelli, A. Liso, P. Gorello, F. Mandelli, C. Mecucci, M.F. Martelli, Translocations and mutations involving the nucleophosmin (NPM1) gene in lymphomas and leukemias, Haematologica 92 (2007) 519–532.
[12] B. Falini, C. Mecucci, E. Tiacci, M. Alcalay, R. Rosati, L. Pasqualucci, R. La Starza, D. Diverio, E. Colombo, A. Santucci, B. Bigerna, R. Pacini, A. Pucciarini, A. Liso, M. Vignetti, P. Fazi, N. Meani, V. Pettirossi, G. Saglio, F. Mandelli, F. Lo-Coco, P.G. Pelicci, M.F. Martelli, Cytoplasmic nucleophosmin in acute myelogenous leukemia with a normal karyotype, N. Engl. J. Med. 352 (2005) 254–266.
[13] B. Falini, N. Bolli, J. Shan, M.P. Martelli, A. Liso, A. Pucciarini, B. Bigerna, L. Pasqualucci, R. Mannucci, R. Rosati, P. Gorello, D. Diverio, G. Roti, E. Tiacci, G. Cazzaniga, A. Biondi, S. Schnittger, T. Haferlach, W. Hiddemann, M.F. Martelli, W. Gu, C. Mecucci, I. Nicoletti, Both carboxy-terminus NES motif and mutated tryptophan(s) are crucial for aberrant nuclear export of nucleophosmin leukemic mutants in NPMc + AML, Blood 107 (2006) 4514–4523.
[14] B. Falini, I. Nicoletti, M.F. Martelli, C. Mecucci, Acute myeloid leukemia carrying cytoplasmic/mutated nucleophosmin (NPMc + AML): biologic and clinical features, Blood 109 (2007) 874–885.
[15] M. Okuwaki, A. Sumi, M. Hisaoka, A. Saotome-Nakamura, S. Akashi, Y. Nishimura, K. Nagata, Function of homo- and hetero-oligomers of human nucleoplasmin/nucleophosmin family proteins NPM1, NPM2 and NPM3 during sperm chromatin remodeling, Nucleic Acids Res. 40 (2012) 4861–4878.
[16] M. Okuwaki, The structure and functions of NPM1/nucleophosmin/B23, a multifunctional nucleolar acidic protein, J. Biochem. 143 (2008) 441–448.
[17] V.M. Namboodiri, I.V. Akey, M.S. Schmidt-Zachmann, J.F. Head, C.W. Akey, The structure and function of *Xenopus* NO38-core, a histone chaperone in the nucleolus, Structure 12 (2004) 2149–2160.
[18] H.H. Lee, H.S. Kim, J.Y. Kang, B.I. Lee, J.Y. Ha, H.J. Yoon, S.O. Lim, G. Jung, S.W. Suh, Crystal structure of human nucleophosmin-core reveals plasticity of the pentamer–pentamer interface, Proteins 69 (2007) 672–678.
[19] C.G. Grummitt, F.M. Townsley, C.M. Johnson, A.J. Warren, M. Bycroft, Structural consequences of nucleophosmin mutations in acute myeloid leukemia, J. Biol. Chem. 283 (2008) 23326–23332.
[20] L. Federici, B. Falini, Nucleophosmin mutations in acute myeloid leukemia: a tale of protein unfolding and mislocalization, Protein Sci. 22 (2013) 545–556.
[21] D. Marasco, A. Ruggiero, C. Vascotto, M. Poletto, P.L. Scognamiglio, G. Tell, L. Vitagliano, Role of mutual interactions in the chemical and thermal stability of nucleophosmin NPM1 domains, Biochem. Biophys. Res. Commun. 430 (2013) 523–528.
[22] F. Scaloni, L. Federici, M. Brunori, S. Gianni, Deciphering the folding transition state structure and denatured state properties of nucleophosmin C-terminal domain, Proc. Natl. Acad. Sci. U. S. A. 107 (2010) 5447–5452.
[23] F. Scaloni, S. Gianni, L. Federici, B. Falini, M. Brunori, Folding mechanism of the C-terminal domain of nucleophosmin: residual structure in the denatured state and its pathophysiological significance, FASEB J. 23 (2009) 2360–2365.
[24] S. Chiarella, L. Federici, A. Di Matteo, M. Brunori, S. Gianni, The folding pathway of a functionally competent C-terminal domain of nucleophosmin: protein stability and denatured state residual structure, Biochem. Biophys. Res. Commun. 435 (2013) 64–68.
[25] D. Fantini, C. Vascotto, D. Marasco, C. D'Ambrosio, M. Romanello, L. Vitagliano, C. Pedone, M. Poletto, L. Cesaratto, F. Quadrifoglio, A. Scaloni, J.P. Radicella, G. Tell, Critical lysine residues within the overlooked N-terminal domain of human APE1 regulate its biological functions, Nucleic Acids Res. 38 (2010) 8239–8256.
[26] M. Hisaoka, S. Ueshima, K. Murano, K. Nagata, M. Okuwaki, Regulation of nucleolar chromatin by B23/nucleophosmin jointly depends upon its RNA binding activity and transcription factor UBF, Mol. Cell. Biol. 30 (2010) 4952–4964.
[27] E. Colombo, J.C. Marine, D. Danovi, B. Falini, P.G. Pelicci, Nucleophosmin regulates the stability and transcriptional activity of p53, Nat. Cell Biol. 4 (2002) 529–533.
[28] C. Lee, B.A. Smith, K. Bandyopadhyay, R.A. Gjerset, DNA damage disrupts the p14ARF-B23(nucleophosmin) interaction and triggers a transient subnuclear redistribution of p14ARF, Cancer Res. 65 (2005) 9834–9842.
[29] Y. Jian, Z. Gao, J. Sun, Q. Shen, F. Feng, Y. Jing, C. Yang, RNA aptamers interfering with nucleophosmin oligomerization induce apoptosis of cancer cells, Oncogene 28 (2009) 4201–4211.
[30] S.S. Gadad, R.E. Rajan, P. Senapati, S. Chatterjee, J. Shandilya, P.K. Dash, U. Ranga, T.K. Kundu, HIV-1 infection induces acetylation of NPM1 that facilitates Tat localization and enhances viral transactivation, J. Mol. Biol. 410 (2011) 997–1007.
[31] D. Wang, A. Baumann, A. Szebeni, M.O. Olson, The nucleic acid binding activity of nucleolar protein B23.1 resides in its carboxyl-terminal end, J. Biol. Chem. 269 (1994) 30994–30998.
[32] T.S. Dumbar, G.A. Gentry, M.O. Olson, Interaction of nucleolar phosphoprotein B23 with nucleic acids, Biochemistry 28 (1989) 9495–9501.
[33] L. Federici, A. Arcovito, G.L. Scaglione, F. Scaloni, C. Lo Sterzo, A. Di Matteo, B. Falini, B. Giardina, M. Brunori, Nucleophosmin C-terminal leukemia-associated domain interacts with G-rich quadruplex forming DNA, J. Biol. Chem. 285 (2010) 37138–37149.
[34] A. Gallo, C. Lo Sterzo, M. Mori, A. Di Matteo, I. Bertini, L. Banci, M. Brunori, L. Federici, Structure of nucleophosmin DNA-binding domain and analysis of its complex with a G-quadruplex sequence from the c-MYC promoter, J. Biol. Chem. 287 (2012) 26539–26548.
[35] S. Burge, G.N. Parkinson, P. Hazel, A.K. Todd, S. Neidle, Quadruplex DNA: sequence, topology and structure, Nucleic Acids Res. 34 (2006) 5402–5415.
[36] A. Siddiqui-Jain, C.L. Grand, D.J. Bearss, L.H. Hurley, Direct evidence for a G-quadruplex in a promoter region and its targeting with a small molecule to repress c-MYC transcription, Proc. Natl. Acad. Sci. U. S. A. 99 (2002) 11593–11598.
[37] C. Vascotto, D. Fantini, M. Romanello, L. Cesaratto, M. Deganuto, A. Leonardi, J.P. Radicella, M.R. Kelley, C. D'Ambrosio, A. Scaloni, F. Quadrifoglio, G. Tell, APE1/Ref-1 interacts with NPM1 within nucleoli and plays a role in the rRNA quality control process, Mol. Cell. Biol. 29 (2009) 1834–1854.
[38] M. Poletto, C. Vascotto, P.L. Scognamiglio, L. Lirussi, D. Marasco, G. Tell, Role of the unstructured N-terminal domain of the hAPE1 (human apurinic/apyrimidinic endonuclease 1), Biochem. J. 452 (2013) 545–557.
[39] R.L. Rich, D.G. Myszka, Advances in surface Plasmon resonance biosensor analysis, Curr. Opin. Biotechnol. 11 (2000) 54–61.
[40] G.B. Fields, R.L. Noble, Solid phase peptide synthesis utilizing 9-fluorenylmethoxycarbonyl amino acids, Int. J. Pept. Protein Res. 35 (1990) 161–214.

Please cite this article as: P.L. Scognamiglio, et al., G-quadruplex DNA recognition by nucleophosmin: New insights from protein dissection, Biochim. Biophys. Acta (2014), http://dx.doi.org/10.1016/j.bbagen.2014.02.017

[41] C. Griesinger, G. Otting, K. Wuthrich, R.R. Ernst, Clean TOCSY for H-1 spin system-identification in macromolecules, J. Am. Chem. Soc. 110 (1988) 7870–7872.
[42] A. Kumar, R.R. Ernst, K. Wuthrich, A two-dimensional nuclear overhauser enhancement (2D NOE) experiment for the elucidation of complete proton–proton cross-relaxation networks in biological macromolecules, Biochem. Biophys. Res. Commun. 95 (1980) 1–6.
[43] C. Dalvit, Efficient multiple-solvent suppression for the study of the interactions of organic solvents with biomolecules, J. Biomol. NMR 11 (1998) 437–444.
[44] C. Bartels, T.H. Xia, M. Billeter, P. Guntert, K. Wuthrich, The program XEASY for computer-supported NMR spectral analysis of biological macromolecules, J. Biomol. NMR 6 (1995) 1–10.
[45] B.A. Johnson, Using NMRView to visualize and analyze the NMR spectra of macromolecules, Methods Mol. Biol. 278 (2004) 313–352.
[46] S. Schwarzinger, G.J. Kroon, T.R. Foss, P.E. Wright, H.J. Dyson, Random coil chemical shifts in acidic 8 M urea: implementation of random coil shift data in NMRView, J. Biomol. NMR 18 (2000) 43–48.
[47] D.S. Wishart, C.G. Bigam, A. Holm, R.S. Hodges, B.D. Sykes, 1H, 13C and 15N random coil NMR chemical shifts of the common amino acids. I. Investigations of nearest-neighbor effects, J. Biomol. NMR 5 (1995) 67–81.
[48] T. Herrmann, P. Guntert, K. Wuthrich, Protein NMR structure determination with automated NOE assignment using the new software CANDID and the torsion angle dynamics algorithm DYANA, J. Mol. Biol. 319 (2002) 209–227.
[49] R. Koradi, M. Billeter, K. Wuthrich, MOLMOL: a program for display and analysis of macromolecular structures, J. Mol. Graph. 14 (1996) 51–55 (29–32).
[50] K. Wüthrich, NMR of Proteins and Nucleic Acids, John Wiley & Sons, New York, 1986.
[51] N.E. Shepherd, H.N. Hoang, G. Abbenante, D.P. Fairlie, Single turn peptide alpha helices with exceptional stability in water, J. Am. Chem. Soc. 127 (2005) 2974–2983.
[52] S. Chiarella, A. De Cola, G.L. Scaglione, E. Carletti, V. Graziano, D. Barcaroli, C. Lo Sterzo, A. Di Matteo, C. Di Ilio, B. Falini, A. Arcovito, V. De Laurenzi, L. Federici, Nucleophosmin mutations alter its nucleolar localization by impairing G-quadruplex binding at ribosomal DNA, Nucleic Acids Res. 41 (2013) 3228–3239.
[53] M. Hisaoka, K. Nagata, M. Okuwaki, Intrinsically disordered regions of nucleophosmin/B23 regulate its RNA binding activity through their inter- and intra-molecular association, Nucleic Acids Res. 17 (2014) 1180–1195.
[54] S. Banuelos, B. Lectez, S.G. Taneva, G. Ormaza, M. Alonso-Marino, X. Calle, M.A. Urbaneja, Recognition of intermolecular G-quadruplexes by full length nucleophosmin. Effect of a leukaemia-associated mutation, FEBS Lett. 587 (2013) 2254–2259.
[55] D. Diana, B. Ziaco, G. Colombo, G. Scarabelli, A. Romanelli, C. Pedone, R. Fattorusso, L.D. D'Andrea, Structural determinants of the unusual helix stability of a de novo engineered vascular endothelial growth factor (VEGF) mimicking peptide, Chemistry 14 (2008) 4164–4166.
[56] I.E. Sanchez, T. Kiefhaber, Hammond behavior versus ground state effects in protein folding: evidence for narrow free energy barriers and residual structure in unfolded states, J. Mol. Biol. 327 (2003) 867–884.

Please cite this article as: P.L. Scognamiglio, et al., G-quadruplex DNA recognition by nucleophosmin: New insights from protein dissection, Biochim. Biophys. Acta (2014), http://dx.doi.org/10.1016/j.bbagen.2014.02.017

ACKNOWLEDGEMENTS

A great deal of my gratitude goes to Prof. Gianluca Tell, who has been mentor, source of inspiration and friend.

I am immensely grateful to the past and present members of the GT lab: Lisa, Giulia, Arianna, Elena, Carlo, Damiano, Laura, Erika, Milly, and Marta, who have always been kind, friendly and ready to help in any situation. In particular, I would like to express my gratitude to Matilde, for her invaluable help in the lab and for being always ready to share a smile.

Thanks also to the people in the LMG lab, to Dr. David Wilson III and his group in particular, because they provided a stimulating environment and they made me feel at home even thousand miles away.

All my colleagues deserve a huge acknowledgement: Federica, on top of everyone, then Paolo, Enrico, Andrea, and Davide, just to name a few, because they shared and breathed with me the PhD experience, inside and especially outside the lab.

A really extraordinary acknowledgement goes to Andrea, who has been more than a friend, more than a colleague, more than a roommate, more than anything else.

I conclude by thanking Michela. No words in any language will be enough to express how grateful I am for her contribute to this thesis and to my life…THANK YOU!